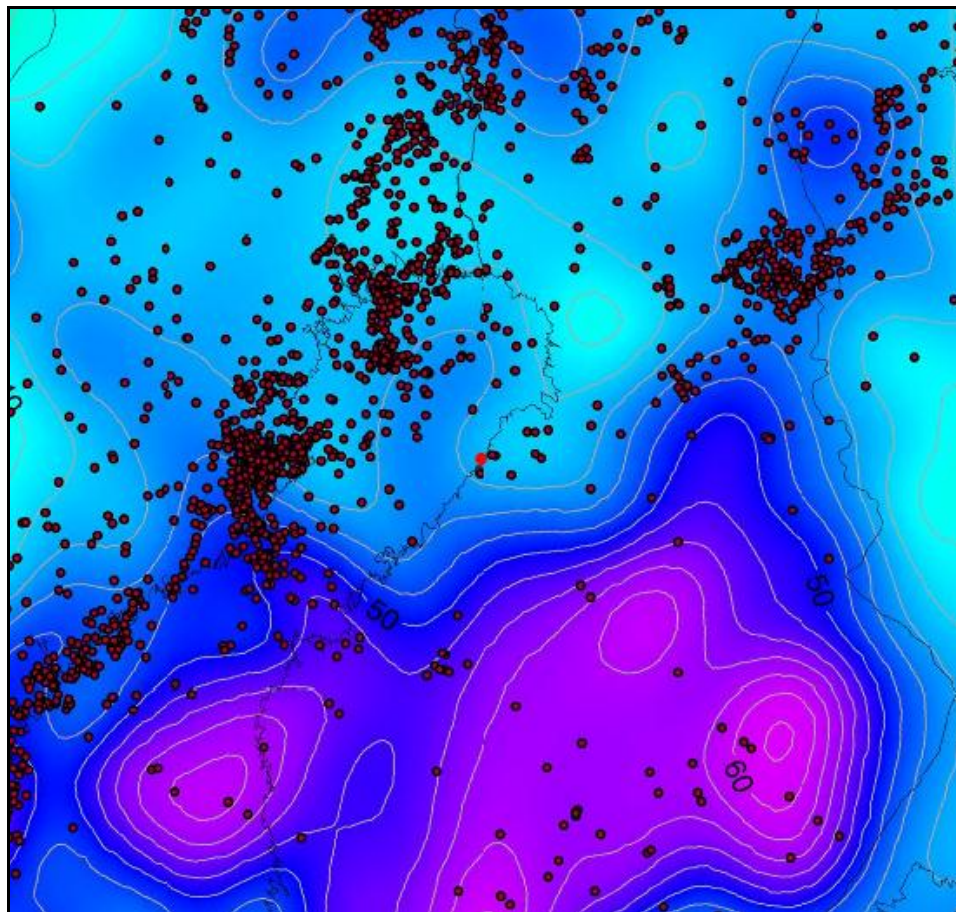


INSTITUTE OF SEISMOLOGY
UNIVERSITY OF HELSINKI

REPORT S-63

**SEISMOTECTONIC FRAMEWORK AND
SEISMIC SOURCE AREA MODELS IN FENNOSCANDIA,
NORTHERN EUROPE**



edited by
Annakaisa Korja and Emilia Kosonen

Helsinki 2015

Editor-in-Chief: Pekka Heikkinen
Guest Editors: Annakaisa Korja and Emilia Kosonen
Corresponding author: Annakaisa Korja
Department of Geosciences and Geography
Institute of Seismology
P.O.Box 68
FI-00014 University of Helsinki
Finland
Email: Annakaisa.Korja@ helsinki.fi

Publisher: Institute of Seismology
P.O. Box 68
FI-00014 University of Helsinki
Finland
Phone: +358-294-1911 (switchboard)
Fax: +358-2941-51598
<http://www.helsinki.fi/geo/seismo/>

ISSN 0357-3060
ISBN 978-952-10-9583-2 (PDF)
ISBN 978-952-10-5078-7 (Paperback)
Unigrafia
Helsinki 2015

Seismotectonic framework and seismic source area models in Fennoscandia, northern Europe

Host organization: **Institute of Seismology, Department of Geosciences and Geography, University of Helsinki**

ISUH - Institute of Seismology, University of Helsinki

Korja, Annakaisa (scientific leader)
Hellqvist, Niina
Koskinen, Paula
Kosonen, Emilia
Mäntyniemi, Päivi
Uski, Marja
Valtonen, Outi

GTK - Geological Survey of Finland

Airo, Meri-Liisa
Huotari-Halkosaari, Taija
Kallio, Jarmo
Laine, Mirva
Nironen, Mikko
Sutinen, Raimo

SGU - Geological Survey of Sweden

Grigull, Susanne
Stephens, Michael

UU – University of Uppsala

Högdahl, Karin
Lund, Björn

Preface

The following people have written the different sections in the text:

Summary

Annakaisa Korja has written the summary.

Section 1

Annakaisa Korja has written section 1.

Section 2

Susanne Grigull (Sweden) and Meri-Liisa Airo, Taija Huotari-Halkosaari and Mikko Nironen (Finland) have presented the geological and geophysical data used in the respective countries in sections 2.1 to 2.5; Karin Högdahl has written about the submarine data in the Gulf of Bothnia in section 2.6; Susanne Grigull, Raimo Sutinen and Emilia Kosonen have written about the faults active during the Quaternary period in section 2.7; and Björn Lund, Marja Uski and Päivi Mäntyniemi have written section 2.8 on the seismicity data in Sweden and Finland. Päivi Mäntyniemi prepared the historical earthquake database and the respective table and figures. Annakaisa Korja has written the section 2.9.

Section 3

Michael Stephens, Mikko Nironen and Annakaisa Korja have presented the major lithotectonic units in the study area in section 3.1.1.

Mikko Nironen and Annakaisa Korja have written the parts of section 3.1.2 that concern the deformation zones in the Karelia and Inari lithotectonic units, the Central Finland lithotectonic unit and the Southern Finland unit. Michael Stephens has written the parts of section 3.1.2 that concern the deformation zones in the Ljusdal lithotectonic unit, the Bothnia-Skellefteå lithotectonic unit and the lithotectonic units inside the Caledonian orogen.

Karin Högdahl and Michael Stephens have written section 3.1.3 on the faults in the Gulf of Bothnia.

Raimo Sutinen, Emilia Kosonen and Björn Lund have written section 3.2 on the glaciation cycles during the Quaternary period. Colby Smith and Lars Rodhe (SGU) have commented section 3.2.

Section 4

Marja Uski and Björn Lund have written subsection 4.1. Päivi Mäntyniemi has written subsection 4.2. Marja Uski, Annakaisa Korja and Björn Lund have written subsection 4.3.

Section 5

Paula Koskinen and Annakaisa Korja have written subsections 5.1-5.3 and Annakaisa Korja has written subsection 5.4. Marja Uski, Björn Lund and Annakaisa Korja have written the subsections 5.5-5.7.

Section 6

Paula Koskinen and Annakaisa Korja have written section 6.

Section 7

Annakaisa Korja and Nina Hellqvist have completed the literature review in section 7 summarizing current seismotectonic and previous seismic source area models in Fennoscandia.

Section 8

Annakaisa Korja has written section 8.1.

Michael Stephens has written the general methodology and result for spatial model 1 in section 8.2. Michael Stephens and Mikko Nironen have written the geological and tectonic framework descriptions of the Swedish and Finnish source areas respectively. Marja Uski and Björn Lund have written the descriptions of the seismic source geometry and seismological parameters in Finland and Sweden, respectively. Päivi Mäntyniemi has written the parts on historical earthquakes in model 1.

Susanne Grigull and Annakaisa Korja have written the general methodology and result for spatial models 2 and 3 in section 8.3. Susanne Grigull, Annakaisa Korja and Emilia Kosonen have written geological and tectonic framework. Björn Lund and Marja Uski have written the descriptions of source areas (seismic source geometry and seismological parameters). Päivi Mäntyniemi has written the parts on historical earthquakes in models 2 and 3.

Section 9

Annakaisa Korja has written the discussion. Päivi Mäntyniemi has written the comments on historical earthquakes in subchapters 9.2 and 9.5.1. Mikko Nironen, Marja Uski, Päivi Mäntyniemi and Björn Lund have commented the discussion.

Section 10

Annakaisa Korja has outlined the conclusions. Mikko Nironen, Päivi Mäntyniemi, Marja Uski and Björn Lund have commented the conclusions.

Section 11

Emilia Kosonen has compiled the references.

Appendices

Appendix 1 Mirva Laine, Taija Huotari-Halkosaari and Mikko Nironen have summarized the geological and geophysical studies previously carried out by GTK for Fennovoima Oy. Outi Valtonen and Annakaisa Korja have written the section on geodetic studies and the instrumental seismic monitoring at the target site. Päivi Mäntyniemi has written the section on historical seismicity in the vicinity of the Hanhikivi site. Annakaisa Korja has written the summary and collected the conclusions and suggestions from the previous studies.

Appendix 2 was compiled by Päivi Mäntyniemi.

Appendix 3 was compiled by Emilia Kosonen and Taija Huotari-Halkosaari.

Appendix 4 was produced by Emilia Kosonen.

Summary

A. Korja

This study aims to identify seismic source areas and to address the seismotectonic framework as a basis for a seismic hazard evaluation at the potential nuclear power plant site at Hanhikivi, Pyhäjoki, Northern Ostrobothnia, Finland. The study has been carried out for Fennovoima Oy by geoscientific expert groups from both Finland (Institute of Seismology University of Helsinki) (ISUH), Geological Survey of Finland (GTK) and Sweden (University of Uppsala, Geological Survey of Sweden) using the latest documented geological, geophysical and seismological data sets from both countries. The study area comprises a circle with 500 km radius around the Hanhikivi site including land and marine areas of Finland and Sweden.

The study has been carried out in six working stages. **Task 1** provided a review summarizing the existing and ongoing geological and geophysical studies carried out around the Hanhikivi site by GTK, the Finnish Geodetic Institute (FGI) and ISUH. The results of stage 1 are summarized in Appendix 1. **Task 2** involved the compilation and description of a regional-scale geological and geophysical upgradable database for present and future studies in the site area. The metadatabase is described in Appendix 3 and the methodology used to evaluate historical seismicity is described in Appendix 3. **Task 3** presented an overview of the paleotectonic evolution and the Quaternary glacial history and the current tectonic framework inside the study area. **Task 4** described seismicity and earthquake source parameters of the study area. **Task 5** involved a review of the current conceptual seismotectonic models and previous seismic source area models for Fennoscandia. **Task 6** identified and described alternative spatial models for seismic source areas in the study area.

Task 1: (*Appendix 1*) Previous studies describing the geological and geophysical features around the Hanhikivi site have been launched in regional (25-300 km), near-regional (5-25 km) and site-vicinity (<5 km) scales. Hanhikivi is located on bedrock composed of rocks belonging to the so-called Svecofennian Domain. The area in the vicinity of the Hanhikivi site is framed to the south and north by NNE-SSW and NW-SE oriented deformation zones that are part of the Raahe-Ladoga shear complex. However, no regional-scale deformation zones seem to cross the site area. None of the significant fracture zones has been active during post-glacial time. The closest known active post-glacial fault zone is in Västerbotten, Sweden, 180 km west of Hanhikivi site. Based on the available data sets, it was concluded that no post-glacial faults could be identified in the near-regional and site-vicinity areas around the Hanhikivi site and that the existence of post-glacial fault structures (and capable faults) in the near-regional study area (25 km) is unlikely. However, the data sets do not cover the study area completely. Geophysical surveys have been recommended for more precise structural studies of the fracture zones in onshore and offshore studies. To gain information on the local-scale (in mm scale) horizontal movements within the study area, a local dense network of permanent GNSS stations should be established for a minimum period of five years.

The historical seismicity data available for Northern Ostrobothnia between 1740 and 1930 suggest that many of the largest historical earthquakes have been felt at Hanhikivi. A virtual seismic history has therefore been compiled. A special feature is that the known historical earthquakes occurred in different countries and in different directions from the site. The estimated intensities at Hanhikivi site have not been larger than I=4-5 (EMS-98). The

compiled seismic history is not long enough to capture the recurrence times of earthquakes of magnitude above 4.

The spatial coverage of the national seismic network in Northern Ostrobothnia was too sparse for detailed or regional seismicity studies around potential power plants. Based on a recommendation by the University of Helsinki, Fennovoima Oy decided to build a local network of 10 stations within a radius of 50 km from the Hanhikivi site.

Task 2: The current study is based on the following previously existing GIS data sets from: 1) the Geological Surveys of Finland and Sweden; including lithological, structural, airborne magnetic and Bouguer gravity anomaly maps, post-glacial faults and the interpretation of shallow marine seismo-acoustic data from the Gulf of Bothnia; and 2) the Universities of Helsinki and Uppsala; including an updated instrumental and historical seismicity database, Moho topography, and the interpretation of deep seismic reflection data (BABEL, FIRE). In addition, freely available topographic data (GLOBE) from the Globe Task Team and bathymetric data (GEBCO) from the British Oceanographic Data Centre have been used. The data sets are supplied with adequate metadata information (Appendix 3) and are archived in an ArcGIS-based database at Fennovoima Oy.

The parametric earthquake catalogue FENCAT covers the years 1375–2011. Macroseismic datapoint (MDP) datasets have been complied for 20 historical earthquakes, which has led to some changes in the non-instrumental part of the FENCAT. The instrumental dataset from FENCAT has been supplemented with a preliminary version of the 2012 earthquake catalogue and a micro-earthquake catalogue for 2000–2013 in Sweden. Mining-induced seismic events as well as events with questionable seismic origin have been removed from the data within or close to the study area.

Task 3: The northern part of the Fennoscandian Shield is surrounded by the Caledonian orogenic belt to the west, the North Atlantic continental platform to the north and the East European platform to the south and east. Offshore, in the Gulf of Bothnia, Meso-Neoproterozoic and Lower Paleozoic sedimentary rocks provide a cover to the crystalline bedrock.

We have divided the bedrock addressed in this study into thirteen lithotectonic units. The majority of these units contain rocks with a distinct tectonothermal history and are mostly separated from each other by regional-scale, ductile and brittle deformation zones or an angular unconformity. The major part of the study area consists of seven lithotectonic units (Karelia, Inari, Central Finland, Southern Finland, Ljusdal, Bothnia-Skellefteå, and Norrbotten) that attained their current architecture during orogenic activity at 2.0–1.8 Ga. The northeastern part of the study area (Karelia, Inari and Norrbotten) contains Archean crust affected by NeoArchean orogeny and later Paleoproterozoic extension at 2.5–2.0 Ga prior to orogenic reworking at 2.0–1.8 Ga. Latest Paleoproterozoic and Mesoproterozoic magmatic rocks and Mesoproterozoic sedimentary provinces, which formed around and after 1.6 Ga in extensional paleotectonic environments, form a unit located mostly in and around the Gulf of Bothnia and the White Sea. These rocks are well-preserved, unaffected by later orogenic activity and complete the Precambrian lithotectonic framework in the Fennoscandian Shield. Ediacaran–Cambrian and Ordovician sedimentary rocks form a platformal cover and together form their own lithotectonic unit. The Caledonian orogen

(0.5–0.4 Ga) in the northwestern part of the study area has been divided into four lithotectonic units.

Deformation zones that were formed during transpressional-compressional and transtensional-extensional events are described for different groups of lithotectonic units. Seismic reflection profiles suggest that most of the ductile deformation zones are limited to the upper crust. They seem either to terminate or to flatten out at the upper-middle crustal boundary, which serves as a major décollement. Only a few major shear complexes extend to the middle-lower crustal boundary and even fewer penetrate the Moho boundary (in central Lapland and along the Raahe-Ladoga shear complex).

During the Quaternary Period (ca. 2.6 Ma–present), the study area was affected by several climate oscillations, from warm to cold with interglacial and glacial phases, respectively, and associated loading and unloading events. In Fennoscandia, there are sediments preserved from three large glaciations (Elsterian, Saalian and Weichselian) and two interglacials (Holstein and Eem) that interrupted the glaciation stages. The last deglaciation period, starting at 18 ka BP, reached southern Finland at 13 ka, stagnated during the colder Younger Dryas at 13-11.5 ka and reached the Gulf of Bothnia at 10 ka; the remainder of the glacier had melted completely by 9 ka. The sedimentary formations deposited during the last glacial cycle are the ones that are best preserved. During the deglaciation period, the sedimentary material was deposited in rivers and lakes, and the bedrock started to rebound to its original position. The highest Baltic Sea shorelines are situated at different altitudes in Fennoscandia, depending on the differences in crustal depression and rebound velocities as well as the sea-level changes during different Baltic Sea stages. The rebounding is not only expressed in retreating sea level observations but also along post-glacial faults. Post-glacial faults suggest sudden stress release and earthquake activity. The onset of the Fennoscandian fault activity started at the end of the deglaciation phase, and the maximum fault instability was reached during the Younger Dryas and Early Holocene period 13-10 ka BP.

Vertical ground motion taking place in Fennoscandia is mostly attributed to glacial isostatic adjustment (GIA), commonly referred to as post-glacial rebound. It is caused by the slow return flow of mantle material back to its original position below the depression of the lithosphere caused by the ice load during the latest glaciation. The still remaining isostatic imbalance is being adjusted by slow land uplift. The latter is centered in northeastern Sweden and the Bay of Bothnia i.e. within the study area. According to a recent land uplift model, the maximum rate of uplift is 8–9 mm/a. The strain field in central Fennoscandia, where the rate of post-glacial rebound is the highest, is dominated by an extension rate of 5 nanostrain/a. The southeastern parts are compressed at strain rates -6 and -1 nanostrain/a.

The orientation of the overall maximum horizontal stress field in northern Europe is WNW–ESE to NW–SE. The azimuth of the plate motion direction relative to North America in Finland is between 115° and 132° and the azimuth increases from south to north. In the northern part of the study area, the minimum principal stress (σ_3) is vertical, the maximum horizontal stress is horizontal and mostly reverse faulting takes place. In the Bothnia regions, where vertical stresses overcome horizontal ones, the maximum principal stress (σ_1) is vertical and normal faulting takes place.

The stress indicators suggest that changes in topography and in thickness of the crust and lithosphere may cause local and regional changes in the stress field in Fennoscandia.

Offshore areas are associated with topographical depressions and thinner crust than the surrounding onshore areas in most cases. A few exceptions are found. The thickest parts of the crust are characterized by subdued topography whereas the highest mountains in the Scandes to the west are characterized by the lack of crustal roots and thinner crust. This suggests that the mountains are not isostatically compensated from below and that other forces are acting on the Fennoscandian margin. It is noted that the present land-uplift maximum is loosely spatially associated with the area hosting the thin to normal crust and that the seismically active areas around the northern part of the Gulf of Bothnia (Bay of Bothnia and southern Lapland) have risen/rebounded slower than model predictions. The negative deviation suggests that either the model has to be updated or that rebounding has been hindered by local structure. It seems that plate boundary forces, GIA and seismicity have complex interwoven relationships that need to further studied in the future.

Task 4: Northern Ostrobothnia is situated in a seismically quiet continental intraplate setting in the northern part of the Fennoscandian Shield. Current tectonic and seismic activity in the study area is caused by processes associated with both intraplate and plate margin processes: opening of the North Atlantic Ocean, post-glacial rebound and local stress caused by local mass anomalies.

Higher seismic activity is found along the east coast of Sweden, in the Gulf of Bothnia, in Lapland, and in the Kuusamo and Wiborg areas. Instrumentally recorded earthquakes in the study area have magnitudes between M_L 0 and 5.2 and have taken place from shallow crustal depths down to 40 km. Some historical earthquakes may have exceeded magnitude 5 in the study area. The seismicity in the study area is clustered along NE-SW-trending zones that are parallel to the Norwegian margin and the Mid-Atlantic ridge. A slight change in the general seismicity pattern takes place across an N-S-trending zone running east of the Finnish-Swedish national border (Pajala shear zone and its northerly continuation). East of this zone, the seismic activity rates are lower and the NE-SW trend is less obvious.

The reliable depth estimates available indicate that the majority of the earthquakes seem to have occurred in the upper 17 km of crust. By the definition that lower limit of the seismogenic zone is where 99% of the earthquakes occur; the results suggest that the seismogenic layer reached down to the depth of 31 km. In the Wiborg batholith, the Skellefteå area (Bothnia-Skellefteå lithotectonic unit) and the Kuusamo district as well as along the Hirvaskoski and Oulujärvi shear zones in the Karelia lithotectonic unit, the depth distribution differs from the general pattern. The earthquake swarms in the Wiborg batholith are unusually shallow, mostly occurring within the first 1–2 km of crust. In the Skellefteå area, roughly 50 % of the events occur in the middle and lower crust, at depths between 15 and 45 km. In the Kuusamo area and along the Hirvaskoski and Oulujärvi shear zones, the seismicity took place down to 30 km and > 50% occurred in the middle crust, at depths below 15 km.

The focal mechanisms in the study area show a combination of mostly strike-slip and reverse faulting conditions. In south-central Sweden, strike-slip is the most common mechanism while reverse mechanisms are more common further to the north. In Finland, reverse and strike-slip mechanisms occur intermixed over the whole country.

Deformation zones that are optimally oriented in the present stress field can potentially be reactivated. The deformation zones archived in the structural database were analysed for

their length and azimuth and they were assigned a potential reactivation type (reverse, normal or strike slip) according to their azimuth alone. The earthquakes in the seismically most active area, close to Skellefteå along the western coast of the Gulf of Bothnia and its northeasterly continuation, appear to cluster around the shoreline and along post-glacial faults, which are mostly oriented optimally for reverse or strike slip faulting. Fault systems in many directions that are optimal for reactivation transect the seismically active Kuusamo area.

Stage 5: Currently, most authors agree that the sources of the seismicity in Fennoscandia are multiple and diverse in nature, ranging from plate-wide to local scales. The dominant driving forces of seismicity are related to opening of the North Atlantic Ocean, post-glacial rebound and lateral variations in lithospheric structure. The current seismotectonic models for Fennoscandia favor combinations of different sources of stress as the origin of seismicity.

One of the models has claimed that the Scandinavian passive margin has a hyperextension architecture that developed during large magnitude extension associated with the opening of the North Atlantic Ocean. Based on topographic and lithospheric thickness data, Scandinavia has been divided into distal margin, proximal margin, hinterland and craton parts that are separated from each other by a taper break, an escarpment and a hinterland break-in slope, respectively, all associated with high seismicity belts. This model suggests that seismicity is concentrated along the boundaries steered by extensional tectonics during the opening and spreading of the North Atlantic Ocean, and further developed throughout the cooling and ongoing accommodation period. The seismically active structures have been and are being reactivated in connection with the loading and unloading events during the latest glaciation period.

Several papers have argued that second order stress fields associated with post-glacial rebound account for most of the seismicity in Fennoscandia. A conceptual rebound dome-forebulge model has been proposed to explain the current seismicity patterns as a response to migrating post-glacial doming of the center and subsidence of the surrounding basins. Post-glacial uplift models are most commonly based on geodetic measurements that show concentric ellipsoidal patterns of both uplift and horizontal displacement around the maximum uplift center. It should be remembered that the GPS maps show residuals after the removal of the standard plate movement, i.e. absolute movement towards the NE and relative SE movement away from North America (ridge push). Since the spatial distribution of the registered earthquakes exhibits little to no correlation with the pattern of rebound in Fennoscandia and the level of seismicity is rather low, it has been concluded that there is no clear evidence that the rebound stress is still able to trigger seismicity in Fennoscandia today. However, post-glacial rebound has had a much more important role in earthquake generation in late-glacial and early post-glacial times.

The present study area has at least partly been included in six previous seismic source area models and six hazard maps. Three seismic hazard estimates have been calculated for Hanhikivi site. In a map of median seismic hazard (horizontal peak ground acceleration or PGA), an area of enhanced hazard with maximum values of 0.15–0.20 m/s² was identified in the Bay of Bothnia and its surroundings. The highest hazard (0.20–0.25 m/s²) was recognized in the Kuusamo district. The smallest hazard values, below 0.1 m/s², were identified in southern Finland. Although the northern and western areas have a large affect on the

seismic hazard calculations, the most influential seismic source area was inferred to be the Raahel-Ladoga shear complex, where the site is located.

Task 6: In the current study, three alternative seismic source area models have been identified and described by two independent groups. Group 1 produced spatial model 1 and focused their analysis on the potential reactivation of geologically ancient features. They have used data sets bearing on historical and instrumental seismicity, lithology, deformation zones including brittle components (faults), lineaments defined on the basis of magnetic and gravity data, and broader crustal structure including Moho depth. Group 2 produced the spatial models 2 and 3. They focused their analysis on the recently active structures using data sets bearing on recent high-quality seismicity data, post-glacial faults (PGF), topography, bathymetry, lineaments defined on the basis of magnetic data and the current stress field. Model 3 is a slightly modified version of spatial model 2 and contains additional polygons.

Discussion and conclusions: The updated seismicity catalogue is more complete and its location precision is better than the FENCAT catalog. The new seismic catalogue is well-suited for earthquake studies and hazard estimations, provided that the magnitudes are homogenized prior to the calculations. Based on a subdataset of the most recent earthquake data (2000-2012), most of the earthquakes (80%) occur in the upper crust down to 17 km in depth, a minority (19%) in the middle crust (17-31 km) and only a few in the lower crust 31-45 km (1%). If the lower limit of the seismogenic zone is the depth above which 99% of the earthquakes occur, the results suggest that the seismogenic layer reaches down to the depth of 31 km. The layer seems to be rather uniform across Fennoscandia. We suggest that the middle to lower crustal boundary may add compositional and rheological constraints to the depth extent of the seismogenic zone in the study area. It is suggested that the décollement controlling the depth extent of fault zones is controlling the lower limit of present seismicity within a given source area.

The seismically active areas are located in areas with crustal thickness <50 km. Where the crustal thickness gradient trends in a NE-SW direction, as along the faulted western margin of the Bothnian Sea and along the Auho-Kandalaksha fault zone in the Kuusamo area, the gradient seems to be associated with a zone of increased seismicity. This observation should be studied in more detail in the future.

It is suggested that seismically active Western Lapland fault system is underlain by an inverted rift system which may have inherited its elastic properties from the Paleoproterozoic rifting phase. The relationships between precollisional inverted rift structures of the lower crust, the Western Lapland fault system and orthogonal PGF faulting should be studied more carefully before any final conclusions. We suggest that the wide range of fault plane solutions documented within the Pärvie Fault could be signaling the movement of a complex thrust system. The implied link between increased seismicity in Kuusamo and Hirvaskoski shear zones and Auho-Kandalaksha fault zones to inverted rift structures should also be looked at.

The three seismic source area models (Models 1, 2 and 3) are closely related because: 1) Seismicity is linked to reactivation of old faults in the present stress field. 2) Post-glacial faults are associated with reactivation of old faults. 3) Topography is influenced by the structure and composition of the Precambrian bedrock. 4) The current tectonic stress field

might be influenced by the structure of the Precambrian bedrock. The boundaries within the seismic source area models are strongly steered by the instrumentally detected earthquake patterns. Hence, a key uncertainty concerns the analysis of the earthquakes; their source location, magnitude and focal mechanism.

There are major similarities and only minor differences between the models. The minor differences are found in the offshore areas in the Bay of Bothnia where structural control of neither the Precambrian faults nor the PGFs or bathymetry is very good and the seismic location accuracy is the poorest.

When comparing the models developed in this study with existing models, it is clear that increased amount of data has enabled to draw smaller polygons in the vicinity of the increased zones of seismicity. Models 1, 2 and 3 resemble most clearly the Saari et al. (2009) seismic source area model that has been used as a national reference model. Although Models 1,2 and 3 are more detailed they comply with the large scale features outlined by the latest European scale reference model SHARE (Giardini et al., 2013).

The distribution of Models 1-3 polygon boundaries are aligned with the major tectonic boundaries presented in Redfield and Osmundsen (2013). The western polygons could be classified as located in the hinterland of the Scandes, the high seismicity polygons overlapping with the hinterland-break-in-slope, and the eastern blocks are located with the craton part. The seismicity zone is located in close proximity to the western boundary of the Bay of Bothnia basin that was active already in the Mesoproterozoic and maybe even earlier.

The major source of seismicity is the opening of the Atlantic only secondly come local sources such as post-glacial rebound or local changes in topography or crustal thickness. The relationship between post-glacial rebound and seismicity patterns is problematic and not easy to solve. First of all, the known PGFs are not parallel to the isolines of the rebound ellipsoid. We note, however, that the zones of increased seismicity in the western flank of the Gulf of Bothnia are parallel and along the long axes of the GIA anomaly. The elongation axis of GIA ellipsoid is parallel to the Norwegian margin and opening of the Atlantic and thus inherited from the previous tectonic processes. The direction of the long axis of the ellipsoid is orthogonal to and the short axis is parallel to the maximum horizontal stress in Fennoscandia stemming from the opening of the Atlantic. It seems that plate boundary forces, GIA and seismicity have complex interwoven relationships that need to be further studied in the future.

Keywords: *seismicity, seismotectonics, seismic source areas, Fennoscandia, Precambrian, postglacial faults, database, nuclear power plant site, Hanhikivi*

Contents

1	Introduction	15
1.1	Background.....	15
1.2	Outline of the study area	17
1.3	Objective and scope	19
2	Data framework and databases	20
2.1	Magnetic and gravity field data.....	20
2.2	Bathymetric and topographic data	30
2.3	Outcrop data	32
2.4	Lithological map database.....	34
2.5	Structural map database	38
2.6	Submarine data in the Gulf of Bothnia.....	46
2.7	Faults active during the Quaternary period	49
2.8	Seismicity database	55
2.8.1	Earthquake database.....	55
2.8.2	Seismic networks and changes in detection capability.....	59
2.9	Deep seismic reflection lines.....	61
3	Geological framework	63
3.1	Paleotectonic evolution.....	63
3.1.1	Major lithotectonic units	63
3.1.2	Ductile shear zones, faults and lineaments.....	71
3.1.3	Faults affecting sedimentary cover rocks in the Gulf of Bothnia	81
3.2	Glaciation cycles in the Quaternary period	89
3.2.1	The Weichselian glaciation (115 – 11.5 ka)	91
3.2.2	Weichselian deglaciation and the Holocene Epoch in northern Europe	94
3.2.3	Faults active during the late Weichselian deglaciation.....	96
4	Seismicity and seismic parameters	102
4.1	Seismicity.....	102
4.2	Historical seismicity	103
4.3	Fault plane solutions	106
5	Current tectonic framework.....	113
5.1	Plate movement and current stress field	113
5.2	Orientation of the maximum horizontal stress	114
5.3	Surface strain.....	116

5.4 Changes in the stress field imposed by changes in crustal and lithospheric thickness	119
5.5 Seismogenic thickness and the depth range of deformation zones and earthquakes	125
5.5.1 Crustal layering and depth extent of the ancient deformation zones	125
5.6 Rheological layering	127
5.7 Observed depth of seismicity.....	129
6 Deformation zones in the current stress field.....	132
6.1 Orientation of deformation zones in the context of the current stress field	132
6.2 Structural line orientations and seismicity.....	135
7 Current seismotectonic and previous seismic source area models	138
7.1 Seismotectonic models	138
7.2 Seismic source area models	144
8 Identification and description of seismic source areas.....	152
8.1 Basis for modeling	152
8.2 Spatial model 1.....	154
8.2.1 General methodology and result	154
8.2.2 Description	159
8.3 Spatial models 2 and 3	184
8.3.1 General methodology and result	184
8.3.2 Description	191
9 Discussion	212
9.1 The database and the completeness of the compiled data sets.....	213
9.2 Seismicity.....	216
9.3 Geological and geophysical boundaries and shear zones	218
9.4 Seismogenic zone	223
9.5 Alternative seismic source area (SSA) models	225
9.5.1 Uncertainties of the SSA models	230
9.6 Comparison to existing SSA models	233
9.7 Comparison to conceptual models.....	238
10 Conclusions	242
11 References	245
Appendices	269
Appendix 1. Previous studies around the Hanhikivi site	269
Appendix 2. On historical earthquake data	269
Appendix 3. Metadatabase	276
Appendix 4. Seismic source area coordinates	277

1 Introduction

A. Korja

1.1 Background

Fennovoima Oy is planning to build a new nuclear power plant (NPP) at the Hanhikivi site situated in the municipality of Pyhäjoki, Northern Ostrobothnia, Finland (Fig. 1.1.1). The safety standards for a NPP require that the level of seismic hazard is evaluated. This report is exclusively focused on a description of the seismotectonic background information necessary for the assessment of hazard associated with vibratory motion due to natural earthquakes at the Hanhikivi site. The characterization of other potentially destructive earthquake effects and seismic hazard phenomena involving permanent ground displacement (e.g. liquefaction and ground collapse) are outside the scope of this project. International recommendations (such as IAEA 2010 guidelines) are followed in order to perform a site-specific probabilistic seismic hazard assessment (PSHA) at Hanhikivi.

For the analysis to be successful the regional geological and seismological framework should be well described and the potential seismic sources should be analyzed and described quantitatively. The following geological and geophysical information is needed in hazard calculation: tectonic framework, seismic source geometry, distance of the source to the site, activity and recurrence of the seismic sources, and seismological parameters including: earthquake magnitude, style of faulting and fault length, distance to site and local site conditions.

International guidelines for the planning of NPP facilities (IAEA 2010, section 4.1.) require that the above-mentioned information is compiled into a database and a seismotectonic model, from where all the required information could be retrieved when evaluating seismic hazard. A seismotectonic model describes the relationships between geological, geophysical, geotechnical and seismological databases and thus provides a foundation for the calculation of the seismic hazard.

Several geological, geophysical and seismic studies have been conducted around the Hanhikivi site with the help of geoscientific consultants, the Geological Survey of Finland (GTK), the Finnish Geodetic Institute (FGI), the Institute of Seismology at the University of Helsinki (ISUH) and ÅF consultants (ÅF) (see Appendix 1). However, the data sets generated by these studies have not been merged into a unified database. Merging of the datasets into a database is one of the priorities of this project report.

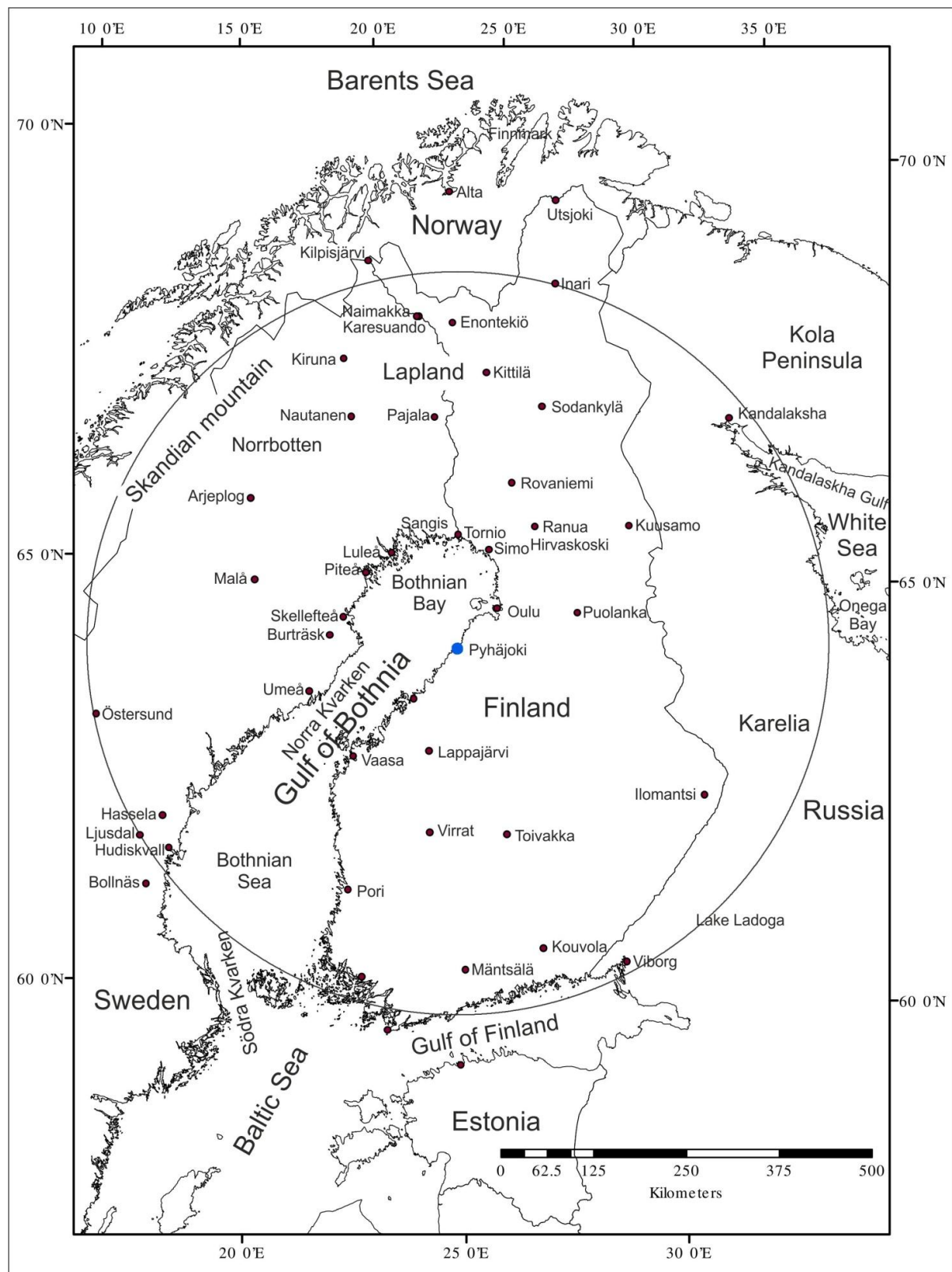


Figure 1.1.1 Map of Fennoscandia and the 500 km radius study area around the Hanhikivi site. Locations mentioned in the text are shown in the map.

There have been three previous evaluations of the seismic hazard at the Hanhikivi site (Mäntyniemi, 2008a; Saari et al., 2009; Korja et al., 2011). These have been based on three different seismic source area models using data from Finland and to lesser extent from Sweden. Since the Hanhikivi site is

situated along the western coast of Finland and only 65 km from the Finnish-Swedish national border, earthquakes in eastern Sweden and the Gulf of Bothnia are felt also at Hanhikivi (Mäntyniemi 2012a,b; FENCAT). It is therefore pertinent that Swedish geoscientific data sets are included in the databases and taken into account in seismic hazard assessments.

1.2 Outline of the study area

The Hanhikivi site is situated in a continental intraplate setting in the northern part of the Fennoscandian Shield; it is surrounded by the Caledonian orogenic belt to the west, the North Atlantic continental platform to the north and the East European platform to the south and east (Fig. 1.2.1). Offshore, in the Gulf of Bothnia, Meso- and Neoproterozoic as well as Cambrian to Ordovician sedimentary rocks form a cover on the rocks belonging to the shield. The latest plate tectonic event that has affected the study area is the opening and spreading of the Atlantic Ocean that initiated 60 Ma ago. This ongoing event has subjected the area to a long-standing tectonic stress-field oriented in a WNW-ESE direction. During the Pleistocene glaciations, the area has been subjected to repeated glacial cycles and associated loading and unloading events. The present geomorphology was largely shaped during the last Weichselian glacial period (Hirvas, 1991; Lundqvist, 1992; Donner, 1995; Fredén, 2002) and the area is still rebounding (see section 5.3).

The intraplate seismicity in the Hanhikivi site vicinity is low (Fig. 1.2.1). Higher seismic activity is found along the eastern coast of Sweden, in the Gulf of Bothnia, and in the Lapland and Kuusamo areas. The highest seismic activity in Fennoscandia is found along the Norwegian coast and the eastern coast of Sweden, parallel to the continental margin. Current tectonic/seismic activity in the northern part of the Fennoscandia is caused by a complex interplay of intraplate and plate margin processes; the opening of the northern Atlantic Ocean, glacial isostatic adjustment (GIA) and local stress caused by local mass deficit or excess (gravitational potential energy) (Fjeldskaar et al., 2000; Bungum et al., 2010; Redfield and Osmundsen, 2013).

To understand the effect of these global and regional processes on the current seismicity and seismic hazard, we have studied an area with a 500 km radius around Hanhikivi. According to IAEA (2010, p. 8), the size of the relevant region may vary, but its radial extent is typically 300 km. In intraplate settings in particular, more distant seismic sources may have to be considered. The study area includes Finland, northeasternmost Norway, Sweden north of latitude 60°N and northwesternmost Russia (Fig. 1.1.1). The study area includes all the seismotectonically similar areas whereas it excludes the part of the Caledonian orogen and the passive continental margin of the North Atlantic that has considerably higher rate of seismicity.

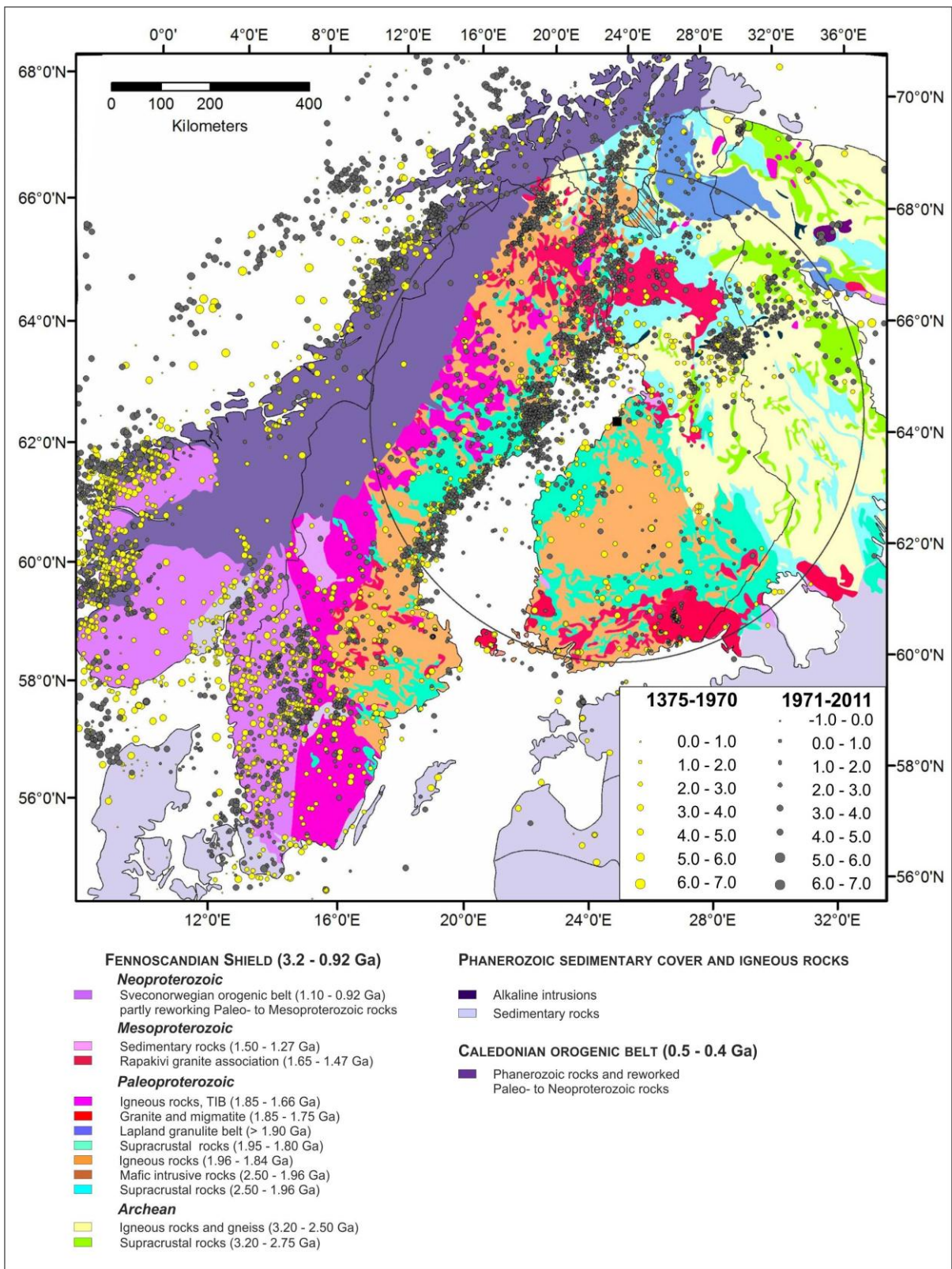


Figure 1.2.1. Seismicity (FENCAT database in Chapter 3) and major geological units of Fennoscandia modified from Lahtinen et al. (2005). Hanhikivi site: black box.

1.3 Objective and scope

This study focuses on gathering geological, geophysical and seismological background information required by seismic hazard assessment, on setting up an upgradable database and on outlining alternative seismic source areas. The analysis is based on literature reviews, on overviews of previous studies in the area, and on recycling and merging of existing data sets stored at the Geological Surveys of Finland (GTK) and Sweden (SGU), as well as at the Universities of Helsinki (ISUH) and Uppsala (UU). Key historical earthquakes in the study region have been re-appraised and the respective information has been collected into a database of historical earthquakes (see Appendix 2). Since the focus of this report is to define regional patterns of seismicity (source areas) and to describe their differences in seismicity and geological evolution/framework, we have used 1: 1 million scale data sets.

A seismotectonic model describes both the spatial relationships between seismicity and tectonic framework and the processes producing the current seismicity. The first phase in developing seismotectonic models is to outline seismic source regions – areas with different seismicity patterns and tectonic history.

The study has six tasks. The *first* task is to review and summarize the existing and ongoing geological and geophysical studies carried out around the Hanhikivi site by GTK, FGI and ISUH (Appendix 1). The *second* task is to compile and describe a regional-scale geological and geophysical upgradable database for the present and future studies of the site area (Section 2 and Appendix 3). The *third* task is to present an overview of the paleotectonic evolution, Quaternary glacial history and current tectonic framework inside the study area. The *fourth* task is to describe seismicity and earthquake source parameters of the study area. The *fifth* task is to review and evaluate the current conceptual seismotectonic models and seismic source region models for Fennoscandia. The *sixth* task is to identify and describe seismic source regions and to outline alternative source area models for seismic hazard calculations for the Hanhikivi site area.

2 Data framework and databases

In this section, we will describe the data sets used in this study and how they are archived and arranged in the database delivered to Fennovoima Oy in the context of the current project. The map compilations are based on previously published lithological, structural and geophysical maps and databases: lithological, structural, aeromagnetic and Bouguer anomaly maps, bathymetry, topography, instrumental and historical seismicity and post-glacial faults. The data are supplied with adequate metadata information (Appendix 3) and stored in an ArcGIS-based database which will be administered by Fennovoima Oy.

Databases at the Geological Survey of Sweden (SGU) and the Geological Survey of Finland (GTK) as well as Finnish Geodetic Institute (FGI) are constantly being updated. The data delivered to the Fennovoima database therefore represents the most up-to-date material available at the time of designing phase of the seismic source areas at workshop in November 2013. Similarly, the earthquake catalogues at the University of Uppsala and at the Institute of Seismology in the University of Helsinki are constantly changing, both with new events and with updated analysis of older events. The earthquake data delivered to the Fennovoima database represent the state of the SNSN (Swedish National Seismic Network) and FNSN (Finnish National Seismic Network) catalogues on the 30th June, 2013, and the 31st December, 2012, respectively.

2.1 Magnetic and gravity field data

Grigull, S., M.-L. Airo, T. Huotari-Halkosaari & M. Nironen

Airborne magnetic measurements have been carried out over most of Sweden (Fig. 2.1.1). Lines were usually flown in N–S or E–W direction at a speed of 230 km/h, a line spacing of 200 m, and a measurement interval of 40 m before, and 17 m after 1995. Flight altitude was 30 m before, and 60 m after 1995. The resulting magnetic anomaly maps (Fig. 2.1.2) are available at resolutions 200 m x 200 m or 50 m x 50 m. For this study, the magnetic maps with resolution 50 m x 50 m were used. SGU has collected new magnetic data during 2012 in the very northern part of the Gulf of Bothnia, southeast of Kalix (Fig. 2.1.3). The lines for these data were flown in an E–W direction and at a line spacing of 400 m.

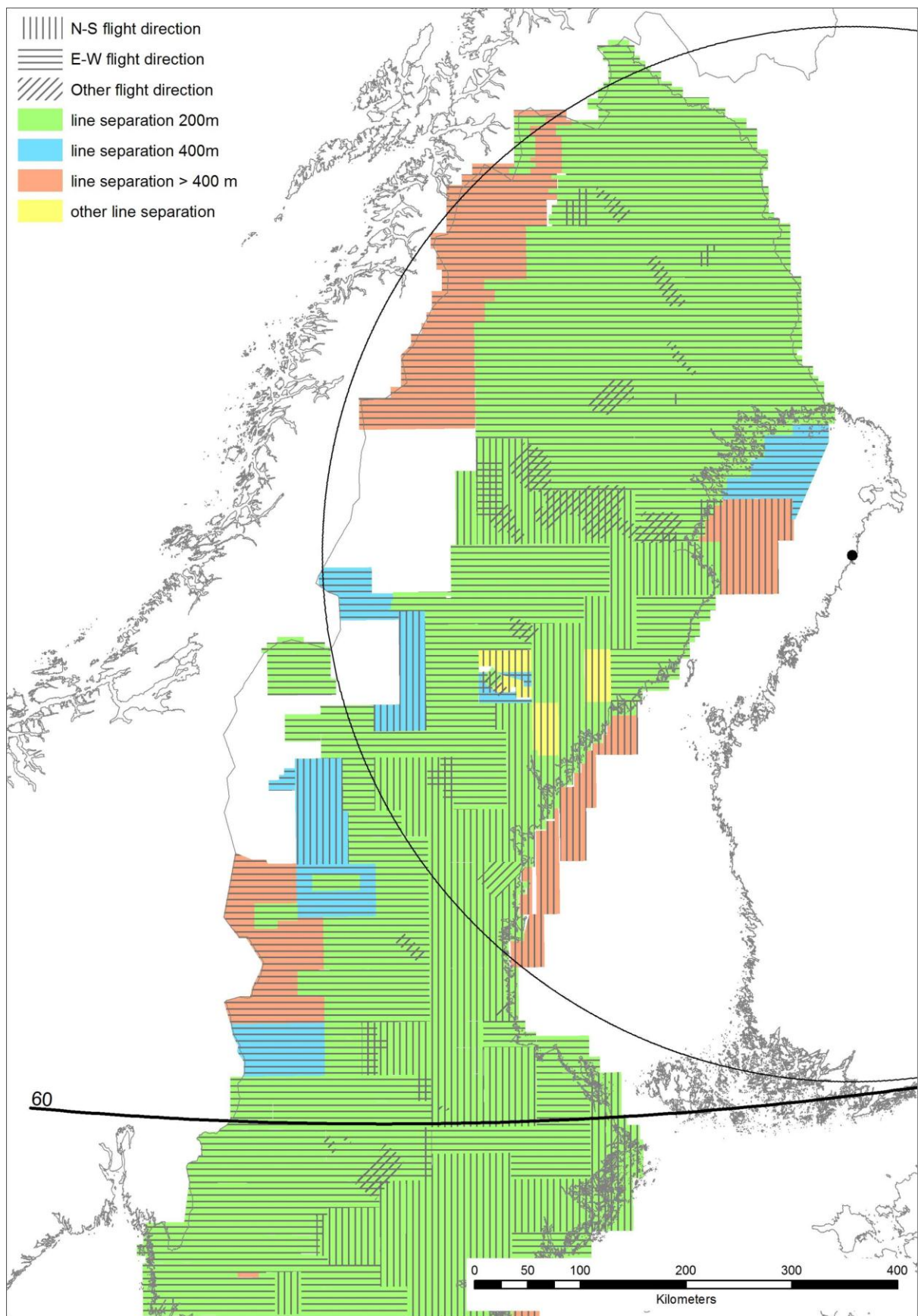


Figure 2.1.1. Degree of coverage of Sweden with airborne magnetic data. Flight line directions and line spacing are indicated. Hanhikivi site: black dot.

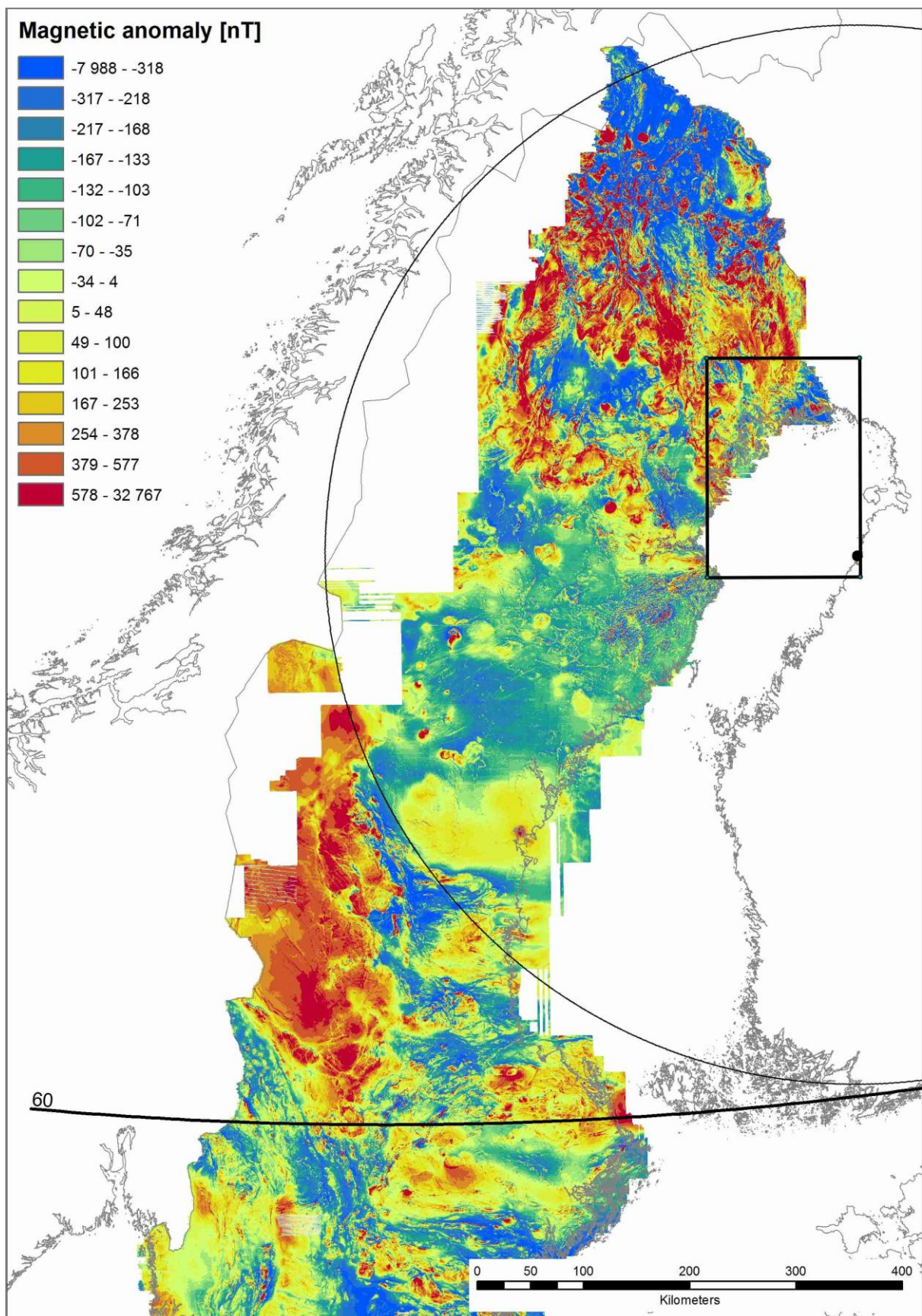


Figure 2.1.2. Total magnetic field anomaly map of Sweden (SGU). The magnetic anomalies are shown after subtracting the geomagnetic reference field DGRF 1965.0. Blue colours indicate lack of magnetic minerals and red colours indicate high concentration of magnetic minerals. The rectangle marked with a black line defines the area shown in Figure 2.1.3.

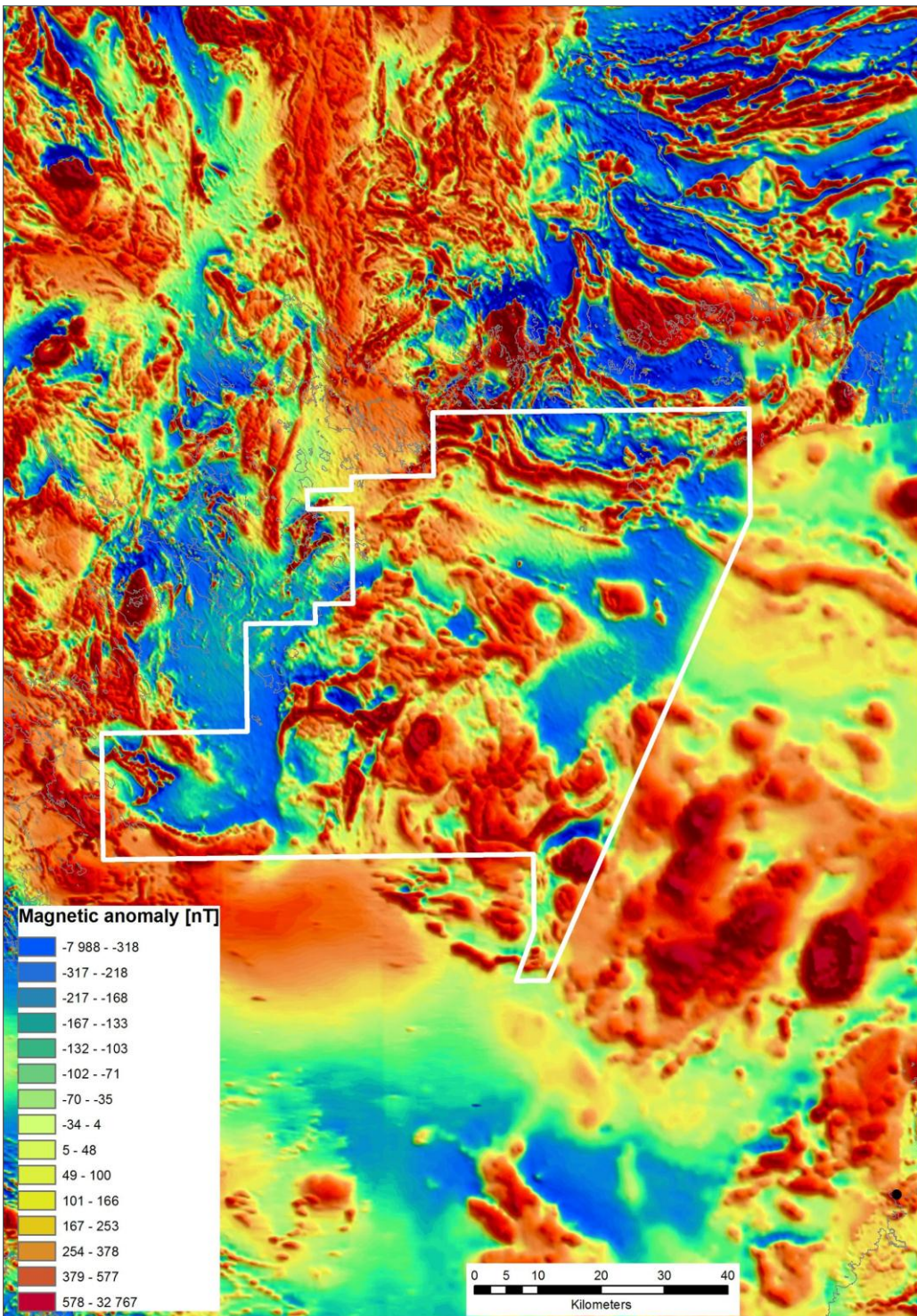


Figure 2.1.3. Area (inside white line) where new airborne magnetic data were collected by SGU during 2012 southeast of Kalix (see also Figure 2.1.2). These new data have been integrated with lower resolution data to the east in Finland and to the south and with higher resolution data to the north and west. The magnetic anomalies are shown after subtracting the geomagnetic reference field DGRF 1965.0.

The available Swedish gravity data is of variable frequency and extent. Currently, 180 719 gravity measurement sites are listed in SGU's databases and their distribution inside the study area is shown

in Figure 2.1.4. The targeted distance between measurement sites lies between 1.5 and 2.0 km. However, especially within the Caledonian orogen, the measurement sites lie farther apart (c. 4 km on average). The resulting Bouguer anomaly map shows that north of latitude 60°N gravity varies from -100 to +10 mGal (Fig. 2.1.5).



Figure 2.1.4. Distribution of gravity measurement sites in Sweden.

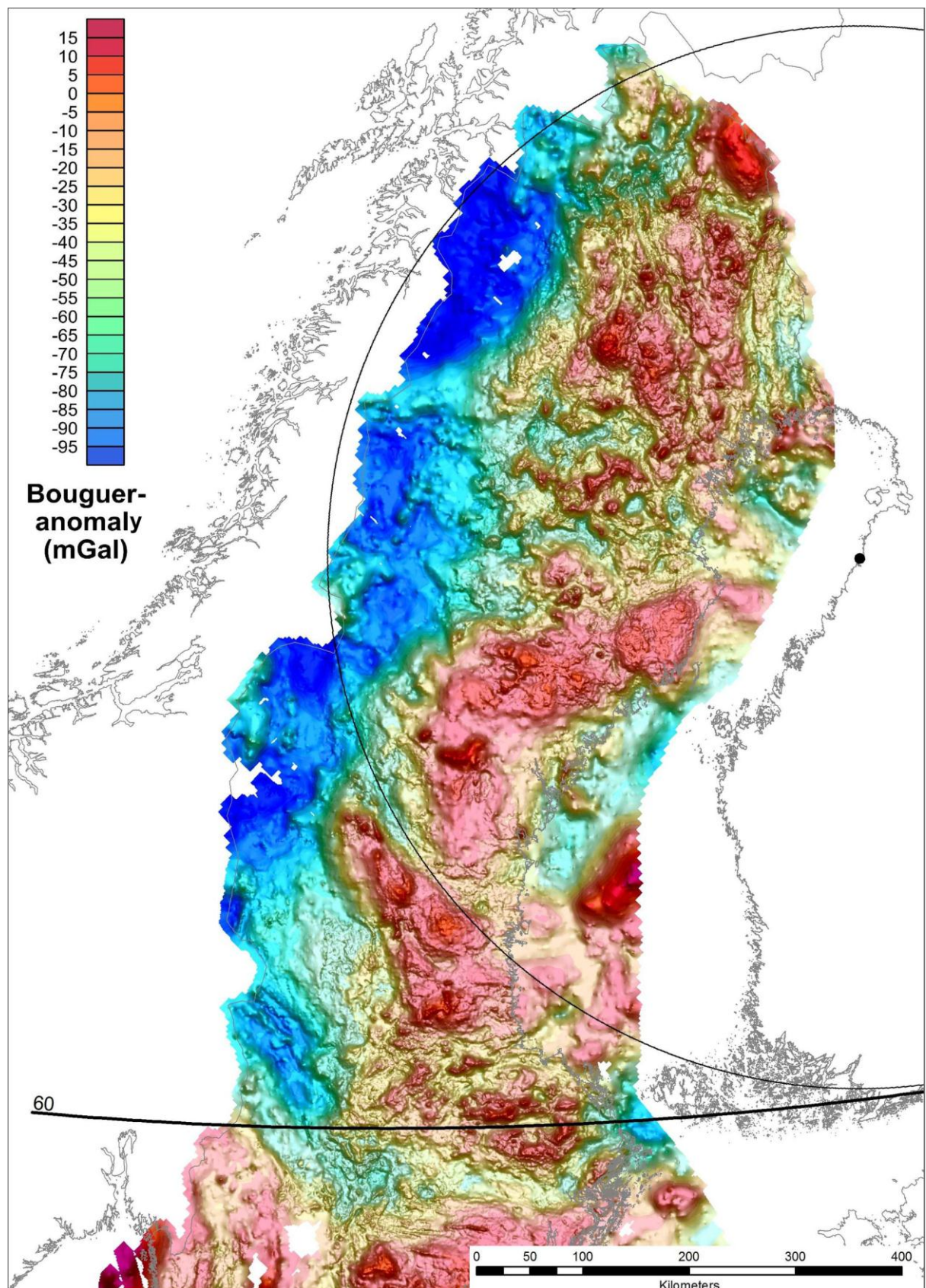


Figure 2.1.5. Bouguer anomaly map of Sweden (SGU). The Bouguer anomalies are calculated using RG82 reference field. Blue colours indicate low densities and red colours indicate high densities of the crust.

The magnetic data sets used here in the analysis of structures over Finland are based on GTK's countrywide airborne geophysical surveys conducted during two systematic national survey programmes. During the First National Airborne Geophysical Mapping Programme (the so-called high-altitude programme) in 1952-1972, the survey altitude was 150 m and flight-line separation 400 m. These surveys covered also the Finnish offshore areas. Following this programme, the Second National Airborne Geophysical Mapping Programme (finished in 2007) was conducted systematically at the nominal survey altitude of 30 m and with a flight-line spacing of 200 m. The flight direction was east-west or north-south. These high-resolution, multi-component geophysical data (magnetic, electromagnetic and radiometric datasets) formed the basis for detailed structural investigations (Airo et al., 2011b). The airborne magnetic grid of GTK (cell size 50/50m) covers the continental and coastal areas of Finland (Fig. 2.1.6) and was used here for the detailed structural investigations. The interpretation of geological structures also benefited from the use of Bouguer anomaly grid of Finland (by FGI and GTK, Elo, 1997) and of the Fennoscandian Shield, grid cell size ~1000/1000m (Fig. 2.1.7). In the region of the Gulf of Bothnia, we also used the "high-altitude" data grid and scanned contour maps. Large scale structural framework was interpreted using the Fennoscandian Shield magnetic data at the cell size of 500/500m (see example in figure 2.1.8).

A semi-automatic method for detection of zones of gravity minima which may correspond to fault and shear zones was applied to the gravity data of Finland. Bouguer anomaly data (by FGI and GTK) were analyzed for curvature minima by using a raster analysis method implemented by US Geological Survey for Oasis Montaj (Phillips, 2007). The method determines the existence of local gravity minima points with associated strike direction. These points were vectorized in ArcGIS and compared with structural zones (fault and shear zones) interpreted from aeromagnetic data (Figure 2.1.9). This kind of procedure was conducted over whole Finland to analyze the regional distribution of geophysically interpreted fault and shear zones.

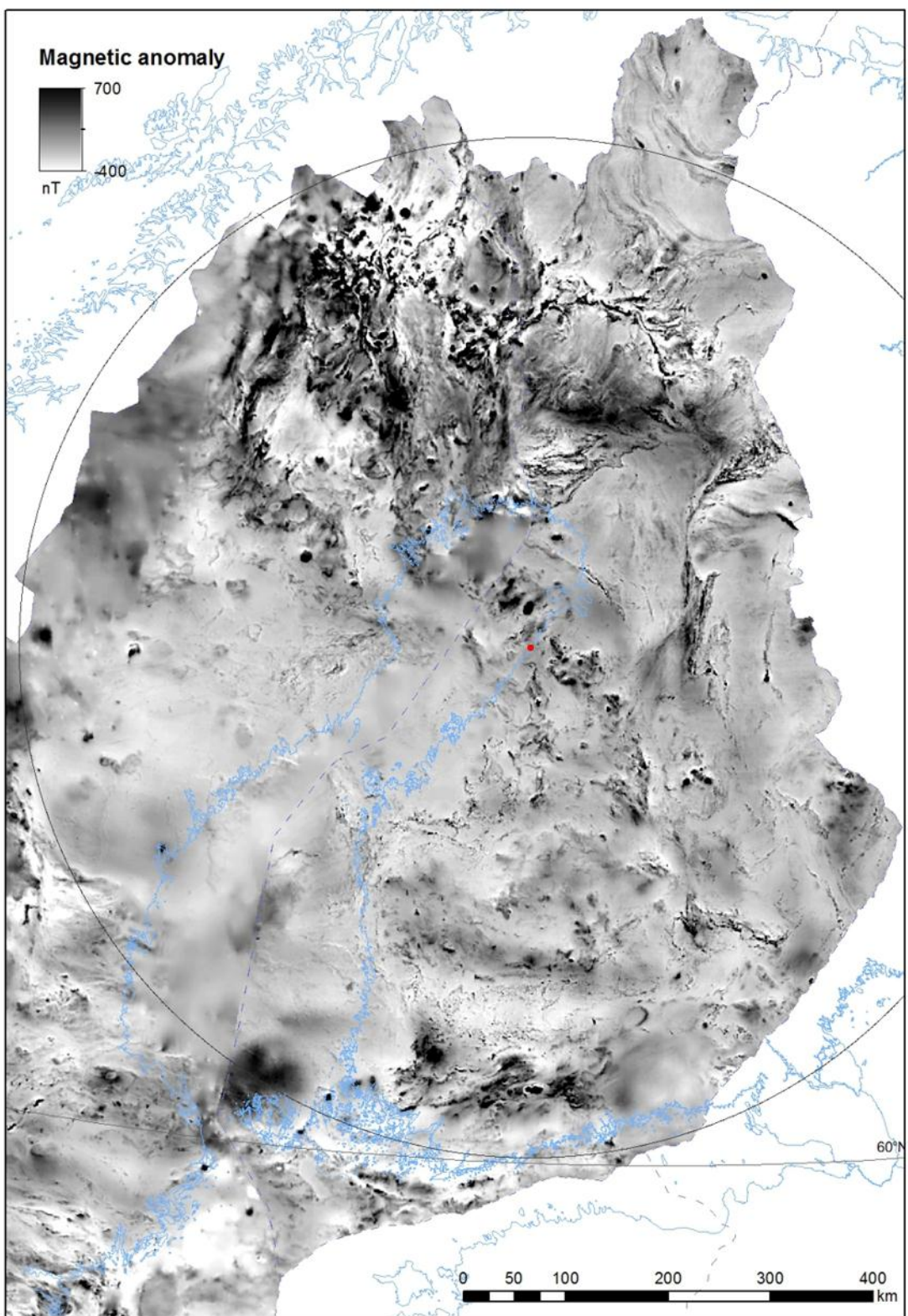


Figure 2.1.6. Combined total magnetic field anomaly map of Finland (Copyright GTK) and Sweden (Copyright SGU). The magnetic anomalies are shown after subtracting the geomagnetic reference field DGRF 1965.0. White colour indicates low and black colour indicates high magnetic field intensity. Hanhikivi site: red dot.

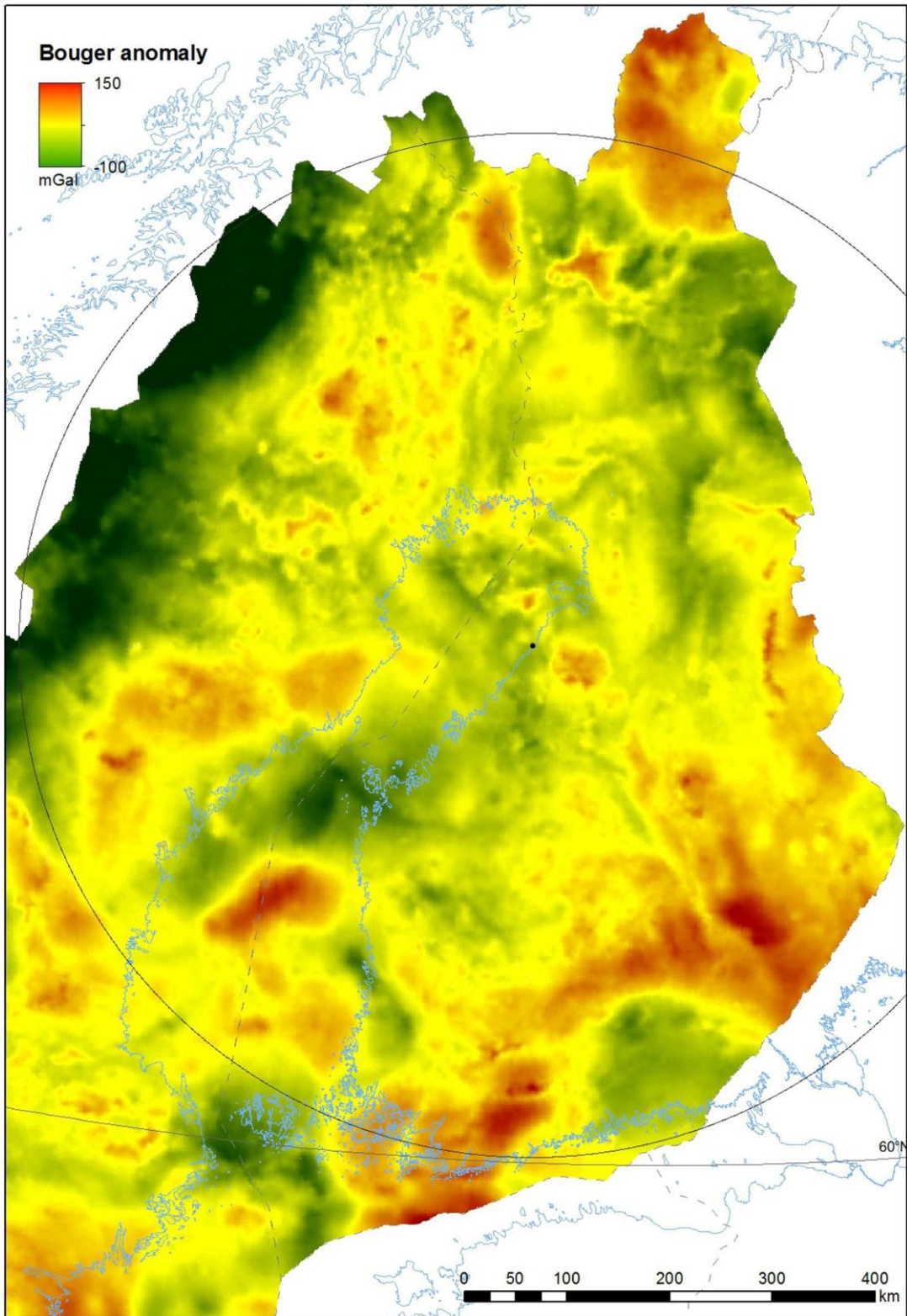


Figure 2.1.7. Combined Bouguer anomaly map of Finland (Copyright FGI and GTK, Elo 1997) and Sweden (Copyright SGU). The Bouguer anomalies are calculated using ISGN-71 reference field. Green colours indicate low densities and red colours indicate high densities of the crust.

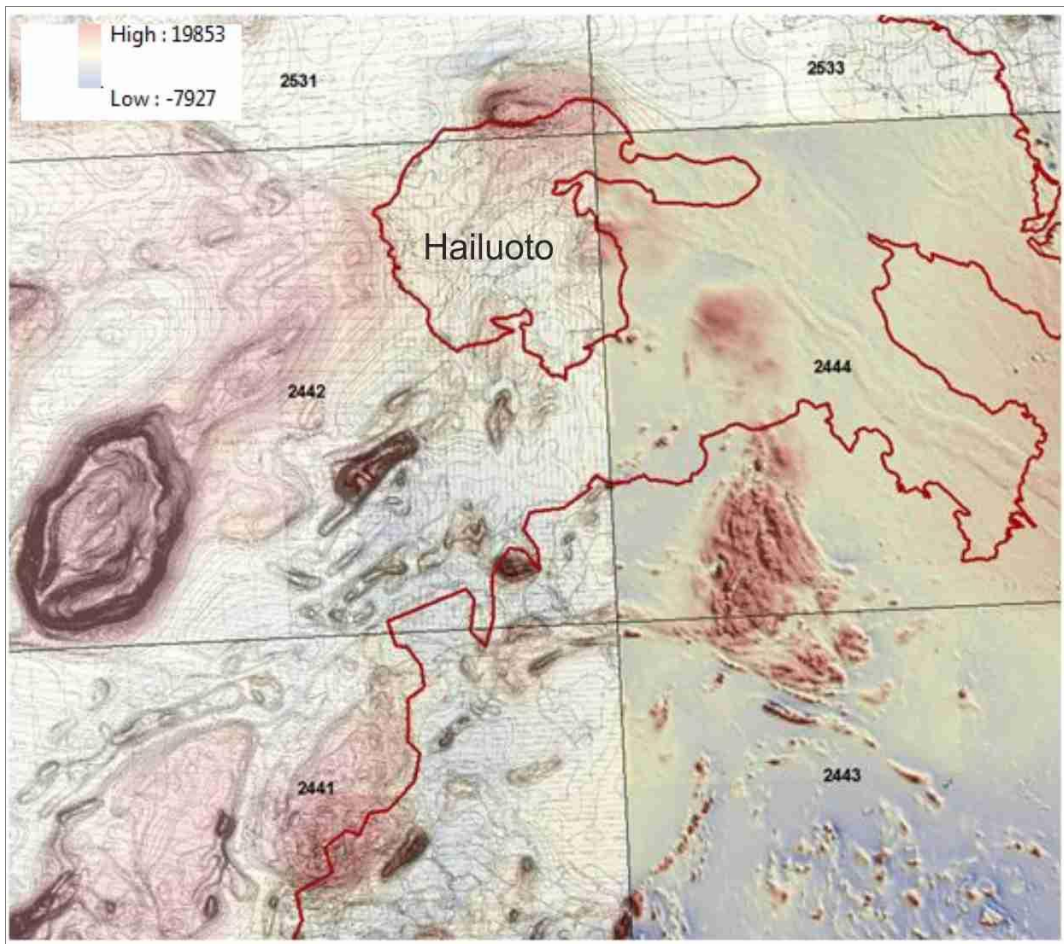


Figure 2.1.8. An example of magnetic data sets used in the structural interpretation of Finland. Magnetic contour maps from offshore (e.g., map sheet 2442) are compared with the more detailed airborne magnetic data from on-shore of the Finnish coast (map sheet 2444). Colour scale from blue (low) to red (high) magnetic field intensity. The north-south extent of a map sheet is 30 km. Red line represents the Finnish coastline.

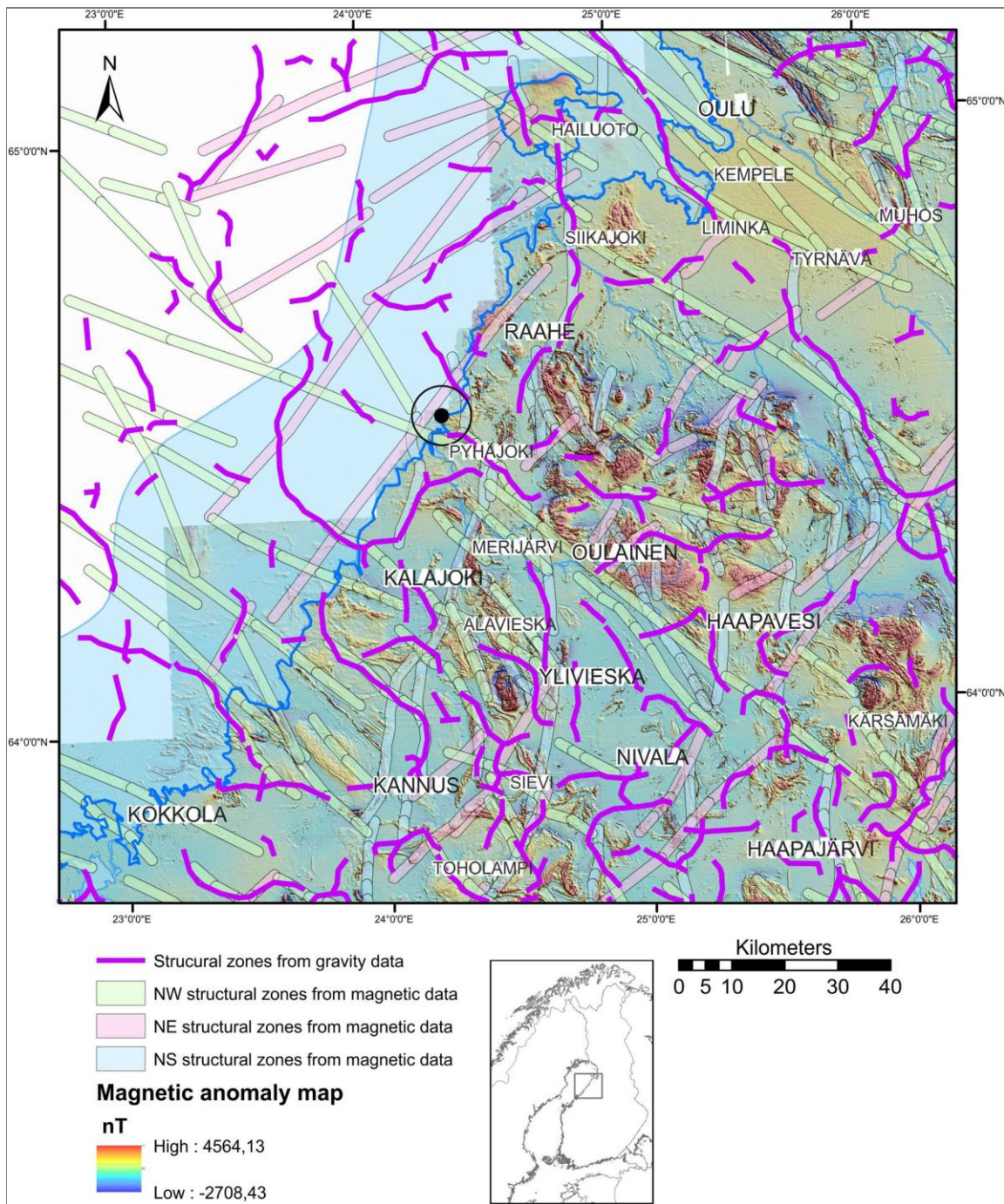


Figure 2.1.9. Main structural zones in areas surrounding Pyhäjoki, inferred from gravity and aeromagnetic minima. Aeromagnetic anomaly map as background.

2.2 Bathymetric and topographic data

S. Grigull, M.-L. Airo, T. Huotari-Halkosaari & M. Nironen

The bathymetric dataset used in this study was extracted from the British Oceanographic Data Centre (BODC) and is referred to as the General Bathymetric Chart of the Oceans (GEBCO) (IOC, IHO & BODC, 2003; https://www.bodc.ac.uk/data/online_delivery/gebco/). The dataset is in the geographic WGS84 coordinate system. Data interval is a global one arc-minute grid. Depressions are calculated against mean sea level and only negative deviations are found. Dark blue indicates large

deviations and deep depressions, light blue indicates small deviations and shallow depressions. Topographic ridges or depressions are denoted as steep gradients expressed as an abrupt change in colour (Fig. 2.2.1).

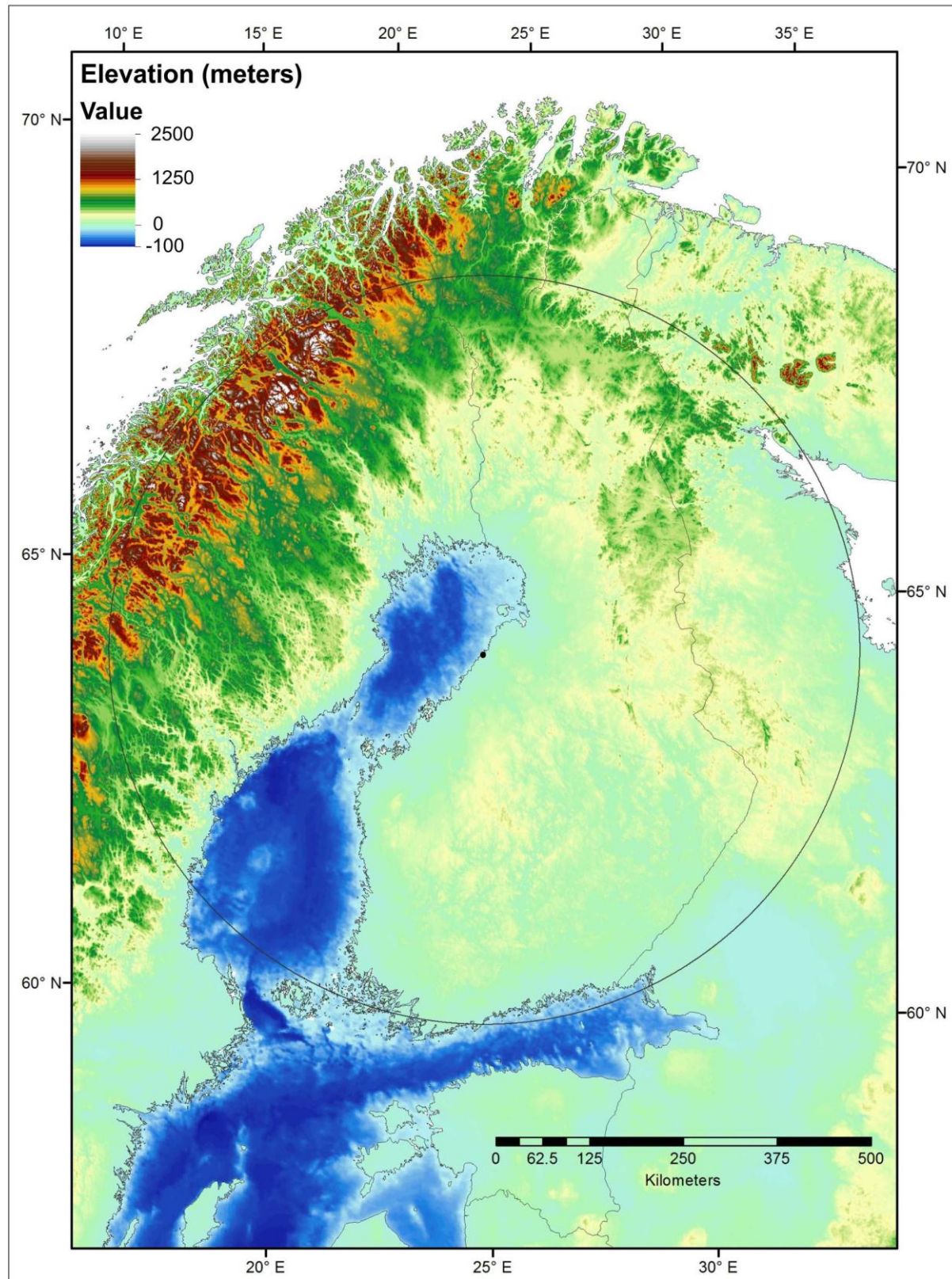


Figure 2.2.1 Topographic and bathymetric datasets.

The topographic dataset used was downloaded from the Global Land One-km Base Elevation Project (GLOBE) database (Globe Task Team et al., 1999; URL: <http://www.ngdc.noaa.gov/mgg/topo/globe.html>) to cover the whole study area (Fig. 2.2.1). The selected C tile (latitude 90N-50S, longitude 0W-90E) is a raster file in the geographic WGS84 coordinate system. Cell size is 30 arc-seconds of latitude and longitude. Elevations are calculated against mean sea level and the C tile area elevations vary from -12 to +4010 meters. Brown/orange indicates large deviations and high topographies; turquoise/green indicates small deviations and low topography. Topographic ridges or depressions are denoted as steep gradients expressed as an abrupt change in colour.

2.3 Outcrop data

S. Grigull, M.-L. Airo, T. Huotari-Halkosaari & M. Nironen

Outcrop data (field observation points), together with the geophysical data described above, provide the base input for the development of the 2D geological models represented in the lithological and structural map databases described below. The density of field observation points for the bedrock in Sweden that have been archived in digital format varies over the country (Fig. 2.3.1). SGU's outcrop database currently counts 256 794 observation points in total for the whole of Sweden; around 160 700 of these points lie north of latitude 60°N. However, it should be noted that many observation points in the remaining part of the country, which form the basis for the geological mapping work, are not included in the digital outcrop database. This information is analogue in character and is archived at SGU in the form of hand-written field notebooks.

Outcrop data of Finland was not used as a base input. As described below, the derivatives of outcrop data, i.e. lithological maps were used instead. The 1:100 000 scale bedrock maps contain information of metamorphic grade, primary structural observations in individual outcrops, and interpretations of deformation zones.

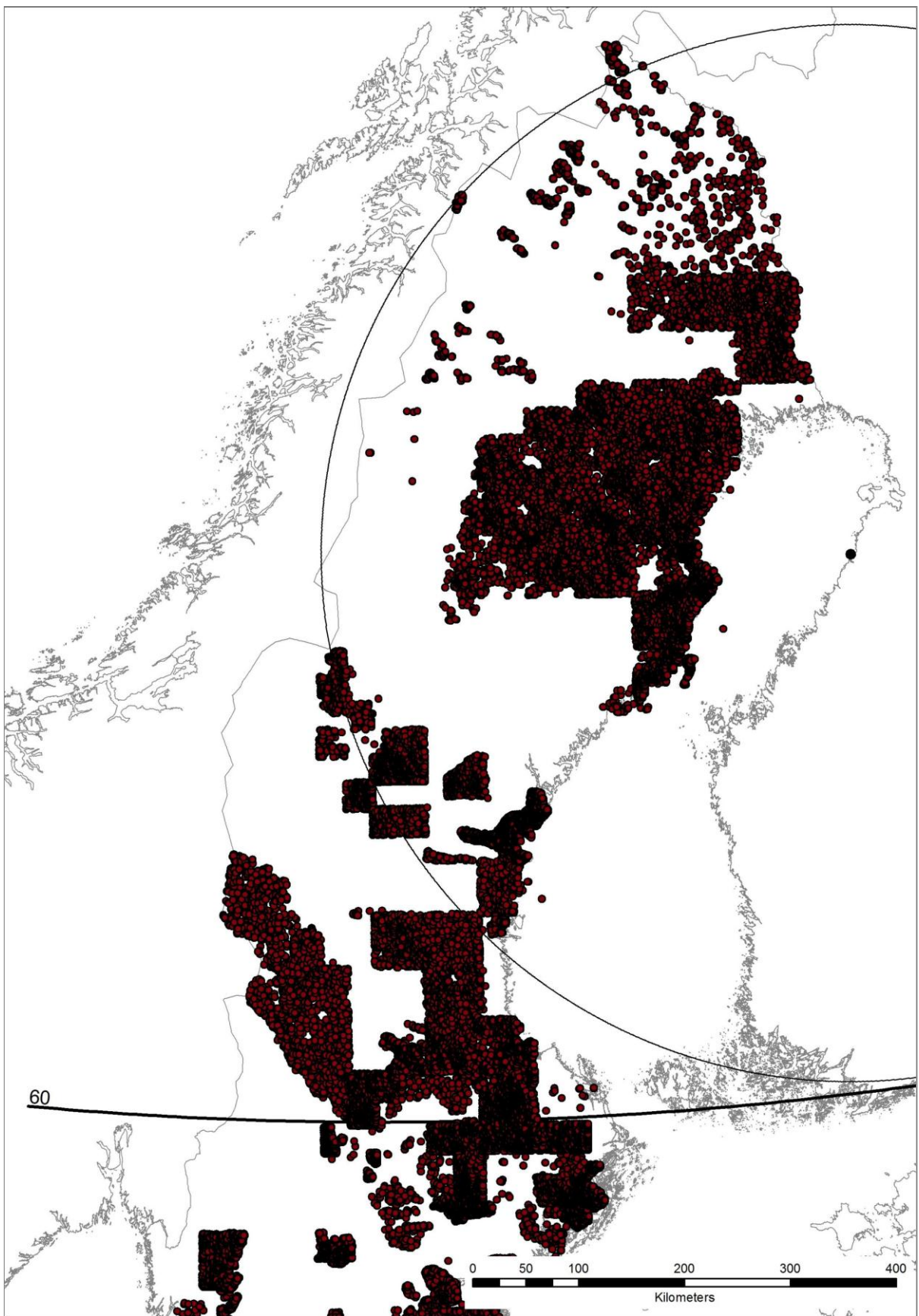


Figure 2.3.1. Distribution of bedrock geological observation points in digital format in Sweden.

2.4 Lithological map database

S. Grigull, M.-L. Airo, T. Huotari-Halkosaari & M. Nironen

The lithological map database of Sweden (Fig. 2.4.1) used for this project is a generalised version of the recently published national 1:1 000 000 (1:1 M) bedrock map (Bergman et al., 2012). The 1:1 M bedrock map of Sweden is based on larger scale, more detailed geological maps (e.g. 1:50 000 and 1:250 000), which, in turn, are based on field observations (section 2.3) as well as on the interpretation of geophysical data (section 2.1). In the lithological map database for the Fennovoima project, the number of lithological units in Sweden was reduced from 146 in the original 1:1 M bedrock map of Sweden (Bergman et al., 2012) to 21 in the Fennovoima database. These 21 units are further attributed to the following seven major lithotectonic units (unit numbers in brackets refer to Figure 2.4.1):

1. Caledonian orogen (units 1, 2).
2. Platformal sedimentary cover rocks on the Fennoscandian Shield (unit 3).
3. Proterozoic (post-1.8 Ga) magmatic and sedimentary provinces (units 4, 5, 6, 7, 8).
4. Sveconorwegian orogen (units 9, 10, 11).
5. Blekinge-Bornholm orogen (units 12, 13).
6. Syn-orogenic rocks (1.9–1.8 Ga) in the context of and inside the 2.0–1.8 Ga orogen (units 14, 15, 16, 17, 18, 19).
7. Archean (3.2–2.7 Ga) and Paleoproterozoic (2.5–2.0 Ga), pre-orogenic rocks in the context of and inside the 2.0–1.8 orogen (units 20, 21).

The study area contains lithologies of all groups except group 5 (Blekinge-Bornholm orogen). Lithologies are delivered as polygon data.

All lithological map information at GTK in Finland, regardless of scale, is stored in a primary map database (DigiKP). In addition, a database generalized from the primary one, suitable for use at the scale 1:200 000, is available (Digi200). However, the database most suitable for the Fennovoima project, at the scale 1:1 000 000 (Digi1M), is currently being updated. Therefore, the map database delivered to the Fennovoima database is the latest published map database compiled at the scale 1:1 000 000 and printed at the scale 1: 2 000 000, referred to as the Geological map of the Fennoscandian Shield (Koistinen et al., 2001; Fig. 2.4.2). Spatial reference: datum WGS84, map projection Gauss-Krueger, central meridian 21°E, false easting 1500 m. The web-address for the data is:

http://arkisto GTK.fi/metatieto/description_of_geological_and_geophysical_maps_of_the_fennoscandian_shield.pdf

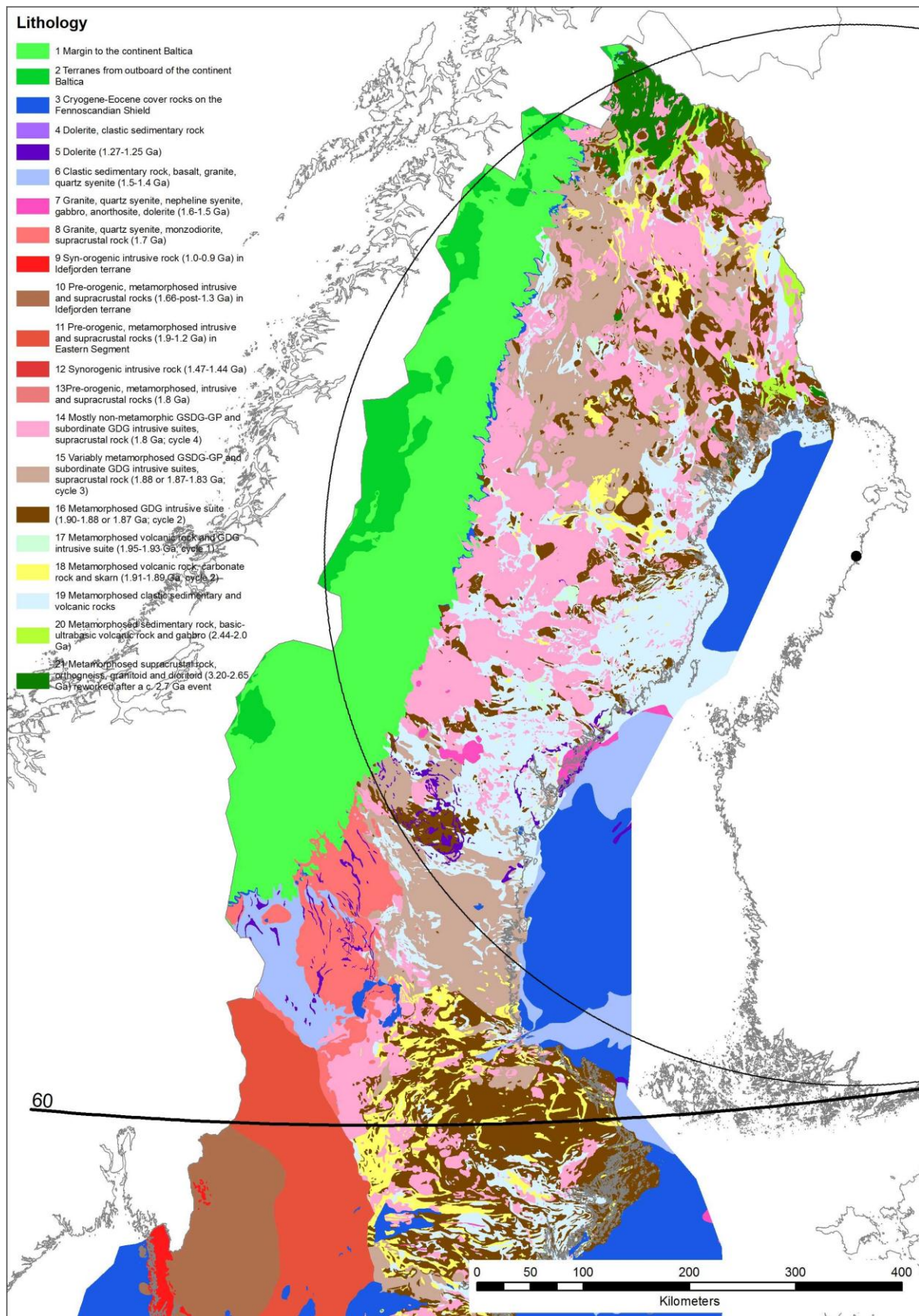
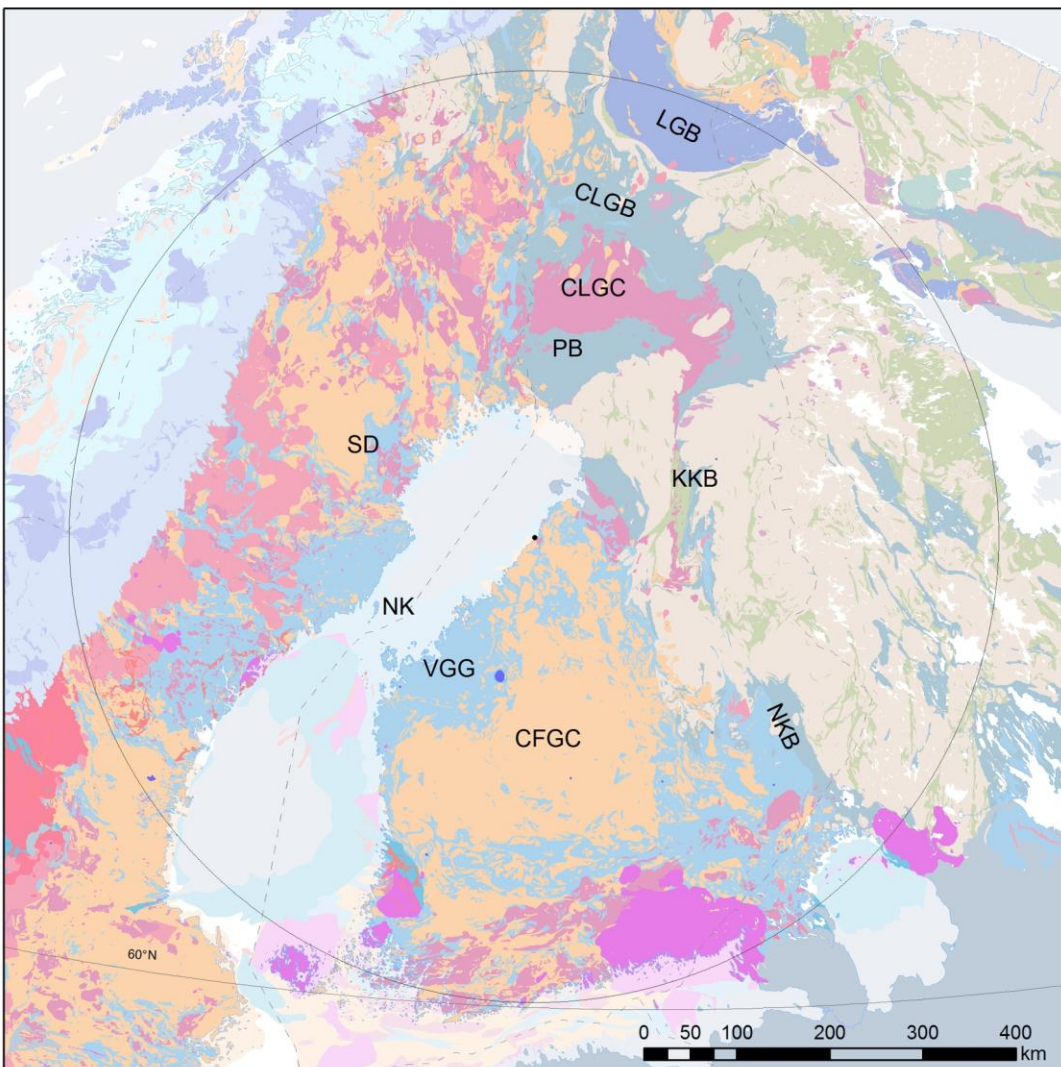


Figure 2.4.1. Generalised lithological map of Sweden.



Meteorite impact rocks and site	
Impact melt, impact breccia/Impact site	[Blue square]
Neoproterozoic (and possibly Mesoproterozoic) and Phanerozoic rocks outside the Caledonian orogenic belt	
Vendian to Cambrian and Devonian alkaline igneous rocks	[Light blue]
Upper Riphean (and possibly older) Vendian and Phanerozoic sedimentary rocks	[Dark blue]
Caledonian orogenic belt	
Archaean rocks along the shortened Baltoscandian continental margin	[Orange]
Supracrustal rocks in exotic and outboard terranes	[Light orange]
Neoproterozoic and Palaeozoic (Cambrian to Devonian) rocks along the shortened Baltoscandian continental margin	[Medium blue]
Proterozoic rocks (c. 2.30-0.90 Ga) along the shortened Baltoscandian continental margin	[Dark blue]
Lower Palaeozoic intrusive rocks in exotic and outboard terranes	[Light orange]
FENNOSCANDIAN SHIELD	
Mesoproterozoic to Palaeoproterozoic (1.71-1.61 Ga and possibly older) rocks	
Granitoid, syenitoid, dioritoid, gabbroid, dolerite and metamorphic equivalents, supracrustal rocks (c. 1.71-1.66 Ga and possibly older)	[Red]
Granite, syenitoid, dioritoid, gabbroid and metamorphic equivalents (c. 1.65-1.47 Ga)	[Magenta]
Lapland granulite belt	[LGB]
Central Lapland greenstone belt	[CLGB]
Central Lapland granitoid complex	[CLGC]
Peräpohja belt	[PB]
Skellefte mining district	[SD]
Kainuu-Kuusamo belt	[KKB]
Finnish North Karelia belt	[NKB]
Central Finland granitoid complex	[CFG C]
Vaasa granitoid complex	[VGC]
Norra Kvarken	[NK]
Palaeoproterozoic rocks (1.96-1.75 Ga)	
Supracrustal rocks (c. 1.95-1.85 Ga and possibly older), predominantly metasedimentary	[Light blue]
Granite, pegmatite (c. 1.85-1.75 Ga)	[Magenta]
Granitoid, syenitoid, dioritoid, gabbroid and metamorphic equivalents, metavolcanic rocks (c. 1.96-1.86 Ga, in part as young as c. 1.84 Ga); 765	[Orange]
Granitoid, syenitoid, dioritoid and gabbroid, supracrustal rocks (c. 1.86-1.84 and c. 1.82-1.76 Ga)	[Light orange]
Palaeoproterozoic rocks in Lapland-White Sea granulite belt	
Granulitic rock, amphibolite, anorthosite (rocks of uncertain age, in time range 2.30-1.90 Ga)	[Dark blue]
Palaeoproterozoic rocks (2.50-1.96 Ga)	
Intrusive rocks, predominantly mafic and ultramafic	[Magenta]
Supracrustal rocks, predominantly mafic/ultramafic metavolcanic and metasedimentary rocks	[Dark blue]
Archaean rocks	
Intrusive rocks (c. 3.20-2.50 Ga and possibly older), orthogneiss, migmatitic gneiss	[Light brown]
Supracrustal rocks (c. 3.20-2.75 Ga and possibly older)	[Green]

Figure 2.4.2. Generalised lithological map of Fennoscandia (modified from Koistinen et al., 2001). LGB = Lapland granulite belt, CLGB = Central Lapland greenstone belt, CLGC = Central Lapland granitoid complex, PB = Peräpohja belt, SD = Skellefte mining district, KKB = Kainuu-Kuusamo belt, NKB = Finnish North Karelia belt, CFGC = Central Finland granitoid complex, VGC = Vaasa granitoid complex, NK = Norra Kvarken.

A set of printed bedrock map sheets at the scale 1:100 000 that have been published over Finland were used as an addition to the lithological database. The maps do not cover the whole of Finland (Fig. 2.4.3). The maps contain information of bedrock areas, observation sites, drilling sites, primary structural observations, ore minerals, and metamorphic index minerals. A printed explanation exists for most of the map sheets. In addition to the Geological map of the Fennoscandian Shield, data bearing on the Central Finland Granitoid Complex bedrock map (Nironen et al., 2000) was used.

For licence reasons, the lithologies in the Russian and Norwegian parts lying within the 500 km circle are delivered in raster format (Copyright GTK 1999, applied to original data owned by the Geological Survey of Norway (NGU) and the Northwest Regional Geological Centre of Russia (NWRGC)).

The Bedrock Map of Finland (Korsman et al., 1997) was used as source material for the Geological map of the Fennoscandian Shield (Koistinen et al., 2001). This material was updated with structural and lithological map information at 1:1 000 000 scale from the Raahe-Ladoga shear complex and with the research data available. The sources of information for the Gulf of Bothnia region and the Gulf of Finland were Lundqvist et al. (1996) and Koistinen (1994), respectively.

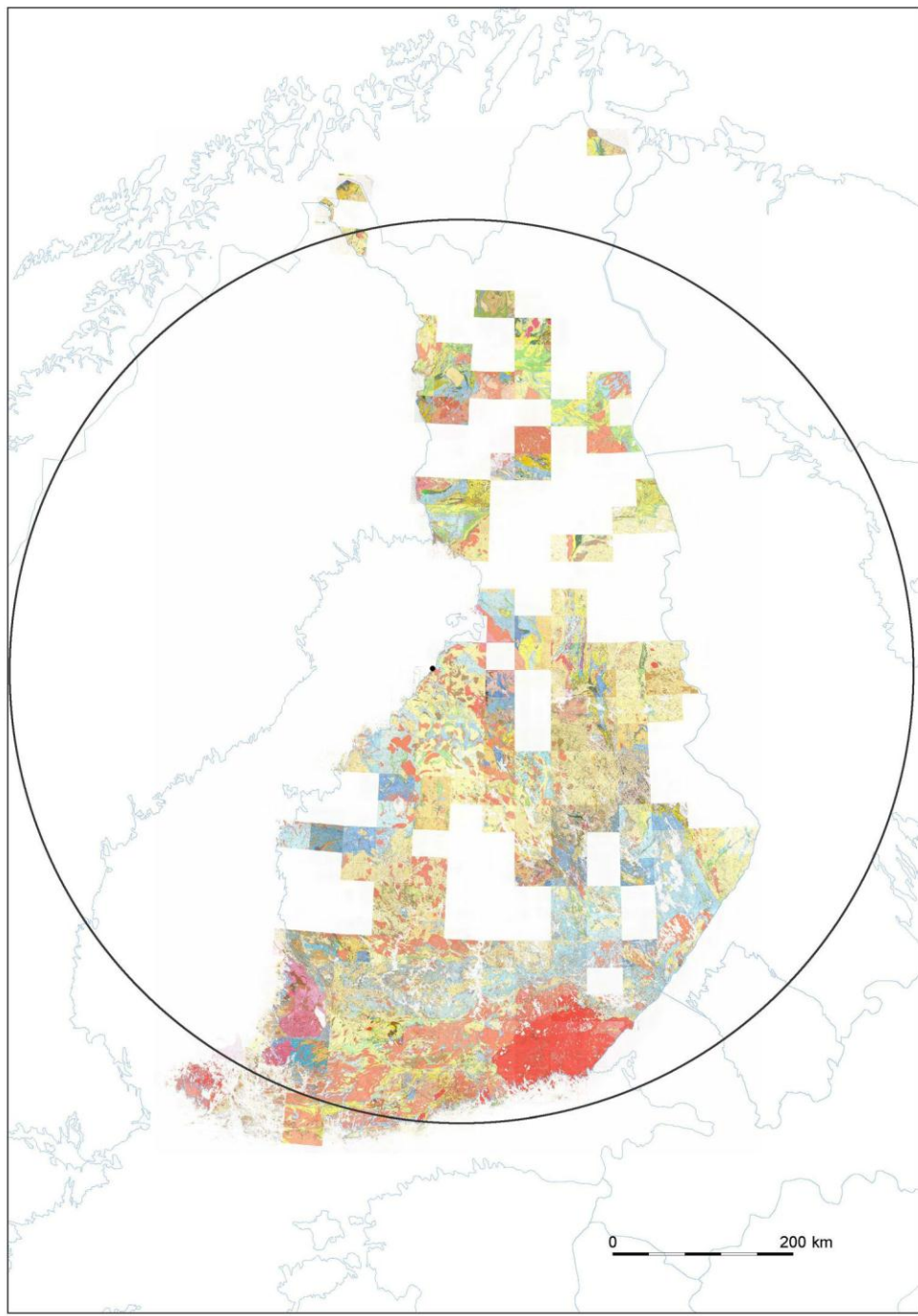


Figure 2.4.3. Coverage of bedrock maps at the scale 1:100 000 in Finland.

2.5 Structural map database

S. Grigull, M.-L. Airo, T. Huotari-Halkosaari & M. Nironen

Ancient deformation zones as well as dykes in Sweden were extracted as line data from the 1:1 M national bedrock database (Bergman et al., 2012). Where possible, the ancient deformation zones were categorised according to their kinematic character (Fig. 2.5.1). Due to their long tectonic history, most of these deformation zones are assumed to have been reactivated several times. A

clear distinction of these zones according to deformation style, i.e. brittle or ductile, was not possible.

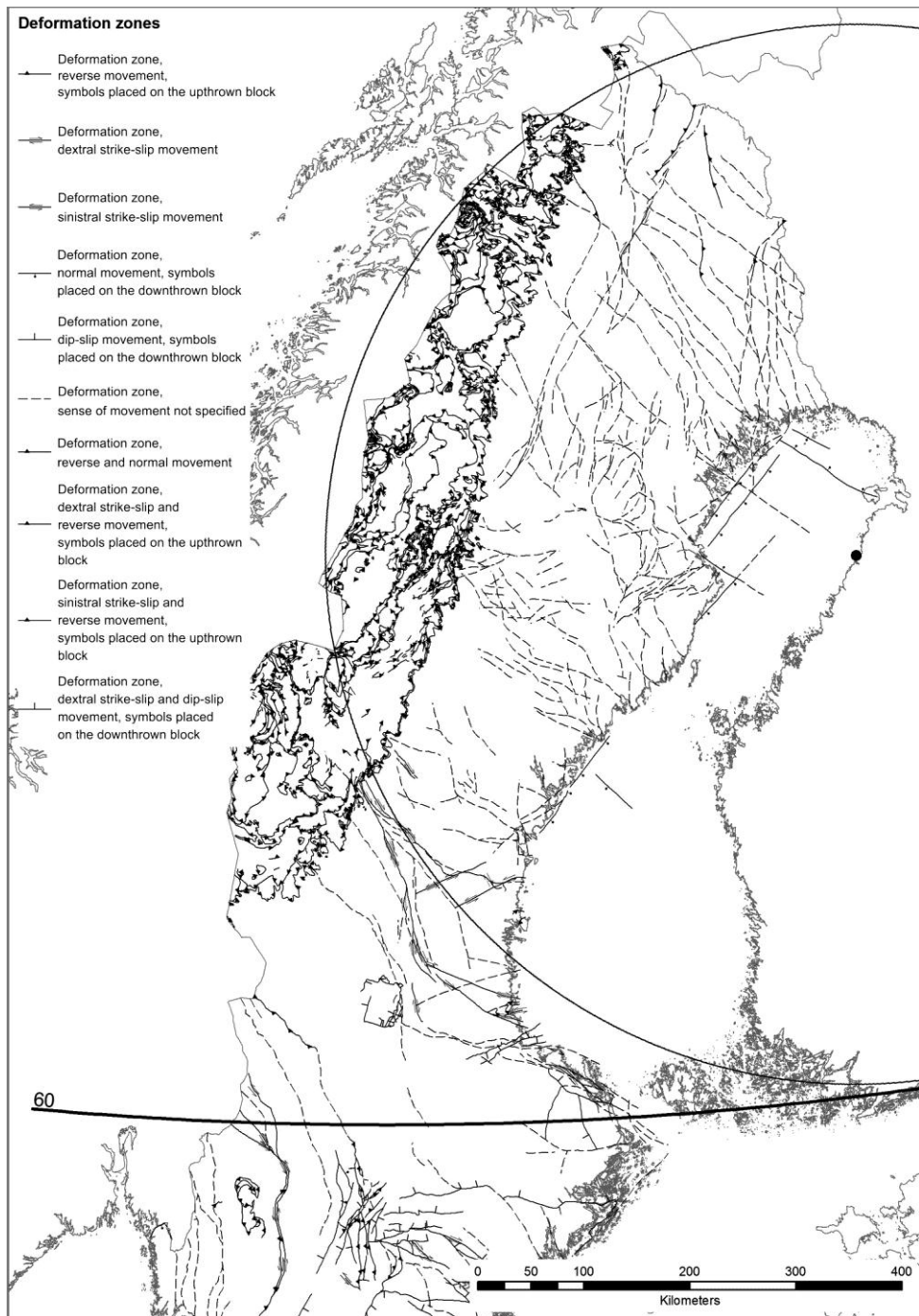


Figure 2.5.1. Deformation zones and their kinematic character in Sweden.

Based on a comparison with structures apparent in the 1:1 M airborne total magnetic field anomaly map of Sweden as well as some larger scale (1:250 000) geological data, the location and extent of the ancient deformation zones have been considered sufficiently accurate on a 1:1 M scale. This quality control work has been a significant component in the work completed at SGU from May 2013 onwards under the auspices of the Fennovoima project.

Some modifications were made to deformation zones in the northernmost part of Sweden, and in the northern part of the Gulf of Bothnia (Bay of Bothnia), making use of the new airborne geophysical data collected by SGU during 2012. The original line data representing the brittle-ductile deformation zones in the Fennovoima database were slightly adjusted, extended, or newly drawn following magnetic minima on the magnetic anomaly map (section 2.1). The modifications are presented in Figure 2.5.2. Some minor modifications along the national border between Finland and Sweden were also made when integrating the two separate data sets in Sweden and Finland (Fig. 2.5.3). These modifications involved the removal of minor discrepancies in the position of deformation zones on each side of the national border, and the removal of zones in Finland with a trace length at the ground surface not conformable with the 1:1 M scale of resolution adopted in this study. The modifications were carried out with the help of the total magnetic field anomaly maps for Sweden and Finland (Figs. 2.1.2 and 2.1.6).

The deformation zones were interpreted from GTK's countrywide airborne geophysical data sets: magnetic, electromagnetic (apparent resistivity) and, to a lesser extent, gamma radiation (Hautaniemi et al., 2005). Moreover, the bedrock map of Finland (1:1 000 000) and printed 1:100 000 bedrock maps (Fig. 2.4.3) were used for the location of ancient deformation zones. The structural data from Russia were interpreted from lower-quality geophysical data that were provided for compilation of the Geological map of the Fennoscandian Shield 1: 2 000 000 (Koistinen et al., 2001). The Rapakivi area lineaments (Fig. 2.5.5) were drawn according to aeromagnetic data and the interpretations was already published in Uski et al. (2006).

An interpretation of lineaments in the offshore area beneath the Gulf of Bothnia (Fig. 2.5.6) was carried out using airborne magnetic and Bouguer anomaly data for the Fennoscandian shield (Korhonen et al., 2002a,b).

The old morphological lineaments

The interpretation of the old morphological lineaments from Finland is made using 10 m x 10 m DEM with elevation contours (© National Land Survey of Finland). The lineaments in the old study area having a radius of 150 km around Pyhäjoki (Kuivamäki et al. 2011; Kukkonen 2011) in Figure 2.5.7 are categorized in 4 groups by length: Group 4: < 1 km, Group 3: 1-5 km, Group 2: 5-20 km and Group 1: > 20 km. In the new 500 km area around Hanhikivi only categories 1 and 2 are presented in the database. The interpretations of the lineaments in the 500 km area around Hanhikivi are the same as for the interpretations for the whole Finland, but they are cut according to circle boarder. The lineaments from Karelia region are drawn using topographic maps and Landsat figures (Landsat TM742 Suomi). The precision of the interpretation is not at the same level for Karelia region as for

Finland (scale is approximate 1:200 000-1:400 000). The lineament interpretation from the bottom of Lake Ladoga was not made due to lack of depth data. The Group 1: > 20 km lineaments in 500 km area are presented in the Figure 2.5.8. The geophysical study from the Russia is based on the geological and topographical data. Some background information can be found from the reports by Kuivamäki et al. (2011) and Kukkonen (2011).

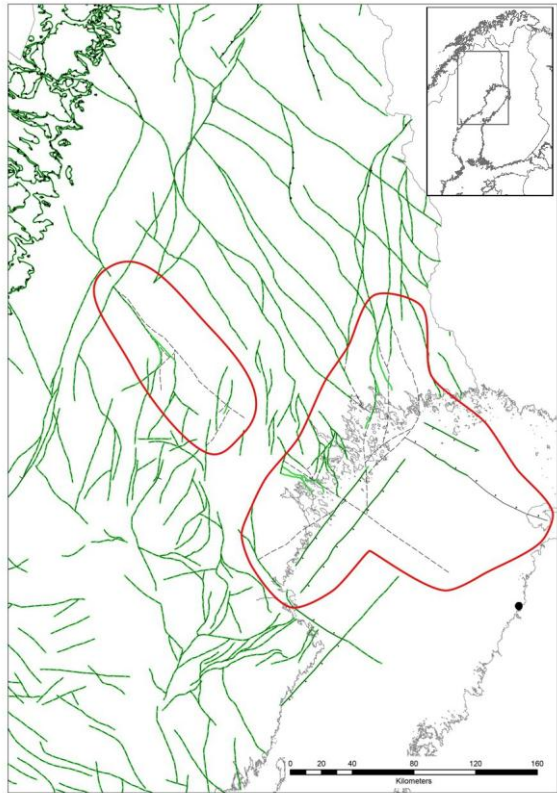


Figure 2.5.2. Map showing modifications made to deformation zones in the northernmost part of Sweden using the SGU airborne magnetic data from 2012. The green lines correspond to the original data set extracted from Bergman et al. (2012) and the black lines correspond to the few modified lines.

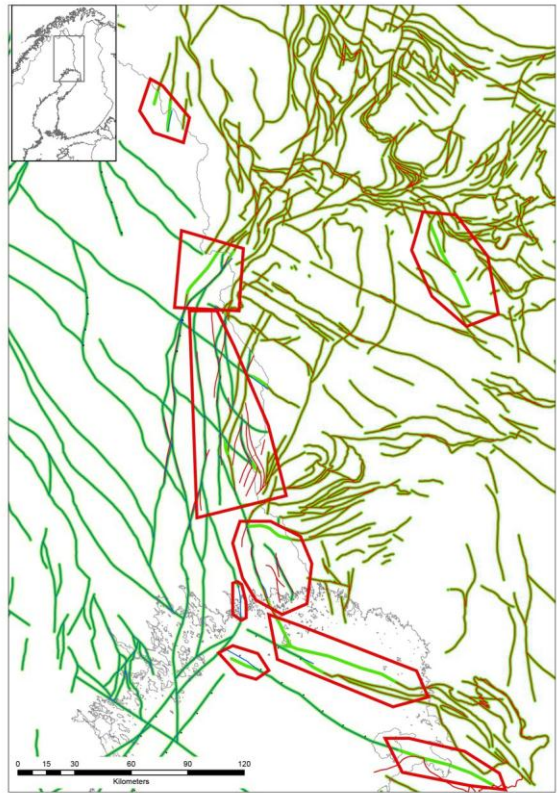


Figure 2.5.3. Map showing modifications made to deformation zones across the border between Finland and Sweden in connection with integration of the respective data sets. The green lines correspond to the resulting deformation zones in the Fennovoima database and the red and blue lines correspond to the original data sets in Finland and Sweden, respectively.

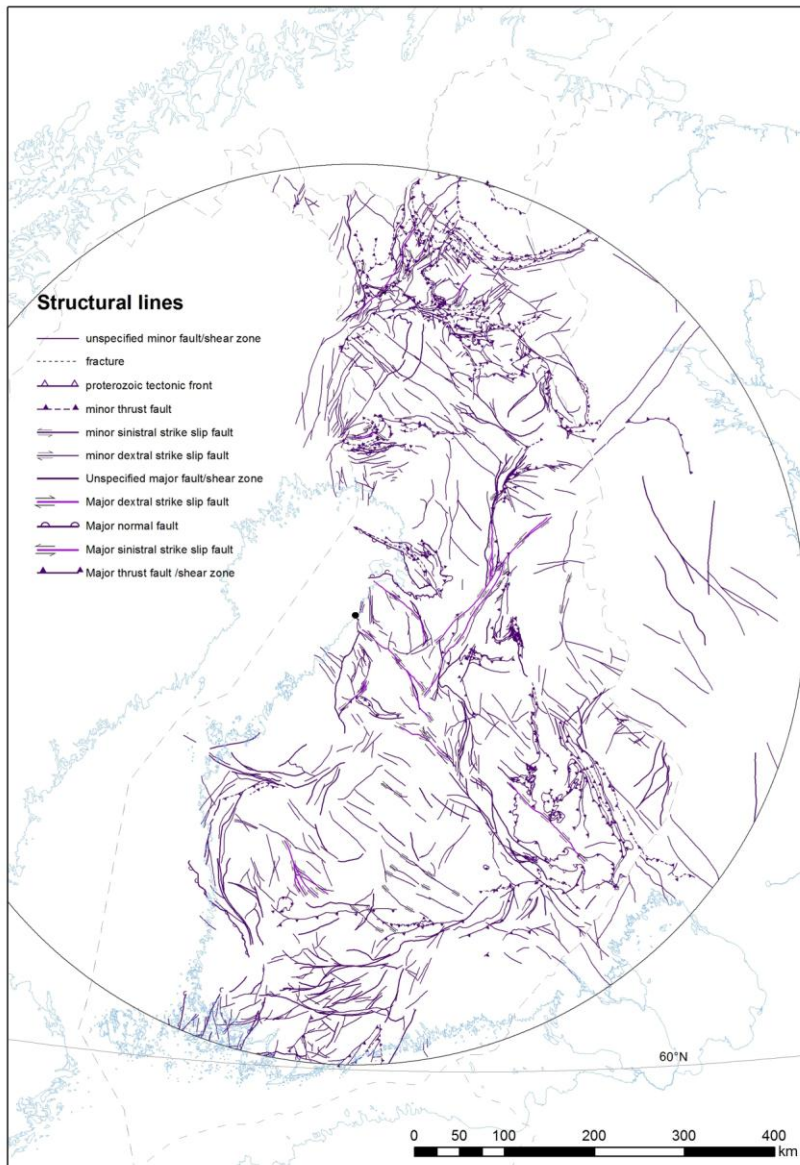


Figure 2.5.4. Deformation zones and their kinematic character in Finland.

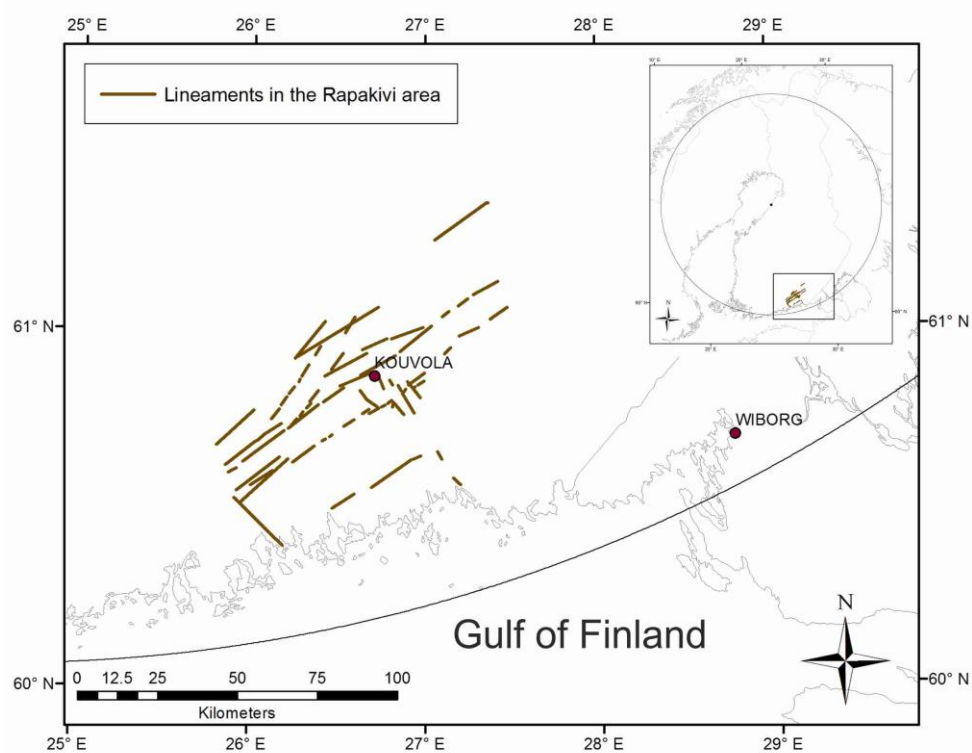


Figure 2.5.5. Lineaments in the Rapakivi area in southeastern Finland according to Uski et al. (2006).

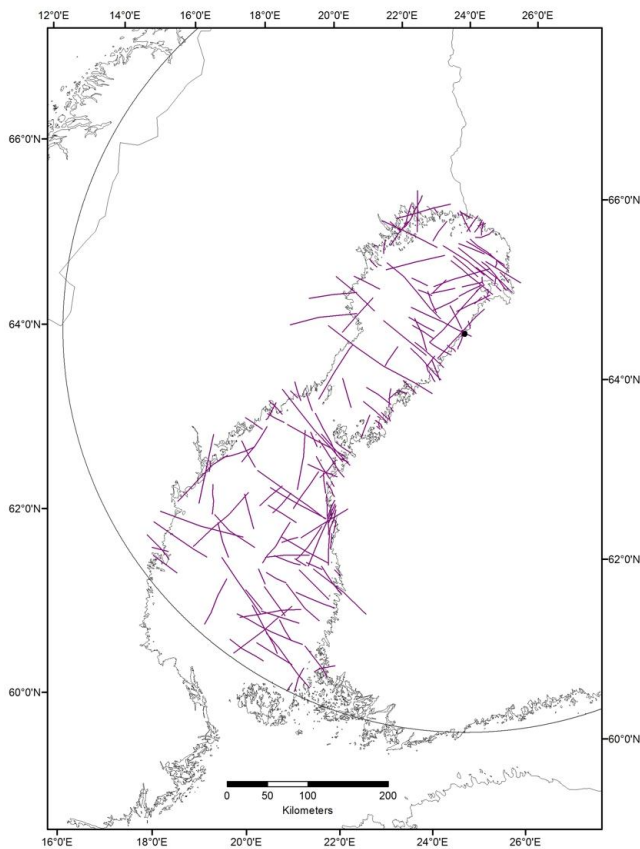


Figure 2.5.6. Lineaments in the Gulf of Bothnia based on an interpretation of airborne magnetic high altitude data and Bouguer anomaly data (GTK).

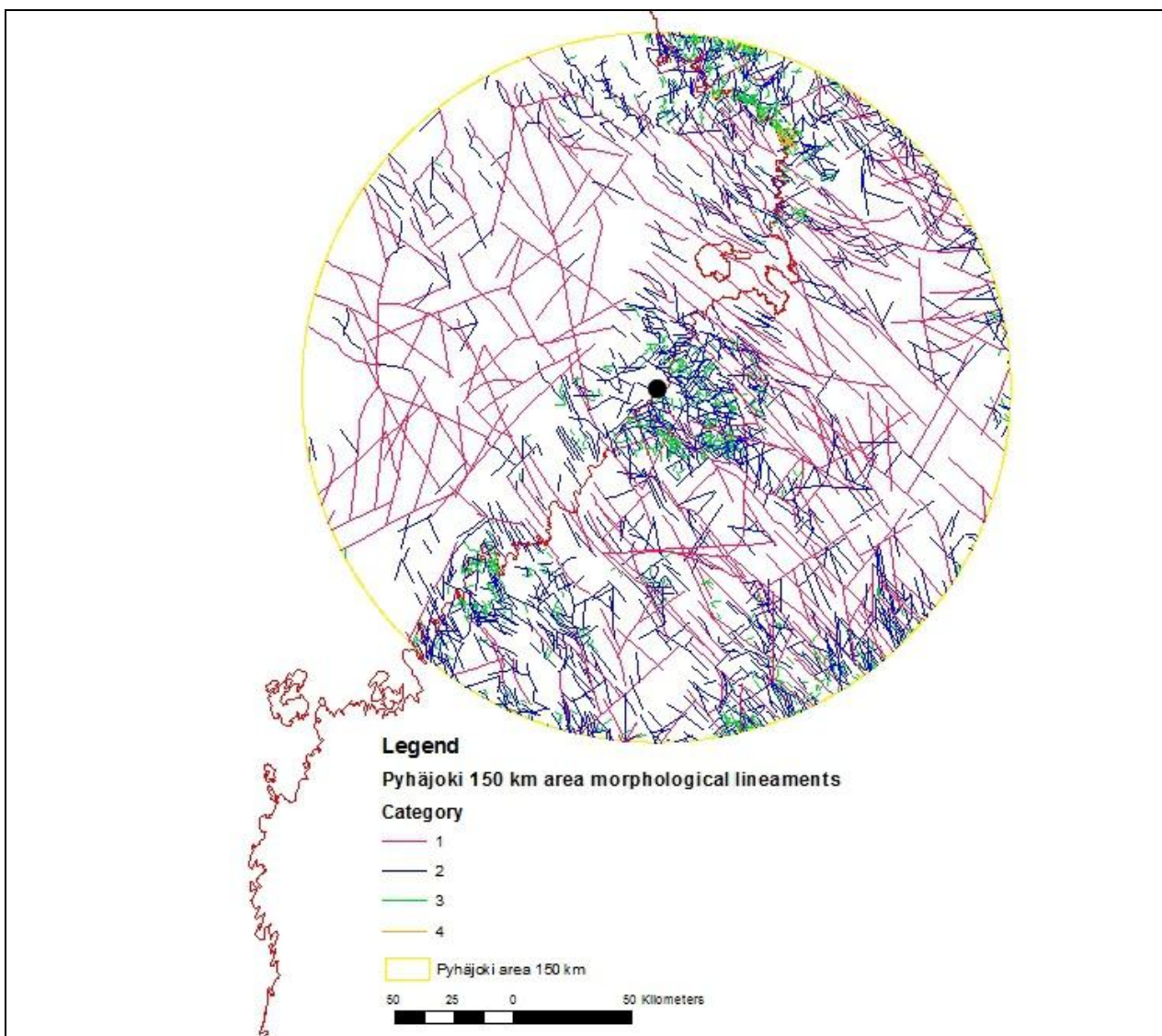


Figure 2.5.7. The lineaments in the old 150 km study area around Hanhikivi (Kuivamäki et al., 2011) are categorized in 4 groups by length: Group 4: < 1 km, Group 3: 1-5 km, Group 2: 5-20 km and Group 1: > 20 km.

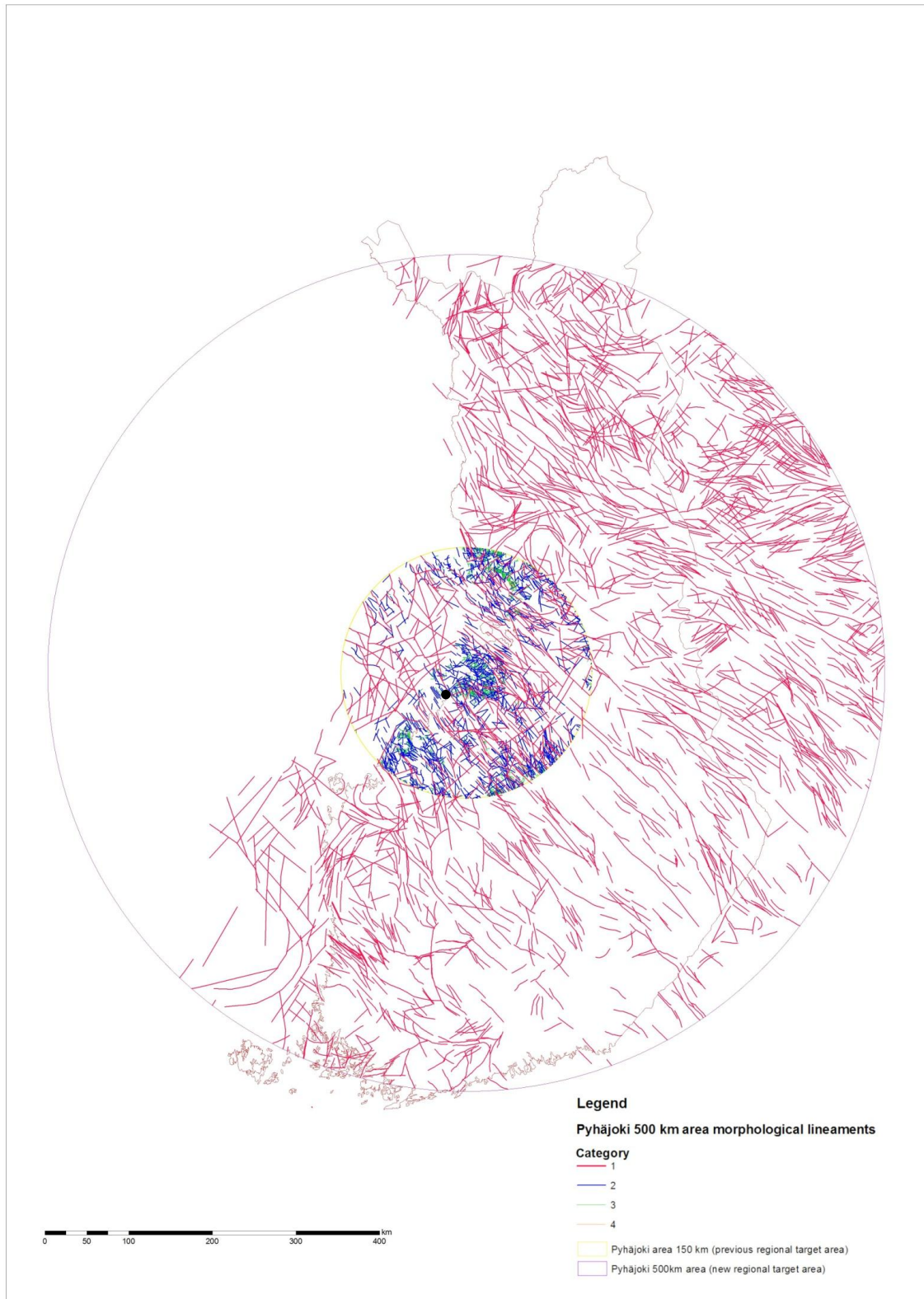


Figure 2.5.8. Morphological lineaments around Hanhikivi. The smaller circle is 150 km and the larger 500 km around Hanhikivi. The lengths of the lineaments are in 4 groups: Group 1 > 20 km, Group 2 5-20 km, Group 3 1-5 km and Group 4 < 1 km. Only group 1 is visualized from the 500 km area around Hanhikivi.

2.6 Submarine data in the Gulf of Bothnia

K. Högdahl

Apart from the focused input completed during previous work in the Bay of Bothnia (see Appendix 1) and the regional lineament interpretation based on geophysical data along the whole of the gulf (see section 2.5). The geology beneath the Gulf of Bothnia has been studied by using both shallow and deep seismo-acoustic methods (Winterhalter, 1972; Axberg, 1980; Wannäs, 1989; BABEL Working Group, 1990). Here we only describe the shallow marine reflection studies focusing on the sedimentary cover that have been used to identify active deformation zones in the offshore areas. The BABEL data sets (BABEL Working Group, 1993) are used as literature reference and the deeper structures inferred from these data are not addressed here.

The southern part of the Gulf of Bothnia (Bothnian Sea) was initially investigated by Winterhalter (1972) using eco-soundings and continuous seismic reflection profiling, covering a total length of 1 850 km (Fig. 2.6.1); samples were also collected on the sea bottom. The sound velocity in water was set to 1 425 m/s and the penetration depth in the Paleozoic sedimentary rocks was generally 100 m. The acoustic boundaries were tentatively correlated to the stratigraphy from a drill core at Finngrundet, NNE of Gävle, and compared with sound velocities collected on the Finnish mainland.

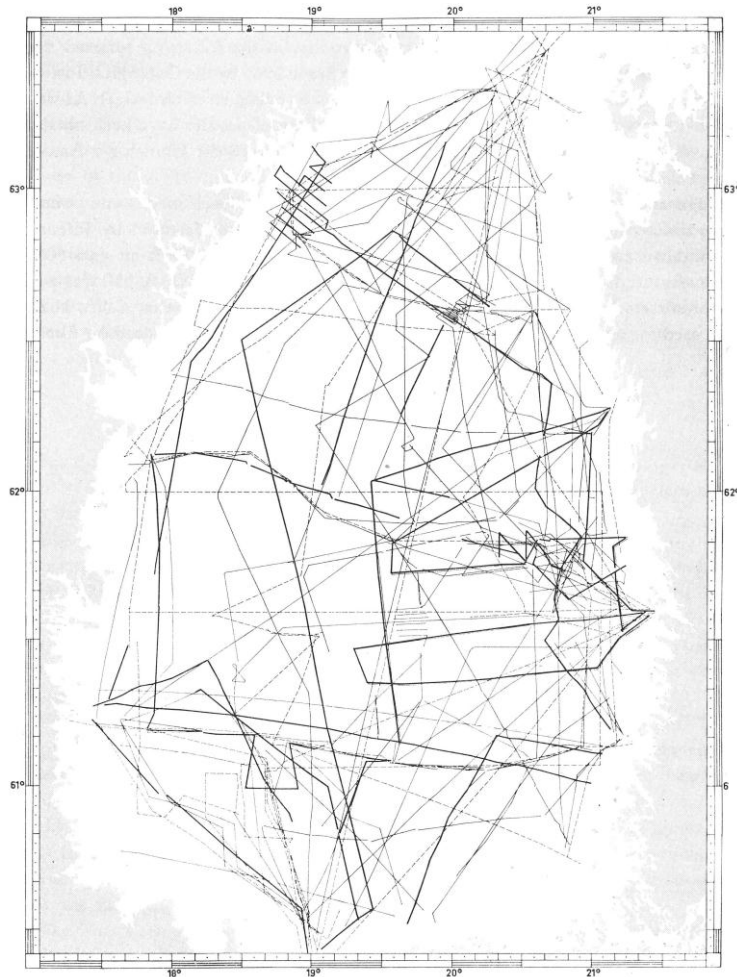


Figure 2.6.1. Location of continuous reflection seismic profiles and eco-sounding measurements in the southern part of the Gulf of Bothnia (Bothnian Sea) after Winterhalter (1972).

During 1972–1978, additional continuous reflection seismic profiling and eco-sounding were carried out along 8 000 km of section lines (Fig. 2.6.2A) in the Bothnia Sea (Axberg, 1980); 10 measurements of continuous refraction seismic soundings were also carried out (Fig. 2.6.2B). The sound velocity in water was calculated to 1 430 m/s and the penetration depth ranged from 50–300 m. The vertical resolution of bedrock layers was normally 2–6 m but spanned between 0.6 and 16 m depending on the sound velocity of the rocks and the applied frequency band (50–900 Hz). Five of the acoustic boundaries were compared with and correlated to the stratigraphy along two drill cores collected at Västra Banken (R3) and Finngrundet (R7), NNE of Gävle (Fig. 2.6.2B).

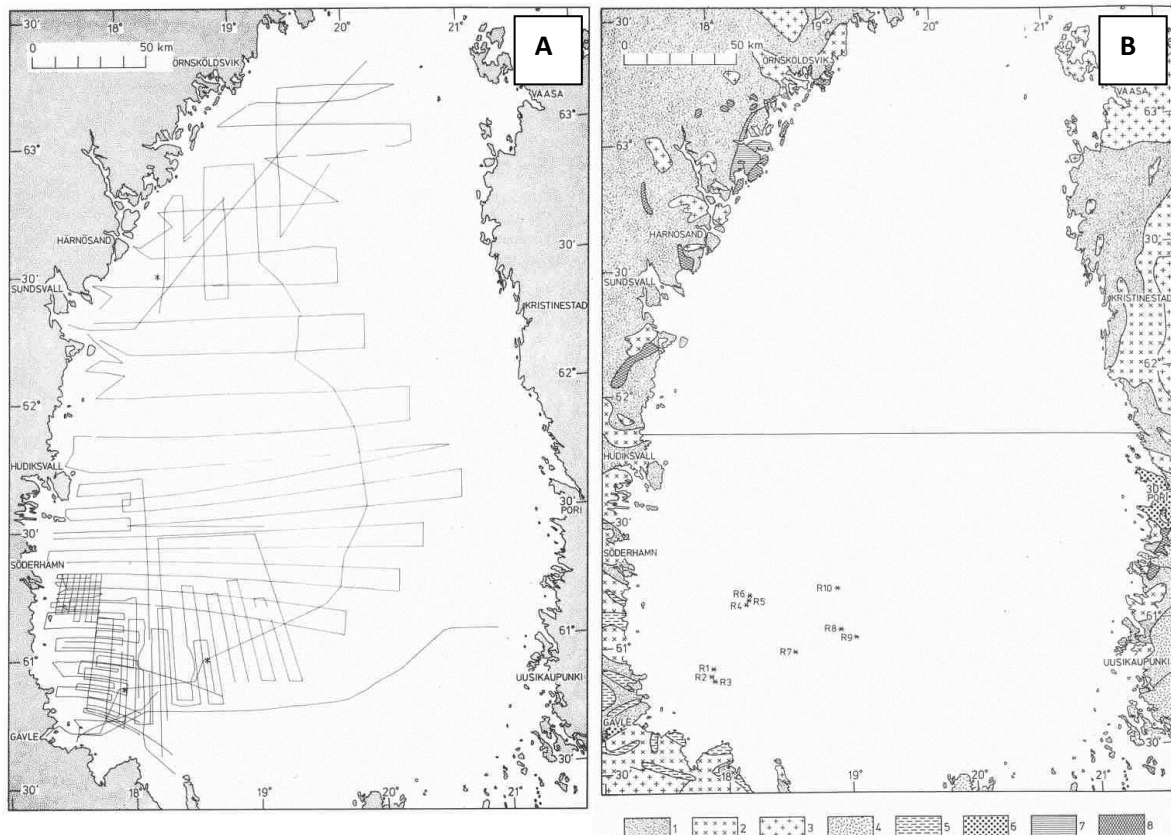


Figure 2.6.2. A) Location of continuous reflection seismic profiles and eco-sounding measurements in the southern part of the Gulf of Bothnia (Bothnian Sea) after Axberg (1980). B) Location of 10 refraction seismic stations in the Bothnian Sea after Axberg (1980). The two southernmost asterisks (R3 and R7) mark the locations of Västra Banken (to the southwest) and Finngrundet (to the northeast). The reader is referred to Figure 5 in Axberg (1980) for the explanation to the rock units shown on land in Figure 2.6.2B.

During 1978–1980, continuous reflection seismic profiling and eco-sounding along 2 800 km of section lines (Fig. 2.6.3A) were carried out in the Bay of Bothnia, in the northern part of the Gulf of Bothnia (Wannäs, 1989); 62 sonobouy refraction seismic measurements were also shot (Fig. 2.6.3B). The reflection seismic data were collected using an analogue, single-channel seismic reflection profiler (Wannäs, 1989). The penetration depth with this method is variable, being a function of water depth and sound velocities in the rocks below, and of the ratio between the sound velocities of

the water and the Quaternary deposits. The sound velocity in water was calculated to 1 430 m/s. The range of the vertical resolution was not provided in Wannäs (1989). The acoustic boundaries were compared with data collected on land in the Finnish mainland and on Hailuoto Island, and correlated to the stratigraphy in one drill core from the same island that covers some of the acoustic boundaries.

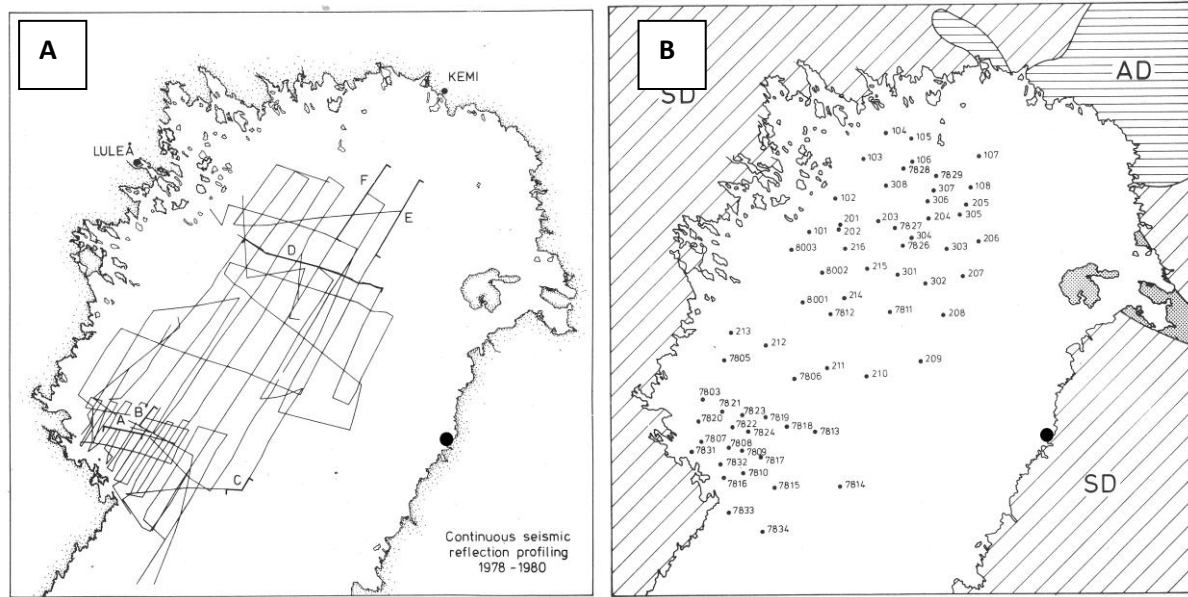


Figure 2.6.3. A) Location of continuous reflection seismic profiles in the northern part of the Gulf of Bothnia (Bay of Bothnia) after Wannäs (1989). B) Location of the 64 sonobouy refraction seismic stations in the Bay of Bothnia after Wannäs (1989). The reader is referred to Figure 3 in Wannäs (1989) for the explanation to the rock units shown on land in Figure 2.6.3B.

All these data have been used to calculate the sound velocities in the sedimentary cover rocks, and to determine the depth to the seismic markers and, thereby, the water depth, the thickness of the sedimentary rocks and the depth to the crystalline basement. The data were also used to identify the locations of faults that disturb the sedimentary cover rocks and their inferred vertical component of displacement.

The data collected by Winterhalter (1972) are stored at the Geological Survey of Finland. The seismic data collected by Axberg (1980) and Wannäs (1989) were recorded on tape and stored as analogue data at the Department of Earth Sciences, Stockholm University. However, in connection with relocation of this institution from central Stockholm and its reorganisation on several occasions, it is difficult to evaluate exactly how much of the original data are currently preserved. None of these data have been converted to modern digital formats. Inspection of primary data was not completed in this study and the evaluation presented here solely makes use of the interpretations presented in Winterhalter (1972, 2000), Axberg (1980) and Wannäs (1989).

In the acoustic-seismic sounding study by Rantataro et al. (2011) in the Bay of Bothnia (Appendix 1, Fig. A1.2), lineaments interpreted by Wannäs (1989) and Kuivämäki et al. (2011) were observed typically as bedrock depressions, but no indications of post-glacial faulting were found in the investigated area.

2.7 Faults active during the Quaternary period

S. Grigull, R. Sutinen & E. Kosonen

Munier & Fenton (2004) and Lagerbäck & Sundh (2008) describe criteria for the identification of post-glacial faults (PGF), including points such as the faults cutting overlying Quaternary deposits, displacement of both late and post-glacial deposits and reactivation occurring close in time to local deglaciation.

The knowledge about the location, displacement properties and length of these faults is largely based on geological work focused on the northern half of Sweden since the 1970's (Lundqvist and Lagerbäck, 1976; Lagerbäck and Henkel, 1977; Lagerbäck, 1979, 1990; Lagerbäck and Sundh, 2008). Post-glacial faults in northern Finland were first discovered by Kujansuu (1964, 1972). These findings were later confirmed by Kuivämäki et al. (1998). Lagerbäck and Sundh (2008) described the methods used to identify the presently known faults active during the Quaternary in Sweden and summarised the present state of knowledge of nine major confirmed fault systems (Fig. 2.7.1). Potential fault candidates were identified using aerial photographs to discover the location and frequency of landslides developed in glacial tills and spatially related fault traces. Field reconnaissance studies were carried out mostly involving trenching across the fault scarps and studying soft sediment deformation structures (Lagerbäck and Sundh, 2008). An interpretation and catalogue of paleoseismicity in Sweden have also been presented by Mörner (2005) and a detailed search for PGFs was carried out during the site investigations for a repository for spent nuclear fuel in Östhammar and Oskarshamn (Lagerbäck and Sundh, 2003; Lagerbäck et al., 2004a,b; Lagerbäck et al. 2005a,b; Lagerbäck et al. 2006 [six SKB reports]).

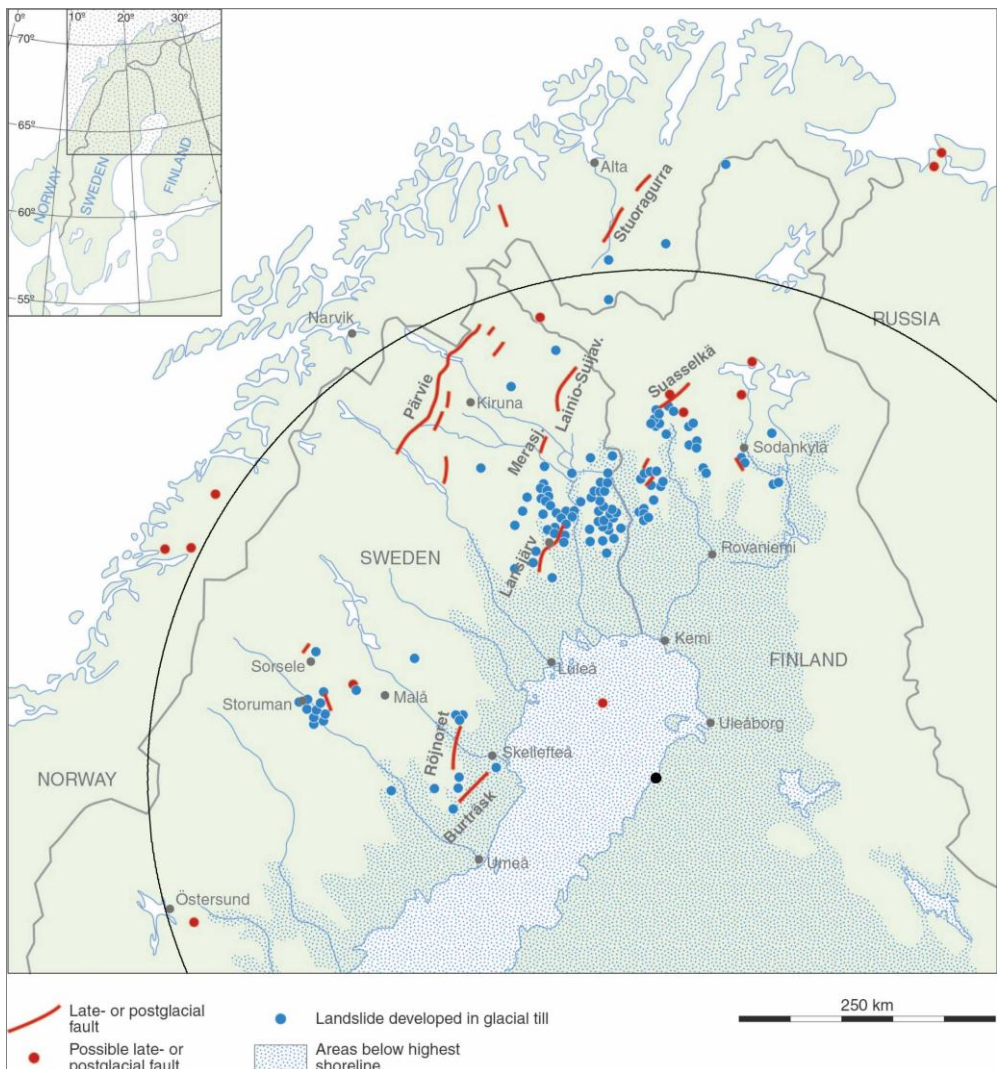


Figure 2.7.1. Distribution of landslides and faults with Quaternary movement in the northern part of Finland, Norway and Sweden. Image after Figure 2 in Lagerbäck and Sundh (2008).

The PGF database consists of known post-glacial faults in Sweden, Finland and Norway as well as possible post-glacial faults in Finland and Sweden area (Fig. 2.7.2). Line data representing the surface expression of faults with confirmed Late Pleistocene or Holocene movement have been extracted from the SGU regional (1:250 000) bedrock database as well as from a separate SGU 1:250 000 Quaternary database. In addition to the faults described by Lagerbäck and Sundh (2008), other post-glacial faults have recently been identified by Quaternary geologists at SGU interpreting high resolution digital elevation models (DEM) derived from LiDAR data. The DEM were also used here to identify landslide scars and landslide clusters, as well as nearby linear features potentially representing faults that may have moved during the Late Pleistocene or Early Holocene and caused these landslides. One formerly unknown fault near Bollnäs (Fig. 2.7.2) was discovered using this method, and a surmised second fault was confirmed as having been active during post-deglaciation time (Ismunden fault in Lagerbäck and Sundh (2008) 25 km southeast of Östersund). The fault near to Bollnäs has recently been trenched (Smith et al., 2014), and faulted soft-sediment structures were

discovered, strongly indicating late- to post-glacial fault movement. Both newly discovered faults (Smith et al., 2014; Mikko et al., 2014) are included in the current Fennovoima database (Fig. 2.7.2). Stereo airphoto interpretation from the 1960's and more recently a 10 m resolution digital elevation model (DEM) by the National Land Survey of Finland have been applied to detect PGFs. The current airborne LiDAR-data allows precise detection of even minor ruptures under the forest canopies (Fig. 2.7.3) as well as reconnaissance of earthquake induced morphological features, such as landslides (Sutinen et al., 2013). New post-glacial faults (Isovaara, Kultima, Paatsikkjoki, Palojarvi) have been found and identified from Finland in past years (Sutinen et al., 2013, 2014) and added to the Fennovoima database (Fig. 2.7.2).

The possible post-glacial faults in the Storuman/Sorsele and Malå region (Sweden), first mentioned during Quaternary mapping (Johansson and Ransed, 2003; Ransed and Wahlroos, 2007), have been included in the database as a separate dataset (Fig. 2.7.2). The Sorsele and Malå faults have been drawn according to Lagerbäck and Sundh (2008). The possible post-glacial faults in Finland, Vaalajärvi, Siyliövaara, Kotijänkä and Sevetti (Fig. 2.7.2) are also included in the database, since most of them are cited in past literature as post-glacial faults (Kujansuu 1964, Kuivamäki et al. 1998); they are currently considered as possible post-glacial faults and await further analysis. The Stuoragurra and Nordmannvik post-glacial faults were drawn according to Lagerbäck and Sundh (2008).

During the process of compiling the current structural lines database, it emerged that most of the late- or post-glacial faults are situated parallel, and spatially close, to ancient deformation zones or even coincide with them. This relationship between ancient crustal zones of weakness and the fault zones active during the Quaternary has already been suggested by Lagerbäck and Henkel (1977). For this reason, the initiative was taken to complete a more detailed lineament study around the known late- or post-glacial faults in Sweden using the magnetic data described in section 2.1 and an interpretation of the total magnetic field anomaly map generated by SGU and shown in Figure 2.1.2. On a 1:100 000 scale map, magnetic minima were traced and compared to available larger scale maps. The resulting line data are also included in the current Fennovoima database and an example is provided in Figure 2.7.4.

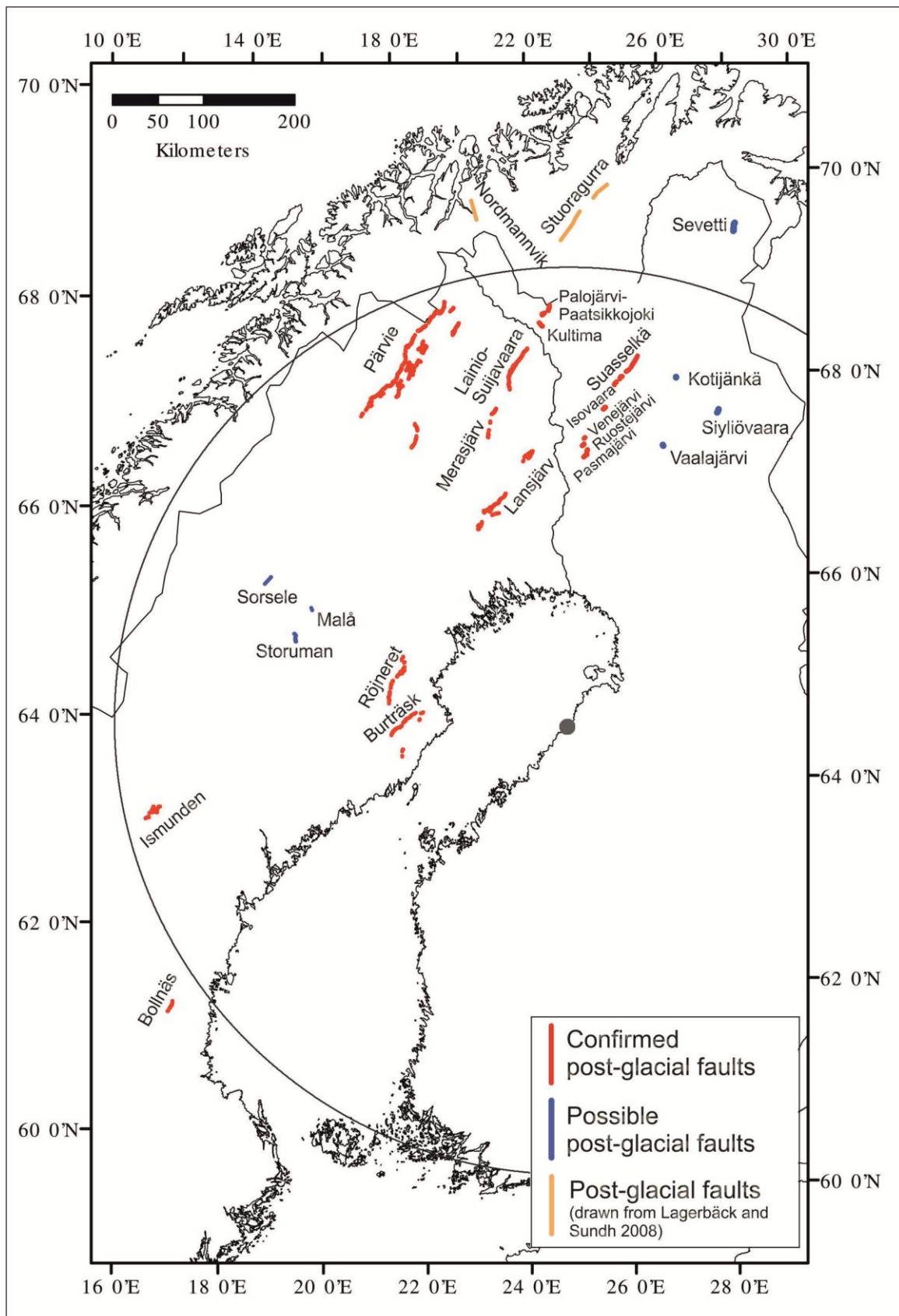


Figure 2.7.2. Fault traces active during the Quaternary as stored in the SGU and GTK databases (red). The location of the traces is based on regional bedrock and Quaternary geology maps as well as on LiDAR derived DEM studies recently undertaken by SGU. Fault traces possible active during Quaternary in Finland and Sweden are shown in blue. Post-glacial faults in Norway are drawn after Lagerbäck and Sundh (2008). Hanhikivi site: grey dot.

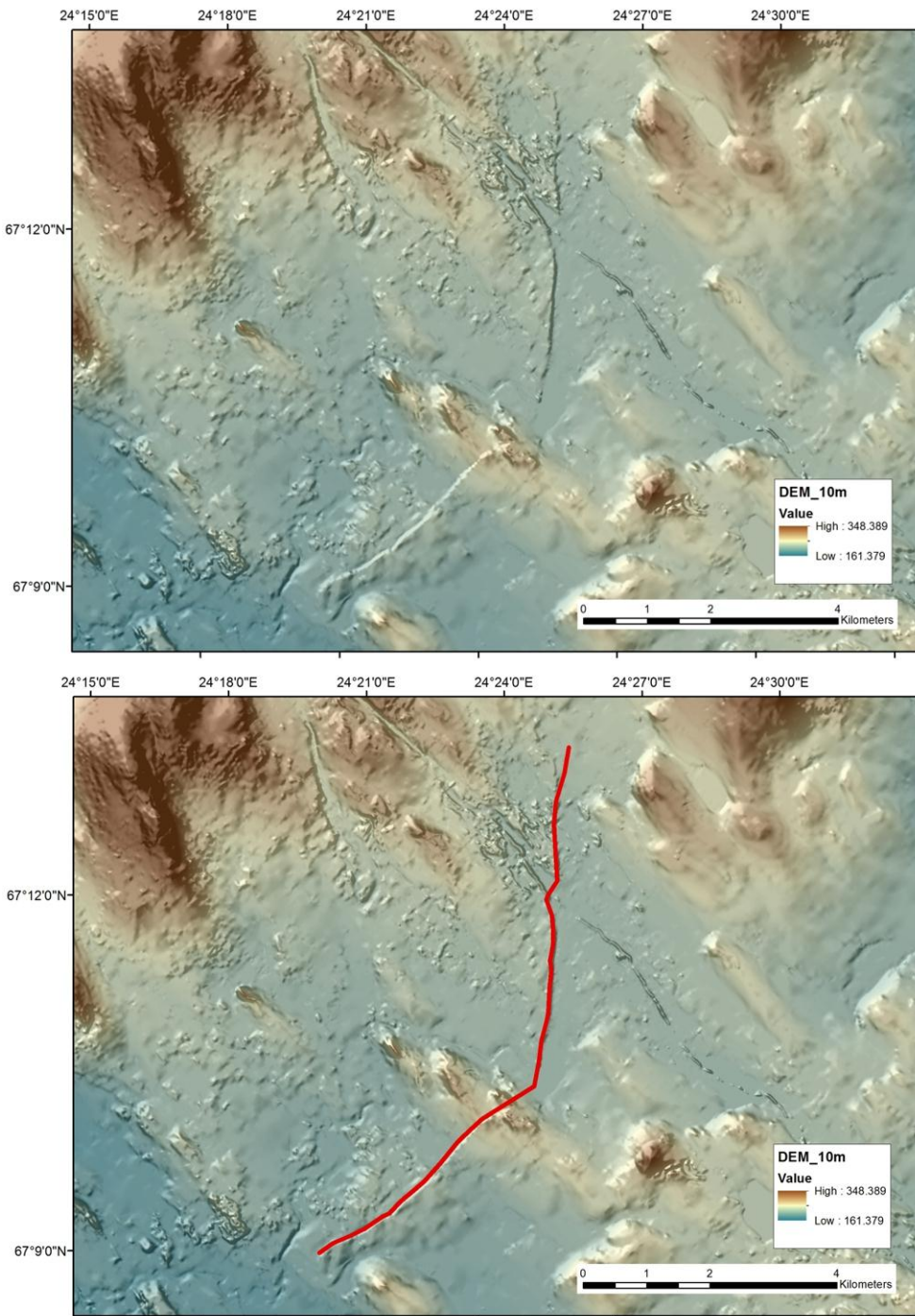


Figure 2.7.3. The Pasmajärvi/Ruokojärvi fault section identified from 10-m DEM data (Digital elevation model 10m © National Land Survey of Finland 2014). On the bottom the Pasmajärvi/Ruokojärvi fault trace is identified and edited on the Fennovoima database. See location of the fault in Figure 2.7.2.

In this study, the locations and lengths of the known faults that have been active during and after glaciations in Finland were checked against the topographical (10 m resolution DEM) (Fig. 2.7.3) and geophysical data (magnetic and airborne electromagnetic data (FDEM)) with all the validated seismic data in the Fennovoima project. Due to the loose data coverage of gravity data, these data have not been analyzed against the post-glacial faults. Drilling and field studies at the Isovaara (Sutinen et al.,

2013) and Pasmajärvi/Ruokojärvi faults have been carried out in 2012 (GTK). Interpretation of Pasmajärvi/Ruokojärvi fault field results is still under investigation (GTK).

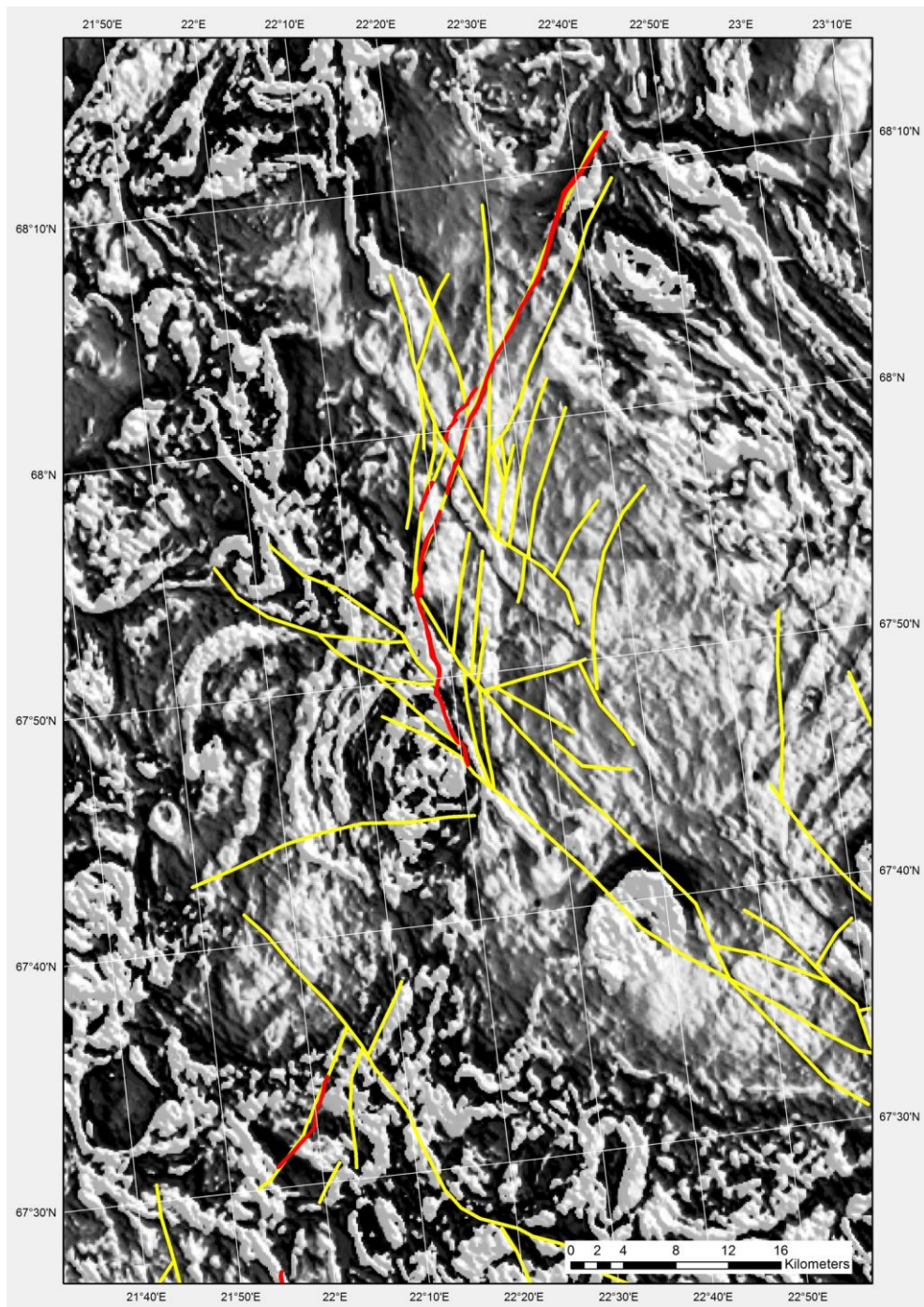


Figure 2.7.4. Detailed section of the Lainio-Suijavaara fault in Norrbotten. The fault trace seems to follow ancient structures (yellow lines) within the bedrock that are expressed as lineaments defined by magnetic minima on the magnetic anomaly map in the background. See location of the fault in Figure 2.7.2. Dark colours: low magnetic susceptibility, light colours: high magnetic susceptibility.

2.8 Seismicity database

B. Lund, M. Uski & Mäntyniemi, P.

The study area is situated in the Fennoscandian Shield, where geological conditions are favourable for detecting and recording seismic signals. The ancient, stable Precambrian crust is seismologically quiet and transfers seismic waves well due to its low attenuation properties. The parametric Fennoscandian earthquake catalogue FENCAT has been used as a primary seismicity reference in this project. FENCAT is a compilation of earthquake reports from cooperating seismological agencies in the Nordic countries, Estonia and NW Russia.

2.8.1 Earthquake database

The parametric earthquake catalogue FENCAT (Ahjos and Uski, 1992; with updates at http://www.seismo.helsinki.fi/english/bulletins/catalog_northeurope.html) is the most comprehensive source of seismicity data available in the study region. It covers the years 1375–2011 (Figs. 2.8.1.1 and 2.8.1.2). Besides the earthquake magnitude and epicentral coordinates, it provides the macroseismic parameters area of perceptibility and maximum intensity for the non-instrumental earthquakes and also for many instrumental earthquakes. Reliable depth estimates are available for only a number of the most recent earthquakes.

In addition, a preliminary version of the 2012 earthquake catalogue has been prepared for this project. It is based on earthquake reports from the Finnish (FNSN) and Swedish (SNSN) national seismic networks. For the current project, the SNSN has provided a supplementary data set not included in the metadatabase (Appendix 3) or open-access FENCAT, including all micro-earthquakes detected within Sweden since August 2000 (Fig. 2.8.1.3). The locations are routine processing, single event locations, and no effort has been made here to further refine the location of the events. Mining-induced seismic events, such as rock bursts and mine collapses, as well as events with questionable seismic origin (e.g., frost shocks, events interpreted as misidentified blasts) have been removed from the data sets.

Besides earthquake parameters, macroseismic data point (MDP) datasets have been prepared for key historical earthquakes in the study region (see Appendix 2, Table A2.1). Effects of local and regional earthquakes have been reported in writing throughout centuries. The textual information is helpful for seismicity studies provided that the rigorous rules of historical seismology are followed. Consulting primary written documentary materials reporting felt earthquake effects has led to a more comprehensive understanding and re-appraisal of the earthquakes. The investigated earthquakes noteworthy in seismic hazard assessment are listed in Table 2.8.1.1.

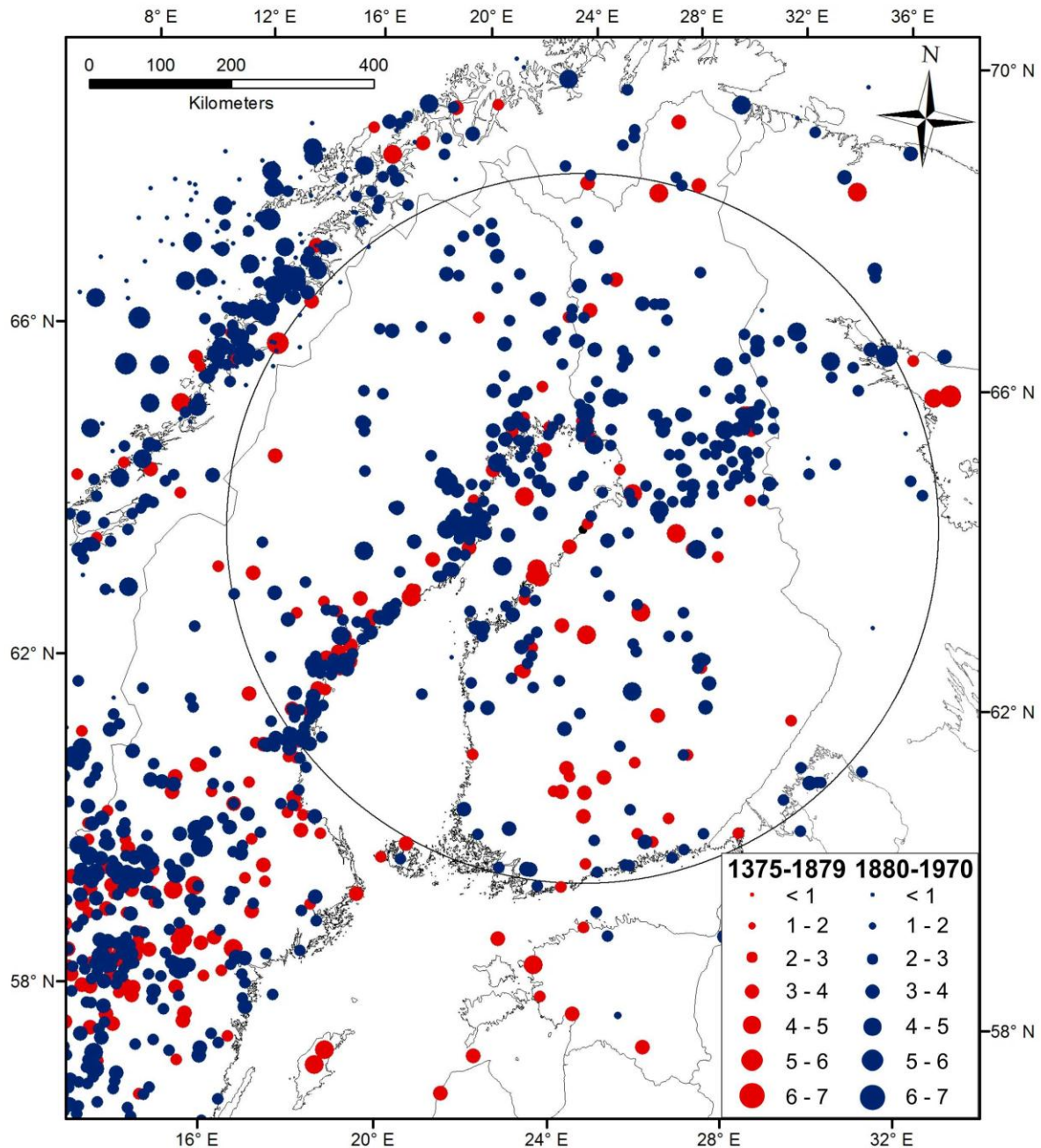


Figure 2.8.1.1. FENCAT earthquake catalogue covering the years 1375-1970.

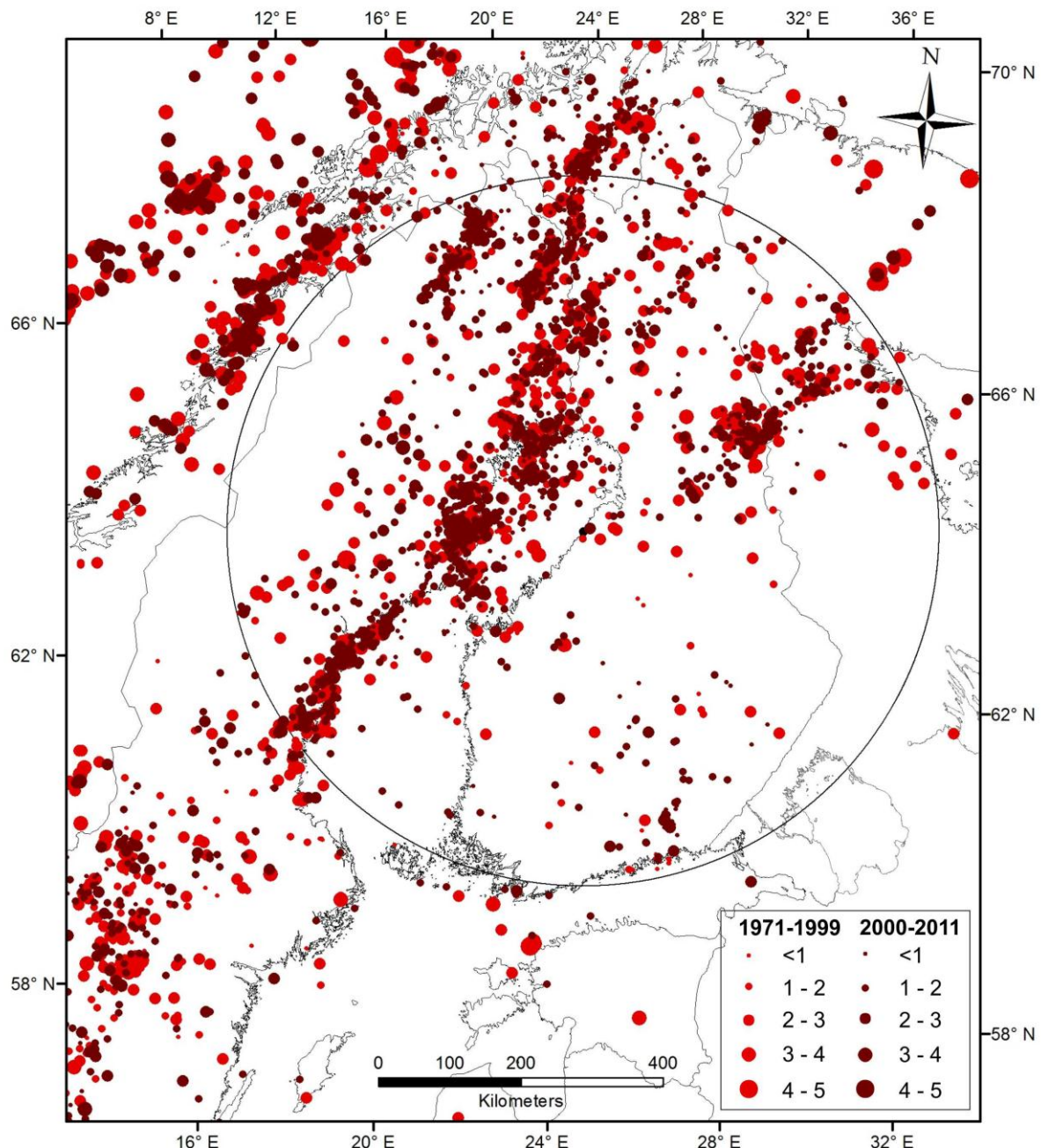


Figure 2.8.1.2. FENCAT earthquake catalogue covering the years 1971-2011 and preliminary version of the 2012 earthquake catalogue.

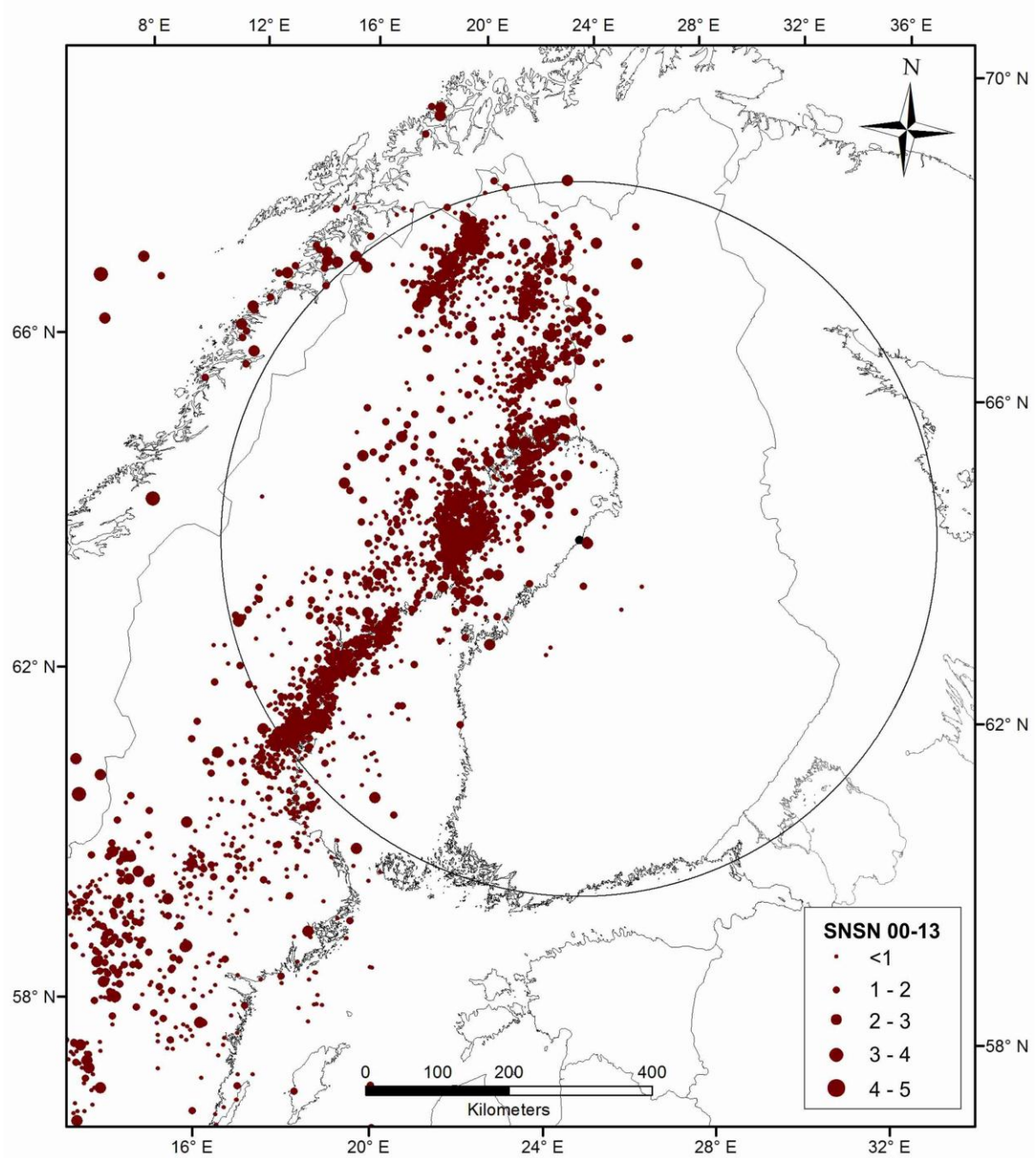


Figure 2.8.1.3. SNSN supplementary data set including micro-earthquakes detected within Sweden since August 2000.

Table 2.8.1.1. Updated historical earthquakes in the FENCAT catalogue.

source	year	month	day	hour	min	sec	lat	lon	uncer time	depth	depth code	mag	mag scale	int	code	macro ref	area	reg code
PAN	1542	0	0	0	0		66.0	35.0	-?	15		4.4	M	VI	?		150	U
PAN	1626	5	14	0	0		66.0	35.5	-C	35		5.1	M	VI	?		350	U
REN	1626	6	22	0	0		64.5	27.0	-B	18	m	4.6	M	VI			185	F
REN	1758	12	31	0	30		68.8	26.4	BC	31	m	4.7	M	V			175	F
REN	1777	3	29	18	0		63.9	23.1	DB	19	m	4.0	M	V			110	F
REN	1882	6	15	13	0		65.8	24.2	CB	20	m	4.6	M	VI	*	MOB	200	F
REN	1882	6	23	6	0		65.6	24.5	CB	27	m	4.9	M	VI	*	MOB	270	F
BAT	1931	11	16	0	20	49	62.5	25.8	AA	15	m	4.5	M	VI	*	KAR	155	F
BAT	1931	11	16	19	30		62.5	25.8	BA	16	m	3.9	M	V	*	KAR	90	F
BAT	1957	8	2	9	15	51	63.2	32.5	BA	0		0.0					0	U
PAN	1958	1	17	9	42	23	65.6	34.0	BB	0		0.0					0	U

NOTE: Different parametric solutions are available for the earthquakes marked in blue. The earthquakes marked in red above have no magnitude in FENCAT, but Nikonov (2004, p. 212) lists them with magnitudes. Explanations of the columns can be found http://www.seismo.helsinki.fi/bulletin/list/catalog_format.html.

2.8.2 Seismic networks and changes in detection capability

The instrumental era began in the Fennoscandian Shield in 1904, when a long-period Wiechert seismograph was installed in Uppsala, Sweden. A long-period Mainka seismograph was installed in Helsinki, Finland in 1924. However, the related seismograms are of little practical value for the study of local earthquakes. The first short-period seismographs were installed in the region in 1956, and all earlier earthquake observations are defined as historical in this report. The time period between 1956 and 1970 can be called semi-instrumental, because the analysis of local earthquakes was not yet fully based on instrumental data. The seismicity record available spans three centuries, about 250 years of which rely on non-instrumental historical data.

The Finnish (FNSN) and Swedish (SNSN) national seismic networks are nowadays the main contributors of seismic observations in the study region (Fig. 2.8.2.1). Prior to 2000, SNSN operated six permanent seismic stations in Sweden and the catalogue was complete for earthquakes down to an approximate magnitude 2. The Swedish Defence Research Agency (FOI, previously FOA) has operated a seismic array station at Hagfors since the early 1970s, as part of the Swedish contribution to international nuclear test ban treaties. From 1980 onwards, FOA operated a number of seismic stations first in southern and then northern Sweden, recording local earthquakes with magnitudes down to zero. Operations were phased out during the early 1990s. Phase readings from the recorded

SNSN and FOA earthquakes were reported to FENCAT. A rapid expansion of the SNSN commenced in 2000 and, by the end of 2012, 60 additional permanent stations had been constructed and instrumented.

All SNSN stations have broadband instruments with frequency bands of 120 s, 60 s and 30 s to 50 Hz and, since 2008, all stations transmit continuous waveform data at 100 Hz sampling frequency to Uppsala. Since August 2000, the automatic SIL system has been in operation in Uppsala (Böðvarsson and Lund, 2003), providing detection and location capabilities that allow the SNSN to record earthquakes of magnitudes down to -1. After analyst review and manual relocation, phase picks for events that are large enough to be recorded outside of Sweden ($\sim M_L > 1$ events) are supplied to FENCAT. The SNSN is currently complete to approximately magnitude 0.3 within the network (Böðvarsson et al., 2006). For the SNSN standard processing, the epicentral uncertainties are on the order of 2 km (B. Lund, pers. comm., 2011).

A significant upgrade of FNSN occurred during the late 1970's when digital tripartite arrays in southern and central Finland became fully operational, allowing for systematic use of instrumental detection, location and magnitude determination methods. Today, the FNSN consists of 26 on-line stations (Fig. 2.8.2.1), 4 operated by the University of Oulu and 22 by the Institute of Seismology at the University of Helsinki (ISUH). One of the stations is a small-aperture seismic array (FINES), others have three-component broad-band seismographs. The latest extension comprised four stations deployed around the planned Hanhikivi NPP in March-April 2013 (Appendix 1). All stations are connected to the ISUH via Internet or satellite and provide continuous waveform data at 40 Hz (array) or 100-250 Hz sampling frequency. In addition to the on-line stations, 4 three-component short-period stations recording in an off-line mode provide supplementary data for FENCAT processing. Three of the stations belong to a portable network that has been in operation in the Kuusamo region since 2003.

Since 2007, the ISUH has had an in-house designed automatic seismic data processing system, which utilizes the available on-line three-component and array stations in Finland and in the neighbouring countries (Figure 4 in Tiira et al., 2011). After analyst review and manual relocation, phase picks for local earthquakes are forwarded to final FENCAT processing.

The FNSN has relatively large inter-station distances, on average 90 km. For the FNSN standard processing, the epicenter location uncertainty is estimated to be 2-5 km within the network (Korja et al., 2011a). The instrumental earthquake catalogue has different levels of completeness. Tiira et al. (2011) estimated the local earthquake catalogue in the area with a 50 km radius surrounding Hanhikivi to be complete down to magnitude 1.5 from 1979 onwards. Today the automatic seismic

data processing system provides automatic event detection and location capabilities down to magnitude 1 and 1.5 within and at the outskirts of the virtual network, respectively.

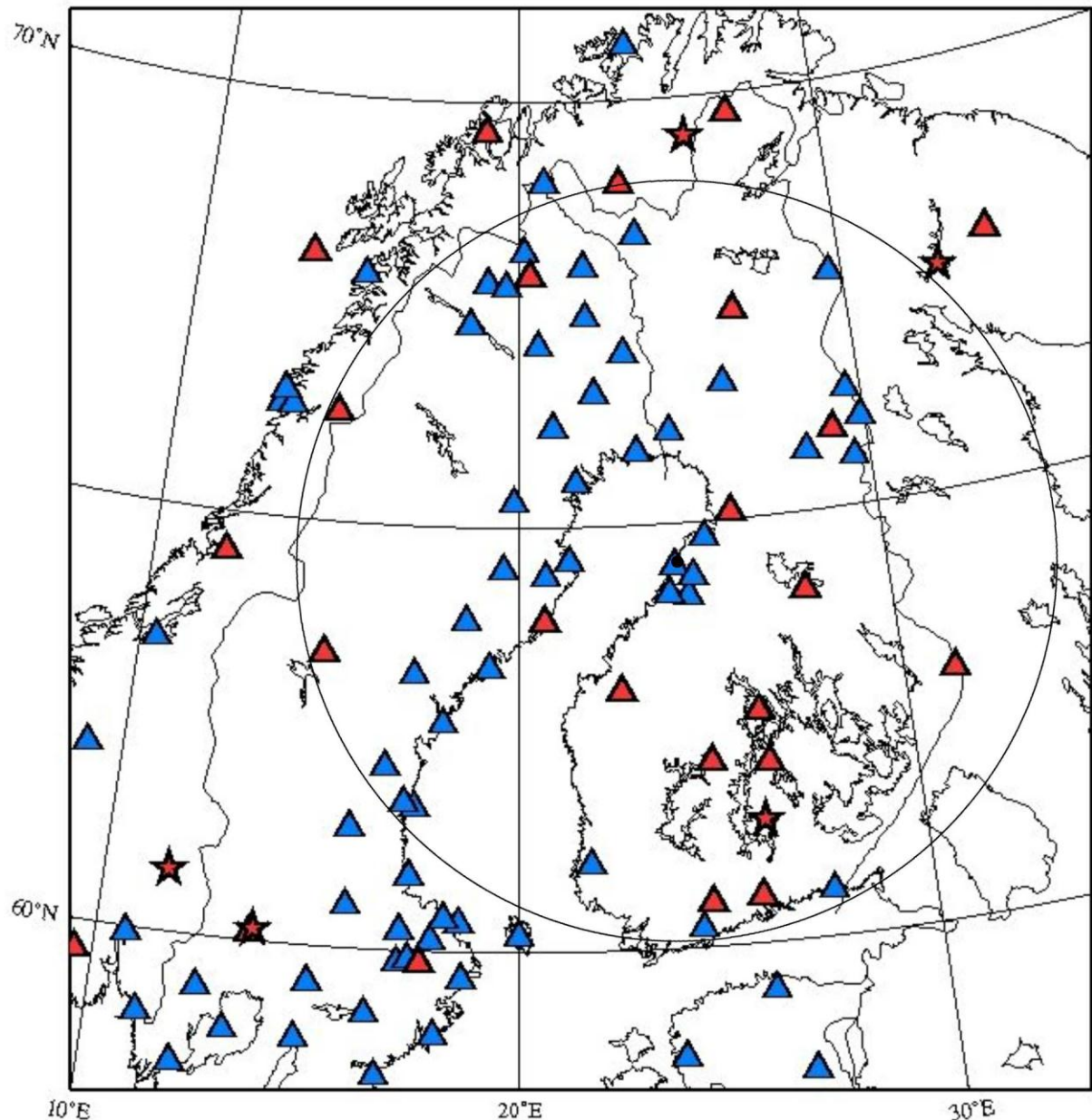


Figure 2.8.2.1. Seismograph stations in Fennoscandia. Triangle denotes a single station and star a seismic array. Stations operational in the 1990's are in red colour, those installed in the 2000's in blue.

2.9 Deep seismic reflection lines

A. Korja

The near vertical reflection sections used in this report are based on the final stack sections from BABEL profiles 1, 2, 3, 4, 6 and 7 and FIRE 1-4 (Fig. 2.9.1). Acquisition parameters and full processing sequence have been described by BABEL Working Group (1993) and Kukkonen and Lahtinen (2006). The data are presented as instantaneous amplitude sections and the post processing sequence is

described in Korja and Heikkinen (2005, 2008). BABEL profiles 1-7 comprise 1230 km of marine seismic profiles in the Gulf of Bothnia. Airgun shot interval has been 75 m, multiplicity of data coverage is 20-24 and the depth extent of the profiles is 70 km. FIRE profiles 1, 2, 3 and 4 comprise 2100 km of land seismic profiles in areas with only minor Quaternary sedimentary cover. Vibroseis interval has been 50 m, multiplicity of data coverage is 90 and the depth extent of the profiles is 80 km.

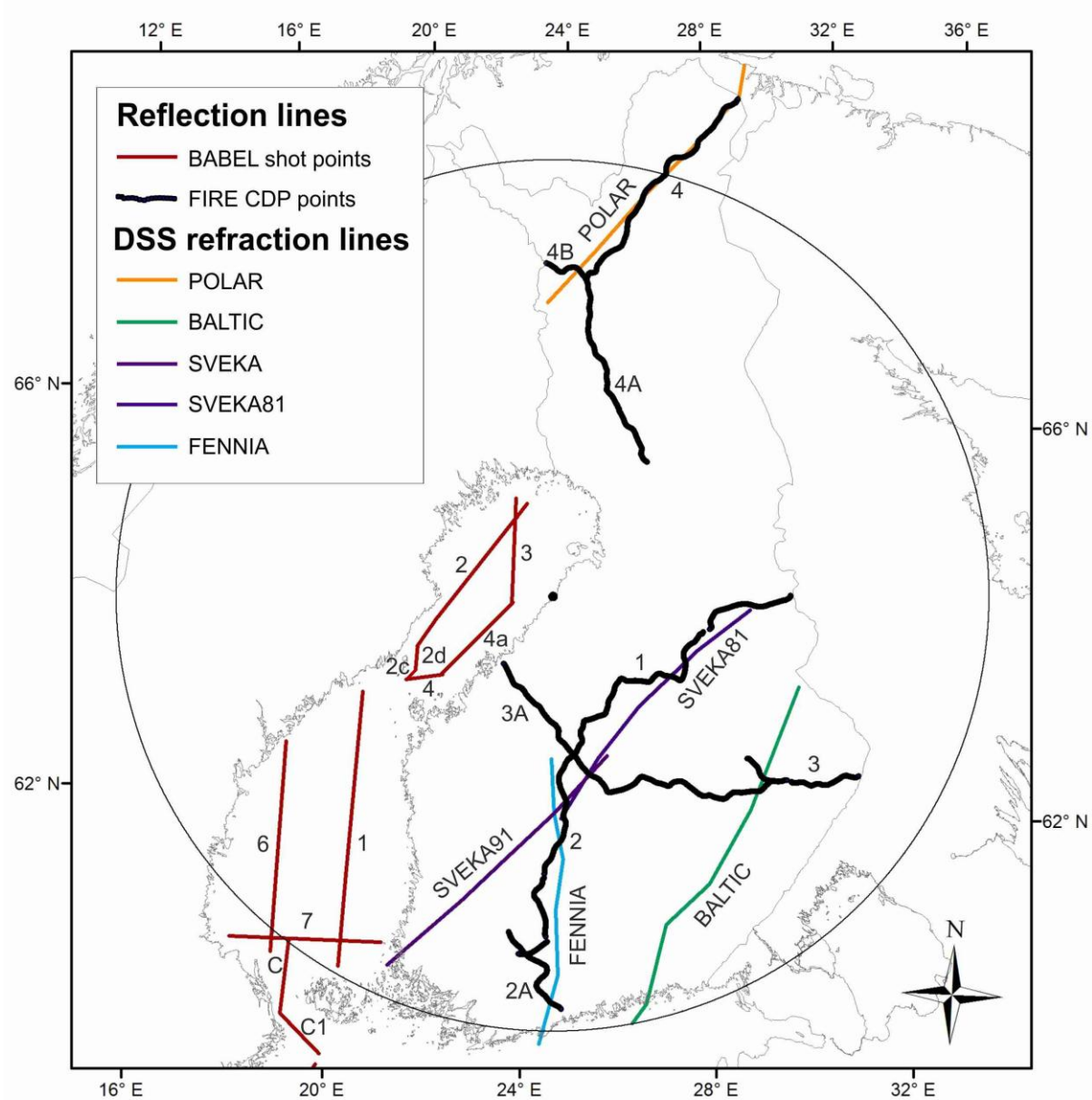


Figure 2.9.1. A map showing the location of deep seismic refraction and reflection lines mentioned in the text. Refraction lines are named and reflection lines are numbered. BABEL lines are marked with red lines and FIRE lines with black lines.

3 Geological framework

3.1 Paleotectonic evolution

3.1.1 Major lithotectonic units

M. Stephens, M. Nironen & A. Korja

The currently used nomenclature for the geological framework and paleotectonic evolution of the bedrock in the northern part of Europe (Gaál and Gorbatshev, 1987) mixes together lithodemic (e.g. Karelia Province, Svecfennian Domain, Transscandinavian Igneous Belt) and tectonic (e.g. Svecfennian orogeny, Caledonides, Platform Cover) concepts. In order to avoid confusion in conceptual understanding and to take account of currently ongoing developments on the structural framework in the Fennoscandian Shield at the geological surveys in Finland and Sweden, an alternative division of the bedrock into lithotectonic units is adopted here. The term "lithotectonic unit" is defined in the international literature as "an assemblage of rocks that is unified on the basis of structural or deformational features, mutual relations, origin, or historical evolution. It may be igneous, sedimentary, or metamorphic" (Neuendorf et al., 2005).

Based on the bedrock national databases for Finland and Sweden (Korsman et al., 1997; Bergman et al., 2012), the Fennoscandian Shield database (Koistinen et al., 2001) and recent broader syntheses of the stratigraphy, structure and tectonic evolution of the geological framework (Hölttä et al., 2008; Lahtinen et al., 2008; Bingen et al., 2008, Stephens and Wahlgren, 2008; Stephens and Weihed, 2013), we have divided the bedrock in the study area with 500 km radius around Hanhikivi into thirteen lithotectonic units (Fig. 3.1.1.1). The majority of these units contain rocks with a distinct tectonothermal history and are separated from each other by regional-scale, ductile and brittle deformation zones or an angular unconformity.

The major part of the study area consists of seven lithotectonic units (Karelia, Inari, Central Finland, Southern Finland, Ljusdal, Bothnia-Skellefteå, and Norrbotten; Fig. 3.1.1.1) that attained their current architecture during orogenic activity at 2.0–1.8 Ga. The terms "Svecfennian orogeny" and "Svecokarelian orogeny" are avoided due to the lack of agreement between geoscientists in Finland and Sweden on the usage of these two terms. The units in the northeastern half of the study area (Karelia, Inari and Norrbotten) contain Archean crust affected by Neoarchean orogeny and later Paleoproterozoic extension at 2.5–2.0 Ga prior to orogenic reworking at 2.0–1.8 Ga (e.g. Gaál and Gorbatshev, 1987; Lahtinen et al., 2005).

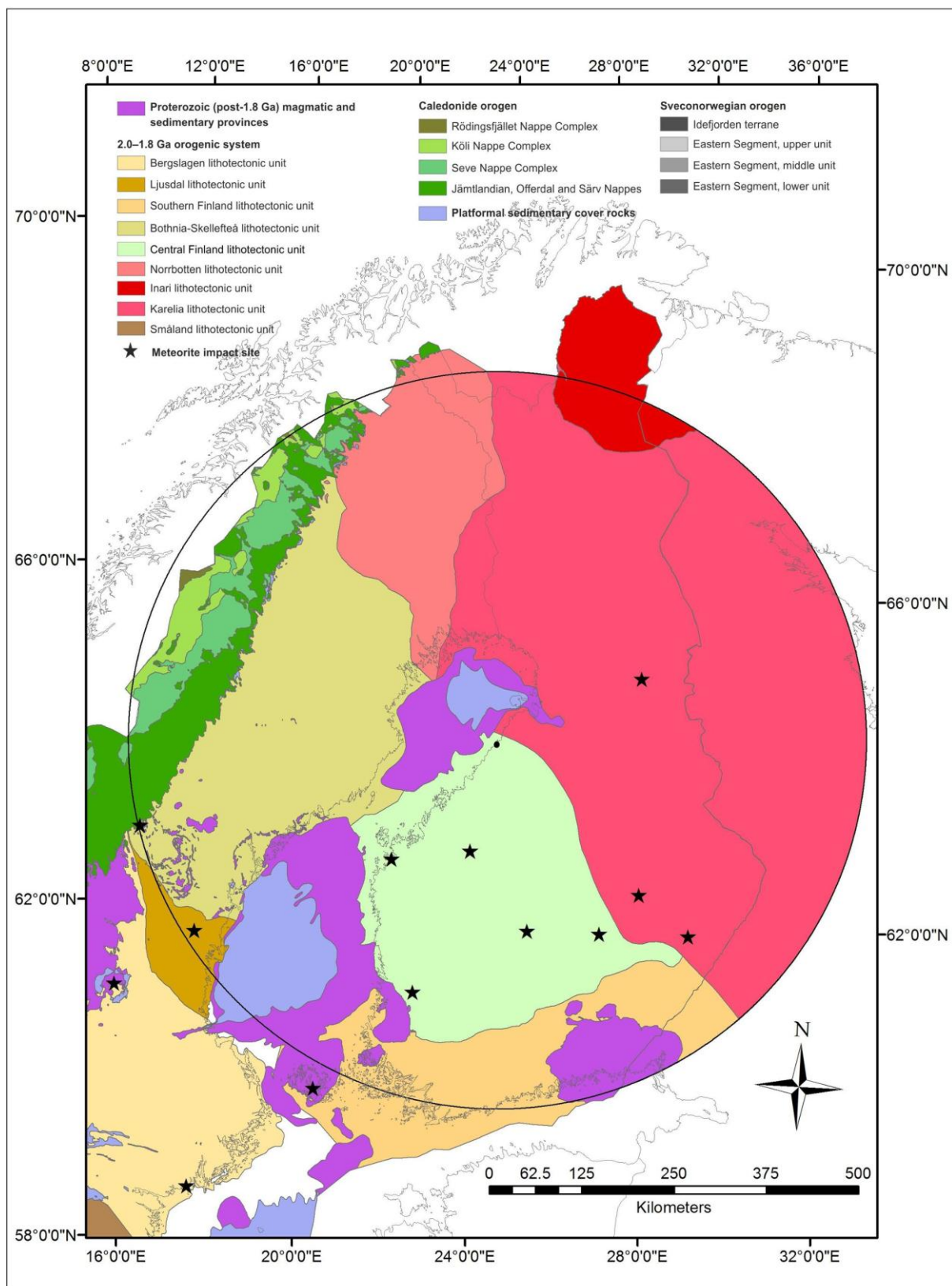


Figure 3.1.1.1. Major lithotectonic units extracted from the national bedrock databases at the scale 1:1 M for Sweden and Finland. Hanhikivi site: black dot.

Mesoproterozoic magmatic and sedimentary provinces and, in southeastern Finland, even latest Paleoproterozoic magmatic rocks, which formed around and after 1.6 Ga in extensional

paleotectonic environments, build together a separate lithotectonic unit inside the study area (Fig. 3.1.1.1) after the orogenic development during 2.0–1.8 Ga. These rocks are well-preserved, unaffected by later orogenic activity and complete the Precambrian lithotectonic framework in the Fennoscandian Shield. In part, there is a major angular unconformity between these rocks and the underlying lithotectonic units.

Ediacaran–Cambrian and Ordovician sedimentary rocks form a platformal cover on top of the Fennoscandian Shield and together form their own lithotectonic unit (Fig. 3.1.1.1). This unit is preserved in the eastern foreland to and beneath the allochthonous thrust sheets in the 0.5–0.4 Ga Caledonian orogen. The boundary between this lithotectonic unit and the underlying units is again, in part, a major angular unconformity.

The Caledonian orogen dominates the northwestern part of the study area and has been divided into four lithotectonic units (Fig. 3.1.1.1). These units were derived from different parts of the shortened margin of the continent Baltica, both the rifted continental margin and the continent-ocean transition zone, from outboard terranes derived from the Iapetus Ocean, and from exotic continental terranes with respect to the continent Baltica.

The remainder of section 3.1.1 addresses the paleotectonic evolution inside the study area during the later part of the Phanerozoic, following the Caledonian orogeny. A short presentation of inferred meteorite impact structures inside the study area completes this section.

Lithotectonic units in the 2.0–1.8 Ga orogenic system and alternative paleotectonic models

The Karelia lithotectonic unit (Fig. 3.1.1.1), in the eastern part of the study area, is dominated by Archean magmatic and migmatitic metamorphic rocks (Fig. 2.4.2.) affected by a Neoarchean orogeny, Paleoproterozoic (2.5–2.0 Ga) extensional events and later orogeny at 2.0–1.8 Ga. This unit is delineated by the Pajala shear zone (Kärki et al., 1993; Bergman et al., 2006) and its northern continuation to the west, the Raahe-Ladoga shear complex to the southwest (Kärki et al., 1993), and the White Sea graben to the east-northeast.

Intracratonic and marginal basins developed during 2.5–2.0 Ga extension of the Archean continent. The earliest rifting phase, at 2.5–2.45 Ga, is seen as NE-SW trending layered intrusions and NE-SW and NW-SE trending mafic dykes, indicating two orthogonal extension directions (Vuollo and Huhma, 2005). Subsequent dyke swarms, dated at 2.32 Ga, 2.2 Ga, 2.1 Ga and 1.98 Ga, appear to show a shift from E-W trend to NW-SE trend. The rocks were subsequently affected, to variable extent, by ductile deformation and metamorphism at 1.9–1.8 Ga (e.g. Corfu and Evans, 2002; Lahtinen et al., 2005). During this orogeny, many of the extensional faults (dykes) were reactivated and inverted, and the

western part of the Archean continent acted as basement to thin-skinned thrusting of ophiolite-bearing allochthons (in the Finnish North Karelia and Kainuu-Kuusamo belts and the Central Lapland greenstone belt) (Fig. 2.4.2; Koistinen, 1981; Hanski, 1997; Peltonen and Kontinen, 2004; Peltonen et al., 2008; Patison et al., 2006; Korja et al., 2006a,b). These rocks were later intruded by granitoids (Fig. 2.4.2). Tiira et al. (2014) described an inverted rift basin previously recognised by Patison et al. (2006) below the thrust units of Central Lapland. The NW-SE directed sub-vertical transfer faults in the paleo-rift system (NW-SE) appear to have survived several later tectonic events.

In the northernmost part of the study area, the Karelia lithotectonic unit is situated in the footwall to a major thrust complex (Lapland granulite belt and Tanaelv sequence) containing 2.0–1.9 Ga sedimentary and magmatic rocks (Daly et al., 2006; Patison et al., 2006). The latter were deformed and metamorphosed under high-pressure granulite conditions around 1.9 Ga; orogenic activity with ductile deformation, some magmatism and lower grade metamorphism continued until 1.8 Ga (Daly et al., 2006; Tuisku and Huhma, 2006). These syn-orogenic rocks are included here in the Inari lithotectonic unit (Fig. 3.1.1.1).

The bedrock in the western and central parts of the study area, west of the Pajala shear zone and southwest of the Raahe-Ladoga shear complex, consist predominantly of 2.0–1.8 Ga old metasedimentary and magmatic rocks, which are syn-orogenic with respect to the 2.0–1.8 Ga orogenic event. Five lithotectonic units have been identified (Central Finland, Southern Finland, Ljusdal, Bothnia-Skellefteå and Norrbotten; Fig. 3.1.1.1). A characteristic feature of all these units is the presence of siliciclastic sedimentary rocks, predominantly deposited as turbidites, as well as traces of magmatic provinces; the magmatic rocks span in age from 1.95–1.78 Ga. The Norrbotten lithotectonic unit, in the northern part of the study area (Fig. 3.1.1.1), comprises both Archean (3.2–2.6 Ga) magmatic rocks and Paleoproterozoic (2.5–2.0 Ga) sedimentary and mainly basic magmatic rocks that are stratigraphically overlain or intruded by the 2.0–1.8 Ga syn-orogenic rocks. These rocks resemble those in the western part of the Karelia lithotectonic unit but are separated from it by the Pajala shear complex and its northerly extension (Lahtinen et al., 2005).

The rocks in these five lithotectonic units were affected by ductile deformation and metamorphism under high temperature and low pressure conditions, in part reaching amphibolite to granulite facies and, in several areas, including migmatization during the 2.0–1.8 Ga orogeny. The extent of these secondary processes varies in space and time, and this variation is an important criterion for the division into lithotectonic units.

Major crustal thickness variation across the Gulf of Bothnia (see section 5 and Grad et al. 2009) as well as a difference in the age of plutonic activity in northern Sweden (large proportion of crust

comprises 1.8 Ga magmatic rocks; number 14, Fig. 2.4.1) and central Finland indicate a major tectonic break in the Gulf of Bothnia area. Berthelsen and Marker (1986) have suggested a major NE–SW-trending deformation zone (Baltic-Bothnian megashear) running parallel to the east coast of Sweden. Thus, the Central Finland lithotectonic unit to the southeast of the Gulf of Bothnia has been separated from the Bothnia-Skellefteå lithotectonic unit to the northwest.

Pronounced tectonic reworking of the rocks around 1.83–1.82 Ga, under high-grade metamorphic conditions, followed an earlier tectonothermal event around 1.87–1.86 Ga in the Southern Finland (Ehlers et al. 1993, Väisänen and Hölttä 1999, Pajunen et al. 2008) and Ljusdal (Högdahl et al. 2008, 2011; Wik et al., 2009) lithotectonic units (Fig. 3.1.1.1). In sharp contrast, the effects of the younger tectonothermal evolution around 1.8 Ga in the Central Finland, Bothnia-Skellefteå and Norrbotten units (Fig. 3.1.1.1), as in the Karelia and Inari lithotectonic units to the northeast, are restricted to ductile deformation along high-strain zones or belts and possibly large-scale folding. The main phase of deformation and metamorphism in the Central Finland, Bothnia-Skellefteå and Norrbotten units occurred around 1.88–1.86 Ga (Korsman et al., 1999; Bergman et al., 2001; Rutland et al., 2001; Kathol and Weihs, 2005; Pajunen et al., 2008; Skyttä et al., 2012).

The generally accepted paleotectonic model for the 2.0–1.8 Ga orogenic system invokes both accretionary orogenic activity related to ongoing subduction processes with amalgamation of outboard microcontinents to an ancient Archean craton, followed by terminal continent-continent collision at 1.8 Ga (e.g. Nironen, 1997; Lahtinen et al., 2005, 2008; Korja et al., 2006b; Korja and Heikkinen 2005, 2008). This setting resembles that in the current Alpine–Himalayan–Indonesian orogenic system (Ward, 1987; Brown, 2009). There are also clear similarities to the paleotectonic evolution in the Trans-Hudson orogen in the Canadian Shield (St-Onge et al., 2006).

The alternative model involves solely accretionary tectonics related to ongoing subduction processes along a single active continental margin, with longer periods of retreating and shorter periods of advancing subduction (Hermannsson et al., 2008; Stephens et al., 2009). This setting corresponds to the current circum-Pacific orogenic system (Brown, 2009) and builds on earlier pioneering work in the Fennoscandian Shield by, for example, Hietanen (1975), Gaál (1982) and Park (1985). The alternative model does not include a terminal continent-continent collision at 1.8 Ga, but permits the accretionary tectonic processes to continue after this time.

Meso- and Neoproterozoic magmatism and sedimentation related to intra-cratonic rifting

Mesoproterozoic magmatic rocks, which formed around 1.6–1.4 Ga, are conspicuous inside the study area in the central part of Sweden, beneath the Gulf of Bothnia and in southern Finland (Fig. 3.1.1.1). They consist of granite, spatially associated with gabbro, anorthosite and monzodiorite and dolerite

dykes (Fig. 2.4.2) (Andersson, 2001; Rämö and Haapala, 2005). These rocks are flanked or overlain by siliciclastic sedimentary rock (so-called “Jotnian sandstone”) and locally 1.5 Ga basalt and felsic porphyry (Kohonen and Rämö 2005, Söderlund et al., 2005; Pokki et al., 2013a,b). Both the rocks and the structures preserved beneath the Gulf of Bothnia are the subject of a more focused study in section 3.1.3 below.

Intracratonic rifting related temporally to Gothian accretionary orogenic activity, which is preserved southwest of the study area inside the Sveconorwegian orogen (Fig. 3.1.1.1), has been proposed as the steering tectonic mechanism for the 1.6–1.5 Ga rapakivi magmatism (Åhäll et al., 2000). Rämö and Haapala (2005) also invoked intracratonic rifting. Heinonen (2012) suggested that the rifting is associated with break-up of a supercontinent (Columbia/Hudsonland). Similarly, a foreland response to the Hallandian-Danopolonian orogenic event (1.5–1.4 Ga) in the Blekinge–Bornholm orogen in the southeasternmost part of Sweden and in Denmark can be inferred for the formation of the sandstone basins and 1.5 Ga magmatic activity. Large-scale rifting also took place in the eastern part of the study area where the Lake Ladoga basin and White Sea rift were formed during the Meso-Neoproterozoic (Baluev, 2006; Kohonen and Rämö, 2005; Koistinen et al., 2001).

During the Meso- to Neoproterozoic Era (1.3–0.5 Ga), the cratonic area responded to the major tectonic events taking place at the peripheral plate margins. Intracratonic rifting preceding the Sveconorwegian orogeny (1.3–1.2 Ga), the possible development of a peri-Timan basin/pассив margin in the north (1.1 Ga), the break-up of the supercontinent Rodinia and opening of the Iapetus Ocean (600 Ma) or the development of the Timanide orogen (0.62–0.53 Ga) north of the study area left minor magmatic traces. These intrusive rocks include: 1) Mesoproterozoic (1.27–1.25 Ga) dolerite sills and dykes (Kohonen and Rämö 2005, Söderlund et al. 2005) in central Sweden, the Gulf of Bothnia and southwestern Finland; 2) Mesoproterozoic (1.20 Ga) kimberlite fields close to Kuhmo in eastern Finland (Kohonen and Rämö, 2005; Söderlund et al., 2005; O’Brien et al., 2005); 3) Mesoproterozoic (1.1–1.0 Ga) alkaline ultrabasic dykes in both the Swedish and Finnish parts of Lapland in the northern part of the study area; 4) Neoproterozoic kimberlite fields at Kuopio-Kaavi in eastern Finland; and 5) a Neoproterozoic (0.59–0.58 Ga) alkaline, carbonatitic intrusive complex close to Sundsvall in Sweden (Kresten et al., 1997; Rukhlov and Bell, 2010).

Platformal sedimentary cover rocks in the eastern foreland to and beneath the Caledonian orogen

Following assembly of the supercontinent Rodinia, which resulted from the Sveconorwegian orogeny in Scandinavia, erosion and the final establishment of a sub-Cambrian peneplain prevailed. After the subsequent break-up of Rodinia and the opening of the Iapetus Ocean around 600 Ma, a

transgressive platformal sequence was deposited on top of the Precambrian crystalline rocks in the Fennoscandian Shield.

Platformal Ediacaran–Cambrian sandstone and overlying Cambrian shale, including black oil shale, are exposed inside the study area along the eastern erosional front of the Caledonian orogen (thin strip in Fig. 3.1.1.1). Cambrian (and possibly Ediacaran) sandstone and Ordovician limestone and shale are also preserved in the submarine area beneath the Gulf of Bothnia (Fig. 3.1.1.1). The boundary between the lithotectonic units represented by the platformal sedimentary cover rocks and the crystalline basement is a major angular unconformity along the Caledonian front, while both faulted and primary unconformable contacts to the underlying crystalline basement are present in the Gulf of Bothnia. More details on both the rocks and the structures preserved beneath the Gulf of Bothnia are presented in section 3.1.3 below.

Tectonostratigraphic units in the 500–400 Ma Caledonian orogen and paleotectonic setting

The Caledonian orogen consists of allochthonous thrust sheets arranged in a systematic tectonostratigraphic sequence (Kulling, 1972; Roberts and Gee, 1985) above autochthonous platformal sedimentary cover rocks and older Proterozoic and Archean rocks belonging to the Bothnia-Skellefteå and Norrbotten lithotectonic units (Fig. 3.1.1.1). Sedimentation and magmatic activity that took place in connection with continental rifting are conspicuous in the structurally lower thrust sheets (Jämtlandian, Offerdal and Särv Nappes, and Seve Nappe Complex; Fig. 3.1.1.1). Rocks formed in connection with a glaciation at high southerly latitudes during the later part of the Neoproterozoic, during ultimate continental break-up and formation of the Iapetus Ocean at 600 Ma and along the subsequent passive margin development to the continent Baltica are also present in these nappes. Subsequently, foreland basin sedimentation related to the initiation of convergence and orogenesis took over during the Ordovician and Silurian and is well-preserved in the lowest thrust sheets (Jämtlandian Nappes; Fig. 3.1.1.1).

Sedimentation and magmatic activity with an oceanic affinity, which occurred in connection with destruction of the Iapetus Ocean during the late Cambrian to Silurian (510–430 Ma), are present in the structurally higher thrust sheets (Köli Nappe Complex; Fig. 3.1.1.1); exotic terranes derived from the continental margin of Laurentia are also preserved in the overlying Rödingsfjället Nappe Complex (Fig. 3.1.1.1). A conspicuous feature of the higher thrust sheets is the occurrence of several fragments of ophiolite derived from ancient oceanic back-arc basins.

Ductile deformation and metamorphism during the Caledonian orogeny was related to continent-arc collisions and ultimately a terminal collision between the Baltica and Laurentia during the latest

Ordovician to Devonian (450–390 Ma). Eclogites, which formed at different times during the Ordovician to Devonian (e.g. Krogh et al., 1974; Root and Corfu, 2012; Spencer et al., 2013) signal the complexity of the collisional events along this ancient margin. Finally, during the Devonian, extensional collapse, sinistral strike-slip deformation and major folding of thinned thrust sheets followed in the western parts of the orogen.

Late Paleozoic paleotectonic activity – final assembly of the supercontinent Pangaea

During the period 400 to 250 Ma, when amalgamation of the supercontinent Pangea was finalized, the study area was located in the foreland to the Hercynian-Variscan orogen to the south, the North Barents Sea-Arctica orogen (Gee et al., 2006) to the north and the Magnitogorsk arc (390–350 Ma) to the northeast (Brown et al., 2006; Nikishin et al., 1996). The only imprint in the rock record inside the study area is the occurrence of alkaline plutons at Iivara and Sokli (360 Ma) in the Eastern Finland area as well in the Kola Peninsula (Fig. 2.4.2). During the Permian (295–275 Ma), extensional deformation and associated volcanic and magmatic activity prevailed in the Oslo rift, Norway. During the same period, dextral transtensional deformation and intrusion of basic dykes occurred along the Sorgenfrei-Tornquist Zone, in the southernmost part of Sweden.

Break-up of Pangaea and opening of the North Atlantic Ocean

After 250 Ma, sedimentary and, locally, magmatic rocks are preserved on land in the southernmost part of Sweden and in offshore areas surrounding the Fennoscandian Shield in Norway and Russia. In particular, major thicknesses of sedimentary material accumulated offshore in connection with continental extension and the development of a passive continental margin prior to and following opening of the North Atlantic Ocean around 60 Ma. More details concerning the character of this passive margin are presented in the section describing current seismotectonic models in section 7.

During the early part of the Mesozoic, differential subsidence controlled by transtensional deformation occurred along the Sorgenfrei-Tornquist Zone in southernmost Sweden (Erlström and Sivhed, 2001). Volcanic activity was also prevalent in this area during the Jurassic and Cretaceous. The tectonic environment radically changed during the later part of the Cretaceous and the earliest part of the Paleogene, i.e. 95–60 Ma, when a marine transgression and inversion tectonics with dextral transpressional deformation along the Sorgenfrei-Tornquist Zone took place (Erlström and Sivhed, 2001). The compressional tectonic event during the Late Cretaceous and into the Paleogene corresponds temporally with the initiation of the Alpine orogeny in southern Europe and the collision between Africa and Eurasia.

An attempt to reconstruct the tectonic history of the shield area after 100 Ma, i.e. from the Late Cretaceous to the Quaternary, on the basis of the plate tectonic history around its margins, was

presented by Muir Wood (1995). From 60 Ma and onwards, the North Atlantic Ocean started to open and to spread. During this time, plate motions associated with spreading of the North Atlantic Ocean have dominated the geodynamics of northern Europe. After approximately 12 Ma, during the Neogene period, a maximum principal stress in a WNW–ESE or NW–SE horizontal direction, steered by ridge push from the mid-Atlantic ridge and, as a consequence, the relative plate motion between the Eurasian and American plates, has prevailed in northern Europe (Muir Wood, 1995). More details concerning the current stress field and surface strain are presented in section 5.

Meteorite impact structures

Several meteorite impact structures have been identified in the Fennoscandian Shield and its sedimentary overburden (Wickman, 1988; Henkel and Pesonen, 1992; see Fig. 3.1.1.1). Inside the study area in Sweden, impact structures that occurred during the Ordovician and Cretaceous periods have been recognised at Lockne near to Östersund (Lindström et al., 2008) and at Dellen close to Hudiksvall (Deutsch et al., 1992; Wik et al., 2009), respectively; impact melt is preserved at Dellen. The Cretaceous (77 Ma) Lappajärvi meteorite crater in Ostrobothnia, with a diameter of c. 15 km, is the largest reliably documented impact structure in Finland (Lehtinen, 1976; Reimold, 1982). Impact melt and breccia are preserved at Lappajärvi. Other inferred impact structures (Sääksjärvi, Iso-Naakkima, Saarijärvi, Söderfjärden, Lumparn) are small and their ages are unknown (Dypvik et al., 2008).

3.1.2 Ductile shear zones, faults and lineaments

M. Nironen, A. Korja & M. Stephens

Ductile to brittle transition, timing of cratonization and the evolution of fault systems

The interpretation of predominantly airborne geophysical (magnetic, gravity and electromagnetic) and digital topographic data in combination with geological field data have been the primary sources of information for the identification of deformation zones in the bedrock (Fig. 3.1.2.1). In Finland, the voluminous data along the FIRE reflection seismic profiles (Kukkonen and Lahtinen, 2006) have provided a valuable addition to the identification of deformation zones. By contrast, geological field data, addressing stratigraphic, structural and metamorphic relationships between rock units, in combination with reflection seismic data along a few profiles in central Sweden have been the primary sources of information in the Caledonian orogen, in the westernmost part of the study area.

The paleotectonic evolution in the Karelia and Norrbotten lithotectonic units suggests crustal stabilization following orogeny during the later part of the Neoarchean. However, together with younger (2.5–2.0 Ga), mainly sedimentary and volcanic rocks formed in connection with extensional

deformation, this ancient continental nucleus was tectonically reworked, to variable extent, during the later orogenic activity at 2.0–1.8 Ga. Final establishment of a cratonic condition could not have taken place until after 1.8 Ga in a larger part of these two units.

K-Ar isotope data from the Central Finland lithotectonic unit indicate that at 1.85 Ga the rocks presently at the erosion surface had cooled beneath 500 °C deep in the crust, under ductile deformation conditions. As the result of exhumation these rocks had been uplifted to higher crustal levels with temperatures below 300 °C and brittle deformation regime by 1.78 Ga (Haudenschild, 1995). On the basis of ^{40}Ar - ^{39}Ar data immediately south of the Ljusdal lithotectonic unit (Bergslagen unit) and inside the Southern Finland unit, a brittle regime was established between 1.8 and 1.7 Ga (Söderlund et al., 2009) or after 1.8 Ga (Torvela et al., 2008), respectively.

There are very few studies of the evolution of the character, kinematics and timing of deformation in the brittle tectonic regime inside the Fennoscandian Shield, including the study area. Most attention has been on the early ductile deformation. The determination of paleostress fields in combination with low-temperature geochronology work at Forsmark (Stephens and Wahlgren, 2008; Sandström et al., 2009; Saintot et al., 2011) and Oskarshamn (Stephens and Wahlgren, 2008; Drake et al., 2009; Viola et al., 2009) in southeastern Sweden, south of the study area, has demonstrated the reactivation of pre-existing ductile deformation zones or the formation of new zones in the brittle deformation regime during 1.5–1.4 Ga (Hallandian-Danopolonian), 1.1 Ga (Sveconorwegian), 0.4 Ga (Caledonian) and even Permian far-field tectonic events (see section 3.1.1). The brittle Sveconorwegian event at Forsmark, for example, caused a marked inversion of the kinematics along structures with WNW–ESE or NW–SE strike compared to the ductile strain around 1.8 Ga (Saintot et al., 2011). Similarly, K-Ar dating of illite at Olkiluoto in southwestern Finland revealed brittle deformation related to Sveconorwegian inferred build-up (1.1–1.0 Ga) and collapse (1.0–0.9 Ga; Viola et al., 2013).

Bearing in mind the poor understanding of the brittle deformational history inside especially the Fennoscandian Shield, the focus in the text below on the major deformation zones is directed to the ductile strain close to the time of their formation. However, since stratigraphic time markers are available in the Gulf of Bothnia, which provide a broader insight into the significance of faulting in this part of the study area from the Mesoproterozoic until after the Ordovician, attention on the faults affecting the rocks preserved in the Gulf of Bothnia is placed in a separate section (3.1.3).

Karelia and Inari lithotectonic units in the 2.0–1.8 Ga orogenic system

As indicated in section 3.1, NE-SW and NW-SE trending mafic dykes were reactivated during the 2.0–1.8 Ga orogeny. Thrusting towards the northeast is seen in the Finnish North Karelia belt (Fig. 2.4.2; e.g. Koistinen, 1981; Ward, 1987; Kohonen, 1995), and towards the east in the Kainuu-Kuusamo belt (Fig. 2.4.2; Tuisku and Laajoki, 1990). During subsequent transpression deformation partitioned into shear zones between rigid Archean blocks. The northern part of the Kainuu-Kuusamo belt developed into the N-S trending dextral, ductile, subvertical Hirvaskoski shear zone (Fig. 3.1.2.1; Kärki et al., 1993). The NE-SW trending, sinistral, subvertical Oulunjärvi shear zone deforms the Hirvaskoski shear zone. The Auho fault at the northwestern margin of the Oulunjärvi shear zone is a semi-brittle structure that extends further northeast and, together with other faults in Russia, forms a NNE-SSW trending fault set, here called the Auho-Kandalaksha fault zone. The Auho-Kandalaksha fault zone (Fig. 3.1.2.1) consists of several parallel faults extending from central Finland up to the Kandalaksha Gulf in northwestern Russia (Elo, 1991a). Magnetic and gravity data suggest sinistral movement or shear and steep dips for the faults (Elo, 1991b).

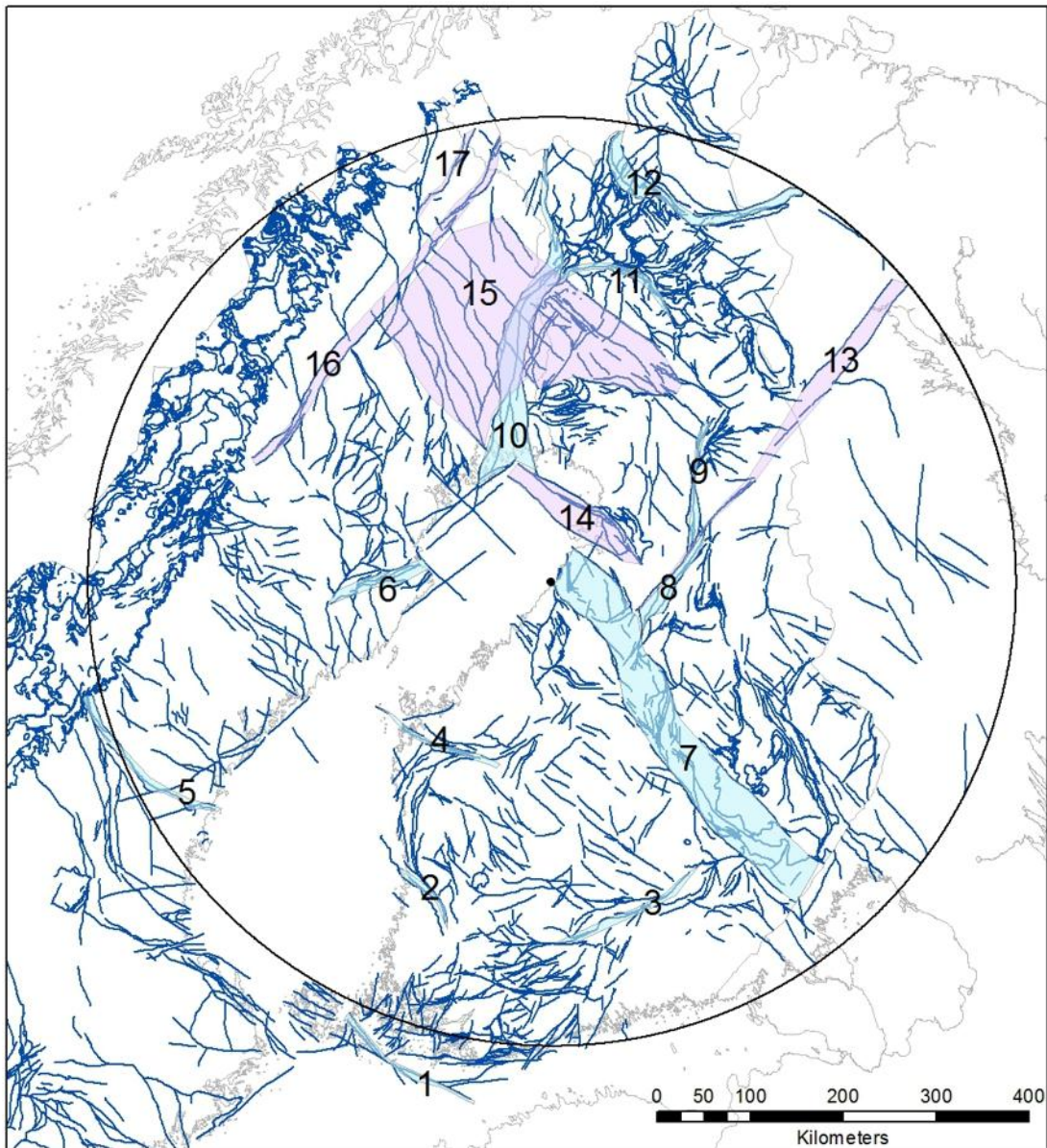


Figure 3.1.2.1. Major Paleoproterozoic deformation zones extracted from the national bedrock databases at the scale 1:1 M for Sweden and Finland and modified slightly in the context of this study (see section 2.5). Zones or complexes of zones showing ductile shear deformation with or without brittle deformation are shown in blue colour, brittle deformation zones (fault zones) are shown in pink colour. 1- Sottunga-Jurmo shear zone; 2- Kynsikangas shear zone; 3- Kuortti shear zone; 4- Malax shear zone; 5- Hassela shear zone; 6- Burträsk shear zone; 7- Raahe-Ladoga shear complex; 8- Oulunjärvi shear zone; 9- Hirvaskoski shear zone; 10- Pajala shear zone; 11- Venejoki shear zone; 12- Vuotso shear zone; 13- Auho-Kandalaksha fault zone; 14- Muhos fault zone; 15- Western Lapland fault system; 16 -Karesuando-Arjeplog deformation zone; 17- Kiruna-Naimakka deformation zone.

Ductile deformation zones with E-W strike dominate in the Peräpohja belt (Figs. 2.4.2 and 3.1.2.1; e.g. Laajoki, 2005). FIRE 4 seismic data suggest that only minor shortening occurred in this belt after initial basin development (Patison et al., 2006). The central Lapland part of the Karelia lithotectonic unit may be divided structurally into three parts. In the western part (in the Kittilä greenstone), a set

of east-bending convex shear zones have been interpreted as thrusts with displacement towards the east—northeast (Lehtonen et al., 1998; Hölttä et al., 2007). In the northern part, another set of roughly N-S trending shear zones have been interpreted as thrusts with displacement towards the west—southwest (Hölttä et al., 2007). The variable tectonic movement directions may be partly explained by later folding of the thrusts. In the eastern part, sub-horizontal thrusts, with displacement towards the south, were inferred by Evins and Laajoki (2002). They associated this thrust nappe tectonics to the composite (Archean-Proterozoic) Lapland-Kola orogen (including the Inari lithotectonic unit) with Archean continental crust (the Karelia lithotectonic unit). The dominant thrust system inside the Inari lithotectonic unit, with thrusting towards the southwest, is the result of the same collision between 1.93 and 1.91 Ga (Gaál et al., 1989; Daly et al., 2006). The thrust system continues into a shear zone, named here as the Vuotso shear zone (Fig. 3.1.2.1), flanking the southern margin of the Inari lithotectonic unit.

The boundary between central and southern Lapland is marked by the crustal scale deformation zone referred to as the Venejoki shear zone (Patison et al., 2006), curving around the Central Lapland granitoid complex (Figs. 2.4.2 and 3.1.2.1). South of this zone, the deformation zones are either NW-SE or NE-SW trending brittle-ductile faults (Airo, 1999), which are still active in southern Lapland (Uski et al., 2003). Tiira et al. (2013) suggested that the shear zones originated during the 2.5-2.4 Ga rifting event.

Ductile and brittle deformation zones with N-S, NE-SW and NNW-SSE trends comprise the complex deformation belt referred to as the Pajala shear zone (Kärki et al., 1993; Bergman et al., 2001, 2006), the western border of which defines the boundary between the Norrbotten (to the west) and Karelia (to the east) lithotectonic units (Figs. 3.1.1.1 and 3.1.2.1). Bergman et al. (2006) suggested a polyphase tectonothermal evolution in two lithotectonic units during the time span 1.86–1.74 Ga with different histories on both sides of the Pajala shear zone. Wikström et al. (1996) also suggested that ductile deformation along the Pajala shear zone took place earlier around 1.88 Ga. At least parts of the Pajala shear zone with N-S strike show an east-side-up and sinistral displacement during its development (Wikström et al., 1996; Bergman et al., 2001). The eastern border of the Pajala shear zone more or less follows the Swedish national boundary. In the north, the shear zone diminishes into a single shear zone that continues northwards into Norway; the sense of shear in that part is unknown.

Ductile and brittle deformation zones with N-S strike, which belong to the southernmost extension of the Pajala shear zone (Fig. 3.1.2.1), terminate southwards against a deformation zone with NW-SE strike. This zone corresponds to a fault that disturbs the sedimentary cover in the Bay of Bothnian (see section 3.1.3 and Fig. 3.1.2.1) but it also lies close to or along the blind surface separating the

Norrbotten and Karelia lithotectonic units to the north and the Bothnia-Skellefteå and Central Finland lithotectonic units to the south (Figs. 3.1.1.1 and 3.1.2.1; Öhlander et al., 1993; Mellqvist et al., 1999). This zone continues to the southeast in Finland as part of the Raahe-Ladoga shear complex.

A set of NW-SE striking faults extend from the Norrbotten lithotectonic unit through the Pajala shear zone to the Karelia lithotectonic unit. The faults overprint the N-S shear zones in the Pajala shear zone, and offset NE-SW striking lithologies in the Karelia lithotectonic unit. They are narrow and probably semi-brittle but the sense of movement in these faults is unknown. Here these faults are collectively named as the Western Lapland fault system (Fig. 3.1.2.1). Faults with similar NW-SE strike extend to the Bay of Bothnia; these have been related to the development of the Muhos Basin on the mainland of Finland, containing Mesoproterozoic and Neoproterozoic rocks (Wannäs, 1989; Winterhalter, 2000). Wannäs (1989) called the NW-SE striking lineament system Senja-Oulujoki Tectonic Zone, but since the Muhos basin is slightly more to the north, we have named the zone in Figure 3.1.2.1 as Muhos fault zone.

Lithotectonic units in the 2.0–1.8 Ga orogenic system west of the Gulf of Bothnia

Steeply dipping deformation zones with WNW-ESE to NW-SE or N-S to NNW-SSE strike dominate inside the Ljusdal lithotectonic unit and the major part of the Bothnia-Skellefteå lithotectonic unit (Fig. 3.1.2.1), south of and including the Skellefte mining district (Fig. 2.4.2). A few detailed studies are available that have addressed the character, kinematics and timing of deformation along the deformation zones inside or close to this part of the study area.

Ductile shear displacement with a significant dextral strike-slip component of movement occurred around 1.87–1.86 Ga and later around 1.82–1.81 Ga along the zones or broader shear belts with WNW-ESE to NW-SE strike close to the southwestern border of the study area (Högdahl and Sjöström, 2001; Högdahl et al., 2009). One of these zones, the Hassela Shear Zone (HSZ; Fig. 3.1.2.1; Högdahl and Sjöström, 2001), marks the boundary between the Ljusdal and Bothnia-Skellefteå lithotectonic units. A complex interplay between steeply dipping ductile and brittle shear zones with WNW-ESE (or E-W) and ENE-WSW strike, the latter showing a sinistral strike-slip component of shear in an apparent conjugate relationship, are present along and in the vicinity of the Hassela Shear Zone.

In the northern part of the Bothnia-Skellefteå lithotectonic unit, the most conspicuous structural feature is the Burträsk shear zone, composed of zones with ENE-WSW to NE-SW strike (Figs. 2.4.2 and 3.1.2.1). This shear zone also shows a dextral strike-slip component of displacement and was active in the ductile regime at least around 1.82 Ga (Romer and Nisca, 1995; Weiher et al., 2002).

Some modification in the bulk shortening direction along the orogenic belt is apparent (e.g. HSZ; Fig. 3.1.2.1). Inversion tectonics with transpressive deformation at 1.88–1.86 Ga, following normal faulting, has been inferred along steeply dipping zones with WNW–ESE strike in the Skellefte mining district (Bauer et al., 2011; Skyttä et al., 2012).

North of the Skellefte mining district, in the northernmost of the Bothnia-Skellefteå lithotectonic unit and in the Norrbotten unit, the structural pattern for the regionally significant deformation zones changes radically; steeply dipping zones with NNE–SSW to NE–SW strike, NW–SE strike or N–S to NNW–SSE strike dominate (Fig. 3.1.2.1). Information in the structural map database (Figure 3.1.2.1) and in Bergman et al. (2001) indicates that deformation zones trending NNE–SSW to NE–SW (e.g. Kiruna–Naimakka and Karesuando–Arjeplog deformation zones) show a west-side-up, apparently reverse sense of displacement, while a zone with NW–SE strike further south shows a southwest-side-up, again apparently reverse sense of displacement. These structures were active in the ductile regime at least until 1.8 Ga. The sense of movement along these structures appears to be opposite to that observed along the regionally significant Pajala shear zone to the east, along the boundary to the Karelia lithotectonic unit, and along two steeply dipping zones with N–S to NNW–SSE strike situated between the Karesuando–Arjeplog and Pajala deformation zones (Fig. 3.1.2.1).

Lithotectonic units in the 2.0–1.8 Ga orogenic system east of the Gulf of Bothnia

Within the Central Finland lithotectonic unit (Fig. 3.1.1.1), ductile high strain structures curve around an igneous complex referred to as the Central Finland granitoid complex (Fig. 2.4.2). The complex is bounded by a major NW–SE trending structure, the Raahe-Ladoga shear complex (Korsman and Glebovitsky, 1999) in the northeast, the WNW–ESE trending Malax shear zone in the west, the NW–SE trending Kynsikangas shear zone (Pajunen et al., 2008) in the southwest, and the Kuortti shear zone in the south/southeast (Fig. 3.1.2.1).

Within the granitoid complex, the lineaments are trending NW–SE, NE–SW as well as N–S and E–W. The NE–SW and E–W trending lineaments are imaged by shallow dipping listric reflections whereas the NE–SW and N–S trending lineaments are imaged by subvertical reflections on FIRE1 and FIRE3 lines (Korja et al., 2009). Nironen et al. (2000) have interpreted the NW–SE-lineaments to be shear zones with a dextral strike-slip sense of movement that developed in a transtensional tectonic environment at 1.88–1.87 Ga. Korja et al (2009) suggested that the most of the shear zones were at least reactivated during a lateral spreading event at 1.88 Ga.

The Raahe-Ladoga shear complex (Fig. 3.1.2.1) is a major NW–SE trending crustal feature separating the Karelia lithotectonic unit to the northeast, containing an Archean crustal basement beneath Paleoproterozoic rocks, and the Central Finland lithotectonic unit to the southwest apparently

lacking an Archean crustal component. The boundaries of this shear complex are difficult to delineate exactly; it is at least 350 km long with a maximum width of about 100 km (Korsman and Glebovitsky, 1999; Kärki et al., 2012). It is characterized by linear Bouguer gravity minima (Figs. 2.1.7 and 2.1.9; see Korsman et al., 1999). The shear complex consists of ductile shear zones in varying directions, overprinted by semi-brittle and brittle faults (Pajunen 1986, Kärki et al. 1993, Kärki and Laajoki 1995; Korsman and Glebovitsky, 1999). On the basis of SVEKA deep seismic sounding profile (Fig. 2.9.1) Luosto et al. (1984) and Korsman et al. (1999) suggested that shear zones within the central part of the complex are sub-vertical and extend to the base of the crust. The reflection seismic FIRE 1 and FIRE3 profiles transect a NNW–SSE trending shear complex and they image a set of steeply west-dipping structures (Korja et al., 2006a; Sorjonen–Ward, 2006; Korja and Heikkinen, 2008). The shear zones can be followed from the surface to at least the middle crust.

The sense of horizontal movement and magnitude of displacement along the length of the Raahe-Ladoga shear complex are not fully known. Both dextral (Halden, 1982) and sinistral (Gaál, 1980) horizontal shearing have been suggested along relatively late shear zones. Pajunen (1986) studied a 30 km by 30 km area in the central part of the shear complex and detected a sequence of deformation with dextral strike-slip movement along a vertical shear zone with NW–SE strike, overprinted by a vertical, sinistral ductile shear zone with NNW–SSE strike that is deformed by dextral semi-brittle faults with N-S strike. Dextral shearing has been proposed for two shear zones in the northwestern part of the shear complex (Weiher and Mäki, 1997). Vertical movements also occurred during development of the shear complex (Korsman et al., 1984; Korsman and Glebovitsky, 1999).

Ductile shearing in the central part of the Raahe-Ladoga shear complex initiated at 1.885 Ga (Vaasjoki and Sacco, 1988; Korsman et al., 1999) and ductile deformation was associated with mafic to felsic magmatism from 1.885 Ga to at least 1.87 Ga. Evidence for late brittle deformation (temperatures around 300°C) and development of a metamorphic block structure at 1.78–1.6 Ga is provided by K-Ar ages (Haudenschild, 1988, 1995), and the apatite fission-track method yielded even lower ages of 0.9–0.7 Ga (Lehtovaara, 1976).

In summary, the sequence of deformation in the Central Finland lithotectonic unit can be divided into three phases: 1) Contraction associated with accretion initiated before 1.90 Ga, leading to compressional deformation along the western margin of the Karelia lithotectonic unit; 2) transpressional deformation during continued contraction, leading to mainly dextral shearing and the initial development of the Raahe-Ladoga shear complex at 1.885 Ga; 3) transtensional deformation at around 1.88 Ga, leading to lateral spreading in the Central Finland granitoid complex, development

of a metamorphic block structure and reactivation or development of shear zones with varying senses of movement.

The structural pattern in the Southern Finland lithotectonic unit differs from that in the Central Finland lithotectonic unit (Fig. 3.1.2.1). The intersection of E–W- and WNW–ESE-trending shear zones in the Southern Finland unit gives rise to a lozenge-shaped pattern on the exposure level (Fig. 3.1.2.1). The E–W-trending zones probably have both vertical and horizontal movement components whereas at least some NNE–SSW-trending zones are normal faults (Nironen et al., 2006; Väisänen and Skyttä, 2007). The structural pattern developed at 1.84–1.83 Ga and controlled the emplacement of the 1.84–1.81 granites that occur as rather thin sheets in the Southern Finland lithotectonic unit (Ehlers et al., 1993). The deformational history in this unit at 1.84–1.80 Ga was complicated and involved bulk shortening in varying directions (Pajunen et al., 2008; Skyttä and Mänttäri, 2008). A shear zone network with roughly E–W and NNE–SSW strikes developed after 1.81 Ga (Väisänen and Skyttä, 2007). The shear zones with E–W strike show both vertical and horizontal movement components whereas at least some of the zones with NNE–SSW strike are normal faults (Nironen et al., 2006; Väisänen and Skyttä, 2007). Torvela et al. (2013) suggested that the crustal architecture is characterised by an extensional shear fabric observable in the reprocessed seismic sections of FIRE2a.

Three shear zones extend from southern Finland westward to the Gulf of Bothnia (Fig. 3.1.2.1). In the northernmost of these, the WNW-ESE trending Malax shear zone, the sense of shear is unknown. The zone follows the strike of a peculiar rock association (Vittinki mafic volcanic rocks and chert) that may define an important tectonic boundary. Further south there is the NW-SE trending Kynsikangas shear zone, with inferred kinematic history as sinistral horizontal movement followed by normal faulting (Pietikäinen, 1994). The shear zone developed at 1.87 Ga and was reactivated repeatedly afterwards (Pajunen et al., 2008). The southernmost shear zone, referred to as the Sottunga-Jurmo shear zone (Torvela and Ehlers, 2010), shows dextral transpressional deformation that can be followed more than 150 km. To the northwest in the Gulf of Bothnia, this zone is transected by the Åland rapakivi granite and covered by Paleozoic sedimentary rocks. In the Sottunga-Jurmo shear zone three ductile deformation events, from 1.85 Ga to 1.79 Ga, were followed by semi-brittle deformation (mylonite zones) and brittle deformation (pseudotachylites), the latter bracketed between 1.78 Ga and 1.58 Ga (Torvela et al., 2008).

Caledonian orogen

The Caledonian orogen is dominated by thrusts with top-to-the-southeast displacement (Kulling, 1972; Roberts and Gee, 1985). These structures were active in the ductile and ductile–brittle regimes

mainly during the Silurian, in connection with the terminal collision of the continents Laurentia and Baltica (Gee, 1975; Stephens, 1988; Gee et al., 2010). Some thrust zones, not least those lying internally within the Seve Nappe Complex and Offerdal Nappe, may have been active earlier during the Ordovician, in connection with the accretionary tectonic phase and continent-arc collision (Stephens, 1988).

The thrusts form the boundaries to allochthonous slices of bedrock and the basal thrust forms a detachment in Cambrian black oil shale, placing the allochthonous units on top of autochthonous platformal cover rocks and underlying Precambrian crystalline rocks (Fig. 3.1.2.2). The presence of transported slabs of Proterozoic basement inside the allochthonous sheets indicates the thick-skinned stacking.

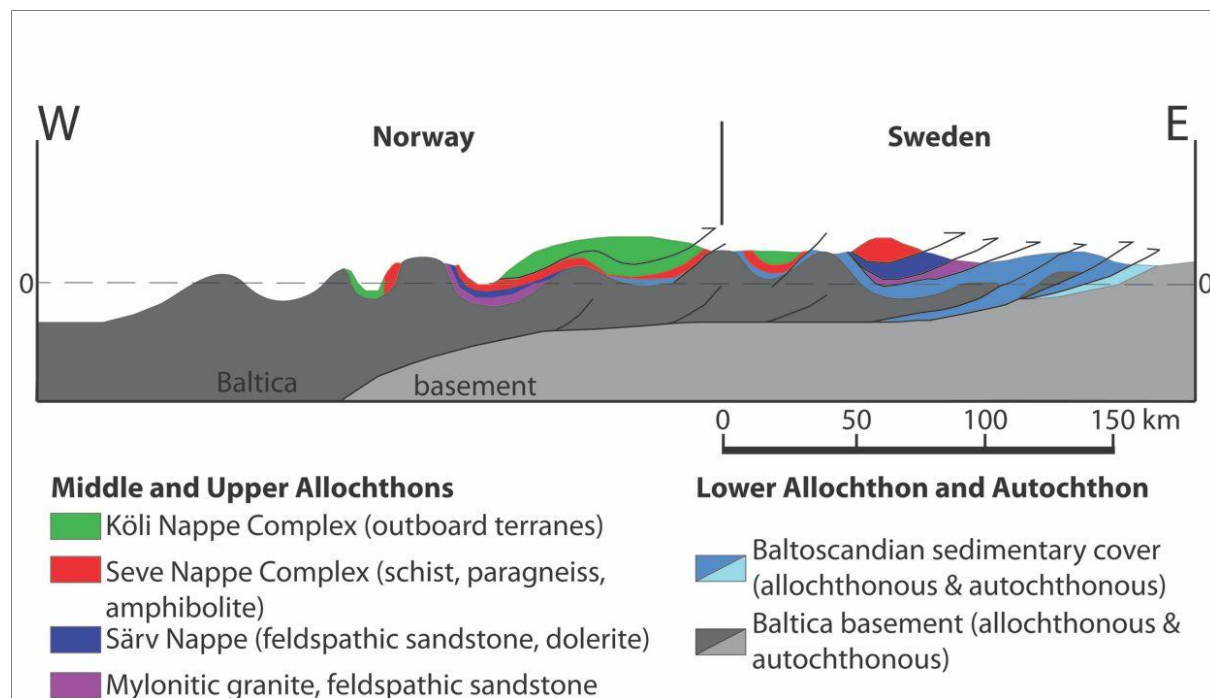


Figure 3.1.2.2. A cross-section through the central part of the Caledonian orogen in Scandinavia showing the gently dipping tectonostratigraphic framework of this orogen (modified after Gee et al., 2010). The Offerdal Nappe corresponds to the unit labelled “Mylonitic granite and feldspathic sandstone” and the Jämtlandian Nappes consist of allochthonous Baltoscandian sedimentary cover and basement in the Lower Allochthon.

The thrusts dip gently, generally westwards (Figs. 3.1.2.1 and 3.1.2.2), but the area is also affected by later, upright folding with axial surface traces parallel to the orogen. These folds rotate the thrust contacts and, thereby, give rise to dips of thrusts to the east and an apparent normal sense of movement. However, the contact between the Seve Nappe Complex, derived from the rifted outer continental margin of Baltica, and the Köli Nappe Complex with its oceanic affinities shows evidence for normal top-to-the-northwest displacement (Trouw, 1986; Greiling et al., 1998) after amalgamation of these two complexes.

3.1.3 Faults affecting sedimentary cover rocks in the Gulf of Bothnia

K. Högdahl & M. Stephens

Lithological and structural framework

The submarine area in the Gulf of Bothnia is underlain by sedimentary cover rocks that lie stratigraphically on top of older Proterozoic crystalline basement (Fig. 3.1.3.1). The bathymetric and topographic high in the Norra Kvarken area separates two fault-controlled sub-basins in the Bothnian Sea to the south and the Bay of Bothnia to the north (Fig. 3.1.3.1).

In the Bothnian Sea, Mesoproterozoic sandstone (Jotnian sandstone), is intruded by 1.27–1.26 Ga (Söderlund et al. 2006; Suominen 1991) dolerites with either NE–SW trends or saucer shapes (Fig. 3.1.3.1; Winterhalter, 1972; Axberg, 1980; BABEL Working Group, 1990, 1993; Korja et al., 2001). The significant thickness (up to 3 km) (Fig. 3.1.3.2; Korja et al., 2001) of the sandstone sequence has been explained by penecontemporaneous subsidence of the basin and down-warping along flexure folds and faults (Axberg 1980) and by collapse of the underlying rapakivi granite body (Korja et al., 2001). In the western part, rocks are overlain by Cambrian sandstone and Ordovician limestone and shale (Fig. 3.1.3.1) up to nearly 400 m thick, which are also disturbed by faulting (Winterhalter, 1972; Axberg, 1980). Sedimentary cover rocks in the Bay of Bothnia are dominated by Mesoproterozoic and Neoproterozoic (Ediacaran?) siltstone and sandstone (referred to as “Middle Riphean and Upper Vendian” in Winterhalter, 2000) overlain by Cambrian sandstone; all rocks are affected by faulting (Fig. 3.1.3.1; Wannäs, 1989; Winterhalter, 2000; Koistinen et al., 2001).

Brittle structures are frequent in the Gulf of Bothnia (Winterhalter, 1972; Axberg, 1980; Wannäs, 1989) and predominantly strike NE–SW to NNE–SSW, NW–SE and less commonly NNW–SSE and N –S (Figs. 3.1.3.2 and 3.1.3.3). Many of these faults and joints have been repeatedly active and are parallel or sub-parallel to structures and lineaments found on land (e.g. Axberg, 1980). Bearing in mind the discussion in section 3.1.2 of the deformation zones on the Swedish and Finnish mainlands, it is likely that some of the major brittle structures preserved in the Gulf of Bothnia have ductile precursors that affected the underlying crystalline basement and have been repeatedly reactivated.

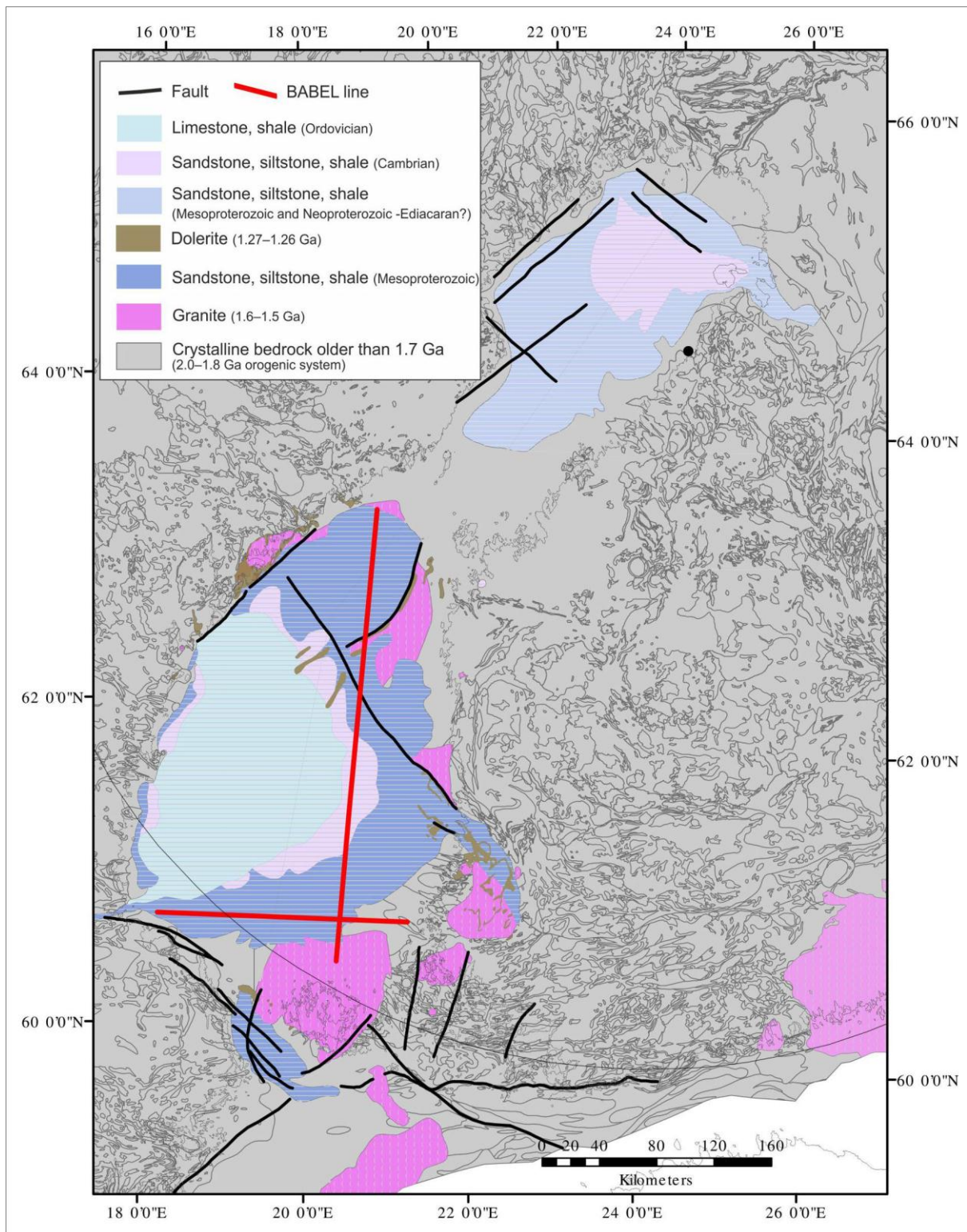


Figure 3.1.3.1. BABEL lines 1 and 7 on a geological map of the Gulf of Bothnia (after Koistinen et al., 2001). Babel profiles 1 (red line; N-S) and 7 (red line; W-E).

The western coast of the Gulf of Bothnia is partly characterised by rather steep fjord-like valleys with elevations reaching to heights of up to 300 m, whereas the eastern coast defines a flat and broad coastal zone (Axberg, 1980; Veltheim, 1962; 1969). The NE–SW to NNE–SSW Bothnian Zone (Axberg, 1980) or Bothnian Fracture Zone (Wannäs, 1989) can be traced along the western coast from the

southern part in the Bothnian Sea and northwards towards Kemi at the northern end of the Bay of Bothnia (Figs. 3.1.3.2 and 3.1.3.3). It is one of the major structural features in the Gulf of Bothnia.

Based on the thickness of the Mesoproterozoic sandstones and the structural features, the Gulf of Bothnia is interpreted to have represented a half-graben rift structure during the Mesoproterozoic (Axberg, 1980). BABEL profiles 1 and 7 imaged both upper crustal and crustal scale listric reflections dipping towards the east (Figs. 3.1.3.1 and 3.1.3.3; Korja and Heikkinen, 1995). Korja and Heikkinen (1995) suggested that the Gulf of Bothnia sedimentary basins are thin-skin basins (Fig. 3.1.3.3) that formed as response to the Mesoproterozoic rifting event. Similar crustal reflection geometries have been described also from the Olkiluoto site (Juhlin and Cosma, 2007; Kukkonen et al., 2011b). Platformal sedimentation prevailed during the Paleozoic.

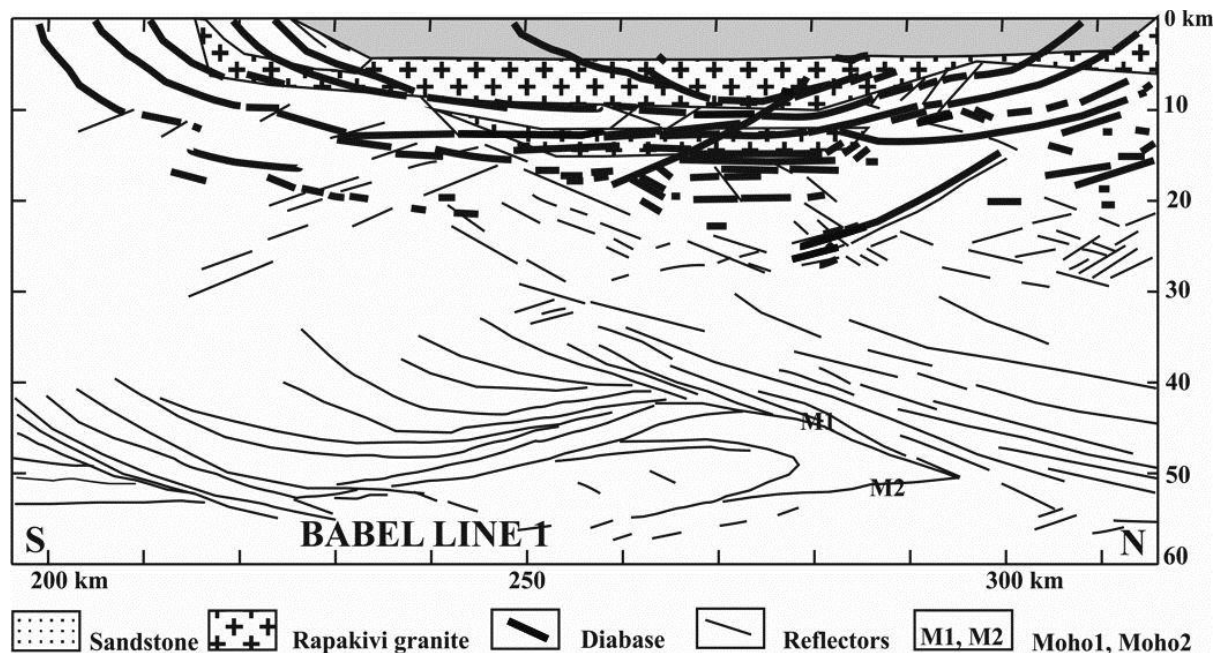


Figure 3.1.3.2. A vertical section of the Northern Bothnian Sea basin along BABEL 1 (Korja et al., 2001). Location of the profile is given in figure 3.1.3.1.

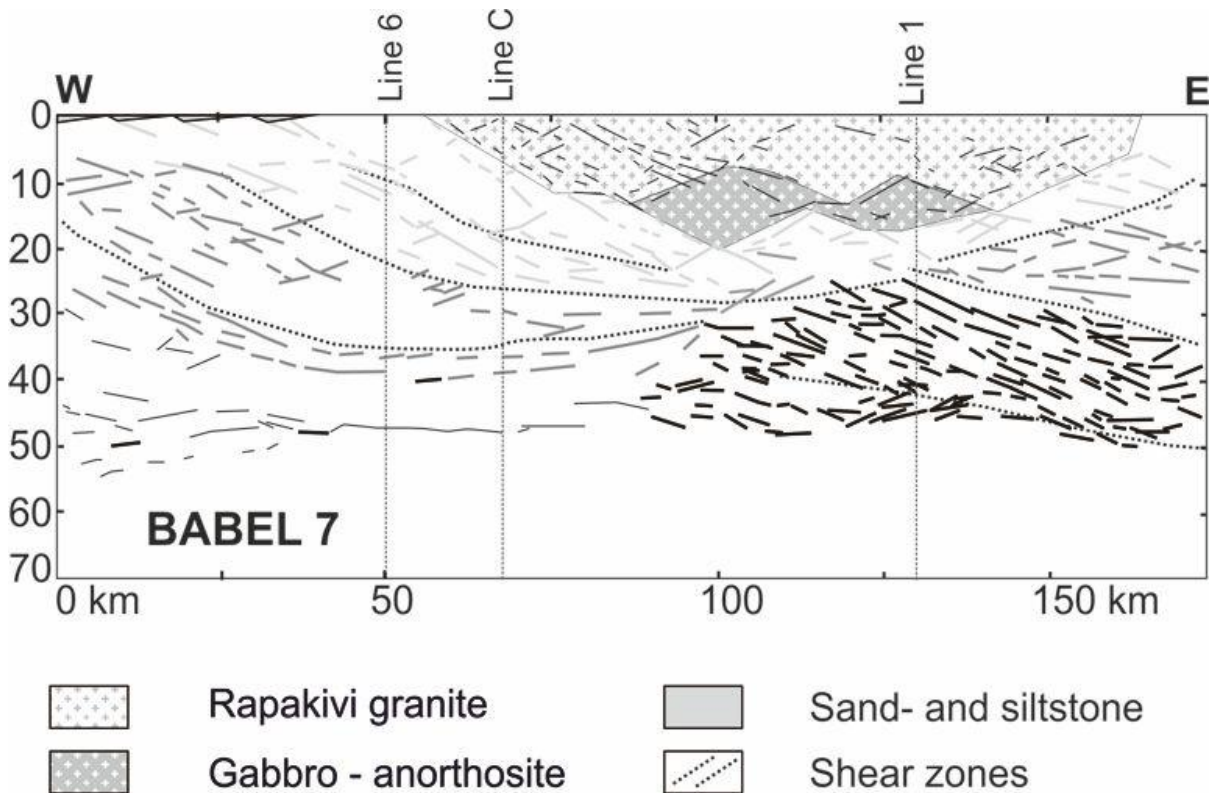


Figure 3.1.3.3. A vertical section of the southern part of the Bothnian Sea basin along BABEL 7 (Korja and Heikkinen, 2005). Location of the profile is given in figure 3.1.3.1.

Character and timing of faulting affecting the sedimentary cover rocks in the Bothnian Sea

In the Bothnian Sea, in the southern part of the Gulf of Bothnia, the NW–SE trending structures are the most persistent, while NE–SW to NNE–SSW faults and joints are more frequent and N–S structures subordinate (Fig. 3.1.3.4A). In part, these structures delimit the extension and preservation of the sedimentary cover rocks. For example, the northern limit of the Paleozoic rocks coincides with the so called "Aranda rift" (Fig. 3.1.3.4), with NW–SE strike, which also hosts a major esker inferred to have been deposited during the Quaternary (Fig. 3.1.3.5; Winterhalter, 1972; Axberg, 1980). Furthermore, the western boundary of the sedimentary rocks commonly follows the NE–SW to NNE–SSW fault system referred to as the Bothnian Zone (Berthelsen and Marker, 1986; Axberg, 1980). According to Wannäs (1989), the continuation of this fault system in the Bay of Bothnia (see below) was established during the 1.1–0.9 Ga Sveconorwegian orogeny (see section 3.1.1). Close to the Swedish coast in the Bothnian Sea, the faults of the Bothnian Zone have accommodated vertical displacement in the order of 1200–1300 m (Axberg, 1980) by repeated fault activity.

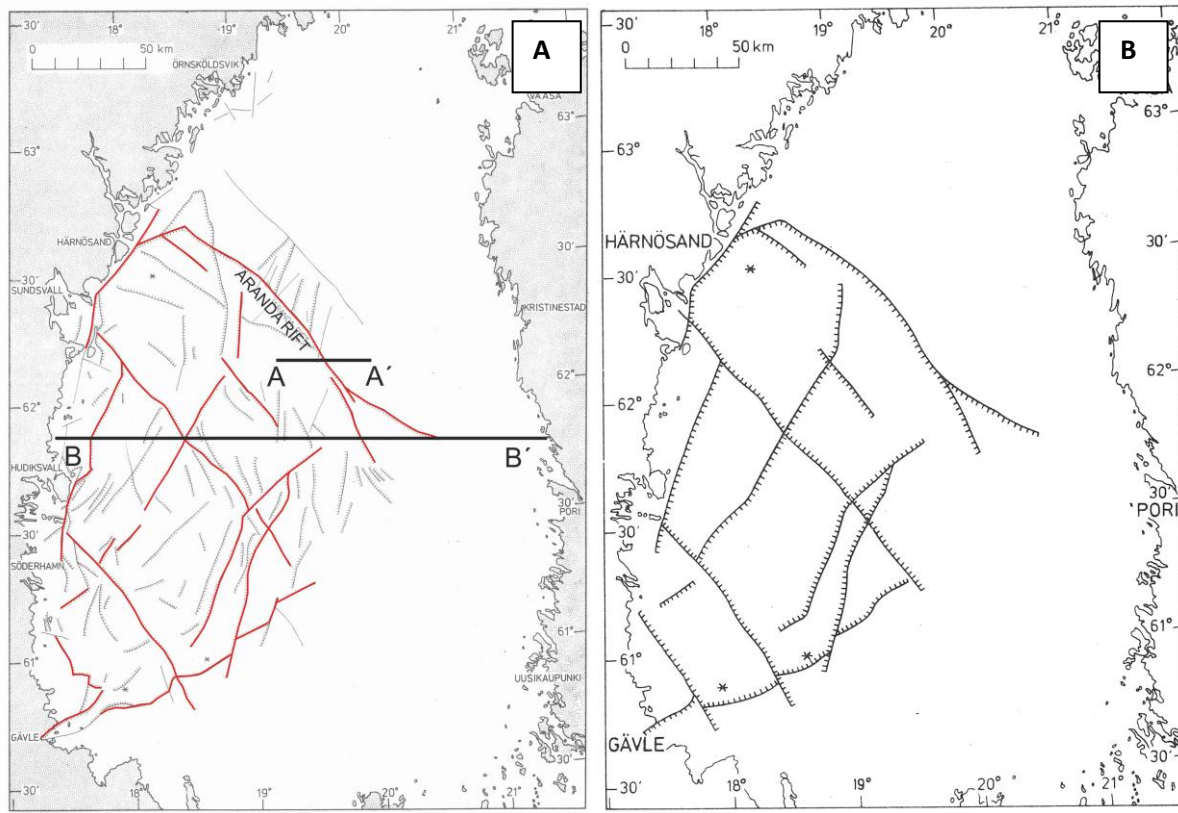


Figure 3.1.3.4. Inferred lineaments and faults in the Bothnian Sea in the southern part of the Gulf of Bothnia. A) Tectonic lineaments inferred to be fault and joint zones after Axberg (1980). NW-SE structures are more persistent, whereas NE-SW to NNE-SSW structures are more common. The red lines mark the more important structures according to Axberg (1980), the black lines mark the location of lines A-A' and B-B' in Figures 3.1.3.5 and 3.1.3.6, respectively. B) Fracture systems in the northern and eastern part of the Bothnian Sea, including the "Aranda rift", after Winterhalter (1972). 1 = Assumed fault line, 2 = Fault line inferred from bathymetric and reflection profiling data, 3 = hachures denote the inferred downthrown side.

The Paleozoic rocks, including Ordovician limestone, are fractured and block faulted (Fig. 3.1.3.6) and displacements between the blocks are commonly in the order of 40–60 m (Axberg, 1980). It has been suggested that the block faulting was caused by reactivation of older structures either during the Caledonian orogeny (Wannäs, 1989) or associated with the uplift of the western part of Scandinavia (Scandian mountain belt) during opening of the North Atlantic Ocean (Axberg, 1980). Activity during the Caledonian orogeny is supported by the occurrence of fluorite-calcite veins in the vicinity of the Gulf of Bothnia, the Baltic Sea and the Gulf of Finland. These veins are indicated to be Paleozoic in age and are often spatially associated with Cambrian sandstone dykes (Alm et al., 2005).

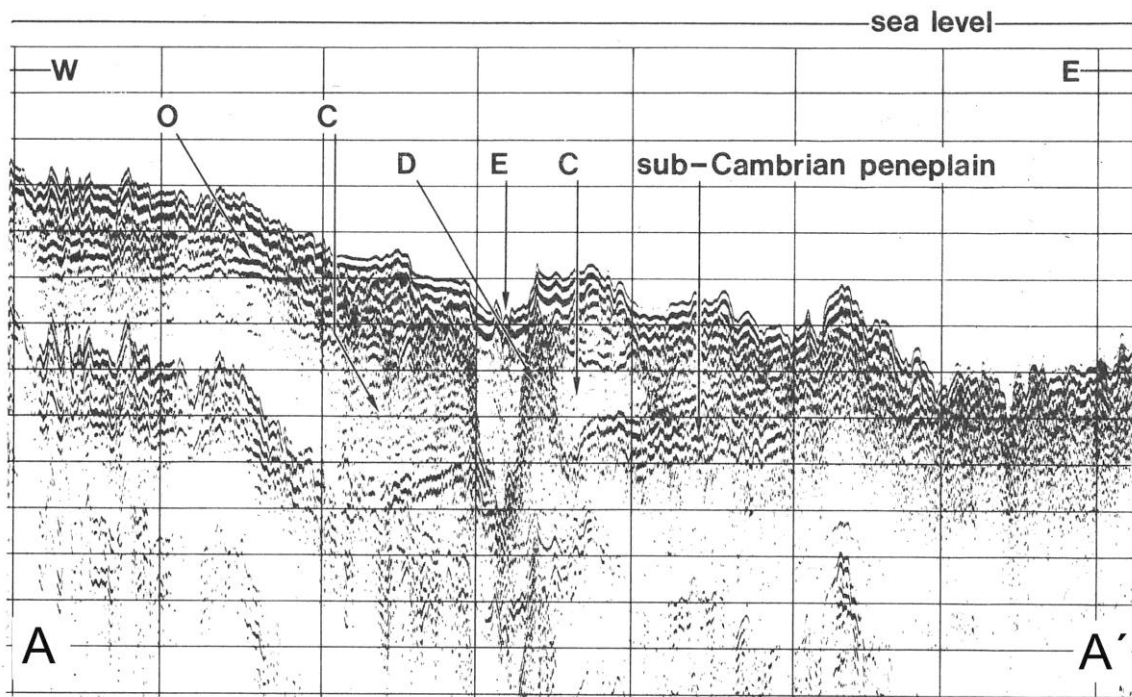


Figure 3.1.3.5. An example of a shallow seismic reflection profile A-A' across the "Aranda rift" hosting the Aranda esker (after Axberg, 1980). A fault marking the rift and esker are marked with "E". The location of the profile B-B' is marked on Figure 3.1.3.4A and more details on this figure can be found in Figure 24 in Axberg (1980).

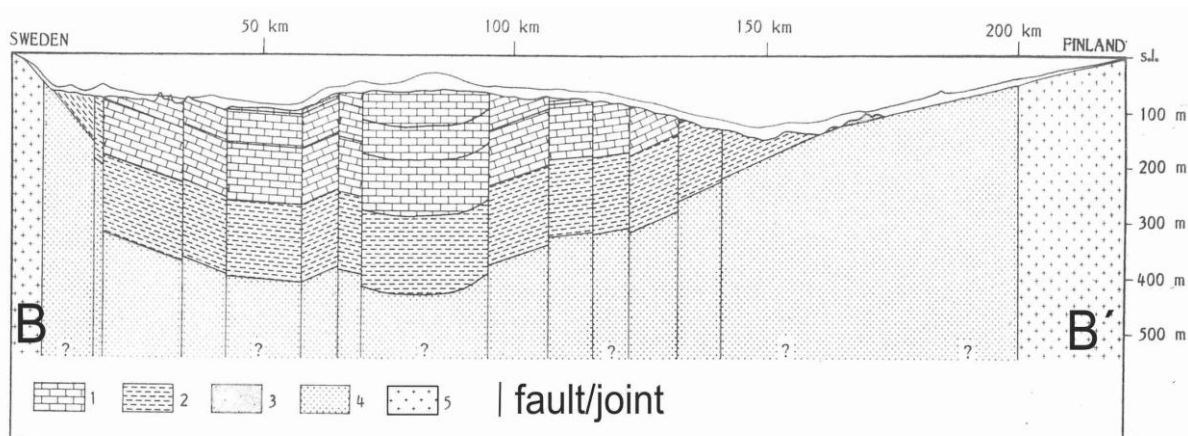


Figure 3.1.3.6. An E-W trending vertical cross-section B-B' through the Bothnian Sea after Axberg (1980). The location of the cross-section B-B' is marked on Figure 3.1.3.4A. 1 = Ordovician limestone and shale, 2 = Cambrian sandstone, 3 = Outliers of Paleozoic rock, 4 = Mesoproterozoic sandstone (so-called "Jotnian sandstone"), 5 = Proterozoic crystalline basement.

Character and timing of faulting affecting the sedimentary cover rocks in the Bay of Bothnia

In the Bay of Bothnia, in the northern part of the Gulf of Bothnia, a number of fault-controlled basin structures have been identified (Wannäs, 1989). The most prominent faults in this area trend NE-SW, NNW-SSE and NW-SE, inferred to be related to the following large-scale structures; the so-called Bothnian Fracture Zone, Ladoga-Bothnian Bay Tectonic Zone and Senja-Oulujoki Tectonic Zone (Fig.

3.1.3.7), respectively (Wannäs, 1989). Reactivation and down-faulting along these fault zones have caused block movements that divided the Bay of Bothnia into a number of rhomboidal segments with different depth to the crystalline basement. In the down-faulted blocks the seismic unit M4, interpreted to be of Cambrian age, is preserved (Fig. 3.1.3.8). The following text addresses, in more detail, information on two of these major structures.

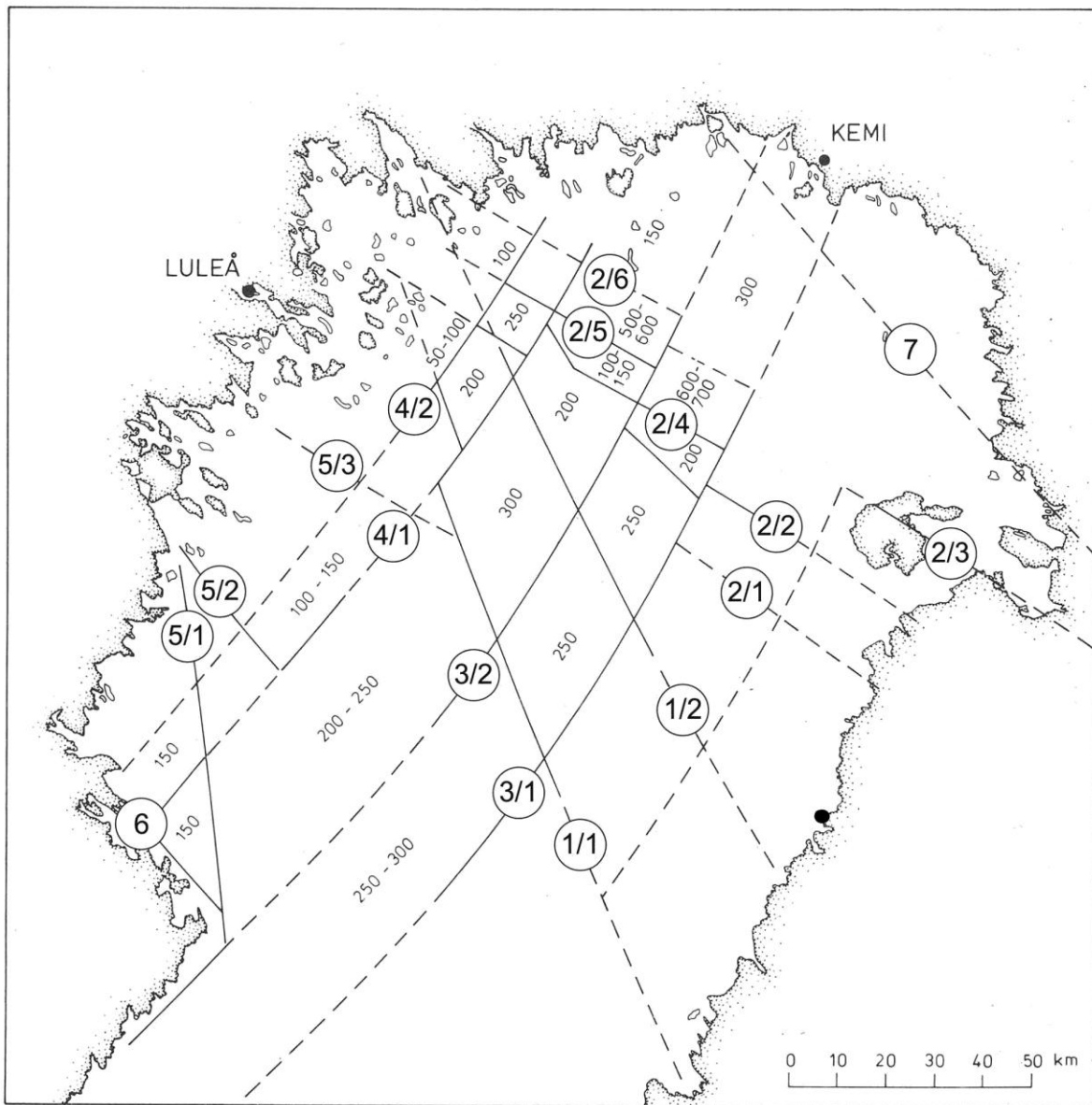


Figure 3.1.3.7. Inferred structures in the Bay of Bothnia in the northern part of the Gulf of Bothnia after Wannäs (1989). 1 = Ladoga-Bothnian Bay Tectonic Zone, 2 = Senja-Oulujoki Tectonic Zone that also delimits the so-called “Muhos basin”, 3 = Bothnian Fracture Zone, 4 = NE-SW fault system parallel to the Bothnian Fracture Zone, 5 = Faults with different orientation in the Piteå-Bjuröklubb area, 6 = Inferred lineament, 7 = Northern boundary of the depression in the Bay of Bothnia. The numbers refer to the depth (metres) to the crystalline basement.

The Bothnian Fracture Zone can be traced from Kemi to Härnösand (Wannäs, 1989) and is most likely associated with the so-called Bothnian Zone south of the Norra Kvarken high (Axberg, 1980). In the Bay of Bothnia, a parallel fault located further to the west is considered to be part of the same system (Wannäs, 1989). Close to the Swedish coast, there is yet another parallel fault set that marks the western limit of the depression in the Bay of Bothnia (4 in Figure 3.1.3.7).

The lineament zone referred to as the Senja-Oulujoki Tectonic Zone by Wannäs (1989) consists of a number of sub-parallel faults with NW–SE strike (Fig. 3.1.3.7). It has been related to the development of the Muhos Basin on the mainland of Finland, containing Mesoproterozoic and Neoproterozoic (Ediacaran?) siltstone and sandstone (Wannäs, 1989; Winterhalter, 2000). In the Bay of Bothnia, these faults occur between the island of Hailouto and Kalix (Fig. 3.1.3.7) and repetitive movements along these structures have been inferred to control the basement morphology (Wannäs, 1989). They have been interpreted as strike-slip faults that, together with intersecting N–S structures, form pull-apart basins ("strike-slip basins" in Wannäs, 1989). Rantataro et al. (2011) have located the deformation with modern seismo-acoustic methods and concluded that the faults have not been active during the Quaternary (Appendix 1).

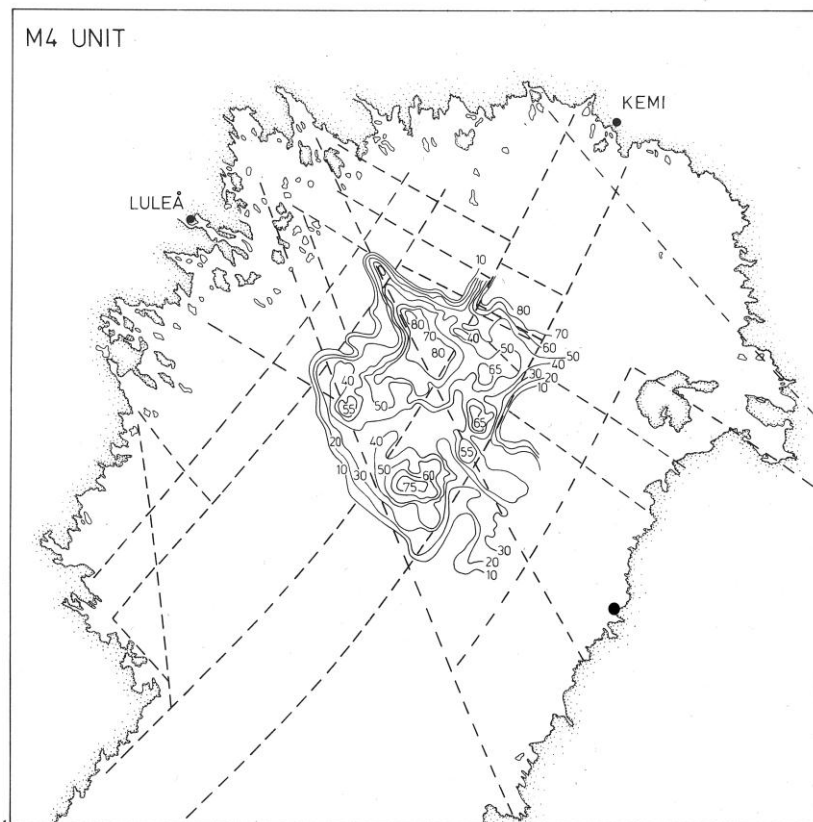


Figure 3.1.3.8. Distribution and thickness of the M4 seismic unit interpreted to represent Cambrian sandstone (from Wannäs, 1989).

The existence of sphalerite, galena and pyrite in the sandstones indicate some hydrothermal activity after their deposition and has been suggested to be rift-related (Wannäs, 1989). Since the timing of

deposition of the sandstones is poorly constrained, the timing of fault activity is also only tentatively known. However, basement blocks showing variable degrees of uplift are draped by sedimentary rocks deposited prior to development of the sub-Cambrian peneplain (Wannäs, 1989). Extensional deformation at least during the later part of the Mesoproterozoic is supported by a large number of 1.1 Ga lamprophyre and carbonatite dykes with N–S trend in the Kalix area (Kresten et al., 1981, 1997), emplaced close to the intersection of different major fault sets.

3.2 Glaciation cycles in the Quaternary period

R. Sutinen, E. Kosonen & B. Lund

The Quaternary Period (ca. 2.6 Ma – present) is divided into two separate epochs, Pleistocene (2.588 Ma-11.5 ka) and Holocene (11.5 ka-present) (Fig. 3.2.1.A). The Quaternary Period is characterized by climate oscillations, from warm to cold with interglacial and glacial phases. During the Early Pleistocene Epoch (2.6-0.8 Ma) there were 41 cold stages, but only 14 of which were sufficiently cold and long to create substantial ice sheets (Ehlers and Gibbard, 2011). Most extensive glaciations in the Quaternary Period occurred during the Middle (781-126 ka) and Late Pleistocene (126-11.5 ka) 5-6 major cold events (Fig. 3.2.1.B) (Gibbard and Cohen, 2008). The climate oscillation evidence is based on Marine Isotope Stages (MIS) from deep sea benthic $\delta^{18}\text{O}$ records (Shackleton, 1997; Lisiecki and Raymo, 2005) (Fig. 3.2.1.B) as little evidence has been found in terrestrial areas. The present Holocene period started approximately 11.5 ka years ago when the last glacial period was ending. In the Fennoscandian area there are traces of last three large glaciations (Elsterian, Saalian and Weichselian) that extended south of the Baltic Sea from the Scandian Mountains. Two interglacials, Holstein (MIS 11) and Eem (MIS 5e), interrupted the main glaciation stages. Clear evidence for the earlier glaciations has not been found from Fennoscandian area. However, the oldest Middle Pleistocene till sheets are found in Don lobe area in SW Russia (Fig. 3.2.2).

These till sheets are underlain and overlain by interglacial sediments containing Tiraspolian age fauna from early Middle Pleistocene. This Don Glaciation, also known as Donian, has been related to MIS 16 stage (see Figure 3.2.1.B), and according to glacial till origin the accumulation center of the ice sheet has been demonstrated to be in NW direction i.e. in Scandinavian province (Alekseev, 1996; Astakhov, 2004; Velichko et al., 2011).

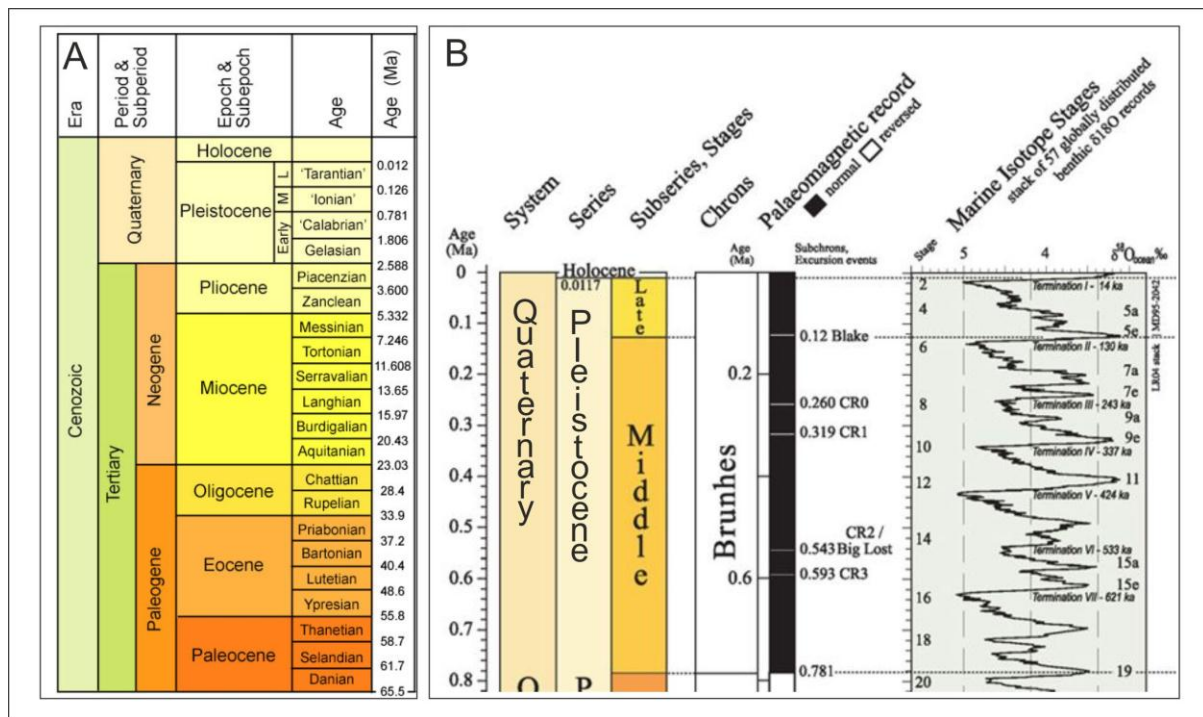


Figure 3.2.1. (A) The definition of the Quaternary system and Pleistocene division according to International Commission on Stratigraphy (ICS) (Gibbard and Head, 2009) (B) Marine Isotope Stages (MIS 19-2) (climate cycles) during Middle and Late Pleistocene period (Lisiecki and Raymo, 2005; Cohen and Gibbard, 2011).

Evidence for the last three large ice sheet's extents have been found throughout Northern Europe, for example, from central and southern Germany and Poland (Fredén, 2002; Svendsen et al., 2004; Litt et al., 2007). The Elsterian glacial phase (MIS 12) and Saalian Complex Stage (MIS 10-6, 400-130 ka) had a larger maximum extent towards the south than the following Weichselian glaciations (MIS 5d-2, 115-11.5 ka). The maximum ice-sheet extent in Eurasia during the Late Saalian (c. 160–140 ka) can be seen in figure 3.2.2. The Late Saalian glaciation (MIS 6) had the largest known ice-sheet in West Siberia during Late Pleistocene as the Weichselian glaciations did not spread as much to the western Siberia area (Svendsen et al., 2004). Saalian till sheet deposits (MIS 10-6) have been recognized in many places in north and west Finland (e.g. Hirvas, 1991; Donner, 1995; Pitkäraanta, 2013). The earlier Elsterian deposits are rare in Sweden and Finland. Eemian interglacial (MIS 5e, 130-115 ka) organic deposits are found in several sites in Sweden and Finland (Robertsson et al., 1997; Robertsson, 2000; Donner, 1995). Figure 3.2.1.1 illustrates the Eemian Sea extent in Fennoscandia (reproduced from Ehlers and Gibbard, 2011).

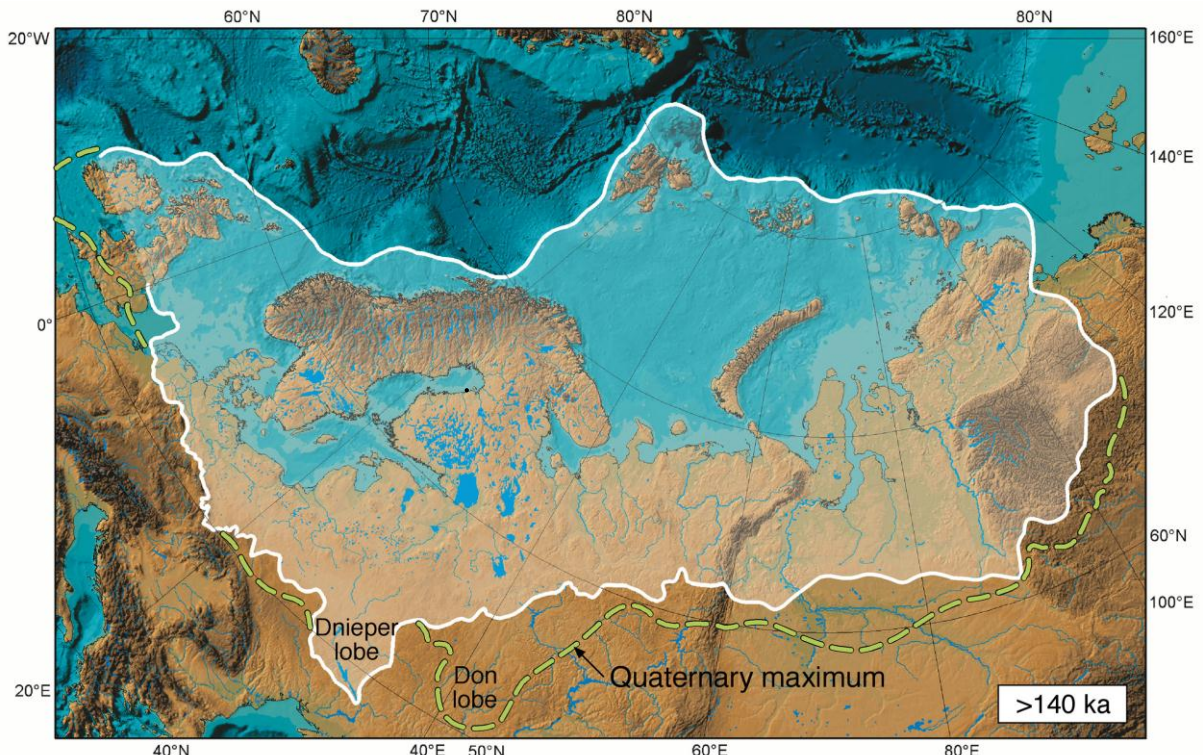


Figure 3.2.2. Maximum extent of Late Saalian ice-sheet in Eurasia (c. 160-140 ka) (figure from Svendsen et al., 2004). The Don lobe shows the maximum ice-sheet extent during the Don glaciations (MIS 16, early Middle Pleistocene).

3.2.1 The Weichselian glaciation (115 – 11.5 ka)

Clear evidence for Late Pleistocene Weichselian glaciations (115 – 11.5 ka) are found in Fennoscandia. Glaciogenic and glaciofluvial deposits from the last glacial periods, Early, Middle and Late Weichselian, can be found in Sweden and Finland (Hirvas, 1991; Lundqvist, 1992; Sutinen, 1992; Donner, 1995; Fredén, 2002; Sohlenius and Hedenström, 2008; Pitkäranta, 2013). The major part of the present soft sediment deposits are generally considered to be Late Weichselian, even though there is no strong evidence for this. The Late Weichselian deposits have buried the earlier remnants. Consequently the extents of the earlier glaciations are more difficult to determine, and there are differences in the Early Weichselian stratigraphy in Swedish and Finnish Lapland as well as uncertainties in the Middle Weichselian glacial extent.

Two end moraine zones (W1 and W2) across northern Finland are the most prominent features evidencing the pre-Late Weichselian ice advance. The end moraine zone in the Pudasjärvi-Oulu region is built of vast masses of sand and gravel, and based on seismic and radar data these coarse-textured deposits vary in thickness from 25 to 60 m (Sutinen, 1992). The ridge formations are covered with a till of Late Weichselian origin. South of the Pudasjärvi end moraine the Late Weichselian till overlies the Eemian (organic) sediments suggesting that the Pudasjärvi end moraine marks the Early Weichselian (W1, MIS 5b) termination (Fig. 3.2.1.1A). The extension of this end

moraine further south along the coast of the Gulf of Baltic is not known. Also, the northern extension in Lapland towards the Arctic Ocean is unknown. The Early and Middle Weichselian moraines (e.g. Veiki moraines), that survived the later glaciations, have been found in a wide area in Swedish Lapland (e.g. Lagerbäck, 1988; Sigfúsdóttir, 2013).

During the early Middle Weichselian (MIS 4, 70-60 ka) it is believed that the ice sheet covered the whole of Sweden and Finland (Fig. 3.2.1.1C) (e.g. Saarnisto & Salonen, 1995; Svendsen et al., 2004; Salonen et al., 2008). Another end moraine zone in Lapland (W2, MIS 3) can be followed from the Pello area in the west to Kittilä and Porttipahta in central Lapland towards Savukoski and cross the Finnish-Russian border to the east (Sutinen, 1992). Based on the radar evidence from the Porttipahta area, the foreset beds of these glaciofluvial formations are tilting south. Between the ‘Porttipahta’ and Pudasjärvi end moraines the Eemian sediments are overlain by two Weichselian sedimentary units, hence, suggesting that the ‘Porttipahta’ end moraine marks the mid-Weichselian (W2, MIS 3) termination. As is the case with W1, no evidence has been found so far to indicate the northern extent. However, the glacial dispersal on the northern side of the W2-termination is extremely complicated and indicates at least three major ice flow phases (Sutinen, 1992; Sutinen et al., 2013).

Weichselian ice sheets have had large differences in volume as well as variations in spatial and temporal extents and the ice sheet accumulation center location has also varied. The Early Weichselian ice sheet has been interpreted to have been the most extensive towards the northeast (Svendsen et al., 2004). The Late Weichselian (MIS 2) on the other hand was the most extensive to the west and south being the largest of the Weichselian period ice sheets. The Late Weichselian last glacial maximum (LGM) border (22 000 years ago) is seen in Figure 3.2.1.1D. The Weichselian period had also many known interstadials, when Fennoscandia was free of ice over 10 000 year long periods. Also Saalian and Elsterian are thought to have undergone several ice free interstadials.

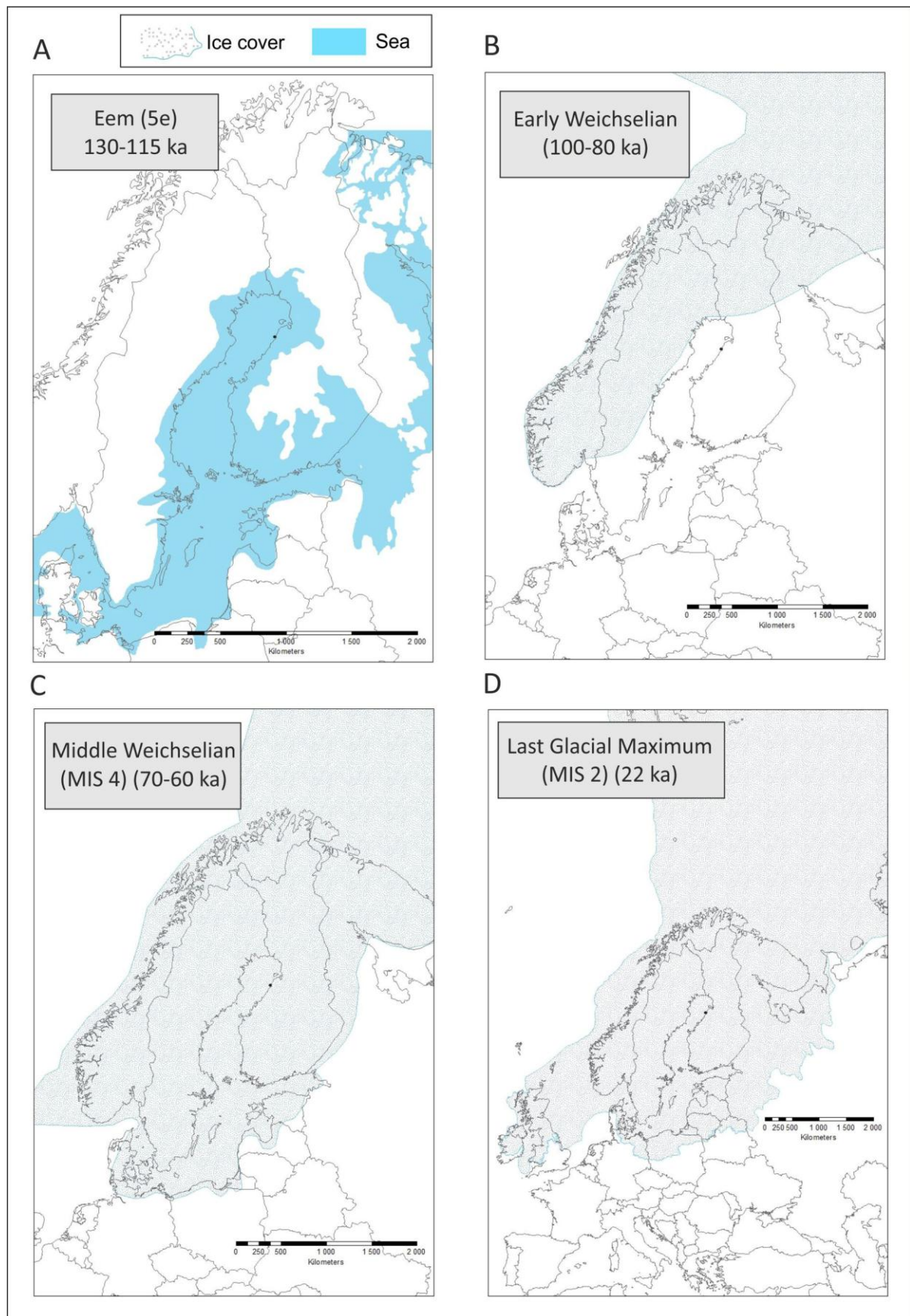


Figure 3.2.1.1. Extent of interglacial Eemian Sea (A), Early (B) and Middle Weichselian (C) glaciations and Late Weichselian Last Glacial Maximum (LGM) (D). A and D are based on Ehlers and Gibbard (2011) and B and C are based on Svendsen et al. (2004).

3.2.2 Weichselian deglaciation and the Holocene Epoch in northern Europe

Deglaciation started c. 18 ka ago, when the ice-sheet started to retreat from its LGM extent in the northern parts of Germany and Poland (Fig. 3.2.1.1) (Ehlers et al., 2011) and northeastern sector of Russia (Lunkka et al., 2001). The retreating ice had several standstills and re-advances. The retreating glacial margin reached southern Sweden c. 14.6 ka and southern Finland c. 13 ka ago. The last major standstill occurred during a cold period called the Younger Dryas (YD) (13-11.5 ka). The large ice-marginal formations in southern Sweden and Finland (Salpausselkä I and II) and western Russia (Kalevala and Rugozero) represent the Younger Dryas end moraines (Fig. 3.2.2.1). These large glaciifluvial deposits were formed on the shores of the Baltic Ice Lake and White Sea Ice Lake that were located in front of the ice margin (Fig. 3.2.2.1). The deglaciation chronology from southern Sweden and Finland (and Russian Karelia) through the YD end moraines to the Bay of Bothnian is based on clay varve chronology (Sauramo, 1923; Cato, 1987), ^{10}Be dating (Rinterknecht et al., 2004), ^{14}C dating and paleomagnetic dating (e.g. Saarnisto & Saarinen, 2001). Two ice stream fans in Lapland, one in Utsjoki in the north and the other in Kuusamo in the southeast, have been linked to the Younger Dryas end moraines in Finnmark, northern Norway and east into Russian Karelia (Sutinen et al., 2009, 2010). The end of the Younger Dryas marks the onset of the present interglacial epoch, the Holocene. During this phase the ice retreat was surprisingly fast, such that in Utsjoki, northernmost Finnish Lapland, the oldest basal peat ages range from 9 220 to 11 200 cal. yr BP (calibrated years before present) (Oksanen, 2006) whereas in Kittilä the oldest basal peat ages are of 10 800 cal. yr BP (Mäkilä and Muurinen, 2008). In addition, the landslide-buried woody remnants of birch (*Betula* ssp.) have yielded cal. 9 730 cal. yr BP in Kittilä (Sutinen, 2005). After the YD, the ice margin retreated more or less continuously in southern and western areas during the early part of the Holocene, reaching the Gulf of Bothnia 10.3 ka ago (Fig. 3.2.3.1).

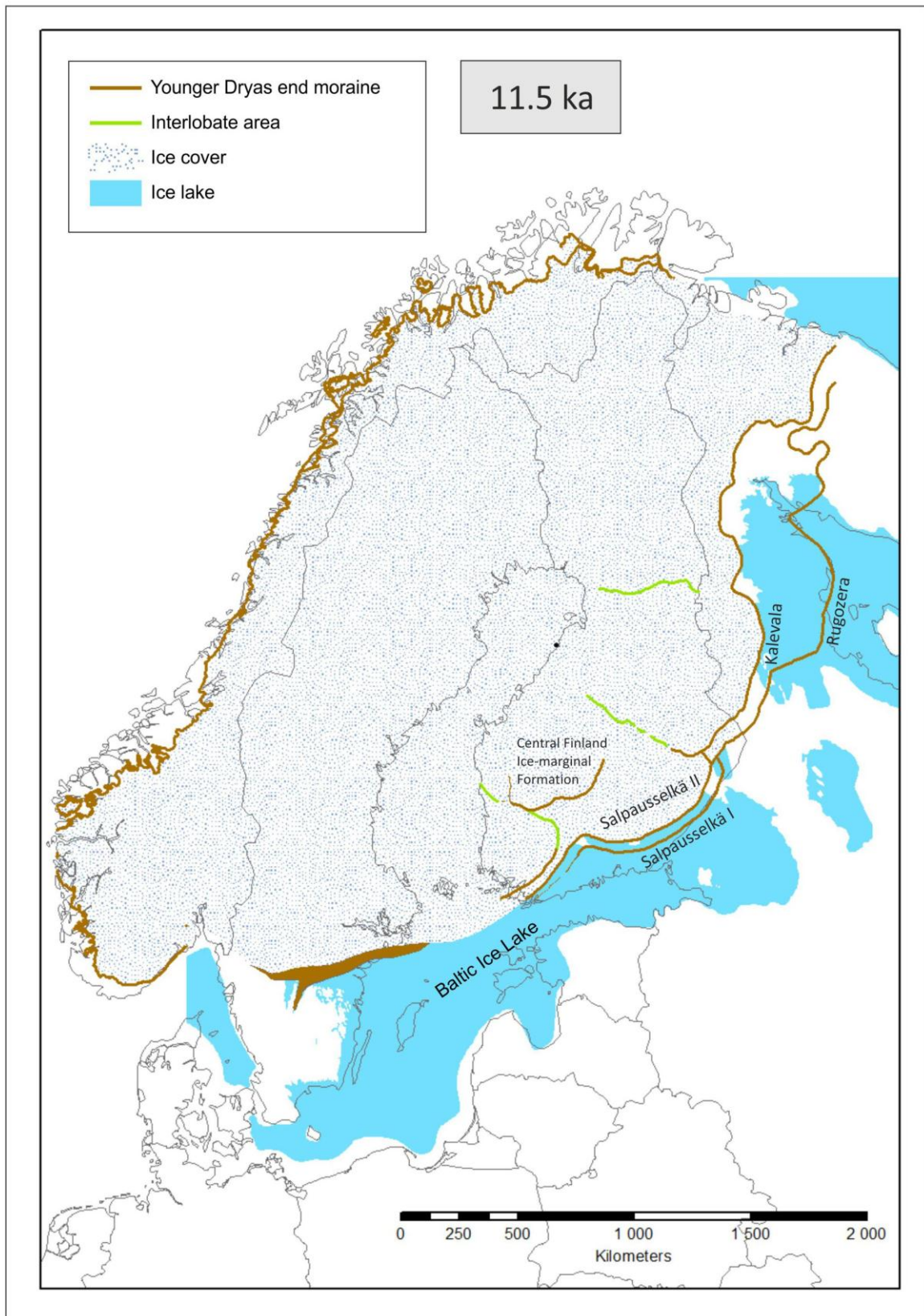


Figure 3.2.2.1. Glacial extent and end moraines during the Younger Dryas standstill phase and the Baltic Ice Lake 11 500 years ago (modified from Ehlers and Gibbard, 2011).

Finland was completely deglaciated by 10 000 years ago, and the last remnants of the ice sheet in Sweden have been dated to 9000-8500 BP (e.g. Lundqvist, 2004; Johansson et al., 2011). The deglaciation curves and known post-glacial faults are seen in Figure 3.2.3.1. After the Baltic Ice Lake (14 000 – 11 550 cal. yr BP) the Baltic Sea area experienced Yoldia Sea (11 550 – 10 700 cal. yr BP) that was followed by Ancylus Lake (10 700 – 9 800 cal. yr BP) and Litorina Sea (9 800 –present cal. yr BP) stages in the Early Holocene (Björck, 1995; Björck, 2008; Andrén et al., 2011). The highest Baltic Sea shorelines are situated at different altitudes in the Fennoscandian area depending on the differences in crustal depression and rebound velocities as well as the sea-level changes during different Baltic Sea stages. Also, an important factor is when the area became ice-free. Ancylus and Litorina shorelines reached the southern Lapland area as the ice had already retreated to the Scandian mountain area. These past Baltic Sea stages have deposited silt and clay sediments along low-lying coastal areas of Sweden and Finland.

The average thickness of the Quaternary sediments in Finland has been estimated to be 8.6 m and the most common thickness being 3-4 m (Okko, 1964). The thickest continuous deposits are found in southwestern Finland (clay deposits) and in the Salpausselkä end moraine zones. In Finland and Sweden, the thickest sediment covers are found in valleys extending to over 100 meters (Lundqvist, 1958; Pitkäranta, 2013). The average bedrock erosion in Sweden during the Quaternary Period has been estimated to be 12 m with 1 meter per glaciation (Påsse, 2004).

3.2.3 Faults active during the late Weichselian deglaciation

The Late Weichselian deglaciation resulted in active faulting of the bedrock in northern Fennoscandia. Approximately a dozen late- or post-glacial reverse fault scarps have been identified in northern Fennoscandia from the 1960s onwards (see section 2.7) (e.g. Kujansuu, 1964; Lagerbäck, 1979; Olesen, 1988; Kuivamäki et al., 1998). The faults have displacements and scarps from a few centimeters to 30 meters high (Lagerbäck & Sundh, 2008; Olesen, 1988; Kuivamäki et al., 1998) and the seismic events may have reached magnitudes of up to 8 or larger (Muir Wood, 1993; Arvidsson, 1996). Post-glacial faults (PGF) in Fennoscandia are shown in Figure 3.2.3.1 and listed in Table 3.2.3.1. The post-glacial faults generally follow old weakness zones which were reactivated in a combination of tectonic, glacial isostatic adjustment (GIA) and local stresses (e.g. Wu et al., 1999; Lund, 2005; Lund et al., 2009). In most of the Lapland area, the spacing of the SW-NE oriented post-glacial faults is about 100 km.

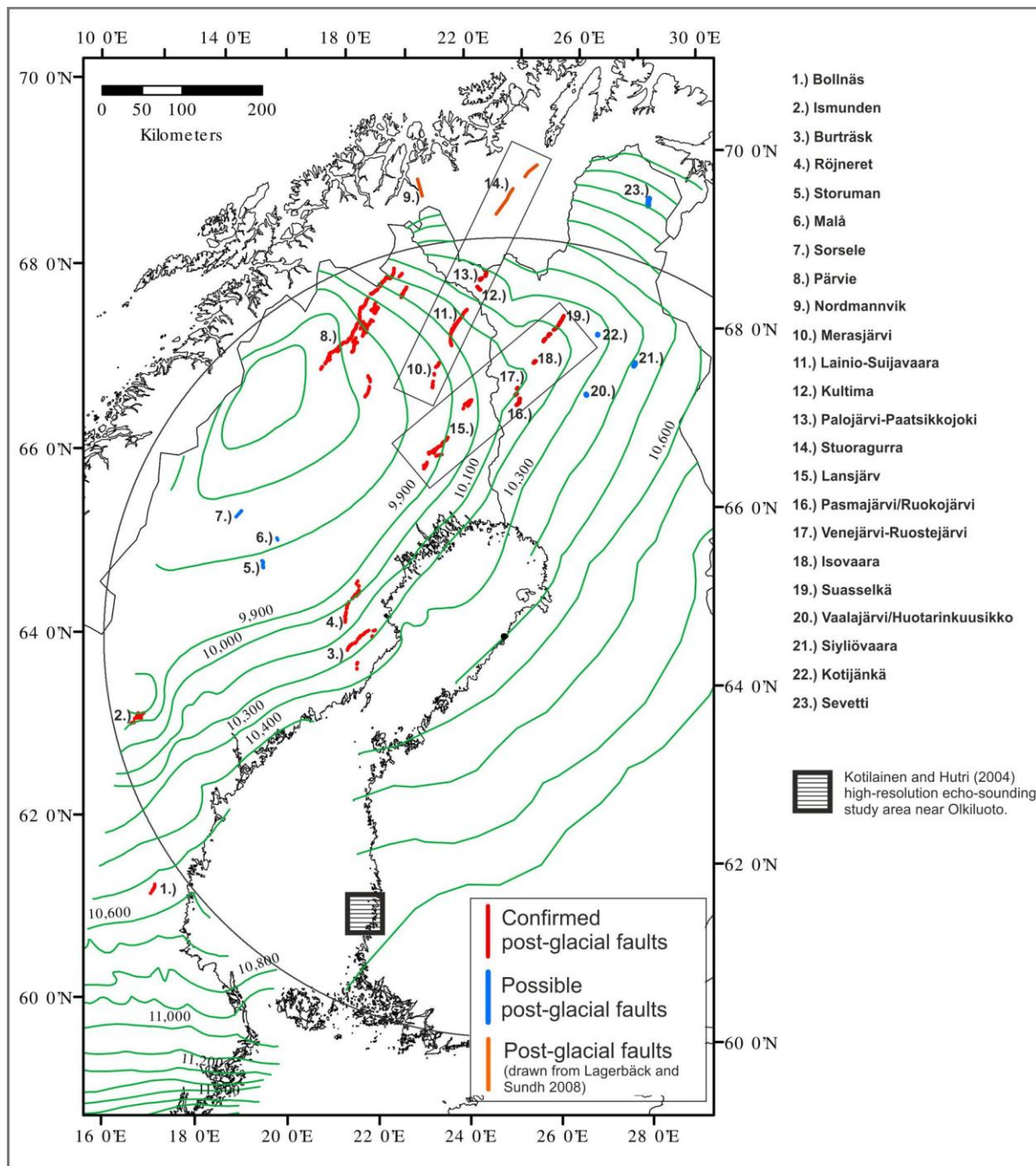


Figure 3.2.3.1. Post-glacial faults and deglaciation curves of the Late Weichselian ice sheet. Deglaciation chronology is based on Lunkka et al. (2004) and Lundqvist (2004). Two long PGF-lines are presented (boxes). PGFs are also presented in section 2.7.

Kilometer scale PGFs have only been found in Fennoscandia (e.g. Munier & Fenton, 2004), in regions undergoing glacio-isostatic uplift. Relative dating of the rupture of the Fennoscandian PGFs is uncertain (Lagerbäck & Sundh, 2008) but one hypothesis is that they ruptured as final deglaciation occurred at a site, such that the first faults to move were the ones in eastern Lapland and Sweden shoreline areas (Muir Wood, 1993) (Fig. 3.2.3.1). The faults have been inferred to form during different phases of the last deglaciation: 1) beneath the retreating ice-sheet, 2) during the uncovering of the ice-sheet and 3) after local deglaciation (Lagerbäck & Witschard, 1983; Lagerbäck

and Sundh, 2008; Sutinen et al., 2013; 2014). Displacement on the post-glacial faults is inferred to have occurred as single events, observed in trenches as single ruptures through glacial sediments and then continued sedimentation, and no conclusive evidence has been found for repeated movements (e.g. Lagerbäck & Sundh, 2008). Indirect observations of dated landslides and sediment disturbances may indicate that the period of increased seismicity may have lasted several thousand years after deglaciation (e.g. Sutinen, 2005; Sutinen et al., 2014; Mörner, 2003).

The NNE trending reverse Pärvie fault system consists of linear series of fault scarps and is a 155 km long fault line. Also two long SW-NE trending PGF-lines continue across the borders in Lapland (see Figure 3.2.3.1). Similar to most PGFs in Sweden, the majority of the PGFs in Finland follow the SW-NE trending geometry. The Suasselkä PGF (see Table 3.2.3.1 and Fig. 3.2.3.1), first reported by Kujansuu (1964), seems to have a continuation to Isovaara PGF and further SW to Pasmajärvi-Ruokojärvi/Venejärvi/Ruostejärvi fault swarm and perhaps even into the Lansjärv fault system in Norrbotten Sweden (see Lagerbäck and Sundh, 2008). In a similar manner, the Palojärvi fault in western Finnish Lapland could be associated not only with the Lainio-Suijavaara PGF-system in Sweden (Sutinen et al., 2014; see Lagerbäck and Sundh, 2008) but also in the NE to the Stuoragurra PGF in Finnmark, Norway (see Olesen, 1988). These features indicate that the PGF lines could be much longer than previously thought.

Other than these two main PGF-lines (Lansjärv/Pasmajärvi/Venejärvi/Ruostejärvi/Suasselkä and Lainio-Suijavaara/Palojärvi/Stuoragurra), some discrete and unverified fault patterns have been described e.g. in central Lapland. The Vaalajärvi/Huotarinkuusikko (Table 3.2.3.1), for example, diverts in orientation from the main stress pattern (Kuivämäki et al., 1998) and therefore these will be further studied as the airborne LiDAR will be available in the near future. The excavation across the Vaalajärvi scarp has shown that there are no clear indications of faulting in the overburden Quaternary deposits and the fault is now classified only as a possible post-glacial fault (Kuivämäki et al., 2001).

In Utsjoki, northernmost Finnish Lapland, a significant concentration of landslides (Sutinen et al., 2009) suggests a high magnitude seismic event. According to the historical earthquake-induced landslide model by Keefer (2002), the area affected by a $M_w \approx 7$ earthquake approximates 10,000 km² and the maximum lateral distance of a landslide from the fault-rupture zone approximates 150 km. Therefore, Stuoragurra may have contributed to the Utsjoki landslides. These slides, however, occurred in a nunatak position at some 11.9 ka (Sutinen et al., 2009). The Sevetti fault (Table 3.2.3.1) is closer to Utsjoki, but this structure has not been verified. In the next few years, airborne LiDAR data will be available for northern Finland and Sweden allowing more thorough investigations (targeted trenchings/ drillings/ datings) of PGFs and earthquake induced landforms.

Table 3.2.3.1. Post-glacial faults in Finland, Sweden and Norway (modified after Lagerbäck and Sundh, 2008; Kuivämäki et al., 1998; Olesen et al., 2004, 2013). * PGFs in 500 km radius from Hanhikivi site. Red shading shows formations that are not fully verified as PGFs.

Fault system	Country	Scarps	Ave scarp height (m) (up thrown side)	Trend	Dip	Length (km)	Fault movement	Estimated activity	Reference
Suasselkä *	Finland	1 major several minor	4-5 (SE)	SW-NE	70°-80° SE	36-48	Reverse	Post-glacial	Kujansuu, 1964
Isovaara*	Finland	1 major	4-6	SW-NE		4	Reverse	Post-glacial	Sutinen et al., 2013
Pasmajärvi/ Ruokojärvi *	Finland	2	4-10 (SE)	SW-NE SSW-NNE	45° SE	4 5	Reverse	Post-glacial	Kujansuu, 1964
Ruostejärvi *	Finland	1	0-3 (NW)	SW-NE		3	Normal	Post-glacial	Kujansuu, 1964; Kuivämäki, 1986
Venejärvi*	Finland	2	0-7 (SE)	SW-NE	70°-90° SE	(2) 10	Reverse	Post-glacial	Kujansuu, 1964
Vaalajärvi*	Finland	2 minor	2	NW-SE		6	Normal ?		Kujansuu, 1964
Kotijänkä*	Finland	1	0-1	N-S		700 m			Kujansuu, 1964
Siyliövaara *	Finland	1	4	SW-NE		4			Sutinen et al., 2007
Palojärvi*	Finland	1 major several minor	4-6	N-SSW		6	Reverse	Deglacial, possible extension of the Lainio-Suijavaara	Sutinen et al., 2014
Paatsikkajo ki*	Finland	2 minor	1-1.5	(W)SW-NE		1-3	Reverse	Post-glacial	Sutinen et al., 2014
Kultima*	Finland	1 major	4-10	NW-SE		4	Reverse	Subglacial	Sutinen et al., 2014
Sevetti	Finland	1 major	4-15	NE-SW(S)		12	Reverse	Possibly subglacial	Sutinen et al., 2009
Pärvie *	Sweden	Several	3-10	NNE		155	Reverse	Deglaciation phase	Lagerbäck, 1979
Lainio- Suijavaara *	Sweden	4	10-30	NNE-SSW to S		3-50	Reverse	During deglaciation	Lagerbäck, 1979
Merasjärvi *	Sweden	1	10-15	SSW-NNE		8	Reverse	Post-glacial	Lagerbäck, 1979
Lansjärv*	Sweden	4 major, Several small	2-10	SSW-NNE		50	Reverse	Post-glacial, under sea	Lagerbäck, 1979
Burträsk *	Sweden	Several	5-15	NE		40	Reverse	Late/post-glacial	Lagerbäck, 1979
Röjnoret *	Sweden	Several	5-15	N		56	Reverse	Post-glacial	
Sorsele*	Sweden		1.5-2	SW-NE		1-2	Reverse	Post-glacial	Ransed and Wahlroos, 2007
Ismunden*	Sweden	2	3-5	ENE-WSW			Reverse		
Bollnäs*	Sweden								under SGU's investigation
Storuman*	Sweden	Several	2-10	NW-SE		10			Johansson and Ransed, 2003
Malå*	Sweden	4	small scarps			1	-		
Stuoragurra	Norway	3 separate sections	7	SW-NE	40°	80	Reverse	Post-glacial	Olesen, 1988
Nordmannvik	Norway	1	1	NW-SE		2	Normal	Post-glacial	Tolgensbakk and Sollid, 1988

Kuivämäki et al. (1998) also studied Russian Karelia structures indicated as post-glacial faults in Lake Onega area (Lukashov, 1995), however, the evidence was not conclusive and these possible post-glacial faults are not included in this study. Using marine geophysical mapping and borehole cores, Jakobsson et al. (2014) suggests that there is an 80 km long fault system in Lake Vättern which may have ruptured in a post-glacial earthquake with 13 m vertical offset at the end of the Younger Dryas

(ca. 11.5 ka). Other post-glacial seismic activities have been reported from southern Sweden, including landslides and turbidites associated with a fault in northern Lake Vättern (Mörner, 1985). There have furthermore been studies on defining features e.g. disturbed sediment structures, bedrock cave systems, landslides to seismo-tectonic or glaciotectonic origin (e.g. Mörner, 2003; Lagerbäck et al., 2005a). In Finland there are also some evidence of microsize (cm-m) post-glacial faults cutting bedrock and the glacial striations in Ilomantsi area (eastern Finland) (Nenonen and Huhta, 1993) and in archipelago SW Finland (See Figure 5 in Kuivamäki et al., 1998).

Even though the recent excavations by Rantataro et al. (2011) in the Bay of Bothnia near Hanhikivi did not reveal any paleoseismic events or structures, the high-resolution echo-sounding profiles from Bothnian Sea sediments near Olkiluoto (Fig. 3.2.3.1) have revealed two sites with post-glacial paleoseismicity structures in sediments (e.g. disturbed structures, submarine slides and slumps, debris-flow structures) (Kotilainen and Hutri, 2004). Hutri et al. (2007) dated these events with paleomagnetic, biostratigraphy and lithostratigraphical methods give estimated age between 10 650 cal. yr BP and 10 200 cal. yr BP. This age estimation is in line with the Northern Fennoscandian paleoseismic events, but occurred a few hundred years after the ice had retreated from the Olkiluoto area (Kukkonen et al., 2010).

Modelling of fault reactivation during glaciations has been performed by e.g. Wu & Hasegawa (1996a,b), Wu et al. (1999), Lund (2005) and Lund et al. (2009). These model predictions suggest that the onset of the Fennoscandian fault activity started at 15 ka BP, and that maximum fault instability was reached during the Younger Dryas and Early Holocene periods 13-10 ka BP. The studies show that the glacially induced stresses are not sufficient to drive fault rupture on their own, but that it is the combination of glacial and tectonic stresses that causes the post-glacial earthquakes. In particular, the tectonic stress field must be reverse for the superposition of glacial and tectonic stresses to act to destabilize faults at the end of deglaciation (e.g. Lund et al., 2009). This is in good agreement with the observation that most of the PGFs strike SW-NE, perpendicular to the direction of ridge-push induced horizontal stresses, and that the fault directions do not follow the outline of the former Fennoscandian ice dome.

The glacial history of Swedish and Finnish Lapland reveal that two large (Elsterian and Saalian) ice sheets and three consecutive Weichselian ice sheets have loaded the region with known PGFs. Lagerbäck and Sundh (2008) found no evidence of reactivation of the faults during the previous Weichselian glacial periods, it is however not known if they ruptured at the end of the earlier Pleistocene glaciations. The modeling results discussed above indicate that faults will reactivate at the end of all glacial periods, if the faults are critically stressed at the start of glaciation. However, as

strain accumulation in the Fennoscandian Shield is low (e.g. Scherneck et al., 2010), it may take 100,000 years or more to reload a fault after a large earthquake.

4 Seismicity and seismic parameters

4.1 Seismicity

M. Uski & B. Lund

Fennoscandia is a stable intraplate region characterized by low to moderate seismicity. Historical earthquakes have magnitudes up to 6.1 (FENCAT). Instrumentally recorded earthquakes have magnitudes between M_L -1 and 5.5 and take place from shallow crustal depths down to 40 km (e.g. Böðvarsson et al., 2006; Uski et al., 2012). Earthquakes in the study area are generally small and there are roughly 2 magnitude ≥ 3 events per year. The seismicity in the study area is clustered along NE–SW-trending zones that are parallel to the Norwegian margin and the opening of the Atlantic Ocean along the Mid-Atlantic ridge (Figs. 1.2.1 and 4.1.1). A slight change in the general pattern takes place across an N–S-trending zone running east of the Finnish-Swedish national border (Pajala shear zone; 10 in Fig. 3.1.2.1). East of this zone, the seismicity rates are lower and the NE–SW trend is less obvious. Underground mining also causes local perturbations in the stress field, resulting in shallow mining-induced/influenced seismicity (e.g. Roth and Bungum, 2003) in and around the large mines of northern Sweden, Kola Peninsula and Pyhäsalmi.

The NE–SW trending earthquake clusters in northern Sweden and Finland have been associated with PGF zones and western flank of the Gulf of Bothnia (Lagerbäck, 1990; Lindblom et al., 2011; Olesen et al., 2013; Uski et al., 2003). The most active NE–SW-trending zone in Finland is the Kuusamo-Kandalaksa zone spatially associated with the Precambrian Auho-Kandalaksha fault zone. Low magnitude seismic swarms occur within the major 1.7–1.6 Ga rapakivi granite batholith (Wiborg batholith) in southeastern Finland and Russia (Uski et al., 2006). The coastal areas of northern Norway are also known for relatively shallow swarm-type seismic activity (Fig. 4.1.1). A total of 10,000 events with local magnitudes up to M_L =3.2 have been recorded in Meløy during 1978-79 (Bungum et al., 1979, 1982). Earthquake swarms or sequences have also been observed in Steigen and Rana (Atakan et al., 1994; Hicks et al., 2000a).

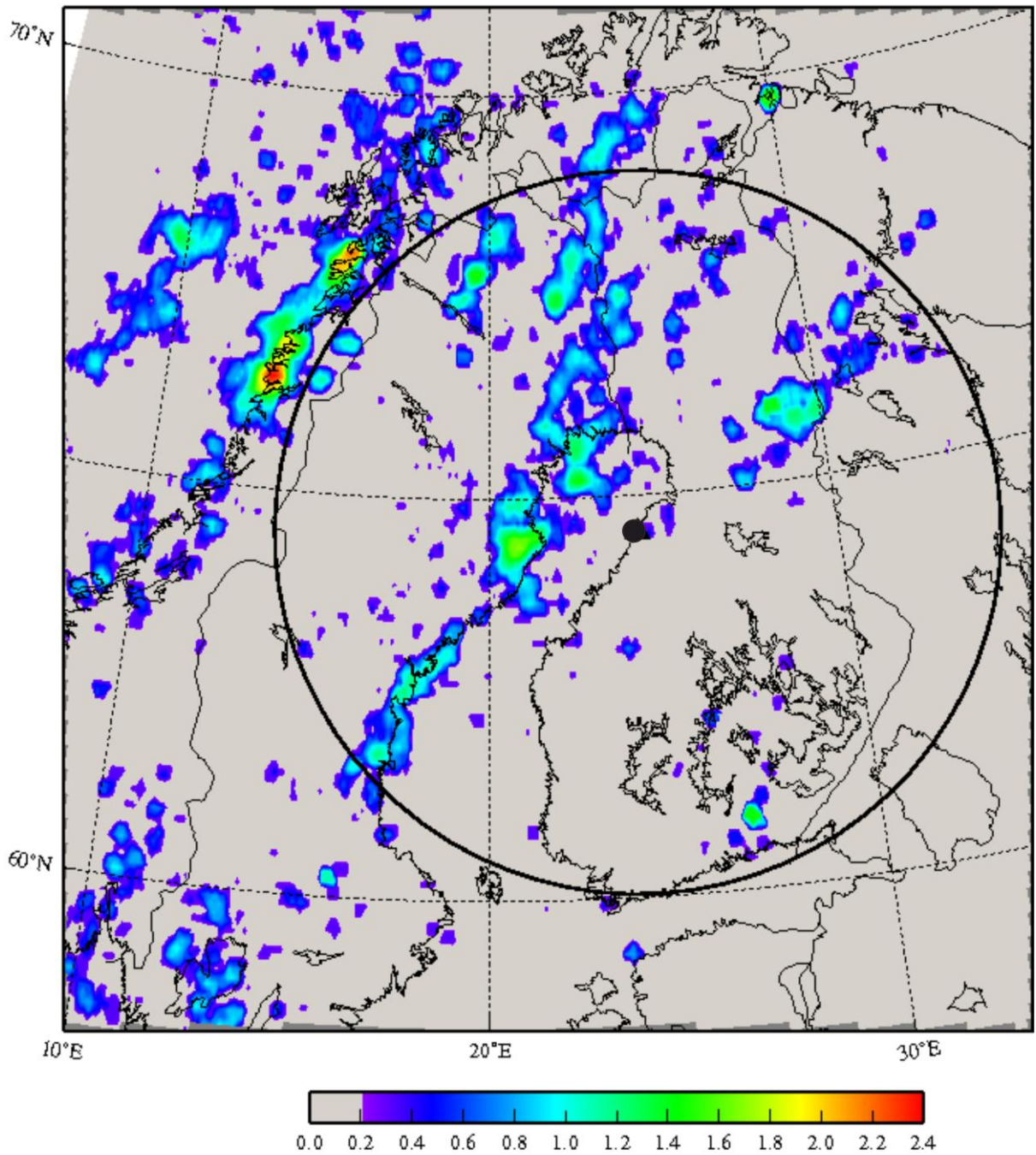


Figure 4.1.1. An earthquake density map of Fennoscandia in the period 1971-2012. The map displays, the cumulative number of instrumentally recorded earthquakes with magnitude ≥ 1 within $12 \text{ km} \times 12 \text{ km}$ grids. The black circle shows the limits of the study area, i.e. the radius of 500 km from Hanhikivi (black dot).

4.2 Historical seismicity

P. Mäntyniemi

The macroseismic record is of great importance in determining the geographical distribution of earthquakes. It is fortuitous that earthquakes occur along the western coast of the Gulf of Bothnia, so locating lesser earthquakes where they were felt often gives acceptable epicenters. The western

coastline of the Gulf of Bothnia has long been recognized as one area of enhanced seismicity in the Fennoscandian Shield. Early ideas about the spatial distribution of accumulating onshore seismicity observations were relatively accurate elsewhere as well, so the Vänern area in Sweden, Kuusamo in Finland, and the Oslo area in southeastern Norway were recognized as areas of recurrent lesser earthquakes. Instrumental studies gradually improved the location accuracy (e.g. Husebye et al., 1978; Bungum and Fyen, 1979).

On the other hand, large earthquakes are more likely to awaken wide interest and to be subjected to detailed studies. Early investigations in the study area were compiled by Moberg (1891, 1901) for the earthquakes of the 15 and 23 June 1882 and 4 November 1898 (UTC), respectively. They were mostly lists of observations sorted according to place, but a classification of the strength of earthquake effects on a three-degree intensity scale was included and the respective isoseismals were plotted on maps.

A renewed interest in large historical earthquakes in Fennoscandian began in the 2000s. For instance, Kebeasy and Husebye (2003) re-assessed the Kattegat earthquake of 1759 and Husebye and Kebeasy (2004) the Lurøy earthquake of 1819. Mäntyniemi (2004a) studied the earthquake of 16 November 1931 and its aftershock in Central Finland, and Mäntyniemi (2008b) reinvestigated the earthquake of 4 November 1898 in northern Finland and Sweden. Tatevossian et al. (2011, 2013) investigated earthquake activity in the Finnish-Russian border region in the spring of 1626 and in the winter of 1758, respectively. Further searches into the primary written materials of earthquake effects were made in the framework of the Hanhikivi projects (Mäntyniemi, 2012a,b; see also Appendix 2). Despite these efforts, many entries in parametric catalogues, such as those of Båth (1956) and Wahlström (1990), do not rely on a comprehensive investigation with macroseismic intensities assessed for each reported locality.

An effective and straightforward way to illustrate the strength of an earthquake is by plotting the area of perceptibility (example in Fig 4.2.1). Such plots show that a number of large-magnitude earthquakes ($M_L > 4$) occurred in the study region and its vicinity between 1882 and 1909, whereas the last thirty years exhibit much lower levels of seismic activity. The observation of temporal variation of seismicity is by no means novel, but nevertheless important for assessing seismicity and seismic potential. Although two and a half centuries is a very short time at plate interiors and a rather modest extension of the seismicity record back in time, it turns out to be very helpful.

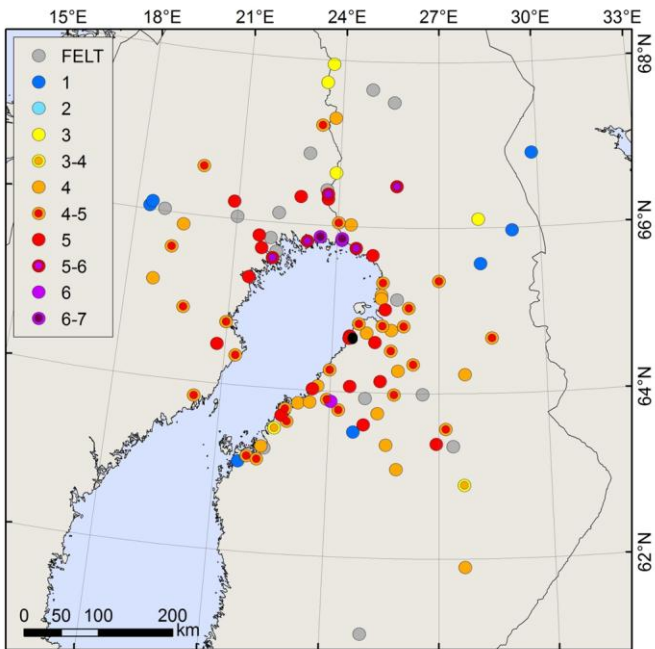


Fig. 4.2.1 An example of an area of perceptibility on 23 June 1882 (Mäntyniemi and Wahlström 2013). The respective earthquake magnitude is estimated at 4.6 on the moment magnitude scale. During the instrumental era, no such large areas of perceptibility have been recorded. The numbers are macroseismic intensities on the European Macroseismic Scale (Grünthal, 1998). Intensity 3 stands for weak ground shaking.

It is inviting to think that these large earthquakes occurred within the clusters of microearthquakes that sharpen up in recent seismicity maps based on an improved coverage of seismograph stations. However, associating an individual historical earthquake to a given fault or area is affected by uncertainties, and it is not possible to pinpoint the locations of these earthquakes. The areas of perceptibility spread over a large area, illustrating the capability of different parts of it to produce an earthquake of magnitude above 4. The areas of perceptibility of the earthquakes of 15 and 23 June 1882 and 4 November 1898 overlap largely, but not completely. The accuracy of location is sufficient to state that the respective epicentres were located in the Bay of Bothnia area, offshore or inland, which makes them important historical earthquakes in the study area.

The macroseismic observations may help to estimate the recurrence times of large earthquakes. It has been proposed that there may be some evidence for repeat earthquakes in the seismicity record of the study area. The earthquakes of 14 July 1765, 31 December 1908 and 15 June 2010 may have been located in the vicinity of Skellefteå and were of magnitude around 3.5-3.8 (Mäntyniemi, 2012b). All these earthquakes were reportedly felt on both the western and eastern coasts, but not at the bottom of the Bay of Bothnia. GregerSEN et al. (1991) defined earthquakes of magnitude 3.5 or larger as rare in the present-day seismicity pattern, so the claimed repeat Skellefteå earthquakes exceed this threshold slightly. It is speculated that the available seismicity record is not sufficient to capture the recurrence times of earthquakes of magnitude above 4 anywhere within the study area.

4.3 Fault plane solutions

M. Uski, A. Korja & B. Lund

Focal mechanisms are generally classified using Andersonian faulting theory (Anderson, 1951). He realized that the surface of the Earth must be a principal plane of stress, containing two of the three principal stress directions (σ_1 , σ_2 , σ_3). Hence the third principal stress direction is oriented normal to the Earth's surface. Two of the three principal stresses are horizontal (σ_H and σ_h) and one is vertical (σ_v). The value and direction of the principal stress defines the mode of faulting. If Mohr-Coulomb failure criterion is applicable and a coefficient of friction is 0.6 then the direction of rupturing can be predicted (Fig. 4.3.1). In a strike-slip stress regime, the maximum and the minimum principal stress are horizontal ($\sigma_H > \sigma_v > \sigma_h$), and rupturing takes place at approximately 30° angle to the maximum principal stress (σ_H). Reverse/thrust faulting takes place when the minimum principal stress is vertical ($\sigma_h > \sigma_h > \sigma_v$). The faults would strike perpendicular to the direction of σ_H , the dip direction is parallel to σ_H and dip angle is ~30°. Normal faulting only happens when maximum principal stress (σ_1) is vertical ($\sigma_v > \sigma_H > \sigma_h$), in which case the strike of the fault is *parallel to $\sigma_H = \sigma_2$* and the dip of the fault is ~60° (~30° to σ_1) (Fig. 4.3.2).

In Figure 4.3.2 the faulting mechanisms are associated with earthquake focal mechanisms, so called beach balls. They are projections on a horizontal plane of the quadrants of compression and tension of the lower half of a focal sphere surrounding the earthquake source. Fault plane solutions for the study area are presented in Figure 4.3.3 and Table 4.3.1.

The focal mechanisms in the study area show a combination of mostly strike-slip and reverse faulting conditions (Fig. 4.3.3). Slunga (1991) showed that in south-central Sweden, earthquake focal mechanisms are generally of strike-slip type and point to a NW-SE direction for the maximum horizontal stress. Reverse mechanisms occur more frequently further to the north. Recent focal mechanism determinations along the Swedish northeast coast (Fig. 4.3.3) corroborate these results as they show predominantly strike-slip faulting. In Finland, reverse and strike-slip mechanisms occur intermixed over the whole country.

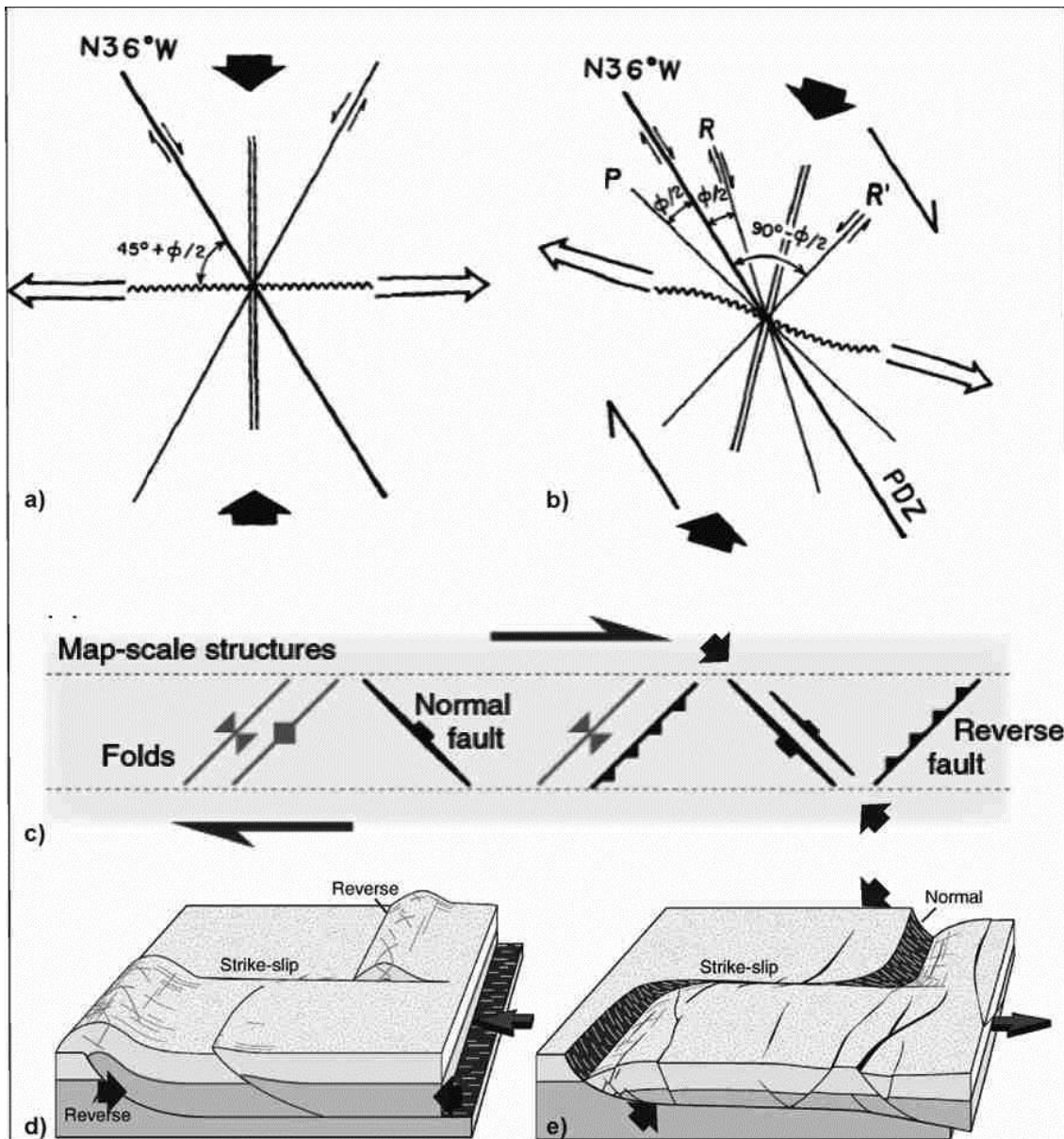


Figure 4.3.1. The relationships between compressional horizontal stress vectors and fault types. a) Coulomb-Anderson model of pure shear and b) Riedel model of right simple shear model for vertical dextral faults after Sylvester (1988). Double line represents orientation of extension (T) fractures and wavy line orientation of fold axes. P = P -fracture, R and R' are synthetic and antithetic shears, respectively, PDZ = principal displacement zone and Φ = angle of internal friction. Short black arrows denote the shortening axis and open arrows the elongation axis. c) Large scale structures forming along a dextral strike-slip zone after Fossen (2010). Transfer faults are strike-slip faults that form parallel to the direction of maximum horizontal stress in (d) contractional or (e) extensional settings after Fossen (2010).

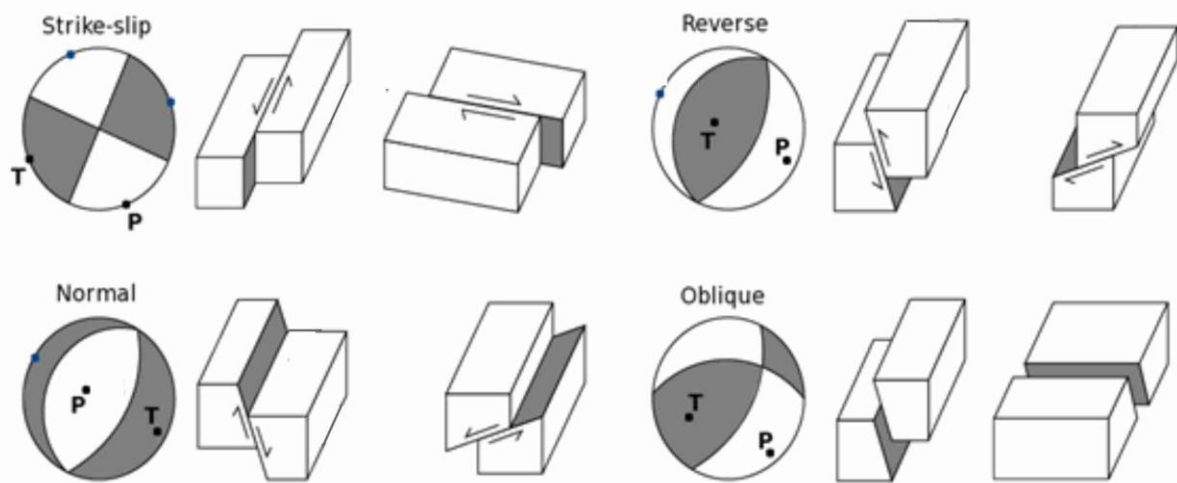


Figure 4.3.2. Earthquake focal mechanisms on stereographic projections (“beach balls”) and their associated faulting mechanisms modified after Shearer (2009). Fault mechanics are shown for both of the possible fault planes. Abbreviations: P - compression axis, T - tension axis.

Strike-slip is the dominant component of motion in and around the Gulf of Bothnia, although some normal faulting solutions have also been reported. First results from the Ostrobothnia local seismic network agree well with the general pattern. The mechanisms determined so far (no. 37-39, Table 4.3.1, Fig. 4.3.3) are of strike-slip type with a small component of extension, indicating transtension. The preferred nodal planes are trending approximately NNW-SSE, i.e. parallel to lineaments within the Raahe–Ladoga shear complex (Valtonen et al., 2014). Also in central Finland, a composite focal mechanism determined for the M_L 3.8 Lappajärvi event (no. 3, Table 4.3.1, Fig. 4.3.3) and its aftershock indicates strike-slip movement along N-S striking sub-vertical fault plane (Slunga and Ahjos, 1986).

In the Wiborg batholith, composite fault-plane solutions for the 2003 and 2011 earthquake swarms correspond to dip-slip motion along WSW-ENE and SW-NE striking subvertical fault planes (no. 30 and 36, Table 4.3.1, Fig. 4.3.3). In a nearby area, source mechanisms of 15 micro-earthquakes are characterized by strike-slip or reverse motion along subvertical structures (Saari, 1998). Thrust/reverse mechanisms have also been computed for two shallow events in southern Finland (no. 27 and 33, Table 4.3.1, Fig. 4.3.3).

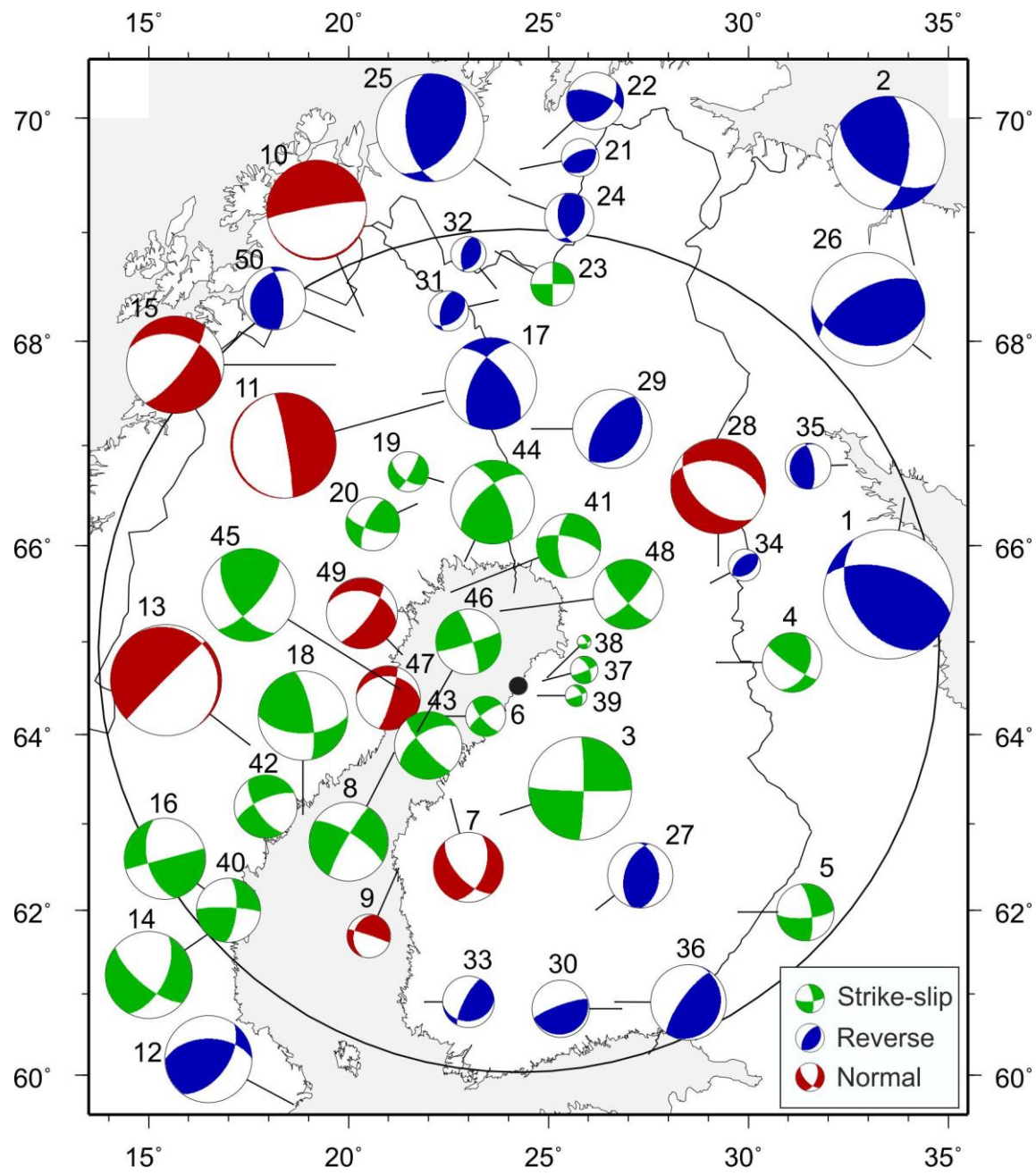


Figure 4.3.3. Focal mechanisms for events in Table 4.3.1. The area of a beach ball is scaled to magnitude

Table 4.3.1. A compilation of focal mechanisms for a selected set of earthquakes within the study area. Beach balls are shown in figure 4.3.3.

Ev.no	Date (YrMonDay)	Lat. °N	Lon. °E	M _L	Strike	Dip	Rake	Ref.*
1	19670520	66.60	33.70	4.8	287	57	64	A
2	19810410	68.70	37.20	4.2	122	52	39	A
3	19790217	63.08	23.92	3.8	1	85	-4	B
4	19801128	64.78	29.20	2.2	125	81	48	B
5	19810327	61.98	29.75	2.1	351	73	-17	B
6	19830428	64.20	22.43	1.5	139	73	-15	B
7	19830825	63.28	22.55	2.6	138	61	-134	B
8	19840302	63.80	21.14	2.9	302	73	-173	B
9	19840315	62.49	21.25	1.6	288	87	-122	B
10	19670413	68.10	20.80	3.7	260	85	-90	C
11	19750811	67.50	22.50	3.9	350	85	-90	C
12	19791223	59.63	18.62	3.1	36	54	51	C
13	19830929	63.89	17.53	4.1	225	88	-82	C
14	19860125	61.80	16.90	3.2	130	70	-146	C
15	19870419	67.80	19.80	3.6	38	74	-127	C
16	19870723	61.70	17.50	3.0	75	90	-35	C
17	19880516	67.50	22.00	3.4	320	60	40	C
18	19890725	63.03	18.82	3.2	90	57	-57	C
19	19870527	66.61	22.42	1.5	30	80	-34	D
20	19870718	66.50	21.23	2.0	205	70	20	D
21	19890109	69.46	24.64	1.7	45	30	70	E
22	19890713	69.63	25.27	2.5	45	45	35	E
23	19891116	68.75	23.60	1.9	0	90	0	E
24	19910413	69.29	24.08	2.6	30	45	120	E
25	19960121	69.34	24.00	3.8	174	53	64	E
26	19990817	67.84	34.56	4.3	240	60	70	F
27	20000511	62.02	26.25	2.4	358	42	76	G
28	20000915	65.79	29.23	3.5	133	47	-69	G
29	20010502	67.17	24.62	2.9	35	30	90	G
30	20030509	60.81	26.83	2.1	250	80	90	H
31	20070116	68.38	23.73	1.5	193	57	66	I
32	20070225	68.47	23.69	1.3	191	56	78	I
33	20070103	60.91	21.91	1.9	207	76	69	J
34	20060117	65.64	29.03	1.2	226	50	83	K
35	20060218	66.80	32.49	1.7	351	70	79	K
36	20111201	60.90	26.67	2.8	216	75	95	L
37	20130526	64.59	24.87	1.0	333	61	-9	M
38	20131207	64.62	24.98	0.5	333	66	-26	M
39	20131216	64.42	24.73	0.8	335	51	-9	M
40	20061020	62.03	17.62	2.4	5	70	8	N
41	20080918	65.52	22.56	2.4	282	67	-151	N
42	20081120	62.61	17.93	2.3	246	70	-154	N
43	20090505	63.68	21.48	2.5	237	57	-166	N
44	20090722	65.84	22.91	3.1	229	62	154	N
45	20100615	64.49	21.30	3.5	145	58	24	N
46	20110131	64.03	21.72	2.4	342	80	176	N
47	20111216	64.40	20.99	2.4	274	32	-15	N
48	20120518	65.33	23.80	2.6	44	75	165	N
49	20121002	64.87	21.34	2.6	286	38	-26	N
50	20130411	68.09	20.14	2.3	213	29	127	N

* References: A: Assinovskaya (1986); B: Slunga and Ahjos (1986); C: Arvidsson and Kulhanek (1994); D: Arvidsson (1996); E: Bungum and Lindholm (1996); F: Roth and Bungum (2003); G: Uski et al. (2003); H: Uski et al. (2006); I: Uski and Korja (2007); J: Saari (2008); K: Uski et al. (2012); L: Smedberg et al. (2012); M: Valtonen et al. (2014); N: SNSN database, Böðvarsson and Lund (2003).

In western Finnish Lapland, northern Sweden and Finnmark in northern Norway, the seismicity is mostly related to the PGFs, with events generally occurring to the southeast of the faults as expected due to their reverse mechanisms with southeasterly dip directions (e.g. Lindblom et al., 2011). Some additional events occur diffusely around the faults. Focal mechanisms computed for two earthquakes in northwestern Finland indicate thrust/reverse motion along fault planes striking NE-SW or NNE-SSW (no. 31, 32, Table 4.3.1, Fig. 4.3.3). The results agree well with focal mechanisms computed in the Stuoragurra fault zone in Finnmark, northern Norway (no. 21-25, Table 4.3.1, Fig. 4.3.3). The M_L 2.9 event in Kolari (no. 29, Table 4.3.1, Fig. 4.3.3) is among the strongest events observed in the region. The fault plane solution of this event suggests a pure thrust-faulting mechanism along gently dipping, NE-SW oriented fault surfaces (Uski et al., 2003). The solution agrees well with surface expressions of the nearby Venejärvi-Ruostejärvi-Pasmajärvi PGFs, which have been interpreted to be part of a listric fault system (Kuivamäki et al., 1998).

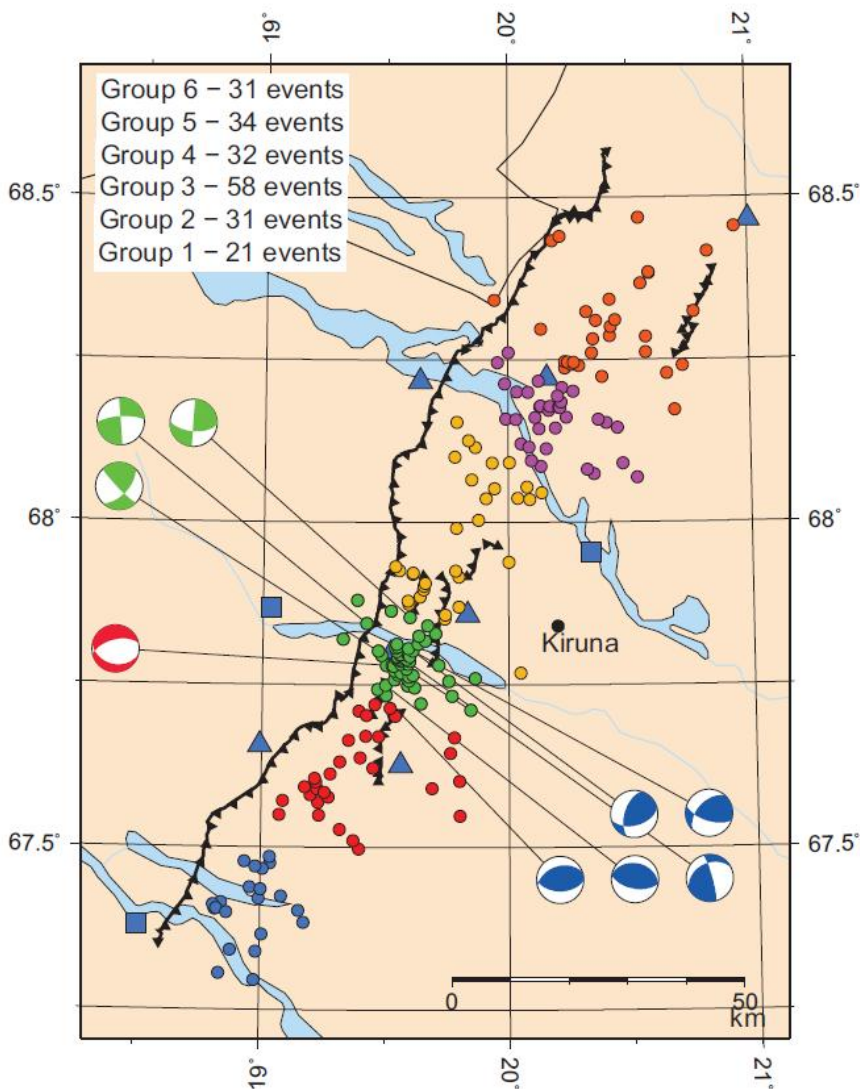


Figure 4.3.4. Fault plane solutions around Pärvie post-glacial fault system (Lindholm and Lund, 2011).

In the vicinity of the Pärvie post-glacial fault, the focal mechanisms are very variable, both in terms of faulting regime and nodal plane directions (Fig. 4.3.4; Lindblom and Lund, 2011). A majority of the 212 mechanisms show dominant sinistral strike-slip faulting, 25 % have reverse faulting and 15 % normal faulting. The strain along the fault is in general reverse with obliquity toward strike-slip. This indicates transpressional regime.

Available source mechanisms for the Kuusamo region suggest dominantly reverse or thrust type faulting along NNE–SSW striking fault planes, albeit contrasting mechanisms and variable styles of fault slip are also found. A normal faulting mechanism has been computed for the M_L 3.5 earthquake that occurred in Kuusamo on September 15 2000 (no. 28, Table 4.3.1, Fig. 4.3.3; Uski et al., 2003).

The source mechanism for the M_L 4.8 Kandalaksha event implies predominantly reverse motion along a fault plane with NW–SE strike (no.1, Table 4.3.1, Fig. 4.3.3). A reverse mechanism with different strike orientation, N-S, has been computed for a shallow earthquake that took place on 18 February 2006 at the western flank of the Kandalaksha Gulf (no. 35, Table 4.3.1, Fig. 4.3.3).

5 Current tectonic framework

5.1 Plate movement and current stress field

P. Koskinen & A. Korja

Although the absolute motion of Northern Europe in the no-net-rotation (NNR) reference frame is northeastward (Kreemer et al., 2003), the largest component affecting the stress field in both the western Eurasian and North American plates is the rotation around their common Euler pole. This causes the spreading of the Atlantic Ocean and orients the maximum horizontal stress directions in Northern Europe in a WNW–ESE to NW–SE direction (Kreemer et al., 2003; Heidbach et al., 2008). This observation is supported by a study by Gölke and Coblenz (1996), where they modeled the origins of the European stress field (Fig. 5.1.1). They concluded that regardless of the boundary forces at the southern and eastern margins, the orientation of the overall maximum horizontal stress field in Europe remains WNW-ESE to NW-SE and the magnitude of the horizontal tectonic stresses in the continental regions are in the order of 20-30 MPa when averaged over a 100 km thick lithosphere.

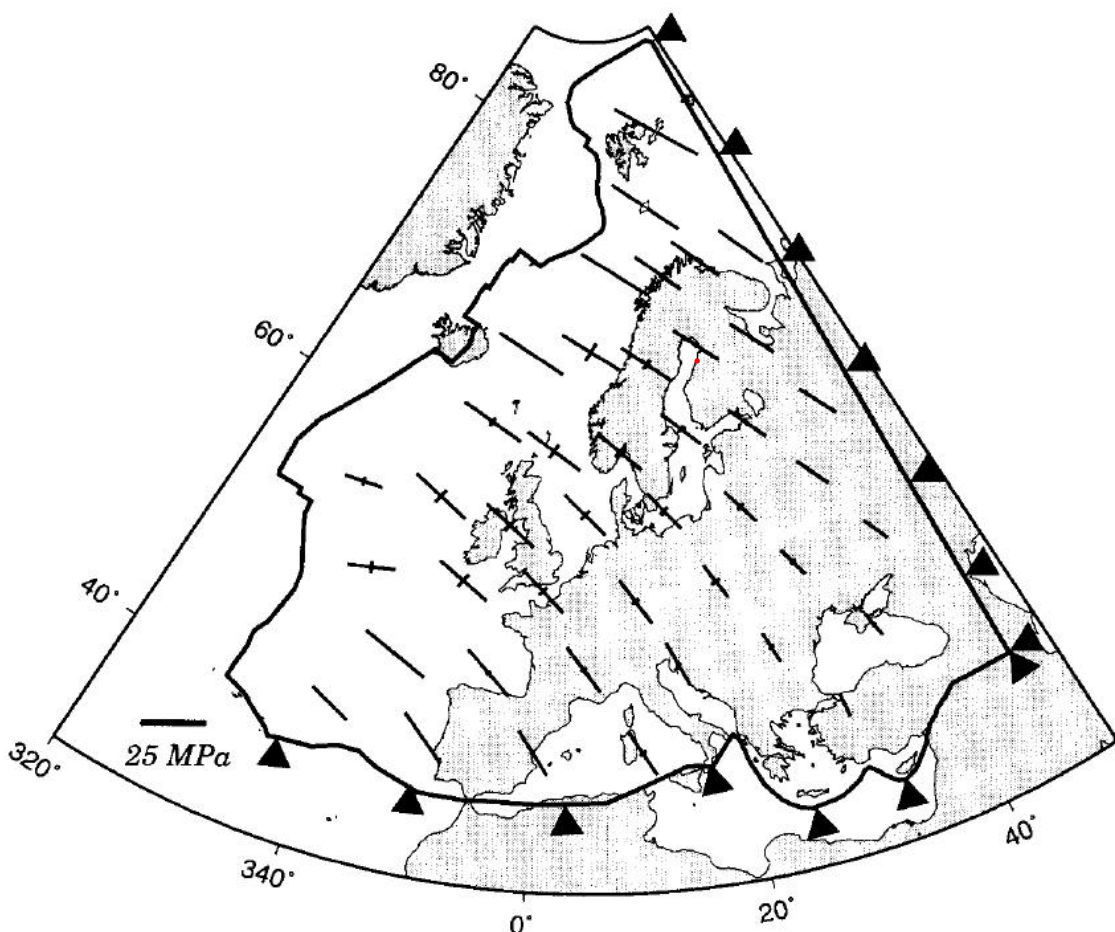


Figure 5.1.1. A modeled for European stress field (Gölke and Coblenz, 1996).

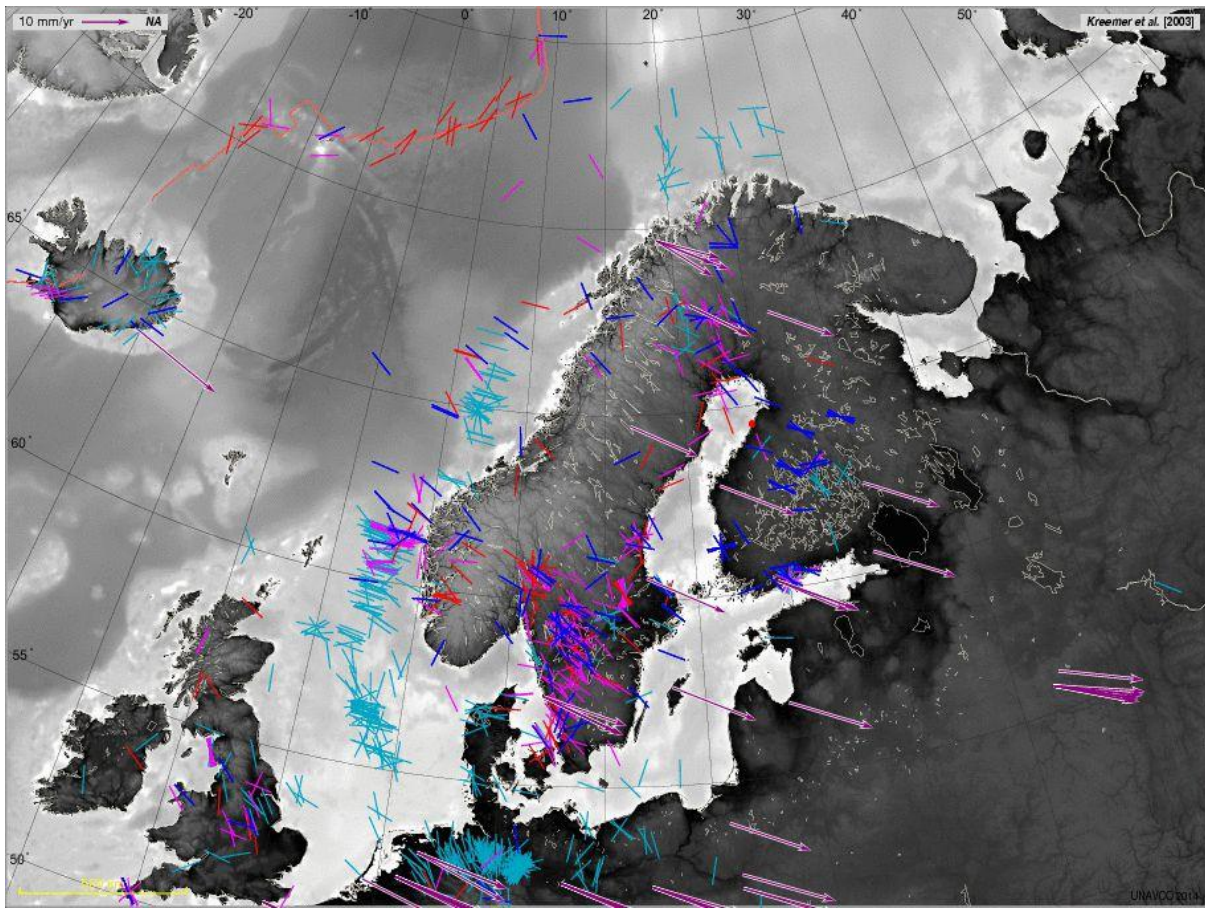


Figure 5.1.2. A comparison of the stress indicators (classes A-D; Heidbach et al., 2008) and the movement of Fennoscandia relative to North America (Jules Verne Voyager, 2011). Purple vectors are observed geodetic velocities that have been rotated into a best-fit model reference frame for the model GSRM 1.2. Stress regimes are indicated with colours: pink- normal ($\sigma_v > \sigma_H > \sigma_h$), green- strike-slip ($\sigma_H > \sigma_v > \sigma_h$); light blue and blue – thrust ($\sigma_H > \sigma_h > \sigma_v$). Hanhikivi site: red dot.

The azimuth of the plate motion direction relative to North America is $\sim 119^\circ$ for southernmost Finland and 128° for northern Lapland, with a standard deviation of $\sim 4^\circ$ when using the ITRF2000 reference frame (UNAVCO Plate Motion Calculator, 2012). Thus, the azimuth falls between 115° and 132° and the azimuth increases from south to north. For Sweden, the same azimuth interval is 110° - 127° . The movement of the Eurasian relative to the North American plate is compared with the observed regional stress field indicators from the World Stress Map 2008 database (Heidbach et al., 2008) in Figure 5.1.2.

5.2 Orientation of the maximum horizontal stress

P. Koskinen & A. Korja

The azimuth data from the World Stress Map (WSM) 2008 database (Heidbach et al., 2008) suggests that the maximum horizontal stress in Fennoscandia is oriented in a WNW-ESE to NW-SE direction (Fig. 5.2.1). The orientation of maximum horizontal crustal stress indicators (σ_H) in Finland and

Sweden are shown in an azimuth histogram in Figure 5.2.2. The data points in classes A-C represent different observation methods and different depths. Because most of the data points are from shallow depths (< 1km), they indicate the state of stress in the upper most crust only. In the upper most crust the stress regime is mainly thrust (reverse) in Finland and Sweden (Fig. 5.2.1). Along the eastern coast of the Bay of Bothnia, both the maximum and minimum principal stresses are horizontal and strike-slip faulting takes place.

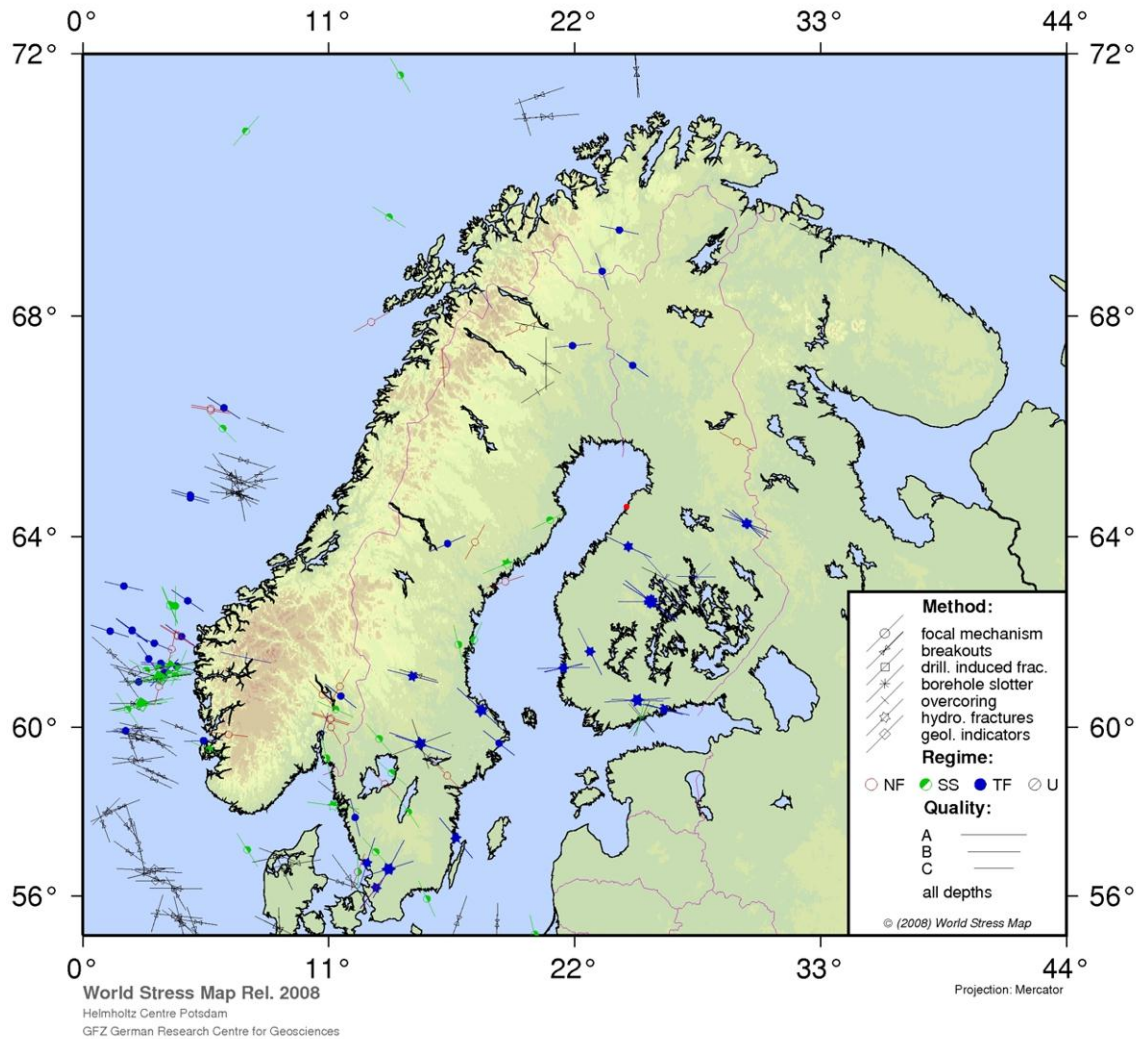
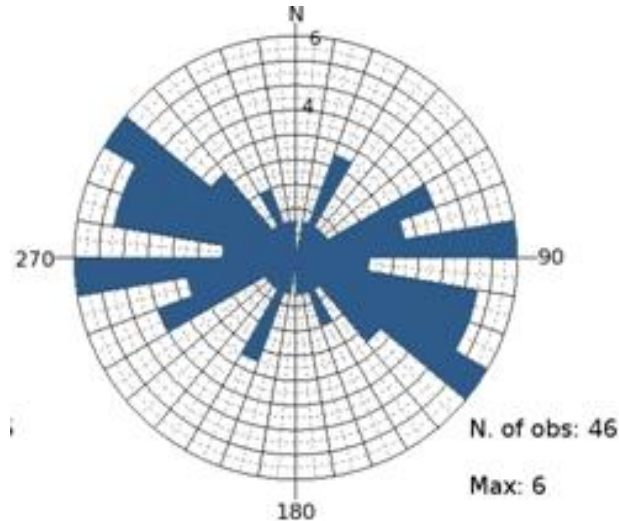


Figure 5.2.1. Orientation of maximum horizontal crustal stress (σ_H) indicators in northern Europe from the World Stress Map database (Heidbach et al., 2008). The methods used for determining the stress orientation are presented with symbols described in the legend. Length of the line indicates quality of the stress indicator (A-C). Stress regimes are indicated with colours: red - NF normal ($\sigma_v > \sigma_H > \sigma_h$); green - SS strike-slip ($\sigma_H > \sigma_v > \sigma_h$); blue - TF thrust ($\sigma_H > \sigma_h > \sigma_v$) and black - U undetermined.

The dominating direction of the maximum horizontal crustal stress indicators (σ_H) is NW–SE (Fig. 5.2.2) with a minor peak in a W–E direction caused by data from southern Finland. The stress map data are corroborated by recent earthquake fault plane solutions in (Table 4.3.1. and Fig. 4.3.3; Bungum and Lindholm, 1996; Saari and Slunga, 1996; Saari, 2008; Uski et al., 2006; Lindholm and

Lund, 2011). Henderson (1991) inverted the focal mechanisms of Slunga (1991) for the causative state of stress. He found a well-constrained direction of maximum horizontal stress in a NW-SE direction indicating a strike-slip stress state for southern Sweden. In northern Sweden, a predominant direction could not be determined.

Figure 5.2.2. A histograms of the orientation of maximum horizontal stress in Finland and Sweden north of latitude 60°N. Data in classes A-C in the WSM database (Heidbach et al., 2008) are presented as degrees from north. Accuracy for quality: A ±15°, B ±15-20°, C ±20-25°



5.3 Surface strain

P. Koskinen & A. Korja

Vertical ground motion taking place in Fennoscandia is mostly attributed to glacial isostatic adjustment (GIA), commonly referred to as post-glacial rebound (Ågren and Svensson, 2007). It is caused by the slow return flow of mantle material back to its original position prior to the depression of the lithosphere by the ice load of the latest glaciation, which ended around 10,000 years ago (Fig. 5.3.1). The still remaining isostatic imbalance is being adjusted by slow land uplift and subsidence. The land uplift is centered in northwestern Sweden and the Bay of Bothnia i.e. within the study area. According to recent land uplift model (Figs. 5.3.2-5.3.3; Milne et al., 2001; Johansson et al., 2002; Ågren and Svensson, 2007; Nørbech et al., 2008), the maximum rate of uplift is 8-9 mm/a. The absolute land uplift calculated by Nørbech et al. (2008) based on velocities from the NKG2005LU model (Nordiska Kommissionen för Geodesi (NKG) model 2005; Ågren and Svensson, 2007) is shown together with the World Stress Map stress indicators (Heidbach et al., 2008) in Figure 5.3.2. Uplift and the trends of PGF faults are compared in Figure 5.3.3.

Recently, Cai and Grafarend (2007) and Scherneck et al. (2010) have reevaluated the strain rates in Fennoscandia using the continuous GPS observations from 36 sites of BIFROST network (Fig. 5.3.4). The uncertainties are still rather large, in the order of 30-50%. The strain rate field in central Fennoscandia, where the uplift rate of post-glacial rebound is the highest, is dominated by extension of 5 nanostrain/a. Compression between -6 and -1 nanostrain/a prevails in the southeastern parts, where the uplift rate is smaller. As noted by Cai and Grafarend (2007), the uplift is also accompanied

by lateral strain in the order of 1-2 nanostrain/a that is caused by the Earth's surface curving, tilting and rising.

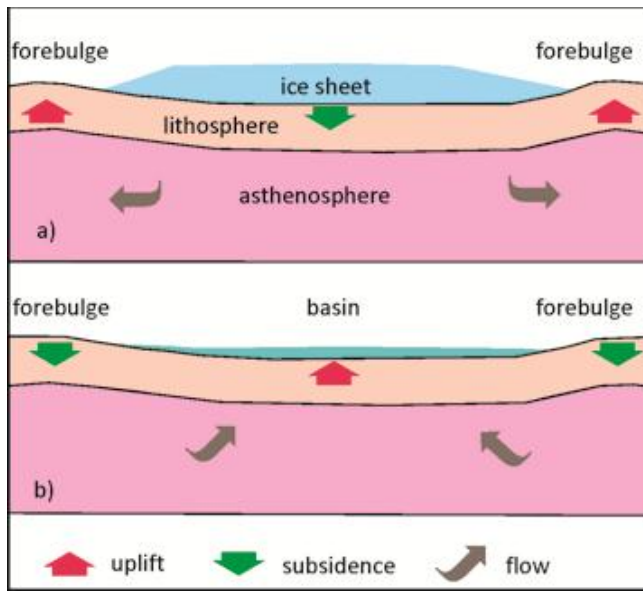


Figure 5.3.1. A schematic model of the uplift and subsidence processes during a) glaciations and b) deglaciation.

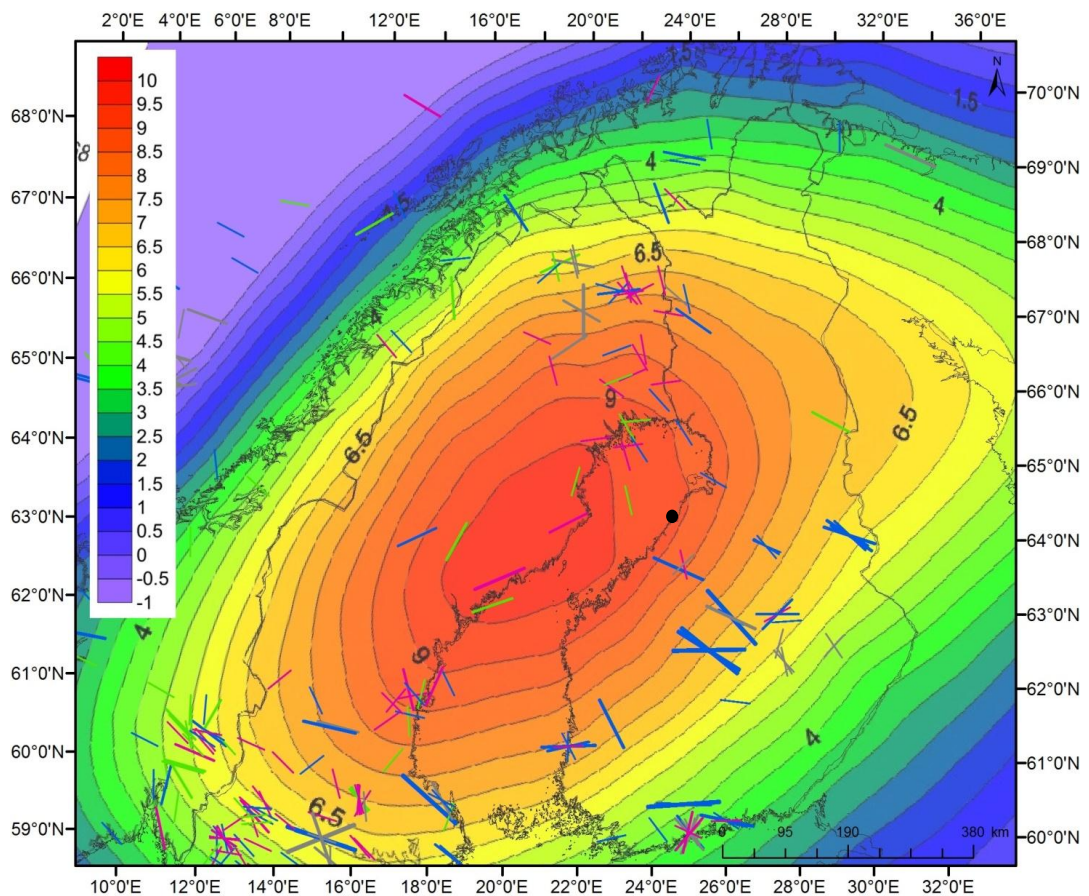


Figure 5.3.2. A comparison of the absolute land uplift velocity model (NKG_RF03vel; Nørbech et al., 2008) and stress indicators (Heidbach et al., 2008). Uplift velocity is expressed in mm/a. Stress regimes are indicated with colours: red -NF normal ($\sigma_v > \sigma_h > \sigma_l$); green -SS strike-slip ($\sigma_h > \sigma_v > \sigma_l$); blue - TF thrust ($\sigma_h > \sigma_l > \sigma_v$). Hanhikivi site: black dot.

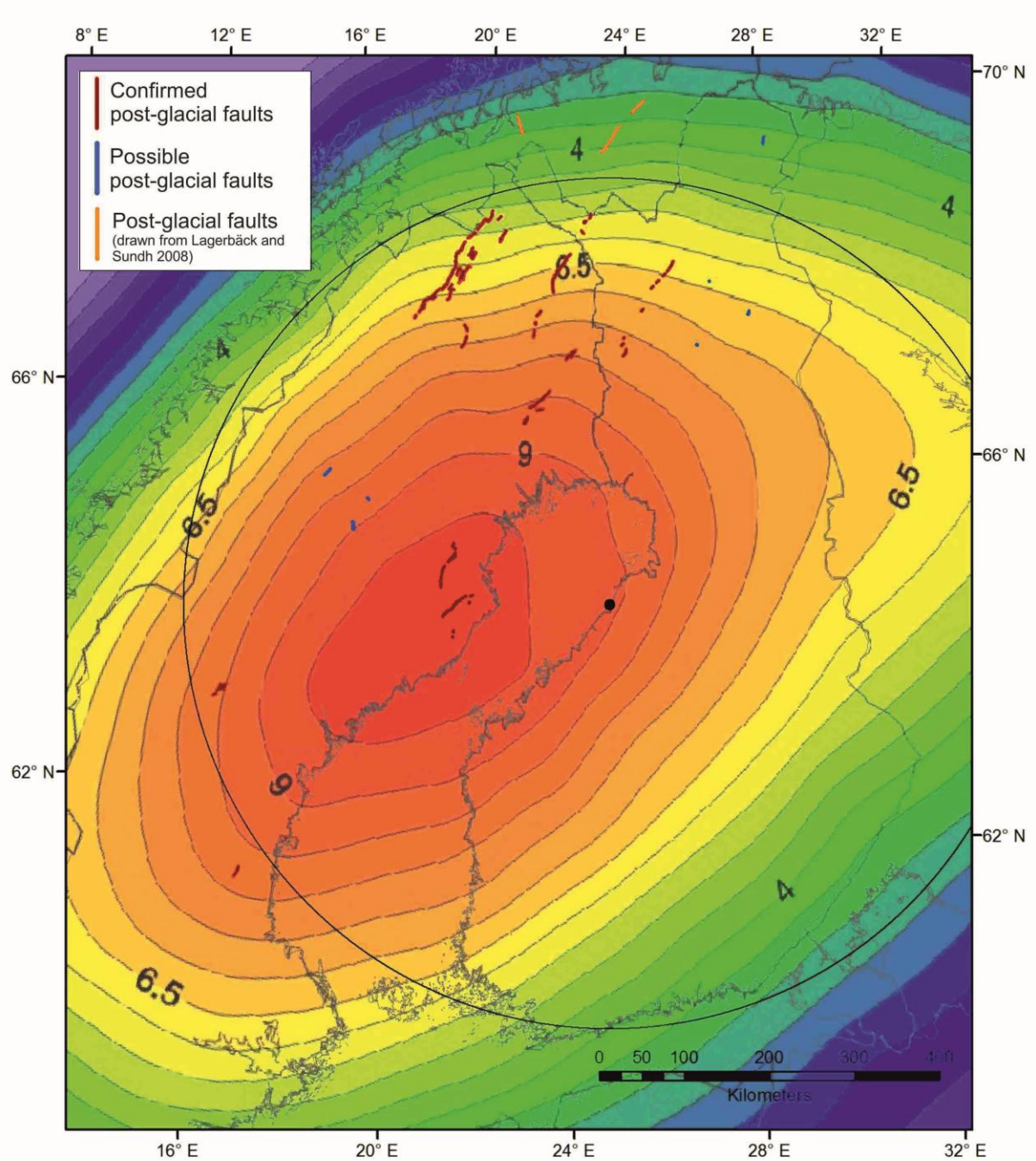


Figure 5.3.3. Absolute land uplift according to the model NKG_RF03vel (Nørbech et al., 2008) and post-glacial faults from Fennovoima database (section 2.7) in Lapland and central Sweden area.

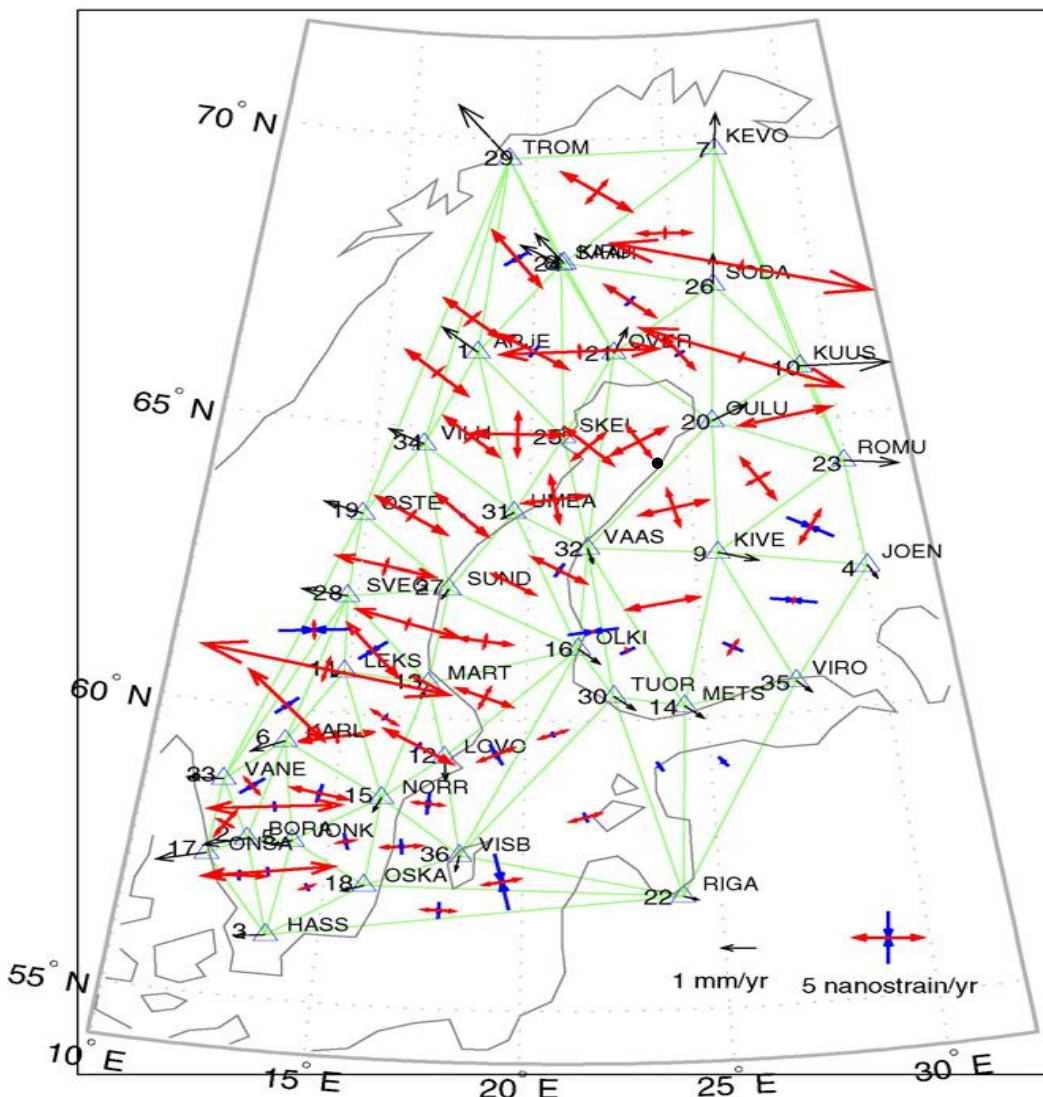


Figure 5.3.4. A map of the principal strain rates and associated residual velocities in Fennoscandia based on GPS triangulation between 36 BIFROST sites. (Cai and Grafarend, 2007). Red arrow – direction of extension; blue arrow – direction contraction; black arrows – direction of residual velocity.

5.4 Changes in the stress field imposed by changes in crustal and lithospheric thickness

A. Korja

Pascal and Cloething (2009) suggested that the stress field in Scandinavia is affected by local and regional changes in the thickness of the crust and lithosphere and in topographic elevation (Fig. 5.4.1) in addition to tectonic forces or rebound stresses. The local changes affect the level of gravitational potential energy (GPE) which in turn modifies the horizontal stresses stemming from plate movements and changes in the plate velocity fields (Ghosh et al., 2009; Pascal and Cloething, 2009; Zhu and Tromp, 2013). Earlier Hagaseva (1985) suggested that the large thickness changes of the crust modify the effect of ridge push forces on continental margins locally. Fejerskov and Lindholm (2000) suggested the change in crustal thickness to affect the local stress fields in Norway.

According to them, in areas with thick rigid crust, the ridge push force is distributed over larger width range and thus the tectonic stress and earthquake activity is reduced. Areas with thinner crust are marked by higher stress levels and seismic activity, respectively.

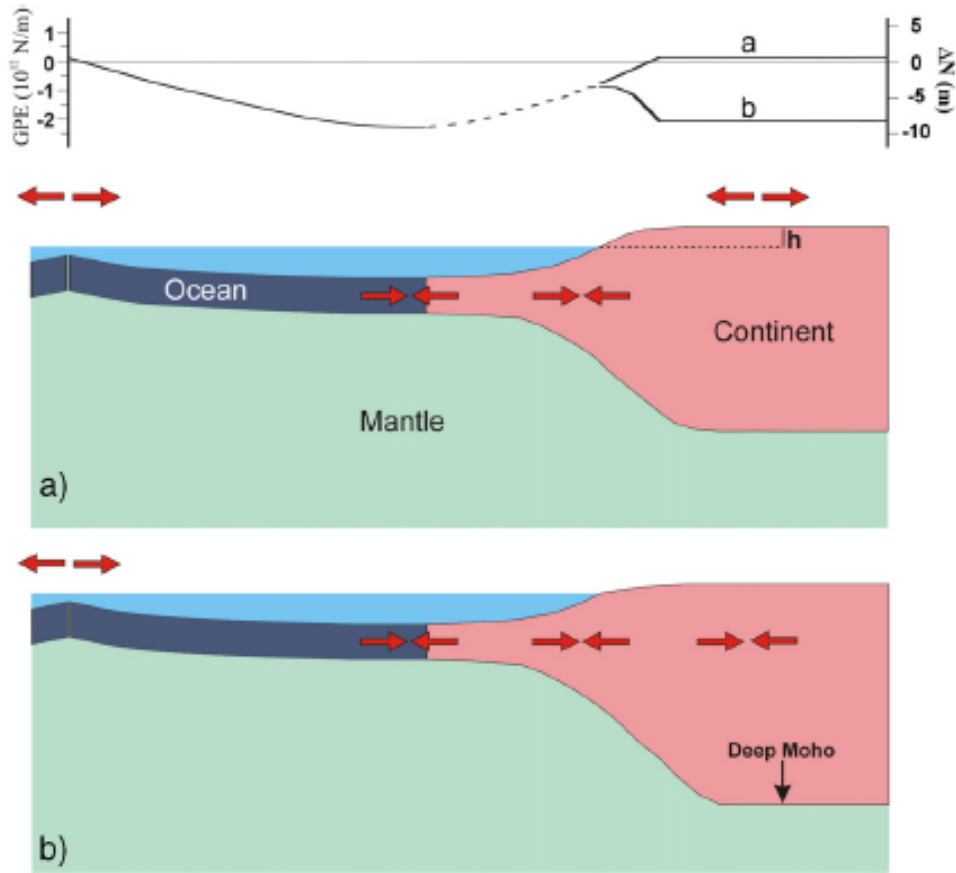


Figure 5.4.1. A cartoon illustrating how gravitational stresses affect a passive continental margin (Pascal and Cloetingh, 2009). The upper panel shows the variation in gravitational potential energy (GPE) and its associated geoid undulations. a) Continental landmasses are elevated and their GPE level exceeds GPE values at mid-oceanic ridges: the continent is under extension and adds a lateral compressive force on its passive margins. b) Continental landmasses are characterized by thick crust and subdued topography: ridge push forces dominate both onshore and offshore.

The study area includes the thick Precambrian core of the continental Eurasian plate (Grad et al., 2009; Fig. 5.4.2). Recently, several authors have published crustal thickness maps or the depth to the Moho boundary maps of Fennoscandia (e.g. Grad et al., 2009; Artemieva and Thybo, 2013). In all of the maps, the crustal thickness varies markedly across the study area. The largest thicknesses (> 50-65 km) are found in central and southern Finland, in the Bothnian Sea and in western Lapland. The Bay of Bothnia and its surroundings, Eastern Lapland, Kola and Karelia and rapakivi areas are characterized by thicknesses around 40 km. Northern and central Sweden are characterized by moderate thicknesses of 45-50 km in depth. A marked thinning of the crust takes place below the Scandes, where the crust thins to 36 km over a short distance.

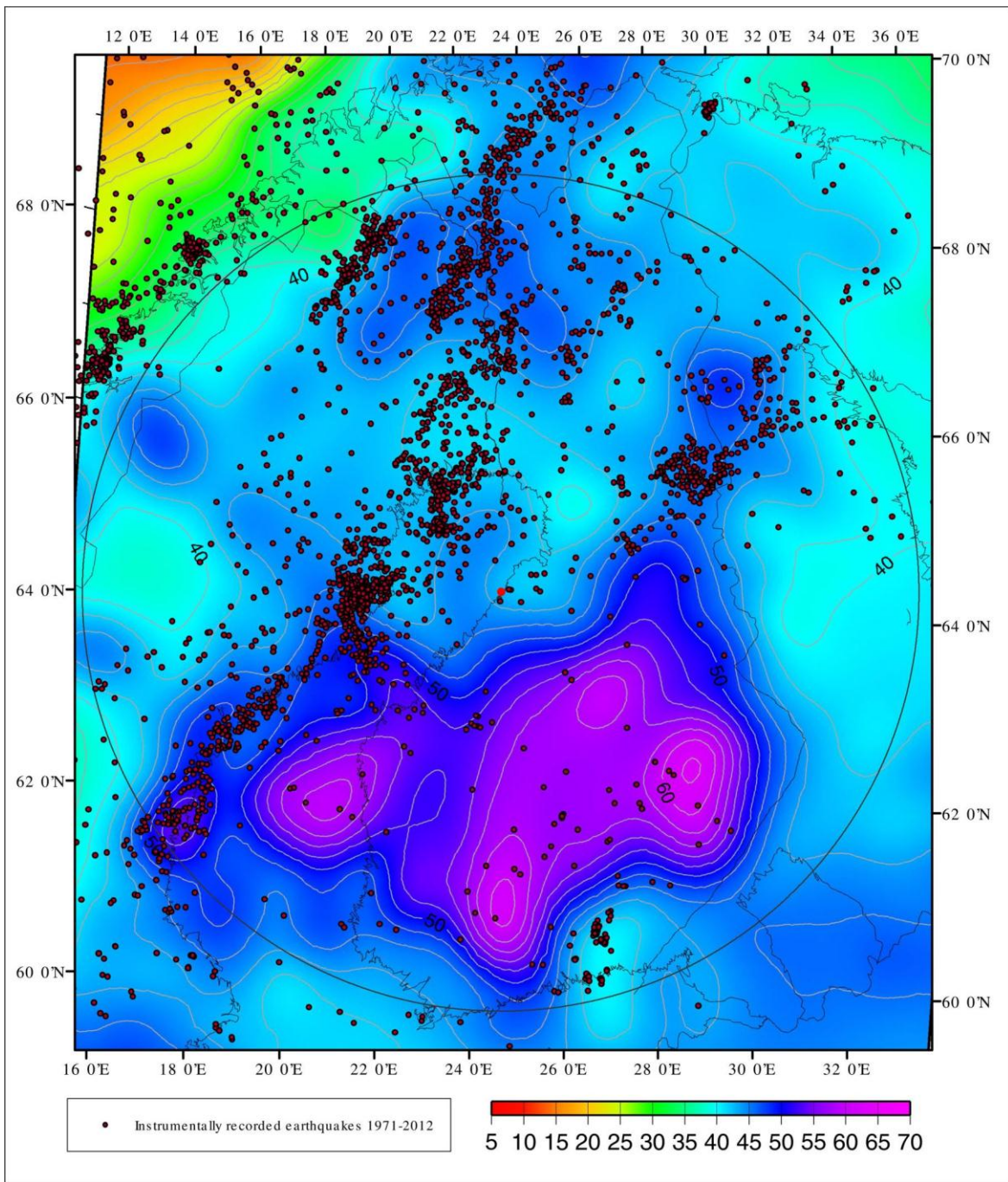


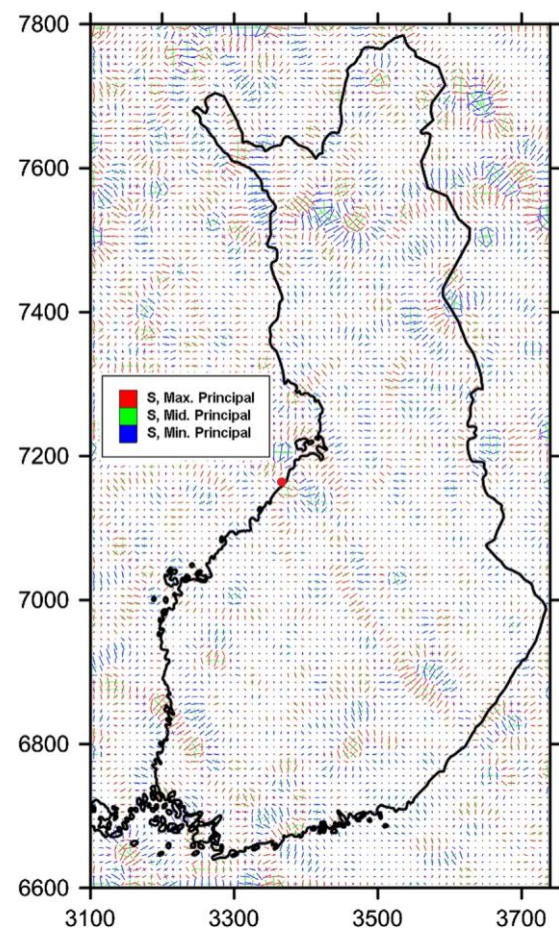
Figure 5.4.2. A Moho-depth map after Grad et al. (2009) and seismicity in Fennoscandia.

The changes from thick (65-55 km) to moderately thick or normal crust (45-48 km) takes places over rather narrow zones, 20-30 km in width, or rather steps. A step in the Moho boundary is displayed as a gradient zone in interpolated maps. Where a step in the Moho is accompanied by a marked change in density, local to regional scale GPE energy anomalies and associated horizontal stress are found. Potential sites are e.g. the southwestern and northwestern part of Central Finland lithotectonic unit or the Norra Kvarken region.

Most of the abrupt changes in the Bouguer map are not stemming from crustal thickness changes but from density changes in the upper crust, which may induce more local anomalies of the stress

field. Elo and Pirttijärvi (2013) have suggested a method where the local stress anomalies (Fig. 5.4.3) created by local lateral density variations (GPE) in the uppermost crust (0-780 m) can be mapped using the vertical gradient of the Bouguer anomaly data. They display the results as maps of principal maximum stress (15-20 MPa) and principal minimum stress (-20 - -15 MPa) representing localities of compression and tension, respectively (Fig. 5.4.3). The most prominent linear features in the stress map are the NW-SE trending red maxima (principal maximum stress anomalies) accompanied by strings of blue minima (principal minimum stress anomalies) associated with large granites within the Raahe-Ladoga shear complex and Satakunta graben southwest of the Kynsikangas shear zone. Yet another anomalous area is found in Central Lapland, where perpendicular set of NW-SE and NE-SW trending maxima and accompanying minima are found in proximity to the Suasselkä PGF.

Figure 5.4.3. A map of the directions of principal maximum (red), medium (green) and minimum (blue) stress components induced by local mass anomalies in the upper most crust (Elo and Pirttijärvi, 2013). The stresses are calculated from the vertical derivative of the Bouguer map of Finland. The maximum value of principal maximum stress is around 15-20 MPa and the maximum value of principal minimum stress is -15 - -20 MPa. Hanhikivi site: red dot.



Recently several authors have published lithospheric thickness maps of Europe (Artemieva et al., 2006; Artemieva, 2009; Jones et al., 2010). In all of these maps, the lithospheric thickness varies markedly across the study area. The changes in the lithospheric thickness mirror those of crustal thickness. Large thicknesses (>200 km) are found in the eastern parts of the Fennoscandian shield, and smaller thicknesses in the Bay of Bothnia and in Lapland. The largest thickness change takes place across the Scandes. Changes in both crustal and lithospheric thicknesses imply changes in the thermal regime of the crust and in the theoretical thickness of the seismogenic zone (Moisio and Kaikkonen, 2012).

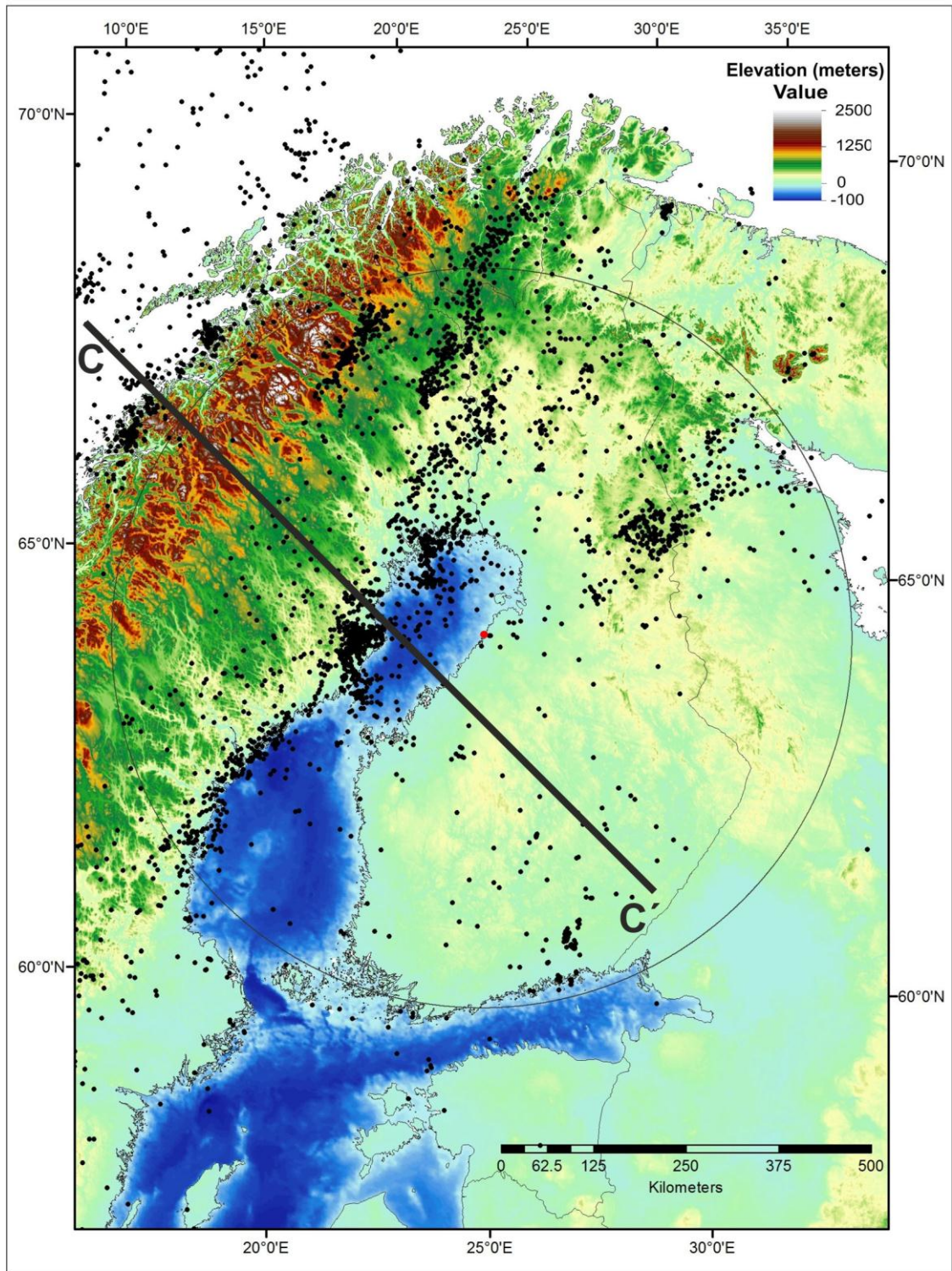


Figure 5.4.4. The correlation of topography and seismicity (instrumental events 1971-2012, Fig. 2.8.1.2) in Fennoscandia. Line C-C' locates a topographic cross-section in figure 5.4.5.

The topography (Figs. 2.2.1 and 5.4.4) changes from east to west and south to north. The changes mimic to some extent the geological boundaries. The most abrupt changes take place in an NW-SE direction (Figs. 5.4.4 and 5.4.5). The platform margin to the Atlantic Ocean changes abruptly in elevation to the Scandian mountain belt along the Norwegian margin which reaches the topographic

heights of 2 km. Fejerskov and Lindholm (2000) have estimated that the topographical load might induce stresses between 10–140 MPa depending on the degree of compensation. The subdued topography in the Precambrian hinterland areas in northern Sweden are shallowly tilting towards the Gulf of Bothnia basin to the east–southeast. In contrast to Sweden, the Finnish topography tilts gently towards the Gulf of Bothnian basin to the west. Although the topography is even more flat-lying it reaches the topographic high of 500 m close to the Archean–Proterozoic boundary zone. A higher topography with a mean height of 400 m prevails along the western flank of the White Sea graben. The sea areas and inland seas that are characterized by topographical depressions have generally thinner crust than the surrounding onshore areas. The thickest parts of the crust are characterized by low topography whereas the highest mountains in the Scandes are characterized by the lack of crustal roots or rather thin crust. This suggests that the mountains are not isostatically compensated from below and that external forces are acting on the Fennoscandian margin.

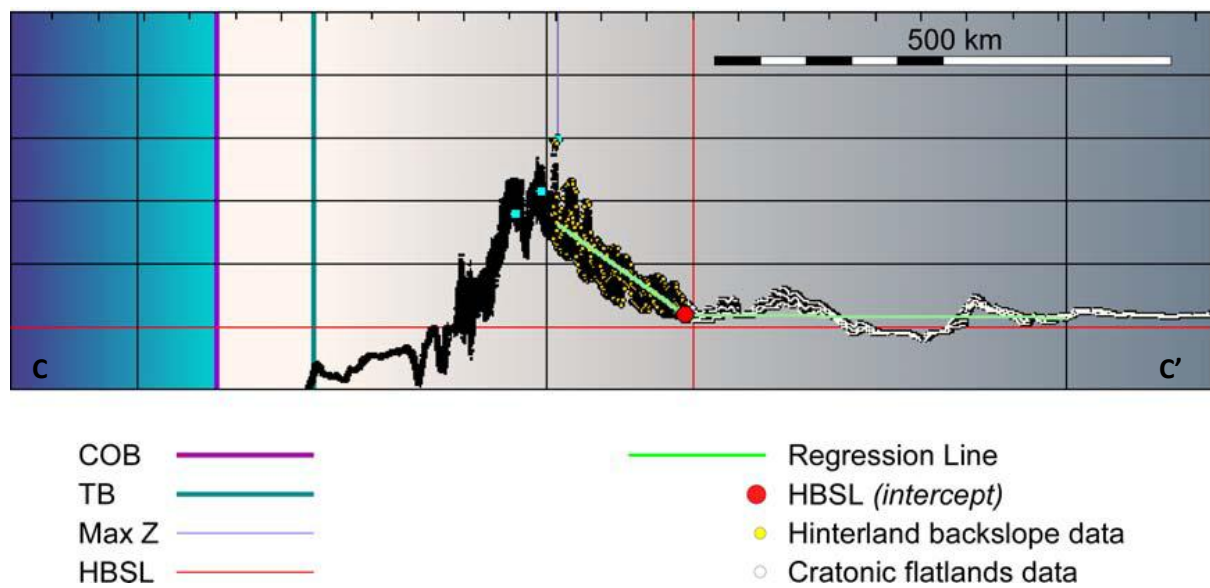


Figure 5.4.5. A topographic cross-section C-C' across Scandinavia by Redfield and Osmundsen (2013). The cross-section is in NW-SE direction i.e. parallel to horizontal stress caused by the opening of the Atlantic. The cross-section reveals a pronounced asymmetry and a well-defined hinterland break-inslope where the change from craton to hinterland takes place. The location of the profile is found in Fig. 5.4.4. and 7.1.2. Abbreviations COB- continent ocean boundary; TB – taper break; MAXZ- maximum height; HBSL- hinterland break inslope.

Because potential energy differences need to equate with time, extension of highly elevated areas is expected with associated regional scale anomalies of the stress field. Topography and seismicity are compared in Figure 5.4.4. Zones of increased seismicity seem to localize close to topographic gradients.

5.5 Seismogenic thickness and the depth range of deformation zones and earthquakes

M. Uski, B. Lund & A. Korja

Earthquakes result from frictional instabilities on sliding surfaces i.e. faults. Slunga (1991) argued that aseismic slip along a fault in Sweden is generally more common than seismic slip. Seismicity is not controlled by the mechanical properties of bulk rocks, but by the properties of faults. A change with depth from stick-slip to stable sliding corresponds to the seismic–aseismic transition that takes place close to the quartz-rich upper-middle crust brittle-ductile transition (e.g., Pasquale et al., 2001). Thus, the lowermost brittle-ductile transition zone in quartz-rich rocks is regarded as the lower boundary of the seismogenic layer – a layer brittle enough for earthquakes to occur. Similar conclusions were already made by Sibson (1982) who hypothesized that the base of the brittle-ductile transition marks the maximum depth of large earthquakes.

Kukkonen and Peltonen, (1999) and later Kaikkonen et al., (2000) have constructed rheological “jelly sandwich” profiles for northeastern Fennoscandia. A rheological “jelly sandwich” model assumes that the upper crust and mantle are strong, brittle layers whereas middle and lower crust consist of a series of alternating weak, ductile layers and strong, brittle layers. Kukkonen and Peltonen (1999) have derived their rheological profile from a xenolith-controlled geotherm for the Kaavi kimberlite field in the Karelian lithotectonic unit. Their model indicates that the first upper brittle-ductile transition takes place below the depth of 30 km but in a close proximity to the middle-lower crustal boundary. Their model further suggests that the upper part of the lower crust (35-45 km) may be brittle, whereas the lower part behaves in a ductile way.

5.5.1 Crustal layering and depth extent of the ancient deformation zones

The thickness of the crust varies considerably (36-65 km) within Fennoscandia (Fig. 5.4.2). The eastern parts have a well-developed three-layer crust comprising of upper (0-15 km), middle (10-32 km) and lower crust (32-65km) with well defined layer boundaries (Korja et al., 1993; Figures FIRE 1 & 3, BABEL 3 & 4). Although the thickness of the crustal layers varies, the boundary of the middle to lower crust is rather smooth and located at around 32 ± 5 km (Korja et al., 1993). The largest differences in thickness values are caused by the presence or absence of mafic, high velocity lower crust. Where the crust is thick (> 50 km), the high velocity layer is thick (5-30 km) and where the crust is thinner the layer is very thin (< 5 km) or absent.

Recently deep seismic reflection profiles have imaged the layered crustal structure in more detail (Fig. 5.5.1.1.; BABEL Working group, 1993; Korja and Heikkinen, 2005, 2008; Kukkonen et al., 2006; Korja et al., 2009). The studies confirm the idea that the crust is layered in large areas and that the

layering is disrupted by major deformation and suture zones. The profiles also suggest that most of the deformation zones outcropping at surface have only a limited vertical extent. They seem to either terminate or to flatten out at the upper-middle crustal boundary, which is inferred to be a major décollement (Fig. 5.5.1.1; Korja and Heikkinen, 2008; Korja et al., 2009). Some major deformation zones or rather tectonic block boundaries extend to the middle-lower crustal boundary and a few even penetrate through the Moho boundary (Venejoki shear zone, Raahe-Ladoga shear complex). The décollement is well-defined and found at a depth of approximately 10 km in the Central Finland lithotectonic unit (Central Finland granitoid complex, the southern part of the Bay of Bothnia) and in central Lapland (Karelia lithotectonic unit; Central Lapland granitoid complex) (Patison et al., 2006; Korja and Heikkinen, 2008; Korja et al., 2009). Inverted rift and rift structure has been imaged from the Peräpohja-Central Lapland area and from the Bothnian Sea, respectively (Korja and Heikkinen, 1995, 2005; Patison et al., 2006; Tiira et al., 2014). The reflective images along the BABEL and FIRE seismic profiles suggest that the latest events – usually extensional – dominate the present crustal architecture and may thus restrict the depth extent of the present seismicity.

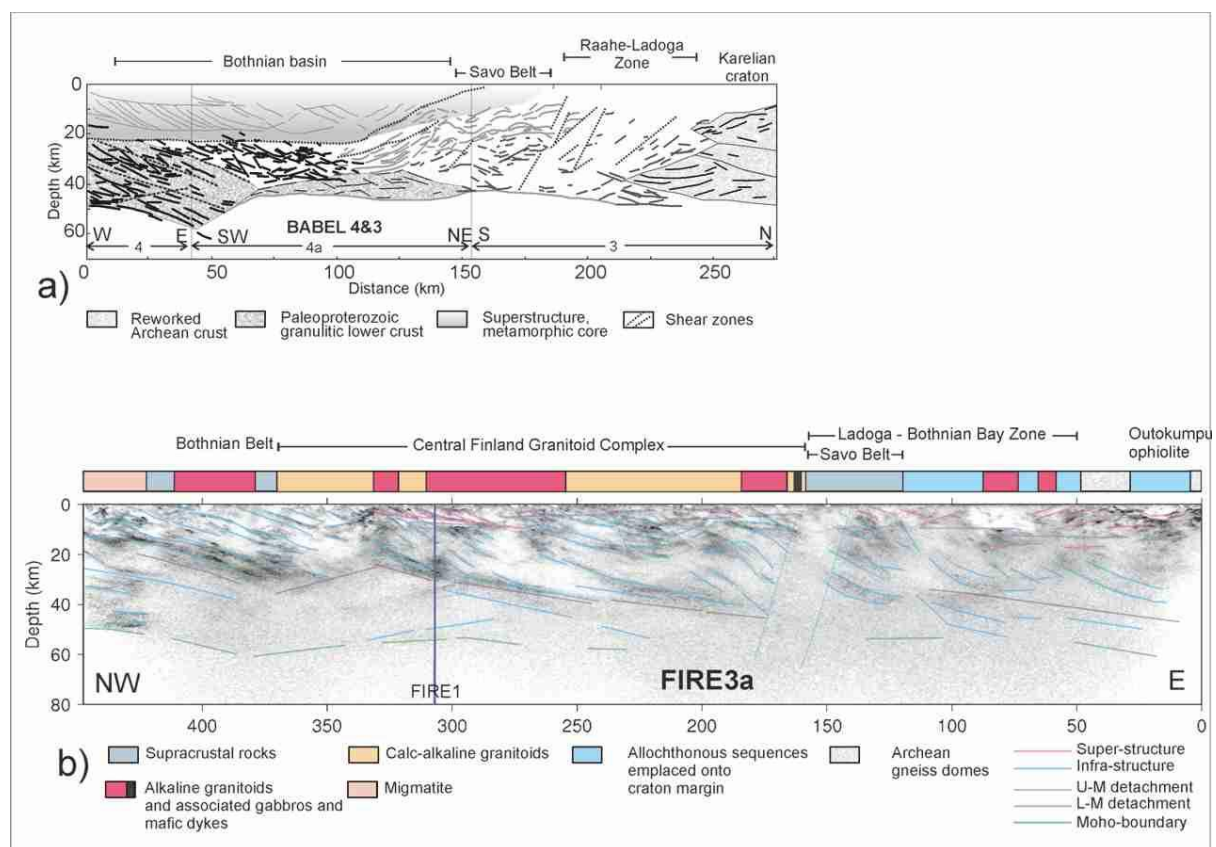


Figure 5.5.1.1. Crustal structure and the depth extent of the fault zones along deep seismic reflection lines. a) BABEL3&4 (Korja and Heikkinen, 2008). Major ductile shear zones are marked with stippled lines and b) FIRE 3 (Korja et al., 2009). Major ductile shear zones are marked with colored lines on the grey-scale section. Locations of the lines are given in figure 2.9.1.

5.6 Rheological layering

M. Uski, B. Lund & A. Korja

Rheological strength envelopes for Finland (Fig. 5.6.1; Table 5.6.1) have been constructed using a xenolith-controlled geotherm for the Kaavi kimberlite field (Kukkonen and Peltonen, 1999) and 3-layer crustal models obtained from DSS profiles (Fig. 2.9.1 and 5.6.2; Kaikkonen et al., 2000; Moisio and Kaikkonen, 2000, 2004, 2006, 2012). The models comprise two relatively weak layers (upper and middle crust) and a strong layer comprising the lower crust. The lowermost parts of the layers are very weak zones. Rheologically weak zones locate above the reflective layer boundaries of the refraction models (Fig. 5.6.1; Moisio and Kaikkonen, 2004). For example in FENNIA model the weak layers are located above velocity jumps 6.20-6.25 km/s and 6.60-7.00 km/s marking the change from upper to middle crust and from middle to lower crust, respectively. The depth of brittle-ductile transition zone (BTZ) is highly dependent on the model parameters. In areas where the crust contains several layers, BTZ is located at around the depth of 10 km (e.g. Central Finland lithotectonic unit), whereas in models and areas where crustal layering is not well-developed BTZ may be found at depths around > 40 km (Moisio and Kaikkonen, 2006, 2012).

Moiso and Kaikkonen (2006) have modeled hypothetical situation where Fennoscandia is subjected to a pressure of 50 MPa. In this case, the stress field is quite uniformly distributed at different crustal layers. The stress intensity in the upper crust had values between 42 and 45 MPa, the middle crust around 50 MPa and the lower crust around 60 MPa. In the models, the state of the stress was mostly governed by elastic parameters rather than by applied rheological structure. At such low stress levels no ductile deformation was generated, no failure took place and only areas close to surface could potentially fail. Another modeling study where wet crustal rheologies were used suggested distinct decoupling of strong upper crust, weak lower crust and strong upper mantle (Moisio and Kaikkonen, 2000). They suggest that decoupling interrupts the transmission of differential stress from the brittle upper crust to the ductile lower crust and upper mantle.

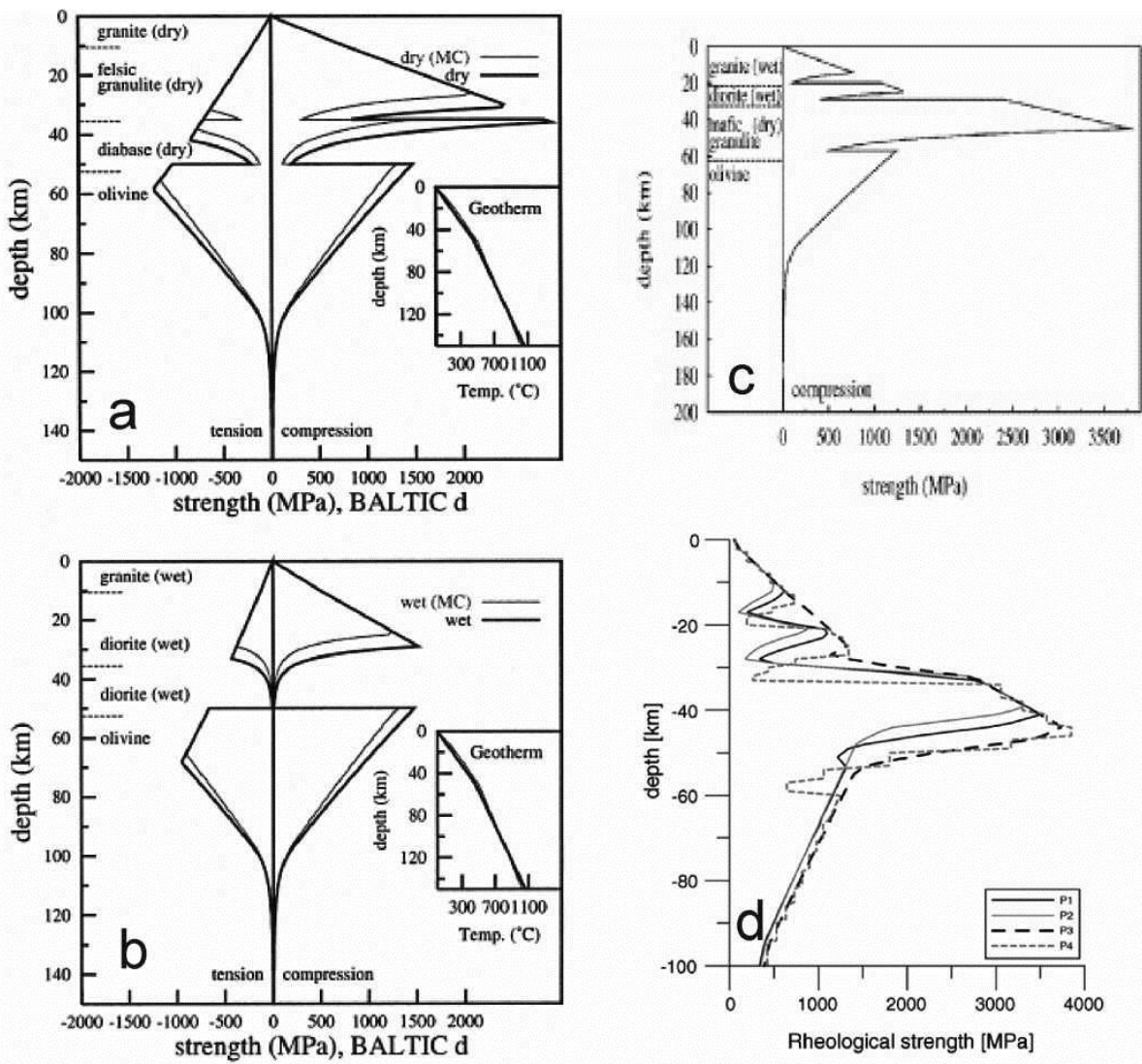


Figure 5.6.1. Examples of rheological strength profiles of Svecofennian crust along DSS profiles a-b) BALTIC profile with dry wet rheologies (Moisio and Kaikkonen, 2000), c) FENNIA-N (wet upper crust, dry lower crust) (Moisio and Kaikkonen, 2004), d) southern and central Finland (Moisio and Kaikkonen, 2006).

Table 5.6.1. An example of material parameters used in layered or jelly-sandwich rheological models of Central Fennoscandian Shield by Moisio and Kaikkonen (2006).

Layers	Petrology	Power law exponent n	Activation energy E_p (kJ mol $^{-1}$)	Initial constant A_p (MPa $^{-n}$ s $^{-1}$)	Thermal conductivity k (W m $^{-1}$ K $^{-1}$)	Heat production A (μ W m $^{-3}$)	Density ρ (kg m $^{-3}$)	Young's Modulus E (GPa)	Poisson's ratio μ
Upper crust	Granite (wet)	1.9	140	2.0E-04	3.0	1.6-0.9	2700	60	0.23
Middle crust	Diorite (wet)	2.4	212	3.2E-02	3.0	0.6-0.3	2800	70	0.25
Lower crust	Mafic granulite (dry)	4.2	445	1.4E+04	3.0	0.1-0.05	2900	80	0.27
Mantle	Olivine (dry)	3.0	510	7.0E+04	4.2	0.02-0.002	3100-3300	70	0.25
	Flow parameters for the Dorn law								
Petrology	Activation energy E_D (kJ mol $^{-1}$)	Initial constant A_D (s $^{-1}$)	Dorn law stress σ_D (GPa)						
Mantle	Olivine	535	5.7E+11	8.5	4.2	0.02-0.002	3100-3300		

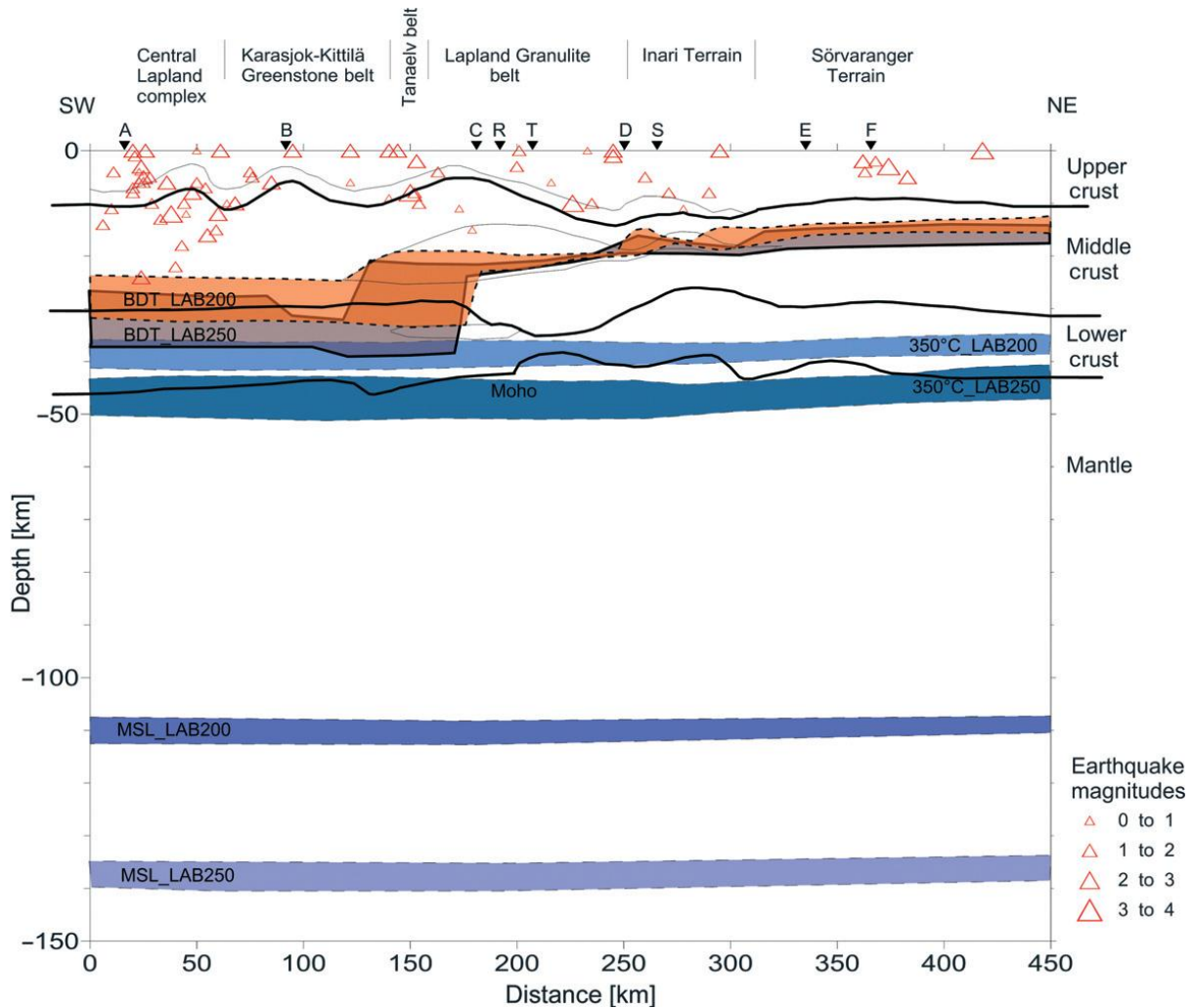


Figure 5.6.2. A vertical cross section of POLAR profile with seismicity and mechanical boundaries and 350 °C isotherm for two alternative LAB models (200 km or 250 km) (Moisio and Kaikkonen, 2012). The colored belts show the variation of modeling results for each boundary. Solid lines mark the main layer boundaries of the refraction model by Janik et al. (2009). The location of the profile is shown in figure 2.9.1. Abbreviations: BDT - brittle-ductile transition; LAB- lithosphere-asthenosphere boundary; MSL-mechanically strong lithosphere.

5.7 Observed depth of seismicity

M. Uski, B. Lund & A. Korja

Earthquakes in the study area seem to occupy a wide focal depth range, from shallow surface levels down to 40 km and even deeper (FENCAT, Section 2.8, Appendix 3). However, prior to 2000, the routinely determined focal depths have been subject to large uncertainties (Ahjos and Uski, 1992). This was mainly due to the sparse coverage of regional seismic stations, which precluded detailed analyses of seismic sources, even though seismological data from the Finnish, Norwegian, Russian and Swedish networks were combined. Since 2000, the station coverage of the SNSN and FNSN (Fig. 2.8.2.1) has significantly improved and, hence, also the earthquake detection and source location capabilities of the networks. However, in routine location process, unconstrained focal depth is the

parameter most sensitive to deficiencies in input data (e.g., phase identification and picking errors, uncertain velocity model). Good azimuthal coverage and distance to the nearest station are also regarded as prime controls for accurate estimation of source depth. A rule of thumb is that the distance to the nearest station should not exceed 1.5 times the source depth. The strict criteria are seldom fulfilled within permanent seismic networks such as the FNSN and SNSN. Thus the shallowest depth estimates have the largest uncertainties.

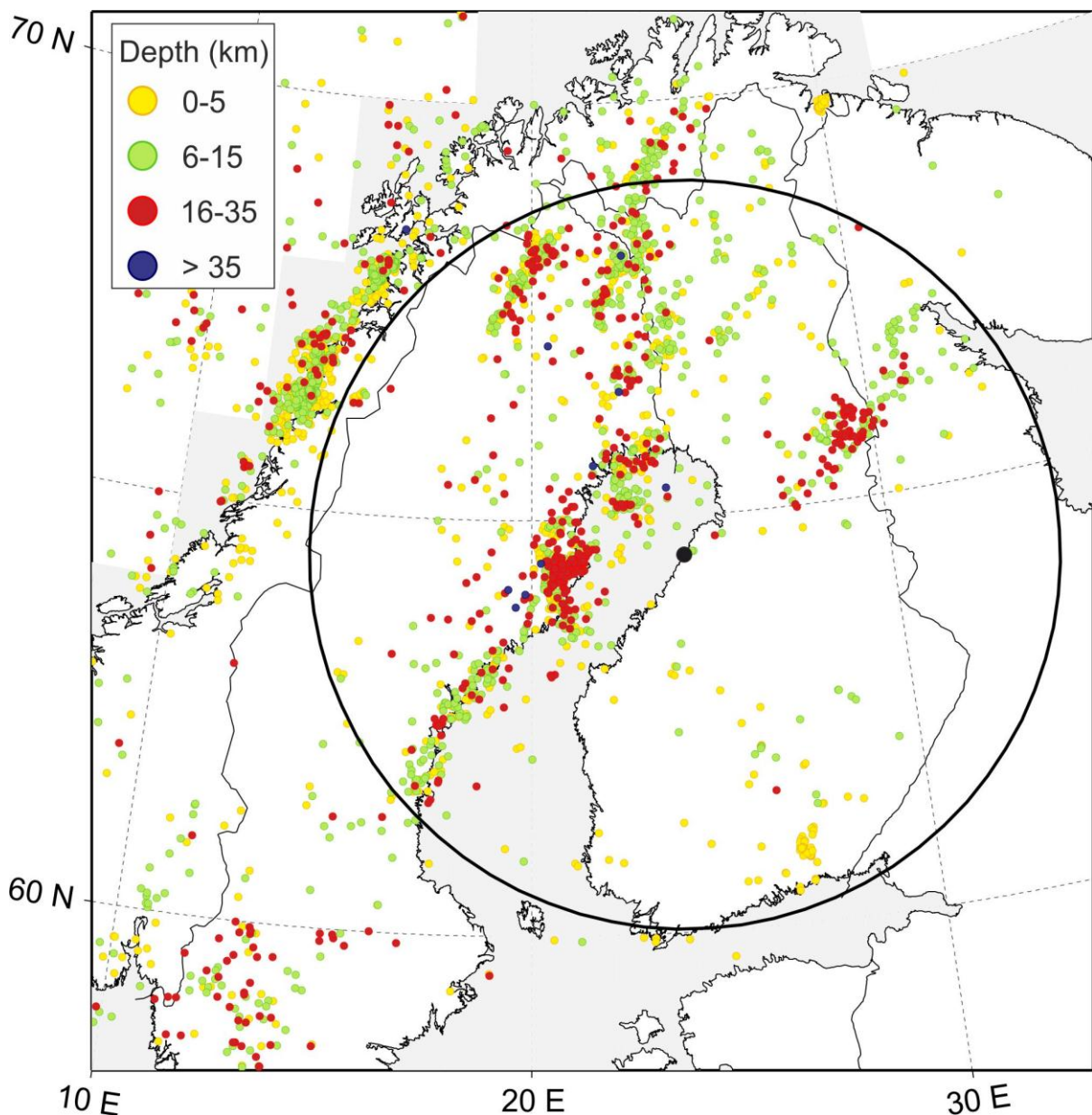


Figure 5.7.1. Depth distribution of earthquakes for the period 2000-2012. Depths routinely fixed to 10 or 15 km are not included

A map of earthquake depth distributions for the period 2000-2012 (Fig. 5.7.1) shows that the majority of earthquakes in the study area occur within the uppermost 15 km of the crust. The depth distribution differs from the general pattern in four areas and zones: Wiborg batholith, the Skellefteå

area, the Kuusamo area and the Hirvaskoski and Oulujärvi shear zones. In the Wiborg batholith, the earthquake swarms are unusually shallow, mostly occurring within the first 1–2 km of crust. In the Skellefteå area, roughly 50 % of the events occur in the middle and lower crust, at depths between 16 and 45 km. In the Kuusamo area and in the vicinity of the Hirvaskoski and Oulujärvi shear zones, the seismicity takes place between depths of a few kilometers and ~30 km. Note that in this region more than half of the events occur in the middle crust between depths of 15 and 30 km. Furthermore, a detailed study of depth distribution within the Kuusamo temporary seismic network (Fig. 5.7.2) suggests that the uppermost crust down to about 8 km is aseismic (Uski et al., 2012). The apparent aseismicity of the uppermost crust has been explained by the excess of strong, high density mafic material within the Kuusamo block.

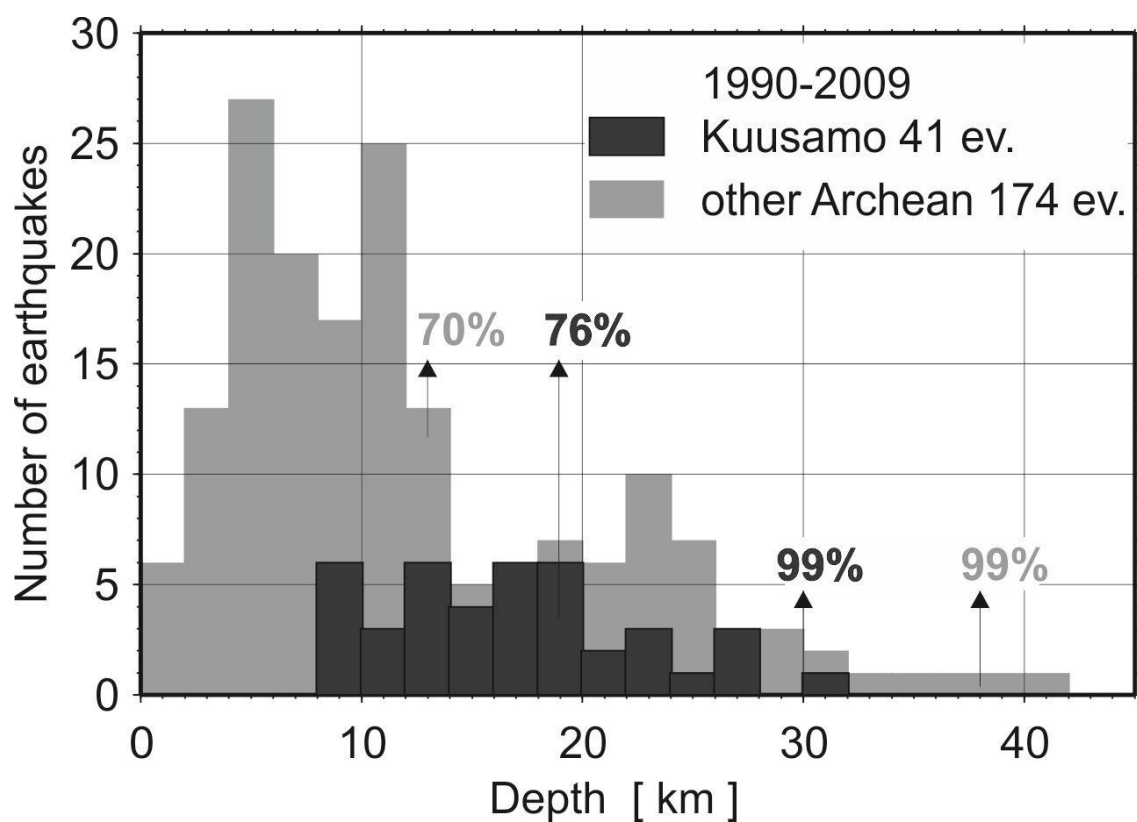


Figure 5.7.2. The focal depth distribution of ‘well-constrained’ earthquakes in northeastern Fennoscandia for 1990–2009 (Uski et al., 2012). Events within 70 km from the centre of the Kuusamo network are highlighted by dark grey and those from the surrounding Karelian lithotectonic unit by light grey. The data are grouped in 2 km intervals. Numbers denote the cumulative percentage of earthquakes occurring above the marked depth).

6 Deformation zones in the current stress field

P. Koskinen & A. Korja

Faulting may take place in either pure shear or simple shear mode. Simple shear is rotational and forms a greater variety of structures than pure shear (Fig. 4.3.1b). According to Andersson (1951) pure shear faulting takes place when the maximum principal stress is parallel to the maximum shortening axis (Fig. 4.3.1a). Because bedrock is rarely neither homogenous nor isotropic and it is unlikely that both conjugate faults are active simultaneously, most major faults form in simple shear mode. They are also mostly formed by reactivation of old joints and extension fractures (Sylvester, 1988).

In pure shear mode thrusting takes place perpendicular to compression direction, normal faults are perpendicular to tensional direction (parallel to principal stress) and strike slip faults form at $45 + \phi/2$ angles. In simple shear systems, thrusting and normal faulting takes place similar to pure shear systems, whereas strike-slip faults (principal displacement) happens at a larger angle. This angle depends on coefficient of internal friction ($\tan \phi = \mu$) a constant that varies from 0.47 to 1.0 for solid rocks (Byerlee, 1978), and may be as low as 0.2-0.4 for pre-existing fractures with fault gouge (Sauber et al., 2000). Additional faults called Riedel shears (R) are synthetic shear fractures that form at an angle of $\phi/2$ to the principal displacement plane. These have a conjugate pair called antithetic Riedel shears (R'), which have an opposite sense of slip, at an angle of $90^\circ - \phi/2$ to the principal displacement plane. In a larger map scale normal faults occur perpendicular to the extension axis and reverse faults and folds perpendicular to the contraction axis even within a dominantly strike-slip shear zone (Fig. 4.3.1.c). Strike-slip faults forming parallel to the direction of maximum or minimum horizontal stress are called transfer faults (Fig. 4.3.1.d,e) because they transfer displacement from one fault to another. The tips of transfer faults terminate against other faults or fractures.

6.1 Orientation of deformation zones in the context of the current stress field

The potential of reactivation of the pre-existing deformation zones is dependent on the direction of stress field and cross-angle between the deformation zone and the stress field (Fig. 6.1.1) i.e. how well the structures fulfil the ideal faulting directions criteria. One way to address the problem is to use existing structural databases compiled by the surveys (see chapter 2.5 and Fig. 6.1.1) and stress field values deduced from global stress field databases. One of the underlying problems is that the major deformation zones are curvilinear and not straight lines. The second problem is that many of the structures are not only simplified but also extrapolated from several small and discontinuous structures. The third problem is the reliability of the direction of the maximum horizontal component of the current stress field derived from global databases. Thus any attempts to analyse the

reactivation potential will be based on a number of assumptions on how to limit the continuation of the structures and on the stress field parameters.

Koskinen (2013) and Koskinen and Korja (2014) have evaluated the potential of the structural elements in the lineament database (Figs. 2.5.1, 2.5.4-2.5.6, 2.7.2 and 2.7.4.) to be reactivated in the present stress field (Figs. 5.1.1. and 5.2.1) based on Andersson's (1951) theory of faulting (Fig. 4.3.1b). They have assumed that the direction of the maximum horizontal component of the stress field can be approximated using plate motion data (Fig. 5.1.1) and the World Stress Map indicators (Fig. 5.2.1) in classes A-C. The validity of last assumption maybe questioned as most of the data points in the WSM are from the uppermost kilometre of the crust. However, it can be argued that the observations of the analysed lineaments are also from the surface, and thus the data sets are compatible in this regard. The stress field analysis is corroborated with the plate motion data. Koskinen and Korja (2014) have also assumed that a) only the continuous segments can move in one single seismic event; b) only straight segments are likely to slip during one event; c) bends hinder or at least disrupt slip. Based on these assumptions Koskinen and Korja (2014) have analysed the orientation of the lineaments and their cross-angle with the current stress field vectors.

The structural elements are extracted from the 1: 1 M structural database (Fig. 6.1.1). The orientation may only be analysed from straight segments and thus the lineament nodes have been split into shorter segments with uniform direction. The lineaments are later analysed for geographical orientation as degrees from the north (azimuth) and degrees from stress vector orientation (cross-angle).

The azimuth of maximum horizontal component of the stress field is estimated to lie between 115° and 135° in the study area (Figs. 5.1.1. and 5.2.1). The theoretical azimuth diagram (Fig. 6.1.2) for the study area has been created using Anderson's (1951) faulting theory, Mohr-Coulomb failure criterion, coefficient of friction of $\mu = 0.6$ and 0.2 (Koskinen and Korja 2014). The azimuth diagram shows in which directions different fault types could potentially develop. For imaging purposes, the line-segments of the structural elements have been color-coded after their azimuth indicating fault type (Figs. 6.1.3-6.2.2). If the direction of maximum horizontal stress (σ_H) were between 115° and 135° then the optimal orientation for reverse faulting would be perpendicular to σ_H , (025°-045°; purple). Normal faulting would occur parallel to σ_H (115°-135°; blue) given that the maximum principal stress were vertical. Transfer faults would occur in the same direction (blue). In pure shear domain, strike-slip (SS) faulting would occur in conjugate sets $\pm 30^\circ$ to σ_H , ($m= 0.6$): dextral SS faults would strike 085°-105° (pink), and sinistral SS faults 145°-165° (light green). In simple shear domain, dextral SS faults would thus strike 075°-095° (red) and sinistral SS faults 155°-175° (green). With different experimental set-ups, other faulting modes are possible.

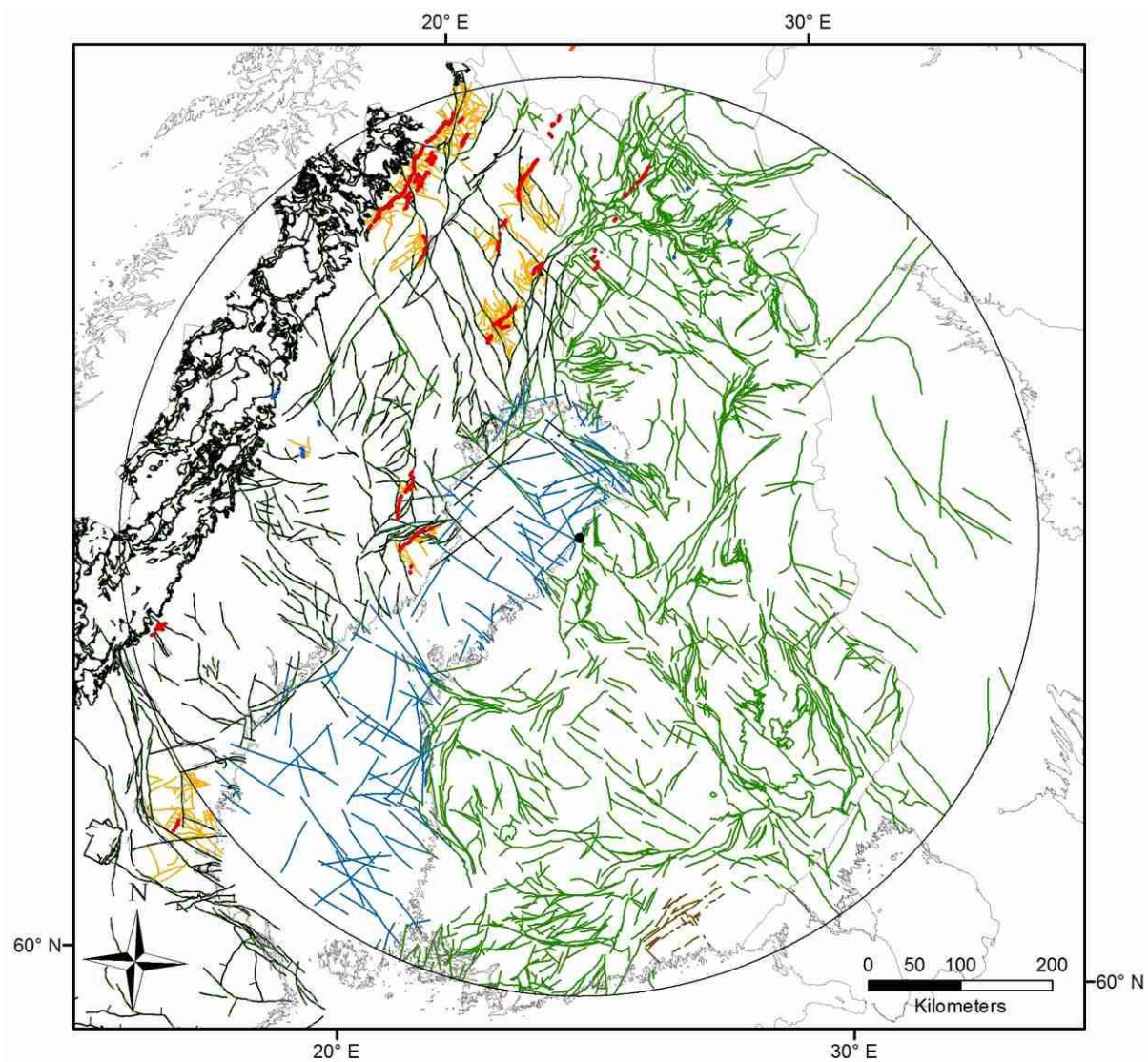
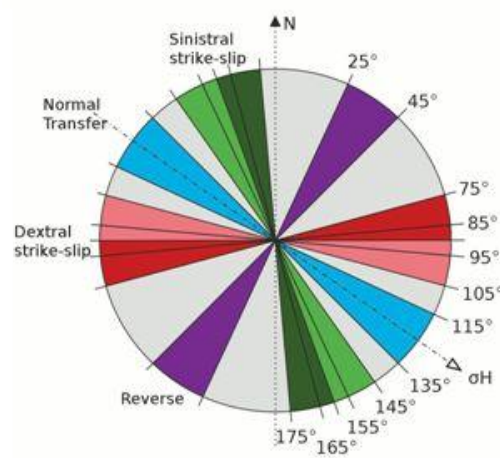


Figure 6.1.1. A subset of structures for which potential reactivation properties are calculated. A compilation of subsets shown in figures 2.5.1, 2.5.4-2.5.6, 2.7.2 and 2.7.4. Hanhikivi site: black dot.

Figure 6.1.2. The theoretical azimuth diagram showing intervals of the optimal orientation categories for reverse, normal and strike-slip regimes in Central Fennoscandia. The intervals have been calculated assigning the direction of maximum horizontal stress (σ_H) between 115° and 135° and coefficient of friction (μ) to 0.2. Strike slip regimes in pure shear domain are in pink and light green. Strike slip regimes in simple shear domain are in red and green.



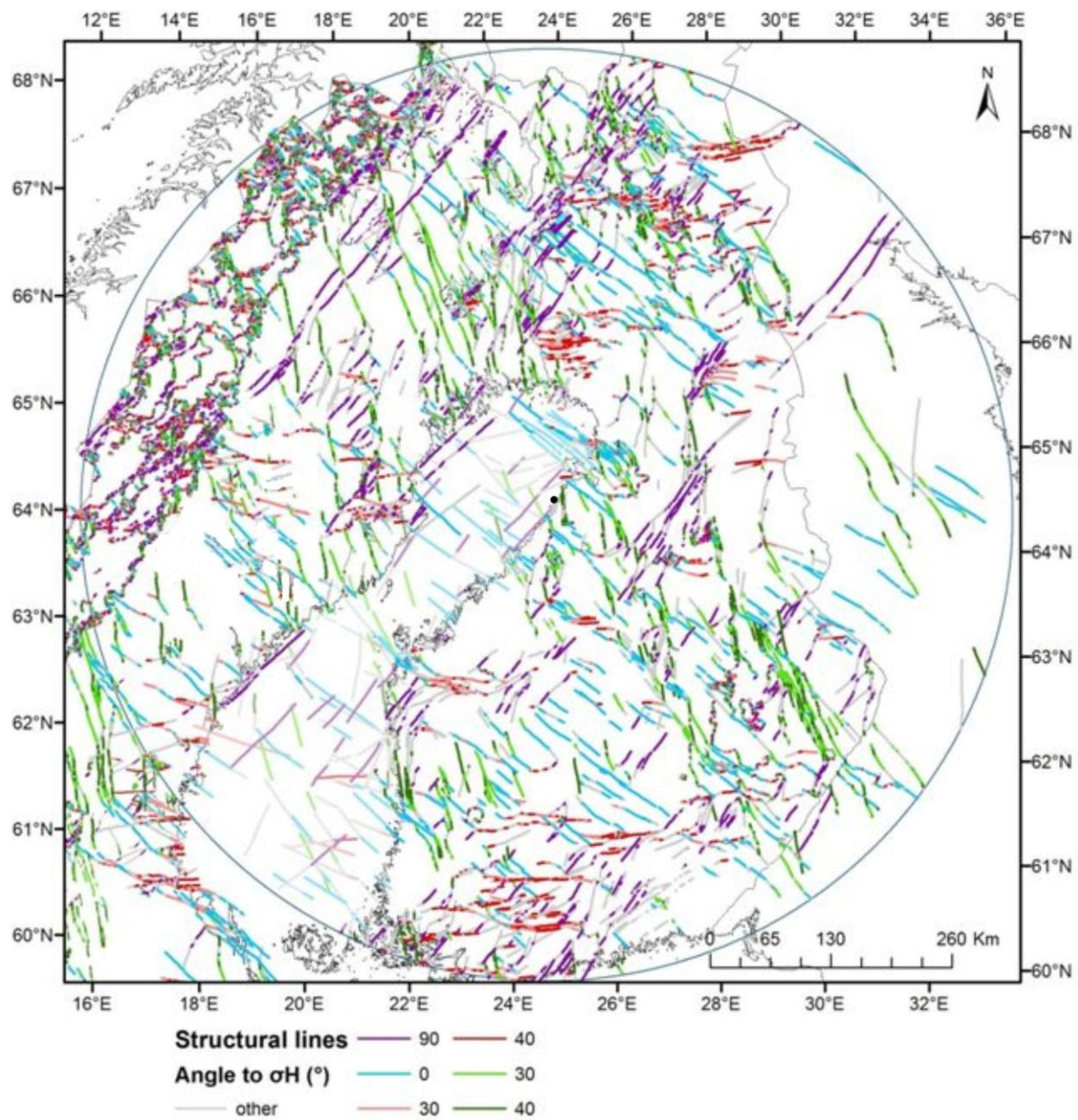


Figure 6.1.3. Orientation of the straight segments of the structural elements in figure 6.1.1. . Colour coding represents the horizontal cross-angle to the maximum horizontal stress direction. Legend: purple –reverse; blue – normal and transfer fault; pink – pure shear dextral strike slip; red- simple shear dextral strike slip; light green – pure shear sinistral strike slip; green - simple shear sinistral strike slip.

6.2 Structural line orientations and seismicity

In Figures 6.2.1 and 6.2.2, the deformation zones are presented together with earthquake epicentres and their magnitudes. Since there are no apparent regional variations in the magnitude of earthquakes in Fennoscandia, no relations between deformation zone trends and earthquake magnitude can be found. However, there are clear regional variations in the number of earthquakes. The most seismically active area is the western shore of the Gulf of Bothnia and its northeasterly

continuation. The earthquakes seem to cluster around the shoreline and post-glacial fault system. Structures are oriented optimally for reverse faulting (purple), associated transfer faulting (blue) and strike-slip (green) (Figs. 6.1.1 and 6.1.2). Earthquake focal mechanisms suggest that the strike-slip and transfer components are more active. The areas of high seismicity in western Finnish Lapland seem to be linked with a reverse and transfer faulting system (purple and blue lines in Figure 6.2.1). Kuusamo is transected by structural elements trending in various orientations (Fig. 6.2.1).

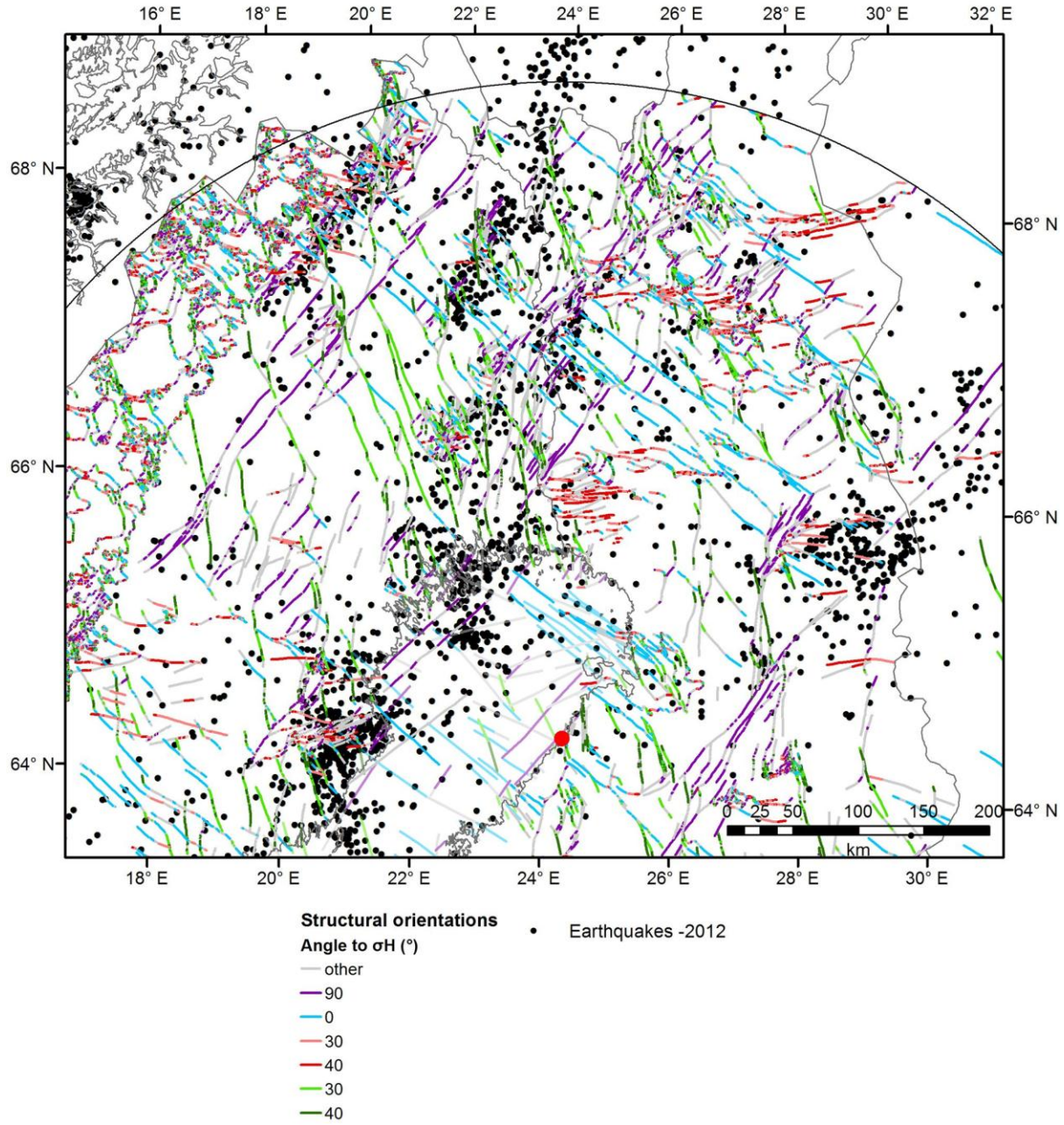


Figure 6.2.1. Orientation of the straight segments of the deformation zones and seismicity in the northern part of the study area. Earthquake data from figures 2.8.1.1-2.8.1.2. Colour coding represents the horizontal cross-angle to the maximum horizontal stress direction. Legend: purple – reverse; blue – normal and transfer fault; pink – pure shear dextral strike slip; red- simple shear dextral strike slip; light green – pure shear sinistral strike slip; green - simple shear sinistral strike slip.

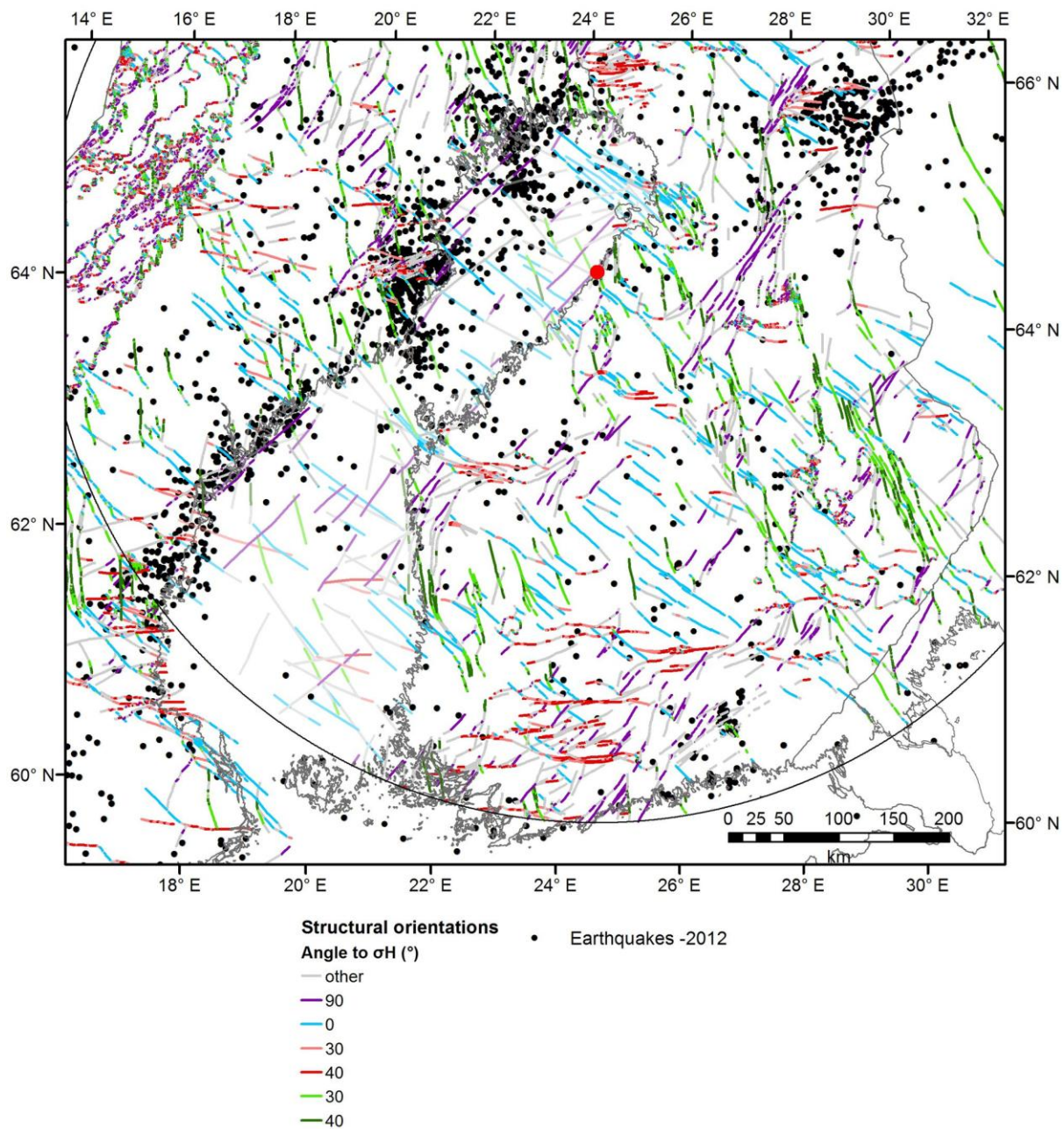


Figure 6.2.2. Orientation of the straight segments of the deformation zones and seismicity in the southern part of the study area. Earthquake data from figures 2.8.1.1-2.8.1.2. Colour coding represents the horizontal cross-angle to the maximum horizontal stress direction. Legend: purple – reverse; blue – normal and transfer fault; pink – pure shear dextral strike slip; red- simple shear dextral strike slip; light green – pure shear sinistral strike slip; green - simple shear sinistral strike slip.

7 Current seismotectonic and previous seismic source area models

A. Korja & N. Hellqvist

7.1 Seismotectonic models

Seismicity and the origin of seismicity in Fennoscandia have been studied for the last hundred years. Currently most authors agree that the sources of the seismicity in Fennoscandia are multiple and diverse in nature, ranging from plate-wide to local scales (Bungum et al., 2010). The dominant driving forces of seismicity are related to a) plate tectonics; and b) post-glacial rebound c) lateral variations in lithospheric structure.

Fjeldskaar et al. (2000) have classified the horizontal stress field generating mechanisms into three groups based on their magnitude and effective distance (Table 7.1.1). The largest stresses are caused by the continental scale (>1000 km) first order stress field associated with plate tectonics, which in Fennoscandia is ridge-push from the Mid-Atlantic ridge (see chapter 5.1). The regional scale second order stress fields (100-1000 km) are caused by regional scale gravitational or compositional inhomogeneities of the crust such as crustal tilting or flexure, mass loading and unloading (Fig. 5.3.1) or large density differences (Fig. 5.4.1). More local, third order stress fields (< 100 km) are generated by local topographic, compositional and structural differences. In the following, we will review the existing seismotectonic models addressing the origin of seismicity in Fennoscandia. Papers referring to national or local seismicity patterns are referred to in the seismicity section 4.

Table 7.1.1. Stress-generating mechanisms in Fennoscandia (Fjeldskaar et al., 2000).

Stress field	Stress generating mechanism
Continental (lateral extent > 1000 km)	Plate tectonic forces
Regional (100-1000 km)	Large-scale density inhomogeneities <ul style="list-style-type: none">- continent-ocean boundary Flexural stresses <ul style="list-style-type: none">- sediment loading- deglaciation Wide topographic loads
Local (<100 km)	Topography (e.g. fjords, mountain ranges) Geological features (e.g. faults)

Redfield and Osmundsen (2013) claimed that the Scandinavian passive margin has a hyperextension architecture that developed during large magnitude extension associated with the opening of the Atlantic Ocean c. 60 million years ago (Fig. 7.1.1). Based on topographic and lithospheric thickness data, they divided Scandinavia into distal margin, proximal margin, hinterland and craton parts (Fig. 7.1.2) that are separated from each other by taper break (TB; distal/proximal margin), escarpment (E; proximal margin/hinterland) and hinterland break in slope (HBSL; hinterland/craton). A topographic

cross-section reveals a pronounced asymmetry and a well-defined hinterland break in slope (HBSL; Fig. 5.4.5). They argued that stretching resulted in a highly attenuated pervasively faulted and permanently weakened distal margin; an extended proximal margin wedge, where most of the thickness reduction of the crust is located; and a flexure in the hinterland.

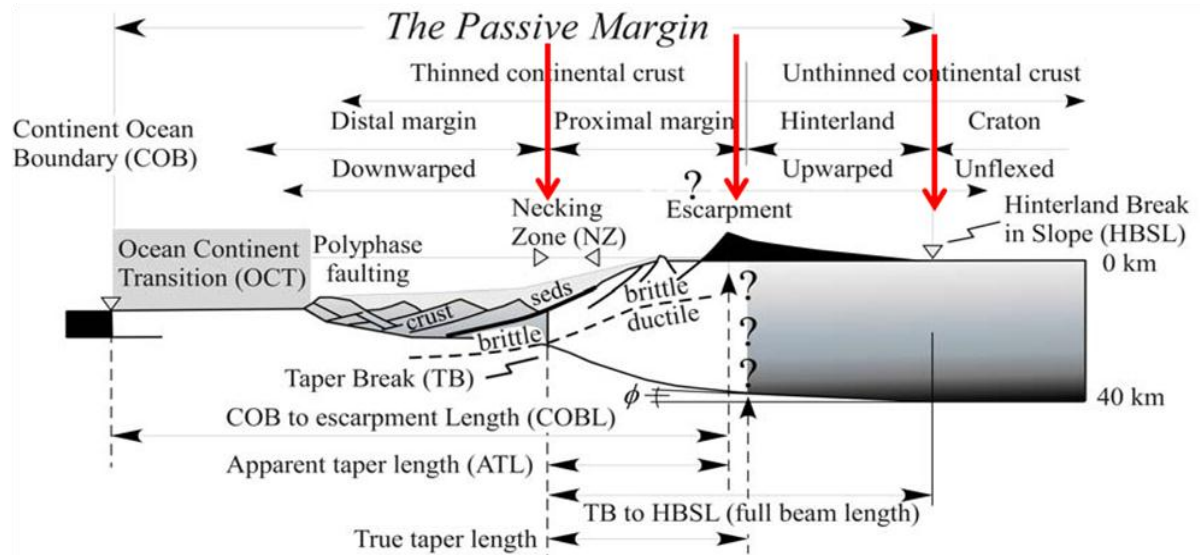


Figure 7.1.1. A hyperextended continental margin model (Redfield and Osmundsen, 2013). A complimentary vertical cross-section of the topography is shown in Fig. 5.4.5.

Redfield and Osmundsen (2013) defined four seismic energy belts located along the older structural boundaries. The seismicity zones defined by Redfield and Osmundsen (2013) are compared with the seismicity earthquake database used in this study (Fig. 7.1.3). The first belt is the offshore belt of seismic activity that runs along the outermost edge of the proximal margin, just inboard of and roughly parallel to the TB (TB; Figs. 7.1.2 and 7.1.3). It is characterized by reverse faults and earthquake hypocenters deeper than 15 km. The second belt of near-shore to onshore seismicity runs along the inner proximal margin edge, roughly parallel to and seaward of the topographic escarpments (Figs. 7.1.2 and 7.1.3). Earthquakes on this belt occur usually at depths shallower than 12 km and their focal mechanism is oblique-normal slip. The third belt marks the transition from unextended but upwarped lithosphere to unextended, unwarped lithosphere that is located just inboard of the HBSL (Figs. 7.1.2 and 7.1.3). This third belt is characterized by small earthquakes ($M_w \leq 2$). Outside our study area Redfield and Osmundsen (2013) found fourth additional seismicity belt that follows the thinned crust of North Sea–Viking graben rift systems outboard of the thicker Horda Platform in the North Sea. Seismically quiet areas are found in the Trøndelag Platform and in the hinterland between the escarpment (E) and the hinterland break in slope (HSBL).

Redfield and Osmundsen (2013) suggested that seismicity is concentrated along the boundaries defined by extensional tectonics, further developed throughout the cooling and ongoing

accommodation period. The structures have been and are being reactivated by the loading and unloading events of the Plio–Pleistocene glaciation period. They concluded that, while the structures originated from an old tectonic event, their present seismic activity is not only associated with ridge push but also with isostatic post-glacial uplift and with erosion associated with the on-going accommodation phase.

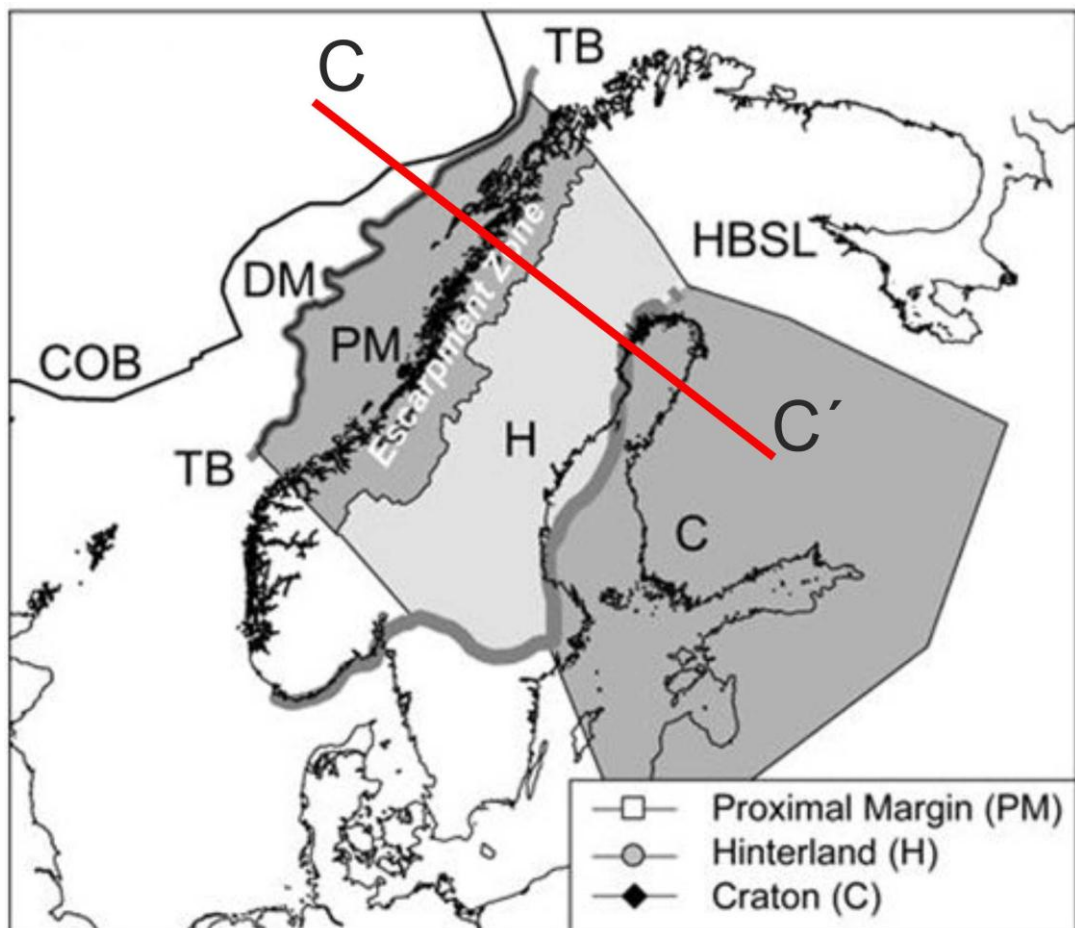


Figure 7.1.2. A map showing the division of Scandinavia into four tectonic domains related to extensional deformation and opening of the Atlantic Ocean (Redfield and Osmundsen, 2013). Line C-C' shows the location of figure 5.4.5. Abbreviations: C – Craton; COB -Continent Ocean Boundary; DM-Distal Margin; H –Hinterland; HBSL- Hinterland break- inslope; PM - Proximal Margin; TB - Taper Break.

Several workers have argued that second order stress fields associated with post-glacial rebound (Fig. 5.3.1) account for most of the seismicity in Fennoscandia (e.g. Muir Wood, 2000; Gudmundsson, 1999). Muir Wood presented a conceptual rebound dome - forebulge model that explains the current seismicity patterns as a response to migrating post-glacial doming of the center and sinking of the surrounding basins (Fig. 7.1.4). Similar relationships between seismicity and post glacial uplift were obtained with rheological modeling by Gudmundsson (1999) and Fjeldskaar et al. (2000). Mörner (1990) suggested that the uploading/unloading is fully compensated at the lithosphere-

asthenosphere boundary (Fig. 5.3.1). Fjeldskaar et al. (2000) also concluded that post-glacial uplift and ridge-push stress act constructively. They also noted that the seismically active areas around the northern part of the Gulf of Bothnia (Bay of Bothnia and southern Lapland) have risen/rebounded slower than predicted by a glacial isostatic adjustment (GIA) model, leaving behind a negative deviation (Fig. 7.1.4). This suggests that either the GIA model has to be updated or that rebound is hindered by local structure. It seems that plate boundary forces, GIA and seismicity have complex interwoven relationships that need to be further studied in the future.

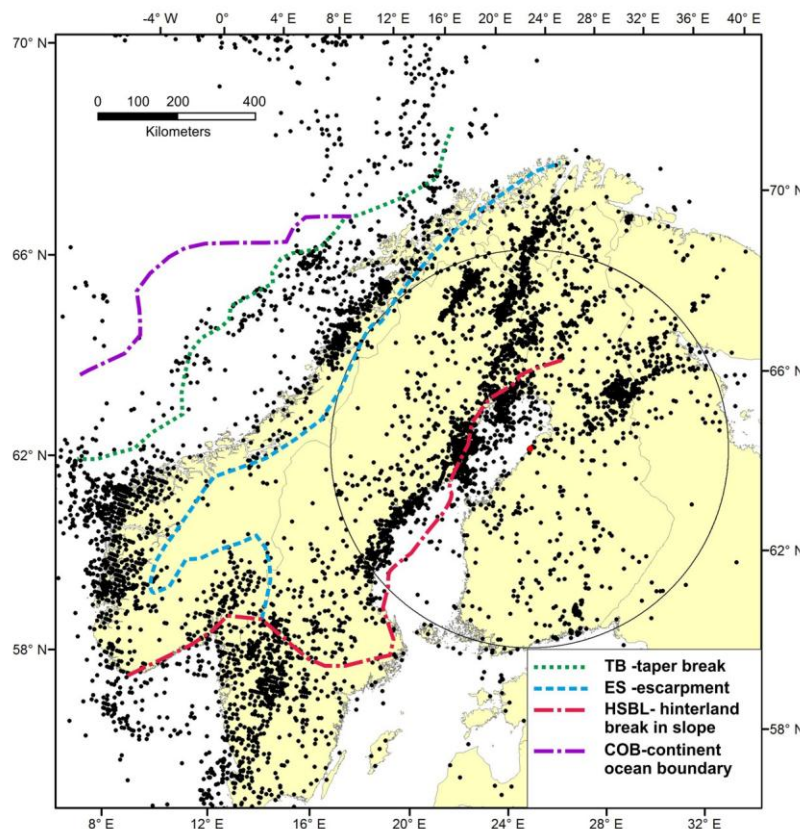


Figure 7.1.3. Tectonic domains after Redfield and Osmundsen (2013) and Fennoscandian seismicity (Fig. 1.2.1). Hanhikivi site: red dot.

Seismotectonic post-glacial uplift models (e.g. Mörner, 1990; Gudmundsson, 1999; Fjeldskaar et al., 2000; Muir Wood, 2000) are most commonly based on geodetic measurements that show concentric ellipsoidal patterns of both uplift around uplift center. More detailed information on the uplift geometries and horizontal displacements are found in recent studies using the BIFROST GPS (Figs. 5.3.2- 5.3.5; Milne et al., 2001; Johansson et al., 2002; Ågren and Svensson, 2007; Nørbech et al., 2008). It should be remembered that the GPS maps show residuals after the removal of the standard plate movement i.e. absolute movement towards the NE and relative SE movement away from North America (see section 5.1. and figure 5.1.2.).



Figure 7.1.4. Areas with significant negative deviations (1.0 mm/a) between the observations and the calculated glacial isostatic uplift (Fjeldskaar et al., 2000). Note the large deviations around the Bay of Bothnia where the rate of seismicity is also high.

According to Muir Wood (2000), deglaciation dominates the current crustal strain field in many high latitude stable continental regions such as Fennoscandia. Muir Wood (2000) made a conceptual model of glacial unloading of the lithosphere that included not just the vertical component of rebound but also the horizontal deformation (Fig. 7.1.5). Vertical stresses are almost always a consequence of the direct and instantaneous application of the glacial loading, while changes in horizontal stresses are functions of the viscoelastic respond to mantle loading/unloading. The strongest seismicity is predicted in the northeast and southwest quadrants of the former fore bulge (Fig. 7.1.5b), whereas the quadrants of aseismicity are located in the northwest and southeast. Seismicity related to the collapse of the fore bulge is found in the Norwegian Sea and the Baltic states. Seismicity in Fennoscandia will continue to slowly decay with declining rebound. The seismicity zones defined by Muir Wood (2000) are compared with the seismicity data used in this study in Figure 7.1.6.

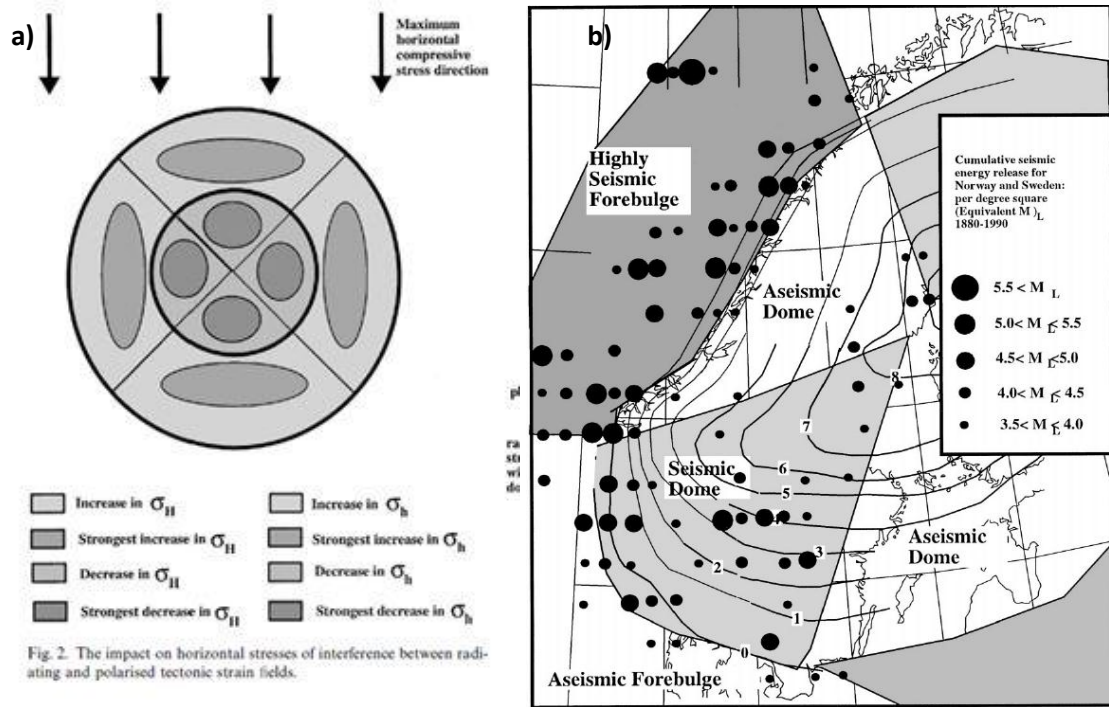


Figure 7.1.5. a) The impact on horizontal stress of interference between radiating and polarized tectonic strain field (Muir Wood, 2000). b) Quadrants of active and inactive seismicity from 1880-1990 in Fennoscandia according to Muir Wood (2000). Uplift rates are shown in mm/a. Most of the intraplate seismicity is associated with rise of the deglaciation dome and fall of the forebulge.

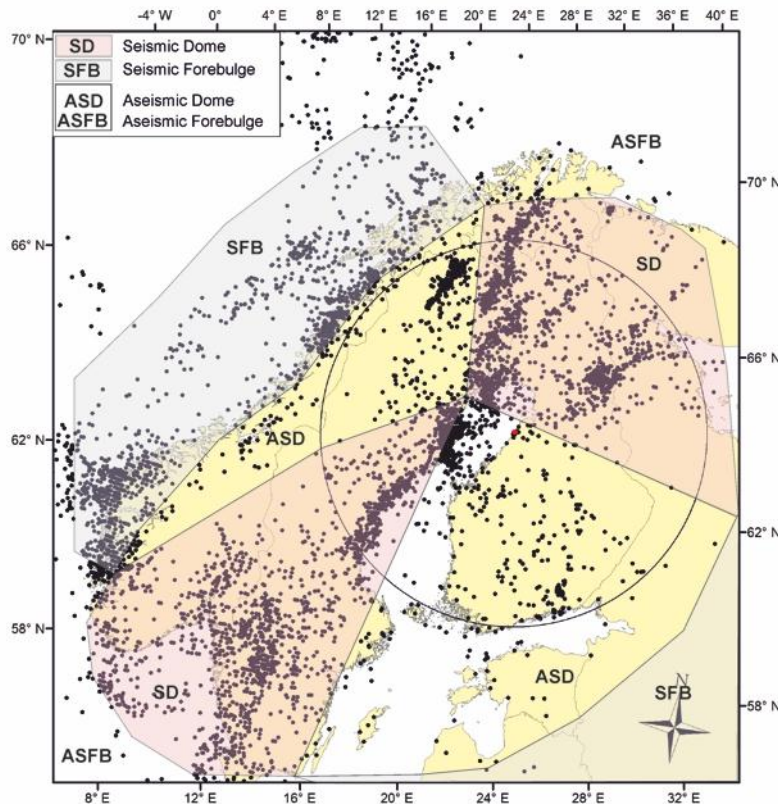


Figure 7.1.6. A comparison of Fennoscandian seismicity (FENCAT) and the quadrants of active and inactive seismicity of the deglaciation dome and the forebulge of Muir Wood (2000).

Wu et al. (1999) have modeled fault instability during and after glaciations. They claim that the flexure of the lithosphere due to glaciations induce large instabilities in the crust at the end of deglaciation. Minor instabilities (1 MPa) still exist at the center of the rebound and the predicted mode of failure is thrusting. Because the level of seismicity is rather low, they conclude that there is no clear evidence that the rebound stress is still able to trigger seismicity in Fennoscandia today. The post-glacial rebound has had a much more important role in earthquake generation in late glacial and early post-glacial times. Wu et al. (1999) noted that the spatial pattern of the earthquakes exhibit little to no correlation with the pattern of rebound in Fennoscandia.

Pascal and Cloetingh (2009) also concluded that post-glacial rebound has had a significant influence in the past on the stress regime in Fennoscandia but that it is not effective today. This is evident through the measurements done in Finnmark where stress-relief structures were found to be consistent with a regional NW-SE compression associated with ridge push forces (Pascal et al., 2005). At present, the stress field is mainly consistent with plate tectonic forces and no clear correlation with glacial unloading can be seen. Other stress sources such as sedimentary loading/unloading and rebound have only local and/or short term significance. Observed variations in lithospheric structure and elevation from the margin towards the continental interiors may produce significant potential stresses which together with tectonic forces exert control on the dynamic evolution of the margin. Pascal and Cloetingh (2009) also proposed that the buoyancy forces created by the Cenozoic uplift of Fennoscandia might have contributed to the observed decreased rates of the spreading of the North Atlantic ridge, similar to that observed in South America.

7.2 Seismic source area models

The Hanhikivi site is included in six existing seismic source area models (Mäntyniemi et al., 1993; NFR/NORSAR and NGI, 1998; Grünthal and the GSHAP Region 3 Working Group, 1999; Wahlström and Grünthal, 2001; Mäntyniemi, 2008a; Saari et al., 2009; Korja et al., 2011; Giardini et al., 2013), hazard maps (Grünthal and the GSHAP Region 3 Working Group, 1999; Wahlström and Grünthal, 2000, 2001; Mäntyniemi et al., 2001; Giardini et al., 2013). Seismic hazard estimates have been calculated for the Hanhikivi site (Mäntyniemi et al., 2001; Mäntyniemi, 2008a; Saari et al., 2009; Korja et al., 2011).

Mäntyniemi et al. (1993) used 8 subregions for Norway, Sweden, Finland, and Denmark (Fig. 7.2.1). Kijko et al. (1993) divided Sweden into the northern and southern parts and further in the Lake Vänern and the eastern coast of the Gulf of Bothnia subregions. Grünthal and the GSHAP Region 3 Working Group (1999) modified the northern subregions of the model somewhat when calculating the seismic hazard of Fennoscandia within the framework of the Global Seismic Hazard Assessment

Program (GSHAP) (Fig. 7.2.2). Seismic hazard in Fennoscandia is low according to GSHAP estimates (Fig. 7.2.3).

In 2001, Wahlström and Grünthal presented yet another updated seismic source region model for Norway, Sweden, Finland, and Denmark. In this model they have used three sets of seismic source regions: a) a revised version of NFR/NORSAR and NGI (1998) used for GSHAP-Global Seismic Hazard Assessment Program (Fig. 7.2.2; Grünthal and the GSHAP Region 3 Working Group, 1999; <http://www.seismo.ethz.ch/static/gshap/ceurope/>) including 31 source regions. b) A model with 21 source regions based on the seismicity distribution. c) A model with 14 source regions based mainly on tectonic maps of Sweden, Finland, and Denmark in addition to 21 regions for Norway and its offshore area from the NFR/NORSAR and NGI (1998) model. As a result, they presented a map of median values of hazard values or horizontal PGA (m/s^2) values for a mean return period of 475 years (Fig. 7.2.4). The highest hazard in Fennoscandia, with values up to $0.45 m/s^2 - 0.70 m/s^2$, is found along the Norwegian coast. An area of enhanced hazard is also found in areas surrounding the Bay of Bothnia, with maximum values of $0.15-0.20 m/s^2$. The highest hazard in the study area is in the Kuusamo district $0.20-0.25 m/s^2$. The smallest hazard values below $0.1 m/s^2$ are found in southern Finland.

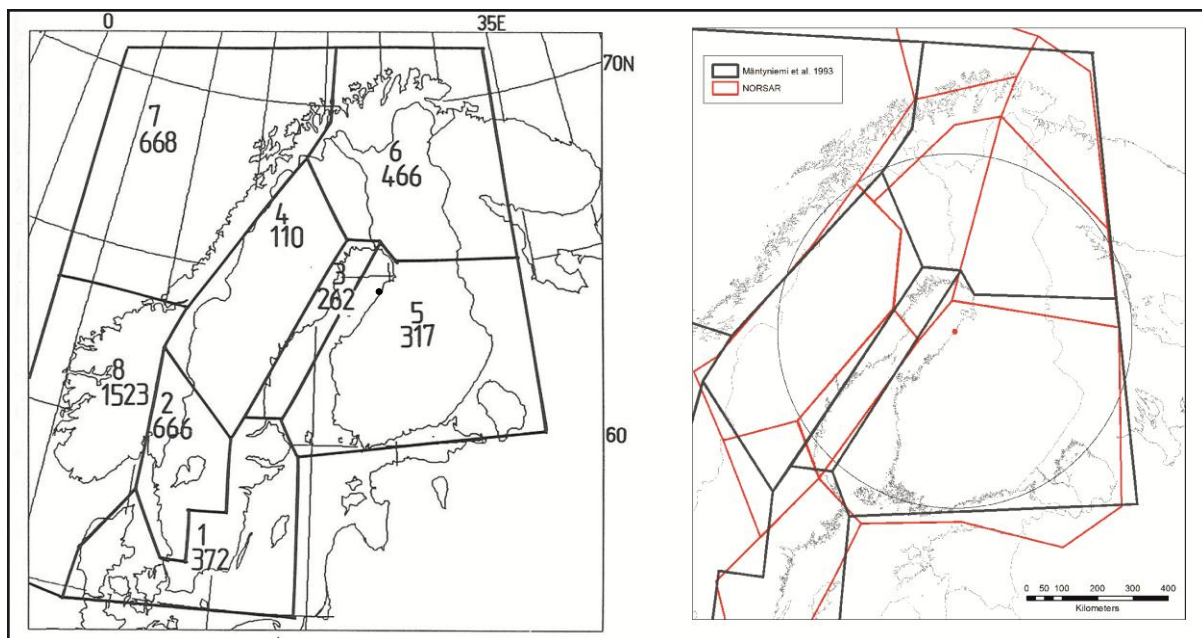


Figure 7.2.1. A Seismic source area model for Fennoscandia (Mäntyniemi et al., 1993). Hanhikivi site: black/red dot.

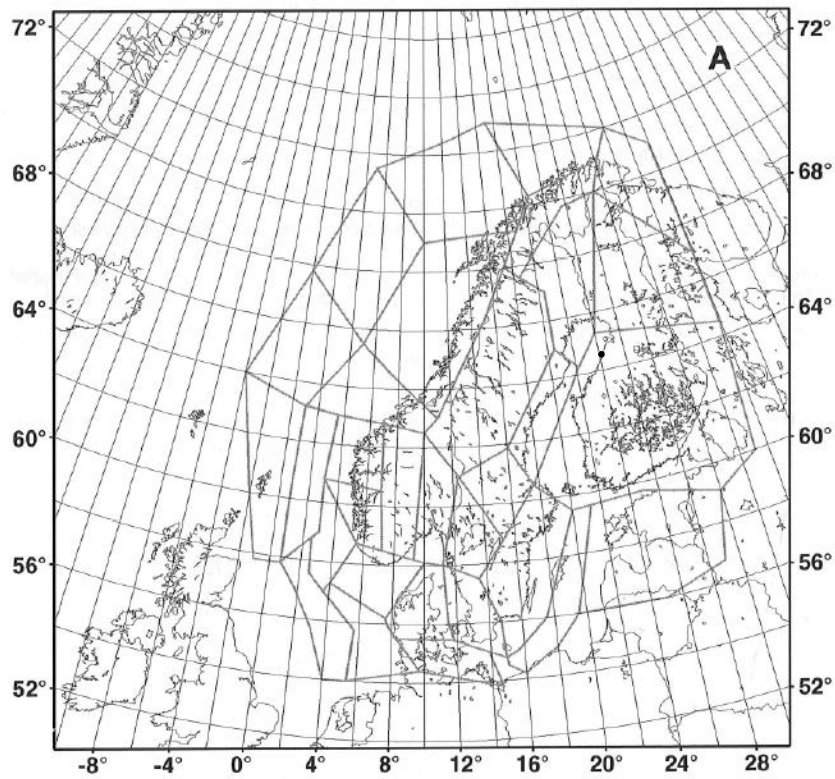


Figure 7.2.2. Source regionalization models and source regions in GSHAP model (Wahlström and Grünthal, 2001).

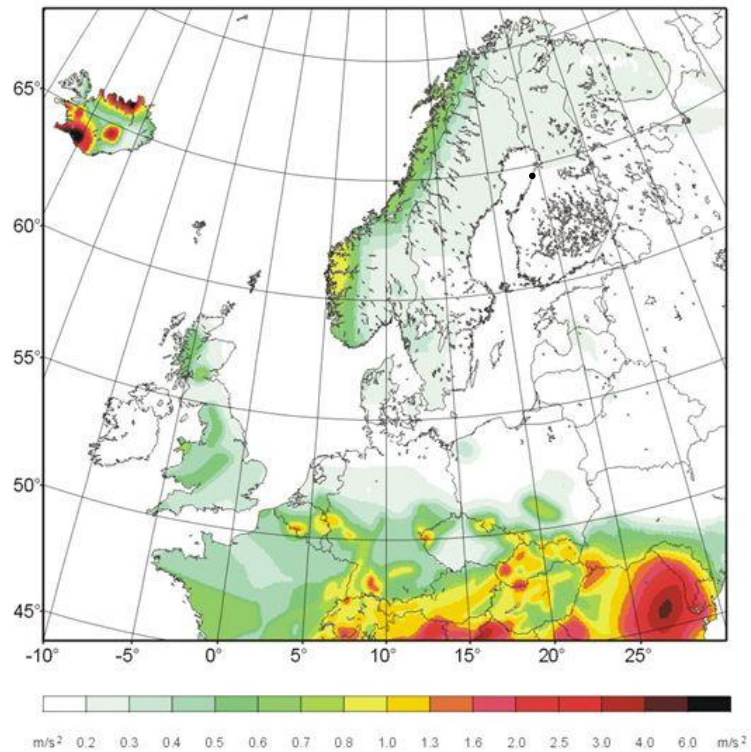


Figure 7.2.3. A homogeneous seismic hazard map for horizontal peak ground acceleration for the probability level of an occurrence or exceedance of 10% within 50 years by GSHAP-Global Seismic Hazard Assessment Program (Grünthal and the GSHAP Region 3 Working Group, 1999).

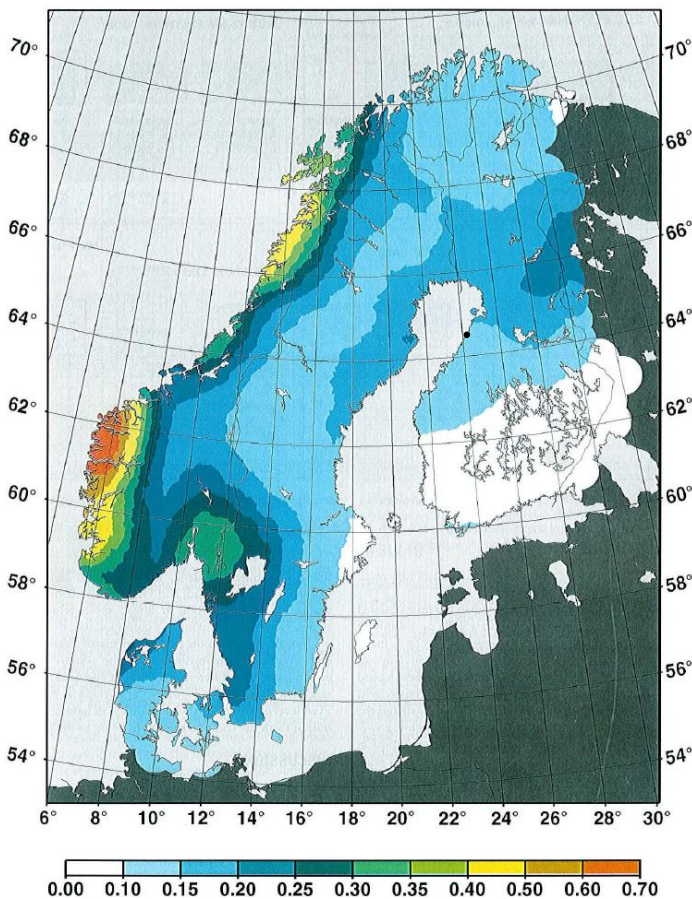


Figure 7.2.4. A map of 90% probability of non-exceedance of horizontal PGA (m/s^2) in 50 years, corresponding to a mean return period of 475 years (Wahlström and Grünthal, 2001). Median hazard values are given.

The EU-project SHARE (Seismic Hazard Harmonization in Europe, <http://www.share-eu.org>) attempted to harmonize the probabilistic hazard assessments of Europe (Fig. 7.2.5) and produced a second version of European areal seismic source zone model (SSZM) (Arvidsson et al., 2010). In Scandinavia, SHARE model is largely based on GSHAP model. According to Arvidsson et al. (2010), the source area models for the Baltic Sea, the Baltic countries and Finland have been largely reworked so that zonation corresponds better to large scale tectonic features and seismicity. The North European seismic source area model (GSHAP; Fig 7.2.2) has been included in EU-project SHARE - Seismic Hazard Harmonization in Europe (<http://www.share-eu.org>), attempting to harmonize the probabilistic hazard assessments of Europe (Fig. 7.2.5) and to establish as a regional reference model. In Sweden two smaller source areas have been merged into one, but the over-all geometry has not changed. Seismic hazard is estimated to be low in the study area and very low in the site vicinity (Fig. 7.2.6). SHARE model is included in the ongoing global seismic hazard assessment mapping initiative GEM - Global Earthquake Model (<http://www.globalquakemodel.org/>). GEM aims to produce a uniform, independent and open access standard for calculation of earthquake hazard.

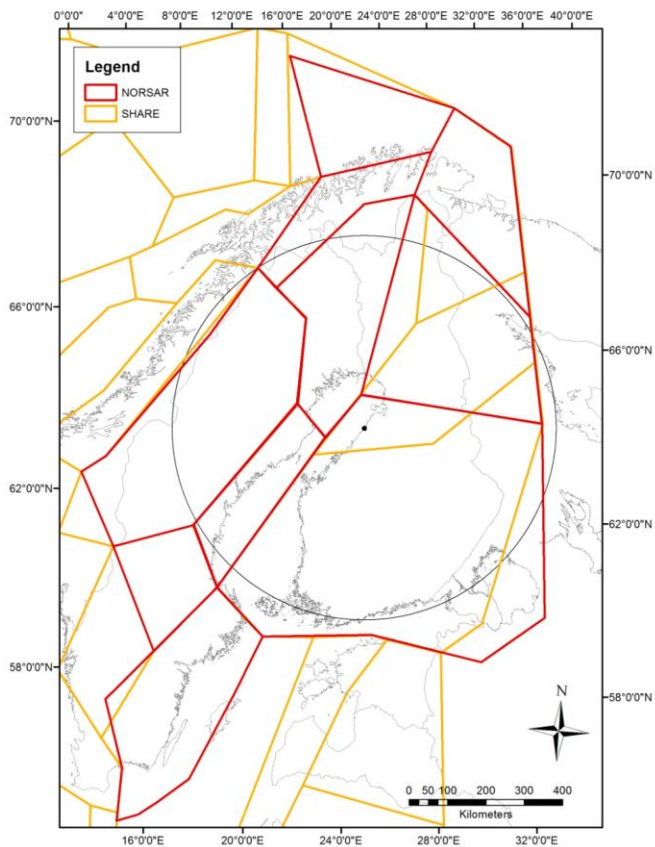


Figure 7.2.5. Seismic source areas of Scandinavia by SHARE (Giardini et al., 2013) modified from GSHAP model (Wahlström and Grünthal, 2001).

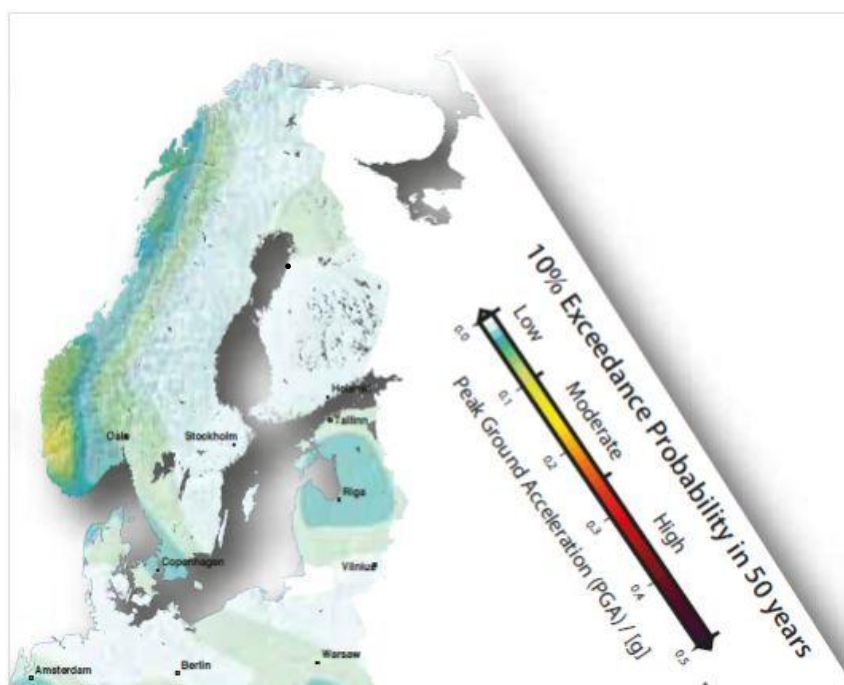


Figure 7.2.6. A Seismic probabilistic hazard map of Fennoscandia by SHARE- Seismic Hazard Harmonization in Europe (Giardini et al., 2013).

Saari (1998) focused on seismic source areas of south-eastern Finland and its vicinity. His source area model is based on observations of seismic activity and tectonic analysis. The model and its revisions (Fig. 7.2.7; Saari, 2008, 2012; Saari et al., 2009) have been used when estimating seismic hazard at NPP sites in Finland. Figure 7.2.6 presents seismicity and seismic source areas within the distance of 500 km from Hanhikivi. The model consists of 10 polygons characterized by areas of either low or moderate seismicity. The polygons in the west and north are trending in NE-SW direction and polygons in the east and south are trending in NW-SE direction.

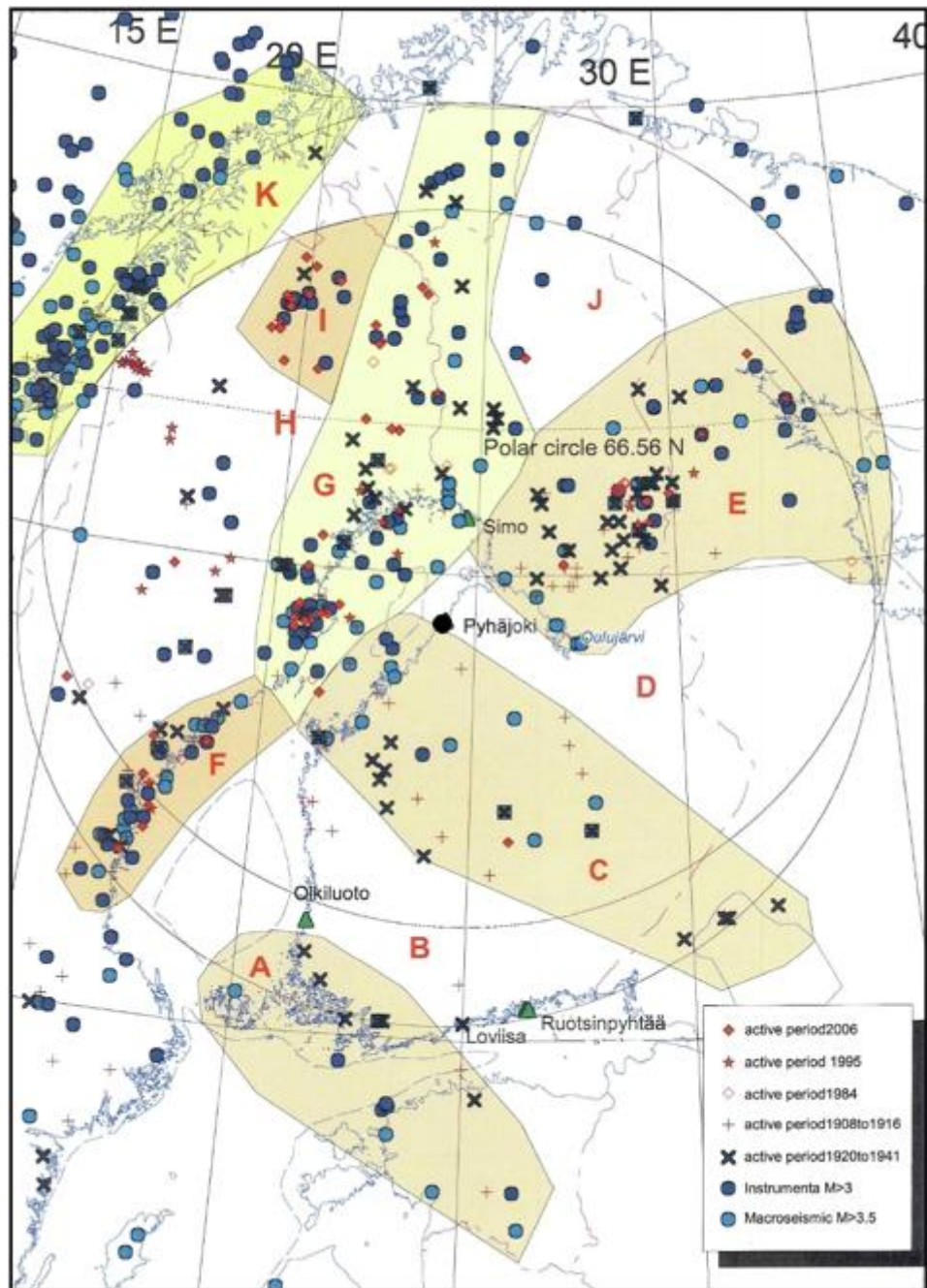


Figure 7.2.7. Seismic source areas and epicenters of earthquakes in 1375 - 2010 according to FENCAT (Saari et al., 2009). The distance of 500 km is from Hanhikivi site is shown by a circle.

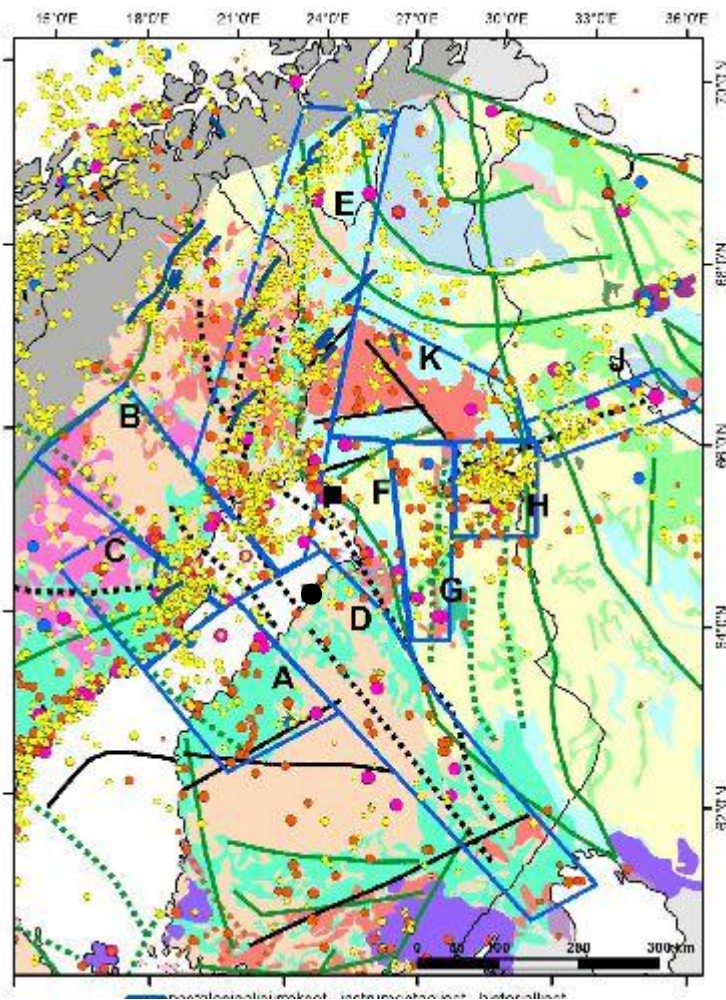


Figure 7.2.8. Seismicity in Fennoscandia according to Korja et al. (2011a). Historical earthquakes are from FENCAT – catalogue and instrumental earthquakes (1971–2010) from the Fennoscandian earthquake catalogue.

Mäntyniemi et al. (2001) prepared a seismic hazard map for Fennoscandia on the basis of knowledge of past seismicity. Probabilities of occurrence of magnitudes were computed for time intervals of one year and 50 and 100 years. No seismic source areas were defined. The peak ground acceleration values along the eastern coast of the Gulf of Bothnia were in the range 0.01–0.015·g for a mean return period of 475 years. They also estimated site-specific hazard for a hypothetical engineering structure located on the eastern coast. Maximum ground amplitude was chosen as the ground-motion descriptor in the site-specific hazard assessment, and seismicity data inside a circle with a 350 km radius from the site were taken into account.

Mäntyniemi (2008a) described the seismicity in the vicinity of three candidate NPP sites in the municipalities of Pyhäjoki, Ruotsinpyhtää and Simo. The seismic source areas defined in the framework of the GSHAP were used when computing a preliminary estimate of site-specific seismic hazard for each site. A peak ground acceleration value 0.12·g corresponding to a 10^{-5} annual probability of exceedance was given for Hanhikivi.

Korja et al. (2011a) outlined alternative seismic source areas around the Hanhikivi site for seismic hazard calculation of the regional area. They suggested that seismicity in northern Finland is mainly

concentrated to ancient weakness zones and faults that have been reactivated in the current stress field. In the report by Korja et al. (2011a), twelve source regions were defined in the areas surrounding the Bay of Bothnia (Fig. 7.2.8). Since the precision in epicenter location turned out to be rather low, it was not possible to attach single earthquakes to single faults or shear zones. For this reason, seismic source areas comprising several faults and larger earthquakes (magnitude over 3.5) were defined. Although the northern and western areas have a large effect on the seismic hazard calculations, the most influential seismic source area is still the Raahe-Ladoga shear complex, where the Hanhikivi site is located. The closest known active post-glacial fault zone is in Västerbotten, Sweden, 180 km west of this site.

8 Identification and description of seismic source areas

In the first part of this report we have described the new digital datasets now available for seismic source area modeling. The seismic data set within the study area is by far larger than those used in previous seismic source area models. We have used large amounts of small magnitude earthquake data from SNSN network that outline the zones of increased seismicity with higher precision than in the previous studies. We have also carefully checked the data to remove mining-induced events and explosions that degrade the quality of some of the previously published seismotectonic studies (e.g. Redfield and Osmundsen, 2013). By adding to the high quality seismic data also other high quality geophysical and geological data sets we augmented the geoscientific information of the study area. The high quality data sets warrant the design of more detailed seismic source area models than those based on fewer data (Saari et al., 2009), focusing on Scandinavia (Wahlström and Grünthal, 2001) or made for regional to global scale reference (SHARE; Giardini et al., 2013).

8.1 Basis for modeling

A. Korja

We have defined seismic source areas as areas with spatially distinct seismicity patterns. These patterns arise since seismic stress release favours pre-existing zones of weakness and, in intracratonic areas, earthquakes tend to occur along reactivated faults, ductile shear zones, failed rifts or other weak zones suitably oriented in the current stress field. A variation in earthquake occurrence and change in seismicity pattern is therefore likely to be due to local changes in the current stress field caused by such heterogeneities in the structural or lithological framework. As stated earlier in the text, we refer to reactivated faults and ductile shear zones in more general terms in this report as deformation zones.

In a seismic source area model, the studied area is divided into polygons with differing seismicity patterns. The patterns may comprise discrete seismogenic structures (i.e. faults), diffuse seismicity belts or regions, where seismicity is not attributable to specific structures, or a combination of the two. The definition of the polygons is based on various geological, geophysical and seismological datasets. A subsequent hazard analysis requires information on the geological and tectonic framework, seismic source geometries and seismological parameters from each polygon. A more detailed list is shown in Table 8.1.1.

Table 8.1.1. Properties of seismic source areas. Geological and tectonic framework and seismic source area geometry columns have been used to define the source areas, whereas seismological parameters have been collected for further studies. PGF = Post-glacial fault

Geological and tectonic framework	Seismic source geometry	Earth quake parameters
Major lithotectonic units based on lithological and structural databases	Presence/absence of seismicity	Largest observed magnitude
Direction of major deformation zones including faults	Direction of seismic zones	Style of faulting/fault plane solutions
Major Quaternary geological units	Activity level	Focal depth
Presence/absence of PGF	Seismogenic thickness	
Age of PGF faulting	Spatial and temporal seismicity patterns	
Direction of topographic/bathymetric ridges or valley		
Current stress field		

In order to avoid unilateral thinking or the adoption of unwarranted preconceptions concerning the sources of seismicity, three alternative seismic source area models, referred to as models 1,2 and 3, have been outlined for hazard assessment by two independent groups in a workshop in November 2013. Group 1 consisted of Meri-Liisa Airo (GTK), Karin Högdahl (UU), Paula Koskinen (ISUH), Päivi Mäntyniemi (ISUH), Mikko Nironen (GTK), Michael Stephens (SGU) and Marja Uski (ISUH). Group 2 consisted of Susanne Grigull (SGU), Taija Huotari-Halkosaari (GTK), Annakaisa Korja (ISUH), Emilia Kosonen (ISUH), Mirva Laine (GTK) and Björn Lund (UU). Jouni Saari was consulted by both groups. Group 1 produced spatial model 1 and focused their analysis on the potential reactivation of geologically ancient structures in the bedrock. They have used data sets bearing on seismicity, lithology, deformation zones including brittle components (faults), lineaments defined on the basis of magnetic and gravity data, and broader crustal structure including Moho depth. Group 2 produced the spatial models 2 and 3. They focused their analysis on the recently active structures using data sets bearing on seismicity, post-glacial faults (PGF), topography, bathymetry, lineaments defined on the basis of magnetic data and the current stress field. Model 3 is a more detailed version of spatial model 2 and contains additional polygons. After drafting the polygons, seismicity and seismic events in each polygon have been described by Uski, Mäntyniemi and Lund (see preface).

Since the description of seismic events are rather standard, most of the descriptions originally made for model 1 could be copied to model 2 and 3 with some modifications. Some minor changes to the preliminary boundaries were made based on the detailed investigations on the seismic events close to the boundaries. This was to assure that the boundaries separating areas with different geological and geophysical demands met also the seismological criteria. When drawing the polygon boundaries,

model 1 highlighted seismicity and its interplay with Paleoproterozoic bedrock structures and structural evolution, whereas models 2 and 3 highlighted seismicity and its interplay with post-glacial faulting and topography/bathymetry.

8.2 Spatial model 1

M. Stephens, M. Nironen, M. Uski, B. Lund & P. Mäntyniemi

8.2.1 General methodology and result

The identification of seismic source areas in spatial model 1 made use primarily of the observation from the seismicity data that earthquake epicenters are clustered in several parts of the study area and elsewhere either sparse and diffusely distributed or virtually absent (see section 2.8 and Figs. 2.8.1.1-2.8.1.3).

Focus was placed firstly on defining the boundaries to the clusters or groups of clusters by making use of the major lithotectonic framework (section 3.1.1) and the occurrence of ductile shear zones, ancient (pre-Quaternary) faults and lineaments (sections 3.1.2 and 3.1.3). These features relied, in turn, on the data sets addressed in sections 2.1 to 2.6 above. The paleotectonic evolution throughout the Archean and Proterozoic eons and the Paleozoic era (section 3.1) was a critical input to the descriptions of the source areas. In accordance to the rules summarized earlier, no account was taken in the construction of spatial model 1 to the faults known to be active during the Quaternary period (so-called PGF) or to the detailed interpretation of lineaments defined by magnetic minima in the vicinity of these faults (sections 2.7 and 3.2.3). The parts of the geological and tectonic framework that address glaciation and deglaciation (section 3.2) and the current stress field and plate tectonic regime (section 5) were also not addressed. Following definition of the clusters, areas were identified where virtually no seismic activity has been registered. Finally, the remaining parts of the study area were classified as areas with uncommon and diffuse seismic activity. The result of the exercise described above is shown in Figure 8.2.1 (polygons) and the coordinates defining each polygon are presented in Appendix 4.

Spatial model 1 consists of twelve seismic source areas with more or less clustered seismic activity (areas 1.2, 1.4, 1.5, 1.7, 1.8, 1.9, 1.10, 1.11, 1.14, 1.15, 1.16 and 1.17), two areas in which seismic activity is virtually absent (1.1 and 1.18) and four so-called “rest areas” where the seismic activity is sparse and diffuse. Five areas (1.1–1.5) lie more or less entirely inside Sweden with a minor extension, in two cases (1.1 and 1.2), into Norway; six areas (1.6–1.11) are situated in both Sweden and Finland with minor extension, also in two cases (1.6 and 1.7), into Norway; and seven areas are

either situated entirely in Finland (1.15), occur in Finland, Russia and Norway (1.12) or extend from Finland into Russia (1.13, 1.14, 1.16, 1.17 and 1.18).

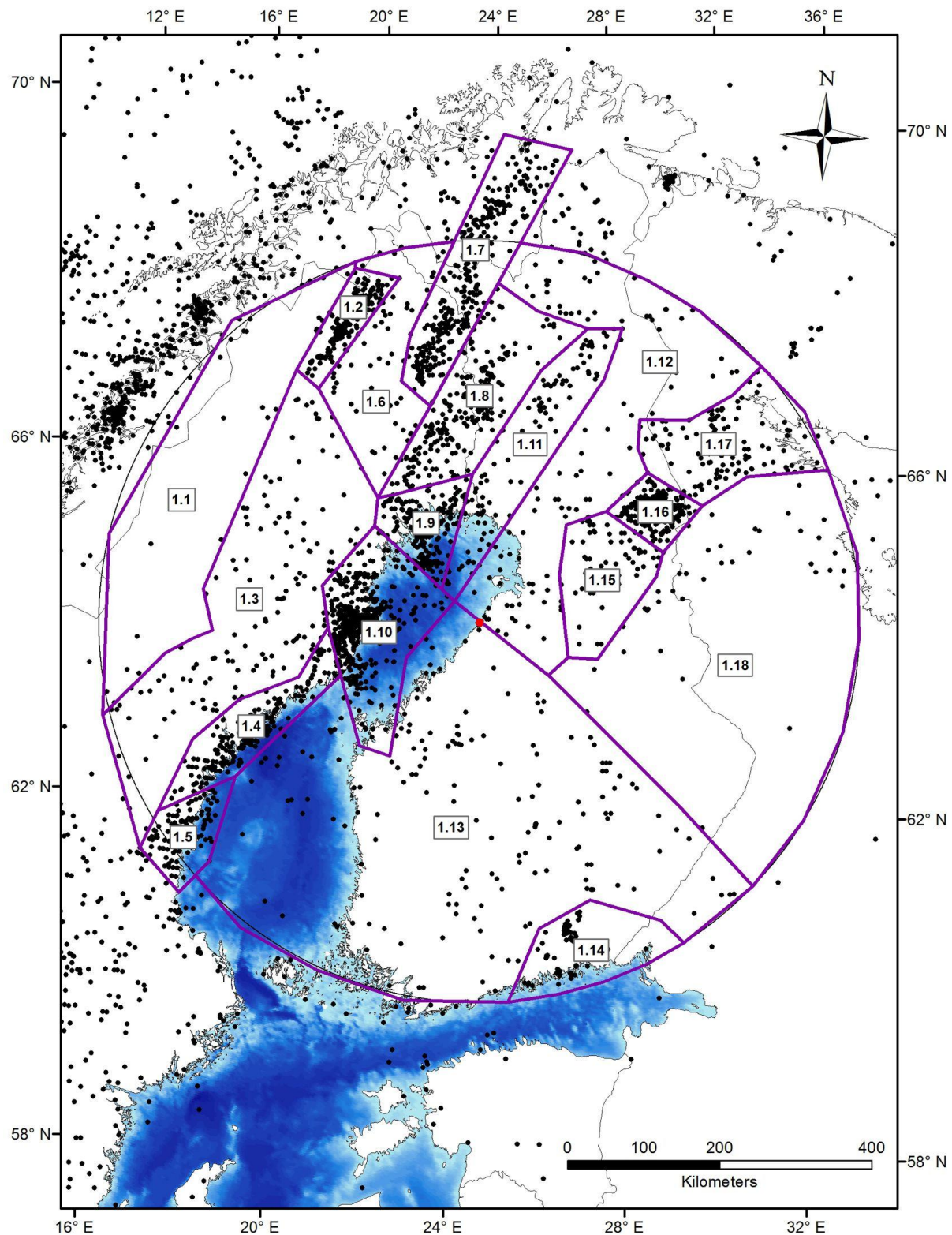


Figure 8.2.1. Earthquake epicenters (based on figures 2.8.1.1-2.8.1.2) and seismic source areas identified in spatial model 1 in the area with 500 km radius centred on the proposed Hanhikivi nuclear power plant, Finland. The bathymetric character of both the Gulf of Bothnia and the Gulf of Finland is also shown. Hanhikivi site: red dot.

The correlation of the proposed seismic source areas to the ancient tectonic framework (Figs. 8.2.2 and 8.2.3) is a prominent feature and motivates the strategy behind spatial model 1. This statement is illustrated by the following broader observations:

- The three groups of clusters close to the western side of the Gulf of Bothnia (1.5, 1.4 and 1.10, Fig. 8.2.1) follow the NE–SW trend of the partly faulted contact between the predominantly Paleoproterozoic crystalline basement, mostly preserved on land to the northwest, and the Proterozoic, Cambrian and, in part, Ordovician sedimentary cover rocks preserved in separate sub-basins on the sea-floor in the Gulf of Bothnia to the southeast (Figs. 8.2.2 and 8.2.3). Even the distinctive tail of earthquake epicenters beneath the Gulf of Bothnia in the Norra Kvarken archipelago corresponds to the basement high separating the sub-basins to the northeast (Bay of Bothnia) and southwest (Bothnian Sea) of this archipelago.
- The seismic source area where virtually no seismic activity has been registered in Sweden (1.1, Fig. 8.2.1) corresponds to the 0.5–0.4 Ga Caledonian orogen with NE–SW trend (Fig. 8.2.2) or, more strictly, if data south of 60°N is taken into consideration, to the Scandian mountain belt (Fig. 2.2.1) that formed in connection with the opening of the North Atlantic Ocean during the Paleogene. These two major tectonic entities correspond spatially very close to each other.
- The seismic source area where virtually no seismic activity has been registered in Finland (1.18, Fig. 8.2.1) corresponds to a part of the crystalline basement in the Fennoscandian Shield composed of Archean rocks (Fig. 8.2.2) that were less affected by younger Paleoproterozoic (2.0–1.8 Ga) orogenic events and were apparently cratonized earlier during the NeoArchean (e.g. Daly et al. 2006, Hölttä et al. 2008).
- The eight seismic source areas with prominent clusters of seismic activity showing a NE–SW or N–S trend in the northeastern part of the study area (1.2, 1.7, 1.8, 1.9, 1.11, 1.15, 1.16 and 1.17; Fig. 8.2.1) are all situated in the part of the crystalline basement in the foreland to the Caledonian orogen (Fennoscandian Shield), where Archean rocks form the structural basement (Fig. 8.2.2) and have been reworked, together with Paleoproterozoic rocks, by the 2.0–1.8 Ga orogenic system, i.e. in the area where cratonization generally occurred later during the Paleoproterozoic era.

The small cluster of epicenters in the southeastern part of Finland (1.14, Fig. 8.2.1) occurs inside a late Paleoproterozoic rapakivi granite suite (Fig. 2.4.2).

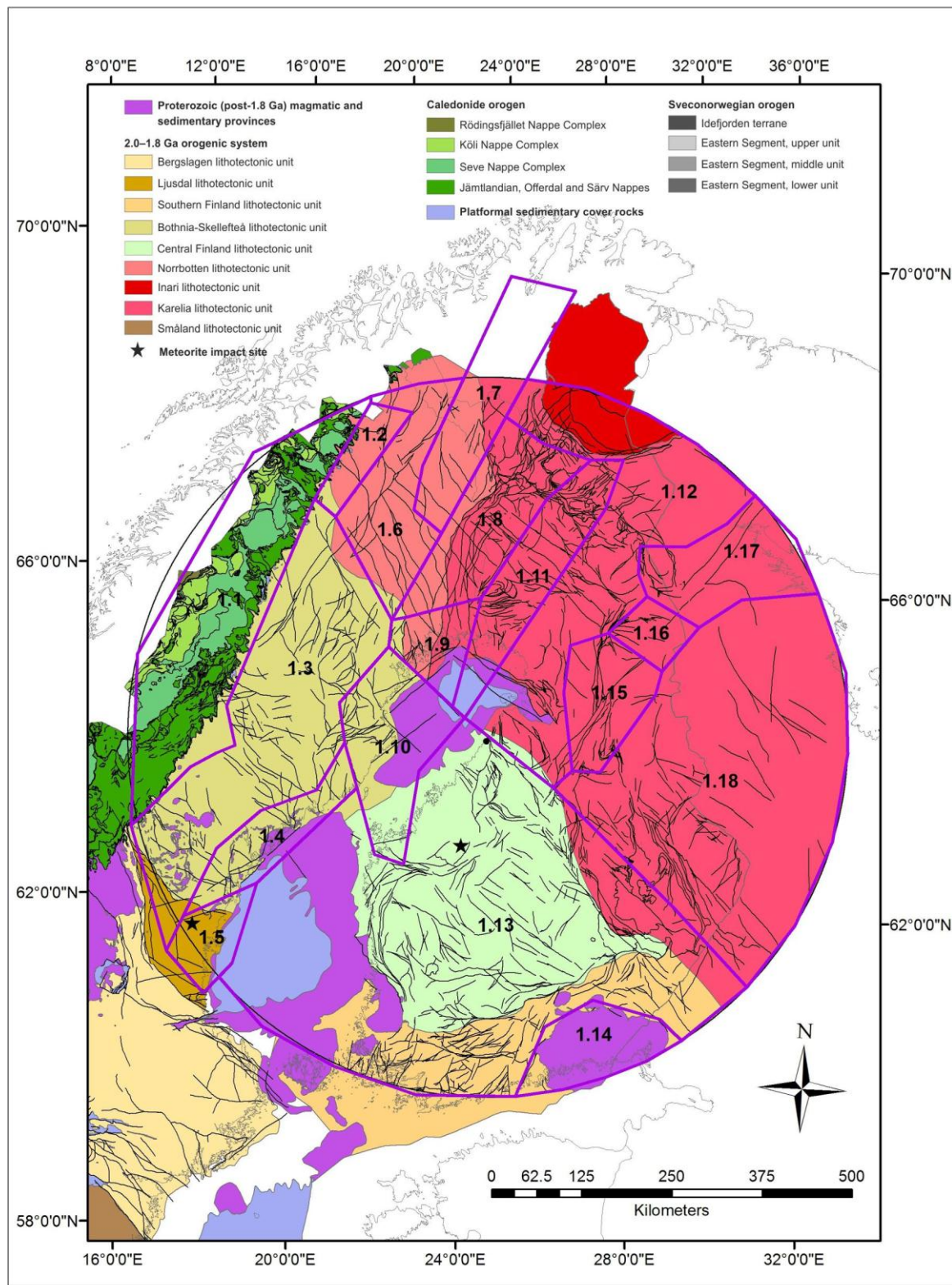


Figure 8.2.2. Seismic source areas identified in spatial model 1 and their relationship to major lithotectonic units (Fig. 3.1.1.1) extracted from the national bedrock databases at the scale 1:1 M for Sweden and Finland. Hanhikivi site: black dot.

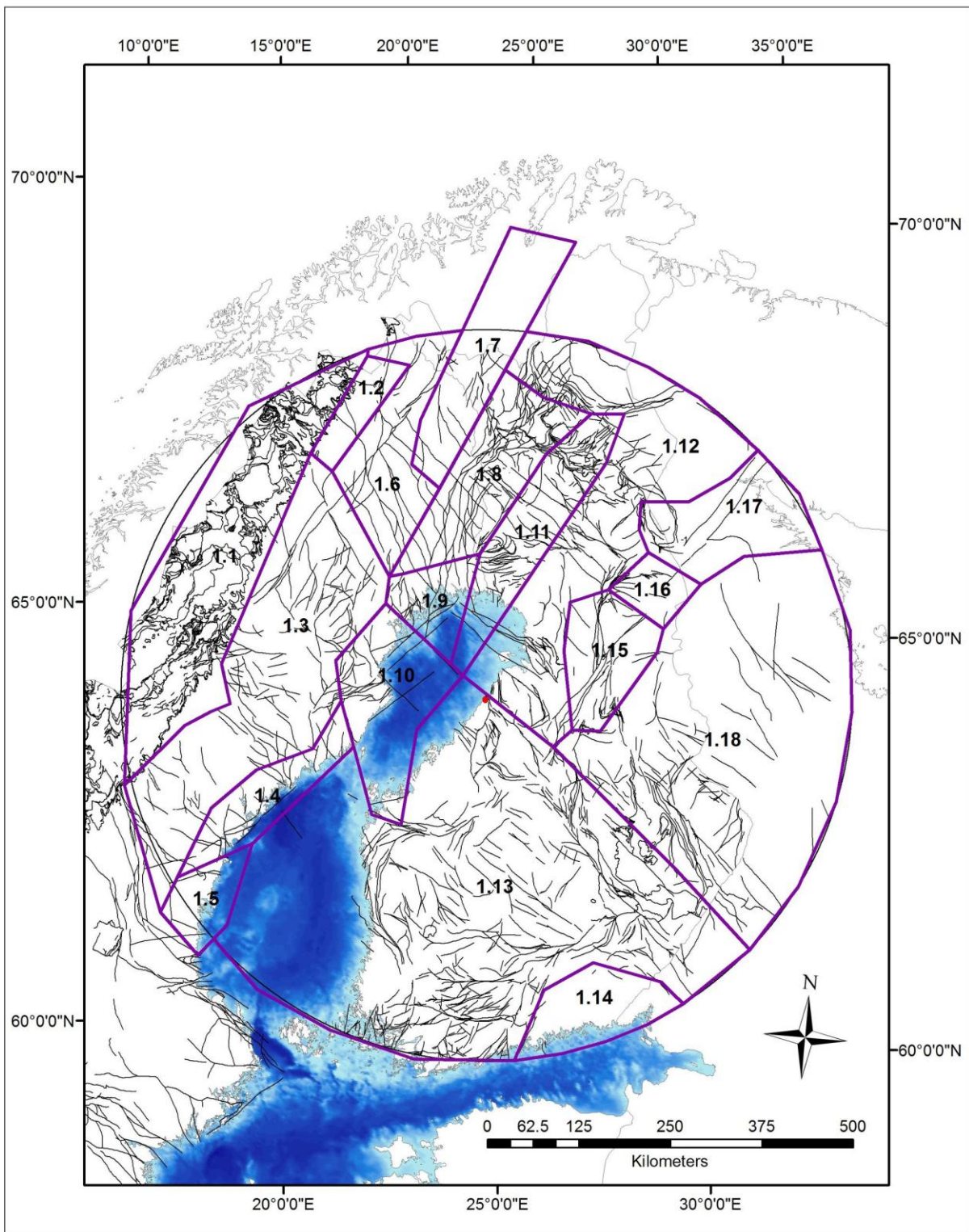


Figure 8.2.3. Seismic source areas identified in spatial model 1 and their relationship to major deformation zones (Fig. 3.1.2.1) extracted from the national bedrock databases at the scale 1:1 M for Sweden and Finland and modified slightly in the context of this study (see section 2).

The following text describes the different source areas with focus on a documentation of the data sets used in the definition of an area, the criteria used to define its boundaries, and the geological and seismological characteristics of the area. The ground surface spatial models for the distribution of major deformation zones, lithological units and lithotectonic units in the bedrock, and the map

showing the airborne magnetic anomalies identified using data collected at 30–60 m above ground level (Fig. 2.1.1 for Sweden) were continually used during the work with each seismic source area, both for the definition of its boundaries and for internal characterisation.

8.2.2 Description

Seismic source area 1.1

The seismicity data in combination with the information bearing on the major lithotectonic units and the major ductile and brittle deformation zones in the bedrock have been used to define and characterise seismic source area 1.1. The seismicity data consists of events both from the historical and instrumental data in the FENCAT catalogues (Figs. 2.8.1.1-2.8.1.2). The major lithotectonic units have been recognised using the combined information in the lithological and structural map databases. The information in these two databases inside source area 1.1 is based mainly on field outcrop data. Apart from some limited seismic reflection data along a W–E profile between Östersund and Norway (see overview in Gee et al., 2010), geophysical data have provided only limited information.

The western boundary of seismic source area 1 corresponds to the western limit of the study area with 500 km radius (Fig. 8.2.1). The eastern boundary has been constructed by essentially following the eastern erosional front of the 0.5–0.4 Ga Caledonian orogen (Fig. 8.2.2), which corresponds closely to the Scandian mountain belt that formed during the Paleogene. A minor modification from this trend was carried out in the north-central part of Sweden, north of Östersund, to include an area where epicentres are absent and regionally significant deformation zones have not been identified (Figs. 8.2.1 and 8.2.3).

Apart from the minor bulge referred to above, which lies within the Bothnia-Skellefteå lithotectonic unit, seismic source area 1.1 occurs entirely within the Caledonian orogen with its prominent NE–SW trend (Fig. 8.2.2). A distinctive feature of this orogenic belt is the occurrence of predominantly sedimentary and, in western areas, magmatic rocks, which formed during the Neoproterozoic to Silurian, that are thrust on top of and consequently allochthonous with respect to the underlying crystalline basement (see, for example, overviews in Roberts and Gee, 1985; Stephens, 1988; Gee et al., 2010; Figs. 3.1.2.2 and 8.2.3). The rocks show variable grades of metamorphism, locally under high-pressure conditions during different tectonic events (490–480 Ma and 450–440 Ma). The occurrence of transported slabs of Proterozoic basement inside the allochthonous sheets indicates the thick-skinned character of the thrust tectonics. The thrusts dip gently, generally westwards (Fig. 8.2.3), but the area is also affected by later, upright folding with axial surface traces parallel to the orogen. These folds rotate the thrust contacts and, thereby, give rise to dips of thrusts to the east

and an apparent normal sense of movement. The tectonostratigraphy was established during the Silurian in connection with a terminal continent-continent collision.

Source area 1.1 has very little seismicity and the events are widely distributed in the area (Fig. 8.2.1). The strongest instrumental event occurred on 17 November 1984 in the northwestern corner of the area and had a magnitude of 2.9. As the area has only one seismic station, in the southernmost corner, the events in the area have poor depth determinations and larger than average uncertainties in the epicentral locations. Focal depths vary between a few kilometres and 35 km, with large uncertainties. The conditions for documenting possible historical earthquakes were not favourable due to a sparse population and short literary tradition. However, the large Norwegian earthquake of 9 March 1866 was reportedly felt in the southern part of this area.

Seismic source area 1.2

The same types of data and information as in seismic source area 1.1 have been used to define and characterise source area 1.2. Furthermore, the major lithotectonic units have been recognised using the combined information in the lithological and structural map databases and the information in these databases is based, in turn, on an integrated evaluation of data derived mainly from field outcrop studies and airborne magnetic field measurements; gravity field measurements have also been used in particularly the interpretation of major lithotectonic units.

The boundaries of source area 1.2 are steered primarily by the reduction in the frequency of epicenters around the source area with its distinctive cluster pattern (Fig. 8.2.1). The western boundary corresponds to the boundary with seismic source area 1.1 and the eastern erosional front of the Caledonian orogen. The eastern boundary is steered mainly by the gradient in seismic activity but partly by ancient geological features. In the south, the boundary follows a deformation zone with NNE–SSW to NE–SW trend that disturbs mainly 1.8 Ga rocks at the ground surface (Fig. 8.2.3); in the Kiruna area in the central part, it follows the structural anisotropy defined by the strike of lithological units; in the north, it lies along a deformation zone with NNE–SSW to NE–SW trend affecting Archean rocks at the ground surface (Fig. 8.2.3). The southern boundary takes account of the fall in frequency of epicenters (Fig. 8.2.1) and lies also close to the boundary two lithotectonic units (Fig. 8.2.2); the Norrbotten lithotectonic unit to the north, containing 1.9–1.8 Ga magmatic rocks with an Archean component in their source rock, and the northern part of the Bothnia-Skellefteå lithotectonic unit to the south, containing similar rocks apparently lacking such a source component (Öhlander et al., 1993; Mellqvist et al., 1999). The northern boundary simply follows the sharp decrease in seismic activity (Fig. 8.2.1).

As indicated above, virtually the whole of seismic source 1.2 lies in the Norrbotten lithotectonic unit (Fig. 8.2.2), with its Archean basement and important metallic mineral deposits, comprising a major component inside the 2.0–1.8 Ga orogenic system. Archean orthogneiss intruded by dolerite (2.3–2.0 Ga) forms a conspicuous lithological component at the ground surface in the northern part of the area (Bergman et al., 2001). These rocks were subsequently affected, to variable extent, by deformation and metamorphism during orogenic activity at 2.0–1.8 Ga (Bergman et al., 2001). The remainder of source area 1.2 at the ground surface consists of Paleoproterozoic (2.4–2.0 Ga), metamorphosed sedimentary and volcanic rocks, which formed prior to the 2.0–1.8 Ga orogenic activity, and younger Paleoproterozoic variably metamorphosed, magmatic and sedimentary rocks, which formed during this activity, all underlain by Archean basement (Bergman et al., 2001). Volcanic rocks with variable composition from basaltic to rhyolitic (1.89–1.88 Ga) and felsic intrusive rocks (1.88–1.86 Ga) are volumetrically conspicuous in the near-surface realm.

Steeply dipping, ductile and brittle deformation zones with NNE–SSW to NE–SW, NW–SE or N–S strike occur within and along the eastern boundary of source area 1.2 (Fig. 8.2.3). Material in the structural map database and Bergman et al. (2001) indicates that one of the deformation zones with NNE–SSW to NE–SW strike in the northeasternmost corner of the source area (Kiruna–Naimakka deformation zone; Fig. 3.1.2.1; Bergman et al., 2001) shows a west-side-up, apparently reverse sense of displacement, while a zone with NW–SE strike further south shows a southwest-side-up, again apparently reverse sense of displacement (Fig. 8.2.3). These structures have affected the rocks described above but their tectonic evolution after 1.8 Ga is poorly constrained. Gently dipping thrusts with top-to-the-southeast displacement are present close to the western boundary of source area 1.2 directly west of the erosional front to and inside the Caledonian orogen (Fig. 8.2.3). These structures formed in connection with the continent-continent collision between Laurentia and Baltica during the period 450–390 Ma (Gee, 1975; Stephens, 1988; Gee et al., 2010). Faults in seismic source area 1.2 inferred to have been active during the Quaternary period are discussed below in spatial models 2 and 3.

Earthquakes in source area 1.2 (Fig. 8.2.1) are strongly correlated in space with the mapped surface trace of the post-glacial Pärvie fault which trends NNE–SSW (see spatial models 2 and 3). Events mostly occur to the southeast of the fault, as expected from its reverse mechanism with southeasterly dip direction. Permanent seismic stations of the SNSN were established in the area in 2003 and, during 2007–2010, a temporary seismic network of eight additional stations operated along the Pärvie fault. SNSN locations in area 1.2 generally have low epicentral uncertainties. Events with well-defined depths indicate that earthquakes occur from very shallow down to 35 km depth. However, the majority of events are confined to the upper 20 km of crust (Lindblom et al., 2011). The

strongest observed earthquake is a shallow M_L 3.6 event that took place on 26 December 1987 about 30 km WSW of Kiruna. No large historical earthquakes are known in this area.

Seismic source area 1.3

The same types of data and information as in source area 1.1 have been used to define and characterise seismic source area 1.3. Furthermore, the major lithotectonic units, the lithological units and the major ductile and brittle deformation zones in the bedrock have been recognised using the same type of data as that presented in source area 1.2.

Source area 1.3 with its sparse and diffuse seismic pattern (Fig. 8.2.1) emerged during the spatial model 1 work as one of two “rest areas” in the northwestern part of the study area following definition of the surrounding source areas 1.1, 1.2, 1.4, 1.5, 1.7, 1.8, 1.9 and 1.10. The boundary between source area 1.3 and the second “rest area” 1.6 was constructed by following approximately the line separating the Norrbotten and Bothnia-Skellefteå lithotectonic units at the ground surface (Fig. 8.2.2). The contact to the Archean rocks inside the Norrbotten lithotectonic unit dips to the south and west.

Virtually the whole of seismic source area 1.3 is situated inside the Bothnia-Skellefteå lithotectonic unit belonging to the 2.0–1.8 Ga orogenic system (Fig. 8.2.2). A rapakivi granite suite and dolerite sills intruded this unit after the 2.0–1.8 Ga orogeny (Fig. 8.2.2). The northernmost and southernmost parts occur inside the neighbouring Norrbotten and Ljusdal lithotectonic units, respectively (Fig. 8.2.2). More information on the geology in these marginal areas is presented in seismic source areas 1.2 and 1.5.

The major part of seismic source area 1.3 consists of migmatitic paragneiss and some better preserved metamorphosed greywacke (1.89 Ga and older), gneissic granitoid and leucocratic granite. In the northern part, magmatic provinces composed of rocks formed at 1.89–1.88 Ga and 1.88–1.86 Ga, the former with major metallic mineral deposits (Skellefte ore district), dominate; older magmatic rocks that formed at 1.95–1.93 Ga are locally present (Kathol and Weiher, 2005). All these rocks are intruded by large volumes of 1.8 Ga and, in southern parts, even 1.85 Ga granites (Lundqvist et al., 1990; Högdahl and Sjöström, 2001; Kathol and Weiher, 2005). Regional polyphase deformation and metamorphism at 1.88–1.86 Ga has been identified in the Bothnia-Skellefteå lithotectonic unit (Rutland et al., 2001; Kathol and Weiher, 2005; Skyttä et al., 2012). Ductile deformation along shear zones continued until 1.8 Ga. The bedrock in the southern part of the source area (see Fig. 8.2.2) is intruded by anorthosite, gabbro and granite belonging to the so-called rapakivi granite suite (1.53–1.51 Ga) and dolerite sills (1.27–1.26 Ga).

Steeply dipping, ductile and brittle deformation zones with WNW–ESE or NNW–SSE strike occur in the central and southern parts of source area 1.3, south of and including the Skellefte ore district (Fig. 8.2.3). North of this district the structural pattern changes radically and regionally significant deformation zones with NNE–SSW to NE–SW strike as well as zones with NW–SE or NNW–SSE strike are present (Fig. 8.2.3). Only a few detailed studies are available that have addressed the tectonic development along the deformation zones. Dextral transpressive deformation around 1.82 Ga has been inferred along the Hassela Shear Zone with WNW–ESE strike in the southernmost part of the source area (Högdahl and Sjöström, 2001) and inversion tectonics with transpressive deformation at 1.88–1.86 Ga following normal faulting has been inferred in the Skellefte ore district to the north (Bauer et al., 2011; Skyttä et al., 2012). Faults in source area 1.3 inferred to have been active during the Quaternary period are discussed below in spatial models 2 and 3.

In source area 1.3, seismicity increases from the Caledonian orogen or Scandian mountain belt in the west eastwards toward the coast and the Gulf of Bothnia (Fig. 8.2.1). There are no clear patterns in the event locations and the seismicity is diffuse (Fig. 8.2.1). Seismic stations are located in the eastern part of the area, making the western seismicity less well-determined. Earthquakes occur from shallow levels down to 40 km depth. Information regarding large historical earthquakes is missing. The Solberg earthquake of 29 September 1983 with magnitude around 4 (Table 4.3.1, No. 13) was located toward the coast in this area (Kim et al., 1985). The area of perceptibility extended to the coastline.

Seismic source area 1.4

The same types of data and information as in seismic source area 1.1 have been used to define and characterise source area 1.4. Furthermore, the major lithotectonic units, the lithological units, the major ductile and brittle deformation zones on land and some of the brittle deformation zones (faults) in the offshore realm, close to the coast of the Gulf of Bothnia, have been recognised using the same type of data as that presented in source area 1.2. Information on faults affecting the sedimentary cover rocks in the Gulf of Bothnia offshore area (Axberg, 1980), with a higher level of data spatial resolution, have also been used in the characterisation of seismic source area 1.4.

The boundaries of seismic source area 1.4 are steered mainly by the reduction in the frequency of epicenters around a broad group of earthquake clusters, the overall trend of which is NE–SW parallel to a fault in the offshore area and more or less parallel to the coastline of the Gulf of Bothnia (Fig. 8.2.1). In the southern part of the source area, this fault forms the boundary between the crystalline bedrock to the northwest and the sedimentary cover in submarine areas to the southeast (Fig. 8.2.2). The southern, northern and eastern boundaries of source area 1.4 have been constructed so as to follow the orientation of deformation zones or the fault in the submarine area with ENE–WSW,

NNW–SSE and NE–SW strike, respectively, which occur in the close vicinity of the gradient in seismic activity (Figs. 8.2.1 and 8.2.3). Since the earthquakes in the north appear to be clustered in a more N–S direction close to a deformation zone with the same orientation (Figs. 8.2.1 and 8.2.3), there was some uncertainty concerning the position of the northern boundary and whether or not a separate source area should be identified. The western boundary of source area 1.4 is more arbitrary in character and steered solely by the reduction in frequency of epicenters (Fig. 8.2.1).

Apart from a small corner in the southwesternmost part of source area 1.4, south of the Hassela Shear Zone, this source area is predominantly situated inside the Bothnia-Skellefteå lithotectonic unit, close to its partly faulted contact to younger Mesoproterozoic and Paleozoic sedimentary rocks to the southeast (Fig. 8.2.2). Rocks belonging to the rapakivi granite suite, dolerite sills and an alkaline complex intruded the rocks in the Bothnia-Skellefteå lithotectonic unit after the 2.0–1.8 Ga orogeny (Fig. 8.2.2).

The Bothnia-Skellefteå lithotectonic unit inside source area 1.4 consists of migmatitic paragneiss and some better preserved metamorphosed greywacke (1.89 Ga and older), gneissic granitoid (1.9 Ga) and leucocratic granite (Lundqvist et al. 1990). The bedrock in this unit is intruded by anorthosite, gabbro and granite belonging to the so-called rapakivi granite suite (1.58 and 1.51 Ga) which, in turn, are overlain, both on land and offshore, by Mesoproterozoic sandstone; 1.27–1.26 Ga dolerite sills and, at one location, an Ediacaran alkaline complex intruded these rocks (Fig. 8.2.2; Winterhalter, 1972, 2000; Axberg, 1980; Lundqvist et al., 1990). Cambrian sandstone and Ordovician shale, sandstone and limestone form the youngest rocks in the source area and are only preserved in the submarine area in the Gulf of Bothnia (Fig. 8.2.2; Winterhalter, 1972, 2000; Axberg, 1980). Seismic reflection data along profiles in the Gulf of Bothnia (e.g. BABEL Working Group, 1990, 1993; Korja and Heikkinen, 2005, 2008) confirm the continuation of the Mesoproterozoic magmatic and sedimentary rocks beneath the Paleozoic cover rocks in the offshore area.

Steeply dipping deformation zones with WNW–ESE to NW–SE and N–S strike, generally with a poorly understood tectonic evolution, occur on land in source area 1.4 (Fig. 8.2.3). Both these sets as well as faults with NE–SW strike have been identified using all the data available in the offshore area (see section 2.6), where they displace the Mesoproterozoic and younger Paleozoic rocks (Winterhalter, 1972, 2000; Axberg, 1980). Formation of faults with NE–SW trend and reactivation of older structures in the crystalline basement are suggested during the Mesoproterozoic and later tectonic evolution. The stratigraphic relationships in the southern part of seismic source area 1.4 show also that all these faults were active at least during or after the Ordovician period. The fault with NE–SW strike close to the coast, northwest of which the earthquake epicenters appear to be clustered, has been inferred to show a southeast-side-down displacement (Axberg, 1980). If some of the earthquake clustering is related to this fault, then it should dip to the northwest, at least at depth,

and have a reverse sense of displacement during or after the Ordovician. The dip-slip displacements along both the NW–SE and N–S fault sets in the offshore area are variable (Axberg, 1980).

Source area 1.4 belongs to the general band of seismicity that lines the Swedish northeast coast (Fig. 8.2.1). The area is well covered by the permanent station network constructed during 2000–2002, making the epicentral locations relatively well-constrained. At a more detailed level of observation inside area 1.4, some events form clusters of seismicity but the majority of the earthquakes occur in a more diffuse pattern (Fig. 8.2.1). Earthquakes occur from shallow depth to almost 40 km depth. The M_L 3.6 Sundsvall earthquake on 4 June 1974 is the strongest instrumental event observed in source area 1.4. It is challenging for studies of historical earthquakes, because the areas of perceptibility may be very incomplete, extending over water toward the east and areas of sparse settlement toward the west. An earthquake felt between Umeå and Härnösand and, in many places in the north, occurred on the morning of 28 July 1888. The area of perceptibility extended to Finland, where ground tremor was noticed in Pietarsaari (Swedish Jakobstad) and the archipelago. The magnitude has been estimated at about M_M 4.

Seismic source area 1.5

The same types of data and information as in seismic source area 1.1 have been used to define and characterise seismic source area 1.5. Furthermore, the major lithotectonic units, the lithological units, the major ductile and brittle deformation zones on land and some of the brittle deformation zones (faults) in the offshore realm, close to the coast of the Gulf of Bothnia, have been recognised using the same type of data as that presented in source area 1.2. As for source area 1.4, information on faults affecting the sedimentary cover rocks in the Gulf of Bothnia offshore area (Axberg, 1980), with a higher level of data spatial resolution, have also been used in the characterisation of seismic source area 1.5.

The boundaries of seismic source area 1.5 are steered mainly by the reduction in the frequency of epicenters around a broad group of earthquake clusters (Fig. 8.2.1). The overall trend of this broad concentration of earthquakes is slightly oblique to the coastline to the Gulf of Bothnia that more or less follows in orientation the boundary between the crystalline bedrock to the west and the sedimentary cover in submarine areas to the east (Fig. 8.2.2). The gradients are commonly situated close to deformation zones with WNW–ESE (southern boundary), ENE–WSW (northern boundary) or NNE–SSW to NE–SW (offshore, eastern boundary) strike and the boundaries have been constructed so as to follow these trends in the three areas (Fig. 8.2.3). As for source area 1.4, the western boundary of source area 1.5 is more arbitrary in character and steered solely by the reduction in frequency of epicenters (Fig. 8.2.1).

The major part of source area 1.5 is situated inside the Ljusdal lithotectonic unit, belonging to the 2.0–1.8 Ga orogenic system, close to the contact with younger Mesoproterozoic and Paleozoic sedimentary rocks to the southeast (Fig. 8.2.2). In the northernmost part of the source area, north of the Hassela Shear Zone and inside the neighbouring Bothnia-Skellefteå unit, Mesoproterozoic dolerite sills (1.27–1.26 Ga) intruded the gneissic bedrock after the 2.0–1.8 Ga orogeny (Fig. 8.2.2).

The bedrock in source area 1.5 is dominated by migmatitic paragneiss (1.89 Ga and older) intruded by gneissic granitoid (1.87–1.84 Ga); diatexitic migmatite and leucocratic granite are more conspicuous north of Hudiksvall, in the northern part of the source area (Wik et al., 2009). Regional polyphase deformation and metamorphism around 1.87–1.86 Ga and 1.83–1.82 Ga has been identified in the Ljusdal lithotectonic unit but only around 1.87–1.86 Ga in the southwestern part of the Bothnia-Skellefteå lithotectonic unit, west of the Gulf of Bothnia (Högdahl et al., 2008, 2011; Wik et al., 2009). In the offshore area, a layered sequence of Mesoproterozoic sandstone that passes upwards and eastwards into Cambrian sandstone and Ordovician shale, sandstone and limestone is preserved above the crystalline bedrock (Fig. 8.2.2; Winterhalter, 1972; Axberg, 1980). Impact melt and breccia inside a shock zone, related to a meteorite impact structure during the Cretaceous (Deutsch et al., 1992), occur in the western part of source area 1.5 around the lake Dellen (Fig. 8.2.2).

Steeply dipping, ductile and brittle deformation zones with WNW–ESE or NNW–SSE strike occur close to the southern and western boundaries of the source area (Fig. 8.2.3; Högdahl et al., 2009; Wik et al., 2009). A significant dextral strike-slip component of ductile shear displacement around 1.87–1.86 Ga and later around 1.81 Ga has been inferred along some of these zones (Högdahl et al., 2009). A complex interplay between steeply dipping ductile and brittle shear zones with E–W and ENE–WSW trend, the latter showing a sinistral strike-slip component of shear, are present in the northern part of the source area. The E–W zones appear to be an easterly continuation of the Hassela Shear Zone with its dextral transpressive deformation around 1.82 Ga (Högdahl and Sjöström, 2001) and probably earlier. Bearing in mind data with a higher level of spatial resolution (see section 2.6), faults with NNE–SSW to NE–SW trend showing predominantly east-side-down displacement are prominent in the offshore area close to the eastern boundary of the source area; more persistent faults with NW–SE strike and northeast-side-down displacement are also present (Fig. 8.2.3). The stratigraphic relationships indicate that these faults were active at least during or after the Ordovician period.

Source area 1.5 belongs to the general band of seismicity that lines the Swedish northeast coast as described in source area 1.4 (Fig. 8.2.1). The area is well-covered by the permanent station network constructed during 2000–2002, making the epicentral locations relatively well-constrained. In area 1.5, many of the events occur in a wide cluster or band trending NE–SW north of the town of Hudiksvall (Fig. 8.2.1). North and south of this cluster there is more diffuse seismicity (Fig. 8.2.1).

Earthquakes occur from shallow levels down to 35 km depth. The strongest event recorded is the M_L 3.4 earthquake on 15 December 1991 offshore Sundsvall. No large historical earthquakes are known in this area.

Seismic source area 1.6

The same types of data and information as in seismic source area 1.1 have been used to define and characterise seismic source area 1.6. Furthermore, the major lithotectonic units, the lithological units and the major ductile and brittle deformation zones in the bedrock have been recognised using the same type of data as that presented in source area 1.2.

Source area 1.6 with its sparse and diffuse seismic pattern emerged during the spatial model 1 work as the second “rest area” in the northwestern part of the study area following definition of the surrounding source areas 1.1, 1.2, 1.7, 1.8 and 1.9 (Fig. 8.2.1). As described above, the boundary between this source area and the second “rest area” 1.3 was constructed by following approximately the line separating the Norrbotten and Bothnia-Skellefteå lithotectonic units at the ground surface (Fig. 8.2.2).

Seismic source 1.6 is situated more or less entirely inside the Norrbotten lithotectonic unit (Fig. 8.2.2), with its Archean basement and important metallic mineral deposits, comprising a major component inside the 2.0–1.8 Ga orogenic system. The Archean rocks are a continuation of the Archean bedrock observed in source area 1.2; they were affected, to variable extent, by deformation and metamorphism during orogenic activity at 2.0–1.8 Ga (Bergman et al., 2001). The remainder of source area 1.2 at the ground surface consists of Paleoproterozoic (2.4–2.0 Ga), metamorphosed sedimentary and volcanic rocks, which formed prior to the 2.0–1.8 Ga orogenic activity, and younger Paleoproterozoic variably metamorphosed, magmatic and sedimentary rocks, which formed during this activity, all underlain by Archean basement (Bergman et al., 2001). Rocks belonging to different magmatic provinces and formed at 1.89–1.88 Ga, 1.88–1.86 Ga and around 1.8 Ga are volumetrically the most conspicuous in the near-surface realm.

Steeply dipping, ductile and brittle deformation zones with NW–SE strike (e.g. Nautanen deformation zone) strongly dominate inside source area 1.6 (Bergman et al., 2001; Fig. 8.2.3). These zones are part of the Western Lapland fault system (Fig. 3.1.2.1) that deforms older structures throughout Lapland. This fault system appears to end at the NNE-SSW to NE-SW trending Karesuando-Arjeplog deformation zone. Zones with N-S strike are locally present in the Karesuando-Arjeplog deformation zone (Bergman et al., 2001; Fig. 8.2.3). The Karesuando–Arjeplog deformation zone shows both west-side-up, apparently reverse dip-slip and a dextral strike-slip sense of displacement (Bergman et al., 2001). The deformation zones in source area 1.6 have affected all the rocks described above.

However, their tectonic evolution after 1.8 Ga is poorly constrained. Faults in source area 1.6 inferred to have been active during the Quaternary period are discussed below in spatial models 2 and 3.

Source area 1.6 is located in the region between some of the better established post-glacial faults identified in northern Sweden (see spatial models 2 and 3). However, such faults have been identified in the southwestern part of the source area (see spatial models 2 and 3) and appear to be spatially associated with ancient, regionally more important zones striking NW–SE as well as a segment of the Karesuando–Arjeplog deformation zone. The area shows a low activity rate diffuse seismicity (Fig. 8.2.1) and has been well-covered by seismic stations since 2004, making epicentral locations relatively well-determined. Earthquake depths range from shallow to 40 km. The strongest event recorded is the M_L 3.7 earthquake on 13 April 1967 about 40 km northwest of Kiruna (Table 4.3.1, No. 10). No large historical earthquakes are known in this area.

Seismic source area 1.7

The same types of data and information as in seismic source area 1.1 have been used to define and characterise source area 1.7. Furthermore, the major lithotectonic units, the lithological units and the major ductile and brittle deformation zones in the bedrock have been recognised using the same type of data as that presented in source area 1.2.

The western, southern and eastern boundaries of seismic source area 1.7 in Sweden proved difficult to define in the context of ancient geological features in the bedrock and were drawn mainly on the basis of the reduction in the frequency of epicenters around the clusters in the central part of the source area (Fig. 8.2.1). The eastern boundary is situated partly in the vicinity of a lithological boundary on the ground surface between intrusive rocks with an age range of 1.89–1.80 Ga to the east and of 1.89–1.86 Ga to the west.

In Sweden, source area 1.7 is situated between the Karesuando–Arjeplog deformation zone (Bergman et al., 2001) to the west and the Pajala shear zone (Kärki et al., 1993; Bergman et al., 2001, 2006) to the east, inside the Norrbotten lithotectonic unit (Fig. 8.2.2). The northern boundary of this unit is not well-constrained. It has been extended tentatively here as far north as a major system of shear zones inside source area 1.7 that strikes NNW–SSE through Finland and into Norway, which appear to link together with the Pajala shear zone (Fig. 8.2.2). The dominant pattern in earthquake locations also appears to turn from NE–SW to NNW–SSE direction in this part of the source area (Fig. 8.2.1 and Fig. 8.2.3). On the basis of these considerations, the northeasternmost part of seismic source area 1.7 inside the study area has been included in the Karelia lithotectonic unit (Fig. 8.2.2).

Source area 1.7 consists of Paleoproterozoic (2.0–1.8 Ga), variably metamorphosed, magmatic and sedimentary rocks, which formed during the 2.0–1.8 Ga orogenic activity, overlying Paleoproterozoic (2.4–2.0 Ga), metamorphosed sedimentary and volcanic rocks, which formed prior to this activity (Bergman et al., 2001); the latter are more conspicuous in the northern part of the source area. All these rocks are underlain by Archean crystalline basement rocks that are not exposed at the ground surface (Bergman et al., 2001). The syn-orogenic lithological units include rocks belonging to different magmatic provinces formed at 1.89–1.88 Ga, 1.88–1.86 Ga and around 1.8 Ga. A conspicuous positive Bouguer gravity anomaly indicative of mass surplus at depth, spatially associated with an anomaly in the total magnetic field, occurs inside source area 1.7 in Sweden directly south of the border to Finland (Figs. 2.1.1 and 2.1.2, respectively).

Steeply dipping, ductile and brittle deformation zones with NW–SE, NNW–SSE or N–S strike are present inside source area 1.7 (Bergman et al., 2001, Korsman et al., 1997; Fig. 8.2.3) and mainly coincide with the trends of the boundaries between major lithological units (Fig. 2.4.1). The tectonic evolution of these structures is, in general, poorly constrained. The NW–SE trending deformation zones are part of the Western Lapland fault system. Faults in source area 1.7 inferred to have been active during the Quaternary period are discussed below in spatial models 2 and 3.

Source area 1.7 encompasses the major post-glacial faults Merasjärvi and Lainio-Suijavaara in Sweden and Stuoragurra in Norway (see spatial models 2 and 3), all of which show appreciable seismic activity (Fig. 8.2.1). Recently, small PGFs have also been found in Enontekiö, in the Finnish part of the source area; the Paatsikkajoki and Palojarvi faults trend NE–SW and NNE–SSW, respectively, and the Kultima fault in a NW–SE direction (Table 3.2.3.1 and see spatial models 2 and 3). The southern segment of the Lainio-Suijavaara fault is spatially associated with one of the regionally important deformation zones with NNW–SSE strike. In Sweden, the activity is well-monitored since the station installations in 2004. The Stuoragurra fault in Norway was investigated with a temporary seismic network in the late 1990's. However, none of these data were available for the current study.

The seismicity in the area is mostly related to the post-glacial faults, with events occurring to the southeast of the faults as expected due to their reverse mechanisms with southeasterly dip directions. Some additional events occur diffusely away from the faults. In Enontekiö, the trends in seismicity range from NNW–SSE, the dominant orientation, to NNE–SSW, i.e. roughly parallel and perpendicular to the major deformation zone.

Events occur from shallow depths down to 35 km depth. The greatest instrumentally recorded earthquake is the 25 February 25 1975 M_L 4.0 event in Finnmark, northern Norway. No notable

historical earthquakes are known for this area. The area has been sparsely populated and devoid of major centers of documentation, so possible earthquakes could have passed unnoticed. Ground tremor was reported from Karasjok, in Norway, at the end of 1758, but the respective epicenter has been placed in Finland (Tatevossian et al., 2013).

Seismic source area 1.8

The same types of data and information as in seismic source area 1.1 have been used to define and characterise source area 1.8. Furthermore, the major lithotectonic units, the lithological units and the major ductile and brittle deformation zones in the bedrock have been recognised using the same type of data as that presented in source area 1.2. In addition, data from the FIRE 4 reflection seismic profile (Patison et al., 2006) were used.

The boundaries of seismic source area 1.8 proved difficult to define in the context of ancient geological features in the bedrock and were drawn mainly on the basis of the reduction in the frequency of epicenters around concentrations mainly in the central and southwestern parts of the source area (Fig. 8.2.1). However, as indicated above, the boundary to source area 1.7 to the west is situated partly in the vicinity of a lithological boundary on the ground surface between intrusive rocks that formed at 1.89–1.80 Ga (east) and 1.89–1.86 Ga (west). Furthermore, the concentrations of earthquake epicenters in the central and southwestern parts of the source area are situated inside or in close vicinity to the major shear belt referred to as the Pajala shear zone (Fig. 8.2.3; Kärki et al., 1993; Bergman et al., 2001, 2006).

The southwestern part of seismic source area 1.8 is situated to the west of the Pajala shear zone and forms a part of the Norrbotten lithotectonic unit. A larger part of the source area occurs within and to the east of the Pajala shear zone and is included here in the Karelia lithotectonic unit (Fig. 8.2.2). Seismicity is generally more diffuse in the northeastern part of the source area, to the east of this shear zone. The northern boundary of the source area has been drawn so that the source area is confined to the Karelia lithotectonic unit and does not include the earthquakes with a different spatial pattern immediately southwest of the Inari lithotectonic unit (Figs. 8.2.1 and 8.2.2).

Source area 1.8 consists of similar rocks as those present in area 1.7. Archean crystalline basement rocks, which are only exposed at the ground surface in the northeastern part of the source area, are overlain by Paleoproterozoic (2.4–2.0 Ga), metamorphosed sedimentary and volcanic rocks. All these rocks formed prior to but were affected by the 2.0–1.8 Ga orogenic activity and are overlain, in turn, by Paleoproterozoic (2.0–1.8 Ga), variably metamorphosed magmatic and sedimentary rocks, which formed during the 2.0–1.8 Ga orogenic activity. The syn-orogenic lithological units include rocks belonging to different magmatic provinces formed at 1.89–1.88 Ga, 1.88–1.86 Ga and around 1.8 Ga.

Ductile and brittle deformation zones with N–S, NE–SW and NNW–SSE trends comprise the complex deformation belt referred to as the Pajala shear zone (Kärki et al., 1993; Bergman et al., 2001, 2006), a major structural component inside source area 1.8 (Fig. 8.2.3). Bergman et al. (2006) suggested a polyphase tectonothermal evolution in the Norrbotten and Karelia lithotectonic units during the time span 1.86–1.74 Ga with different histories on both sides of this zone. Rocks to the west of it were little affected by the younger event around 1.8 Ga and the earlier history around 1.86–1.85 Ga was preserved in this area. Wikström et al. (1996) also suggested that ductile deformation along the Pajala shear zone took place earlier around 1.88 Ga. At least parts of the Pajala shear zone show an east-side-up and sinistral displacement during its development (Wikström et al., 1996; Bergman et al., 2001), i.e. opposite to that observed along the regionally significant Karesuando–Arjeplog deformation zone in source area 1.6 to the west.

A large part of source area 1.8 is also affected by faults with NW–SE strike, on both sides of and cross-cutting the Pajala shear zone (Fig. 8.2.3). These faults are part of the Western Lapland fault system. By contrast, the structural framework is different in the northeastern part of the source area, east of the Pajala shear zone (Fig. 8.2.3). In this area (Central Lapland belt), a set of east-bending convex shear zones dominate the structural pattern (Fig. 8.2.3). These ductile deformation zones have been interpreted as thrusts with displacement towards east or northeast (Lehtonen et al., 1998; Hölttä et al., 2007). In the northernmost part of source area 1.8, another set of shear zones, with roughly N–S strike, have been interpreted as thrusts with displacement towards the west–southwest (Hölttä et al., 2007). The variable kinematics in this area may be partly explained by later folding of the thrusts. In the center of source area 1.8 (east of the Pajala shear zone), a semi-circular area (Central Lapland granitoid complex) is bounded in the north by the Venejoki shear zone (Fig. 3.1.2.1), interpreted on the basis reflection seismic data (Patison et al., 2006) as a thrust zone with displacement towards the north. Faults inside source area 1.8 inferred to have been active during the Quaternary period are discussed below in spatial models 2 and 3.

In Sweden, the seismic activity has been well-monitored since the installation of the northernmost SNSN in 2004. The SNSN network together with the installation of new stations (RNF, TOF) in northern Finland has also improved event location accuracy on the Finnish side of the border. The southwestern and central parts of source area 1.8 are characterized by a moderate amount of low-magnitude seismic activity.

The source area encompasses the Lansjärv post-glacial fault in Sweden and extends into Finland where the Venejärvi, Ruostejärvi and Pasmajärvi post-glacial faults are situated; two post-glacial faults, Isovaara and Suasselkä (Fig. 2.7.2), are also located in the seismically quieter, northeastern

part of the area (see spatial models 2 and 3). The seismicity is located mostly to the southeast of the PGFs, with an appreciable NE–SW band of seismicity (Fig. 8.2.1) connecting the faults in Sweden and Finland. The NW–SE-striking Western Lapland fault system (Fig. 3.1.2.1) traversing the Central Lapland granitoid complex (see above) are prominent in the central part of the area. Intense clustering of earthquake epicenters takes place at locations where such zones and the post-glacial faults intersect. The events occur from shallow depth down to 40 km depth. The largest instrumental event is from the early instrumental recording period. It occurred on 4 September 1968 close to Pello in the Finland-Sweden border zone and had a magnitude of M_L 3.4.

A rather widely noticed earthquake occurred within source area 1.8 on February 17, 1819; it was reportedly felt in places such as Pajala, Kittilä, Muonio and Kolari. Some minor damage (broken windowpanes and stoves) was reported from Kittilä and the macroseismic intensity was $I = 5–6$ (EMS-98). Mäntyniemi (2008b) proposed that the epicenter of the earthquake of 4 November 1898 may have had its origin in this source area. An aftershock was widely felt less than an hour after the main shock. The respective area of perceptibility supports the notion that the epicenter was located in this area rather than in area 1.11.

Seismic source area 1.9

The same types of data and information as in seismic source area 1.1 have been used to define and characterise source area 1.9. Furthermore, the major lithotectonic units, the lithological units, the major ductile and brittle deformation zones on land and some of the brittle deformation zones (faults) in the offshore realm, in the Bay of Bothnia, have been recognised using the same type of data as that presented in source area 1.2. Further Information on possible faults affecting the sedimentary cover rocks in the Bay of Bothnia presented in Wannäs (1989) have also been used in the characterisation of seismic source area 1.9.

The boundaries of source area 1.9 are steered mainly by the reduction in the frequency of epicenters around an area where there is a concentration of earthquake clusters (Fig. 8.2.1). To the west and south, the gradients are situated close to deformation zones with N–S and NW–SE strike, respectively, and these structures have been used to define the western and southern boundaries of the polygon (Fig. 8.2.3). The deformation zone along the southern boundary also corresponds to a bathymetric disturbance in the Bay of Bothnia (Fig. 8.2.3). The boundary on the eastern side has been drawn so as to simply follow the gradient in seismicity (Fig. 8.2.1); it corresponds approximately to the eastern limit of the Pajala shear zone (Kärki et al. 1993, Bergman et al. 2001, 2006) with N–S trend (Fig. 8.2.3). The gradient and boundary on the northern side appears to be independent of and traverses across the Pajala shear zone (Fig. 8.2.3).

Source area 1.9 encompasses a geological highly complex area. The western part of the area, to the west of the Pajala shear zone, is situated more or less entirely inside the Norrbotten lithotectonic unit and the northeastern part, including the rocks in the shear belt referred to as the Pajala shear zone, belongs to the Karelia lithotectonic unit (Fig. 8.2.2). In the southeastern part of source area 1.9, beneath the Bay of Bothnia, these units are stratigraphically overlain by sedimentary cover rocks that were deposited during the Meso- or Neoproterozoic and Cambrian (Fig. 8.2.2). The deformation zone along the southern boundary to source area 1.9 is a fault that disturbs the sedimentary cover but this structure also lies close to or along the blind surface separating the Norrbotten and Karelia lithotectonic units to the north, where 1.9–1.8 Ga magmatic rocks at the ground surface show an Archean crustal input, and the Bothnia-Skellefteå lithotectonic unit to the south, where such rocks are more juvenile and lack an Archean input (Fig. 8.2.2; Öhlander et al., 1993; Mellqvist et al., 1999).

The Precambrian rocks in seismic source area 1.9 resemble those described in the neighbouring area to the north and the reader is referred to source area 1.8 for more information. A conspicuous new lithological component is the occurrence of alkaline ultrabasic dykes that intruded the crystalline bedrock around 1.1 Ga. The sedimentary cover rocks preserved offshore in the Bay of Bothnia consist of Cambrian sandstone overlying reddish Meso- or Neoproterozoic sandstone and siltstone.

Ductile and brittle deformation zones with N–S strike, which belong to the southernmost extension of the Pajala shear zone, appear to terminate southwards against the conspicuous deformation zone with NW–SE strike along the southern boundary of source area 1.9 (Fig. 8.2.3). More information on the tectonic evolution along and on both sides of the Pajala shear zone is presented above in source area 1.8. Zones with N–S, NE–SW and NW–SE strike are prominent on land to the west of the Pajala shear zone (Fig. 8.2.3), while faults with NE–SW, NW–SE and NNW–SSE strike apparently affected the sedimentary cover rocks in the sub-marine area in the Bay of Bothnia (see section 3.1.3). The stratigraphic relationships indicate that these faults were active at least during or after the Cambrian period.

Source area 1.9 may have been the host area of the earthquake of 27 November 1757 felt at the bottom of the Bay of Bothnia and along both the western and eastern coast. Wahlström (1990) gave its magnitude as M_{M} 3.7, but it may have been slightly stronger. The largest instrumental earthquake is the M_{L} 3.6 event that occurred on 6 June 1991 in Luleå. The area has appreciable seismicity (Fig. 8.2.1) but it has not been correlated to a known post-glacial fault (see spatial models 2 and 3). The area has been relatively well-covered since the SNSN network installation in 2004 and one additional permanent station was installed in the area in 2010. There is seismicity along the coastline in a NE–SW direction from Sweden into Finland, but also a well-defined band of seismicity that extends southwards into the Bay of Bothnia and a second one extending in a NW–SE direction in Sweden (Fig.

8.2.1). The offshore events have generally less well constrained locations than the events within the SNSN network. Events occur from shallow levels down to 45 km depth.

Seismic source area 1.10

The same types of data and information as in seismic source area 1.1 have been used to define and characterise source area 1.10. Furthermore, the major lithotectonic units, the lithological units, the major ductile and brittle deformation zones on land and some of the brittle deformation zones (faults) in the offshore realm, close to the coast of the Bay of Bothnia, have been recognised using the same type of data as that presented in source area 1.2. As in source area 1.9, information on faults affecting the sedimentary cover rocks in the Bay of Bothnia offshore area (see section 3.1.3), with a higher level of data spatial resolution, have also been used in the characterisation of source area 1.10.

The boundaries of seismic source area 1.10 are steered mainly by the reduction in the frequency of epicenters around several clusters, situated mainly on land and in the offshore area (Norra Kvarken) between Umeå and Vaasa (Fig. 8.2.1). The southwestern boundary conforms with the boundary deformation zone to source area 1.4 (Fig. 8.2.3), and extends this boundary both to the northwest on land along the zone (Fig. 8.2.3) and to the southeast into the Norra Kvarken area. This area is geologically significant since it marks a bathymetric and topographic high separating two sub-basins filled with sedimentary cover rocks in the Gulf of Bothnia (see section 3.1.3 and Fig. 8.2.2; Winterhalter, 1972, 2000; Axberg, 1980; Wannäs, 1989).

The northern boundary of source area 1.10 follows the fault with NW–SE strike and bathymetric disturbance separating area 1.10 from source areas 1.9 and 1.11 (Fig. 8.2.3). This fault is also geologically significant since it is inferred to mark a blind lithotectonic unit boundary beneath the sedimentary cover (see text above for source area 1.9 and Figure 8.2.2). The southern boundary on the Finnish side of the Gulf of Bothnia has also been placed close to a deformation zone with similar trend (Fig. 8.2.3). The northwestern and southeastern boundaries have been drawn somewhat arbitrarily along the boundaries to the two source areas (1.3 and 1.13, respectively) with sparser and more diffuse seismic activity (Fig. 8.2.1).

The western and southern parts of source area 1.10 are situated in the Bothnia-Skellefteå and Central Finland lithotectonic units, respectively (Fig. 8.2.2). By contrast in the northeastern part, north of Norra Kvarken beneath the Bay of Bothnia, the rocks in these units are stratigraphically overlain by sedimentary cover rocks that were deposited during the Meso- or Neoproterozoic and Cambrian (Fig. 8.2.2).

The Bothnia-Skellefteå lithotectonic unit, inside source area 1.10, consists of migmatitic paragneiss and some better preserved metamorphosed greywacke (1.89 Ga and older), gneissic granitoid and gabbro-diorite (1.9 Ga) and younger (1.8 Ga) granite (Kathol and Weihsed, 2005). Similar lithologies are found in the Vaasa granitoid complex, in the western part of the Central Finland lithotectonic unit (see Fig. 2.4.2). Regional deformation and migmatization, partly diatexitic in character, occurred around 1.88–1.86 Ga (Rutland et al., 2001) prior to the intrusion of the younger granites. However, ductile deformation and metamorphism apparently continued along deformation zones in the Bothnia-Skellefteå lithotectonic unit until at least 1.82 Ga (Romer and Nisca, 1995; Weihsed et al., 2002). The sedimentary rocks overlying the crystalline basement rocks and preserved offshore in the Bay of Bothnia consist of reddish Meso- or Neoproterozoic sandstone and siltstone beneath Cambrian sandstone (Winterhalter, 1972, 2000; Wannäs, 1989).

The most conspicuous deformation zone in source area 1.10 is the complex ductile and brittle Burträsk shear zone southwest of the Skellefteå mining district (Figure 8.2.3; see also Figures 2.4.2 and 3.1.2.1). The shear zone shows a dextral strike-slip component of displacement and was active in the ductile regime at 1.82 Ga (Romer and Nisca, 1995). Apart from the deformation zone with NNW–SSE strike along the southwestern boundary of the source area, regionally significant deformation zones have not been identified on land in the gneisses south of this major shear belt and west of the Gulf of Bothnia (Fig. 8.2.3). By contrast, north of the shear zone, to the west and north of Skellefteå, the structural pattern is more complicated with different sets of zones striking N–S, NW–SE and even NE–SW (Fig. 8.2.3). Sets of faults with similar trend have also been inferred in the offshore area in the Bay of Bothnia. Stratigraphic relationships indicate that these faults were active at least during or after the Cambrian period (Fig. 8.2.3; Wannäs, 1980). In the gneissic rocks of the Central Finland lithotectonic unit, in the southernmost part of source area 1.10, deformation zones with WNW–ESE are present. The southern boundary of source area 1.10 is the Malax shear zone (Fig. 3.1.2.1). The zone follows the strike of a peculiar rock association (Vittinki mafic volcanic rocks and chert) that may define an important tectonic boundary.

Source area 1.10 is Sweden's currently most seismically active area. The area contains the Burträsk and Röjnoret post-glacial faults (see spatial models 2 and 3), which show some spatial relationship to the ENE–WSW to NE–SW shear belt south of Skellefteå and the N–S system of deformation zones west of this town, respectively (see above). The area has been well-monitored by seismic stations since 2001. During 2012, a temporary network of six additional stations was installed around the Burträsk shear zone. A large proportion of the events in the area are aligned along and to the southeast of this fault. Seismicity extends to the northeast past the end of the surface mapped fault scarp into the Bay of Bothnia where it appears to be sparser (Fig. 8.2.1). There is less seismicity associated with the Röjnoret fault, but the area in between the faults contains significant diffuse

seismicity, which continues northward along the coastline (Fig. 8.2.1). Focal depths in the source area are from very shallow down to 45 km depth. In the Skellefteå district, the focal depth pattern differs from the neighbouring source areas as well as from the shallow seismicity pattern on the Finnish side of source area 1.10. Approximately 50% of the events occur in the middle and lower crust, at depths between 15 and 45 km.

The largest instrumental event in the area is from the early instrumental recording period. It occurred on 28 September 1962 close to Burträsk and measured M_L 4.0. During the operational period of the SNSN network, the largest observed earthquake is a strike-slip event of M_L 3.5 that took place on 15 June 2010 at the northeastern extension of the Burträsk fault (Table 4.3.1, No. 45).

The largest earthquake in the study area in the 1900's (9 March 1909, M_L = 4.6 according to FENCAT, M_L = 5 according to Båth, 1956) occurred almost certainly in source area 1.10. No aftershocks are known to have been reported. Three epicenters have been proposed in the published literature, including an offshore epicenter (FENCAT), one on the coast (Båth, 1956), and one tentatively placed close to Skellefteå (Mäntyniemi, 2012b). Several historical earthquakes since 1762 were reportedly felt in this town. The earthquakes of 14 July 1765 and 31 December 1908 were also simultaneously felt on the eastern coast. Several earthquake reports have been reported for the town of Vaasa on the eastern coast. They are probably related to offshore earthquakes. In most cases, no observations in Sweden have been found. Only in one case (earthquake of 26 May 1907) does the area of perceptibility extend from the Swedish territory to Vaasa. The macroseismic data suggest that this may have been a rather deep earthquake.

Seismic source area 1.11

The major lithotectonic units have been recognised using the combined information in the lithological and structural map databases. The information in the lithological database is based mainly on field outcrop data whereas information of the structural database is based mainly on evaluation of data derived from airborne magnetic field measurements. In addition, data from the FIRE reflection seismic profiles (Kukkonen and Lahtinen, 2006) were used. Furthermore, gravity field measurements have been used in the interpretation of major lithotectonic units.

The boundaries of seismic source area 1.11 are difficult to define in the context of ancient geological features in the bedrock and were drawn mainly on the basis of the reduction in the frequency of epicenters around concentrations mainly in the southern and northern parts of the source area (Fig. 8.2.1). The source area is mainly confined to the Karelia lithotectonic unit. The northern boundary roughly follows the margin to the Inari lithotectonic unit (Fig. 8.2.2).

Seismic source area 1.11 consists of Archean crystalline basement rocks, only exposed in the southernmost part of the source area, overlain by Paleoproterozoic (2.4–2.0 Ga), metamorphosed sedimentary and volcanic rocks. These rocks were affected by the 2.0–1.8 Ga orogenic activity and are overlain, in turn, by Paleoproterozoic (2.0–1.8 Ga), variably metamorphosed magmatic and sedimentary rocks, which formed during the 2.0–1.8 Ga orogenic activity. The syn-orogenic lithological units include rocks belonging to different magmatic provinces formed at 1.89–1.88 Ga and around 1.8 Ga.

Ductile deformation zones with E-W strike dominate in the Paleoproterozoic sedimentary and volcanic rocks in the central part of the source area (Peräpohja belt; Korsman et al., 1997; Fig. 8.2.3). Another set of roughly E-W trending ductile shear zones, curving towards NE-SW, are located in the northern part. These zones were interpreted by Evins and Laajoki (2002) as subhorizontal thrusts with displacement towards the south. The central part of source area 1.11 is characterized by NW-SE trending ductile-brittle faults that are part of the Western Lapland fault system (Fig. 3.1.2.1).

In the northeast instrumental seismicity forms a NE-SW-trending pattern that agrees with the small-scale rather than the major structural lines. The pattern is interrupted in central Lapland by NW-SE trending faults constituting the Western Lapland fault system (Fig. 3.1.2.1). The central part of source area 1.11 exhibits sparse and diffuse seismicity. Seismic activity increases towards the Bay of Bothnia area, where epicenters again follow the NW-SE trend. Overall, the local earthquakes are weak and shallow, mostly occurring within the first 15 km of crust. The largest instrumental event in source area 1.11 is from the early instrumental recording period. It occurred on 17 February 1961 in the Bay of Bothnia, about 40 km offshore Oulu and measured M_L 3.7.

This is probably the host area of the 15 June and 23 June 1882 earthquakes. The latter is among the strongest events, if not the strongest, in the seismological record. It is also unique for the Gulf of Bothnia region with two widely felt earthquakes within a time interval of only eight days. The largest intensities ($I = 6–7$ EMS-98) were assigned to Tornio in Finland and Sangis-Kalix area in Sweden (Mäntyniemi and Wahlström, 2013). It is not possible to resolve whether the maximum intensity was 6 or 7, although related documentation could be uncovered in archives. It is not possible to pinpoint whether the epicenter was offshore or onshore. An epicenter given by Båth (1956) to the earthquake of 4 November 1898 (5 November local time) places the $M_L > 4$ earthquake in this source area, but it has later been proposed that the epicenter was located more westward, in this case in source area 1.8 (Mäntyniemi, 2008b).

Seismic source area 1.12

The same types of data and information as in seismic source area 1.11 have been used to define and characterize seismic source area 1.12. The seismicity of the area is sparse and diffuse compared to the adjacent areas, 1.11 in the west and 1.15–1.17 in the east (Fig. 8.2.1). The area is considered as a “rest area” in between source areas with more distinct seismicity pattern. The boundary between this area and the southern “rest area”, 1.13, was constructed by following approximately the seismicity that parallels the Archean-Proterozoic boundary. The northern boundary corresponds to the northern limit of the study area with 500 km radius (Fig. 8.2.1).

Seismic source area 1.12 situates in the Karelia and Inari lithotectonic units (Fig. 8.2.2) and consists of Archean crystalline basement rocks, exposed mainly in the southern and northeastern parts of the source area. These rocks are overlain by Paleoproterozoic (2.4–2.0 Ga), metamorphosed sedimentary and volcanic rocks that are found in both lithotectonic units. These rocks were affected by the 2.0–1.8 Ga orogenic activity and are overlain, in turn, by Paleoproterozoic (2.0–1.8 Ga), variably metamorphosed magmatic and sedimentary rocks, which formed during the 2.0–1.8 Ga orogenic activity. The syn-orogenic lithological units include rocks belonging to different magmatic provinces formed at 1.89–1.88 Ga and around 1.8 Ga. Neoproterozoic sedimentary rocks (Muhos sandstone) are found in the southwestern part of the source area.

The central part of source area 1.12 is affected by deformation zones with NW–SE strike, the same that can be detected in source area 1.2, 1.6–1.8 and 1.11 (Fig. 8.2.3). The central part of source area 1.12 is affected by deformation zones with NW–SE strike, belonging to the Western Lapland fault system. The Vuotso shear zone (see Figure 3.1.2.1), flanks the southern margin of the Inari lithotectonic unit. The shear zone has been interpreted as a set of thrusts with displacement towards southwest (Gaál et al., 1989; Patison et al., 2006).

The instrumental earthquakes have been small, shallow and randomly scattered across the area. There are no distinct seismicity clusters except in the north, where a curved lineament of epicenters correlates with the Vuotso shear zone. A remarkable historical earthquake was felt at Utsjoki and on the Norwegian side of the border at the end of 1758 (Tatevossian et al., 2013). A large earthquake in the early instrumental era occurred on 20 February 1960 and its magnitude is given as M_L4.0. Another large instrumental earthquake in the region is the M_L3.6 event on 21 June 1974 in Ranua.

Seismic source area 1.13

The same types of data and information as in seismic source area 1.11 have been used to define and characterize seismic source area 1.13. This is a source area of quite diffuse seismicity (Fig. 8.2.1). During the spatial model 1 work it emerged as the second “rest area” in the eastern part of the study

area. The southern boundary of the area corresponds to the southern limit of the study area with 500 km radius (Fig. 8.2.1), whereas the NW-SE boundary is constructed by following approximately seismicity that parallels the Archean-Proterozoic boundary. The other boundaries follow definitions of the surrounding source areas 1.4, 1.5, 1.10 and 1.14.

The northeastern part of seismic source area 1.13 belongs to the Karelia lithotectonic unit (Fig. 8.2.2). This part consists of Archean crystalline basement rocks, overlain by Paleoproterozoic (2.4–2.0 Ga) metamorphosed sedimentary rocks; these rocks were affected by the 2.0–1.8 Ga orogenic activity and are intruded by 1.87–1.86 Ga magmatic rocks. Most of seismic source area 1.13 is situated inside the Central and Southern Finland units belonging to the 2.0–1.8 Ga orogenic system. A rapakivi granite suite and dolerite sills intruded this unit after the 2.0–1.8 Ga orogeny, and in the western part, beneath the Bay of Bothnia, the rocks in this unit are stratigraphically overlain by sedimentary cover rocks that were deposited during the Mesoproterozoic and Cambrian (Fig. 8.2.2).

In the central part of the Central Finland lithotectonic unit, east of the Gulf of Bothnia, ductile shear zones curve around the Central Finland granitoid complex (see Figure 2.4.2). In the northeastern part of the igneous complex, a major NW-SE trending structure, the Raahe-Ladoga shear complex, transects the igneous complex. The shear complex consists of ductile shear zones in varying directions, overprinted by semi-brittle and brittle faults (Pajunen, 1986; Kärki et al., 1993; Kärki and Laajoki, 1995). The horizontal movement directions and rates along the length of the shear complex are not known: both dextral (Halden, 1982) and sinistral (Gaál, 1980) horizontal shearing have been suggested along relatively late shear zones. Dextral shearing has been proposed for two shear zones in the northwestern part of the shear complex (Weiher and Mäki, 1997). NW-SE trending dextral shear zones exist in the area of the Central Finland granitoid complex, and Nironen et al. (2000) interpreted that they developed in a transtensional tectonic environment. To the southwest of the Central Finland granitoid complex there is a NW-SE trending shear zone (Kynsikangas shear zone). The inferred deformation history for the zone is sinistral horizontal movement followed by normal faulting (Pietikäinen, 1994).

Within the Southern Finland lithotectonic unit E-W and WNW-ESE trending shear zones cause a lozenge-shaped pattern (Fig. 8.2.3). A shear zone network with roughly E-W and NNE-SSW trends overprints this pattern (Väisänen and Skyttä, 2007). The E-W trending late shear zones have both vertical and horizontal movement components whereas at least some NNE-SSW trending zones are normal faults.

The few earthquakes in southern and central Finland are randomly scattered. However, the largest instrumental earthquake to occur in Finland, the M_L 3.8 event in Lappajärvi on February 17, 1979 is

located within this source area (No. 3, Table 4.3.1). The majority of earthquakes are confined within the first 15 km of crust.

According to non-instrumental earthquake data available, the southernmost Finnish coastline up to the border toward source area 1.10 exhibits low seismicity, the largest earthquake being that felt in the town of Uusikaupunki on 18 April 1926. The magnitude possibly exceeded M_L 3. The upper part of the coastline may have experienced historical earthquakes felt over rather long distances of the coastline. A strong candidate is the earthquake of 29 March 1777. No Swedish observations have been uncovered for this earthquake. The largest earthquake known in central Finland (M_L 4.3 ±0.2) occurred on the early morning of 16 November 1931. It was followed by a widely felt aftershock about 15 hours later (Mäntyniemi 2004b).

Seismic source area 1.14

The same types of data and information as in seismic source area 1.11 have been used to define and characterize seismic source area 1.14 (Fig. 8.2.1.). The area is located at the ground surface within the lithotectonic unit referred to as “Proterozoic (post-1.8 ga) magmatic and sedimentary provinces” (Fig. 8.2.2) and is confined to a 1.65 rapakivi granite (Wiborg granite; Rämö and Haapala, 2005). The southern boundary corresponds to the southern limit of the study area with 500 km radius (Fig. 2.4.2). There are no major lineaments in the source area (Fig. 8.2.3).

Source area 1.14 is separated from the surrounding area 1.13 due to its unique seismicity pattern. The Wiborg granite area is characterized by shallow swarm-type earthquake activity (Uski et al., 2006). The latest swarm has been occurring since December 2011 in and around the town of Kouvola (Table 4.3.1, No. 36). More than 200 earthquakes, with magnitudes ranging from M_L -1 to 2.8, have been recorded so far. The earthquake swarms are unusually shallow, most likely occurring within the first 2 km from the surface. The overall distribution of seismicity follows closely the NE-SW-oriented contacts of rapakivi intrusions, which seem to form local zones of crustal weakness inside the batholith. A shallow shock of M_L 2.9 on 21 July 1982 is the greatest instrumentally recorded event in the area. No aftershocks have been reported for the event.

This source area hosts the oldest earthquake in the Finnish seismicity record, that of 1610. There is an early report of an earthquake swarm in 1751–52. The occurrence during the winter months may cast some doubt on whether it was weather-induced; however, similar seismicity patterns later support the notion that it was of seismic origin. The largest non-instrumental event of M_L 3.1 belongs to the Lapinjärvi earthquake swarm in the 1950's.

Seismic source area 1.15

The same types of data and information as in seismic source area 1.11 have been used to define and characterize seismic source area 1.15. The northern, eastern and western boundaries of source area 1.15 are drawn mainly on the basis of the reduction in the frequency of epicenters that cluster around the two major lineaments, the trends of which are N-S and NNE-SSW (Figs. 8.2.1 and 3.1.2.1). In the northeast, the boundary is controlled by the increased seismicity level within source area 1.16. Since both historical and instrumental seismic data were insufficient to define the southern borders of polygon 1.15, the boundaries are defined such that the southern ends of the Hirvaskoski and Oulunjärvi shear zones (Fig. 3.1.2.1) are included in 1.15.

Seismic source area 1.15 is located in the Karelia lithotectonic unit (Figs. 8.2.2 and 3.1.2.1). The source area consists mainly of Archean crystalline basement rocks. These rocks are overlain by Paleoproterozoic (2.4–2.0 Ga), metamorphosed sedimentary and (minor) volcanic rocks that are confined in and around shear zones. These rocks were affected by the 2.0–1.8 Ga orogenic activity and are intruded by Paleoproterozoic (1.8 Ga) granites (Korsman et al., 1997).

Seismic source area 1.15 contains two major subvertical shear zones: the N-S trending Hirvaskoski shear zone and a NNE-SSW trending Oulunjärvi shear zone deforming the Hirvaskoski shear zone (Fig. 8.2.3). The Hirvaskoski shear zone has been interpreted an ancient thrust belt (thrusting towards east) that was subsequently deformed with a dextral shear component (Tuisku and Laajoki, 1990; Kärki et al., 1993). The sense of shear in the Oulunjärvi shear zone was sinistral (Kärki et al., 1993). Deformation style varied from ductile to semi-brittle, and a NNE trending semi-brittle fault (Auho fault) continues north towards seismic source area 1.16.

Earthquakes cluster at the intersection of the Hirvaskoski and Oulunjärvi shear zones and follow their strike to the north and northeast. However, the trends in earthquake distribution imply activity along NW-SE to NNW-SSE oriented smaller scale faults within the major deformation zones. The seismogenic layer extends from few km below the surface down to a depth of about 30 km. Nearly 50 % of the events occur in the middle crust, at depths between 15 and 30 km.

There are some interesting historical earthquakes probably associated with this source area. The earthquake of 10 April 1902 had a very rare area of perceptibility that extended across the border to Russia. Its magnitude exceeded M_L4. A lesser earthquake occurred on 26 December 1911. The uncertainty associated with the June 1626 epicenter is large, but the earthquake was felt within this source area (Tatevossian et al., 2011). The strongest instrumental earthquake is a magnitude M_L 2.9 event on 9 November 1990 in Puolanka.

Seismic source area 1.16

The same types of data and information as in seismic source area 1.11 have been used to define and characterise seismic source area 1.16. This area, Kuusamo, is the seismically most active area in Finland. The boundaries of the area are based solely on the higher rate of seismicity and the distinctive cluster pattern with relation to the neighboring source areas (Fig. 8.2.1).

The area is located in the Karelia lithotectonic unit (Fig. 8.2.2). It consists of Archean crystalline basement rocks intruded by Paleoproterozoic (2.4–2.0 Ga), mafic layered intrusions and dykes. It is also partly overlain by coeval sedimentary and volcanic rocks. The area was reactivated and metamorphosed during the 2.0–1.8 Ga orogenic activity.

The area is transected by a complex system of NNE-SSW and NW-SE oriented major shear zones and their minor conjugates. The NNE-SSW trending Auho-Kandalaksha fault zone (Fig. 3.1.2.1) consists of several parallel faults extending across source areas 1-15-1.17 from central Finland up to the Kandalaksha Gulf in northwestern Russia (Elo, 1991a). Magnetic and gravity data suggest sinistral movement or shear and steep dips for the faults (Elo, 1991b). The NW-SE trending faults are considered to be continuation of the Western Lapland fault system that stretches over a vast area (including source areas 1.2, 1.6-1.8, 1.11-1.12) from northern Norway to the central Lapland granitoid (Berthelsen and Marker, 1986; Elo, 1991a; Airo, 1999). In addition, roughly WNW-ESE oriented belt of layered intrusions seems to act as a zone of crustal weakness in the local stress field. The most intense clustering of earthquake epicenters coincides with the area where the above mentioned three major lineaments intersect (Uski et al., 2003, 2006). The seismogenic layer extends from few kilometers below the surface down to a depth of about 30 km, i.e., close to the basement of the middle crust. More than half of the events occur in the middle crust, at depths below 15 km. The central part of the area that is occupied by layered mafic intrusions appears to be aseismic down to 6-7 km depth (Uski et al., 2012).

The historical seismicity record begins in 1731 and largely consists of recurrent microearthquakes. The area has been poorly covered by seismic stations until 2005 when a dense temporary network of 4-7 stations became operational. Earthquake determinations before 2005 may therefore contain large uncertainties, whereas the later determinations are well constrained. The largest earthquake (18 August 1926) in this source area has magnitude above M_L 4. The largest instrumentally recorded earthquake is the M_L 3.5 event on 15 September 2000 in Kuusamo (Table 4.3.1, No. 28).

Seismic source area 1.17

Seismic source area 1.17 is located in the Karelia lithotectonic unit (Fig. 8.2.2). The area consists of Archean crystalline basement rocks, partly overlain by Paleoproterozoic (2.4–2.0 Ga),

metamorphosed sedimentary and volcanic rocks. These rocks were affected by the 2.0–1.8 Ga orogenic activity.

The resolution of the geophysical data for interpretation of lineaments is poor in this source area. A NNW-SSE trending lineament exists in the westernmost part of the area, and on lithological basis it probably is a thrust fault. The NNE-SSW trending Auho-Kandalaksha fault zone that continues from source area 1.16 can be discerned.

The same types of data and information as in seismic source area 1.11 have been used to define and characterize seismic source area 1.17. The boundaries do not follow specific ancient geological features in the bedrock and were therefore drawn mainly on the basis of the reduction in the frequency of epicenters (Fig. 8.2.1). The southern and northern limits are based primarily on distribution of epicenters around the broad NNE-SSW trending Auho-Kandalaksha fault zone. The western boundary coincides with the decreased activity rate NNW of the Kuusamo area, and the eastern boundary corresponds to northeastern limits of both the study area and the deformation zone.

Seismicity seems to follow the NNE-SSW trend of the Auho-Kandalaksha fault zone, although roughly NW-trending clusters are also visible. The events are shallower than in the neighboring Kuusamo area: less than 10 % of the events have focal depth exceeding 15 km. Here also, the deepest events seem to concentrate within a zone occupied by mafic layered intrusions. However, due to lack of seismic stations in the area, uncertainties in earthquake source parameters may be high.

An earthquake was felt at the bottom of the Bay of Kandalaksha on 17 December 1758, and it is possible that the observations were made in the vicinity of the epicenter. The maximum intensity may have been up to I=6–7 (EMS-98), because damages to the masonry parts of dwellings were reported (Tatevossian et al., 2013).

The only instrumental earthquake of magnitude greater than 4.0 in northeastern Fennoscandia was located on the eastern fringes of this area. The event took place on 20 May 1967 in the Kandalaksha Gulf and was assigned with magnitudes ranging from 4.8 to 5.2 (Table 4.3.1, No. 1).

Seismic source area 1.18

The same types of data and information as in seismic source area 1.11 have been used to define and characterise seismic source area 1.18. Seismicity of the source area is diffuse, and evidence of seismic activity diminishes toward south (Fig. 8.2.1). The boundaries of seismic source area 1.18 do not follow specific ancient geological features in the bedrock except in the south where the boundary has the same NW-SE trend as the Archean-Proterozoic boundary. The eastern boundary of the area

corresponds to the eastern limit of the study area with 500 km radius (Fig. 8.2.1), whereas the southern boundary is drawn up by following the Raahe-Ladoga shear complex with its NW-SE trend (Fig. 3.1.2.1). Zones of enhanced seismic activity (source areas 1.15-1.17) dictate the northwestern and northern boundaries of area 1.18.

Seismic source area 1.18 is located in the Karelia lithotectonic unit (Fig. 8.2.2). The source area consists of Archean crystalline basement rocks, partly overlain by Paleoproterozoic (2.4–2.0 Ga), metamorphosed sedimentary and volcanic rocks. These rocks in the western part of the seismic source area were affected by the 2.0–1.8 Ga orogenic activity but the effects of this activity diminish eastwards.

The western part of the area is characterized by slightly curving, generally NNW-SSE trending lineaments that have been interpreted as thrust faults (thrusting towards NE at 1.91-1.88 Ga; Kohonen, 1995). The resolution of the geophysical data for interpretation of lineaments is poor in the eastern part of the source area.

The few instrumental events have been weak, shallow and randomly scattered. In addition, lack of seismic stations in the Russian side of the border has precluded detailed analyses of earthquake mechanisms. The strongest event, the M_L 3.7 earthquake on 24 August 1991, is located at the northeastern corner of the source area, close to the Kandalaksha seismicity zone (area 1.17). No notable historical earthquakes are known in this source area. It could be explained by a lack of documentation due to sparsely distributed population and a border area. However, the area appears quite devoid of earthquake epicenters in the instrumental era as well.

8.3 Spatial models 2 and 3

S. Grigull, A. Korja, E. Kosonen, B. Lund, M. Uski & P. Mäntyniemi

8.3.1 General methodology and result

The identification of seismic source areas in spatial models 2 and 3 made use primarily of the seismicity data and the observation that earthquake epicenters in the study area 1) occur in clusters, 2) are generally sparse and diffusely distributed or 3) are virtually absent (sections 2.8 and 4). The seismic data used in the modeling work consists of events both from the SNSN and the FENCAT catalogues (Figs 2.8.1.1-2.8.1.3). Focus was placed on defining the boundaries to these three different styles of seismic activity by making use of the data bearing on faults active during the Quaternary as described in sections 2.7 (Fig. 2.7.2) and 3.2. In model 3, bathymetric and topographic information was also used (section 2.2). No account was taken in spatial models 2 and 3 to lithological information (sections 2.1, 2.3-2.4), geologically ancient structures (sections 2.1–2.3, 2.5

and 2.6) or to parts of the geological and tectonic framework that address the paleotectonic evolution (section 3.1). Although the airborne magnetic anomaly patterns reflect in the first hand the ancient geological structures, the post-glacial faults were studied in the context of the magnetic data in order to look for evidence for reactivation during the Quaternary period along the ancient structures (see section 2.7).

Spatial model 3 is a modification of model 2, where larger polygons were broken up into smaller polygons resulting in source areas more strongly focused on the seismically active faults and the clusters in seismic activity. The results of the exercise described above are shown in Figures 8.3.1–8.3.3 for model 2 and in Figures 8.3.4–8.3.6 for spatial model 3. The coordinates defining each polygon in the two models are presented in Appendix 4.

Spatial model 2 consists of twelve seismic source areas (Fig. 8.3.1) of which seven areas contain earthquake clusters (2.3, 2.4, 2.5, 2.6, 2.7, 2.9 and 2.12), two areas are considered seismically quiet (2.1 and 2.10), and three areas show generally sparse and diffusely distributed seismicity (2.2, 2.8 and 2.11). One area straddles the Swedish-Norwegian border (2.1), four areas lie completely within Sweden (2.2, 2.3, 2.4 and 2.5), and two areas extend across the border between Sweden and Finland (2.6 and 2.7), with area 2.7 also covering small parts of Norway and Russia. Areas 2.8, 2.9, 2.10 and 2.12 are situated both in Finland and Russia, and polygon 2.11 includes the Finnish and Russian mainland as well as parts of Sweden's marine territory in the southern Gulf of Bothnia. The following four source areas in model 2 contain one or more faults known to be active during the Quaternary: 2.2, 2.3, 2.5 and 2.7 (Fig. 8.3.2).

Model 3 consists of 21 polygons (Fig. 8.3.4) of which twelve areas contain earthquake clusters (3.2, 3.4, 3.5, 3.6, 3.8, 3.9, 3.11, 3.12, 3.15, 3.18, 3.12 and 3.17), two are considered quiet (3.1 and 3.19), and seven areas show sparse and diffusely distributed seismicity (3.3, 3.7, 3.10, 3.13, 3.14, 3.16 and 3.20). Apart from some minor adjustments, the following six source areas are congruent in spatial models 2 and 3, and will only be described in detail in model 2: 2.1/3.1, 2.2/3.3, 2.3/3.4, 2.8/3.16, 2.10/3.19, 2.12/3.21.

Of the 21 source areas, two areas straddle the Swedish-Norwegian border (3.1 and 3.2), six polygons lie completely within Sweden (3.3, 3.4, 3.5, 3.6, 3.7 and 3.8), three areas extend across the Swedish-Finnish border (3.9, 3.10 and 3.11) and two areas are shared by Sweden, Finland and Norway (3.12 and 3.13). Area 3.14 lies in Finland and Norway and only area 3.15 lies completely within Finland. Polygons crossing the border from Finland to Russia are 3.16, 3.17, 3.18, 3.19 and 3.21. Area 3.20 includes the Finnish and Russian mainland as well as parts of Sweden's marine territory in the

southern Gulf of Bothnia. The following six source areas in model 3 contain one or more faults known to be active during the Quaternary: 3.2, 3.3, 3.6, 3.11, 3.12 and 3.15 (Fig. 8.3.6).

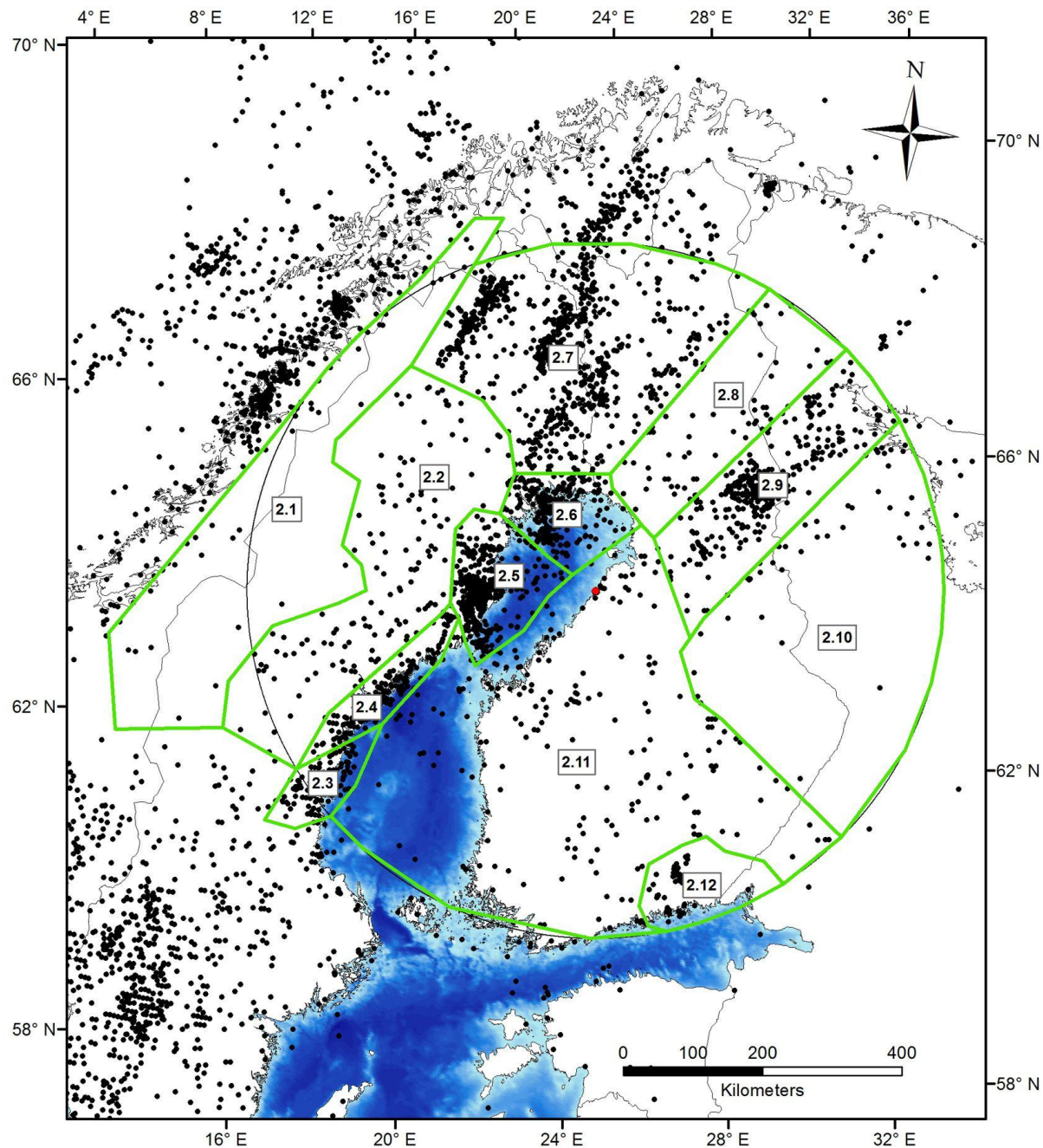


Figure 8.3.1. Earthquake epicenters (Figs. 2.8.1.1-2.8.1.2) and seismic source areas identified in spatial model 2 in the area with 500 km radius centred on the proposed Hanhikivi nuclear power plant, Finland. The bathymetric character of both the Gulf of Bothnia and the Gulf of Finland is also shown.

The work with spatial models 2 and 3 has clearly shown that most earthquake clusters are spatially related to the occurrence of single fault lines or fault systems that show evidence for Pleistocene and Holocene movement. This relationship is reflected in the choice of polygon geometries in both

models. The following text describes the different source areas with focus on the criteria used to define the boundaries and the geological and seismological characteristics of each area.

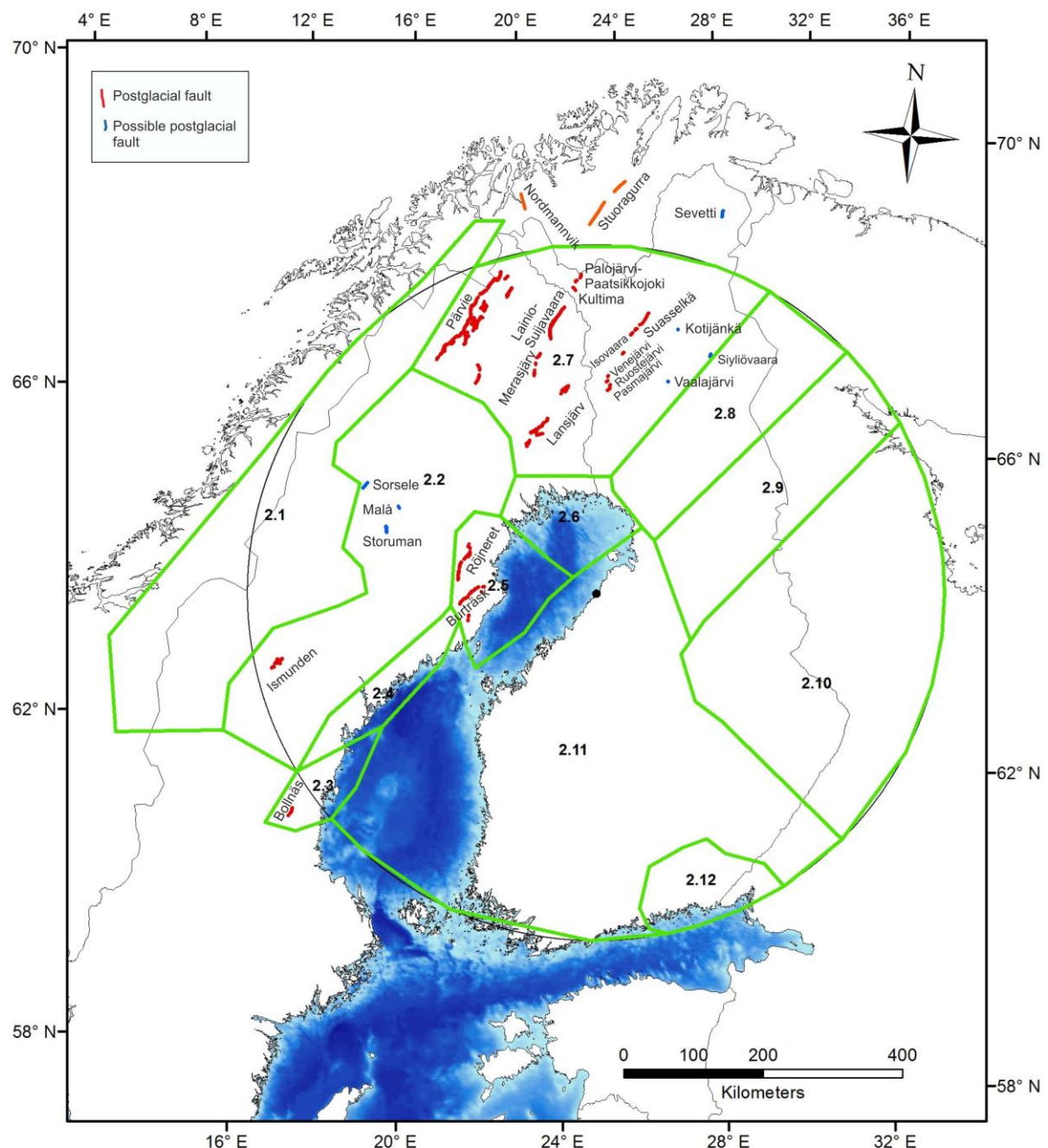


Figure 8.3.2. Seismic source areas identified in spatial model 2 and their relationship to faults inferred to have been active during the late Pleistocene or Holocene on the basis of Quaternary geological data (Fig. 2.7.2). The bathymetric character of both the Gulf of Bothnia and the Gulf of Finland is also shown.

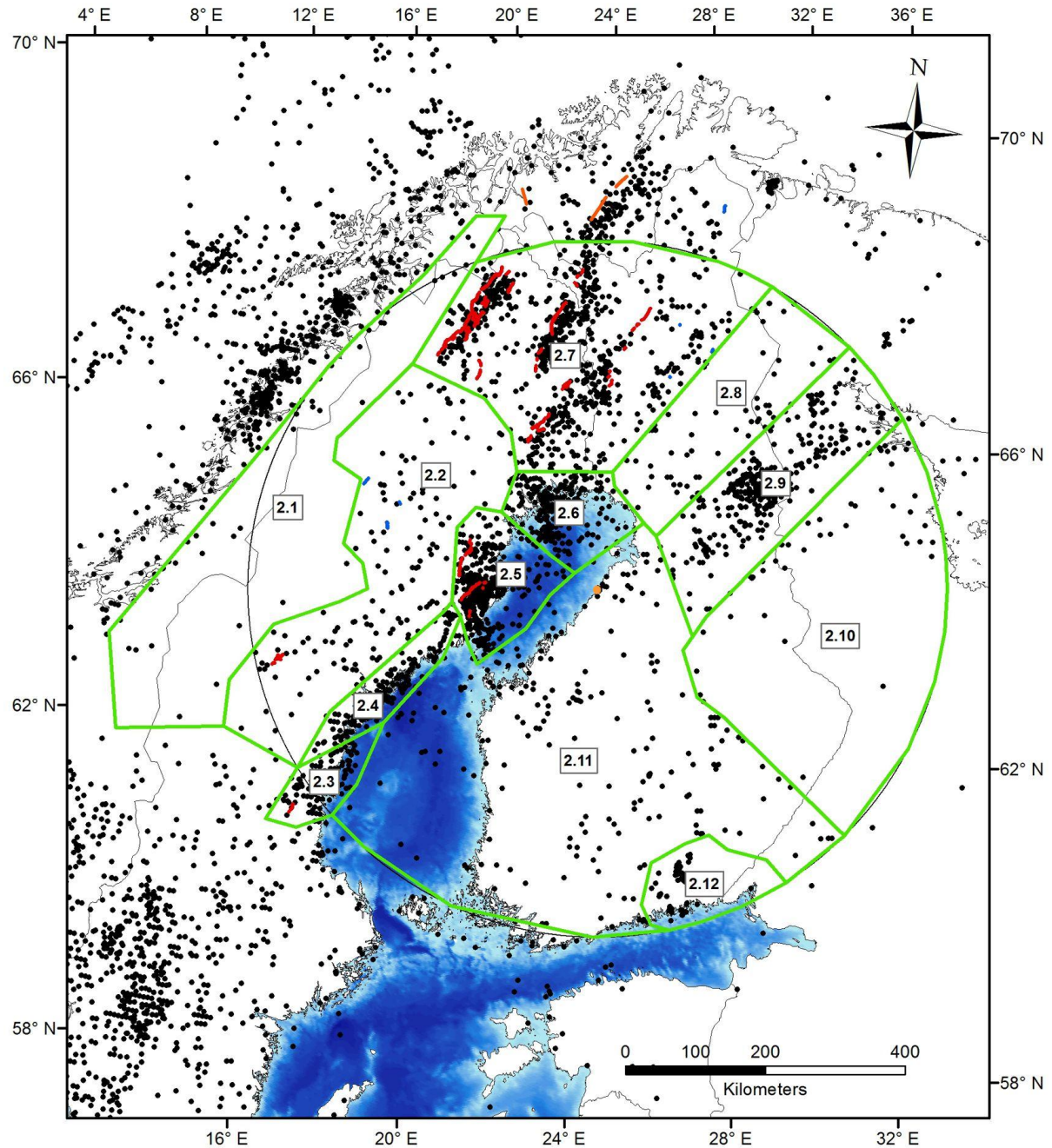


Figure 8.3.3. Earthquake epicenters, seismic source areas identified in spatial model 2 and their relationship to faults inferred to have been active during the late Pleistocene or Holocene on the basis of Quaternary geological data. The bathymetric character of both the Gulf of Bothnia and the Gulf of Finland is also shown. Hanhikivi site: orange dot.

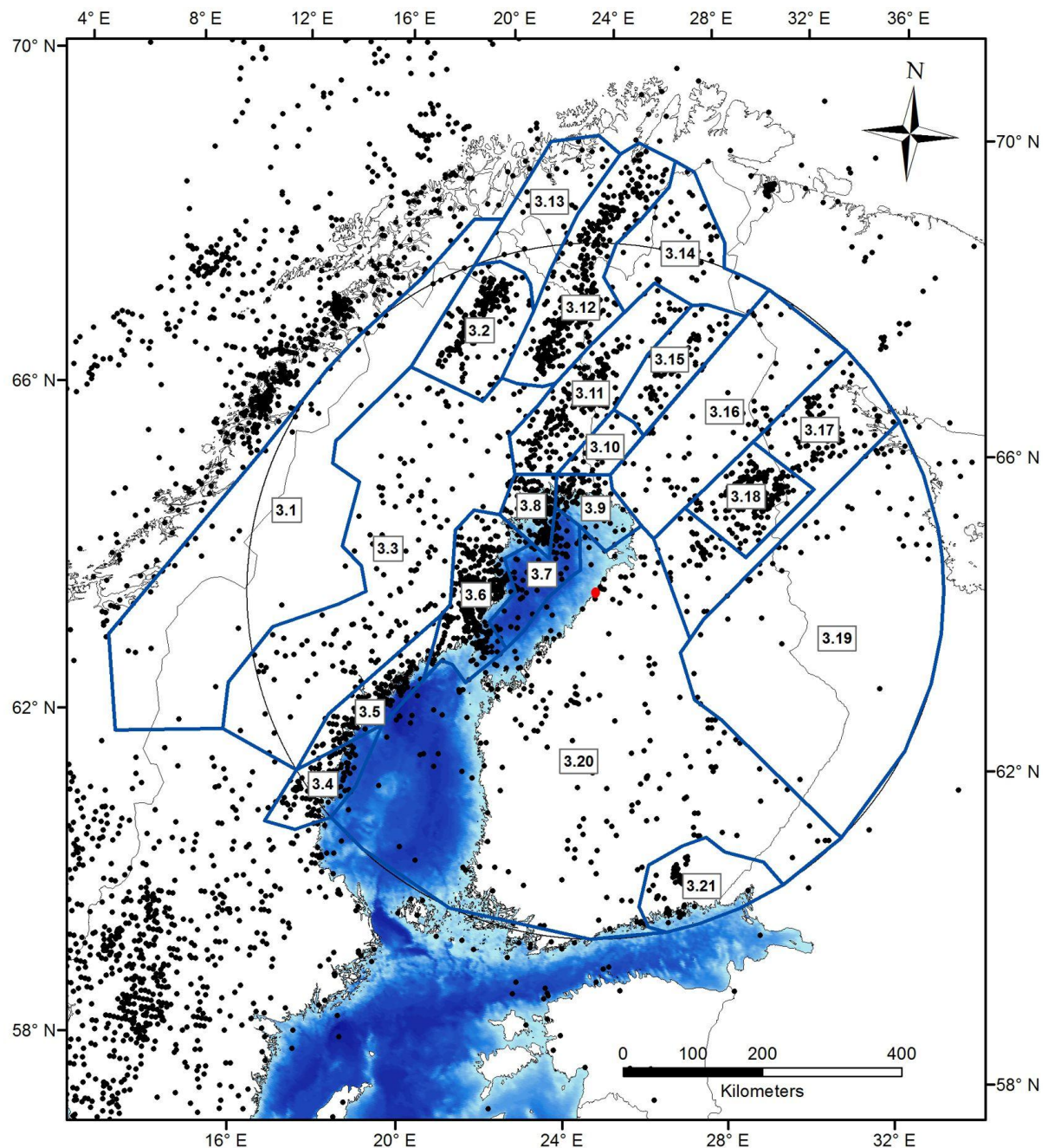


Figure 8.3.4. Earthquake epicenters (Fig. 2.8.1.1-2.8.1.2) and seismic source areas identified in spatial model 3 in the area with 500 km radius centred on the proposed Hanhikivi nuclear power plant, Finland. The bathymetric character of both the Gulf of Bothnia and the Gulf of Finland is also shown.

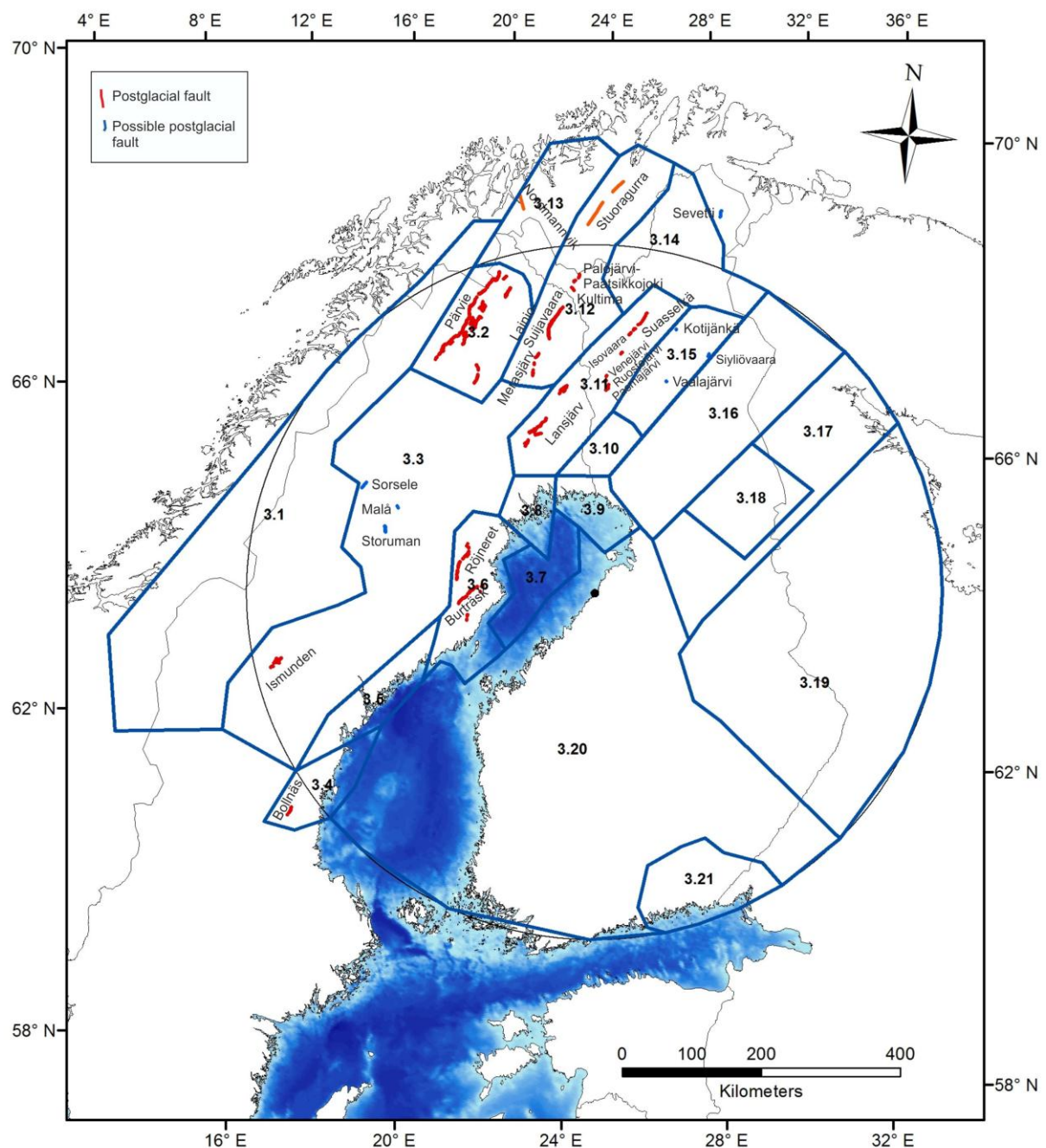


Figure 8.3.5. Seismic source areas identified in spatial model 3 and their relationship to faults inferred to have been active during the late Pleistocene or Holocene on the basis of Quaternary geological data (Fig. 2.7.2). The bathymetric character of both the Gulf of Bothnia and the Gulf of Finland is also shown.

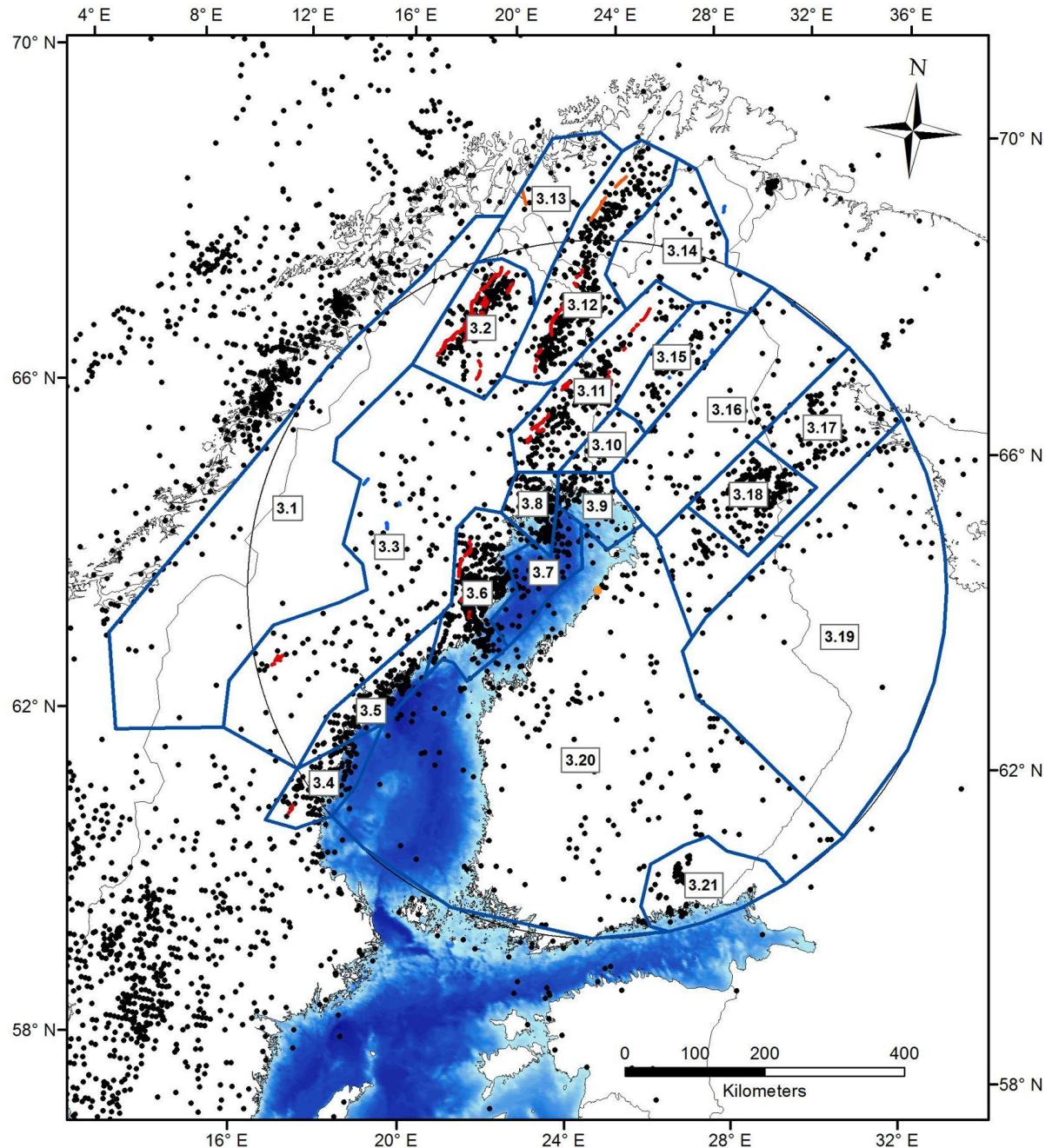


Figure 8.3.6. Earthquake epicenters, seismic source areas identified in spatial model 3 and their relationship to faults inferred to have been active during the late Pleistocene or Holocene on the basis of Quaternary geological data. The bathymetric character of both the Gulf of Bothnia and the Gulf of Finland is also shown.

8.3.2 Description

Seismic source area 2.1

Seismic source area 2.1 extends NE–SW and more or less straddles the border between Norway and Sweden. The source area is one of the two seismically quiet areas in spatial model 2 (Fig. 8.3.1). No evidence for Quaternary faulting has been found in this area. Its western boundary is delineated by the abrupt transition from low seismic activity to relatively high activity along the west coast of

Norway (Fig. 8.3.1). The northeastern boundary of the source area is also marked by an abrupt transition from seismically quiet to a cluster of high activity around the Pärvie fault system in source area 2.7 (Fig. 8.3.1). The boundary shared with polygon 2.2 is somewhat arbitrary but follows approximately the transition from almost no seismicity to increased diffuse seismicity (Fig. 8.3.1). Seismic source area 2.1 corresponds to the Scandian mountain belt. The reader is referred to seismic source area 1.1 in spatial model 1 for the area's relationship to ancient geological features (lithotectonic affiliation, lithology and geologically ancient structures).

Source area 2.1 has very little seismicity and the events are widely distributed in the area. Since there is no seismic station in the area, the events have poor depth determinations and larger than average uncertainties in the epicentral locations. Focal depths vary between a few kilometres and 35 km, with large uncertainties. However, according to the parameterization given in FENCAT, the epicenter of the large Norwegian earthquake of 31 August 1819 was located in this source area. The area of perceptibility extended to the eastern coast of the Gulf of Bothnia. The respective magnitude is assessed at 5.8 based on the studies of Ambraseys (1985) and Muir Wood (1988). Husebye and Kebeasy (2004) proposed a lower magnitude. The largest instrumental event in the area is the MS 3.8 event that occurred on 29 April 1978 in the west coast of Norway, i.e outside the study area with a 500-km radius.

Seismic source area 2.2

Seismic source area 2.2 extends NE–SW and is slightly SE-arcuate (Fig. 8.3.1). Seismicity in this area is generally sparse and diffusely distributed (Fig. 8.3.1). Three minor faults with recorded displacement during the Quaternary are reported within the source area: Storuman, Sorsele and Ismunden. (Fig. 8.3.2; Lagerbäck and Sundh, 2008). Recent work with a LiDAR-derived high resolution DEM at SGU rendered it questionable if the linear features east of Storuman are indeed faults with recorded Quaternary displacement. The existence of a fourth fault west of Malå was suspected but is no longer considered likely after a thorough study by SGU of newly available LiDAR data in the area. There are no clear patterns in the seismic event locations, and no epicenter clusters could unambiguously be attributed to any of these faults (Fig. 8.3.3). The western boundary of the seismic source area is the somewhat arbitrarily defined boundary to polygon 2.1. The eastern boundary is defined by the transition from diffuse to clustered seismicity in polygons 2.3, 2.4, 2.5, 2.6 that extend along the west coast of the Gulf of Bothnia (Fig. 8.3.1). The northern boundary of seismic source area 2.2 delineates the southernmost extent of the clustered seismicity around the faults active during the Quaternary that are included in source area 2.7 (Fig. 8.3.1). The reader is referred to seismic source area 1.3 in spatial model 1 for the area's relationship to ancient geological features.

All seismic stations but one are located in the eastern part of the area, making the seismicity in the west less well-determined. In source area 2.2, seismicity increases somewhat from the Scandian mountain belt in the west towards the coast of the Gulf of Bothnia in the east (Fig. 8.3.1). Earthquakes occur from shallow levels down to 40 km depth. No large historical earthquakes are known for this source area. Possible earthquakes in particular close to the mountains could easily have passed unreported due to the sparse population and lack of documentation centres. The largest instrumental event, the Solberg earthquake of 29 September 1983 with magnitude around 4 (Table 4.3.1, No. 13) was located toward the coast in this area (Kim et al., 1985). The area of perceptibility extended to the coastline.

Seismic source area 2.3

Seismic source area 2.3 extends NE–SW and its western, southern and eastern boundaries are mainly steered by the reduction in frequency of epicenters around the source area (Fig. 8.3.1). At least one fault with reported Quaternary movement (the recently discovered Bollnäs fault; ongoing activities at SGU) occurs in the southwestern corner of the source area outside the study area (Fig. 8.3.2). The northern border to seismic source area 2.4 was drawn along a NE–SW-trending break in the seismicity pattern along the coastline (Fig. 8.3.1). The reader is referred to seismic source area 1.5 in spatial model 1 for the area's relationship to ancient geological features.

Source area 2.3 belongs to the general band of seismicity that lines the northeastern coast of Sweden. The area is well-covered by the permanent station network constructed during 2000–2002, making the epicentral locations relatively well-constrained. In source area 2.3, many of the events occur in a wide NE–SW trending cluster north of the town of Hudiksvall (Fig. 8.3.1) and slightly oblique to the Swedish coastline of the southern Gulf of Bothnia (NNE–SSW). North and south of this band there is more diffuse seismicity (Fig. 8.3.1). Earthquakes occur from shallow levels down to 35 km depth. The largest historical earthquake reported occurred on 21 December 1886 and had a magnitude of around 3.9. The largest instrumental event is the M_L 3.4 earthquake on 15 December 1991 offshore Sundsvall.

Seismic source area 2.4

Seismic source area 2.4 extends NE–SW and its western and eastern boundaries are mainly steered by the reduction in frequency of epicenters around the source area, i.e. in areas 2.2 and 2.11, respectively (Fig. 8.3.1). The southern end corresponds to the boundary shared with polygon 2.3 and the northern boundary abuts against area 2.5, which contains two faults active during the Quaternary (Fig. 8.3.2) and forming a different type of earthquake cluster (Fig. 8.3.1). Most of the seismicity in area 2.4 occurs in a NE–SW-oriented belt along the western shore of the southern part

of the Gulf of Bothnia (Fig. 8.3.1). However, an approximately N-S trending string of earthquake events in the northernmost part of the polygon seems to form a separate earthquake cluster (Fig. 8.3.1). In spatial model 2, this cluster has been included in source area 2.4 whereas, in model 3, it has been attributed to a separate area (3.6).

No faults with Quaternary movement have been described in area 2.4. However, this may be due to the fact that the area is located below the highest shoreline formed after the latest glaciation, so that erosion may have eliminated morphological proof of a potentially active fault or that it is covered under thick post-glacial sediments. It is questionable though whether a potential step in the basement rock could have been eroded under water. The reader is referred to seismic source area 1.4 in spatial model 1 for the area's relationship to ancient geological features.

Source area 2.4 belongs to the general band of seismicity that lines the northeastern coast of Sweden (Fig. 8.3.1). The area is well-covered by the permanent station network constructed during 2000–2002, making the locations of the epicenters relatively well-constrained. In area 2.4, some events form clusters of seismicity but the majority of the earthquakes occur in a more diffuse pattern. Earthquakes occur from shallow depth down to almost 40 km depth. A number of historical earthquakes with magnitude around 4 are known for this area, including those of August 1723, 14 November 1751, 10 March 1930 and 10 October 1935. The macroseismic dataset for the earthquake of 28 July 1888 has been revised (Appendix 2). The area of perceptibility extended westward to seismic source area 2.2 and to Finland. The M_L 3.6 Sundsvall earthquake on 4 June 1974 is the largest instrumental event observed in source area 2.4.

Seismic source area 2.5

Seismic source area 2.5 is more or less triangular in shape (Fig. 8.3.1). Apart from using the transition from clustered to diffuse seismicity (Fig. 8.3.1), bathymetric data for the northern part of the Gulf of Bothnia (Bay of Bothnia) were used to define the SE-facing and NE-facing boundaries. To the southeast, the polygon edge was drawn parallel to the NE–SW-trending margin of the Bay of Bothnia coinciding with a reduction in frequency of epicenters towards polygon 2.11 (Fig. 8.3.1). To the northeast, the polygon edge is delineated by a bathymetric high trending NW–SE and separating the Bay of Bothnia into two separate segments (Fig. 8.3.1). The bathymetric high coincides with a break in the seismicity pattern towards a different cluster included in polygon 2.6 (Fig. 8.3.1). To the west, source area 2.5 shares a boundary with polygon 2.2, defined by the transition from clustered (2.5) to diffuse (2.2) seismicity (Fig. 8.3.1). The SW-facing boundary of polygon 2.5 follows another topographic and bathymetric high known as Norra Kvarken, which divides the Gulf of Bothnia into northern and southern sub-basins (Winterhalter, 1972; Axberg, 1980; Wannäs, 1989) and also seems to coincide with a break in the seismicity pattern (Fig. 8.3.1).

Source area 2.5 is Sweden's currently most seismically active area and seismicity in the area is clustered mainly around two major faults that were active during the Quaternary (Lagerbäck and Sundh, 2008); the NE–SW-trending Burträsk fault and the N–S trending Röjnoret fault to the west and southwest of Skellefteå, respectively (Figs. 8.3.2 and 8.3.3). The reader is referred to seismic source area 1.10 in spatial model 1 for the area's relationship to ancient geological features and the historical seismicity there.

The area has been well-monitored by seismic stations since 2001. In 2012, a temporary network of six additional stations was installed around the Burträsk fault. A large proportion of the events in the area are aligned along and to the southeast of the Burträsk fault. Seismicity extends to the northeast past the end of the surface-mapped fault scarp into the Bay of Bothnia. There is less seismicity associated with the Röjnoret fault, but the area in between the faults contains significant diffuse seismicity, which continues northward along the coastline. Focal depths are from very shallow down to 45 km depth. The largest instrumental event in the area is from the early instrumental recording period. It occurred on 28 September 1962 close to Burträsk and measured M_L 4.0. During the operational period of the SNSN network, the largest observed earthquake is a strike-slip event of M_L 3.5 that took place on 15 June 2010 at the northeastern extension of the Burträsk fault (Table 4.3.1, No.45).

Seismic source area 2.6

Seismic source area 2.6 comprises the northernmost part of the Gulf of Bothnia as well as a slim strip around the Swedish and Finnish coastline approximately from Piteå in Sweden to Kuivaniemi in Finland (Fig. 8.3.1). The area includes one E–W- and one N–S-oriented cluster of earthquakes on the western side of the Bay of Bothnia merging into more diffuse seismicity on its eastern side towards source area 2.11 (Fig. 8.3.1). This boundary as well as the northeastern boundary was drawn somewhat arbitrarily but with respect to the decrease in earthquake frequency towards the east and northeast, respectively (Fig. 8.3.1). The southeastern boundary was also drawn to follow the shallow basinal part of the Bay of Bothnia along the eastern shore. To the north, the area abuts against polygon 2.7 containing several different seismic clusters that seem to follow a more NE–SW trend (Fig. 8.3.1). To the west, the boundary is simply defined by the abrupt change from clustered (2.6) to diffuse seismicity (2.2) and the southwestern boundary corresponds to the border shared with polygon 2.5 (Fig. 8.3.1). Events occur from shallow levels down to 45 km depth. The largest instrumental event in source area 2.6 is from the early instrumental recording period. It occurred on 17 February 1961 in the Bay of Bothnia, about 40 km offshore Oulu and measured M_L 3.7.

Despite the high earthquake frequency, it has not been possible to correlate the seismicity to a known fault active during the Quaternary. This may be due to the fact that the area is located below the highest shoreline, and that erosion may have eliminated morphological proof of a potentially active fault (see also text above). Lagerbäck and Sundh (2008) suggested a location for a "possible late- or post-glacial fault" in the northern part of the Bay of Bothnia, which would be situated in seismic source area 2.6. The reader is referred to seismic source area 1.9 in spatial model 1 for the area's relationship to ancient geological features.

This seismic source area may have been the host area of the earthquake of 27 November 1757 felt at the bottom of the Bay of Bothnia and along both the western and eastern coast. Wahlström (1990) gave its magnitude as $M_{\text{M}}3.7$, but it may have been slightly stronger. This is almost certainly the host area of the 15 June and 23 June 1882 earthquakes. The latter is among the strongest events, if not the strongest, in the seismological record. It is also unique for the Gulf of Bothnia region with two widely felt earthquakes within a time interval of only eight days. The largest intensities ($I = 6-7 \text{ EMS-98}$) were assigned to Tornio in Finland and Sangis-Kalix area in Sweden (Mäntyniemi and Wahlström, 2013). It is not possible to resolve whether the maximum intensity was 6 or 7, although related documentation could be uncovered in archives. It is not possible to pinpoint whether the epicenter was offshore or onshore.

The land and near-shore area of source area 2.6 have been relatively well covered since the SNSN network installation in 2004 and one additional permanent station was installed in the area in 2010. FNSN additional station was added in the area in 2010 to enhance the areas event location accuracy. The offshore events have generally less well-constrained locations than the events within the SNSN or FNSN networks. The Finnish and Swedish joint-processing analysis has been working since 2010 and coastal areas seismic networks have improved during the years 2010-2013.

Seismic source area 2.7

The northern boundary of seismic source area 2.7 corresponds to the border of the study area with its 500 km radius around the target site for the nuclear power plant (Fig. 8.3.1). The other polygon edges were drawn according to the drop in earthquake frequencies and lack of faults active during the Quaternary towards the west and east of the source area (Fig. 8.3.1). The southernmost border is shared with polygon 2.6 and corresponds to a break in the seismicity cluster orientation (Fig. 8.3.1).

Seismic source area 2.7 contains several fault systems inferred to have been active during the Quaternary (Lagerbäck and Sundh, 2008; Kuivamäki et al., 1998) and with earthquake epicenters clustered around these faults (Fig. 8.3.3). The following verified faults are included in source area 2.7: Pärvie, Merasjärvi, Lainio-Suijavaara, Lansjärv, Palojärvi-Paatsikkjoki, Kultima,

Pasmajärvi/Ruokojärvi-Ruostejärvi-Venejärvi, Isovaara and Suasselkä (Fig. 8.3.2). These fault systems trend NE–SW, and seismicity is recorded mainly in the hanging-walls of these faults. Exceptions in Finland are Pasmajärvi-Ruostejärvi-Venejärvi, Isovaara and Suasselkä fault systems that are optimally oriented but no clear seismicity is found in the hanging-wall side. The area has also possible post-glacial faults Vaalajärvi, Siyliövaara and Kotijänkä near the eastern edge of the area (see section 3.2.3.). The Siyliövaara, Kotijänkä and Vaalajärvi faults are situated within a NE-SW oriented corridor of high seismic activity, but the surface traces are oriented in three different directions, SW-NE, N-S and NW-SE, respectively. The region with known PGFs has been affected by three consecutive Weichselian ice caps (see section 3.2). The topographical lineaments (glaciofluvial esker formations) are oriented mostly on SW-NE and NW-SE directions.

Four earthquake clusters are dominant in polygon 2.7 (Fig. 8.3.1). The westernmost cluster trends NNE–SSW and is very likely produced by the Pärvie fault system (Fig. 8.3.2). This system consists of a moderately east-dipping main fault to the west and west-dipping faults at various distances from the main fault further to the east (Lagerbäck and Sundh, 2008). Both fault dip directions show hanging wall up (reverse) movement and seismicity is restricted to the areas between these faults. Lagerbäck and Sundh (2008) attribute also an arcuate, east-facing fault scarp around 60 km to the southeast of the main Pärvie fault line to the Pärvie fault system (Lagerbäck and Sundh, 2008). However, the fault seems to be seismically inactive at the moment since no earthquake cluster could be associated with it. The second earthquake cluster also trends NNE–SSW and occurs in the hanging walls of the Merasjärvi-Lainio-Suijavaara fault system in Sweden and Palojarvi-Paatsikkjoki fault system in Finland (Fig. 8.3.2); east-side-up (reverse) movement has also been inferred here from field studies (e.g. Lagerbäck and Sundh, 2008; Sutinen et al., 2014). The reverse NW–SE trending Kultima fault is also located in the cluster (Sutinen et al., 2014). The seismicity follows the NNE–SSW trend towards the Stuoragurra fault system situated outside the study area in Norway (Fig. 8.3.2). Further to the east of this cluster, the third earthquake cluster occurs along the NE–SW oriented Lansjärv-Suasselkä fault systems starts from Länsjärv fault (Sweden), continues northeastwards as Pasmajärvi-Ruokojarvi/ Venejärvi/ Ruostejärvi fault system (Finland) through Isovaara fault to Suasselkä fault system (Kujansuu, 1964; Kuivamäki et al., 1998) (Fig. 8.3.2). The fourth earthquake cluster that is located further to the east is also trending in NE–SW direction (Fig. 8.3.1). Discrete and unverified post-glacial faults Vaalajärvi, Kotijänkä and Siyliövaara are located in this cluster (Fig. 8.3.2). In between the zones of fault-related seismicity, there are quieter areas with sparse and diffuse seismicity (Fig. 8.3.1). The reader is referred to seismic source areas 1.2, 1.6, 1.7, 1.8, 1.9 and 1.11 in spatial model 1 for the area's relationship to ancient geological features.

The Swedish section of the area has had seismic station coverage since the installation of the northernmost SNSN network in 2004 and a temporary network was installed at the Stuoragurra fault

in Norway in the late 1990's: However, none of the data generated from this temporary network were available for this study. Since 2007 the FNSN seismic network coverage has been good in the Lapland area. Earthquakes occur in the area from shallow levels down to 40 km depth. The deeper level earthquakes (> 15 km) are only found in the western section of the 2.7 area. The largest instrumental earthquake is the M_L 3.9 event that occurred on 11 August 1975 about 50 km northwest of Pajala (Table 4.3.1, No. 11).

It has been proposed that the epicenter of the earthquake of 4 November 1898 (5 November local time) was located in this area (Mäntyniemi, 2008b). Another interesting earthquake occurred on 17 February 1819 along the river valley (seismic source area 1.8 of model 1). However, the earthquake of 31 December 1758 was not located inside source area 2.7 (Tatevossian et al., 2013).

Seismic source area 2.8

The seismic source area 2.8 is in NE-SW direction and there is no evidence of Quaternary faulting. Longest topographical lineaments are in ESE-WNW direction that follows the esker formation and retreating ice-margin direction. Mostly the area is characterized with hummocky moraine deposits. The northeastern corner reaches over the Russian border and near the Kola Peninsula area and the border was drawn to follow the 500 km study area radius. Otherwise the edges were drawn to separate the low seismicity area 2.8 from the increasing seismicity areas 2.6, 2.7 and 2.9 (Fig. 8.3.1). The northwestern border separates the area 2.8 area from area 2.7 characterized by PGF active during the Quaternary (Fig. 8.3.2). The southeastern border is parallel to the NE-SW oriented seismicity cluster in the Kuusamo area 2.9. The reader is referred to seismic source area 1.12 in spatial model 1 for the area's relationship to ancient geological features.

The area has low seismicity and the earthquakes are sporadically distributed. Earthquake depths are from shallow down to about 20 km. The western part of the area is well-monitored since 2007. The event location accuracy decreases towards the Finnish-Russian border. In the early instrumental era, a large earthquake has occurred on 20 February 1960 and the magnitude has been estimated to be at around 4.

Seismic source area 2.9

The seismic source area 2.9 is NE-SW direction and in area has no evidence of Quaternary faulting. However, the area exhibits the most intense seismicity in Finland (Fig. 8.3.1). The seismic source area is located on Finnish and Russian territory. The southeastern area includes the Oulunjärvi area and the northeastern side reaches the Kandalaksha Gulf in White Sea, Russia (Fig. 8.3.1). The polygon edges were drawn to follow the decreasing seismic activity as the area is surrounded by the lowest seismicity areas (2.8, 2.10 and 2.11) in Finland. The shape of the polygon imitates the areas SW-NE

oriented seismicity pattern. The southwestern border was drawn to detach the decreasing earthquake frequency seen in area 2.11. There is no clear main lineament direction in the area, but the esker formations are oriented in E-W pattern to show the retreating ice-margin direction (Fig. 8.2.2). The Early Weichselian (W1) termination end-moraines are found in the western corner of the seismic source area. The reader is referred to seismic source area 1.15, 1.16 and 1.17 in spatial model 1 for the area's relationship to ancient geological features. The seismic source area forms also topographically higher area in the Finland side.

Source area 2.9 is the most active seismic area in the eastern part of the study area with a 500 km radius around Hanhikivi. The earthquakes appear more or less in SW-NE-oriented pattern and, in the central part of the area, there is a large cluster of earthquakes. The topographically highest area, Kuusamo highland, coincides with the high seismicity cluster. These events are diffused uniformly in the seismicity area, but small swarms also appear. The area has clearly the deepest events in Finland. The source depths vary from shallow levels down to about 30 km, i.e., close to the base of the middle crust. Since mid 2000s, the Kuusamo area has been well-monitored by a local network comprising 3-7 temporal stations along with 2 permanent stations. Three of the temporal stations are still in operation. The eastern part of the area has no seismic stations and the good location and depth accuracy in the Finnish side changes to moderate and poor in the Russian side of the national border.

The largest historical earthquake in Kuusamo had magnitude above ML4 and occurred on 18 August 1926. There are some other interesting historical earthquakes associated with this source area. The earthquake of 10 April 1902 had a very rare area of perceptibility that extended across the border to Russia. Its magnitude exceeded ML4. A lesser earthquake occurred on 26 December 1911. The respective epicenters were located west of Kuusamo. The uncertainty associated with the June 1626 epicenter is large, but the earthquake was felt within this source area (Tatevossian et al., 2011). The earthquake of 17 December 1758 possibly occurred in this source area, close to the Bay of Kandalaksha (Tatevossian et al., 2013). The only instrumental earthquake of magnitude greater than 4.0 in northeastern Fennoscandia locates on the eastern fringes of this area. The event took place on 20 May 1967 in the Kandalaksha Gulf and was assigned with magnitudes ranging from 4.8 to 5.2 (Table 4.3.1, No. 1). In Kuusamo, the strongest instrumentally recorded earthquake is the M_L 3.5 event on 15 September 2000 (Table 4.3.1, No. 28).

Seismic source area 2.10

The seismic source area 2.10 is triangular shape area starting from Eastern Finland (Karelia) area and widening to Russian Karelia side (Fig. 8.3.1). The area reaches also the Russian Kandalaksha Gulf and Onega Bay in White Sea. The area is the seismically quietest area in Finland side and there is no evidence of post-glacial faults found in the area. However, there are some evidence of microsize (cm)

post-glacial faults cutting bedrock and the glacial striations in Ilomantsi area, eastern Finland (Nenonen and Huhta, 1993; Kuivamäki et al., 1998). The polygon edges were drawn to separate the seismically active Kuusamo area 2.9 in north and the border was drawn parallel to the SW-NE oriented cluster of events. The eastern border corresponds to the border of the study area (500 km radius). The western and southwestern border was drawn to separate the slightly increasing seismicity in central Finland area. The seismic source area 2.10 was first area in the study region to be deglaciated after the last glacial maximum (see section 3.2.2). No clear dominant geophysical lineament direction was found in the area; however, the topographical and glaciofluvial esker formations are oriented in SE-NW and SSE-NNW direction. The reader is referred to seismic source area 1.18 in spatial model 1 for the area's relationship to ancient geological features.

The area is seismically very quiet in Finland and also in the Russian part of the study area. There are no instrumentally recorded events in the southern part of the triangular area. Increase in seismic activity is seen in the northeastern corner near the Kandalaksha area. Some seismic events seem to follow the geophysical lineaments in the Russian area. The area has sparse seismic network (1 station in FNSN network) and the location and depth accuracy changes from moderate to poor towards the eastern part.

The largest event, the M_L 3.7 earthquake on 24 August 1991, is located at the northeastern corner of the source area, close to the seismically more active source area 2.9. No notable historical earthquakes are known in this source area. It could be explained by a lack of documentation due to sparsely distributed population and a border area. However, the area appears quite devoid of earthquake epicenters in the instrumental era as well.

Seismic source area 2.11

The seismic source area 2.11 is large area in southern and central Finland. The polygon edges were drawn so that western border is connected with the Sweden side seismically active areas 2.3, 2.4, 2.5 and 2.6 and the border is located on Gulf of Bothnia area (Fig. 8.3.1). The northern part of the border in Bay of Bothnia is drawn to follow the basins shallow part in Finland side. In Bothnian Sea area the border is close to Sweden shoreline leaving the deep basin inside the seismic source area 2.11. The border in northeastern corner was drawn to separate the increasing seismicity trend in area 2.9. There is no evidence of post-glacial faults in the area (Fig. 8.3.2). Most of the western and southern area in Finland was located under the highest shoreline during the ancient phases (Baltic Ice Lake, Yoldia Sea, Anculys Lake, Litorina Sea) of Baltic Sea and the possible formed scarps have been destroyed by the wave action. However, there are evidence of microsize (cm) post-glacial faults cutting the bedrock and the glacial striations in southwestern coastal area, for example in Kustavi Island (Kujansuu, 1964). The area has the longest topographical patterns formed on the advancing

ice-margins (drumlins) and retreating ice-margin direction with long glaciofluvial esker formations SE-NW direction and the standstill ice-marginal (delta, sandur-delta etc.) formations SW-NE direction. The longest lineaments are in the direction of SE-NW, N-S, and SW-NE. The reader is referred to seismic source area 1.10, 1.12 and 1.13 in spatial model 1 for the area's relationship to ancient geological features.

The seismic source area has a low seismic activity and the events are widely distributed. No clear pattern or epicenter clusters are found in this area. However, the largest instrumental earthquake to occur in Finland, the M_L 3.8 event in Lappajärvi on February 17, 1979 (Table 4.3.1, No. 3) is located within this source area. The largest non-instrumental earthquake occurred in central Finland on 16 November 1931 (magnitude in the range 4.1 – 4.5). Interesting historical earthquakes occurred on the eastern coast of the Gulf of Bothnia (the reader is referred to source area 1.13 of model 1). The earthquakes occur from shallow depths down to about 30 km. In the Finnish mainland, source area 2.11 is well-covered by FNSN and event locations are relatively well constrained. In coastal and sea areas the event location accuracy has improved since the expansion of SNSN in 2000. A number of new stations have also been constructed in the Finnish and Estonian coasts in 2000s (Fig. 2.8.2.1).

Seismic source area 2.12

The seismic source area 2.12 is located in the S-SE corner of the study area. The area is surrounded by the 2.11 area and the study area border in south. The area was separated from the seismic source area 2.11 due to the different seismicity pattern. Orientations of largest geophysical lineaments are mostly in SW-NE and NW-SE direction. The reader is referred to seismic source area 1.14 in spatial model 1 for the area's relationship to ancient geological features.

The area is seismically active and it has many small earthquake swarms (Table 4.3.1, No. 30 & 36). The swarms have no clear unified pattern, but there can be seen one small SE-NW oriented cluster and few round centered clusters. The largest swarms are located in the middle of the seismic area 2.12. The swarm events are unusually shallow, most likely occurring within the first 2 km from the surface. A shallow shock of M_L 2.9 on 21 July 1982 is the largest instrumentally recorded event in the area. No aftershocks have been reported for the event. Earthquake swarms also known from the historical era, in 1751–52 and 1951–52 in particular. The largest historical event of M_M 3.1 belongs to the 1951-52 swarm. The area has been well-monitored since 2003. The eastern part has lower location accuracy due to lack of seismic stations in the Russian part of the study area.

Seismic source area 3.1

Source area 3.1 corresponds to source area 2.1 in spatial model 2.

Seismic source area 3.2

Seismic source area 3.2 extends NNE–SSW (Fig. 8.3.4) and encompasses the system of faults referred to generally as the Pärvie fault (Fig. 8.3.5). The seismicity in source area 3.2 is strongly correlated with the surface trace of this fault system (Fig. 8.3.6). The Pärvie fault system consists of a moderately east-dipping main fault to the west and west-dipping faults at various distances from the main fault further to the east (Lagerbäck and Sundh, 2008). Both fault dip directions show hanging wall up (reverse) movement and seismicity is restricted to the areas between these faults. An arcuate, west-facing fault scarp 60 km to the southeast of the main Pärvie fault line is also attributed to the Pärvie fault system (Lagerbäck and Sundh, 2008). However, the fault seems to be seismically inactive at the moment since no earthquake cluster could be associated with it. The polygon boundaries were drawn tightly around the Pärvie fault system and the related earthquake cluster, utilizing the decrease of epicenter frequency outside the fault system. The reader is referred to seismic source area 1.2 and 1.6 in spatial model 1 for the area's relationship to ancient geological features.

Permanent seismic stations of the SNSN were established in the area in 2003 and, during 2007–2010, a temporary seismic network of eight additional stations operated along the Pärvie fault system. SNSN locations in area 3.2 generally have low epicentral uncertainties. Events with well-defined depths indicate that earthquakes occur from very shallow levels down to 35 km depth. The largest event observed in source area 3.2 is from the early instrumental recording period. It occurred on 13 April 1967 about 40 km northeast of Kiruna and measured M_L 3.7 (Table 4.3.1, No. 10). Only two non-instrumental earthquakes are known for this source area, and both of them have been assigned a magnitude around 3.

Seismic source area 3.3

Source area 3.3 corresponds to source area 2.2 in spatial model 2 apart from minor adjustments in the northern part of area 3.3 which were necessary due to the breaking up of polygon 2.7 into smaller polygons focused around the northern faults with Quaternary movement.

Seismic source area 3.4

Source area 3.4 corresponds to source area 2.3 in spatial model 2.

Seismic source area 3.5

Source area 3.5 extends NE–SW, and its western and eastern boundaries are mainly steered by the reduction in frequency of epicenters around the source area in areas 3.3 and 3.20 (Fig. 8.3.4). The southern end corresponds to the boundary shared with source area 3.4. The northern boundary

abuts against area 3.6 which contains two faults active during the Quaternary (Fig. 8.3.5) and forming a different type of earthquake cluster. Source area 3.5 corresponds almost to source area 2.4 in spatial model 2. However, the approximately N-S trending string of earthquake events in the northernmost part of area 2.4 has been excluded from source area 3.5 and attributed to 3.6. No faults with Quaternary movement have been described in area 3.5. However, this may be due to the fact that the area is located below the highest shoreline, so that erosion may have eliminated morphological proof of a potentially active fault (see also earlier text).

Seismic source area 3.5 belongs to the general NE–SW-oriented band of seismicity that lines the western coast of the Gulf of Bothnia in Sweden (Fig. 8.3.4). The area is well-covered by the permanent station network constructed during 2000–2002, making the epicentral locations relatively well-constrained. In area 3.5, some events form clusters of seismicity but the majority of the earthquakes occurs in a more diffuse pattern. Earthquakes occur from shallow depth to almost 40 km depth. A number of historical earthquakes with magnitude around 4 are known for this area, including those of August 1723, 14 November 1751, 10 March 1930 and 10 October 1935. The macroseismic dataset for the earthquake of 28 July 1888 has been revised (Appendix 2). The area of perceptibility extended westward to seismic source area 3.3 and eastward to Finland. The M_L 3.6 Sundsvall earthquake on 4 June 1974 is the largest instrumental event observed in source area 3.5.

Seismic source area 3.6

Source area 3.6 extends in a more or less N–S direction (Fig. 8.3.4). Apart from using the transition from clustered to diffuse seismicity (Fig. 8.3.4), bathymetric data for the northern part of the Gulf of Bothnia (Bay of Bothnia) was used to define the eastern and southern boundaries. The eastern boundary follows the margin of the basin defined by the Bay of Bothnia, coinciding with a reduction in frequency of epicenters towards source area 3.7 (Fig. 8.3.4). The southern boundary follows a bathymetric and topographic high at Norra Kvarken, which divides the Gulf of Bothnia into northern and southern sub-basins (Winterhalter, 1972; Axberg, 1980; Wannäs, 1989) and which also seems to coincide with a break in the seismicity pattern (Fig. 8.3.4). To the northeast, the polygon edge is delineated by the on-shore continuation of a bathymetric high trending NW–SE separating the Bay of Bothnia into two separate segments; the bathymetric high also coincides with a break in the seismicity pattern towards a different cluster included in source area 3.8 (Fig. 8.3.4). To the west, source area 3.6 shares a boundary with area 3.3, defined by the transition from clustered (3.6) to diffuse (3.3) seismicity (Fig. 8.3.4). Additionally, area 3.6 incorporates the N–S extending string of seismic events in its southern part that was previously attributed to source area 2.4 in spatial model 2 (Figs. 8.3.1 and 8.3.4).

Source area 3.6 is Sweden's currently most seismically active area and seismicity in the area is clustered mainly around two major faults that were active during the Quaternary (Lagerbäck and Sundh, 2008); the NE–SW-trending Burträsk fault and the N–S trending Röjnoret fault to the west and southwest of Skellefteå, respectively (Figs. 8.3.5 and 8.3.6).

The largest earthquake in the study area in the 1900's (9 March 1909, $M_L = 4.6$ according to FENCAT, $M_L = 5$ according to Båth, 1956) occurred either in this source area or offshore in source area 3.7. FENCAT locates the epicenter offshore, whereas Båth (1956) and Mäntyniemi (2012b) located it in source area 3.6. A number of earthquakes with magnitude around 4 have occurred in this source area, including those of 13 April 1929, 7 January 1935 and 28 September 1962. A magnitude 4.4 has been assigned to the earthquake of 26 May 1907. The respective macroseismic dataset has been revised in this project (Appendix 2).

Source area 3.6 has been well-monitored by seismic stations since 2001. During 2012, a temporary network of six additional stations was installed around the Burträsk fault. A large proportion of the events in the area are aligned along and to the southeast of the Burträsk fault. Seismicity extends to the northeast past the end of the surface mapped fault scarp into the Bay of Bothnia. There is less seismicity associated with the Röjnoret fault, but the area in between the faults contains significant diffuse seismicity, which continues northward along the coastline. Focal depths range from very shallow depths down to 45 km. The largest instrumental event in source area 3.6 is from the early instrumental recording period. It occurred on 28 September 1962 close to Burträsk and measured $M_L = 4.0$. During the operational period of the SNSN network, the strongest observed earthquake is a strike-slip event of $M_L = 3.5$ that took place on 15 June 2010 at the northeastern extension of the Burträsk fault (Table 4.3.1, No. 45).

Seismic source area 3.7

Seismic source area 3.7 frames the margins of the basin in the Bay of Bothnia and includes its deepest parts; the area contains the seismicity in the bay east of the coastal source areas 3.6 and 3.8 (Fig. 8.3.4). Earthquake occurrence in the area decreases from the Swedish toward the Finnish coast. The area is mostly located outside of the SNSN, implying that earthquake locations are less well-constrained in the Bay. Focal depths are generally poor and there is not enough accuracy at the time to set a lower occurrence depth. The Finland coastal area has been well-monitored with FNSN since 2010. An additional seismic station network around Hanhikivi has been installed in 2012. The Finnish and Swedish joint-processing analysis has been working since 2010. The seismic source area has good location accuracy from 2010 onwards.

The FENCAT catalogue locates the historical earthquakes of 27 November 1957, 14 July 1765 and 31 December 1908 in source area 3.7, besides that of 9 March 1909 (see above). Due to location uncertainties, the earthquakes of 1765 and 1908 could also have occurred in source area 3.6, and the earthquake of 1757 possibly in source area 3.8. All the four datasets have been revised in this project (Appendix 2). The largest instrumental event in source area 3.7 is from the early instrumental recording period. It occurred on 23 January 1965 and measured M_L 3.3. During the operational period of the SNSN network, the largest observed earthquake is the M_L 2.9 event that took place on 9 December 2003.

Seismic source area 3.8

Source area 3.8 includes the seismicity along the coast north of Luleå and also a zone of dense seismicity stretching from the north coast out into the Bay of Bothnia (Fig. 8.3.4). The eastern boundary of the area, shared with source areas 3.7 and 3.9, was chosen to follow a N–S-oriented high in the bathymetric data, bounding the western margin of the northern part of the Bay of Bothnia (Fig. 8.3.4). The boundary towards source area 3.11 was drawn somewhat arbitrarily but follows a change in the type of seismic event cluster orientation from more or less N–S to more NE–SW (Fig. 8.3.4). The western boundary is shared with source area 3.3 with its diffuse type of seismicity (Fig. 8.3.4).

No faults with Quaternary movement have been reported for this area. However, this may be due to the fact that the area is located below the highest shoreline so that erosion on land may have eliminated morphological proof of a potentially active fault (see also earlier text). Offshore, there may well be potentially active faults present which have not yet been discovered.

Station coverage has been relatively good since the SNSN station installation in 2004, and increasingly so since the installation of additional stations in 2010. However, some of the seismicity in the Bay of Bothnia is outside of the SNSN network and, thus, has lower location accuracy. Earthquakes in the area occur from shallow depths down to 45 km. The largest instrumental earthquake is the M_L 3.6 event that occurred on 6 June 1991 in Luleå.

Seismic source area 3.9

Seismic source area 3.9 includes the seismicity along the northern coast, in the border region between Sweden and Finland, and in the northernmost part of the Bay of Bothnia (Fig. 8.3.4). The source area extends in a NW–SE direction and its southwestern border is drawn along a bathymetric high defining the northernmost margin of the basin defined by the Bay of Bothnia trending NW–SE (Fig. 8.3.4). Earthquake frequency in the polygon seems higher in its western part than its eastern and northern parts, so that the northern and eastern boundaries were drawn somewhat arbitrarily

against areas of very low seismicity (Fig. 8.3.4). Both detection capabilities of the SNSN and location accuracy for epicenters diminish east of the network. FNSN Tornio station was added in 2010 to enhance the areas event location accuracy. Seismic events in FENCAT located using stations in both Finland and Sweden have smaller uncertainties. Earthquakes occur down to 35 km depth.

This is probably the host area of the 23 June 1882 earthquake, which is among the strongest events, if not the strongest, in the seismicity record of the study area. It is not possible to pinpoint whether the epicenter was offshore or onshore. It has been preceded by a lesser earthquake on 15 June 1882. It is not attested to by a large dataset, and the epicenter could also be located in the neighboring source areas. The macroseismic datasets of the two earthquakes have been revised by Mäntyniemi and Wahlström (2013). The largest instrumental earthquake in this source area has occurred in Kalix on 22 July 2009 with magnitude M_L 3.1 to 3.4 (Table 4.3.1, No. 44).

Seismic source area 3.10

Seismic source area 3.10 extends NE–SW and is an area of sparse and diffusely distributed seismicity, away from the more active north coast and not associated with a fault active during the Quaternary (Figs. 8.3.4 and 8.3.5). This area emerged as a “rest area” after dividing up source area 2.7 in spatial model 2 into smaller areas that are more focused around the faults active during the Quaternary, such as the Lansjärv fault in source area 3.11 to the northwest of area 3.10. Earthquakes in the area occur in shallow depths (> 12 km). The largest instrumental earthquake in source area 3.10 is the M_L 2.7 event that took place on 12 October 1996 in Ylitornio. The SNSN has very limited accuracy in this area. The FNSN has new seismic station installed in Tornio (area 3.9) in 2010 that enhance the area’s accuracy from moderate to good. The reader is referred to seismic source area 1.11 in spatial model 1 for the area’s relationship to ancient geological features. An interesting historical earthquake (among the largest in the study area) is that of 4 November 1898. Mäntyniemi (2008b) proposed a new epicenter that would be in this source area.

Seismic source area 3.11

Source area 3.11 extends NE–SW and frames the area from Lansjärv post-glacial fault in Sweden to the Suasselkä fault system in Finland (Fig. 8.3.5). All polygon boundaries correspond to areas where seismicity clearly decreases away from the faults; the western and eastern polygon edges were drawn such that they are parallel to the surface traces of the Lansjärv, Pasmajärvi-Ruostejärvi-Venejärvi, Isovaara and Suasselkä fault area (Fig. 8.3.6). The reader is referred to seismic source area 1.8 in spatial model 1 for the area’s relationship to ancient geological features.

In Sweden, the seismic activity has been well-monitored since the installation of the northernmost SNSN in 2004. Seismic network FNSN in Finland is well covered in this area giving a good accuracy on

earthquake epicenter locations since 2007. The seismicity is located mostly to the southeast of the NE–SW trending fault lines, with an appreciable NE–SW-trending corridor of seismicity making a connection between the faults in Sweden and Finland very likely (Fig. 8.3.6). Not as clear seismicity pattern is found from the southeast side of the Pasmajärvi-Ruostejärvi-Venejärvi fault system. There is also a decreasing trend in the seismic activity towards the northeastern edge of the area. Events occur from shallow depth down to 40 km depth. The deeper events are found in southwestern area. A rather widely noticed earthquake occurred in this source area on 17 February 1819. The largest instrumental event in source area 3.11 is from the early instrumental recording period. It occurred on 4 September 1968 close to Pello in the Finland-Sweden border zone and measured M_L 3.4.

Seismic source area 3.12

Source area 3.12 extends NNE–SSW and includes the Merasjärvi and Lainio-Suijavaara faults in Sweden, Kultima, Paatsikkjoki and Palojarvi in Finland and the Stuoragurra fault in Norway, all of which show a similar trend and appreciable seismic activity (Figs. 8.3.5 and 8.3.6). All polygon boundaries were drawn where seismicity clearly decreases away from the faults (Fig. 8.3.6). The western and eastern polygon edges were drawn such that they are parallel to the surface traces of the Merasjärvi-Lainio-Suijavaara-Kultima-Paatsikkjoki-Palojarvi-Stuoragurra fault system. The reader is referred to seismic source area 1.7 in spatial model 1 for the area's relationship to ancient geological features.

In Sweden, the seismic activity is well-monitored since the station installations in 2004. In Finland, the seismic network is well-monitored since 2007 giving the good determination accuracy in Sweden, Finland and southern part of Norway area. The Stuoragurra fault in Norway was investigated with a temporary seismic network in the late 1990's. However, none of these data were available for this study and the location accuracy reduces towards Stuoragurra fault and Barents Sea. The seismicity in the area is mostly related to the post-glacial faults, with events occurring to the southeast of the faults as expected due to their reverse mechanisms with southeasterly dip directions (Lagerbäck and Sundh, 2008; Sutinen et al., 2014). Some additional seismic events occur diffusely away from the faults. Events occur from shallow depths down to 35 km. The only known earthquake with magnitude above 3 in this source area occurred on 12 December 1848. The largest instrumental event in source area 3.12 is the M_L 4.0 earthquake on 25 February 1975 in Finnmark, northern Norway. No notable historical earthquakes are known for this area.

Seismic source area 3.13

The seismic source area 3.13 extends in SW-NE direction and runs from northern Sweden through Kilpisjärvi area in Finland to Norway and finally reaching the Barents Sea on northeast (Fig. 8.2.4).

The eastern and southern boundaries correspond to the areas where seismicity increases and the eastern border is parallel to the Merasjärv-Stuoragurra fault system in area 3.12. The southern border separates the seismically active Pärvie post-glacial fault system in area 3.2. The western border was drawn to include the Quaternary active fault Nordmannvik in the seismic source area (Tolgensbakk and Sollid, 1988). The area has very low seismicity and no clear seismicity pattern can be connected to the NW-SE-trending Nordmannvik post-glacial fault (Fig. 8.3.6). The only historical earthquake known in this source area occurred on 3 April 1930 and has been assigned a magnitude of 4.4. The largest instrumental event, the M_L 3.0 earthquake on 26 November 1992, locates about 60 km east of the Nordmannvik fault. The events in source area 3.13 are occurring from shallow depths down to 30 km. The Kilpisjärvi area has contained permanent seismic network station since 2003 providing relatively good coverage for the southern part of the seismic source area. The reader is referred to seismic source area 1.6 in spatial model 1 for the area's relationship to ancient geological features in the southern part of the area.

Seismic source area 3.14

The seismic source area 3.14 is part of the 2.7 post-glacial fault area in spatial model 2. The area has no evidence of Quaternary faults and it has low seismic activity (Fig. 8.3.6). Southern and western boundaries outline the SW-NE oriented seismicity patterns and the fault systems active during the Quaternary. The northwestern edge was defined to exclude the weakening seismicity and decreasing elevation towards the Barents Sea. The Sevetti fault (seen in Figure 8.3.5) is located just outside of the northeastern edge. This fault has been classified as a possible post-glacial fault as its structure has not been verified yet and was therefore excluded from the area. Also no seismicity pattern can be connected to this fault. There have been reported many early post-glacial landslides in the Utsjoki area referring to high-magnitude seismic events (Sutinen et al., 2009). However, the vicinity of Stuoragurra fault in west (area 3.12) could have affected the Utsjoki area (see section 3.2.3). In the topographical lineaments the directions SW-NE and NW-SE are quite even. The last ice retreating direction and most of the glaciofluvial eskers in the area are oriented in SW-NE direction. The reader is referred to seismic source area 1.12 in spatial model 1 for the area's relationship to ancient geological features in southern part of the area.

The area has sparse seismicity and the events occur in shallow depths (above ~11 km). The earthquake of 31 December 1758 and magnitude above 4 may have occurred in the source area (Tatevossian et al., 2013). The largest instrumental event in the area is the M_L 3.5 earthquake on 7 November 1977 in Inari. The area is in the outer border of FNSN seismic network and the uncertainties in event location increase towards the Barents Sea.

Seismic source area 3.15

Seismic source area 3.15 is one part of spatial model 2 area 2.7. All polygon boundaries were drawn where the seismicity was decreasing around the SW-NE oriented seismicity cluster. The Kotijänkä, Vaalajärvi (Huotarinkuusikko) and Siyliövaara faults are located in the area. All of these faults are classified as possible post-glacial faults (see section 3.2.3) (Kuivamäki, 1998; Olesen et al., 2004; Sutinen et al., 2007). The Siyliövaara fault is situated 20 km S from artificial Lake Loka in NE part of the area and it is trending to SW-NE. There are several topographical lineaments nearby that have the same orientation as this fault. The fault follows the magnetic anomaly and it is also near gravity minimum. Kotijänkä (also known as Porttipahta) fault is situated in SW corner of artificial Lake Porttipahta and it is not associated with clear topographical or geophysical lineaments. The Kotijänkä fault is trending nearly to N-S direction. There are some topographical lineaments near the fault that have the same N-S direction. Vaalajärvi fault is located 15 km SW from Sodankylä town and it is trending to SE-NW direction. The fault itself is not associated with clear topographical or geophysical features; however, most of the topographical faults seen in area 3.15 have the same SE-NW trend. Longest topographical lineaments in the polygon are in the direction of NW-SE and SW-NE. The reader is referred to seismic source area 1.11 and 1.12 in spatial model 1 for the area's relationship to ancient geological features.

The seismic source area 3.15 is seismically active and the seismicity is focused on the southeastern side of the area. Even though the area is seismically active the seismicity has no clear pattern related to Kotijänkä or Siyliövaara faults. However, seismic activity is seen in the NE side of Vaalajärvi fault (Fig. 8.3.6). Vaalajärvi fault is classified as normal fault with W-SW side as hanging wall (Kuivamäki, 1998). The earthquakes occur from shallow down to 21 km depth. The largest instrumental event in source area 3.15 is from the early instrumental recording period. It occurred on 20 March 1965 in Sodankylä and measured M_L 3.5. No large historical earthquakes are known in this source area. The FSN seismic station network coverage has been good in the area since 2007.

Seismic source area 3.16

Source area 3.16 corresponds to source area 2.8 in spatial model 2.

Seismic source area 3.17

The seismic source area 3.17 is part of seismic source area 2.9 in spatial model 2. The area 2.9 was divided to separate the large earthquake cluster located in the central part of the area near Russian border to its own area 3.18 (Fig. 8.3.4). The seismic source area 3.17 has no evidence of Quaternary faulting. The seismic source area is located on the territory of Finland and Russia. The polygon edges were drawn following the seismic activity and the area is surrounded by the lowest seismicity areas

(3.16, 3.19 and 3.20) in Finland and Russia. The reader is referred to seismic source area 1.15 and 1.17 in spatial model 1 for the area's relationship to ancient geological features and historical earthquakes there.

The source area 3.17 is a seismically active area. The events are concentrated in the northwestern and central parts of the source area with decreasing seismicity towards the southeastern border. In the northeastern Russian side of the area WSW-ENE and S-N oriented earthquake clusters can be seen (Fig. 8.3.4). The southwestern side of the area is well-monitored but in the northeastern part the estimates of source parameters are more uncertain due to the lack of Russian seismic stations. The events vary from shallow levels down to about 30 km depth. The only instrumental earthquake of magnitude greater than 4.0 in northeastern Fennoscandia locates on the eastern fringes of this area. The event took place on 20 May 1967 in the Kandalaksha Gulf and was assigned with magnitudes ranging from 4.8 to 5.2 (Table 4.3.1, No. 1).

Seismic source area 3.18

The seismic source area 3.18 is part of seismic source area 2.9 in spatial model 2. The polygon edges were drawn to separate Finland's seismically most active area from seismic source area 3.17 (Fig. 8.3.4). Seismic source area 3.18 is located on Kuusamo highland area with elevation varying from 350-500 m a.s.l. being 200 meters higher than the surrounding western and northern areas. The highland (400 m) area continues to northeast to seismic source area 3.17. The reader is referred to seismic source area 1.15 and 1.16 in spatial model 1 for the area's relationship to ancient geological features and the historical seismicity.

Source area 3.18 is the most active seismic area in Finland. The earthquakes are more or less equally spread in the area and the events occur from shallow depths down to about 30 km. Since mid 2000s, the area has been well-monitored by a local network comprising 4-7 temporal stations along with 2 permanent stations. Three of the temporal stations are still in operation. The strongest instrumentally recorded earthquake in Kuusamo is the M_L 3.5 event on 15 September 2000 in Kuusamo (Table 4.3.1, No. 28).

Seismic source area 3.19

Source area 3.19 corresponds to source area 2.10 in spatial model 2.

Seismic source area 3.20

Source area 3.20 corresponds to source area 2.11 in spatial model 2.

Seismic source area 3.21

Source area 3.21 corresponds to source area 2.12 in spatial model 2.

9 Discussion

A. Korja

The Hanhikivi site at Pyhäjoki, Ostrobothnia, Finland is situated in a low seismicity intraplate area where recent seismic hazard evaluation by international and national scientific groups have found that the hazard is indeed low (Figs. 7.2.4 and 7.2.6; Wahlström and Grünthal, 2001; Giardini et al., 2013; Mäntyniemi, 2008a; Saari et al., 2009; Korja et al., 2011a). Nevertheless, the hazard for a potential nuclear power plant site has also to be assessed locally (IAEA, 2010). Hazard estimations are inherently difficult in areas of low seismicity since the earthquake data sets are small and thus their statistical analyses may pose problems. This problem can be tackled by increasing the number of observations. The amount of earthquake observations can be increased by adding historical events and by installing seismic stations that capture small but numerous events. Hazard calculations are based on knowledge on the distribution of seismicity, regional geology and seismotectonics and on scientific theories on the driving mechanisms of seismicity. In this report we have gathered background information and data for hazard calculations for the Hanhikivi site. We have collected and organized the data into an ArcGIS-based database, from which the data can be retrieved in future studies. This will ensure that data and results are accessible for future projects and inspections.

The project has had six tasks: 1) to review and summarize the existing and ongoing geoscientific studies around the Hanhikivi site (Appendix 1), 2) to compile and describe a regional-scale geological and geophysical upgradable database for the present and future studies of the site (Appendix 3), 3) to present an overview of the paleotectonic evolution, Quaternary glacial history and current tectonic framework inside the study area (Chapters 3, 5, 6), 4) to describe seismicity and earthquake source parameters of the study area (Chapter 4), 5) to review and evaluate the current conceptual seismotectonic models and seismic source region models for Fennoscandia (Chapter 7), 6) to identify and describe seismic source regions and to outline alternative source area models for seismic hazard calculations for the Hanhikivi site area (Chapter 8).

In following, we will discuss the completeness of the compiled database, distribution of seismicity, the lithotectonic units and the orientation of shear zones post glacial faults in respect to the current stress field. We will also discuss the new seismic source area Models 1-3 and compare the models to the conceptual seismotectonic models of Fennoscandia and with previously published seismic source area models from the study area.

9.1 The database and the completeness of the compiled data sets

Along the guidelines of IAEA (2010) we have established an upgradable database on the geological, geophysical and seismological data used in this report and to be used in seismic hazard assessments. The data collected during the project have been stored in an ArcGIS database with metadata described in Appendix 3 and the datasets in Chapter 2.

The study area is a 500 km radius circle around the Hanhikivi site. It is larger in size than in the previous geological and geophysical studies (≤ 300 km; Appendix 1) and the same size as in the last hazard evaluation study by Saari et al. (2009). Hence the geological and geophysical data sets are more extensive as they cover a wider area. The previous studies have relied mainly on the data from Finland that covers only little over half of the study area. The data sets from the Swedish part have consisted on publicly available data sets that have been less detailed and more extrapolated. The current data set is thus more extensive and its precision is more uniform across the study area. Because the current dataset covers the entire study area the results should be less biased towards Finland than in the previous studies where Swedish data has had less impact. It is also noted that the all the datasets are now for the first time in one single database and thus it is easier to correctly compare different subsets.

Based on observation data sets at the geological surveys of Finland and Sweden and on a literature review we have compiled and added a PGF data set to the database. The PGFs have uniform coordinate information on the identified and verified PGFs from Finland and Sweden for the first time. The data can now more easily be compared with other digital datasets as was done also in this study. Some of the faults are marked on their exact locations as they have been checked against 10-m DEM data (see Figure 2.7.3) and some have been drilled or examined by on-site excavation on Quaternary deposits. The uncertainty in the position of the inferred PGFs in Sweden is approximately 1 km or less. Close to possible deep drilling sites (ICDP- the International Continental Drilling Programme; Kukkonen et al., 2010, 2011a) the location precision is much higher. The database contains also “possible post-glacial faults” that are still under investigation by SGU and GTK and these sites and data should be verified later. It has to be borne in mind that not all PGFs have yet been found in the Fennoscandia area. The most challenging areas are the offshore areas that are less data-intensive and the large lowland areas that were under the influence of the ancient Baltic Sea phases after deglaciation (13 000-2000 years ago). In these areas the sedimentation processes may have covered and obliterated the potential PGF features. However, new approaches e.g. LiDAR, microseismicity studies, marine seismics and satellite images might prove useful in search for new PGFs.

Structural datasets in the database are largely based on geological interpretations of aeromagnetic datasets in different scales. The rule of thumb is that the precision of the hand drawn structural lines cannot exceed that of line width of 1 mm (in 1:1M maps 1mm equals 1km). In the previous studies (Korja et al., 2011), 1:1M or larger scale maps were used in the Finnish territory and 1:5M scale maps (Koistinen et al., 2001) in the Swedish territory. Thus by using 1:1M scale data also in Sweden, the lateral location uncertainty of deformation zones in the western part of the study area has decreased from 5 km to 1 km. Recall that although some of the deformation zones are up to 8 km wide in nature they have been approximated with only one line in the database. In addition, the lineaments crossing the national border were adjusted to fit data from both sides (Fig. 2.5.3). Although the changes to individual lineaments were small, the large scale picture is clearer. For instance, the regional continuation of the NW-SE trending Western Lapland fault system from Finland to Sweden is more evident than in the previous compilations. It can also be inferred that the Western Lapland fault system transects the much older N-S trending Pajala shear zone. Both structural entities are associated with increased seismicity. Understanding of the regional coverage of the Western Lapland fault system is especially important as it is orthogonal to NE-SW trending PGF faults or rather to the reverse faults facilitating PGF.

Information on bedrock, structural trends and lineaments of the offshore study area i.e. Gulf of Bothnia, is mostly based on geophysical datasets and to lesser degree on geological sampling. The resolution of the offshore data is poorer than in land areas and thus the positioning of the structural trends is less precise. Fracture zones have also been mapped with marine acoustic methods. The regional scale acoustic profiles (Fig. 2.6.1-2.6.3) were collected already in the 1970's and 1980's by Winterhalter (1972), Axberg (1980) and Wannäs (1989). These datasets have severe limitations, the most important being the very low positioning accuracy of the seismic profiles. The second limitation is that the original datasets are analogue recordings on paper and the third is the low energy contents of the air-guns. The new shallow marine seismic dataset (Appendix 1; Rantataro et al., 2011; Alanen et al., 2013) have been compared with morphological and magnetic lineaments and Wannäs lineaments (Fig. A1.4-A1.5). In some of the checked locations, there were hints of fractures co-locating with aeromagnetic and morphological lineaments within couple of hundred meters. In other locations, there were no indications of fractures. The nearest possible Wannäs lineament (lineament 122) is situated at about 14 km southwest from Hanhikivi. The existing shallow marine seismic profiling data does not reach into that area. It seems that the major lineaments outlined by Wannäs (1989) are matched by parallel lineaments in contemporary topographic, bathymetric and aeromagnetic maps (Kuivamäki et al., 2011; Airo et al., 2011a) and acoustic datasets (Rantataro et al., 2011; Alanen et al., 2013). The contemporary lineaments are, however, off-set by several hundreds of meters to kilometers from the suggested position by Wannäs. Even if the analogue

recordings could be digitized (this may take years) it is not clear if any new relevant information would be gained. We suggest that the old data sets should only be used in a regional scale (1: 1M). For more detailed information new data with GPS positioning should be acquired.

The current seismicity database has been improved by deleting misinterpreted mining explosions from the Swedish data in FENCAT, by adding subsets of microearthquakes recorded by denser seismic networks of SNSN in 2000-2012 and OBF in 2013, and by re-appraising the location and magnitudes of a few historical earthquakes. The addition of new datasets has not changed the general spatial distribution of seismicity (Figs. 2.8.1.2 and 2.8.1.3). With increased station density the location precision is better and the clusters and trends of seismicity have become sharper or condensed. Also the other focal parameters are more precisely determined allowing for a more reliable estimation of focal depths (Fig. 5.7.1) and fault plane solutions (Fig. 4.3.2-4.3.3). Because the data sets are more complete and the location precision is better, the merged data are well-suited for studying the intraplate seismicity of Fennoscandia.

Because different agencies have calculated magnitudes using different equations and parameters in the FENCAT catalogue and the current catalogues, the magnitudes are not comparable. The magnitudes should be homogenized before hazard calculation. We conclude that the updated seismicity catalogue is well-suited for earthquake studies and hazard estimations, provided that the magnitudes are homogenized prior to the calculations.

The addition of SNSN data set has increased the location precision especially close to the PGF faults in Sweden and the OBF data in the proximity of the Hanhikivi site. As an example of the high precision of the SNSN data is our new observation made at the workshop in October 2013. There is a N-S directed trend of microseismicity aligned with and on top of a parallel magnetic lineament (Fig. 9.1.1). We suggest that this fault is active and that it should be checked for evidence of post-glacial faulting.

By checking the earthquake catalogue data for mining explosions we have added the reliability of the datasets in scientific earthquake studies. A good example of problems related to using publicly available, unchecked catalogues is the study by Redfield and Osmundsen (2013). They have used the automatic seismic event list published by International Seismological Centre (ICS; <http://www.isc.ac.uk/>) to study the origin seismicity in Fennoscandia. Unfortunately the seismic events included explosions in addition to earthquakes. The data set includes several seismic events M>3 that are explosions in Finland alone. If these events were earthquakes, it would have major consequences for hazard estimations.

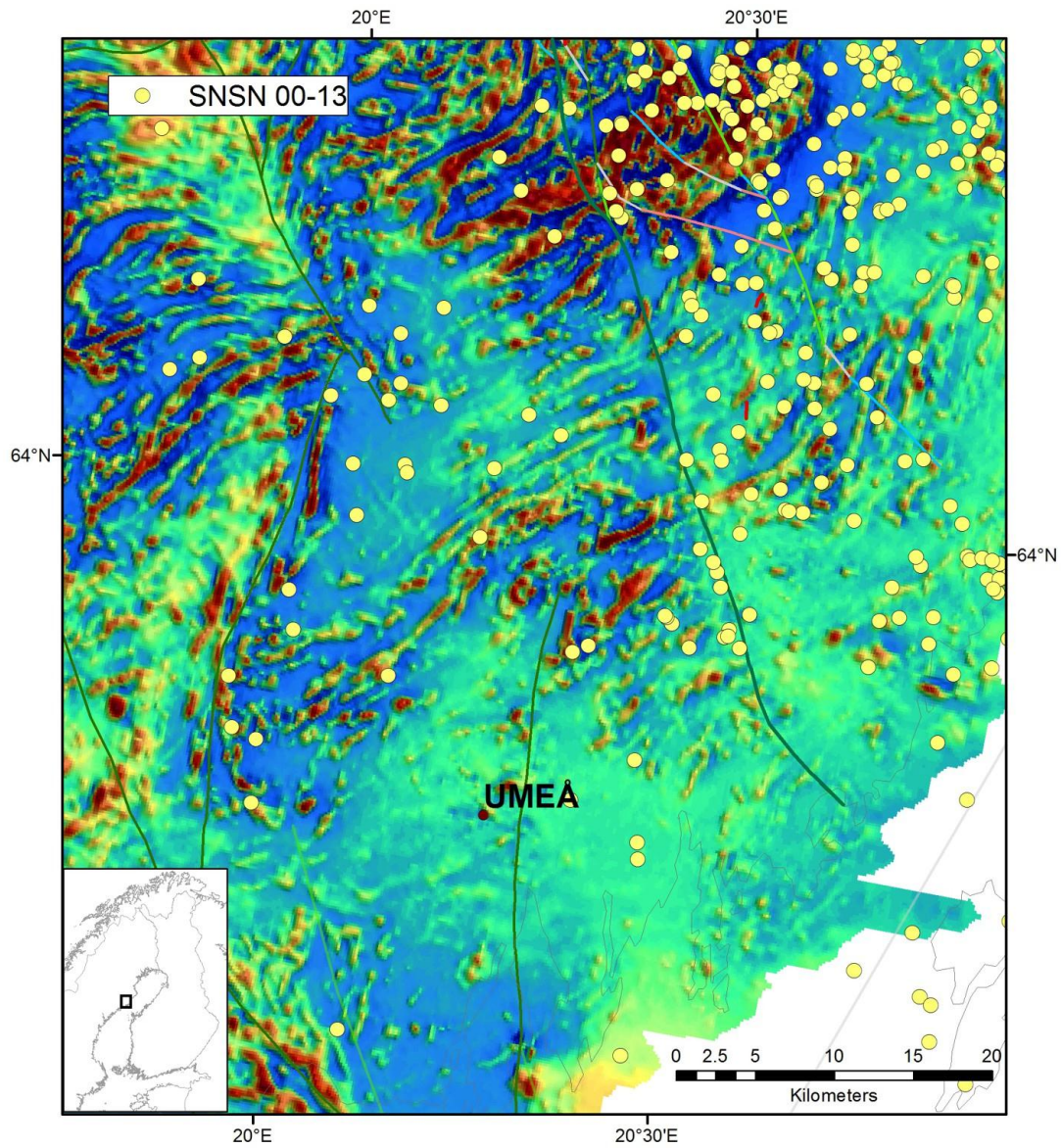


Figure 9.1.1. Seismicity and aeromagnetic map and lineaments in north of Umeå. Note how the microearthquakes align with an existing aeromagnetic lineament suggesting an active fracture.

9.2 Seismicity

A. Korja & P. Mäntyniemi

Earthquakes are instant releases of stress and energy that has been accumulating over long periods of time in Fennoscandia. Opening of the Atlantic initiated a tectonic stress field some 60 Ma ago and changes in the stress fields take place over millions of years. Glaciation cycles produce an additional component to the stress field that have lifetime of 10 000 a/cycle, and even minor, more local third order stresses stemming from gravitational potential energy differences seem to have existed from millions to billions of years. The only stress-field component that may change in short intervals of years to ten years is the local man-made component derived from underground mining and construction. It is thus more than likely that the stress generating mechanisms and hence also the

regional scale stress field is quite permanent in the Fennoscandian Shield within the lifetime of a nuclear power plant.

It is not quite clear, how much of the internal deformation and block movements are taken up by seismic movements and how much is aseismic. Aseismic movement should be much more common as earthquakes are located in places where frictional sliding is hindered and stress piles up. What is the recurrence time of the stress build-up in individual structures? Are the earthquakes always happening along the same fractures or does the seismicity shift from place to place also in low seismicity areas? What is the length of seismic cycle?

The time interval covered by the seismicity record available has not captured the full seismic potential of the study region, being much shorter than the seismic cycle. Even if the hypothesis of large earthquakes with very long recurrence times in the study region is rejected, evidence of earthquakes in intraplate areas with little previous seismicity has to been taken into account. For instance, the Saguenay region (Province of Québec, Canada) experienced an unexpected m_b 5.9 earthquake on 25 November 1988. Within a radius of 50 km from the epicenter, only earthquakes with magnitude 3 or less had been registered earlier (North et al., 1989). Another set of unanticipated earthquakes occurred close to Kaliningrad on 21 September 2004; the largest of them with a magnitude M_w5.2 (Gregersen et al., 2007). There are hardly any records of previous seismicity in Kaliningrad and its vicinity. Some earthquakes in unidentified faults in intraplate areas have also been very disastrous (such as the Latur, India earthquake of 1993).

In the study region, the known earthquakes with magnitude M>4 appear quite sporadically distributed, and it is difficult to assess them in terms of possible recurrence. Some such as the Solberg earthquake of 29 September 1983 with magnitude around 4 (Kim et al., 1985) occurred outside the zones of enhanced seismicity, whereas some large historical earthquakes may have occurred within them. For instance, the 1926 earthquake probably occurred in the Kuusamo area, which today exhibits microearthquakes.

On the plate boundaries, the location of the hazard can often be mapped quite well, whereas in many parts of plate interiors both the location and the timing of earthquake constitute the greatest uncertainty. Stein and Liu (2009) discussed how the slow deformation rates at plate interiors mean that aftershock sequences last for hundreds of years after the main shock. They argued that the aftershock sequences following the past large earthquakes, including those in New Madrid, Missouri (1811–1812); Charlevoix, Quebec (1663); and Basel, Switzerland (1356) still continue. An implication of this to seismic hazard assessment is that locations of large future earthquakes are not delineated by cluster of small earthquakes. This rather supports the notion that the available seismicity record

cannot be used to infer the locations of future earthquakes in the region, which is in accordance with the occurrence of surprise earthquakes. However, if some seismicity observed today is indeed aftershocks of previous large earthquakes, it would imply that there is decreasing seismicity that would at some point come to an end. Basically it is not impossible that a large earthquake occurred many centuries ago, but whether the aftershocks are still occurring is an open question.

Occurrences of very large (Paleo)earthquakes in the study region have been dated to have taken place shortly after the deglaciation, thus belonging to a stress regime different from that of today. However, some authors have claimed large-magnitude earthquakes considerably younger than the paleoevents. Lukashov (1995) proposed a 2300-year interval of higher seismicity in the Lake Onega Domain, Russian Karelia. According to Mörner (2009), large-magnitude paleoearthquakes have occurred in Sweden in the Late Holocene.

9.3 Geological and geophysical boundaries and shear zones

Korja, A

In chapter three the geological background information has been described using the concept of lithotectonic units which have similar tectonic histories and structural grains. The study area includes eleven lithotectonic units that were delineated based on major structural unconformities and other structural criteria. The lithotectonic units have been described in relation to the Paleoproterozoic orogen and Caledonian orogen. Sedimentary and magmatic rocks that have not been emplaced in either of the two orogenies and belong to intervening rift stages have also been described. The resulting map is simple enough for large scale studies. This approach emphasizes the effect of orogenies on the structural development of the terranes and stresses the importance of orogenic folding and faulting as source of structures that can be later reactivated in the current stress field. The classification overlooks the possibility that precollisional rift structures could be inverted and later be reactivated in following orogenies and during the current stress field.

From Figures 9.3.1-9.3.3 it is apparent that seismicity in the central Fennoscandian Shield is associated with gravitational potential energy differences rising from local and regional variations of the topography and bathymetry, crustal thickness and post-glacial rebound anomalies (Fig. 5.4.1). In general, the changes in seismicity patterns are not associated with lithotectonic boundaries (Fig. 9.3.2). Noticeable exceptions are found at the western boundaries of the Mesoproterozoic units, of the Norbotten-Karelia contact, perhaps also a slight change along southern contact of the Inari unit. The Caledonian unit does not host any earthquakes.

The maps indicate that the areas with thick or overthickened crust (> 50 km) have only moderately seismic activity and the earthquakes are shallow (Figs. 5.4.2 and 9.3.3). The seismically active areas

are located in areas with normal thickness crust (<50 km). Where the crustal thickness change is trending in NE-SW direction, like in western flank of the Bothnian Sea and the Auho-Kandalaksha fault zone, the gradient seems to be associated with a zone of increased seismicity. This association should be studied in more detail before any final conclusion can be made.

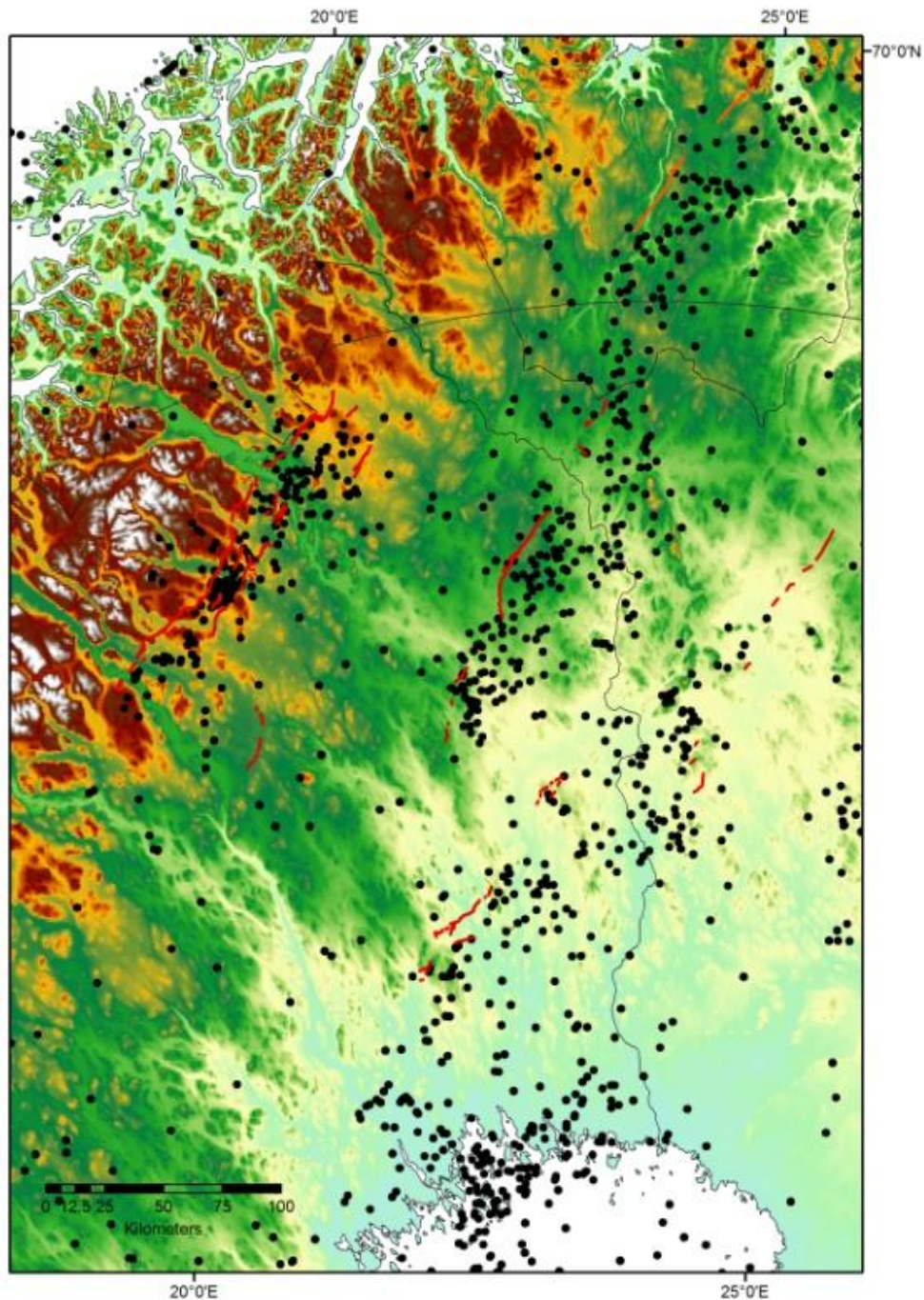


Figure 9.3.1. Topography, PGFs and seismicity. A combination of figures 2.2.1, 2.7.2, 2.8.1.1 and 2.8.1.2. Trends of seismicity and PGFs trend loosely parallel to the topographic gradients.

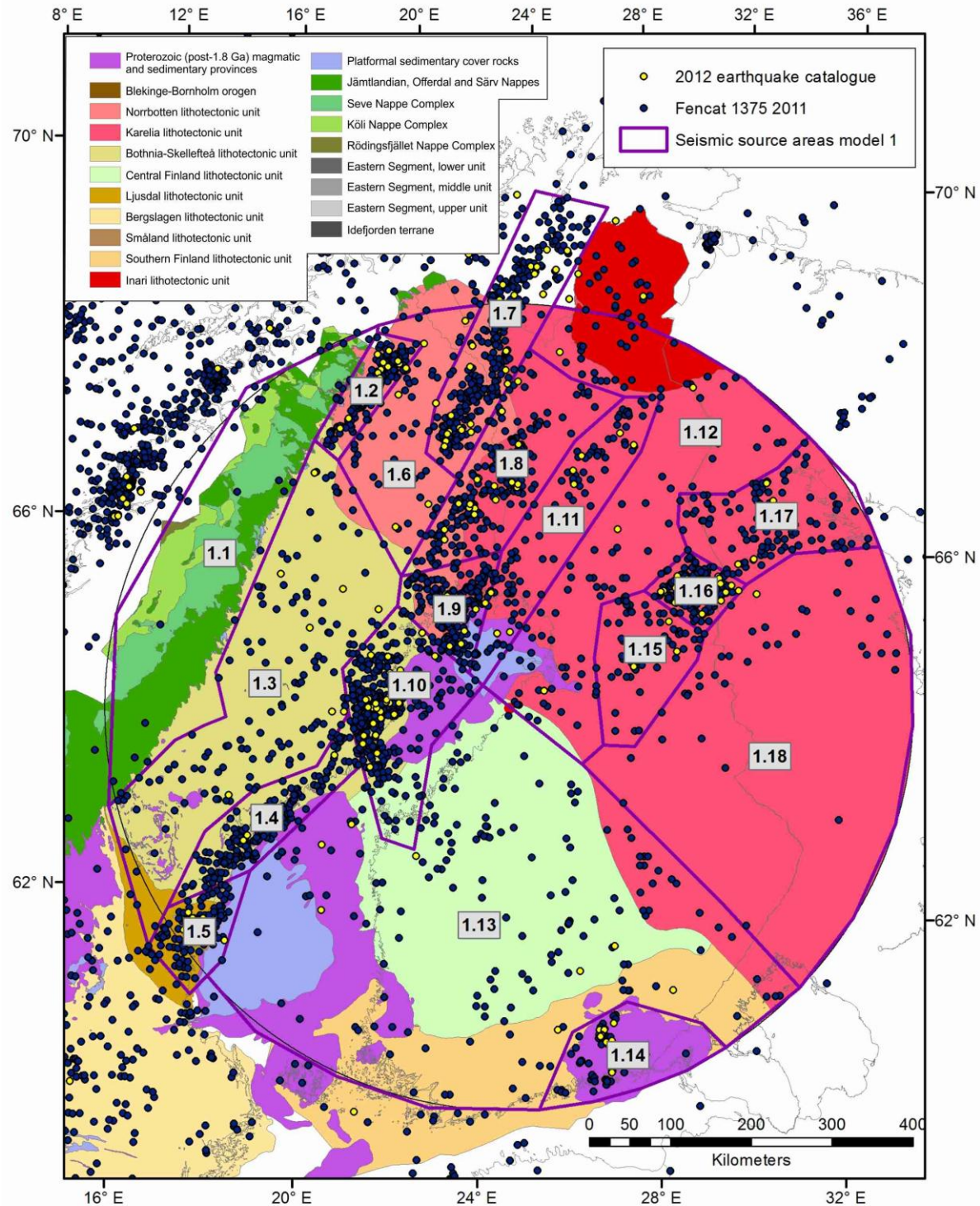


Figure 9.3.2. Lithotectonic units, seismicity and Model 1. A combination of figures 3.1.1.1, 2.8.1.1, 2.8.1.2 and 8.2.1. Hanhikivi site: red dot.

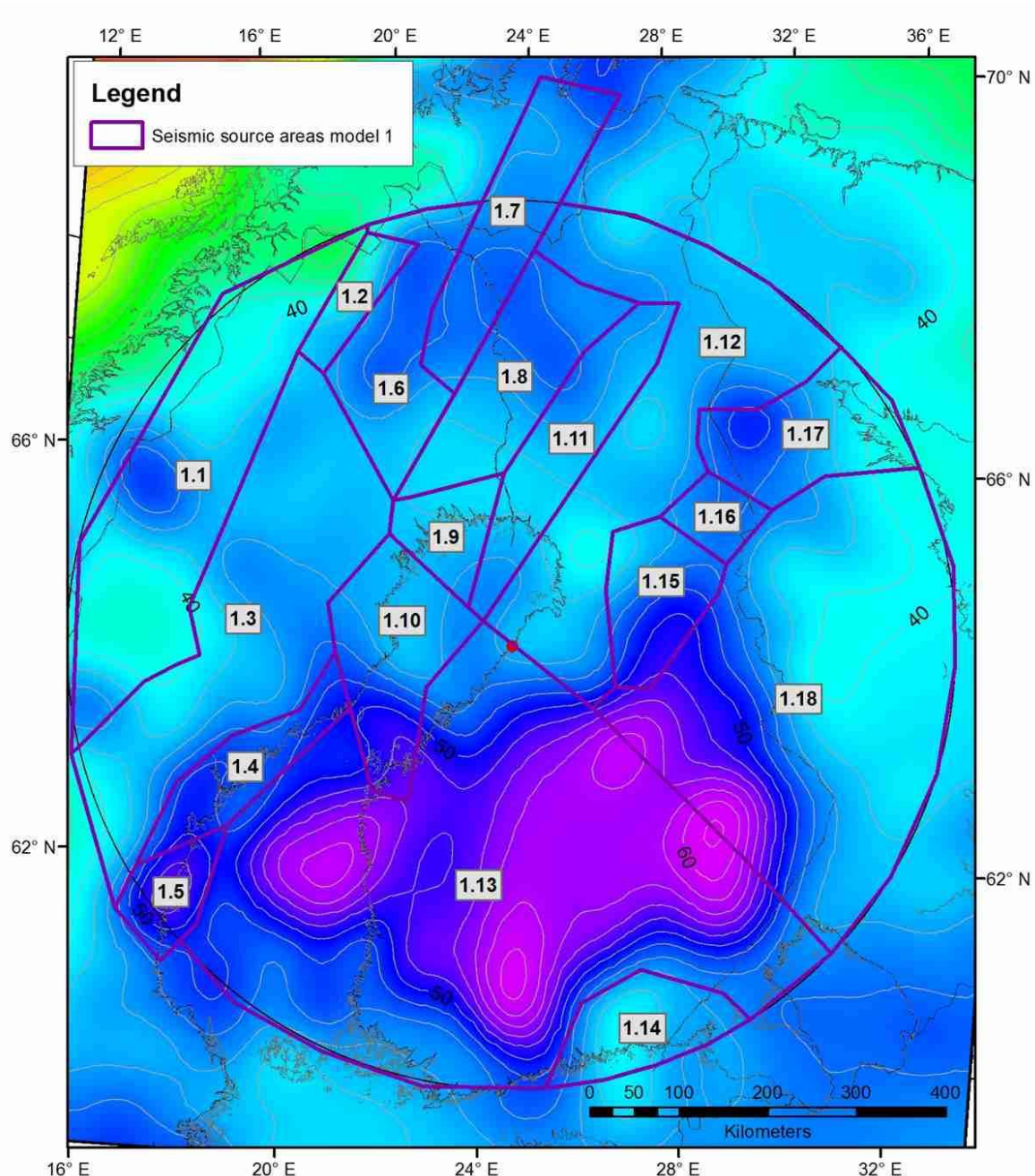


Figure 9.3.3. A depth to the Moho-map, distribution of seismicity and Model 1. A combination of figures 5.4.2 and 8.2.1.

Figure 9.3.4 outlines the major shear zones in Central Fennoscandian Shield. They are color-coded after azimuthal deviation from the present stress field maximum. This helps to visualize distribution of faults that are in perfect orientation to be reactivated as normal, reverse or strike-slip faults in the present tectonic stress field. Only 34 fault plane solutions are included in the stress indicators (Fig. 5.2.1., Heidbach et al., 2008) from where the stress field is calculated. The rest of the fault plane solutions can be used to test the azimuthal deviation map.

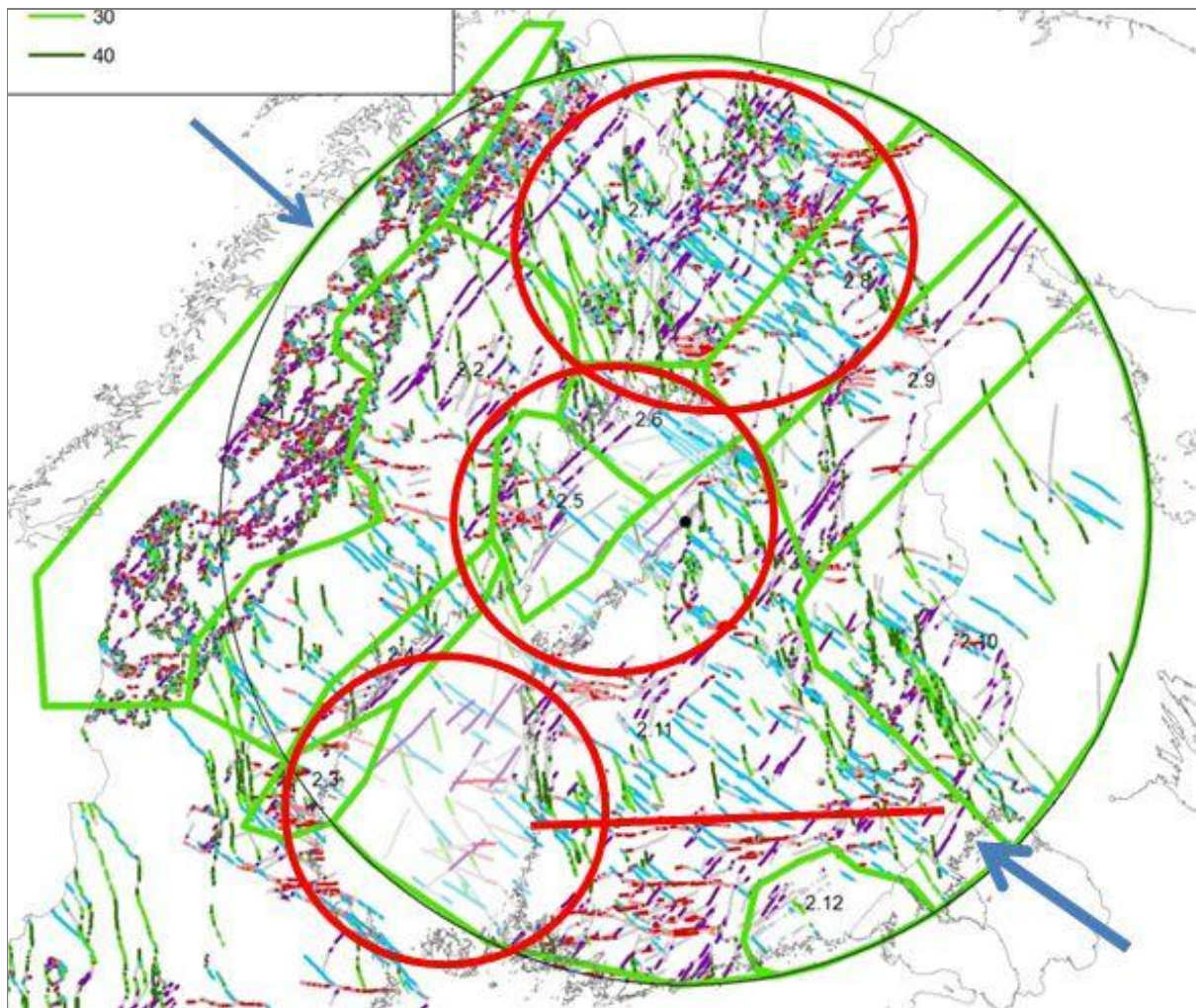


Figure 9.3.4. Deformation zones and Model 2. A combination of figures 3.1.2.1 and 8.3.1. Ellipsoids point out areas where Model polygons transect larger structural domains. Hanhikivi site: black dot.

Another interesting observation from the map is that e.g. in the Central Finland granitoid complex (Fig. 9.3.4; northern part of Model 2) the suggested release mechanism is the same as the one prevailing during its formation in the Precambrian. (For more detailed descriptions of the fault zones in Central Finland see: Nironen et al., 2000; Sorjonen-Ward, 2006; Korja et al., 2009). That is thrust faults in the current stress field have once been moving as thrust faults in the Precambrian, transfer faults have been described as transtensional faults etc. This observation suggests that the stress field stemming from the opening of the North Atlantic is partly reactivated per-existing weak zones of the Eurasian plate (Fennoscandia). Pascal and Cloetingh (2009) suggested that similarly to South-Atlantic also the North Atlantic opening may have partly inherited an older stress field.

Koskinen (2013) and Koskinen and Korja (2014) noted that in Finland only in Lapland seismicity patterns could be linked with individual reactivated fault zones. There seismicity seems to be associated with the reactivation of the pre-existing orthogonal pair of NE-SW and NW-SE faults, associated with reverse (PGF) and transfer faults (Fig. 9.3.4). Tiira et al. (2013) suggested that the set

of NW-SE striking strike slip faults (Western Lapland fault zone) that transect Central Lapland may have inherited their direction from the transfer faults of the buried Paleoproterozoic Lapland rift. It is suggested that the lower crust has attained its elastic properties already in the Paleoproterozoic rifting phase and that those lower crustal properties have been inherited through the different inversion periods as suggested by Watts and Burov (2003). It is not clear whether the Western Lapland fault zone and Lapland paleorift structures are just parallel to each other, or if they have a more profound relationship.

Overall, the relatively young fault sets with presumably brittle-ductile deformation appear to be confined to the area underlain by Archean crust (Fig. 3.1.1.1) or rather Archean crust that was extended and dismembered during Paleoproterozoic rifting event. The consequence of this is that areas underlain by Archean crust host old inverted crustal scale deformation zones. It might be that because they were once formed in brittle environment they might continue to be more susceptible to be reactivated than the ones that were formed as ductile shear zones in the Paleoproterozoic. This reasoning could explain the existence of PGF faults in Lapland.

PGF faults are usually associated with reactivated fault systems. For instance a thrust system may have complex internal 3D structures composed of synthetic, antithetic and transfer parts that are associated with fault plane solutions indicating reverse, normal and strike slip regimes respectively. In the NE-SW trending Pärvie Fault, the earthquakes affiliated with the main fault and synthetic faults to it would produce fault plane solutions compatible with NE-SW striking reverse faults with varying dips. Earthquakes affiliated with the antithetic faults would have fault plane solutions suggesting NE-SW striking normal faults with opposing dips. Earthquakes associated with the transfer/strike slip faults should suggest movement in NW-SE direction along rather steep faults. These would compensate for the different velocities of the different parts of the fault. We suggest that the wide range of fault plane solutions documented within the Pärvie Fault (Lindblom and Lund, 2011; Lindholm et al., 2011) could be signaling the movement of a complex thrust system.

9.4 Seismogenic zone

A seismogenic zone is defined as a zone where the majority of earthquakes takes place. The depth of the seismogenic zone is time and place dependent. In the study area, earthquakes occur at depths between 0 and 45 km (Fig. 9.4.1). Most of the earthquakes (2000-2012) (80%) occur in the upper crust down to 17 km in depth, a minority (19%) in the middle crust (17-31 km) and only a few in the lower crust 31-45 km (1%). Lamontagne and Ranalli (1996) suggested that the lower limit of the seismogenic zone is where 99% of the earthquakes occur. According to this definition the thickness of the seismogenic zone is 31 km in the study area. Kaikkonen et al. (2000) deduced quite similar

values for Finland (eastern part of the study area) by using FENCAT earthquake catalogue data from the years 1965–1997. They evaluated that most of the earthquakes (80%) take place at depths between 0 km and 14 km, 19 % between depths of 14 and 31 km, and less than 1% at deeper levels and that the seismogenic thickness above which (99%) of the earthquakes occur is 31 km. Our results confirm the result that the seismogenic layer is at the depth of 31 km. The layer seems to be rather uniform across Fennoscandia.

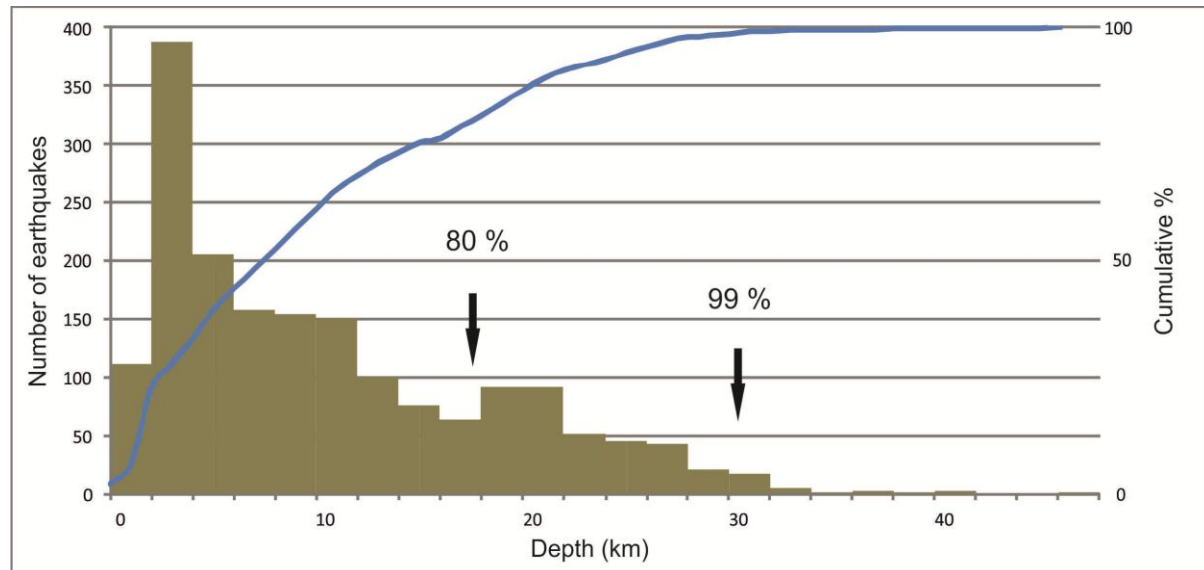


Figure 9.4.1. A histogram of depth distribution of earthquakes in 2000-2012.

Kaikkonen et al. (2000) associated the lower boundary of the seismicity (31 km) with 350 °C isotherm related to transition from velocity weakening to velocity strengthening in granitic rocks (Scholz, 1990). In the study area, the isosurface is located between depths of 30-45 km, when wet rheologies are assumed (Fig. 5.6.1). The isosurface is in close proximity to the seismically determined boundary between high velocity gabbroic lower crust and granodioritic middle crust found between depths of 34 to 42 km (Korja et al., 1993). We suggest that the middle-lower crustal boundary may add compositional and rheological constraints to the depth extent of seismogenic zone in the study area.

After numerical modeling studies where wet crustal rheologies applicable to Finnish crust were used, Moisio and Kaikkonen (2000) suggested that distinct decoupling of strong upper crust, weak lower crust and strong upper mantle (Moisio and Kaikkonen, 2000). They suggested that decoupling interrupts the transmission of differential stress from the brittle upper crust to the ductile lower crust and upper mantle. This corroborates the idea that seismogenic layer is restricted to the middle and upper crust in the study area.

According numerical experiments by Moisio and and Kaikkonen (2006, 2012) the depth of the modelled brittle-ductile transition zone is highly dependent on the number of layers and other model

parameters. In areas where the crust is clearly layered, BTZ is located at around the depth of 10 km (e.g. Central Finland lithotectonic unit), whereas in other areas it may be found at larger depths down to 40 km (Karelia lithotectonic unit). The observed depth distribution (Fig. 5.7.1) is generally in agreement with the rheological models by Moisio and Kaikkonen (2006, 2012). In Central Finland, where crustal layering with a pronounced décollement zone between upper and middle crust is found (Korja and Heikkinen, 2008), the majority of well-defined earthquakes are confined to the upper crust. Note that small to moderate size earthquakes tend to occur along pre-existing zones of weakness with a limited depth extent. Only few of the major large shear zones or rather block boundaries have continuations to the middle crust and even fewer to the lower crust. One of such regions could be Norra Kvarken from where deep earthquakes have been reported (Fig. 5.7.1). From the same area BABEL reflection profiles have identified a paleo-subduction and collision zone accompanied by a step in the Moho and deep penetrating NE dipping shear zones (Fig. 5.5.1.1; BABEL Working Group 1990; Korja and Heikkinen, 2005). It is suggested that the décollement controlling the depth extent of fault zones is controlling the lower limit of present seismicity within a given source area.

In the Kuusamo area and Hirvaskoski and Auho-Kandalaksha deformation zones (Karelia lithotectonic unit) which on one hand belong to the precollisional rift areas and, on the other hand, to areas where the high velocity lower crust is either thin or missing, earthquakes occur deeper, down to 30 km in depth. Although the earthquakes take place at deeper levels and over half of the earthquakes occur between 15 km and 30 km, the events are still located above the onset of brittle-ductile transition as argued by Uski et al. (2012) and thus they are placed within the seismogenic zone (31 km). The implied link between increased seismicity in Kuusamo and Hirvaskoski and Auho-Kandalaksha deformation zones to inverted rift structures should be looked more carefully into.

9.5 Alternative seismic source area (SSA) models

We have outlined three alternative models in section 8. The models were designed by two independent expert groups (see section 8). Group 1 drafted Model 1 (Figs. 8.2.1-8.2.3 and 9.5.1) that is based on geological, historical and instrumental seismicity data in the database (Figs. 2.8.1.1-2.8.1.2), lithotectonic units (Fig.3.1.1.1) and deformation zones found in structural, aeromagnetic or Bouguer anomaly maps (Section 2.1 and 2.5). The model draws from the influence of Paleoproterozoic bedrock structures and structural evolution on the source of seismicity. Group 2 drafted Models 2 and 3 (Figs. 8.3.1-8.3.6 and 9.5.2) and Model 3 is a more detailed version of Model 2. They focused their analysis on the recently active structures using data sets bearing on instrumentally recorded seismicity (1971-2012 + SNSN extra data; Figs. 2.8.1.2-2.8.1.3), post-glacial faults (PGF; Fig. 2.7.2), topography and bathymetry (Fig. 2.2.1), lineaments defined on the basis of

magnetic data and the current stress field (Fig. 5.2.1-5.2.2). Model 3 is an evolved version of spatial model 2 and contains additional minor polygons. The location of the Hanhikivi site was not included in the maps used in the workshop. This has resulted in the fact that the site is right on the polygon margin in Model 1.

Although two independent expert groups have drafted Models 1 and 2 (3) and have used mostly different data sets, the three models share many similarities and have only minor deviations (Table 9.5.1). The similarities can be seen in Figures 9.5.1 - 9.5.3. The models are similar in that the majority of the polygons are overlapping in shape and size for the most parts. Some discrepancies are found on the margins. Most of the differences are found in the offshore areas (Fig. 9.5.4), where structural control of neither the Precambrian deformation zones nor the PGFs or bathymetry is not optimal. The similarity of the models stems from the fact that both groups have used seismicity as the primary descriptor and other materials as secondary descriptors. The models are quite similar because 1) seismicity is linked to reactivation of old faults in the present stress field, 2) post-glacial faults are associated with reactivation of old faults, 3) topography is influenced by the structure and composition of the Precambrian bedrock, 4) the current tectonic stress field might be influenced by the structure of the Precambrian bedrock. It is concluded that the three seismic source area Models 1, 2 and 3 are closely related.

In these models, the spatial grouping of earthquakes has been the major decision criteria and other criteria come only as second. The polygon boundaries are located between the areas of increased seismicity i.e. in the in between areas, which results in certain freedom in drafting the polygons. In this project, two expert groups produced rather similar sets of polygons, which add to the credibility of the models. The closeness of the sub-parallel parts of the polygon lines could perhaps be used as an error estimate of the line positions. Polygons characterized by increased seismicity have deviation around \pm 15 km. Polygons with less earthquakes the boundaries are less well defined and thus deviations are in the order of 5-50 km for large polygons (250- 500 km wide) and in the order 25-50 km for smaller polygons (40-100 km wide). The smallest polygons have the largest error estimates and thus they are the most unreliable polygons.

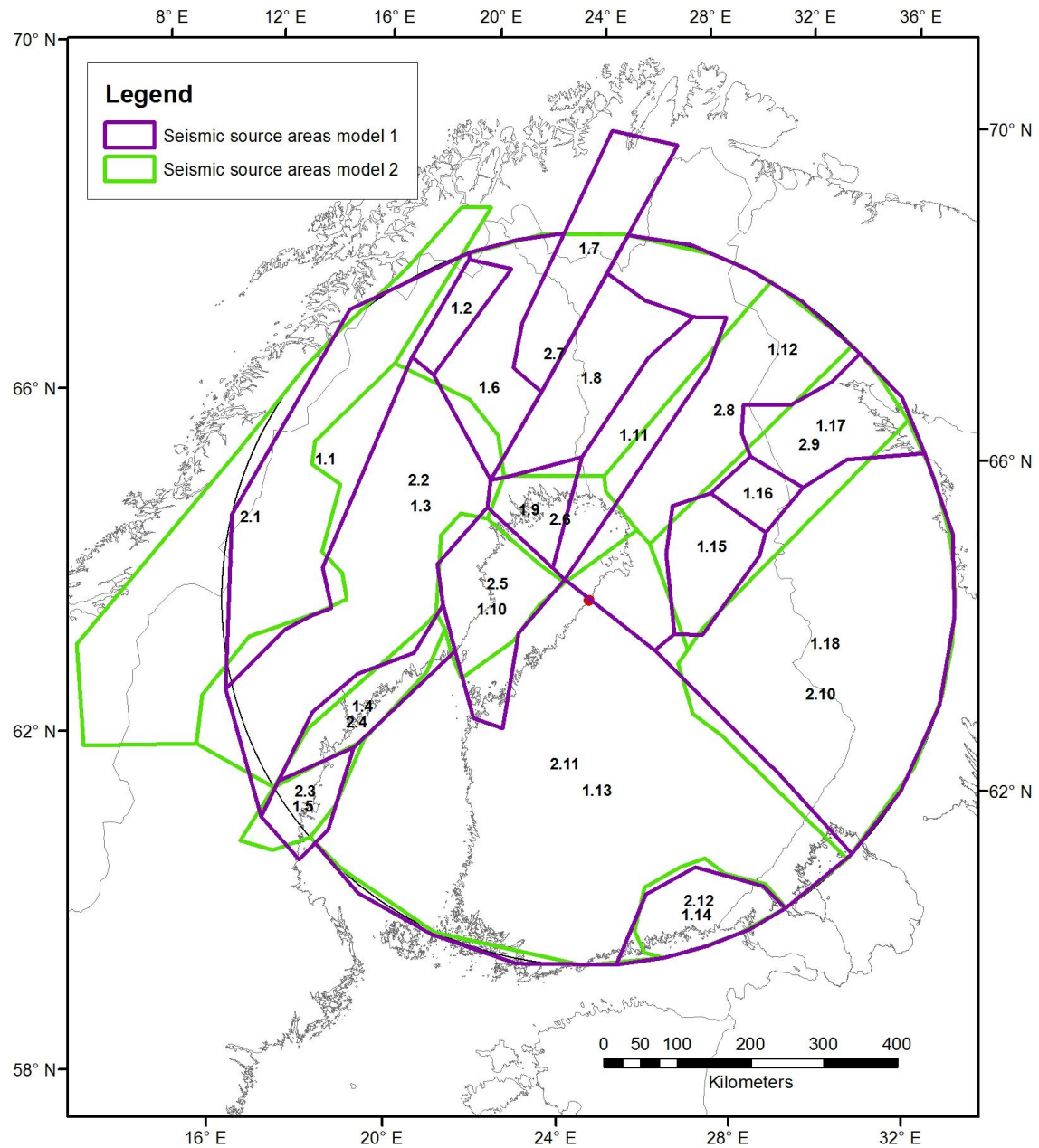


Figure 9.5.1. Overlapping of Models 1 and 2.

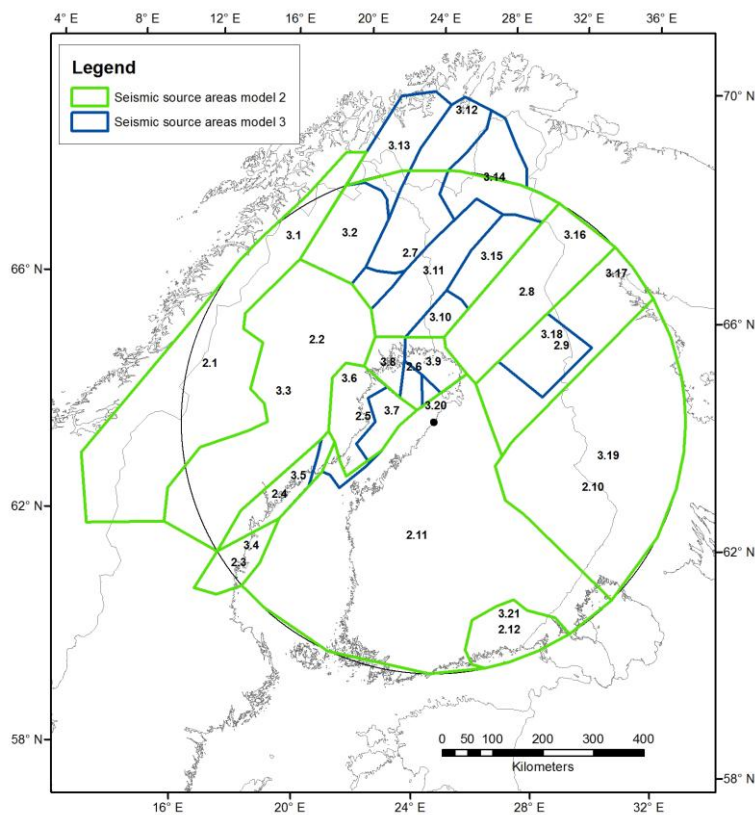


Figure 9.5.2. Overlapping of Models 2 and 3. Model 3 is a more detailed version of Model 2 and it has extra polygons included within the larger polygons of Model 2.

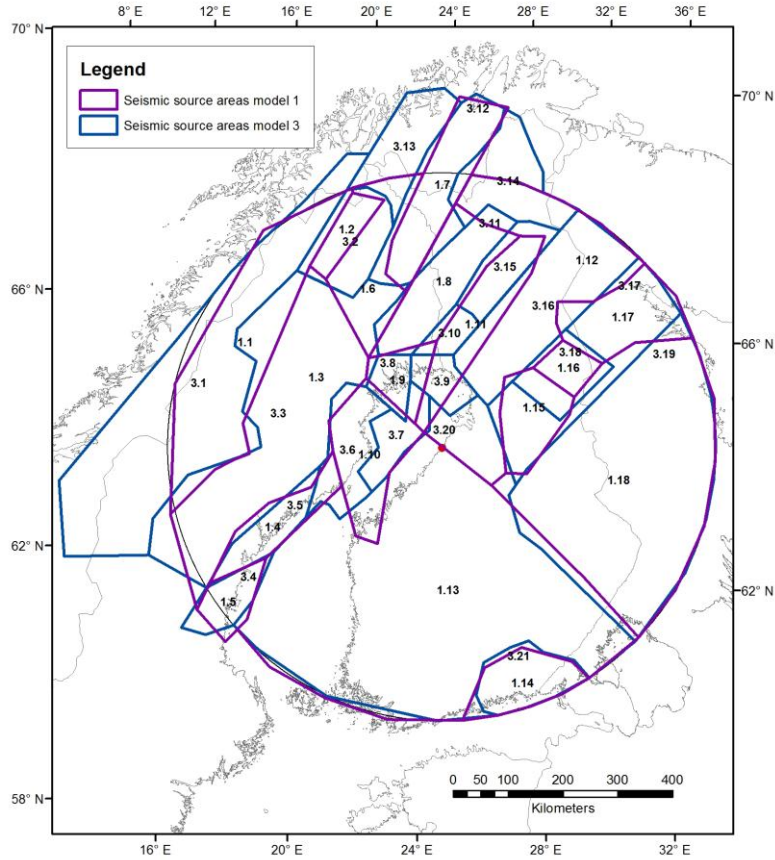


Figure 9.5.3. Overlapping of Models 1 and 3. Note that the models have many similarities and only minor major deflections.

Table 9.5.1. A comparison of polygons in Models 1, 2 and 3. Model 3 has extra subpolygons that are included within the larger polygons of Model 2. These subpolygons are listed in groups that begin with the same row. Polygons with overlapping geometries are placed on the same row. Polygons of Model 3 that have only minor overlapping with Model 1 are in brackets, whereas larger polygons of Model 1 that spread over several smaller polygons of Model 3 are highlighted in colours. Polygons with large parts outside the study area have a note on the observation column as well as those located offshore.

Model 2	Model3	Model 1	obs
2.1	3.1	1.1	outside
2.2	3.3	1.3	
2.3	3.4	1.5	
2.4	3.5	1.4	
2.5	3.6	1.10	offshore
- " -	3.7	1.10	offshore
2.6	3.8	1.9	offshore
- " -	3.9	1.11	offshore
- " -	- " -	1.9	offshore
- " -	- " -	1.12	
- " -	(3.7)	1.10	offshore
2.7	3.2	1.2	
- " -	3.12	1.7	outside
- " -	3.11	1.8	
- " -	3.10	1.11	
- " -	3.15	1.11	
- " -	(3.14)	(1.12)	outside
- " -	(3.13)		outside
2.8	3.16	1.12	
2.9	3.17	1.17	
- " -	- " -	1.15	
- " -	3.18	1.16	
2.10	3.19	1.18	
2.11	3.20	1.13	
- " -	- " -	(1.12)	
- " -	- " -	(1.10)	
2.12	3.21	1.14	

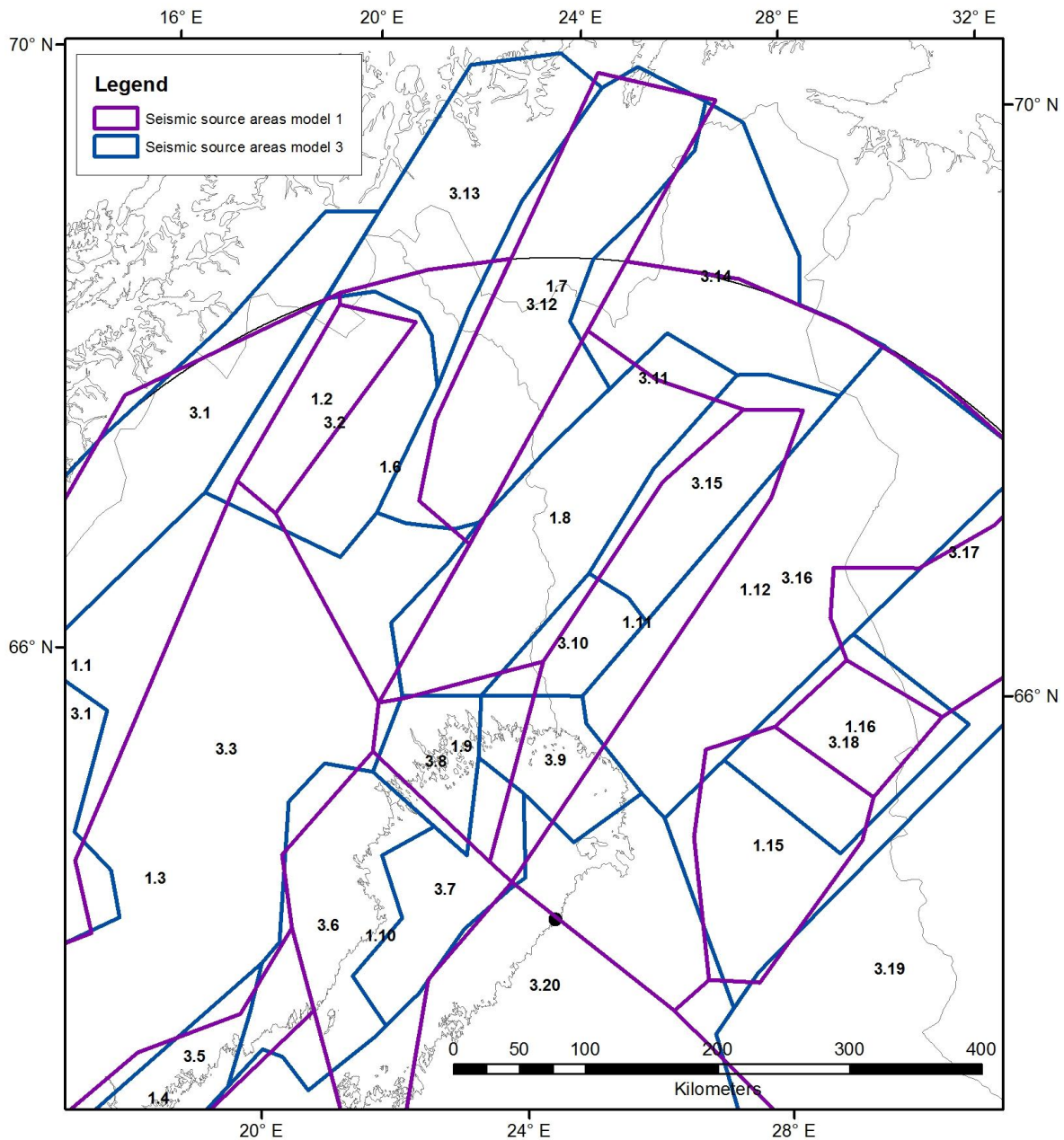


Figure 9.5.4. Discrepancies in the offshore and outside model areas of Models 1 and 3.

9.5.1 Uncertainties of the SSA models

A. Korja & P. Mäntyniemi

In the three seismic source area models presented in this report, the main uncertainty concerns the construction of the boundaries between polygons. These boundaries are strongly steered by the instrumentally detected earthquake patterns presented in Chapter 4.1. Hence a key uncertainty concerns the registration of the occurrence and position of the earthquakes: the source location, magnitude and focal mechanism.

The first uncertainty involves the precision of the earthquake source location (see Section 4.1). The precision (2-5 km within the networks) is sufficient for mapping the areas of enhanced seismicity and relating the events with wide deformation zones, but not for defining any individual fault as a

capable fault. The correlation is further complicated by the fact that deep structure of the deformation zones is mostly unknown. Seismic reflection data from the area suggest that the style of deformation changes with depth and that upper and middle crust may be detached (see Fig. 5.5.1; Korja and Heikkinen, 2008). This implies that it may not be possible to extend the structures observed at surface to great depths and to correlate earthquakes at depth with outcropping structures or lineaments.

As is mentioned in Section 4.1, the bulk of routinely determined focal depths in FENCAT may contain large uncertainties, the shallowest depths in particular. The depth distribution is best resolved within the areas where dense temporary networks have been operational. Waveform modeling of depth-sensitive phases has provided additional constraints on focal depth estimation, verifying, for example, the unusually shallow depth pattern in Wiborg batholith area (source areas: 1.14 and 2.12; Uski et al., 2006) and the mid-crustal activity within the Kuusamo block (Fig. 5.7.2.; source areas: 1.16 and 3.18; Uski et al., 2012). However, convincing data on seismic activity within the lower crust (depths below \sim 32 km) are still lacking.

There are no apparent regional variations in the magnitude of earthquakes in central and eastern Fennoscandia, and thus no relations between deformation zone trends and earthquake magnitude can be found. We emphasize that magnitudes used in this study are those provided by the different seismological agencies for FENCAT and they have to be homogenized prior to hazard calculations. In addition, possible systematic magnitude differences between historical and instrumental data should be evaluated.

It is reasonable that earthquakes were on average better recorded in the instrumental than the non-instrumental era. In the semi-instrumental period, however, the instrumental observations may be of poorer quality than macroseismic ones, in areas where the detection threshold and location accuracy of existing seismograph networks were low. In Finland, the 1930's were covered quite well by macroseismic observations, while the data quantity and quality in the semi-instrumental era in the 1960's were rather poor and inconsistent. The data quality of two historical earthquakes that occurred close together in time in the distant past may differ significantly, and every one of them should be subjected to an individual assessment in order to understand the associated uncertainties.

In historical earthquake data the largest uncertainties of location and magnitude are sometimes associated with the strongest earthquakes whose areas of perceptibility extended to several countries. An example is the Lurøy, Norway earthquake of the 31 August 1819. The felt observations were compiled by Ehrenheim (1824) and Kjellén (1903) for Sweden, and Musketov and Orlov (1893) for Russia, and sometimes the epicenter was subsequently taken to be located in these countries.

Macroseismic maps displaying the whole area of perceptibility were not compiled until Ambraseys (1985) and Muir Wood (1988).

It has been generally noticed that the first efforts to derive parameters, in particular macroseismic magnitudes, tended to overestimate rather than underestimate the value. This has been observed in the study area as well. For instance, Penttilä (1978) assigned a magnitude of 5.2 to the earthquake of 23 June 1882 at the bottom of the Bay of Bothnia. The upgrading is sometimes attributed to colourful details of primary data that received too much weight in intensity assessments. This does not hold true in the study area, where the primary macroseismic data are matter-of-fact and typically concise. The views of contemporary writers about the nature of earthquakes are the part of reports that ages fast, whereas the observations remain usable throughout centuries. Since the first studies, better intensity scales, better ways of assessing intensity on the basis of textual materials, and more rigorous ways of deriving parameters from intensity data points have been developed. An improved understanding of attenuation has emerged (Husebye et al., 1978). Also more seismicity data have accumulated, and they allow calibration of macroseismic magnitudes against instrumental magnitudes.

Earthquake focal mechanisms (Fig. 4.3.3; Table 4.3.1) provide a unique source of information on the stresses acting deep in the crust. It is, however, important to understand their limitations, because each individual fault plane solution may deviate significantly from the regional pattern. In Finland and Sweden, recent focal mechanisms are computed from P wave polarities and P to S wave amplitude ratios (see references in Section 4.3). However, the best-fitting solutions of small earthquakes are seldom unambiguous. This stems from a sparse distribution of input data on the focal sphere and uncertainties in model parameters (e.g. the velocity model used). The well-constrained fault plane solutions of large events may be uncertain by $\pm 10^\circ$ for all source angles (dip, strike, rake), and even larger uncertainties may be associated with solutions of small events. Small earthquakes are also more influenced by local stress conditions than the large, regionally more significant events. In spite of the uncertainties, the available focal mechanism data give a surprisingly consistent view on prevailing stress directions in the study area (Section 4.3).

Neither of the Models 1 and 2 have used the shear zone classification as a prime descriptor. This has resulted structurally very heterogeneous seismic source areas such as 1.13 and 2.11, which include Central Finland, RLSC, Southern Finland and Bothnian Sea rift basin in one seismic source area. It has also resulted in splitting of the Lapland area into several NE-SW striking source areas, 1.2, 1.7, 1.8, 1.11, 1.12, (1.6, 1.12) following the seismicity patterns that mimic the reverse fault patterns. This splitting of the Lapland into several areas may underestimate the importance of the NW-SE striking

deep strike-slip faults stemming from the rift-stage. We can conclude that the rift stages are not well represented in the Models 1, 2 and 3.

The polygons in source models 1-3 (Section 8) are mainly based on instrumental earthquake locations. Also historical earthquake data were used to define Model 1. Due to the brief observation time of earthquake occurrences, little is known about the episodicity of earthquake activity in Fennoscandia. At active plate boundaries, seismicity may migrate over time along major structures (e.g. North Anatolian Fault Zone). The temporal and spatial variation of activity would most likely affect the source area definitions. Also, as argued by Stein and Liu (2009), intraplate earthquake clusters may in fact be long-lived aftershock sequences caused by large earthquakes. It is not appropriate to estimate earthquake recurrence rates using such data.

9.6 Comparison to existing SSA models

A. Korja

The model by Mäntyniemi et al. (1993) has 4 polygons that overlap with our study area (Fig. 9.6.1.). Hanhikivi is situated in a low seismicity area number 5. The model by Mäntyniemi et al (1993) has much larger polygons that incorporate several polygons of Models 1-3. The NE-SW trending of the polygons in the western part of the study area are roughly included in polygons 3 and 4. The high seismicity polygons are included in polygon 3. The high seismicity polygons of Model 1 are included in polygon 6 of Mäntyniemi et al. (1993). The major difference is found at the boundary between the northern high/intermediate seismicity area and low seismicity region in the south. Mäntyniemi emphasizes similarities of seismicity patterns of Kuusamo-Kandalaksa zone to Lapland whereas Model 1 emphasizes the lithotectonic boundary. Models 1 and 3 have several smaller polygons that are incorporated into the larger polygons of the Mäntyniemi et al. (1993) model.

The GSHAP model has six polygons (1-6) that overlap with our study area (Fig. 9.6.2). Hanhikivi is situated in low seismicity source area 6. The fit between the models is rather good. The shapes and trend in both models are similar but Model 1 and 3 have several smaller polygons that are incorporated in the larger polygons of the GSHAP model.

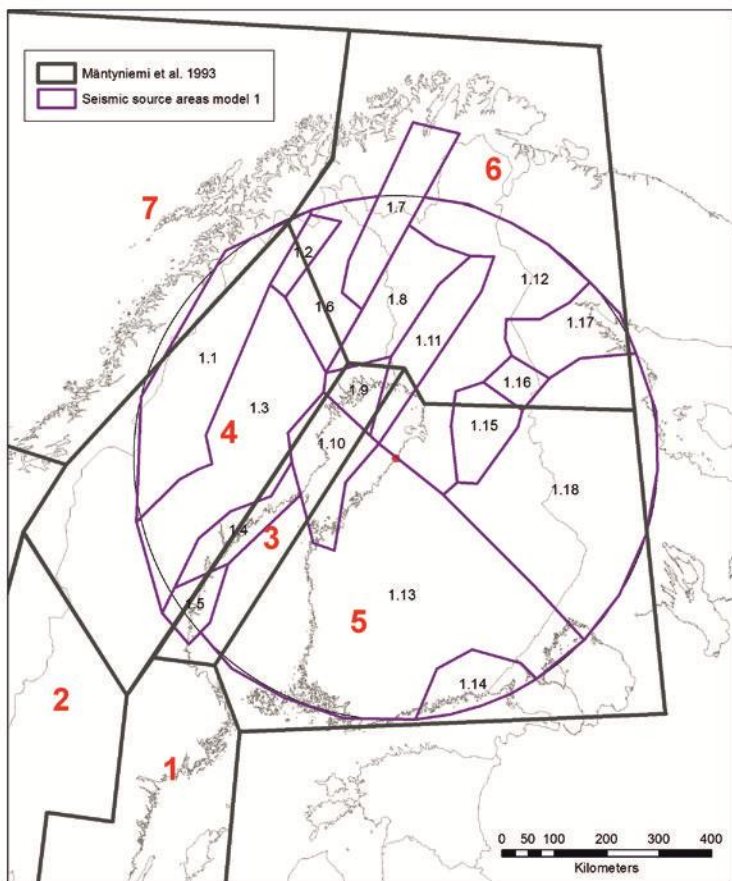


Figure 9.6.1. A comparison of Model 1 and Mäntyniemi et al. (1993) model.

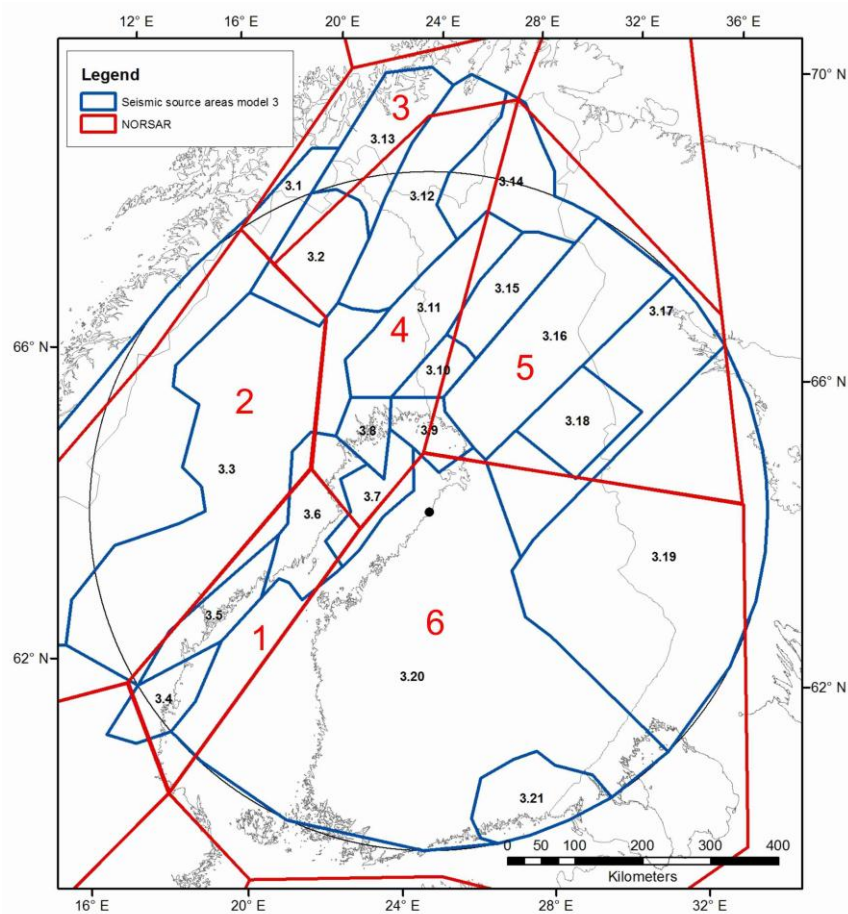


Figure 9.6.2. A comparison of Model 3 and NORSAR A/GSHAP model (Grünthal & the GSHAP Region 3 Working Group, 1999).

The seismic source area model prepared during the EU-project SHARE (Seismic Hazard Harmonization in Europe) includes six polygons (A-G) that overlap our study area (Fig. 9.6.3). Hanhikivi is included in the source area D. The fit between the models is rather good. The shapes and trends in both SHARE model and Models 1-3 are similar, but the latter are more detailed than SHARE model and they contain several additional smaller polygons. SHARE model gives more weight on the Auho-Kandalaksha zone and thus it fits Lapland and the Kuusamo area better than the GSHAP model.

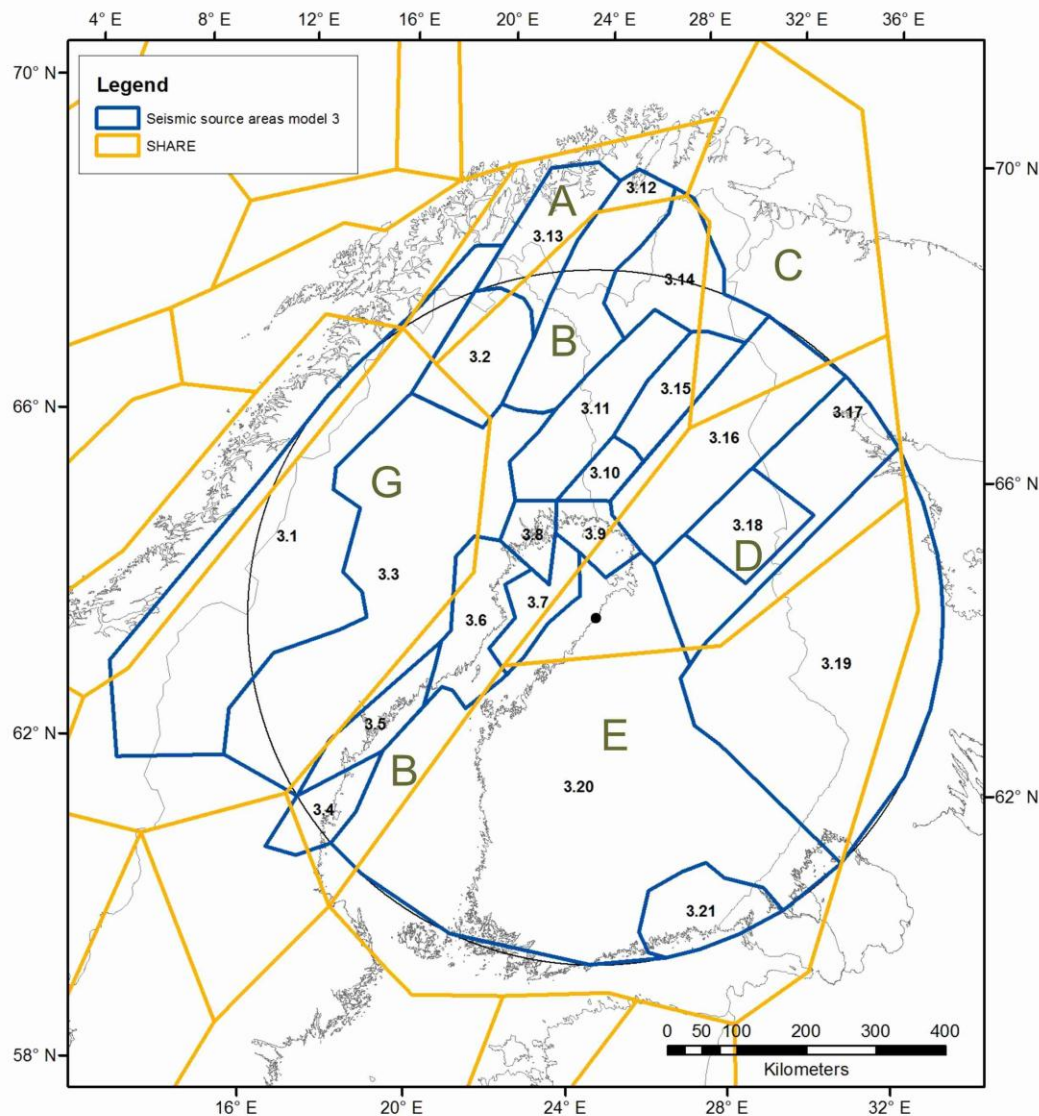


Figure 9.6.3. A comparison of Model 3 and SHARE model (Giardini et al., 2013).

The source area models by Korja et al. (2011a) and Model 1-3 (Fig. 9.6.4) are both displaying a large number of small source areas around the Bay of Bothnia and its surroundings. Major discrepancies are found around Norra Kvarken, Skellefteå area, Raahe-Ladoga shear complex and Hanhikivi area. Two areas (B, K) are trending opposite that to in Model 1-3. The models have only a superficial resemblance pointing out the problems involved in defining small polygons, the large errors and non-

uniqueness.

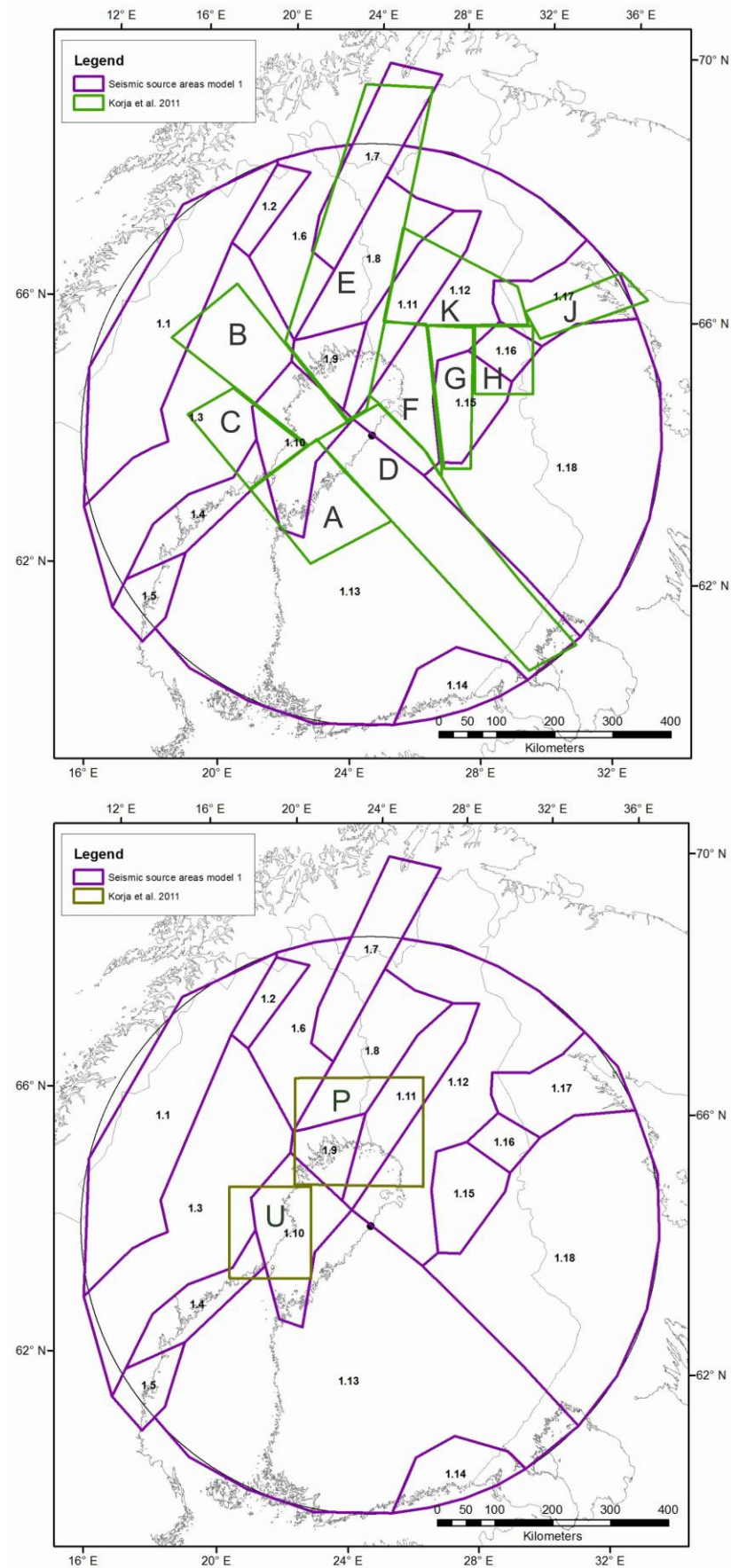


Figure 9.6.4. A comparison of Model 1 and a models by Korja et al. (2011a).

Model 1 resembles most of all Saari et al. (2009) model (Fig. 9.6.5). The Polygons of Model 1 are smaller and more focused on the increased zones of seismicity. The broader shadow zones are classified into the low seismicity areas. The largest discrepancies are found in the Southern Finland low seismicity area, where Saari et al. (2009) have outlined three separate zones and Model 1-3 has no zoning at all. The zoning in Saari et al. (2009) might be an outlier from previous tectonic studies where Raahe-Ladoga shear complex is considered a major tectonic boundary in the Precambrian. It does not seem to be a seismically active area today. Saari et al (2009) emphasize also a major NW-SE trending shear zone Åland to Paldinski (Sottunga-Jurmo shear zone in Fig. 3.1.2.1.) that seem to merge with a major geophysical boundary dividing the East European craton in NW-SE direction. This shear zone falls out of Models 1-3 and thus it has not influenced the seismic source areas in this study.

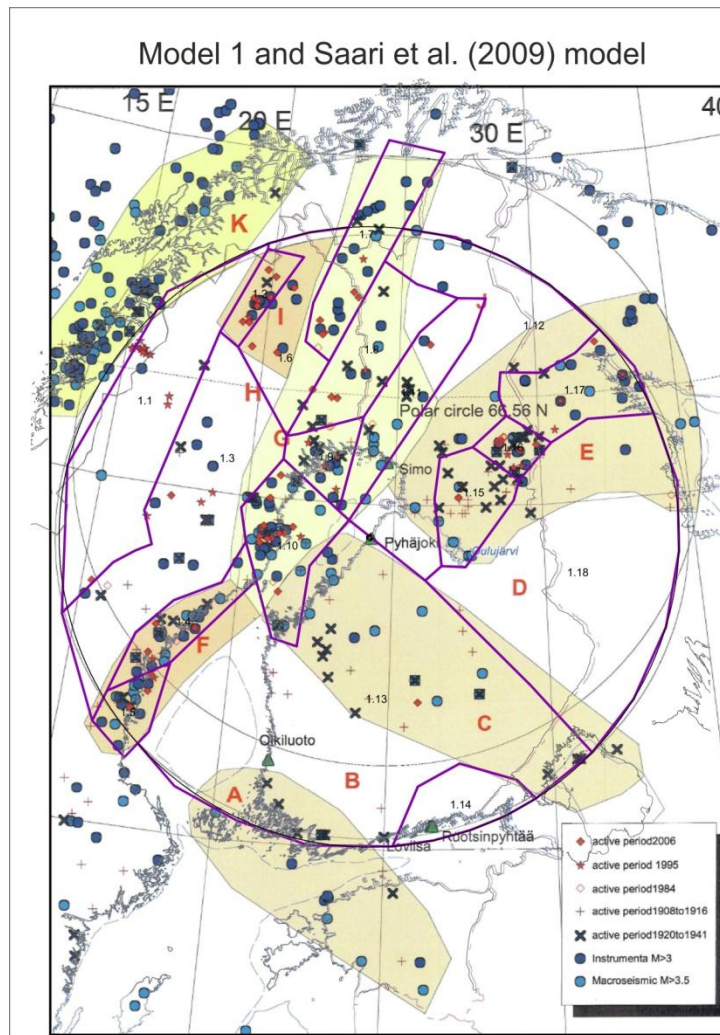


Figure 9.6.5. A comparison of Model 1 and a model by Saari et al. (2009).

The NW-SE striking Raahe-Ladoga shear complex has a complicated fault pattern dominated by steeply dipping to subvertical Proterozoic shear zones at the surface. It can potentially be reactivated as strike slip faults in NW-SE direction with minor amounts of reverse faulting in NE-SW direction

(Fig. 3.1.2.1). The reverse faulting could take place as dip slip faulting on the steep to subvertical faults. The Raahe-Ladoga shear complex is the main structural divider in Finland and it seems to be a seismicity pattern divider as well, yet it does not host many instrumentally detected earthquakes. Within the zone seismicity is subdued with shallow earthquakes. This may be related to the fact that it is mostly located in the thick crust part of Finland. In previous articles dealing with seismicity and tectonics (Talvitie, 1971; Lahtinen et al., 2005; Saari et al., 2009; Korja et al., 2011) the importance of this structural divider has been highlighted, whereas in this paper it has been included in the Central Finland lithotectonic unit and in the low seismicity source areas encompassing Central and southern Finland (1.13, 2.11).

9.7 Comparison to conceptual models

When comparing Model 1 and the conceptual seismogenic model of Redfield and Osmundsen (2013) it is quite clear that the models have much in common (Fig. 9.7.1). The western polygons could be classified as located in the hinterland of Scandes, the high seismicity polygons overlap with the hinterland-break-in-slope and the eastern blocks are located with the craton part. The seismicity zone is located in close proximity to the western boundary of the Bay of Bothnia basin that was active already in the Mesoproterozoic and maybe even earlier. It may well be that the present increased seismicity at the eastern coast of Sweden is linked to an old lithospheric scale weakness zone. The weakness zone may have initiated during the Mesoproterozoic rifting when the western boundary of the Bay of Bothnia basin was formed and it is now reactivated as the the hinterland-break-in slope.

According to Muir Wood (2000), deglaciation dominates the current crustal strain field in many high latitude stable continental regions such as Fennoscandia. His conceptual model predicts the strongest seismicity to take place in the northeast and southwest quadrants of the former fore bulge (Fig. 9.7.2 in pink colour), whereas the quadrants of aseismicity are located in the northwest and southeast (no colour). Muir-Woods conceptual model and Models 1-3 have little in common (Fig. 9.7.2.). The polygons of Model 1 with increased seismic activity in the north are located in both the seismic dome quarter and the aseismic quarter of Muir and Wood's model. The low seismicity polygons are situated in the aseismic quarter. The boundaries do not match well with the Model 1-3 polygon boundaries. Consequently, the Muir-Woods model is not well-supported by Models 1-3.

In Model 1 NE-SW trending polygons have the same direction as the long axes of the GIA anomaly (Fig. 9.7.3). Polygons 1.4, 1.5, 1.11 are along the axes. Also polygons 1.15-1.17 that are associated with the Auho-Kandalaksha fault zone are trending parallel to the GIA ellipsoid. The known PGFs, on the other hand, are not parallel to the isolines of the rebound ellipsoid. The elongation axis of GIA

ellipsoid is parallel to the Norwegian margin and opening of the Atlantic and thus inherited from previous tectonic processes. The direction of the long axes of the ellipsoid is orthogonal to and the short axes parallel to the direction of stress indicators of maximum horizontal stress in Fennoscandia stemming from the opening of the Atlantic.

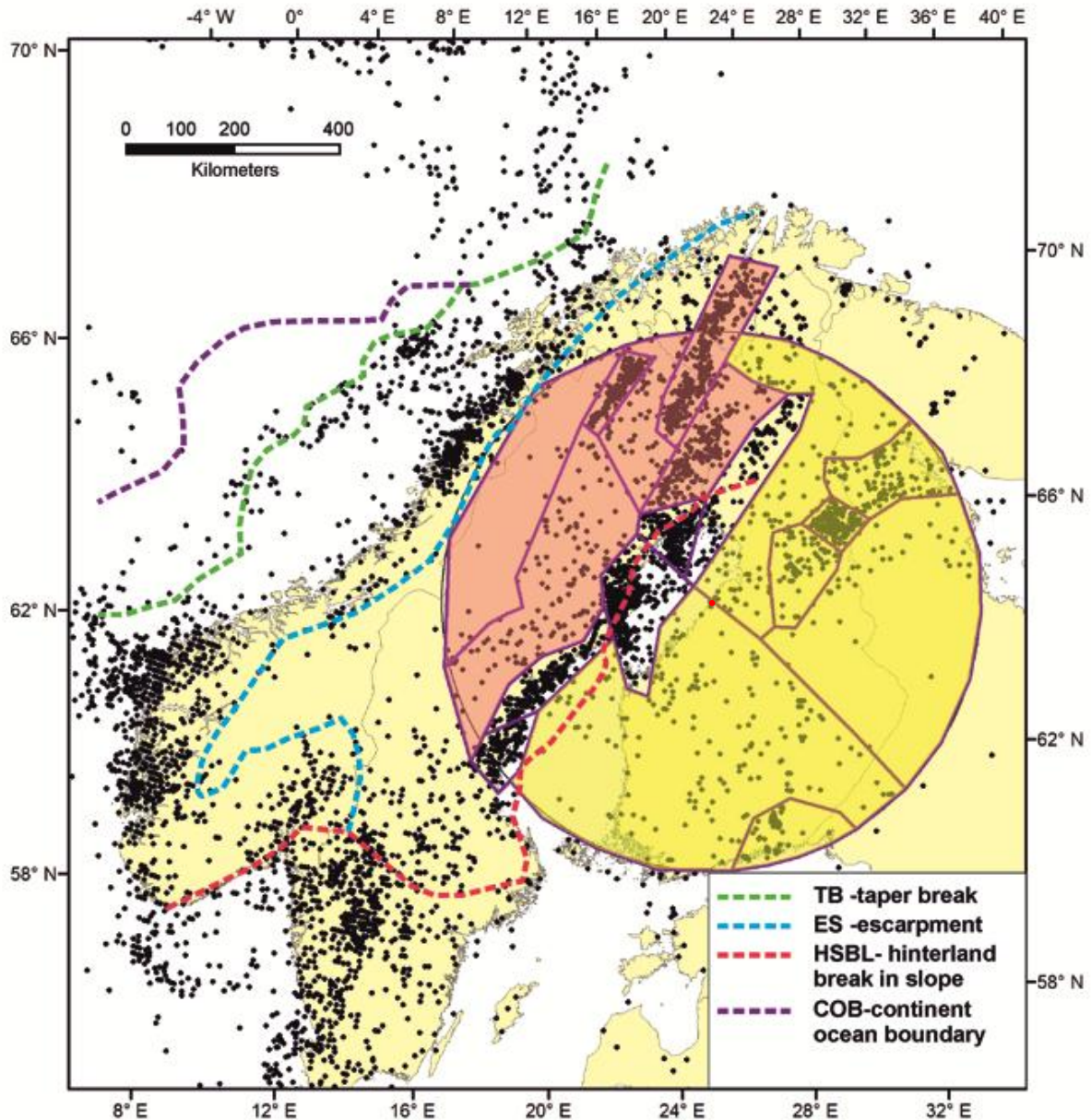


Figure 9.7.1. A comparison of Model 1 and a model by Redfield and Osmundsen (2013).

Plate tectonic forces and ridge push are widely accepted as the first order stress-generating mechanism in Fennoscandia (Slunga, 1991; Hicks et al. 2000b; Fjeldskaar et al., 2000; Böðvarsson et al., 2006; Bungum et al., 2010; Olesen et al., 2013), whereas the relative importance of secondary stress sources, such as erosion, sedimentation, gravitational potential anomalies and post-glacial rebound, remains an open question. According to Böðvarsson et al. (2006), the dominating earthquake mechanism is horizontal movement on sub-vertical structures in a strike-slip regime.

Vertical movement is considered to be less significant than horizontal movement in terms of earthquake generation. Uski et al. (2006) suggested a combination of ridge-push forces and large differences in gravitational potential energy between the Wiborg rapakivi and the surrounding bedrock as the driving mechanism for the swarm type activity in southeastern Finland.

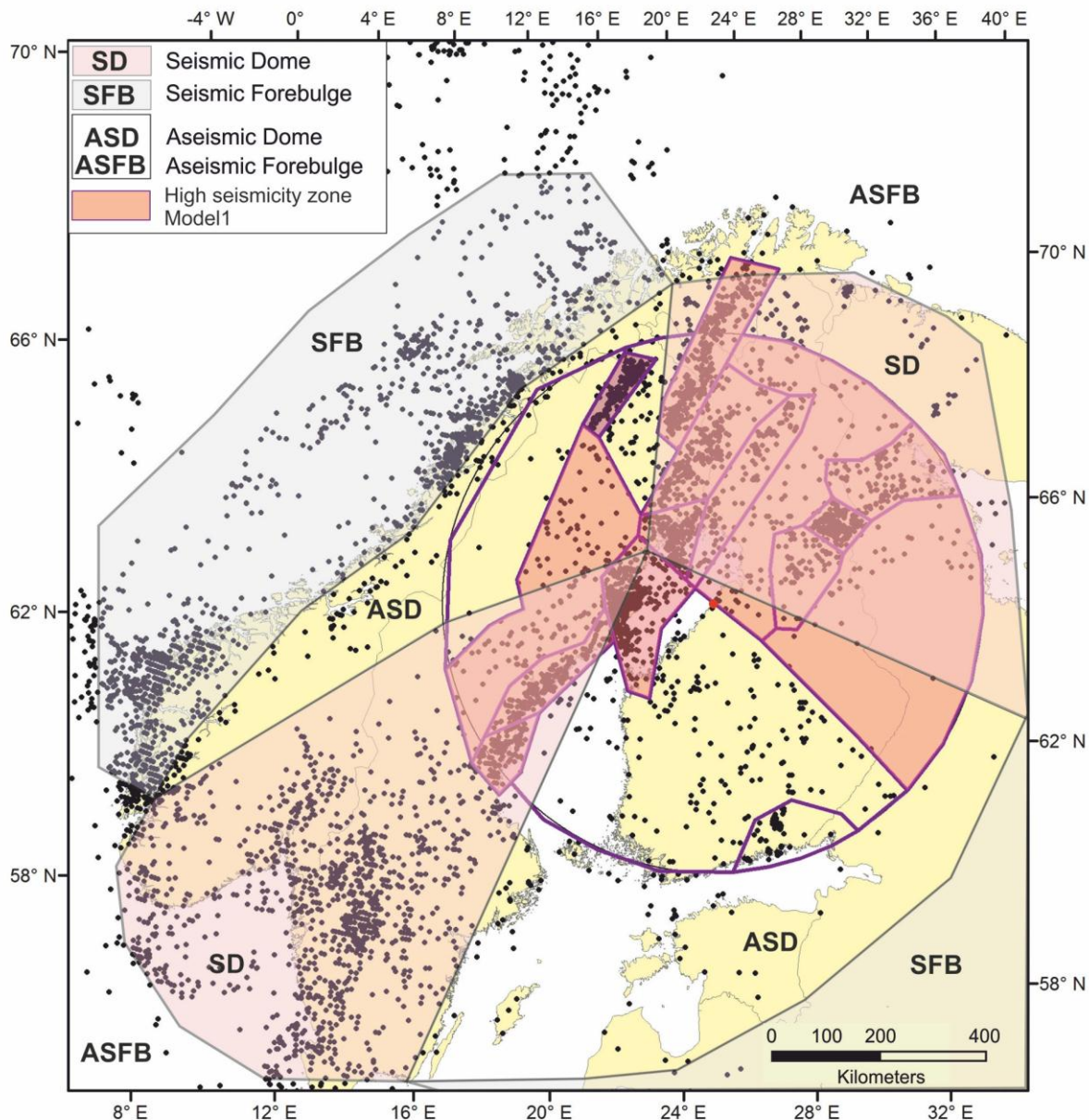


Figure 9.7.2. A comparison of Model 1 and a model by Muir-Wood (2001).

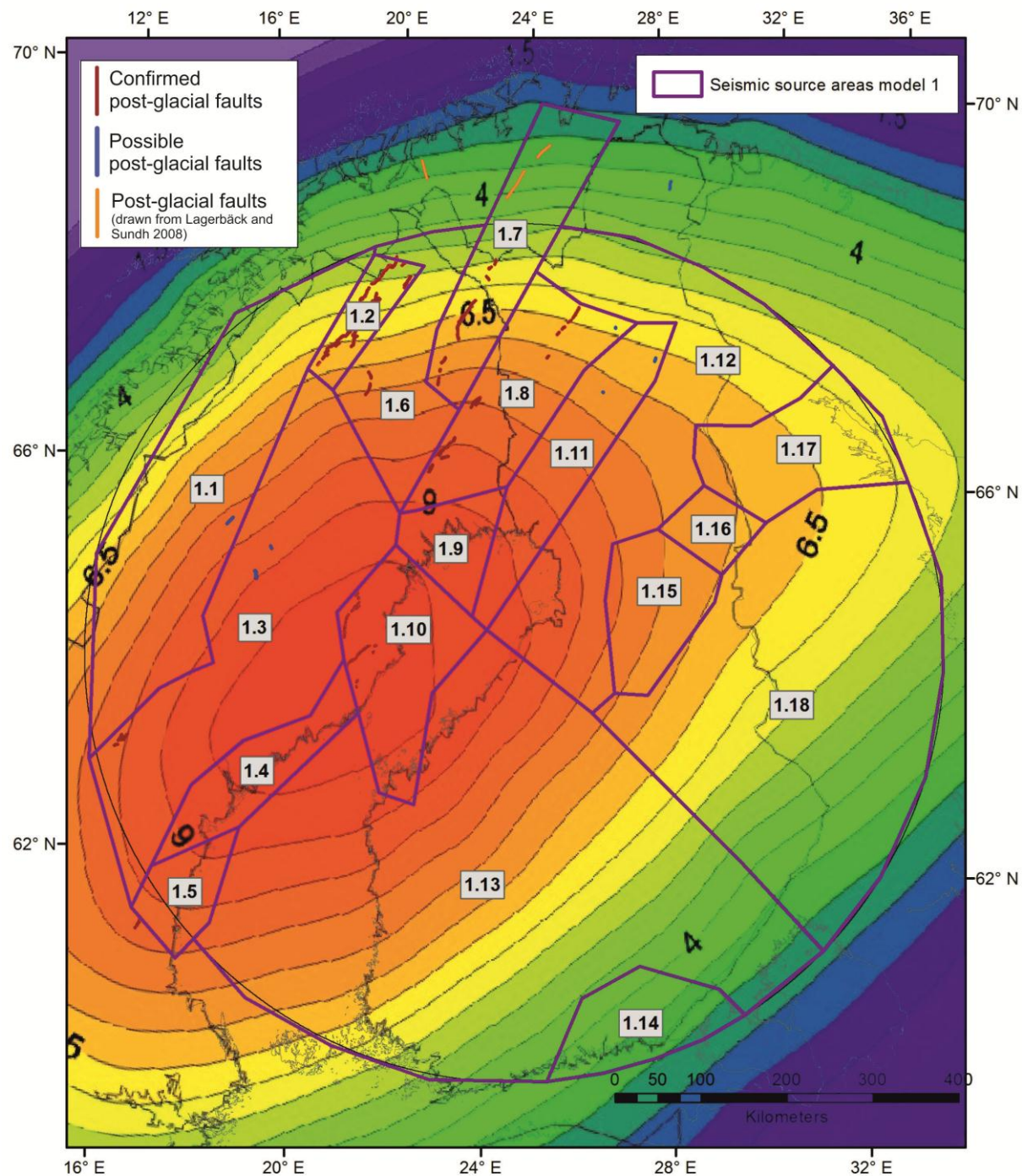


Figure 9.7.3. A comparison of Model 1 and a GIA Uplift model (Fig. 5.3.2. NKG_RF03vel) by Nørbech et al. (2008).

10 Conclusions

A. Korja

The compiled database is digital and upgradable and fulfills the formal database requirements of IAEA. The data and results are accessible for future projects and inspections. Each geological and geophysical dataset is internally of uniform quality over the entire study area. Overlapping data across national borders have been cross-checked and as consequence anomalies along and across the national border zone are easier to interpret. Because the datasets are in a GIS database it is possible directly to compare the data and draw new conclusions.

We conclude that the existing marine acoustic data sets should only be used at regional scale (1: 1M) studies.

The updated seismicity catalogue is more complete and its location precision is better than that of the FENCAT catalogue. We conclude that the new seismic catalogue is well-suited for earthquake studies and hazard estimations, provided that the magnitudes are homogenized prior to the calculations.

Most occurrences of very large (paleo)earthquakes in the study region have been dated to have taken place shortly after the deglaciation, thus belonging to a stress regime different from that of today. It is an open question whether other large (paleo)earthquakes have occurred in the study area more recently.

Lithotectonic unit approach emphasizes the effect of orogenies on the structural development of the terranes and stresses the importance of orogenic folding and faulting as source of structures that can be later reactivated in the current stress field. The classification overlooks the possibility that precollisional rift structures could be inverted and later be reactivated in following orogenies and during the current stress field. The changes in seismicity patterns are not associated with lithotectonic boundaries except at the western boundaries of the Mesoproterozoic units and at Norbotten-Karelia contact.

The seismically active areas are located in areas with thin to normal thickness crust (<50 km). Where the crustal thickness change is trending in NE-SW direction, like in western flank of Bothnian Sea and Auho-Kandalaksha fault zone, the gradient seems to be associated with a zone of increased seismicity.

It is suggested that seismically active Western Lapland fault system is underlain by an inverted rift system which may have inherited its elastic properties from the Paleoproterozoic rifting phase. The

relationships between precollisional inverted rift structures of the lower crust, the Western Lapland fault system and orthogonal PGF faulting should be studied more carefully before any final conclusions. We suggest that the wide range of fault plane solutions documented within the Pärvie Fault could be signaling the movement of a complex thrust system. The implied link between inverted rift structures and the increased seismicity of the Kuusamo area and Hirvaskoski and Auho deformation zones deformation zones could be a topic of further studies.

Earthquakes in the study area are generally small and there are roughly 2 magnitude ≥ 3 events per year. The seismicity in the study area is clustered along NE–SW-trending zones that are parallel to the Norwegian margin and the opening of the Atlantic Ocean along the Mid-Atlantic ridge. Based on a subset of the most recent earthquake data (2000–2012), the majority of the earthquakes (80%) occur in the upper crust down to 17 km in depth, a minority (19%) in the middle crust (17–31 km) and only a few in the lower crust 31–45 km (1%). Our results support the observation by Kaikkonen et al. (2000) that the seismogenic layer stretches to the depths of about 30 km in Finland. We suggest that the middle-lower crustal boundary may add compositional and rheological constraints to the thickness of seismogenic zone in the study area. Furthermore, it is suggested that the upper-middle and middle-lower crustal boundaries that have acted as décollement surfaces in the past, still control the depth extent of fault zones and thus limit the depth extent of present seismicity.

The major source of seismicity is the opening of the Atlantic. Local sources such as post-glacial rebound or local changes in topography or crustal thickness are only secondary sources. The relationship between post-glacial rebound and seismicity patterns is problematic and not easy to solve. First of all, the known PGFs are not parallel to the isolines of the rebound ellipsoid. We note, however, that the zones of increased seismicity in the western flank of the Gulf of Bothnia are parallel and along the long axes of the GIA anomaly (Fig. 5.3.3.). The elongation axis of GIA ellipsoid is parallel to the Norwegian margin and opening of the Atlantic and thus inherited from previous tectonic processes. The direction of the long axes of the ellipsoid is orthogonal to and the short axis is parallel to the maximum horizontal stress in Fennoscandia stemming from the opening of the Atlantic. It seems that plate boundary forces, GIA and seismicity have complex interwoven relationships that should be subjected to futher studied in the future.

The three seismic source area models (Models 1, 2 and 3) are related because: 1) Seismicity is linked to reactivation of old faults in the present stress field. 2) Post-glacial faults are associated with reactivation of old faults. 3) Topography is influenced by the structure and composition of the Precambrian bedrock. 4) The current tectonic stress field might be influenced by the structure of the Precambrian bedrock.

The models are similar in that the majority of the polygons are overlapping in shape and size for the most parts. Some discrepancies are found on the margins. Most of the minor differences between the models are found in the Bay of Bothnia where structural control of neither the Precambrian faults nor the PGFs or bathymetry is optimal and the seismic location accuracy is the poorest.

Although the Models 1-3 have been designed by two different expert groups, they resemble each other. They have many similarities and only minor differences, which adds to the credibility of the models. Because the models are based on a larger amount of additional data, the Models 1-3 are as reliable, if not more, when compared to previous source area models of the area. Although the source area Models 1-3 are more detailed than SHARE - the recently published global scale source area model for EUROPE, they share the same overall geometry in large scale.

The distribution of Model polygon boundaries are aligned with the major tectonic boundaries presented in Redfield and Osmundsen (2013). The western polygons could be classified as located in the hinterland of the Scandes, the high seismicity polygons overlap with the hinterland-break-in-slope and the eastern blocks are located with the craton part. The seismicity zone is located in close proximity to the western boundary of the Bay of Bothnia basin that was active already in the Mesoproterozoic and maybe even earlier.

Acknowledgements:

We are grateful for fruitful discussions during the Fennovoima seismotectonics workshops. The report was greatly improved by the through reviews by the project management group members: Jari Puttonen, Juho Helander and Jouni Saari and the external review group members: David Whipp, Andrej Kijco and Olav Eklund. We also thank Kati Oinonen for her help in drafting the figures and in final editing of the manuscript.

11 References

- Agnew, D.C. & Sieh, K.E., 1978. A documentary study of the felt effects of the great California earthquake of 1857. *Bull Seismol Soc Am* 68(6), 1717–1729.
- Ahjos, T. & Uski, M., 1992. Earthquakes in northern Europe in 1375–1989. *Tectonophysics*, 207, 1–23.
- Airo, M.-L., 1999. Aeromagnetic and petrophysical investigations applied to tectonic analysis in the northern Fennoscandian shield. *Geol. Surv. Finl., Rep. Invest.* 145. 51 pp.
- Airo, M.-L., Leväniemi, H. & Valjus, T., 2011a. Geofysikaalisten aineistojen tulkinta. Geologian tutkimuskeskus, Etelä-Suomen yksikkö, raportti 21.3.2011, 24 s. (Fennovoiman arkistotunnus RE-02-0000092)
- Airo, M.-L., Hautaniemi, H., Korhonen, J. V., Kurimo, M. & Leväniemi, H., 2011b. Airborne geophysical data management and interpretation. In: Nenonen, K. and Nurmi, P. A. (eds.) 2011. *Geoscience for Society : 125th Anniversary Volume*. Geological Survey of Finland, Special Paper 49: 349–358.
- Alanen U., Alvi, K., Hämäläinen J., Kaskela A. & Rantataro J., 2013. Pyhäjoen Hanhikiven edustan merialueen akustis-seismiset tutkimukset 2012. Geologian tutkimuskeskus, tilaustyöraportti 18.1.2013, 13 s. (Fennovoiman arkistotunnus AG-00-0000217)
- Alekseev, M.N., 1996. Possible 'Cromerian Complex' equivalent sequences in the Russian Plain. In: Turner, C. (ed.) *The early Middle Pleistocene in Europe*. 273–277. Balkema, Rotterdam.
- Alm, E., Sundblad, K. & Huhma, H., 2005. Sm-Nd isotope determination of low-temperature fluorite-calcite-galena mineralization in the margins of the Fennoscandian Shield. Swedish Nuclear Fuel and Waste Management Company, SKB Report R-05-66, 68 pp. <http://www.skb.se/publications>.
- Ambraseys, N.N., 1985. The seismicity of western Scandinavia. *Earthquake Engineering Structural Dynamics* 13, 361–399.
- Anderson, E.M., 1951. The dynamics of faulting, Oliver & Boyd, Edinburgh. 206 p.
- Andersson, U.B., 2001. An overview of the geochemical evolution in the Mesoproterozoic (1.58–1.50 Ga) anorogenic complexes of central Sweden. *Zeitschrift für Geologische Wissenschaften* 29, 455–470.
- Andrén, T., Björck, S., Andrén, E., Conley, D., Zillén, L. & Anjar, J., 2011. The Development of the Baltic Sea Basin During the Last 130 ka. In: Harff, J., Björck, S. & Hoth, P. (Eds.) *The Baltic Sea Basin, Central and Eastern European Development Studies (CEEDES)*, Springer-Verlag, Berlin Heidelberg, 75–95.
- Artemieva, I.M., 2009. The continental lithosphere: reconciling thermal, seismic, and petrologic data. *Lithos* 109 (1–2), 23–46.
- Artemieva, I.M. & Thybo, H., 2013. EUNAseis: A seismic model for Moho and crustal structure in Europe, Greenland, and the North Atlantic region. *Tectonophysics*. TECTO-126005 (in press).
- Artemieva, I.M., Thybo, H. & Kaban, M.K., 2006. Deep Europe today: geophysical synthesis of the upper mantle structure and lithospheric processes over 3.5 Ga In: GEE, D. G. & STEPHENSON, R. A. (eds) 2006. *European Lithosphere Dynamics*. Geological Society, London, Memoirs, 32, 11–41.
- Arvidsson, R., 1996. Fennoscandian earthquakes: Whole crustal rupturing related to postglacial rebound. *Science* 274, 744–746.

- Arvidsson, R. & Kulhanek, O., 1994. Seismodynamics of Sweden deduced from earthquake focal mechanisms. *Geophys. J. Int.*, 16, 377–392.
- Arvidsson R. and Grünthal G. and the SHARE Working Group on the Seismic Source Zone Model (2010). D3.1 – Compilation of existing regional and national seismic source zones. 20 p. http://www.share-eu.org/sites/default/files/D3.1_SHARE.pdf
- Assinovskaya, B.A., 1986. Focal mechanisms for earthquakes in the north-eastern part of the Baltic Shield. *Izvestiya, Earth Physics*, Vol. 22, No. 1, 73-75.
- Astakhov, V., 2004. Middle Pleistocene glaciations of the Russian North. *Quaternary Science Reviews* 23, 1285-1311.
- Atakan, K., Lindholm, C.D. & Havskov, J., 1994. Earthquake swarm in Steigen, northern Norway: an unusual example of intraplate seismicity. *Terra Nova* 6, 180-194.
- Axberg, S., 1980. Seismic stratigraphy and bedrock geology of the Bothnian Sea, northern Baltic. *Stockholm Contributions in Geology* 36(3), 153–213.
- BABEL Working Group, 1990. Evidence for Early Proterozoic plate tectonics from seismic reflection profiles in the Baltic Shield. *Nature* 348, 34–38.
- BABEL Working Group, 1993. Integrated seismic studies of the Baltic Shield using data in the Gulf of Bothnia region. *Geophysical Journal International* 112, 305–324.
- Baluev, A.S. 2006. Geodynamics of the Riphean Stage in the Evolution of the Northern Passive Margin of the East European Craton. *Geotectonics* 40, 3, 183–196.
- Bauer, T.E., Skyttä, P., Weihed, P. & Allen, R., 2011. Syn-extensional faulting controlling structural inversion – Insights from the Paleoproterozoic Vargfors syncline, Skellefte mining district, Sweden. *Precambrian Research* 191, 166–183.
- Bergman, S., Kübler, L. & Martinsson, O., 2001. Description of regional geological and geophysical maps of northern Norrbotten county (east of the Caledonian orogen). *Geological Survey of Sweden Ba* 56, 110 pp.
- Bergman, S., Billström, K., Persson, P.-O., Skiöld, T. & Evins, P., 2006. U-Pb age evidence for repeated Palaeoproterozoic metamorphism and deformation near the Pajala shear zone in the northern Fennoscandian shield. *GFF* 128, 7–20.
- Bergman, S., Stephens, M.B., Andersson , J., Kathol, B., & Bergman, T., 2012. Bedrock map of Sweden, scale 1:1 million. *Geological Survey of Sweden K* 423.
- Berthelsen, A. & Marker, M., 1986. 1.9– 1.8 Ga old strike-slip megashears in the Baltic Shield, and their plate tectonic interpretation. *Tectonophysics* 128, 163–181.
- Bingen, B., Andersson, J., Söderlund, U. & Möller, C., 2008. The Mesoproterozoic in the Nordic countries. *Episodes* 31, 29–34.
- Björck, S., 1995. A review of the history of the Baltic Sea, 13.0–8.0 ka BP. *Quaternary International* 27, 19–40.
- Björck, S., 2008. The late Quaternary development of the Baltic Sea basin. In: The BACC Author Team (Eds.) *Assessment of climate change for the Baltic Sea Basin*. Springer-Verlag, Berlin Heidelberg, 398–407.
- Brown, M., 2009. Metamorphic patterns in orogenic systems and the geological record. In: P.A. Cawood & A. Kröner (eds.), *Earth Accretionary Systems in Space and Time*. Geological Society London Special Publications 318, 37–74.
- Brown, D., Spadea, P., Puchkov, V., Alvarez-Marron, J., Herrington, R., Willner, A.P., Hetzel, R., Gorozhanina, Y. & Juhlin, C., 2006. Arc-continent collision in the Southern Urals. *Earth-Sci.Rev.* 79, 261-287.

- Bungum, H. & Fyen, J., 1979. Hypocenter distribution, focal mechanisms, and tectonic implications of Fennoscandian earthquakes, 1954–1978. *Geologiska Föreningens i Stockholm Förhandlingar* 101, 261–273.
- Bungum, H. & Lindholm, C., 1996. Seismo- and neotectonics in Finnmark, Kola and the southern Barents sea: 2. Seismological analysis and seismotectonics. *Tectonophysics* 270, 15–28.
- Bungum, H., Hokland, B.K., Husebye, E.S. & Ringdal, F., 1979. An exceptional intraplate earthquake sequence in Meløy, northern Norway. *Nature*, 280, 32–35.
- Bungum, H., Vaage, S. & Husebye, E., 1982. The Meløy earthquake sequence, northern Norway: source parameters and their scaling relations. *Bull. Seismol. Soc. Am.* 72, 197–206.
- Bungum, H., Olesen, O., Pascal, C., Gibbons, S., Lindholm, C., & Vestøl, O., 2010. To what extent is the present seismicity of Norway driven by post-glacial rebound? *Journal of the Geological Society*, 167, 373–384.
- Byerlee, J.D., 1978. "Friction of rocks". *Pure and Applied Geophysics* 116 (4–5): 615–626.
- Båth, M., 1956. An Earthquake Catalogue for Fennoscandia for the Years 1891–1950. *Sveriges Geologiska Undersökning Ser.C*, No.545, Stockholm, Sweden.
- Böðvarsson, R. & Lund, B., 2003. The SIL seismological data acquisition system - as operated in Iceland and in Swede. In: T. Takanami and G. Kitagawa (eds.), *Methods and Applications of Signal Processing in Seismic Network Operations*, Lecture Notes in Earth Sciences, 98, Springer, Berlin.
- Böðvarsson, R., Lund, L., Roberts, R. & Slunga, R., 2006. Earthquake activity in Sweden. Study in connection with a proposed nuclear waste repository in Forsmark or Oskarshamn. Swedish Nuclear Fuel and Waste Management Company, SKB Report R-06-67, 40 pp. <http://www.skb.se/publications>.
- Cai, J., & Grafarend, E.W., 2007. Statistical analysis of geodetic deformation (strain rate) from the space geodetic measurements of BIFROST Project in Fennoscandia. *J. Geodyn.*, 43, 214–238.
- Cato, I., 1987. On the definitive connection of the Swedish Time Scale with the present. *Sveriges Geologiska Undersökning Ca* 68, 55 pp.
- Cohen K.M. & Gibbard, P., 2011. Global chronostratigraphical correlation table for the last 2.7 million years. Subcommission on Quaternary Stratigraphy (International Commission on Stratigraphy), Cambridge, England.
- Corfu, F. & Evans, P.M., 2002. Late Palaeoproterozoic monazite and titanite U-Pb ages in the Archaean Suomujärvi Complex, N-Finland. *Precambrian Research* 116, 171–181.
- Daly, J.S., Balagansky, V.V., Timmerman, M.J. & Whitehouse, M.J., 2006. The Lapaland-Kola orogen: Palaeoproterozoic collision and accretion of the northern Fennoscandian lithosphere. In: D.G. Gee & R.A. Stephenson (eds.), *European lithosphere Dynamics*. Geological Society London Memoirs 32, 579–598.
- Deutsch, A., Buhl, D. & Langenhorst, F., 1992. On the significance of crater ages: new ages for Dellen (Sweden) and Araguainha (Brazil). *Tectonophysics* 216, 205–218.
- Donner, J., 1995. The Quaternary History of Scandinavia. Cambridge University Press, Cambridge, 200pp
- Downes, G.L., 2004. Procedures and tools used in the investigation of New Zealand's historical earthquakes. *Ann Geophys* 47(2–3), 399–419.
- Drake, H., Tullborg, E.-L. & Page, L., 2009. Distinguished multiple events of fracture mineralization related to far-field orogenic effects in Paleoproterozoic crystalline rocks, Simpevarp area, SE Sweden. *Lithos* 110, 37–49.

- Dypvik, H., Plado, J., Heinberg, C., Håkansson, E., Pesonen, L.J. & Raiskila S., 2008. Impact structures and events – a Nordic perspective. *Episodes* 31(1), 107–114.
- Ehlers J. & Gibbard, P.L., 2011. Quaternary glaciation. In: Singh, V.P., Singh, P. & Haritashya, U.K. (Eds.) *Encyclopedia of Snow, Ice and Glaciers*. Springer: Berlin. 1st edition., 2011, XLVI, 1254 p. 659.
- Ehlers, C., Lindroos, A. & Selonen, O., 1993. The late Svecofennian granite-migmatite zone of southern Finland - a belt of transpressive deformation and granite emplacement. *Precambrian Research* 64, 295-309.
- Ehlers, J., Gibbard, P.L. & Hughes, P.D., 2011. Chapter 1 - Introduction. *Developments in Quaternary Sciences. Quaternary Glaciations - Extent and Chronology. A Closer Look. Volume 15*, Pages 1–14.
- Ehrenheim, V., 1824. Om climaternas rörlighet. Tal hållt vid Praesidii nedläggande uti Kongl. Vetenskaps Akademien. 208 pp. Stockholm.
- Elminen, T., Lohva, J. & Härmä, P., 2008, Ydinvoimalaitoksen mahdollisten sijoituspaikkojen geologiset esiselvitykset, Etelä-Suomen yksikkö, raportti 13.10.2008, 78 s.
- Elo, S., 1991a. Geophysical features indicating deep fractures in the Kuusamo area. *Geol. Surv. Finland, Spec. Paper* 13, 27–37.
- Elo, S., 1991b. Geophysical indications of deep fractures in the Näränkäväära-Syöte and Kandalaksha-Puolanka zones. *Geol. Surv. Finland, Spec. Paper* 13, 43–50.
- Elo, S., 1997. Interpretations of the gravity anomaly map of Finland. In: Pesonen, L. J. (ed.) *The lithosphere in Finland - a geophysical perspective*. *Geophysica* 33 (1), 51-80.
- Elo, S. & Pirttijärvi, M., 2013. The effect of lateral density variations on the state of stress in the uppermost crust in Finland, *International Journal of Rock Mechanics and Mining Sciences*, 63, 131-137.
- Elo, S. & Sipola, V., 2003. Digitaalisten korkeusmallien käytöstä painovoimamittausten käsittelyssä. In: Hyvönen E. & Sandgren E. (Eds.) *Sovelletun geofysiikan XIV neuvottelupäivät*, Rovaniemi, hotelli Pohjanhovi 4. - 5.11.2003 abstraktikokoelma, Vuorimiesyhdistys, Sarja B. 81 pages, in Finnish, ISBN 952-9618-51-4
- Erlström, M. & Sivhed, U., 2001. Intra-cratonic dextral transtension and inversion of the southern Kattegat on the southwest margin of Baltica – Seismostratigraphy and structural development. *Geological Survey of Sweden C 832*, 33 pp.
- Evins, P.M. & Laajoki, K., 2002. Early Proterozoic nappe formation: an example from Sodankylä, Finland, Northern Baltic Shield. *Geological Magazine* 139, 73-87.
- Fejerskov, M. & Lindholm, C.D., 2000. Crustal stress in and around Norway; an evaluation of stress-generating mechanisms. In Nøttvedt. A. (ed.): *Dynamics of the Norwegian margin*, Geological Society, London, Special Publications 167, 451-467.
- Fjeldskaar, W., Lindholm, C., Dehls, JF. & Fjeldskaar, I., 2000. Postglacial uplift, neotectonics and seismicity in Fennoscandia. *Quaternary Science Reviews* 19, 1413-1422.
- Fossen, H., 2010. *Structural Geology*. Cambridge University Press, Cambridge. 463 p.
- Fredén, C. (ed.), 2002. *Berg och jord. Sveriges nationalatlas*. Third edition., 208 pp.
- Gaál, G., 1980. Geological setting and intrusion tectonics of the Kotalahti nickel-copper deposit, Finland. *Bulletin of the Geological Society of Finland* 52, 101-128.
- Gaál, G., 1982. Proterozoic tectonic evolution and late Svecokarelian plate deformation of the Central Baltic Shield. *Geologisch Rundschau* 71, 158–170.

- Gaál, G. & Gorbatschev, R., 1987. An outline of the Precambrian evolution of the Baltic Shield. *Precambrian Research* 35, 15–52.
- Gaál, G., Berthelsen, A., Gorbatschev, R., Kesola, R., Lehtonen, M.I., Marker, M. & Raase, P., 1989. Structure and composition of the Precambrian crust along the POLAR Profile in the northern Baltic Shield. In: Freeman, R., von Knorring, M., Korhonen, H., Lund, C., Mueller, St. (Eds.) *The European Geotraverse, Part 5: The POLAR Profile. Tectonophysics* 162, 1-25.
- Gee, D.G., 1975. A tectonic model for the central part of the Scandinavian Caledonides. *American Journal of Science* 275A, 468–515.
- Gee, D.G., Bogolepova, O.K. & Lorenz, H., 2006. The Timanide, Caledonide and Uralide Orogens in the Eurasian high Arctic, and relationships to the palaeo-continents Laurentia, Baltica and Siberia. In: D. Gee, R. Stephenson (Eds.) *European Lithosphere Dynamics*, Geological Society, London, Memoirs, 32, 507-520.
- Gee, D.G., Juhlin, C., Pascal, C. & Robinson, P., 2010. Collisional Orogeny in the Scandinavian Caledonides (COSC). *Geologiska Föreningens i Stockholm Förhandlingar* 132, 29–44.
- Ghosh, A., Holt, W.E. & Flesch, L.M., 2009. Contribution of gravitational potential energy differences to the global stress field. *Geophys. J. Int.* 179, 787-812.
- Giardini, D., Woessner, J., Danciu, L., Valensise, G., Grünthal, G., Cotton, F., Akkar, S., Basili, R., Stucchi, M., Rovida, A., Stromeyer, D., Arvidsson, R., Meletti, F., Musson, R., Sesetyan, K., Demircioglu, M.B., Crowley, H., Pinho, R., Pitilakis, K., Douglas, J., Fonseca, J., Erdik, M., Campos-Costa, A., Glavatovic, B., Makropoulos, K., Lindholm, C. & Cameelbeeck, T., 2013. Seismic Hazard Harmonization in Europe (SHARE): Online Data Resource, <http://portal.share-eu.org:8080/jetspeed/portal/>, doi: 10.12686/SED-00000001-SHARE, 2013.
- Gibbard, P. & Cohen K.M., 2008. Global chronostratigraphical correlation table for the last 2.7 million years. *Episodes*, 31, No.2, 243-247.
- Gibbard, P. & Head, M.J., 2009. The definition of the Quaternary System/Period and the Pleistocene Series/Epoch. *Quaternaire* 20, 125-133.
- GLOBE Task Team and others (Hastings, David A., Paula K. Dunbar, Gerald M. Elphingstone, Mark Bootz, Hiroshi Murakami, Hiroshi Maruyama, Hiroshi Masaharu, Peter Holland, John Payne, Nevin A. Bryant, Thomas L. Logan, J.-P. Muller, Gunter Schreier & John S. MacDonald), eds., 1999. The Global Land One-kilometer Base Elevation (GLOBE) Digital Elevation Model, Version 1.0. National Oceanic and Atmospheric Administration, National Geophysical Data Center, 325 Broadway, Boulder, Colorado 80305-3328, U.S.A.
- Grad, M., Tiira, T. & ESC Working Group, 2009. The Moho depth map of the European Plate. *Geophys. J. Int.* 176, 279–292.
- Gregersen, S., Korhonen, H. & Husebye, E.S., 1991. Fennoscandian dynamics: Presentday earthquake activity. *Tectonophysics* 189, 333–344.
- Gregersen, S., Wiejacz, P., Dębski, W., Domanski, B., Assinovskaya, B., Guterch, B., Mäntyniemi, P., Nikulin, V.G., Pacesa, A., Puura, V., Aronov, A.G., Aronova, T.I., Grünthal, G., Husebye, E.S. & Sliaupa, S., 2007. The exceptional earthquakes in Kaliningrad district, Russia on September 21, 2004. *Physics of the Earth and Planetary Interiors* 164: 63–74.
- Greiling, R.O., Garfunkel, Z. & Zachrisson, E., 1998. The orogenic wedge in the central Scandinavian Caledonides: Scandian structural evolution and possible influence on the foreland basin. In: Sundquist, B & Stephens, M.B. (eds.), *Tectonics and Geological History of some Phanerozoic Orogens*. GFF 120, 181–190.
- Grünthal, G., (Ed.) 1998. European Macroseismic Scale 1998. *Cahiers du Centre Européen de Géodynamique et de Séismologie* 15, Luxembourg.

- Grünthal, G. & the GSHAP Region 3 Working Group, 1999. Seismic Hazard Assessment for Central, North and Northwest Europe: GSHAP Region 3. Annali di Geofisica 42, 999-1011. <http://www.seismo.ethz.ch/static/gshap/ceurope/report.html>
- Gudmundsson, A., 1999. Postglacial crustal doming, stresses and fracture formation with application to Norway. Tectonophysics 307, 407-419.
- Gölke, M. & Coblenz, D., 1996. Origins of the European regional stress field. Tectonophysics, 266, 11-24.
- Halden, N.M., 1982. Structural, metamorphic and igneous history of migmatites in the deep levels of a wrench fault regime, Savonranta, eastern Finland. Transactions of the Royal Society of Edinburgh: Earth Sciences 73, 17-30.
- Hanski, E., 1997. The Nuttio serpentinite belt, Central Lapland: An example of Paleoproterozoic ophiolitic mantle rocks in Finland. Ofioliti 22, 35-46.
- Hasegawa, H. S., Adams, J. & Yamazaki, K., 1985. Upper Crustal stresses and vertical stress migration in eastern Canada. Journal of Geophysical Research, 90(B5), 3637-3648.
- Haudenschild, U., 1988. K-Ar age determination on biotite and muscovite in the Pihtipudas-lisalmi and Joroinen areas, eastern Finland. In: Korsman, K. (Ed.) Tectono-metamorphic evolution of the Raahe-Ladoga zone. Geological Survey of Finland, Bulletin 343, 33-50.
- Haudenschild, U., 1995. The Vaaraslahti pyroxene granitoid intrusion and its contact aureole: isotope geology. In: Hölttä, P. (Ed.) Relationship of granitoids, structures and metamorphism at the eastern margin of the Central Finland Granitoid Complex. Geological Survey of Finland, Bulletin 382, 81-89.
- Hautaniemi, H., Kurimo, M., Multala, J., Leväniemi, H. & Vironmäki, J., 2005. The "Three In One" aerogeophysical concept of GTK in 2004. In Airo, M.-L. (Ed): Geological Survey of Finland, Special Paper 39, 21-74.
- Heidbach, O., Tingay, M., Barth, A., Reinecker, J., Kurfeß, D. & Müller, B., 2008. The World Stress Map database release 2008. doi:10.1594/GFZ.WSM.Rel2008, 2008. Database last accessed 15th of June 2013 at: <http://www.world-stress-map.org>
- Heinonen, A., 2012. Isotopic evidence for the origin of Proterozoic massif-type anorthosites and their relation to rapakivi granites in southern Finland and northern Brazil. Department of Geosciences and Geography A; no. A18. 44 p.
- Henderson, J., 1991. An estimate of the stress tensor in Sweden using earthquake focal mechanisms. Tectonophysics 192, 231-244.
- Henkel, H. & Pesonen, L.J., 1992. Impact craters and craterform structures in Fennoscandia. Tectonophysics 216, 31-40.
- Hermansson, T., Stephens, M.B., Corfu, F., Page, L.M. & Andersson, J., 2008. Migratory tectonic switching, western Svecofennian orogen, central Sweden: Constraints from U/Pb zircon and titanite geochronology. Precambrian Research 161, 250-278.
- Hicks, E.C., Bungum, H. & Lindholm, C.D., 2000a. Seismic activity, inferred crustal stresses and seismotectonics in the Rana region, Northern Norway. Quaternary Science Reviews 19, 1423-1436.
- Hicks, E.C., Bungum, H. & Lindholm, C.D., 2000b. Stress inversion of earthquake focal mechanism solutions from onshore and offshore Norway. Norsk Geologisk Tidsskrift, 80, pp. 235-250
- Hietanen, A., 1975. Generation of potassium-poor magmas in the northern Sierra Nevada and the Svecofennian of Finland. U.S. Geological Survey Journal of Research 3, 631-645.
- Hirvas, H., 1991. Pleistocene stratigraphy of Finnish Lapland. Geological survey of Finland Bulletin 354, 123pp.

- Hiärne, U.L., 1706. Den korta anledningen, til åthskillige malm och bergarters, mineraliers och jordeslags &c. efterspörjande och angifwande. Del 2: Den beswarade och förklarade anledningens andra flock, om jorden och landskap i gemen. Stockholm, tryckt af Mich. Laurelio, 133–416.
- Husebye, E.S. & Kebeasy, T.R.M., 2004. A re-assessment of the 31st of August 1819 Lurøy earthquake – Not the largest in NW Europe. Norwegian Journal of Geology 84, 57–66.
- Husebye, E.S., Bungum, H., Fyen, J. & Gjøystdal, H., 1978. Earthquake activity in Fennoscandia between 1497 and 1975 and intraplate tectonics. Nor. Geol. Tidsskr. 58, 51–68.
- Hutri, K.-L., Heinsalu, A., Kotilainen, A.T. & Ojala, A.K.E., 2007. Dating early Holocene palaeoseismic event(s) in the Gulf of Bothnia, Baltic Sea. Boreas, 36, 56–64.
- Högdahl, K. & Sjöström, H., 2001. Evidence for 1.82 Ga transpressive shearing in a 1.85 Ga granitoid in central Sweden: implications for the regional evolution. Precambrian Research 105, 37–56.
- Högdahl, K., Sjöström, H., Andersson, U.B. & Ahl, M., 2008. Continental margin magmatism and migmatisation in the west-central Fennoscandian Shield. Lithos 102, 435–459.
- Högdahl, K., Sjöström, H. & Bergman, S., 2009. Ductile shear zones related to crustal shortening and domain boundary evolution in the central Fennoscandian Shield. Tectonics 28 (TC1003, doi:10.1029/2008TC002277), 18 pp.
- Högdahl, K., Majka, J., Sjöström, H., Persson Nilsson K., Claesson, S. & Konecný P., 2011. Reactive monazite and robust zircon growth in diatexites and leucogranites from a hot, slowly cooled orogen: implications for the Palaeoproterozoic tectonic evolution of the central Fennoscandian Shield, Sweden. Contributions to Mineralogy and Petrology, 22 pp.
- Hölttä, P., Väisänen, M., Väänänen, J. & Manninen, T., 2007. Paleoproterozoic metamorphism and deformation in Central Lapland, Finland. In: Ojala, V.J. (Ed.) Gold in the Central Lapland Greenstone Belt, Finland. Geological Survey of Finland, Special Paper 44, 7–56.
- Hölttä, P., Balagansky, V., Garde, A.A., Mertanen, S., Peltonen, P., Slabunov, A., Sorjonen-Ward, P. & Whitehouse, M., 2008. Archaean of Greenland and Fennoscandia. Episodes 31, 13–19.
- International Atomic Energy Agency (IAEA), 2010. Seismic hazards in site evaluation for nuclear installations. Specific safety guide SSG-9, Vienna, 60 pp.
- IOC, IHO & BODC, 2003. Centenary Edition of the GEBCO Digital Atlas, published on CD-ROM on behalf of the Intergovernmental Oceanographic Commission and the International Hydrographic Organization as part of the General Bathymetric Chart of the Oceans, British Oceanographic Data Centre, Liverpool, U.K.
- Jakobsson, M., Björck, S., O'Regan, M., Flodén, T., Greenwood, S.L., Swärd, H., Lif, A., Ampel, L., Koyi, H. & Skelton, A., 2014. Major earthquake at the Pleistocene-Holocene transition in Lake Vättern, southern Sweden. Geology. doi:10.1130/G35499.1
- Janik T., Kozlovskaya, E., Heikkinen, P., Yliniemi, J. & Silvennoinen, H., 2009. Evidence for preservation of crustal root beneath the Proterozoic Lapland-Kola orogen in the northern Fennoscandian shield derived from P- and S- wave velocity models of POLAR and HUKKA wide-angle reflection and refraction profiles and FIRE4 reflection transect. J. Geophys. Res. 114, B06308, doi:10.1029/2008JB005689.
- Johansson, K. & Ransed, G., 2003. Map of the Quaternary deposits 23H Stensele, scale 1:100 000. Sveriges geologiska undersökning, Ak 43.
- Johansson, J.M., Davis, J.L., Scherneck, H.-G., Milne, G.A., Vermeer, M., Mitrovica, J.X., Bennett, R.A., Jonsson, B., Elgered, G., Elósegui, P., Koivula, H., Poutanen, M., Rönnäng, B.O. & Shapiro, I.I., 2002. Continuous GPS measurements of postglacial adjustment in Fennoscandia, 1. Geodetic Results. J. Geophys. Res., Vol. 107, Issue B8, ETG 3-1-ETG 3-27.

- Johannson, P., Lunkka, J.-P. & Sarala, P., 2011. Chapter 9 - The Glaciation of Finland. Developments in Quaternary Sciences. Quaternary Glaciations - Extent and ChronologyA Closer Look. Volume 15, Pages 105–116.
- Jones, A.G., Plomerova, J., Korja, T., Sodoudi, F. & Spakman, W., 2010. Europe from the bottom up : a statistical examination of the central and northern European lithosphere-astenosphere boundary from comparing seismological and electromagnetic observations. *Lithos* 120 (1-2), 14-29.
- Juhlin, C. & Cosma C., 2007. A 3D surface seismic pilot study at Olkiluoto, Finland: Acquisition and processing report. Eurajoki, Finland: Posiva Oy. Working Report 2007-65. 47 p.
- Jules Verne Voyager, 2011. http://jules.unavco.org/Voyager/ILP_GSRM Last accessed 20th of October 2013.
- Kaikkonen, P., Moisio, K. & Heeremans, M., 2000. Thermomechanical lithospheric structure of the central Fennoscandian Shield. *Phys. Earth Planet. Inter.*, 119, 209-235.
- Kathol, B. & Weihed, P. (eds.), 2005. Description of regional geological and geophysical maps of the Skellefte District and surrounding areas. Geological Survey of Sweden Ba 57, 197 pp.
- Kebeasy, T.R.M. & Husebye, E.S., 2003. Revising the 1759 Kattegat earthquake questionnaires using synthetic wavefield analysis. *Physics of the Earth and Planetary Interiors* 139, 269-284. Keefer, D.K., 2002. Investigating landslides caused by earthquakes - A historical review. *Surveys in Geophysics* 23, 473-510.
- Kjellén, R., 1903. Meddelanden om jordstötar i Sverige före 1846. *Geologiska Föreningens i Stockholm Förhandlingar* 25, pp. 129–170, 191–228.
- Kijko, A., Skordas, E., Wahlström, R. & Mäntyniemi, P., 1993. Maximum likelihood estimation of seismic hazard for Sweden. *Natural Hazards* 7: 41–57.
- Kim, W.-Y., Kulhánek, O., van Eck, T. & Wahlström, R., 1985. The Solberg, Sweden, Earthquake of September 29, 1983. Report No.1-85, Seismological Department, University of Uppsala, Sweden, ISSN 0280-3070
- Kohonen, J., 1995. From continental rifting to collisional shortening - Paleoproterozoic Kaleva metasediments of the Höytäinen area in North Karelia, Finland. Geological Survey of Finland, Bulletin 380, 79 pp.
- Kohonen, J. & Rämö, O.T., 2005. Sedimentary rocks, diabases, and late cratonic evolution. In: Lehtinen, M., Nurmi, P. and Rämö, T. (Eds.) *The Precambrian Bedrock of Finland - Key to the evolution of the Fennoscandian Shield*. Elsevier Science B.V, 563-604.
- Koistinen, T., 1981. Structural evolution of an early Proterozoic strata-bound Cu-Co-Zn deposit, Outokumpu, Finland. *Transactions of the Royal Society of Edinburgh, Earth Sciences* 72, 115-158.
- Koistinen, T. (Ed.) 1994. Precambrian basement of the Gulf of Finland and surrounding area 1 : 1 000 000. Geological Survey of Finland.
- Koistinen, T., Stephens, M.B., Bogatchev, V., Nordgulen, Ø., Wennerström, M. & Korhonen, J., 2001. Geological map of the Fennoscandian Shield, scale 1 : 2 000 000. Geological Surveys of Finland, Norway and Sweden and the North-West Department of Natural Resources of Russia.
- Korhonen, J. V., Aaro, S., All, T., Elo, S., Haller, L. Å., Kääriäinen, J., Kulinich, A., Skilbrei, J. R., Solheim, D., Säävuori, H., Vaher, R., Zhdanova, L. & Koistinen, T., 2002a. Bouguer anomaly map of the Fennoscandian Shield: IGSN 71 gravity system, GRS80 normal gravity formula. Bouguer density 2670 kg/m³, terrain correction applied. Anomaly continued upwards to 500 m above ground: scale 1:2 000 000.

- Korhonen, J.V., Aaro, S., All, T., Nevanlinna, H., Skilbrei, J. R., Säävuori, H., Vaher, R., Zhdanova, L. & Koistinen, T., 2002b. Magnetic anomaly map of the Fennoscandian Shield: DGRF-65 anomaly of total field. Anomaly continued upwards to 500 m above ground: scale 1:2 000 000.
- Korja, A. & Heikkinen, P.J., 1995. Proterozoic extensional tectonics of the central Fennoscandian Shield: Results from the Baltic and Bothnian Echoes from the Lithosphere experiment. *Tectonics* 14, 504-517.
- Korja, A. & Heikkinen, P.J., 2005. The accretionary Svecfennian orogen – Insight from the BABEL profiles. *Precambrian Research* 136, 241–268.
- Korja, A. & Heikkinen, P.J., 2008. Seismic images of Paleoproterozoic microplate boundaries in the Fennoscandian Shield. In: K.C. Condie & V. Pease (eds.), When did plate tectonics begin on planet Earth? Geological Society of America Special Paper 440, 220–248.
- Korja, A., Korja, T., Luosto, U. & Heikkinen, P., 1993. Seismic and geoelectric evidence for collisional and extensional events in the Fennoscandian Shield - implications for Precambrian crustal evolution. *Tectonophysics* 219, 129-152.
- Korja, A., Heikkinen, P. & Aaro, S., 2001. Crustal structure of the northern Baltic Sea palaeorift. *Tectonophysics* 331, 341-358.
- Korja, A., Lahtinen, R., Heikkinen, P., Kukkonen, I.T. & FIRE Working Group, 2006a. A geological interpretation of the upper crust along FIRE 1. In: Kukkonen, I.T. & Lahtinen, R., (Eds.) Finnish Reflection Experiment FIRE 2001-2005. Geological Survey of Finland, Special Paper 43, 45-76.
- Korja, A., Lahtinen, R. & Nironen, M., 2006b. The Svecfennian Orogen: a collage of microcontinents and island arcs. In: D. Gee, R. Stephenson (Eds.) European Lithosphere Dynamics, Geological Society, London, Memoirs, 32, 561-578.
- Korja, A., Kosunen, P. & Heikkinen, P., 2009. A case study of lateral spreading: the Precambrian Svecfennian Orogen. Geological Society, London, Special Publications 321, 225-251.
- Korja, A., Kortström, J., Lindblom, P., Mäntyniemi, P., Uski, M. & Valtonen, O., 2011. Seismisten aineistojen kerääminen ja tulkinta Pyhäjoen alueelta. Tilaustutkimuksen raportti, Seismologian instituutti, HY. 64 p.
- Korsman, K. & Glebovitsky, V. (eds.) 1999. Raahe-Ladoga Zone structure-lithology, metamorphism and metallogeny : a Finnish-Russian cooperation project 1996-1999. Map 2: Metamorphism of the Raahe-Ladoga Zone 1:1 000 000. Espoo: Geological Survey of Finland.
- Korsman, K., Hölttä, P., Hautala, T. & Wasenius, P., 1984. Metamorphism as indicator of evolution and structure of the crust in Eastern Finland. Geological Survey of Finland, Bulletin 328, 40 pp.
- Korsman, K., Koistinen, T., Kohonen, J., Wennerström, M., Ekdahl, E., Honkamo, M., Idman, H. & Pekkala, Y. (Eds.), 1997. Suomen kallioperäkartta– Berggrundskarta över Finland – Bedrock map of Finland 1:1 000 000. Geological Survey of Finland, Espoo, Finland.
- Korsman, K., Korja, T., Pajunen, M., Virransalo, P. & GGT/SVEKA Working Group, 1999. The GGT/SVEKA Transect: structure and evolution of the continental crust in the Palaeoproterozoic Svecfennian orogen in Finland, *International Geology Review*, 41, 287-333.
- Kortström, J., Lindblom, P. & Korja, A., 2011. Seismiset asemat TOF ja OUF, Raportti T-83, Seismologian Instituutti, Helsingin Yliopisto, Helsinki, 15 s.
- Kortström, J., Uski, M., Tiira, T. & Korja, A., 2012. Data processing and analysis system for the Pyhäjoki seismic network, Report T-86, Institute of Seismology, University of Helsinki. 15 pp.
- Koskinen, P., 2013. Orientation of faults and their potential for reactivation in the present stress field in Finland. M.Sc. thesis, University of Helsinki, Finland.
- Koskinen, P. and Korja, A. 2014. Orientation of faults in the present stress field – Work Report. Institute of Seismology, University of Helsinki, Report S-60, pp. 24.

- Kotilainen, A. & Hutri, K-L., 2004. Submarine Holocene sedimentary disturbances in the Olkiluoto area of the Gulf of Bothnia, Baltic Sea: a case of postglacial palaeoseismicity. *Quaternary Science Reviews*, 23, pp. 1125-1135.
- Kousa, J. & Lundqvist, Th., 2000. Svecofennian Domain. In: Lundqvist, Th., Autio, S. (Eds.) *Description to the Bedrock Map of Central Fennoscandia (Mid-Norden)*. Geological Survey of Finland, Special Paper 28, 47-75.
- Kreemer, C., Holt, W.E. & Haines, A.J., 2003. An integrated global model of present-day plate motions and plate boundary deformation. *Geophys. J. Int.*, 154, 8-34. Updates on the model at: <<http://gsrm.unavco.org/>>
- Kresten, P., Åhman, E. & Brunfelt, A.O., 1981. Alkaline ultramafic lamprophyres and associated carbonatite dykes from the Kalix area, northern Sweden. *Geologische Rundschau* 70, 1215–1231.
- Kresten, P., Rex, D.C. & Guise P.G., 1997. ^{40}Ar - ^{39}Ar ages of ultramafic lamprophyres from the Kalix area, northern Sweden. In Th. Lundqvist (ed.): *Radiometric dating results 3*. Geological Survey of Sweden C 830, 14–19.
- Krogh, T.E., Mysen, B.O. & Davis, G.L., 1974. A Palaeozoic age for the primary minerals of a Norwegian eclogite. *Carnegie Institute Washington Yearbook* 73, 575–576.
- Kuivämäki, A., 1986. Havaintoja Venejärven ja Ruostejärven postglasialisista siiroksista. (In Finnish). Abstract: Observations of the Venejärvi and Ruostejärvi postglacial faults. Geol. Surv. Finland, Nuclear Waste Disposal Research Report YST-52. 20 pp.
- Kuivämäki, A., Vuorela, P. & Paananen, M., 1998. Indications of postglacial and recent bedrock movements in Finland and Russian Karelia. Geol. Surv. Finland, Nuclear Waste Disposal Research Report YST-99. 92 pp.
- Kuivämäki, A., Paananen, M. & Vuorela, P. 2001. Postglacial faults and bedrock movements in Finland. Final report of investigations in 1987-2001. Geological Survey of Finland, Espoo.
- Kuivämäki, A., Wennerström, M., Vaarma, M., Härmä, P., Nyholm, T. & Turunen, T., 2011. Simon Karsikon ja Pyhäjoen Hanhikiven mahdolisilla ydinvoimalan sijoitusalueilla ja niiden ympäristössä mahdollisesti tapahtuneiden nuorten (postglasialisten) kallioliikuntojen selvittäminen. Vaihe I – kallioperäaineistojen kokoaminen, tulkinta ja analysointi. Geologian tutkimuskeskus, Etelä-Suomen yksikkö, raportti 31.3.2011, 41 s. (Fennovoiman arkistotunnus RE-02-0000093)
- Kujansuu, R., 1964. Nuorista siirroksista Lapissa. (Summary: Recent Faulting in Lapland). *Geologi* 16, 30–36.
- Kujansuu, R., 1972. On landslides in Finland Lapland. *Geological Survey of Finland, Bulletin* 256, 1-22.
- Kukkonen, I., 2011. Yhteenvetoraportti postglasialisten siirrosten selvityksistä Simon Karsikon ja Pyhäjoen Hanhikiven mahdolisilla ydinvoimalan sijoitusalueilla. Geologian tutkimuskeskus, Etelä-Suomen yksikkö, raportti 24.5.2011, 13 s. (Fennovoiman arkistotunnus RE-02-0000098)
- Kukkonen, I.T. & Peltonen, P., 1999. Xenolith-controlled geotherm for the central Fennoscandian Shield: implications for lithosphere-asthenosphere relations. *Tectonophysics*, 304, 301-315.
- Kukkonen, I.T. & Lahtinen, R., (Eds.) 2006. *Finnish Reflection Experiment FIRE 2001-2005*. Geological Survey of Finland, Special Paper 43, 247 pp.
- Kukkonen, I.T., Heikkinen, P., Ekdahl, E., Hjelt, S.-E., Yliniemi, J., Jalkanen, E. & FIRE Working Group, 2006. Acquisition and geophysical characteristics of reflection seismic data on FIRE transects, Fennoscandian Shield. In: Kukkonen IT, Lahtinen R (eds) *Finnish Reflection Experiment FIRE 2001-2005*. Geological Survey of Finland, Special Paper 43, 13-43.
- Kukkonen, I.T., Olesen, O. & Ask, M.V.S., 2010. Postglacial faults in Fennoscandia: targets for scientific drilling. *GFF* 132 (1), 71-81.

- Kukkonen, I.T., Ask, M.V.S. & Olesen, O., 2011a. Postglacial Fault Drilling in Northern Europe: Workshop in Skokloster, Sweden. *Scientific Drilling* No. 11, 56-59.
- Kukkonen, I. T., Heikkinen, P., Heinonen, S., Laitinen, J. & HIRE Working Group of the Geological Survey of Finland, 2011b. Reflection seismics in exploration for mineral deposits: initial results from the HIRE project. *Geological Survey of Finland, Special Paper* 49, 49–58.
- Kulling, O., 1972. The Swedish Caledonides. In: Strand, T. & Kulling, O. (Eds.), *Scandinavian Caledonides*.
- Kärki, A. & Laajoki K., 1995. An interlinked system of folds and ductile shear zones – late stage Svecokarelian deformation in the central Fennoscandian Shield, Finland. *Journal of Structural Geology* 17, 9, 1233-1247.
- Kärki, A., Laajoki, K. & Luukas, J., 1993. Major Palaeoproterozoic shear zones of the central Fennoscandian Shield. *Precambrian Research* 64, 207–223.
- Kärki, A., Korja, T., Mahmoud, M., Pirttijärvi, M., Tirronniemi, J., Tuisku, P. & Woodard, J., 2012. Structure of the Raahe–Ladoga Shear Complex. *Lithosphere* 2012 – Seventh symposium on the structure, composition and evolution of the lithosphere in Finland. Geological Survey of Finland, Espoo, November 6-8, 2012, Programme and extended abstracts. Institute of Seismology, University of Helsinki, Report S-56, 55-58.
- Kärkkäinen, N. & Lohva, J., 2008. Ydinvoimalaitoksen mahdollisten sijoituspaikkojen kallioperän malmipotentiaaliselvitys, Etelä-Suomen yksikkö, rapportti 16.12.2008, 58 s.
- Laajoki, K., 2005. Karelian supracrustal rocks. In: Lehtinen, M., Nurmi, P.A., Rämö, O.T. (Eds.) *Precambrian Geology of Finland – Key to the Evolution of the Fennoscandian Shield*. Elsevier B.V., Amsterdam, 279-342.
- Lagerbäck, R., 1979. Neotectonic structures in northern Sweden. *Geologiska Föreningens i Stockholm Förhandlingar* 100, 263–269.
- Lagerbäck, R., 1988. The Veiki moraines in northern Sweden - widespread evidence of an Early Weichselian deglaciation. *Boreas* 17, 469-486.
- Lagerbäck, R., 1990. Late Quaternary faulting and paleoseismicity in northern Fennoscandia, with particular reference to the Lansjärvi area, northern Sweden. *Geologiska Föreningens i Stockholm Förhandlingar* 112, 333–354.
- Lagerbäck, R. & Henkel, H., 1977. Studier av neotektonisk aktivitet i mellersta och norra Sverige, flygbildsgenomgång och geofysisk tolkning av recenta förkastningar (with a short English summary). KBS Teknisk Rapport 19, Kärnbränslesäkerhet, Stockholm, 35 pp.
- Lagerbäck, R. & Witschard, F., 1983. Neotectonics in Northern Sweden – geological investigations. SKBF/KBS Technical Report 83-58. Svensk Kärnbränslehantering AB, Stockholm, 58 pp.
- Lagerbäck, R. & Sundh, M., 2003. Searching for evidence of late- or postglacial faulting in the Forsmark region. Results from 2002. SKB P-03-76, Svensk Kärnbränslehantering AB.
- Lagerbäck, R. & Sundh, M., 2008. Early Holocene faulting and paleoseismicity in northern Sweden. *Geological Survey of Sweden C* 836, 80 pp.
- Lagerbäck, R., Sundh, M. & Johansson, H., 2004a. Searching for evidence of late- or postglacial faulting in the Forsmark region. Results from 2003. SKB P-04-123, Svensk Kärnbränslehantering AB.
- Lagerbäck, R., Sundh, M. & Svedlund, J.-O., 2004b. Searching for evidence of late- or postglacial faulting in the Oskarshamn region. Results from 2003. SKB P-04-192, Svensk Kärnbränslehantering AB.

- Lagerbäck, R., Sundh, M., Svedlund, J.-O. & Johansson, H., 2005a. Searching for evidence of late- or postglacial faulting in the Forsmark region. Results from 2002-4. SKB R-05-51, Svensk Kärnbränslehantering AB.
- Lagerbäck, R., Sundh, M., Svantesson, S.-I. & Svedlund, J.-O., 2005b. Searching for evidence of late- or postglacial faulting in the Forsmark region. Results from 2004. SKB P-05-232, Svensk Kärnbränslehantering AB.
- Lagerbäck, R., Sundh, M. & Svantesson, S.-I., 2006. Searching for evidence of late- or postglacial faulting in the Oskarshamn region. Results from 2005. SKB P-06-160, Svensk Kärnbränslehantering AB.
- Lahtinen, R., Korja, A. & Nironen, M., 2005. Paleoproterozoic tectonic evolution. In: M. Lehtinen, P.A. Nurmi & O.T. Rämö (eds.), *Precambrian Geology of Finland – Key to the Evolution of the Fennoscandian Shield*. Elsevier B.V., Amsterdam, 481–532.
- Lahtinen, R., Garde, A.A. & Melezhik, V.A., 2008. Paleoproterozoic evolution of Fennoscandia and Greenland. *Episodes* 31, 20–28.
- Lamontagne, M. & Ranalli, G., 1996. Thermal and rheological constraints on the earthquake depth distribution in the Charlevoix, Canada, intraplate seismic zone. *Tectonophysics* 257, 55-69.
- Lehtinen, M., 1976. Lake Lappajärvi, a meteorite impact site in western Finland. Geological Survey of Finland, Bulletin 282, 92 pp.
- Lehtonen, M., Airo, M.-L., Eilu, P., Hanski, E., Kortelainen, V., Lanne, E., Manninen, T., Rastas, P., Räsänen, J. & Virransalo, P., 1998. Kittilän vihreäkivialueen geologia. Lapin vulkaniittiprojektiin rapportti. Summary: The stratigraphy, petrology and geochemistry of the Kittilä greenstone area, northern Finland. A report of the Lapland Volcanite Project. Geological Survey of Finland, Report of Investigation 140, 144 p.
- Lehtovaara, J., 1976. Apatite fission track dating of Finnish Precambrian intrusives. *Annales Academiae Scientiarum Fennicae. Series A III, Geologica – Geographica* 117., 94 pp.
- Lindblom, E. & Lund, B., 2011. Focal mechanisms and the state of stress along the Pärvie end-glacial fault, northern Sweden. In: Lindblom, E. *Microearthquake Study of End-glacial Faults in Northern Sweden*. Phil.lic thesis in seismology, University of Uppsala, Sweden.
- Lindblom, E., Lund, B., Tryggvason, A., Uski, M., Juhlin, C., Böövarsson, R. & Roberts, R., 2011. Microearthquake activity on the Pärvie end-glacial fault, northern Sweden. In: Lindblom, E. *Microearthquake Study of End-glacial Faults in Northern Sweden*. Phil.lic thesis in seismology, University of Uppsala, Sweden.
- Lidberg, M., Johansson, J.M., Scherneck, H.-G. & Milned, G.A., 2010. Recent results based on continuous GPS observations of the GIA process in Fennoscandia from BIFROST. *Journal of Geodynamics* 50, 8–18. ISSN 0264-3707, DOI: 10.1016/j.jog.2009.11.010.
- Lindström, M., Schmitz, B., Sturkell, E. & Ormö, J., 2008. 33rd IGC excursion guide "Paleozoic Impact Craters", 54 pp.
- Lisiecki, L.E. & Raymo, M.E., 2005. A Plio-Pleistocene Stack of 57 Globally Distributed Benthic $\delta^{18}\text{O}$ Records. *Paleoceanography* 20, PA1003, 17 pp.
- Litt, T., Behre, K.-E., Meyer, K.-D., Stephan, H.J. & Wansa, S., 2007. Stratigraphische Begriffe für das Quartär des norddeutschen Vereisungsgebietes. *Eiszeitalter und Gegenwart* 56 (1/2), 7. 7-65.
- Lukashov, A.D., 1995. Paleoseismotectonics in the northern part of Lake Onega (Zaonezhkij Peninsula, Russian Karelia). Geological Survey of Finland, Nuclear Waste Disposal Research, Report YST-90. 36 pp.
- Lund, B., 2005. Effects of Deglaciation on the Crustal Stress Field and Implications for Endglacial Faulting: A Parametric Study of Simple Earth and Ice Models. Swedish Nuclear Fuel and Waste Management Co., Stockholm. Technical Report TR-05-04, 68 pp.

- Lund, B., Schmidt, P. & Hieronymus, C., 2009. Stress evolution and fault stability during the Weichselian glacial cycle. Tech. Rep. TR-09-15, Swedish Nuclear Fuel and Waste Management Co. (SKB), Stockholm, Sweden. 106 p.
- Lundqvist, J., 1958. Studies of the Quaternary History and Deposits of Värmland, Sweden. Sveriges Geologiska Undersökning, Ser. C. 559, 57 pp.
- Lundqvist, J., 1992. Glacial stratigraphy in Sweden. Geological Survey of Finland, Special Paper 15, 43–59
- Lundqvist, J., 2004. Glacial history of Sweden. Developments in Quaternary Sciences. Quaternary Glaciations- Extent and Chronology — Part I: Europe. Vol 2, Part 1, Pages 401-412.
- Lundqvist, J. & Lagerbäck, R., 1976. The Pärvie Fault: A late-glacial fault in the Precambrian of Swedish Lapland. Geologiska Föreningens i Stockholm Förhandlingar 98, 45–51.
- Lundqvist, T., Gee, D.G., Kumpulainen, R., Karis, L. & Kresten, P., 1990. Beskrivning till berggrundskartan över Västernorrlands län. Geological Survey of Sweden Ba 31, 429 pp.
- Lundqvist, T., Bøe, R., Kousa, J., Lukkarinen, H., Lutro, O., Roberts, D., Solli, A., Stephens, M.B. & Weiher, P., 1996. Bedrock map of Central Fennoscandia 1 : 1 000 000. Geological Survey of Finland (GSF), Geological Survey of Norway (NGU), Geological Survey of Sweden (SGU).
- Lunkka, J.P., Saarnisto, M., Gey, V., Demidov, I. & Kiselova, V., 2001. Extent and age of the Last Glacial Maximum in the southeastern sector of the Scandinavian Ice Sheet. Global and Planetary Change 31, 407–425.
- Lunkka, J.-P., Johansson, P., Saarnisto, M. & Sallasmaa, O., 2004. Glaciation of Finland. In: Ehlers, J & Gibbard, P.L. (editors). Quaternary Glaciations – Extent and Chronology. Elsevier. 93-100.
- Luosto, U., Lanne, E., Korhonen, H., Gutterch, A., Grad, M., Materzok, R. & Perchuc, E., 1984. Deep structure of the Earth's crust on the SVEKA profile in central Finland. Annales Geophysicae 2, 5, 559-570.
- Marotta, A.M., Mitrovica, J.X., Sabadini, R. & Milne, G., 2004. Combined effects of tectonics and glacial isostatic adjustment on intraplate deformation in central and northern Europe: Applications to geodetic baseline analyses. *Journal of Geophysical Research: Solid Earth* 109.B1, DOI: 10.1029/2002JB002337.
- McCue, K., 2004. Australia: historical earthquake studies. Ann Geophys 47(2–3), 387–397.
- Mellqvist, C., Öhlander, B., Skiöld, T. & Wikström, A., 1999. The Archaean–Proterozoic Palaeoboundary in the Luleå area,northern Sweden: field and isotope geochemical evidence for a sharp terrane boundary. Precambrian Research 96, 225–243.
- Midzi, V., Bommer, J.J., Strasser, F.O., Albini, P., Zulu, B.S., Prasad, K. & Flint, N.S., 2013. An intensity database for earthquakes in South Africa from 1912 to 2011. Journal of Seismology 17, 1183–1205.
- Mikko, H., Smith, C.A., Lund, B., Ask, M., Munier, R. 2014. Neotectonic faulting in Sweden: Surface expression from a LiDAR based digital elevation model. Abstract, 31st Nordic winter meeting, Lund, p. 139
- Milne, G.A., Davis, J.L., Mitrovica, J.X., Scherneck, H.-G., Johansson, J.M., Vermeer, M. & Koivula, H., 2001. Space-geodetic constraints on glacial isostatic adjustment in Fennoscandia. Science 291, 2381– 2385.
- Moberg, K.A., 1891. Jordskalfven i Finland år 1882 (Earthquakes in Finland in 1882). Fennia 4(8), 36 pp. (in Swedish)
- Moberg, K.A., 1901. Jordskalfvet den 5 Nov. 1898. (Earthquake of the 5th of November 1898). Fennia 18(6), 28 pp. (in Swedish)

- Moisio, K. & Kaikkonen, P., 2000. Rheological structure and numerical geodynamical modelling in the Fennoscandian Shield. In: Pesonen, L.J., Korja, A. and Hjelt, S.-E., 2000 (Eds.) *Lithosphere 2000: A Symposium on the Structure, Composition and Evolution of the Lithosphere in Finland*. Programme and Extended Abstracts, Espoo, Finland, October 4-5, 2000. Institute of Seismology, University of Helsinki, Report S-41, p. 71-75.
- Moisio, K. & Kaikkonen, P., 2004. The present day rheology, stress field and deformation along the DSS profile FENNIA in the central Fennoscandian Shield. *Journal of Geodynamics*, 38: 161-184.
- Moisio, K. & Kaikkonen, P., 2006. Three-dimensional numerical thermal and rheological modelling in the central Fennoscandian Shield. *J. Geodyn.*, 42, 95–114.
- Moisio, K. & Kaikkonen, P., 2012. Thermal and rheological structures along the seismic POLAR profile in the northern Fennoscandian Shield. *Terra Nova* 25, 2–12. doi: 10.1111/j.1365-3121.2012.01084.x
- Muir Wood, R., 1988. The Scandinavian earthquakes of 22 December 1759 and 31 August 1819. *Disasters* 12, 223–236.
- Muir Wood, R., 1993. A review of the seismotectonics of Sweden. SKB Report TR-93-13, Svensk Kärnbränslehantering AB.
- Muir Wood, R., 1995. Reconstructing the tectonic history of Fennoscandia from its margins: The past 100 million years. Swedish Nuclear Fuel and Waste Management Company, SKB Report TR-95-36. <http://www.skb.se/publications>.
- Muir Wood, R., 2000. Deglaciation Seismotectonics: a principal influence on intraplate seismogenesis at high latitudes. *Quaternary Science Reviews*, 19, 1399-1411.
- Munier, R. & Fenton, C., 2004. Appendix 3: Review of postglacial faulting. In: Munier, R. and Hökmark, H. *Respect distances, Rationale and means of computation*. R-04-17, 157-218.
- Musketov, I. & Orlov, A., 1893. *Katalog zemletrasenii Rossiiskoi Imperii. Zapiski Imper. Russ. geograf. objestv.*, vol. 26.
- Musson, R.M.W., 1986. The use of newspaper data in historical earthquake studies. *Disasters* 10(3), 217–223.
- Musson, R.M.W., 1995. Historical seismicity of South China from European sources: example of the Hong Kong Newspaper Press. *Acta Seismol Sin* 8(3), 487–490.
- Mäkilä, M. & Muurinen, T., 2008. Kuinka vanhoja ovat pohjois-Suomen suot? *Geologi*, 60, 179-184. (In Finnish with English summary).
- Mäntyniemi, P., 2004a. Pre-instrumental earthquakes in a low-seismicity region: A reinvestigation of the macroseismic data for the 16 November 1931 events in Central Finland using statistical analysis. *Journal of Seismology* 8: 71–90.
- Mäntyniemi, P., 2004b. A list of previously unknown earthquakes in Finland between 1877 and 1887 based on newspaper reports. *Geophysica* 40(1–2), 15–22.
- Mäntyniemi, P., 2005. A tale of two earthquakes in the Gulf of Bothnia, Northern Europe in the 1880s. *Geophysica* 41, 73-91.
- Mäntyniemi, P., 2008a. Seismisyshistorioiden tarkastelu ja YVL 2.6 –ohjeiston mukaisen suunnittelumaanjäristyksen määrittäminen ydinvoimaloiden mahdollisille sijoituspaikoille Pyhäjoella, Ruotsinpyhtää ja Simossa (An investigation of the seismic histories and estimation of a design earthquake according to YVL 2.6 guidelines to possible nuclear power point sites in Pyhäjoki, Ruotsinpyhtää and Simo). Unpublished report, 31 pp. and Appendices (in Finnish).
- Mäntyniemi, P., 2008b. The earthquake of 4 November 1898 in northern Europe: New insights. *Journal of Geophysical Research* 113, B11303, doi:10.1029/2007JB005461

- Mäntyniemi, P., 2012a. Pyhäjoen seismisyshistoriasta (On the historical seismicity in Pyhäjoki). Unpublished report, 25 pp. and Appendices (in Finnish).
- Mäntyniemi, P., 2012b. Intraplate Seismicity and Seismic Hazard: The Gulf of Bothnia Area in Northern Europe Revisited. In: Earthquake Research and Analysis - New frontiers in Seismology, Sebastiano D'Amico (Ed.), InTechOpen, pp. 283–298
- Mäntyniemi, P. & Wahlström, R., 2013. Macroseismic reports and intensity assessments for the earthquakes in the Bay of Bothnia area, northern Europe on 15 and 23 June 1882. Institute of Seismology, University of Helsinki, Report S-57, 88 pp.
- Mäntyniemi, P., Wahlström, R., Lindholm, C. & Kijko, A., 1993. Seismic hazard in Fennoscandia: a regionalized study. *Tectonophysics* 227: 205–213.
- Mäntyniemi, P., Kijko, A. & Retief, P., 2001. Parametric-historic procedure for seismic hazard assessment and its application to northern Europe. *Boll. Geofis. teor. appl.* 42, 41–55.
- Mörner, N.-A., 1985. Paleoseismicity and geodynamics in Sweden: *Tectonophysics*, v. 117, p. 139–153. doi:10.1016/0040-1951(85)90242-2.
- Mörner, N.-A., 1990. Glacial isostasy and long-term crustal movements in Fennoscandia with respect to lithospheric and asthenospheric processes and properties. *Tectonophysics* 176, 13-24.
- Mörner, N.-A., 2003. Paleoseismicity of Sweden, a novel paradigm. *Paleogeophysics and Geodynamics*, Stockholm University.
- Mörner, N.-A., 2005. An interpretation and catalogue of paleoseismicity in Sweden. *Tectonophysics* 408, 265–307.
- Mörner, N.-A., 2009. Late Holocene earthquake geology in Sweden. In: Reicherter, K., Michetti, A. M. & Silva, P. G. (eds) *Palaeoseismology: Historical and Prehistorical Records of Earthquake Ground Effects for Seismic Hazard Assessment*. Geological Society, London, Special Publications, 316, 179-188.
- Nenonen, J. & Huhta, P., 1993. Quaternary glacial history of the Hattu schist belt and adjacent parts of the Ilomantsi district, eastern Finland. Geological Survey of Finland, Special Paper 17, pp. 185–191.
- Neuendorf, K.K.E., Mehl, Jr., J.P. & Jackson, J.A. (eds.), 2005. *Glossary of Geology*. American Geological Institute United Book Press, United States of America, 779 p.
- NFR/NORSAR & NGI, 1998. Seismic Zonation for Norway. Report for the Norwegian Council for Building Standardization, 162 pp.
- Nikishin, A.M., Ziegler, P.A., Stephenson, R.A., Cloetingh, S.A.P.L., Fume, A.V., Fokin, P.A., Ershov, A.V., Bolotov, S.N., Korotaev, M.V., Alekseeva, A.S., Gorbachev, V.I., Shipilov, E.V., Lankreijer, A., Bembinova, E.Y. & Shamilov, I.V., 1996. Late Precambrian to Triassic history of the East European Craton: dynamics of sedimentary basin evolution. *Tectonophysics* 268, 23-63.
- Nikonov, A. A., 2004. Istoricheskiye zemletryaseniya (Historical earthquakes), In: Deep structure and seismicity of the Karelian region and its margins, Sharov N. V. (Ed.), Petrozavodsk, 192–213 (in Russian).
- Nironen, M., 1997. The Svecofennian Orogen: a tectonic model. *Precambrian Research* 86, 21–44.
- Nironen, M., Elliott, B.A. & Rämö, O.T., 2000. 1.88-1.87 Ga post-kinematic intrusions of the Central Finland Granitoid Complex: a shift from C-type to A-type magmatism during lithospheric convergence. *Lithos* 53, 37-58.
- Nironen, M., Kuosmanen, E. & Wasenius, P. 2002. Central Finland Granitoid Complex. Bedrock map 1:400 000. Geological Survey of Finland.

- Nironen, M., Korja, A., Heikkinen, P. & FIRE Working Group, 2006. A geological interpretation of the upper crust along FIRE 2 and FIRE 2A. In: Kukkonen, I.T. & Lahtinen, R., (Eds.) Finnish Reflection Experiment FIRE 2001-2005. Geological Survey of Finland, Special Paper 43, 77-103.
- North, R.G., Wetmiller, R.J., Adams, J., Anglin, F.M., Hasegawa, H.S., Lamontagne, M., Du Berger, R., Seeber, L. & Armbruster, J., 1989. Preliminary results from the November 25, 1988 Saguenay (Quebec) earthquake, *Seism. Res. Lett.* 60, 89–93.
- Nørbech, T., Engsager, K., Jivall, L., Knudsen, O., Koivula, H., Lidberg, M., Ollikainen, M. & Weber, M., 2008. Transformation from a common Nordic reference frame to ETRS89 in Denmark, Finland, Norway, and Sweden – status report. In: Knudsen, P. (Ed.), Proceedings of the NKG General Assembly, May 29 – June 2, Copenhagen, Denmark, 2006, Technical Report No. 1, 2008, DTU Space National Space Institute.
- O'Brien, H.E., Peltonen, P. & Vartianen, H., 2005. Kimberlites, carbonatites, and alkaline rocks. In: Lehtinen, M. et al. (eds.) Precambrian geology of Finland – Key to the evolution of the Fennoscandian Shield. Developments in Precambrian geology 14. Elsevier B.V., Amsterdam, pp. 605–644.
- Okko, V. 1964. Maaperä. In: Rankama, K. (Ed.) *Suomen geologia*. Helsinki, Kirjayhtymä, 239–332. (in Finnish).
- Oksanen, P.O. 2006. Holocene development of the Vaisjeäggi palsa mire, Finnish Lapland. *Boreas* 35, 81-95.
- Olesen, O., 1988. The Stuoragurra Fault, evidence of neotectonics in the Precambrian of Finnmark, northern Norway. *Nor. Geol. Tidsskr.*, 68: 107-118.
- Olesen, O., Blikra, L.H., Braathen, A., Dehls, J.F., Olsen, L., Rise, L., Roberts, D., Riis, F., Faleide, J.I. & Anda, E., 2004. Neotectonic deformation in Norway and its implications: a review. *Norwegian Journal of Geology* 84, 3-34.
- Olesen, O., Bungum, H., Dehls, J., Lindholm, C., Pascal, C. & Roberts, D., 2013. Neotectonics, seismicity and contemporary stress field in Norway – mechanisms and implications. In: Olsen, L., Fredin, O. and Olesen, O. (eds.) *Quaternary Geology of Norway*, Geological Survey of Norway Special Publication, 13, pp. 145–174.
- Pajunen, M., 1986. Deformation analysis of cataclastic structures and faults in the Tervo area, Central Finland. In: Korsman, K. (Ed.) *Development of deformation, metamorphism and metamorphic blocks in eastern and southern Finland*. Geological Survey of Finland, Bulletin 339, 16-31.
- Pajunen, M., Airo, M-L., Elminen, T., Mänttäri, I., Niemelä, R., Vaarma, M., Wasenius, P. & Wennerström, M., 2008. Tectonic evolution of the Svecofennian crust in southern Finland. In: Pajunen, M. (Ed.) *Tectonic evolution of the Svecofennian crust in Finland – a basis for characterizing bedrock technical properties*. Geological Survey Finland, Special Paper 47, 15-160.
- Pascal, C. & Cloetingh, S.A.P.L., 2009. Gravitational potential stresses and stress field of passive continental margins: Insights from the South-Norway shelf. *Earth and Planetary Science Letters*, 277, pp. 464-473.
- Pascal, C., Roberts, D. & Gabrielsen, R.H., 2005. Quantification of neotectonic stress orientations and magnitudes from field observations in Finnmark, northern Norway. *Journal of Structural Geology*, 27, 859-870.
- Pasquale, V., Verdoya, M. & Chiozzi, P., 2001. Heat flux and the seismicity in the Fennoscandian Shield. *Phys. Earth Planet. Int.*, 126, 147–162.
- Patison, N.L., Korja, A., Lahtinen, R., Ojala, V.J. & FIRE Working Group, 2006. FIRE seismic reflection profiles 4, 4A and 4B: insights into the crustal structure of northern Finland from Ranua to Näätämö. In: Kukkonen, I.T. & Lahtinen, R., (Eds.) *Finnish Reflection Experiment FIRE 2001-2005*. Geological Survey of Finland, Special Paper 43, 161-222.

- Park, A.F., 1985. Accretion tectonism in the Proterozoic Svecokarelides of the Baltic Shield. *Geology* 13, 725–729.
- Peltonen, P. & Kontinen, A., 2004. The Jormua ophiolite: a mafic-ultramafic complex from an ancient ocean-continent transition zone. In: Kusky, T.M. (Ed.) *Precambrian Ophiolites and Related Rocks. Developments in Precambrian Geology* 13, 35-71.
- Peltonen, P., Kontinen, A., Huhma, H. & Kuronen, U., 2008. Outokumpu revisited: New mineral deposit model for the mantle peridotite-associated Cu–Co–Zn–Ni–Ag–Au sulphide deposits. *Ore Geology Reviews* 33, 559-617.
- Penttilä, E., 1978. Earthquakes in Finland 1610–1976. Institute of Seismology, University of Helsinki, Report S-1, 15 pp.
- Phillips, J.D., 2007. Geosoft eXecutables (GX's) developed by the U.S. Geological Survey, version 2.0, with notes on GX development from Fortran code: U.S. Geological Survey Open-File Report 2007-1355.
- Pietikäinen, K.J., 1994. The geology of the Paleoproterozoic Pori shear zone, southwestern Finland, with special reference to the evolution of veined gneisses from tonalitic protoliths. Ph.D. thesis, Michigan Technological University, 129 pp.
- Pitkäranta, R., 2013. Lithostratigraphy and age of pre-late Weichselian sediments in the Suupohja area, Finland. *Lithostratigraphy and age of pre-Late Weichselian sediments in the Suupohja area, western Finland. Annales Universitatis Turkuensis, Ser. AII* 284, 66 pp.
- Pokki, J., Kohonen, J., Lahtinen, R., Rämö, O. T. & Andersen, T., 2013a. Petrology and provenance of the Mesoproterozoic Satakunta formation, SW Finland. *Geological Survey of Finland, Report of Investigation* 204, pp. 47.
- Pokki, J., Kohonen, J., Rämö, O.T. & Andersen, T., 2013b. The Suursaari conglomerate (SE Fennoscandian shield; Russia) – Indication of cratonic conditions and rapid reworking of quartz arenitic cover at the outset of the emplacement of the rapakivi granites at ca. 1.65 Ga. *Precambrian Research* 233, 132-143.
- Poutanen, M., Häkli, P., Kallio, U., Nyberg, S., Rouhiainen, P. & Saaranen, V., 2011. Geodeettisten havaintoaineistojen kokoaminen, käsitteily ja analyysi Simon-Pyhäjoen alueelta mahdollisen ydinvoimalan sijoitusalueen liikuntamiseksi.
- Putkinen, N. & Valpola, S., 2011. Pyhäjoen Hanhikiven nuoret siirrokset. *Geologian tutkimuskeskus, Länsi-Suomen yksikkö, raportti LSY Y99/9999/2011/9/99*, 2 s. (Fennovoiman arkistotunnus RE-02-0000096)
- Påsse T, 2004. The amount of glacial erosion of the bedrock. SKB TR-04-25, Svensk Kärnbränslehantering AB.
- Ransed, G. & Wahlroos J.-E., 2007. Map of the Quaternary deposits 24H Sorsole, scale 1:100 000. *Sveriges geologiska undersökning K 42*.
- Rantataro, J., Kaskela, A. & Alvi, K., 2011. Simosel - Simo Merigeologia/vaihe 1 v.2011. *Geologian tutkimuskeskus, tilaustyöraportti 31.3.2011*, 9 s + 1 liite (Fennovoiman arkistotunnus RE-02-0000095).
- Redfield, T.F. & Osmundsen, P.T., 2013. The Long –term topographic response of a continent adjacent to a hyperextended margin: a case study from Scandinavia. *Geological Society of America Bulletin*, v. 125, no. ½, p. 184-200.
- Reimold, W.U., 1982. The Lappajärvi meteorite crater, Finland: petrography, Rb-Sr, major and trace element geochemistry of the impact melt and basement rocks. *Geochimica et Cosmochimica Acta* 46, 1203-1225.

- Rinterknecht, V. R., Clark, P. U., Raisbeck, G. M., Yiou, F., Brook, E. J., Tschudi, S. & Lunkka, J. P., 2004. Cosmogenic ^{10}Be dating of the Salpausselkä I Moraine in southwestern Finland. *Quaternary Science Reviews* 23, 2283 - 2289.
- Roberts, D. & Gee, D.G., 1985. An introduction to the structure of the Scandinavian Caledonides. In: Gee, D.G. & Sturt, B.A. (eds.), *The Caledonide Orogen - Scandinavia and related areas*, Chichester, Wiley, 55–68.
- Robertsson, A.-M., 2000. The Eemian interglacial in Sweden, and comparison with Finland. *Geologie en Mijnbouw/Netherlands Journal of Geosciences* 79, 325–333.
- Robertsson, A.-M., Svedlund, J.-O., Andrén, Th. & Sundh, M., 1997. Pleistocene stratigraphy in the Dellen region, central Sweden. *Boreas* 26, 237–260.
- Romer, R.L. & Nisca, D.H., 1995. Svecofennian crustal deformation of the Baltic Shield and U-Pb age of late-kinematic tonalitic intrusions in the Burträsk Shear Zone, northern Sweden. *Precambrian Research* 75, 17–29.
- Root, D. & Corfu, F., 2012. U-Pb geochronology of two discrete Ordovician high pressure metamorphic events in the Seve nappe complex, Scandinavian Caledonides. *Contributions to Mineralogy and Petrology* 163, 769–788.
- Rosberg, J.E., 1912. Jordskalf i Finland 1904–1911 (Earthquakes in Finland 1904–1911). *Fennia*, 32(5), 1–25 (in Swedish).
- Roth, M. & Bungum, H., 2003. Waveform modeling of the 17 August 1999 Kola Peninsula earthquake. *Bull. Seismol. Soc. Am.*, 93, 1559-1572, doi: 10.1785/0120020015.
- Rukhlov, A.S. & Bell, K., 2010. Geochronology of carbonatites from the Canadian and Baltic Shields, and the Canadian Cordillera: clues to mantle evolution. *Mineralogy and Petrology* 98, 11–54.
- Rutland, R.W.R, Skiöld, T. & Page, R.W., 2001. Age of deformation episodes in the Palaeoproterozoic domain of northern Sweden, and evidence for a pre-1.9 Ga crustal layer. *Precambrian Research* 112, 239–259.
- Rämö, O.T. & Haapala, I., 2005. Rapakivi granites. In: Lehtinen, M., Nurmi, P.A., Rämö, O.T. (Eds.) *Precambrian Geology of Finland – Key to the Evolution of the Fennoscandian Shield*. Elsevier B.V., Amsterdam, 533-562.
- Saari J., 1998. Regional and local seismotectonic characteristics of the area surrounding the Loviisa nuclear power plant in SE Finland. Ph.D. thesis. Inst Seismology, Univ. Helsinki, Report S-36, 78p.
- Saari, J., 2008. Seismicity in the Olkiluoto area. Posiva report, POSIVA 2008-04, Posiva Oy, Eurajoki, Finland. 55 p.
- Saari, J., 2012. Seismic activity parameters of the Olkiluoto site. Posiva report, POSIVA-2012-34, Posiva Oy, Eurajoki, Finland. 60 p.
- Saari, J. & Slunga, R., 1996. Fault plane solutions of microearthquakes in the Loviisa region in south-eastern Finland. Posiva report, POSIVA-96-02, Posiva Oy, Eurajoki, Finland. 55 p.
- Saari, J., Heikkinen, P.J., Varpasuo, P., Malm, M., Turunen, E., Karkkulainen, K., Valtonen, O. & Uski, M., 2009. Estimation of seismic hazard in territory of Finland, Report number EXP-500, ÅF-Consult Ltd.
- Saarnisto, M. & Salonen, V-P., 1995. Glacial history of Finland. In: Ehlers, J., Kozarski, S., Gibbard, P. (eds). *Glacial deposits in North-east Europe*. A.A.Balkema, Rotterdam, 3-10.
- Saarnisto, M. & Saarinen, T., 2001. Deglaciation chronology of the Scandinavian Ice Sheet from the Lake Onega Basin to the Salpausselkä End Moraines. *Global and Planetary Change*, volume 31, pages 387-405.

- Sahlström, K.E., 1911. Jordskalf i Sverige 1907–1910 (Earthquakes in Sweden 1907–1910). Sveriges Geologiska Undersökning (Geological Survey of Sweden), Ser.C, No.238, Stockholm, Sweden (in Swedish).
- Saintot, A., Stephens, M.B., Viola, G. & Nordgulen, Ø. 2011: Brittle tectonic evolution and paleostress field reconstruction in the southwestern part of the Fennoscandian Shield, Forsmark, Sweden. *Tectonics* 30, TC4002, doi:10.1029/2010TC002781.
- Salonen, V.-P., Kaakinen, A., Kultti, S., Miettinen, A., Eskola, K.O. & Lunkka, J.P. 2008. Middle Weichselian glacial event in the central part of the Scandinavian Ice Sheet recorded in the Hitura pit, Ostrobothnia, Finland. *Boreas* 37, 38–54.
- Sandström, B., Tullborg, E.-L., Larson, S.Å. & Page, L., 2009. Brittle tectonothermal evolution in the Forsmark area, central Fennoscandian Shield, recorded by paragenesis, orientation and $^{40}\text{Ar}/^{39}\text{Ar}$ geochronology of fracture minerals. *Tectonophysics* 478, 158–174.
- Sauber, J., Plafker, G., Molnia, B.F. & Bryant, M.A., 2000. Crustal deformation associated with glacial fluctuations in the eastern Chugach Mountains, Alaska. *J. Geophys. Res.*, 105(B4), 8055-8077.
- Sauramo, M. 1923. Studies on the Quaternary varve sediments in southern Finland. *Bulletin de la Commision géologique de Finlande* 60, 164 pp
- Scherneck, H.-G., Lidberg, M., Haas, R., Johansson, J.M. & Milne, G.A., 2010. Fennoscandian strain rates from BIFROST GPS: A gravitating, thick-plate approach. *J. Geodyn.*, 50, 19-26.
- Scholz, C.H. 1990. The Mechanics of Earthquakes and Faulting. Cambridge University Press, Cambridge, 439 pp.
- Seeber, L. & Armbruster, J.G., 1987. The 1886–1889 aftershocks of the Charleston, South Carolina, earthquake: a widespread burst of seismicity. *J Geophys Res* 92(B3), 2663–2696.
- Shackleton, N.J., 1997. The deep-sea sediment record and the Pliocene-Pleistocene boundary. *Quaternary International* 40, 33–35.
- Shearer, P.M., 2009. Introduction to Seismology. Cambridge University Press, Cambridge. 396 pp.
- Sibson, R.H., 1982. Fault zone models, heat flow, and the depth distribution of earthquakes in the continental crust of the United States. *Bull. Seismol. Soc. Am.*, 72, 151-163.
- Sigfúsdóttir, Th., 2013. A sedimentological and stratigraphical study of Veiki moraine in northernmost Sweden. *Dissertations in Geology at Lund University*, No. 354, 27 pp.
- Skyttä, P. & Mänttäri, I., 2008. Structural setting of late Svecofennian granites and pegmatites in Uusimaa Belt, SW Finland: Age constraints and implications for crustal evolution. *Precambrian Research* 164, 86-109.
- Skyttä, P., Bauer, T.E., Tavakoli, S., Hermansson, T., Andersson, J. & Weihed, P., 2012. Pre-1.87 Ga development of crustal domains overprinted by 1.87 Ga transgression in the Palaeoproterozoic Skellefte district, Sweden. *Precambrian Research* 206–207, 109–136.
- Slunga, R.S., 1991. The Baltic Shield earthquakes. In: S. Björnsson, S. GregerSEN, E.S. Husebye, H. Korhonen & C.-E. Lund (Eds.), *Imaging and Understanding the Lithosphere of Scandinavia and Iceland*. *Tectonophysics*, 189: 323-3111..
- Slunga, R. & Ahjos, T., 1986. Fault mechanism of Finnish earthquakes, crustal stresses and faults. *Geophysica* 22, 1 – 13.
- Smedberg, I., Uski, M., Tiira, T., Komminaho, K. & Korja, A., 2012. Intraplate earthquake swarm in Kouvola, south-eastern Finland. *Geophysical Research Abstracts*. 2012;14:EGU2012-8446.
- Smith, C.A., Sundh, M., Mikko, H. 2014. Surficial geology indicates early Holocene faulting and seismicity, central Sweden. *International Journal of Earth Sciences (Geologische Rundschau)* 103, 1711-1724

- Sohlenius, G. & Hedenström, H., 2008. Geological development during the Quaternary period. In Söderbäck, B. (ed.), Geological evolution, palaeoclimate and historical development of the Forsmark and Laxemar-Simpevarp areas. Site descriptive modelling SDM-Site. Swedish Nuclear Fuel and Waste Management Company, SKB Report R-08-19, 89–134. <http://www.skb.se/publications>.
- Sorjonen-Ward, P. 2006. Geological and structural framework and preliminary interpretation of the FIRE 3 and FIRE 3A reflection seismic profiles, central Finland. *Geological Survey of Finland, Special Paper 43*, 105–159.
- Spencer, K.J., Hacker, B.R., Kylander-Clark, A.R.C., Andersen, T.B., Cottle, J.M., Stearns, M.A., Poletti, J.E. & Seward, G.G.E., 2013. Campaign-style titanite U-Pb dating by laser-ablation ICP: Implications for crustal flow, phase transformations and titanite closure. *Chemical Geology* 341, 84–101.
- St-Onge, M.R., Searle, M.P. & Wodicka, N., 2006. Trans-Hudson Orogen of North Amererica and Himalaya-Karakoram-Tibetan Orogen of Asia: Structural and thermal characteristics of the lower and upper plates. *Tectonics* 25, TC4006, doi:10.1029/2005TC001907.
- Stein, S. & Liu, M., 2009. Long aftershock sequences within continents and implications for earthquake hazard assessment. *Nature* 462, 87-89.
- Stephens, M.B., 1988. The Scandinavian Caledonides: A complexity of collisions. *Geology Today* 4, 20–26.
- Stephens, M.B. & Wahlgren, C.-H., 2008. Bedrock evolution. In: Söderbäck, B. (ed.), Geological evolution, palaeoclimate and historical development of the Forsmark and Laxemar-Simpevarp areas. Site descriptive modelling SDM-Site. Swedish Nuclear Fuel and Waste Management Company, SKB Report R-08-19, 25–88. <http://www.skb.se/publications>.
- Stephens, M.B. & Weihed, P., 2013. Tectonic evolution and mineral resources in the Fennoscandian Shield, Sweden. In: Allen, R., Jansson N. & Ripa, M. (eds.), Bergslagen: Geology of the volcanic- and limestone-hosted base metal and iron oxide deposits. Geological Survey of Sweden SGA excursion guidebook SWE4, 10–20.
- Stephens, M.B., Ripa, M., Lundström, I., Persson, L., Bergman, T., Ahl, M., Wahlgren, C.-H., Persson, P.-O. & Wickström, L., 2009. Synthesis of the bedrock geology in the Bergslagen region, Fennoscandian Shield, south-central Sweden. *Geological Survey of Sweden Ba* 58, 259 pp.
- Stucchi, M., 1993. Through catalogues and historical records: an introduction to the project «Review of Historical Seismicity in Europe», in *Historical Investigation of European Earthquakes*, edited by M. Stucchi and J. Vogt (CNR, Milano), 1, 3–14.
- Stucchi, M., Albini, P. & Rubbia Rinaldi, G., 2000. Historical earthquake data in Europe and the Euro-Mediterranean Intensity Database. *Euro-Mediterranean Seismological Centre Newsletter* 16, 5–7.
- Suominen, V., 1991. The chronostratigraphy of southwestern Finland with special reference to Postjotnian and Subjotnian diabases. *Geological Survey of Finland Bulletin* 356, 106 pp.
- Sutinen, R., 1992: Glacial deposits, their electrical properties and surveying by image interpretation and ground penetrating radar. *Bulletin de la commission Géologique de Finlande* 359, 123 pp.
- Sutinen, R., 2005. Timing of early Holocene landslides in Kittilä, Finnish Lapland. *Geological Survey of Finland, Special Paper* 40, 53-58.
- Sutinen, R., Jakonen, M., Liwata, P. & Hyvönen E., 2007. Late-Weichselian sheetflow drainage of subglacial Lokka ice lake. *Geol. Surv. Finl. Spec. Paper*. 46, 55-62.
- Sutinen, R., Piekkari, M. & Middleton, M., 2009. Glacial geomorphology in Utsjoki, Finnish Lapland proposes Younger Dryas fault-instability. *Global and Planetary Change*, 69, 16-28.

- Sutinen R., Hyvönen E., Närhi P., Haavikko P., Piekkari M. & Middleton M., 2010. Sedimentary anisotropy diverges from flute trends in south-east Finnish Lapland. *Sedimentary Geology* 232 (3-4), 190-197.
- Sutinen, R., Hyvönen, E. & Kukkonen, I., 2013. LiDAR detection of paleolandslides in the vicinity of the Suasselkä posglacial fault, Finnish Lapland. *International Journal of Applied Earth Observation and Geoinformation* 27, 91-99.
- Sutinen, R., Hyvönen E., Middleton, M. & Ruskeeniemi, T., 2014. Airborne LiDAR detection of postglacial faults and Pulju moraine in Palojärvi, Finnish Lapland. *Global and Planetary Change* 115, 24-32.
- Svendsen, J.I., Alexanderson, H., Astakhov, V.I., Demidov, I., Julian, A.D., Funder, S., Gataulling, V., Henriksen, M., Hjort, J., Houmark-Nielsen, M., Hubberten, H.W., Ingulfsson, O., Jakobsson, M., Kjer, K.H., Larsen, E., Lokrantz, H., Lunkka, J.P., Lys, A., Mangerud, J., Matiouchkov, A., Murray, A., Muller, P., Niessen, F., Nikolskaya, O., Polyak, L., Saarnisto, M., Siegert, C., Siegert, M.J., Spielhagen, R.W., & Ruedige, S. 2004. Late Quaternary ice sheet history of northern Eurasia. *Quaternary Science Reviews* 23, 1229–1271.
- Sylvester, A.G., 1988. Strike-slip faults. *Geol. Soc. Am. Bull.*, 100(11), 1666-1703.
- Söderlund, U., Isachsen, C., Bylund, G., Heaman, L., Patchett, P.J., Vervoort, J.D. & Andersson, U.B., 2005. U-Pb baddeleyite ages and Hf, Nd isotope chemistry constraining repeated mafic magmatism in the Fennoscandian Shield from 1.6 to 0.9 Ga. *Contributions to Mineralogy and Petrology* 150, 174–194.
- Söderlund, U., Elming, S.-Å., Ernst, R.E & Schissel, D., 2006. The central Scandinavian Dolerite Group - protracted hotspot activity or back-arc magmatism? Constraints from U-Pb baddeleyite geochronology and Hf isotopic data. *Precambrian Research* 150, 136–152.
- Söderlund, P., Hermansson, T., Page, L.M. & Stephens, M.B., 2009. Biotite and muscovite ^{40}Ar - ^{39}Ar geochronological constraints on the post-Svecofennian tectonothermal evolution, Forsmark site, central Sweden. *International Journal of Earth Sciences* 98, 1835–1851.
- Talvitie, J., 1971. Seismotectonics of the Kuopio region, Finland. *Bull. Comm. Géol. Finlande*. vol 248, 41 p.
- Talwani, P. & Sharma, N., 1999. Reevaluation of the magnitudes of three destructive aftershocks of the 1886 Charleston earthquake. *Seismol Res Lett* 70(3), 360–367.
- Tatevossian, R.E. & Mäntyniemi, P., 2014. Earthquake scenarios: A practical way to handle alternative solutions to historical earthquakes and to increase the transparency of seismic hazard assessment. *Natural Hazards* 72, 549–564.
- Tatevossian, R.E., Mäntyniemi, P. & Tatevossian, T.N., 2011. On the earthquakes in the Northern Baltic Shield in the spring of 1626. *Natural Hazards* 57: 133–150.
- Tatevossian, R.E., Tatevossian, T.N. & Mäntyniemi, P., 2013. Earthquake activity in Finland and the Russian North in December 1758: rare reports and their interpretation. *Annals of Geophysics* 56(5), 1-18. doi:10.4401/ag-5829.
- Tiira, T., Uski, M., Kortstrom, J., Valtonen, O. & Korja, A., 2011. Pyhäjoki Seismic Network – a Preliminary Proposal, Report T-84, Institute of Seismology, University of Helsinki, Helsinki, 37 pp.
- Tiira, T., Janik., T.Kozlovskaya, E., Grad., M., Korja, A., Komminaho, K., Hegedüs, E., Kocács, C.A, Silvennoinen, H. & Brückl, E., 2013. Crustal architecture of the inverted Central Lapland rift along HUKKA 2007 profile. *Pure and Applied Geophysics*, DOI 10.1007/s00024-013-0725-3.
- Tiira, T., Janik, T., Kozlovskaya, E., Grad, M., Korja, A., Komminaho, K., HEGEDÜS, E., KOVÁCS, C.A., Silvennoinen, H. & BRÜCKL, E., 2014. Crustal architecture of the inverted Central Lapland rift along HUKKA 2007 profile. *Pure and Applied Geophysics* (in press).

- Tolgensbakk, J. & Sollid, J. L. 1988. Kåfjord, kvartærgeologi og geomorfologi 1:50 000, 1634 II. Geografisk institutt, University of Oslo.
- Torvela, T. & Ehlers, C., 2010. Microstructures associated with the Sottunga-Jurmo shear zone and their implications for the 1.83–1.79 Ga tectonic development of SW Finland. Bull. Geol. Soc. Finland 82,5–29.
- Torvela, T., Mänttäri, I. & Hermansson, T., 2008. Timing of deformation phases within the South Finland shear zone, SW Finland. Precambrian Research 160, 277–298.
- Torvela, T., Moreau, J., Butler, R., Korja, A. & Heikkinen, P., 2013. The mode of extension in the orogenic mid-crust revealed by seismic attribute analysis. G3: Geochemistry, Geophysics, Geosystems, vol 14, nr. 4, s. 1069–1086.
- Trouw, R.A.J., 1986. Structural geology of the Marsfjällen area, Caledonides of Västerbotten, Sweden. Geological Survey of Sweden C 689, 115 pp.
- Tuisku, P. & Laajoki, K., 1990. Metamorphic and structural evolution of the Early Proterozoic Puolankajärvi Formation, Finland – II. The pressure-temperature-deformation-composition path. Journal of metamorphic Geology 8, 375–391.
- Tuisku, P. & Huhma, H., 2006. Evolution of migmatitic granulite complexes: implications from Lapland granulite belt, Part II: Isotopic dating. Bulletin of the Geological Society of Finland 78, 143–175.
- UNAVCO Plate Motion Calculator, 2012.
http://www.unavco.org/community_science/science-support/crustal_motion/dxdt/model.html
Last accessed 20th of September 2013.
- Uski, M. & Korja, A., 2007. Hypocenter distribution of earthquakes in north-western Finnish Lapland: preliminary investigation. Abstract in: The 38th Nordic Seismology Seminar, Helsinki, 12–15.6.2007
- Uski, M., Hyvönen, T., Korja, A. & Airo, M.-L., 2003. Focal mechanisms of three earthquakes in Finland and their relation to surface faults. Tectonophysics 363, 141–157.
- Uski, M., Tiira, T., Korja, A. & Elo, S., 2006. The 2003 earthquake swarm in Anjalankoski, south-eastern Finland. Tectonophysics 422, 55–69. doi:10.1016/j.tecto.2006.05.014.
- Uski, M., Tiira, T., Grad, M. & Yliniemi, J., 2012. Crustal seismic structure and depth distribution of earthquakes in the Archean Kuusamo region, Fennoscandian Shield. Journal of Geodynamics 53, 61–80. doi:10.1016/j.jog.2011.08.005
- Vaasjoki, M. & Sakkola, M., 1988. The evolution of the Raahe-Ladoga zone in Finland: isotopic constraints. In: Korsman, K. (Ed.) Tectono-metamorphic evolution of the Raahe-Ladoga zone. Geological Survey of Finland, Bulletin 343, 7–32.
- Valjus, T., 2008. Geofysikaiset kallionpintaselvitykset Ruotsinpyhtäällä, Simossa ja Pyhäjoella, Etelä-Suomen yksikkö, raportti 28.11.2008, 6+58 s.
- Valtonen, O., Uski, M., Korja, A., Tiira, T. & Kortström, J. 2012a. Simulations of a Microearthquake Network, Geophysical Research Abstracts. Vol 14, EGU2012-8121.
- Valtonen, O., Lindblom, P., Komminaho, K., Kortsröm, J., Keskinen, J., Smedberg, I. & Korja, A., 2012b. Suunnitelma Pyhäjoen seismisestä paikallisverkosta, Raportti T-85, Seismologian Instituutti, Helsingin Yliopisto, Helsinki, 19 s.
- Valtonen, O., Uski, M., Tiira, T., Kortström, J. & Korja, A. 2012c. Yhteenveto Pyhäjoen seismisen paikallisverkon ja aineiston käsittelyn suunnittelusta, Seismologian Instituutti, raportti T-87, Helsingin yliopisto, Helsinki, 13 pp.

- Valtonen, O., Kortström, J. & Korja, A., 2012d. Pyhäjoen seisminen paikallisverkko - vaihe 1, Seismologistan Instituutti, raportti T-88. Helsinki, 26 pp.
- Valtonen, O., Uski, M., Korja, A., Tiira, T. & Kortström, J., 2013a. Optimal configuration of a micro-earthquake network, *Advances in Geosciences*, 34, 33-36 pp.
- Valtonen, O., Uski, M., Tiira, T., Kortström, J. & Korja, A., 2013b. Optimal configuration of the local Ostrobothnian seismic network OBF, *XXVI Geofysiikan päivät*, Helsinki, 131-133 pp.
- Valtonen, O., Kortström, J. & Korja, A., 2013c. OBF-verkko - vaiheen 1 loppuraportti, Seismologistan Instituutti, raportti T-89, 17 pp.
- Valtonen, O., Kortström, J. & Korja, A., 2013d. OBF-verkon detektio- ja paikannuskyky – vaiheessa 1 . Seismologistan Instituutti, raportti T-91.
- Valtonen, O., Uski, M., Kortström, J. ja Korja, A. 2014. OBF-verkon toiminta ja seismiset havainnot vuonna 2013, Seismologistan instituutti, raportti T-92. Helsinki, 29 pp
- Velichko, A.A, Faustova, M.A., Pisareva, V.V, Gribchenko, Yu.N., Sudakova, N.G. & Lavrentiev, N.V., 2011. Chapter 26 - Glaciations of the East European Plain: Distribution and Chronology. In: Ehlers and Gibbard (Eds.) *Developments in Quaternary Sciences. Quaternary Glaciations - Extent and Chronology. A Closer Look. Volume 15*, Pages 337–360.
- Veltheim, V., 1962. On the pre-Quaternary geology of the bottom of the Bothnian Sea. *Bull. Comm. Geol. Finlande*, 200, p. 1-166.
- Veltheim, V., 1969. On the pre-Quaternary geology of the Bothnian Bay area in the Baltic Sea. *Bull. Comm. Géol. Finlande*, 239, p. 1-56.
- Vestøl O., 2006. Determination of postglacial land uplift in Fennoscandia from leveling, tide-gauges and continuous GPS stations using least squares collocation. *J. Geodesy*, 80, 248–258, doi:10.1007/s00190-006-0063-7
- Viola, G., Venvik Ganerød, G. & Wahlgren, C.-H., 2009. Unraveling 1.5 Ga of brittle deformation history in the Laxemar-Simpevarp area, southeast Sweden: A contribution to the Swedish site investigation study for the disposal of highly radioactive nuclear waste. *Tectonics* 28, TC 5007, DOI: 10.1029/2009TC002461.
- Viola, G., Zwingmann, H., Mattila, J. & Käpyaho, A., 2013. K-Ar illite age constraints on the Proterozoic formation and reactivation history of a brittle fault in Fennoscandia. *Terra Nova* 25, 236-244.
- Vuollo, J. & Huhma, H., 2005. Paleoproterozoic mafic dikes in NE Finland. In: Lehtinen, M., Nurmi, P.A., Rämö, O.T. (Eds.) *Precambrian Geology of Finland – Key to the Evolution of the Fennoscandian Shield*. Elsevier B.V., Amsterdam, 195-236.
- Väisänen, M. & Hölttä, P., 1999. Structural and metamorphic evolution of the Turku migmatite complex, southwestern Finland. *Bulletin of the Geological Society of Finland* 71, 1, 177-218.
- Väisänen, M. & Skyttä, P., 2007. Late Svecofennian shear zones in southwestern Finland. *GFF* 129, 55-64.
- Wahlström, R., 1990. A catalogue of earthquakes in Sweden in 1375–1890. *Geologiska Föreningens i Stockholm Förhandlingar* 112(3), 215–225
- Wahlström, R. & Grünthal, G., 2000. Probabilistic seismic hazard assessment (horizontal PGA) for Sweden, Finland and Denmark using different logic tree approaches. *Soil Dynamics and Earthquake Engineering* 20, 45–58.
- Wahlström, R. & Grünthal, G., 2001. Probabilistic seismic hazard assessment (horizontal PGA) for Fennoscandia using the logic tree approach for regionalization and nonregionalization models. *Seismological Research Letters*, 72, 1, 33-45.
- Wannäs, K.O., 1989. Seismic stratigraphy and tectonic development of the Upper Proterozoic to Lower Paleozoic of the Bothnian Bay, Baltic Sea. *Stockholm Contributions in Geology* 40(3), 83–168.

- Ward, P., 1987. Early Proterozoic deposition and deformation at the Karelian craton margin in southeastern Finland. *Precambrian Research* 35, 71-93.
- Watts A.B. and Burov, E.B. 2003. Lithospheric strength and its relationship to the elastic and seismogenic layer thickness. *Earth and Planetary Science Letters* 213, 113-131.
- Weihed, P. & Mäki, T. (Eds.) 1997. Research and exploration – where do they meet? 4th Biennial SGA Meeting, August 11-13, 1997, Turku, Finland. Excursion guidebook A2: volcanic hosted massive sulphide and gold deposits in the Skellefte district, Sweden and western Finland. Geological Survey of Finland, Guide 41, 81 pp.
- Weihed, P., Billström, K., Persson, P.-O. & Bergman Weihed, J., 2002. Relationship between 1.90–1.85 Ga accretionary processes and 1.82–1.80 Ga oblique subduction at the Karelian craton margin, Fennoscandian Shield. *GFF* 124, 163–180.
- Wickman F E, 1988. Possible impact structures in Sweden. In: A. Boden and K.-G Eriksson, (eds.), Deep Drilling in Crystalline Bedrock. Volume 1: The Deep Gas Drilling in the Siljan Impact Structure, Sweden and Astroblemes. Springer-Verlag, Berlin.
- Wik, N.-G., Albrecht, L., Bergman, S., Kübler, L. & Sundberg, A., 2009. Malmer, industriella mineral och bergarter i Gävleborgs län. Geological Survey of Sweden RM 130, 310 pp.
- Wikström, A., Skiöld, T. & Öhlander, B., 1996. The relationship between 1.88 Ga pld magmatism and the Baltic–Bothnian shear zone in northern Sweden. In: Brewer, T.S. (ed.), Precambrian Crustal Evolution in the North Atlantic Region. Geological Society Special publication 112, 249–259.
- Winterhalter, B., 1972. On the geology of the Bothnian Sea, an epeiric sea that has undergone Pleitocene glaciation. Geological Survey of Finland, Bulletin 258, 66 pp.
- Winterhalter, B., 2000. Sedimentary rocks underlying the Gulf of Bothnia. In Lundqvist, T. & Autio, S. (eds.), Description to the bedrock map of central Fennoscandia (Mid-Norden). Geological Survey of Finland, Special paper 28, 76–79.
- Wu, P. & Hasegawa, H.S., 1996a. "Induced stresses and fault potential in Eastern Canada due to a realistic load: a preliminary analysis". *Geophysical Journal International* 125: 415-430.
- Wu, P. & Hasegawa, H.S. 1996b. "Induced stresses and fault potential in Eastern Canada due to a realistic load: a preliminary analysis". *Geophysical Journal International* 127: 215–229.
- Wu, P. Johnston, P. & Lambeck, K. 1999: Postglacial rebound and fault instability in Fennoscandia. *Geophysical Journal International* 139, 657-670.
- Zhu, H. & Tromp, J., 2013. Mapping Tectonic Deformation in the Crust and Upper Mantle Beneath Europe and the North Atlantic Ocean. *Science* Vol. 341, no. 6148, pp. 871-875.
- Ågren, J. & Svensson, R., 2007. Postglacial Land Uplift Model and System Definition for the New Swedish Height System RH 2000. Reports in Geodesy and Geographical Information Systems Rapportserie, LMV-Rapport 2007:4, Lantmäteriet, Gävle, Sweden.
- Åhäll, K.-I., Connelly, J. & Brewer, T.S., 2000. Episodic rapakivi magmatism due to distal orogenesis? Correlation of 1.69–1.50 Ga orogenic and inboard “anorogenic” events in the Baltic Shield. *Geology* 28, 823–826.
- Öhlander, B., Skiöld, T. & Elming S.A., BABELWorking Group, Claesson, S. & Nisca, D.H., 1993. Delineation and character of the Archaean–Proterozoic boundary in northern Sweden. *Precambrian Research* 64, 67–84.

Appendices

Appendix 1. Previous studies around the Hanhikivi site

Appendix 2. On historical earthquake data

P. Mäntyniemi

Technical information on the revision of historical earthquakes

According to the IAEA guidelines (2010, p. 12), information about earthquakes in the study area shall be collected and documented before conducting a PSHA for a NPP. This includes historical earthquakes that occurred before the advent of seismic instruments. Various written documentary materials testify of the effects of local and regional earthquakes in the past. The textual information can be utilized in seismicity studies using the rigorous rules of historical seismology. The seismicity record should be extended as far back in time as possible. Macroseismic data provide constraints on earthquake effects when no instrumental records are available. They make an important contribution to loss modeling by seismological and engineering communities.

It was known on the basis of earlier seismological compilations that information on earthquakes observed in the study area is available since the first half of the 1700s. It was judged that chances to uncover usable reports older than 300 years are extremely small. This was based on general considerations of the history of settlement and learning. The semi-nomad indigenous people in Lapland in the north did not prepare written accounts. Town rights were accorded to several harbours and old marketplaces on the coasts of the Gulf of Bothnia in the reign of King Gustaf II Adolf of Sweden between 1611 and 1632, reflecting the growing importance of this region to the Crown. A milestone in learning was the work of U. Hiärne (1706) that included observations of ground tremor in southern Sweden.

The search strategy was to focus on the two and a half centuries of the historical seismicity record available. Efforts were taken to expand the data by re-appraising known earthquakes and searching for possible forgotten earthquakes (forgotten by catalogue compilers) and cases where the parametric entry in a catalogue relies on erroneous information, so-called fake earthquakes.

It was decided that primary written documentary materials should be consulted and maps plotted on the basis of available data. Intensity data points (IDPs) represent the formalization of historical records of earthquake effects. They become macroseismic data through IDPs (Stucchi et al. 2000). An IDP carries at least the information about time, place name and its coordinates, and the respective macroseismic intensity. A historical earthquake is constructed with the help of the IDPs carrying the

same time. The concept of macroseismic data point (MDP) is used when discussing historical earthquakes in the Fennoscandian Shield, because intensity cannot always be assessed due to a lack of detailed documentation available there.

The distribution of population and centres of documentation and learning influences how the effects of local and regional earthquakes can be reported in writing. The study area includes the Gulf of Bothnia, where observations can mainly be obtained from islands not far from the coastline. Sometimes observations were made on boats, for instance on 23 June 1882 (Mäntyniemi and Wahlström, 2013). Offshore seismicity cannot be investigated reliably using historical earthquake observations alone, because it can be hard to separate near-shore earthquakes from those further away at the open sea. Individual earthquakes strong enough to be felt on both coasts are an exception. Settlements concentrated along water-ways, so the coastlines can be studied.

Maps allow a quick evaluation of the quantity, spatial distribution, and intensity values of the MDPs available for a given historical earthquake. The maximum intensity, when available and reliable, immediately tells us about possible damages caused by the earthquake, and the distribution and quantity of the MDPs give insights into the uncertainties associated with the earthquake location and magnitude.

The more extensive non-instrumental catalogue may be helpful in the search for rare earthquakes that have no modern counterparts. In particular, there can be large earthquakes that occur far more seldom than small ones. The study region includes a water area, so offshore seismicity cannot be investigated reliably using historical observations alone, except for individual earthquakes strong enough to be felt on both coasts. It was decided to pay special attention to such cases in this project. No single threshold magnitude can be associated with these earthquakes, because magnitude is coupled with epicenter and the width of the Gulf of Bothnia varies. However, microearthquakes are not felt over very long distances, so an earthquake felt both on the eastern and western coast is relatively large.

Contemporary newspapers have reported felt effects of local and regional earthquakes and constitute a valuable source of information, especially for earthquakes for which seismologists did not distribute questionnaires or conduct field studies. Such reports have been widely used in the assessment of macroseismic intensities worldwide (Agnew and Sieh, 1978; Musson, 1986, 1995; Seeger and Armbruster, 1987; Talwani and Sharma, 1999; Downes, 2004; McCue, 2004; Midzi et al., 2013; among many others). Mäntyniemi (2005) improved the macroseismic data sets of two historical earthquakes in the study area with the help of contemporary newspapers.

The search had to be tailored to the investigated time interval. Newspapers published inside the area of perceptibility and local newspapers distributed inside one to two municipalities are promising sources of earthquake reports, but they appeared in northern Fennoscandia rather late. For instance, the Swedish newspaper *Norrbottens Kuriren*, established in Luleå in 1861, was instrumental in publishing felt reports of the 23 June 1882 earthquake from Swedish Lapland (Mäntyniemi and Wahlström, 2013). National newspapers were the main source of information in the latter half of the 1700s. In addition to focusing on specific time intervals, efforts were taken to systematically browse important newspaper titles, in particular Swedish *Inrikes Tidningar* ("Domestic Papers"), established in 1760.

Archives were searched in specific cases. Further information related to the important earthquake of 23 June 1882 was uncovered; however, it was not sufficient to resolve whether intensity value $I = 6$ or $I = 7$ was closer to the true maximum; it was assigned as $I = 6-7$, reflecting uncertainty following from a lack of detailed information. Mäntyniemi (2012a) listed other sources that were considered in the course of the work. They included previous seismological compilations, such as descriptive earthquake catalogues and studies on individual earthquakes (see, e.g., Wahlström, 1990 for references). One limitation is that possible private correspondences and diaries are hard to locate.

A classification of the quality of written source materials was given in Korja et al. (2011). Individual written accounts were divided into three groups according to how detailed they were and how well the event described could be assessed using seismological criteria. Intensities were assessed on the European Macroseismic Scale (EMS-98; Grünthal, 1998). The MDP maps prepared for the historical earthquakes in the study area are given in Mäntyniemi (2012a,b).

Output of the search

Re-appraisal of known historical earthquakes typically resulted in an improved understanding of the area of perceptibility. In many cases, the newspaper reports referred to places not previously listed as ones where the respective earthquake was felt. The uncovered reports were sometimes located on the outskirts of the area of perceptibility, which increases the confidence in the respective macroseismic magnitude. For instance, Mäntyniemi and Wahlström (2013) revised the macroseismic dataset for the earthquakes of 15 June and 23 June 1882. They listed 80 contemporary newspaper reports, out of which 40 were previously disregarded, fully or partly.

In some cases, the uncovered reports improved the intensity assessment for a given place. In particular, archive documentation related to the Norwegian earthquake of 31 August 1819 was found for Tornio, Finland. With the help of the expanded documentation for this town, it could be confirmed that the intensity was not smaller than $I = 4$ (EMS-98) there. Husebye and Kebeasy (2004,

p. 63) proposed to downgrade this intensity value to “Felt (II?)”, but this is ungrounded in the light of the available documentation.

It was not very surprising that not many new historical earthquakes (i.e. dates) were uncovered. Mäntyniemi (2004b) found seven earthquakes attested to by one or two MDPs in Finland in the late 1800s. This supports the notion that the larger earthquakes (wider areas of perceptibility) have not passed unnoticed by earlier compilers of seismological works. Alternatively, some areas of perceptibility are incompletely reported and cannot be resolved using the documentation available.

The problems of investigating seismicity in border areas are well known (e.g., Stucchi, 1993). The Gulf of Bothnia has been crossed by a state border since 1809, and the older times were often forgotten by seismologists, who typically focused on their own territory only. A straightforward task was to combine the MDPs carrying the same time from Finnish and Swedish publications for a number of earthquakes. They include historical earthquakes from the late 1700s until the early 1900s. For example, the largest earthquake in the study area in the 1900s, on 9 March 1909, was investigated separately by Sahlström (1911) for Sweden and Rosberg (1912) for Finland.

The efforts taken to reappraise important historical earthquakes in the study region prior to this project and during it have resulted in 20 revised macroseismic datasets (Table A2.1). Macroseismic data points (MDPs), i.e. triplets with place coordinates and the respective macroseismic intensity accompanied by the place name, are readily available for these earthquakes. Figure A2.1 shows all the available data points with intensity I=2 or above. There are a total of 1230 such data points associated with the 20 earthquakes (data points with information confined to ‘felt’ were not plotted)

Table A2.1 Sets of Macroseismic Data Points (MDPs) available for historical earthquakes in the study area.

No.	Date of earthquake	#(MDPs)	Remarks
1	27 November 1757	4	Felt on the eastern and western coasts of the Gulf of Bothnia
2	14 July 1765	6	Felt on the eastern and western coasts
3	29 March 1777	8	Felt on the eastern coast
4	31 August 1819	5	Only data points in present-day Finland investigated, epicenter in Norway
5	15 June 1882	28	A transfrontier earthquake
6	23 June 1882	99	A transfrontier earthquake, a possible aftershock on 27 July 1882 a separate report comprising the macroseismic data for earthquake #5 and #6 is available
7	1 April 1883	33	A foreshock on 31 March and two aftershocks on 2 April 1883
8	28 July 1888	34	A transfrontier earthquake, reports mainly from Sweden
9	4 November 1898 A	74	A transfrontier earthquake, local time 5 November 1898, a separate report comprising the macroseismic data for earthquake #9 and #10 is available
10	4 November 1898 B	22	The largest aftershock
11	10 April 1902	115	Felt in Russia too
12	7 August 1906	3	A small earthquake close to the NPP site
13	26 May 1907	33	A transfrontier earthquake, reports mainly from Sweden
14	31 December 1908	16	A transfrontier earthquake, places not specified on the eastern coast
15	9 March 1909	147	A transfrontier earthquake
16	26 December 1911	52	Epicenter east of the NPP site
17	5 February 1915	23	Felt around Vaasa, no data from Sweden
18	18 August 1926	171	Kuusamo, felt observations made in Russia too
19	16 November 1931 A	908	Central Finland, main shock
20	16 November 1931 B	368	Central Finland, the largest aftershock

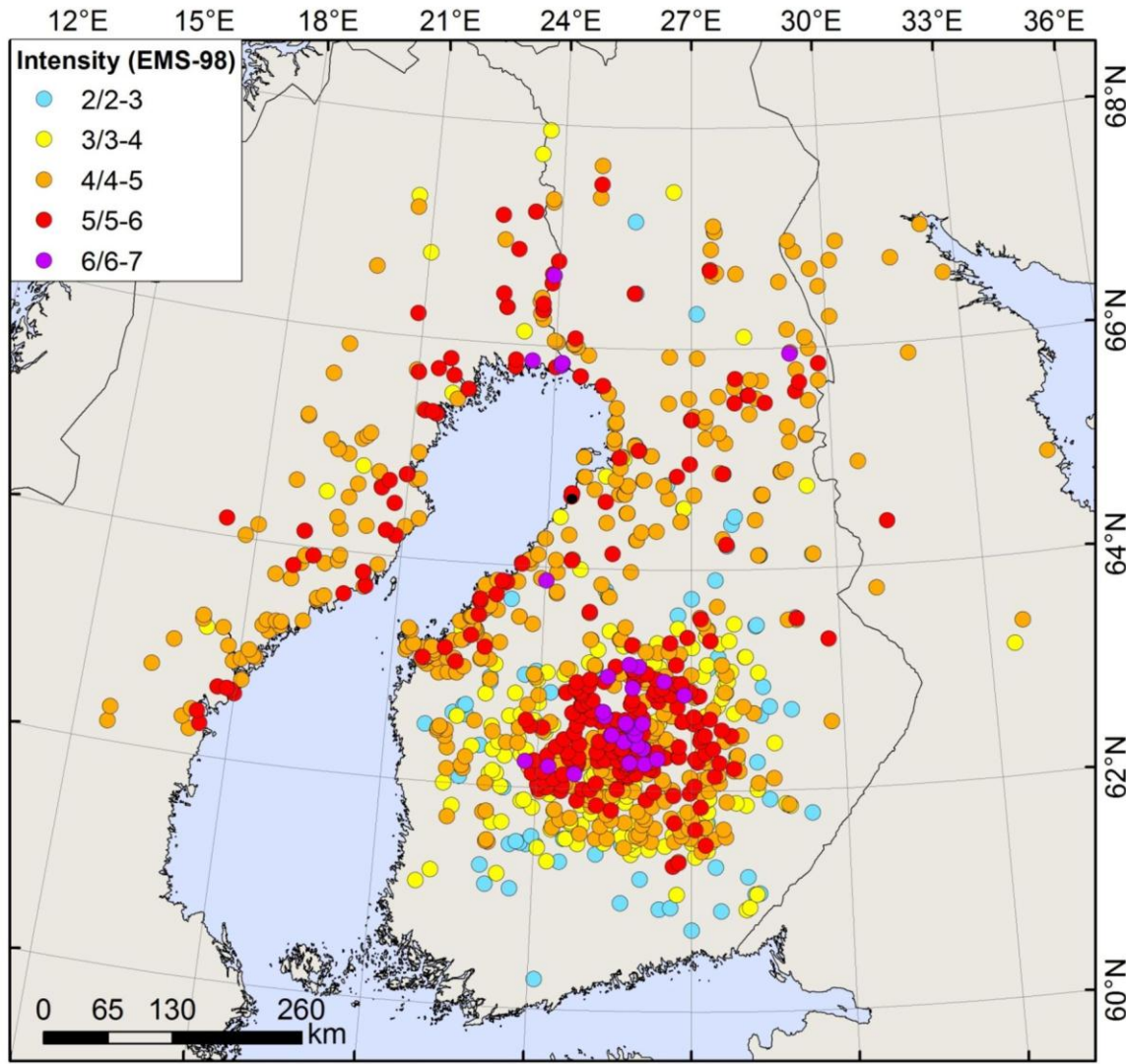


Figure A2.1 The available data points with intensity $I=2$ or above for the 20 historical earthquakes listed in Table A2.1.

Seismic histories

An investigation on the intensities experienced at different places on the Gulf of Bothnia allows seismic histories to be compiled for them. For instance, seismic histories were presented for two coastal towns, Vaasa (Swedish *Vasa*) and Tornio (*Torneå*), from 1730 to 1920. The earthquake effects recorded in writing in Vaasa are attributed to earthquakes in the Gulf of Bothnia and west of it. The maximum effects were estimated at macroseismic intensity $I = 4-5$ (EMS-98). The effects experienced in Tornio are attributed to local earthquakes at the bottom of the Gulf of Bothnia, except for the 1819 Lurøy earthquake in Norway. The maximum intensity recorded in Tornio was estimated at $I = 6-7$ (EMS-98). No historical earthquake was reportedly felt in both towns.

The seismic history of Vaasa shows an absence of earthquake effects between 1787 and 1883. No earthquakes felt in the vicinity of the town, or on both sides of the Gulf of Bothnia, are known from

that time. The gap may follow from a combination of missing reports and an absence of earthquakes. There may have been a seismic quiescence spanning several decades. When the seismicity level increased from 1882 onward, earthquakes surprised observers and no recollections of previous occurrences emerged. The seismic history of Tornio is less intermittent.

In particular, the seismic history of Pyhäjoki from 1740 to 1930 was compiled using the available data (Mäntyniemi, 2012a; see Appendix 1 p. 284). Few primary documents from Pyhäjoki are available, but it can be inferred using reports from surrounding towns that many of the largest known historical earthquakes were felt there. The epicenters of these earthquakes were located in Finnish, Swedish, or Norwegian territory. The estimated intensities experienced at Pyhäjoki were no larger than I = 4 (EMS-98). The compiled seismic history cannot be used to infer the locations of future earthquakes that will be felt in Pyhäjoki and strengths of earthquake effects there.

The revised macroseismic datasets and corresponding MDP maps give an improved understanding of the spatial extent and effects of historical earthquakes in the study area. The most ample datasets allow to reassess macroseismic magnitudes (that can be converted into moment magnitudes) and other macroseismic parameters. The re-assessed parameters are used in computations of seismic hazard for the NPP site.

Appendix 3. Metadatabase

E. Kosonen & T. Huotari-Halkosaari

Stored in Fennovoima Oy
Maintenance: Fennovoima Oy
Contact person: Juho Helander
Address: Salmisaarenaukio 1, FI-00180 Helsinki, Finland

Appendix 4. Seismic source area coordinates

E. Kosonen

Table A4.1. Seismic source areas and coordinates for spatial model 1 (section 8.2).

Polygon	POINT X (m)	POINT Y (m)	Point X	Point Y	Polygon	POINT X (m)	POINT Y (m)	Point X	Point Y
1.1	43226.31	7555019.17	16.1444	67.7484	1.12	336312.61	7186687.29	23.5578	64.7648
1.1	206445.40	7632618.61	19.7607	68.6498	1.12	532281.35	7477019.13	27.7530	67.4076
1.1	205775.80	7623725.81	19.7700	68.5700	1.12	556504.12	7544039.93	28.3520	68.0050
1.1	128073.27	7490607.99	18.3410	67.2981	1.12	511607.14	7544369.76	27.2778	68.0133
1.1	5811.95	7203050.43	16.6431	64.5881	1.12	445633.48	7566867.07	25.6875	68.2101
1.1	17782.94	7148163.17	17.0676	64.1204	1.12	393708.89	7604213.67	24.3971	68.5301
1.1	-8675.45	7137579.81	16.5686	63.9891	1.12	422788.07	7656658.17	25.0683	69.0097
1.1	-43926.36	7118880.27	15.9274	63.7713	1.12	508035.16	7643224.84	27.2000	68.9000
1.1	-126834.64	7037026.60	14.6029	62.9167	1.12	590081.40	7607839.22	29.2095	68.5683
1.1	-117864.42	7275535.98	13.8123	65.0201	1.12	659429.29	7566266.24	30.8432	68.1654
1.1	43226.31	7555019.17	16.1444	67.7484	1.12	739491.23	7494835.51	32.6077	67.4720
1.2	128073.27	7490607.99	18.3410	67.2981	1.12	700915.88	7456292.44	31.6412	67.1562
1.2	205775.80	7623725.81	19.7700	68.5700	1.12	644423.53	7424059.47	30.3000	66.9000
1.2	263591.74	7610516.55	21.2110	68.5070	1.12	579861.00	7424641.29	28.8265	66.9290
1.2	157175.19	7465763.18	19.0834	67.1123	1.12	577263.71	7386545.71	28.7428	66.5881
1.2	128073.27	7490607.99	18.3410	67.2981	1.12	589693.22	7354783.16	29.0000	66.3000
1.3	-126834.64	7037026.60	14.6029	62.9167	1.12	535487.97	7304004.92	27.7775	65.8553
1.3	-43926.36	7118880.27	15.9274	63.7713	1.12	482845.52	7286877.14	26.6264	65.7032
1.3	-8675.45	7137579.81	16.5686	63.9891	1.12	474112.61	7220868.73	26.4488	65.1104
1.3	17782.94	7148163.17	17.0676	64.1204	1.12	485442.84	7112590.04	26.7009	64.1395
1.3	5811.95	7203050.43	16.6431	64.5881	1.12	459149.02	7089457.87	26.1669	63.9298
1.3	128073.27	7490607.99	18.3410	67.2981	1.12	336312.61	7186687.29	23.5578	64.7648
1.3	157175.19	7465763.18	19.0834	67.1123	1.13	336312.61	7186687.29	23.5578	64.7648
1.3	235272.09	7322290.37	21.1808	65.9111	1.13	459149.02	7089457.87	26.1669	63.9298
1.3	230770.24	7285305.47	21.1578	65.5773	1.13	628939.15	6920156.90	29.4942	62.3904
1.3	162231.07	7207243.29	19.8739	64.8183	1.13	728269.53	6812374.62	31.2735	61.3780
1.3	169851.31	7152037.50	20.1583	64.3341	1.13	637428.21	6738087.06	29.5219	60.7545
1.3	130699.07	7086556.33	19.5137	63.7116	1.13	606849.70	6768064.83	28.9778	61.0329
1.3	53238.25	7057640.75	18.0461	63.3658	1.13	514368.41	6794380.36	27.2681	61.2834
1.3	-7996.59	7005905.71	17.0001	62.8271	1.13	447111.04	6757100.65	26.0238	60.9454
1.3	-77831.43	6863552.56	16.1200	61.4700	1.13	406268.53	6660524.78	25.3158	60.0711
1.3	-126834.64	7037026.60	14.6029	62.9167	1.13	269389.98	6662954.06	22.8589	60.0388
1.4	48014.89	6957139.18	18.2160	62.4681	1.13	154833.08	6702512.82	20.7465	60.3117
1.4	-54377.20	6911362.27	16.4074	61.9262	1.13	54636.72	6758301.69	18.8253	60.7103
1.4	-7996.59	7005905.71	17.0001	62.8271	1.13	-4786.41	6827004.07	17.5704	61.2485
1.4	53238.88	7057663.22	18.0460	63.3660	1.13	13529.96	6845991.54	17.8580	61.4400
1.4	130699.07	7086556.33	19.5137	63.7116	1.13	48014.89	6957139.18	18.2160	62.4681
1.4	169851.31	7152037.50	20.1583	64.3341	1.13	186591.05	7089344.08	20.6319	63.7907
1.4	186591.05	7089344.08	20.6319	63.7907	1.13	211286.90	6996853.59	21.2973	62.9861
1.4	48014.89	6957139.18	18.2160	62.4681	1.13	251305.21	6983293.66	22.1044	62.8944
1.5	-54377.20	6911362.27	16.4074	61.9262	1.13	272809.27	7112773.95	22.3408	64.0668

1.5	48014.89	6957139.18	18.2160	62.4681	1.13	336312.61	7186687.29	23.5578	64.7648
1.5	13529.96	6845991.54	17.8580	61.4400	1.14	406268.53	6660524.78	25.3158	60.0711
1.5	-26378.77	6804620.57	17.2357	61.0220	1.14	434768.73	6727702.19	25.8059	60.6797
1.5	-77831.43	6863552.56	16.1200	61.4700	1.14	447111.04	6757100.65	26.0238	60.9454
1.5	-54377.20	6911362.27	16.4074	61.9262	1.14	514368.41	6794380.36	27.2681	61.2834
1.6	157175.19	7465763.18	19.0834	67.1123	1.14	606849.70	6768064.83	28.9778	61.0329
1.6	263591.74	7610516.55	21.2110	68.5070	1.14	637428.21	6738087.06	29.5219	60.7545
1.6	205775.80	7623725.81	19.7700	68.5700	1.14	588359.26	6709629.62	28.6092	60.5130
1.6	206445.40	7632618.61	19.7607	68.6498	1.14	531774.12	6687018.47	27.5752	60.3185
1.6	272362.51	7650281.05	21.3350	68.8692	1.14	472096.48	6670460.27	26.4972	60.1701
1.6	335406.75	7658515.57	22.8842	68.9877	1.14	406268.53	6660524.78	25.3158	60.0711
1.6	278279.10	7536610.23	21.7230	67.8590	1.15	535487.97	7304004.92	27.7775	65.8553
1.6	265976.26	7475083.12	21.5600	67.3000	1.15	610234.45	7250649.53	29.3700	65.3600
1.6	304257.60	7442640.11	22.5006	67.0375	1.15	601477.56	7218450.04	29.1582	65.0741
1.6	235272.09	7322290.37	21.1808	65.9111	1.15	524044.32	7110639.85	27.4937	64.1214
1.6	157175.19	7465763.18	19.0834	67.1123	1.15	485442.84	7112590.04	26.7009	64.1395
1.7	265976.26	7475083.12	21.5600	67.3000	1.15	474112.61	7220868.73	26.4488	65.1104
1.7	278279.10	7536610.23	21.7230	67.8590	1.15	482845.52	7286877.14	26.6264	65.7032
1.7	401380.79	7799286.88	24.3805	70.2806	1.15	535487.97	7304004.92	27.7775	65.8553
1.7	490280.96	7778649.34	26.7440	70.1144	1.16	535487.97	7304004.92	27.7775	65.8553
1.7	304257.60	7442640.11	22.5006	67.0375	1.16	589693.22	7354783.16	29.0000	66.3000
1.7	265976.26	7475083.12	21.5600	67.3000	1.16	661732.80	7311704.49	30.5490	65.8853
1.8	255224.94	7325976.62	21.6100	65.9600	1.16	610234.45	7250649.53	29.3700	65.3600
1.8	235272.09	7322290.37	21.1808	65.9111	1.16	535487.97	7304004.92	27.7775	65.8553
1.8	304024.15	7442175.03	22.4960	67.0332	1.17	589693.22	7354783.16	29.0000	66.3000
1.8	393708.89	7604213.67	24.3971	68.5301	1.17	577263.71	7386545.71	28.7428	66.5881
1.8	445633.48	7566867.07	25.6875	68.2101	1.17	579861.00	7424641.29	28.8265	66.9290
1.8	511607.14	7544369.76	27.2778	68.0133	1.17	644423.53	7424059.47	30.3000	66.9000
1.8	450223.20	7489502.96	25.8335	67.5172	1.17	700915.88	7456292.44	31.6412	67.1562
1.8	359939.20	7353411.77	23.8801	66.2692	1.17	739491.23	7494835.51	32.6077	67.4720
1.8	255224.94	7325976.62	21.6100	65.9600	1.17	796658.86	7434629.63	33.7825	66.8841
1.9	255224.94	7325976.62	21.6100	65.9600	1.17	827117.44	7358813.36	34.2713	66.1784
1.9	359939.20	7353411.77	23.8801	66.2692	1.17	720627.38	7349797.43	31.9017	66.1906
1.9	319444.29	7202129.62	23.1844	64.8944	1.17	661732.80	7311704.49	30.5490	65.8853
1.9	230770.24	7285305.47	21.1578	65.5773	1.17	589693.22	7354783.16	29.0000	66.3000
1.9	235272.09	7322290.37	21.1808	65.9111	1.18	728269.53	6812374.62	31.2735	61.3780
1.9	255224.94	7325976.62	21.6100	65.9600	1.18	628939.15	6920156.90	29.4942	62.3904
1.10	162231.07	7207243.29	19.8739	64.8183	1.18	459149.02	7089457.87	26.1669	63.9298
1.10	230770.24	7285305.47	21.1578	65.5773	1.18	485442.84	7112590.04	26.7009	64.1395
1.10	319444.29	7202129.62	23.1844	64.8944	1.18	524044.32	7110639.85	27.4937	64.1214
1.10	336312.61	7186687.29	23.5578	64.7648	1.18	601477.56	7218450.04	29.1582	65.0741
1.10	272809.27	7112773.95	22.3408	64.0668	1.18	610234.45	7250649.53	29.3700	65.3600
1.10	251305.21	6983293.66	22.1044	62.8944	1.18	661732.80	7311704.49	30.5490	65.8853
1.10	211286.90	6996853.59	21.2973	62.9861	1.18	720627.38	7349797.43	31.9017	66.1906
1.10	186591.05	7089344.08	20.6319	63.7907	1.18	827117.44	7358813.36	34.2713	66.1784
1.10	169851.31	7152037.50	20.1583	64.3341	1.18	865486.93	7249302.23	34.8138	65.1632
1.10	162231.07	7207243.29	19.8739	64.8183	1.18	867993.63	7136855.51	34.5807	64.1605
1.11	359939.20	7353411.77	23.8801	66.2692	1.18	846959.01	7014394.83	33.8811	63.0915

1.11	450223.20	7489502.96	25.8335	67.5172	1.18	794732.72	6898201.80	32.6508	62.1002
1.11	511607.14	7544369.76	27.2778	68.0133	1.18	728269.53	6812374.62	31.2735	61.3780
1.11	556504.12	7544039.93	28.3520	68.0050					
1.11	532281.35	7477019.13	27.7530	67.4076					
1.11	336312.61	7186687.29	23.5578	64.7648					
1.11	319444.29	7202129.62	23.1844	64.8944					
1.11	359939.20	7353411.77	23.8801	66.2692					

Table A4.2. Seismic source areas and coordinates for spatial model 2 (section 8.3).

Polygon	POINT X (m)	POINT Y (m)	Point X	Point Y	Polygon	POINT X (m)	POINT Y (m)	Point X	Point Y
2.1	235956.93	7694414.36	20.3169	69.2299	2.8	729146.71	7505939.91	32.3894	67.5794
2.1	104024.88	7481694.14	17.8201	67.1883	2.8	594498.48	7374194.37	29.1217	66.4726
2.1	-4549.80	7375326.22	15.7954	66.0908	2.8	496939.87	7279005.27	26.9335	65.6330
2.1	-8780.52	7343736.89	15.8272	65.8061	2.8	451960.47	7235047.12	25.9722	65.2351
2.1	29708.05	7316689.03	16.7512	65.6261	2.8	434604.77	7253768.80	25.5921	65.4000
2.1	5234.04	7224746.14	16.5570	64.7788	2.8	392721.08	7306647.74	24.6485	65.8630
2.1	33015.35	7195641.92	17.2267	64.5612	2.8	389732.60	7327353.77	24.5655	66.0476
2.1	38968.48	7159923.10	17.4605	64.2533	2.8	584400.65	7554775.55	29.0275	68.0944
2.1	-57.63	7141402.23	16.7294	64.0354	2.8	617963.95	7592941.35	29.8754	68.4245
2.1	-94640.86	7108986.43	14.9587	63.6026	2.8	729146.71	7505939.91	32.3894	67.5794
2.1	-158633.06	7029027.61	14.0242	62.7909	2.9	522838.35	7118422.11	27.4701	64.1914
2.1	-166448.24	6962371.35	14.1329	62.1939	2.9	504158.64	7091079.21	27.0849	63.9467
2.1	-320617.28	6960199.65	11.2863	61.8732	2.9	481062.40	7154643.87	26.6055	64.5166
2.1	-330142.30	7098841.60	10.4467	63.0476	2.9	451960.47	7235047.12	25.9722	65.2351
2.1	-111066.86	7360250.45	13.5731	65.7725	2.9	496939.87	7279005.27	26.9335	65.6330
2.1	-17340.72	7477603.13	15.0905	66.9687	2.9	594498.48	7374194.37	29.1217	66.4726
2.1	25390.97	7523299.63	15.8643	67.4409	2.9	729146.71	7505939.91	32.3894	67.5794
2.1	118613.98	7608937.23	17.7136	68.3343	2.9	763449.73	7466246.19	33.0994	67.1967
2.1	195078.72	7694017.48	19.2944	69.1834	2.9	804651.61	7404116.52	33.8869	66.6044
2.1	235956.93	7694414.36	20.3169	69.2299	2.9	522838.35	7118422.11	27.4701	64.1914
2.2	104024.88	7481694.14	17.8201	67.1883	2.10	490746.47	7071446.82	26.8124	63.7704
2.2	206456.88	7432599.38	20.2931	66.8690	2.10	522838.35	7118422.11	27.4701	64.1914
2.2	245015.74	7382554.88	21.2729	66.4571	2.10	804651.61	7404116.52	33.8869	66.6044
2.2	253020.94	7328037.34	21.5578	65.9767	2.10	839853.64	7326456.63	34.4662	65.8771
2.2	230848.84	7270065.16	21.1900	65.4413	2.10	860727.10	7249861.67	34.7146	65.1734
2.2	194201.93	7276399.36	20.3906	65.4655	2.10	866264.12	7206969.15	34.7203	64.7859
2.2	167341.02	7247173.25	19.8863	65.1789	2.10	868511.79	7159612.81	34.6474	64.3624
2.2	160415.01	7141063.28	19.9895	64.2271	2.10	864753.98	7098427.09	34.4229	63.8220
2.2	147126.47	7125443.27	19.7543	64.0747	2.10	850478.80	7026542.14	33.9763	63.1963
2.2	55874.25	7045261.76	18.1322	63.2593	2.10	812744.97	6930141.95	33.0510	62.3708
2.2	-14242.33	6983383.76	16.9480	62.6194	2.10	721617.75	6805612.56	31.1413	61.3213
2.2	-60657.00	6903070.12	16.3157	61.8439	2.10	548954.92	6975138.29	27.9633	62.9029
2.2	-166448.24	6962371.35	14.1329	62.1939	2.10	510854.84	7003713.35	27.2155	63.1625
2.2	-158633.06	7029027.61	14.0242	62.7909	2.10	490746.47	7071446.82	26.8124	63.7704
2.2	-94640.86	7108986.43	14.9587	63.6026	2.11	335801.46	7182142.79	23.5522	64.7238
2.2	-57.63	7141402.23	16.7294	64.0354	2.11	434604.77	7253768.80	25.5921	65.4000

2.2	38968.48	7159923.10	17.4605	64.2533	2.11	451960.47	7235047.12	25.9722	65.2351
2.2	33015.35	7195641.92	17.2267	64.5612	2.11	481062.40	7154643.87	26.6055	64.5166
2.2	5234.04	7224746.14	16.5570	64.7788	2.11	504158.64	7091079.21	27.0849	63.9467
2.2	29708.05	7316689.03	16.7512	65.6261	2.11	490746.47	7071446.82	26.8124	63.7704
2.2	-8780.52	7343736.89	15.8272	65.8061	2.11	510854.84	7003713.35	27.2155	63.1625
2.2	-4549.80	7375326.22	15.7954	66.0908	2.11	548954.92	6975138.29	27.9633	62.9029
2.2	104024.88	7481694.14	17.8201	67.1883	2.11	721617.75	6805612.56	31.1413	61.3213
2.3	62224.79	6967702.12	18.4615	62.5789	2.11	638217.79	6738276.46	29.5365	60.7560
2.3	23969.23	6879651.20	17.9641	61.7514	2.11	610295.85	6770584.77	29.0430	61.0546
2.3	-11650.12	6834840.71	17.4229	61.3090	2.11	554501.59	6785041.44	28.0140	61.1960
2.3	-62866.76	6817782.92	16.5330	61.0880	2.11	527613.39	6806303.59	27.5169	61.3897
2.3	-106370.11	6830356.03	15.7018	61.1343	2.11	493217.49	6793735.86	26.8735	61.2778
2.3	-60657.00	6903070.12	16.3157	61.8439	2.11	445154.07	6766214.04	25.9851	61.0269
2.3	62224.79	6967702.12	18.4615	62.5789	2.11	431390.39	6706380.44	25.7515	60.4877
2.4	160415.01	7141063.28	19.9895	64.2271	2.11	445108.19	6677500.58	26.0090	60.2306
2.4	172813.88	7119462.39	20.2901	64.0466	2.11	470858.85	6670199.82	26.4749	60.1677
2.4	147213.57	7060181.38	19.9043	63.4937	2.11	360934.13	6659682.46	24.5026	60.0507
2.4	62224.79	6967702.12	18.4615	62.5789	2.11	158810.89	6704779.67	20.8143	60.3353
2.4	-60657.00	6903070.12	16.3157	61.8439	2.11	33206.86	6790437.11	18.3598	60.9712
2.4	-14242.33	6983383.76	16.9480	62.6194	2.11	-11650.12	6834840.71	17.4229	61.3090
2.4	147126.47	7125443.27	19.7543	64.0747	2.11	23969.23	6879651.20	17.9641	61.7514
2.4	160415.01	7141063.28	19.9895	64.2271	2.11	62224.79	6967702.12	18.4615	62.5789
2.5	194201.93	7276399.36	20.3906	65.4655	2.11	147213.57	7060181.38	19.9043	63.4937
2.5	230848.84	7270065.16	21.1900	65.4413	2.11	172813.88	7119462.39	20.2901	64.0466
2.5	302102.22	7206967.57	22.8123	64.9278	2.11	182358.54	7082151.44	20.5613	63.7228
2.5	335801.46	7182142.79	23.5522	64.7238	2.11	195482.15	7051706.07	20.8842	63.4627
2.5	300362.94	7150943.24	22.8531	64.4254	2.11	265967.04	7102788.98	22.2164	63.9730
2.5	265967.04	7102788.98	22.2164	63.9730	2.11	300362.94	7150943.24	22.8531	64.4254
2.5	195482.15	7051706.07	20.8842	63.4627	2.11	335801.46	7182142.79	23.5522	64.7238
2.5	182358.54	7082151.44	20.5613	63.7228	2.12	638217.79	6738276.46	29.5365	60.7560
2.5	172813.88	7119462.39	20.2901	64.0466	2.12	575225.24	6704344.16	28.3681	60.4683
2.5	160415.01	7141063.28	19.9895	64.2271	2.12	518056.31	6682156.56	27.3264	60.2757
2.5	167341.02	7247173.25	19.8863	65.1789	2.12	470858.85	6670199.82	26.4749	60.1677
2.5	194201.93	7276399.36	20.3906	65.4655	2.12	445108.19	6677500.58	26.0090	60.2306
2.6	253020.94	7328037.34	21.5578	65.9767	2.12	431390.39	6706380.44	25.7515	60.4877
2.6	313121.01	7327892.41	22.8775	66.0165	2.12	445154.07	6766214.04	25.9851	61.0269
2.6	389732.60	7327353.77	24.5655	66.0476	2.12	493217.49	6793735.86	26.8735	61.2778
2.6	392721.08	7306647.74	24.6485	65.8630	2.12	527613.39	6806303.59	27.5169	61.3897
2.6	434604.77	7253768.80	25.5921	65.4000	2.12	554501.59	6785041.44	28.0140	61.1960
2.6	335801.46	7182142.79	23.5522	64.7238	2.12	610295.85	6770584.77	29.0430	61.0546
2.6	302102.22	7206967.57	22.8123	64.9278	2.12	638217.79	6738276.46	29.5365	60.7560
2.6	230848.84	7270065.16	21.1900	65.4413					
2.6	253020.94	7328037.34	21.5578	65.9767					
2.7	104024.88	7481694.14	17.8201	67.1883					
2.7	195127.00	7628587.99	19.4966	68.6018					
2.7	306847.26	7657636.49	22.1747	68.9612					
2.7	419014.77	7657055.72	24.9736	69.0122					
2.7	540709.77	7629025.06	28.0074	68.7698					

2.7	579820.92	7612766.71	28.9619	68.6155
2.7	617963.95	7592941.35	29.8754	68.4245
2.7	584400.65	7554775.55	29.0275	68.0944
2.7	389732.60	7327353.77	24.5655	66.0476
2.7	313121.34	7327892.41	22.8775	66.0165
2.7	253020.94	7328037.34	21.5578	65.9767
2.7	245015.74	7382554.88	21.2729	66.4571
2.7	206456.88	7432599.38	20.2931	66.8690
2.7	104024.88	7481694.14	17.8201	67.1883

Table A4.3. Seismic source areas and coordinates for spatial model 3 (section 8.3).

Polygon	POINT X (m)	POINT Y (m)	Point X	Point Y	Polygon	POINT X (m)	POINT Y (m)	Point X	Point Y
3.1	235956.93	7694414.36	20.3169	69.2299	3.13	195127.00	7628587.99	19.4966	68.6018
3.1	104024.88	7481694.14	17.8201	67.1883	3.13	235956.93	7694414.36	20.3169	69.2299
3.1	-4549.80	7375326.22	15.7954	66.0908	3.13	305244.51	7805464.03	21.8228	70.2807
3.1	-8780.52	7343736.89	15.8272	65.8061	3.13	373214.98	7814324.13	23.6115	70.4028
3.1	29708.05	7316689.03	16.7512	65.6261	3.13	404547.69	7787798.80	24.4771	70.1789
3.1	5234.04	7224746.14	16.5570	64.7788	3.13	343412.94	7702073.63	23.0131	69.3821
3.1	33015.35	7195641.92	17.2267	64.5612	3.13	303725.36	7621110.97	22.1687	68.6326
3.1	38968.48	7159923.10	17.4605	64.2533	3.13	279912.82	7561579.60	21.7109	68.0833
3.1	-57.63	7141402.23	16.7294	64.0354	3.13	275608.18	7600820.79	21.5246	68.4303
3.1	-94640.86	7108986.43	14.9587	63.6026	3.13	266083.16	7617489.57	21.2557	68.5713
3.1	-158633.06	7029027.61	14.0242	62.7909	3.13	232318.89	7633586.49	20.3907	68.6845
3.1	-166448.24	6962371.35	14.1329	62.1939	3.13	195127.00	7628587.99	19.4966	68.6018
3.1	-320617.28	6960199.65	11.2863	61.8732	3.14	410173.24	7559966.23	24.8379	68.1393
3.1	-330142.30	7098841.60	10.4467	63.0476	3.14	380287.16	7611245.81	24.0608	68.5877
3.1	-111066.86	7360250.45	13.5731	65.7725	3.14	398215.48	7658729.72	24.4521	69.0202
3.1	-17340.72	7477603.13	15.0905	66.9687	3.14	431778.12	7690988.45	25.2688	69.3198
3.1	25390.97	7523299.63	15.8643	67.4409	3.14	474469.24	7740586.71	26.3384	69.7720
3.1	118613.98	7608937.23	17.7136	68.3343	3.14	483113.22	7777480.03	26.5554	70.1035
3.1	195078.72	7694017.48	19.2944	69.1834	3.14	511052.96	7761806.98	27.2891	69.9633
3.1	235956.93	7694414.36	20.3169	69.2299	3.14	535224.51	7702232.42	27.8982	69.4270
3.2	104024.88	7481694.14	17.8201	67.1883	3.14	554274.55	7660163.59	28.3600	69.0466
3.2	195127.00	7628587.99	19.4966	68.6018	3.14	553702.40	7624052.73	28.3262	68.7230
3.2	232318.89	7633586.49	20.3907	68.6845	3.14	580393.87	7612499.10	28.9757	68.6130
3.2	266083.16	7617489.57	21.2557	68.5713	3.14	617963.95	7592941.35	29.8754	68.4245
3.2	275608.18	7600820.79	21.5246	68.4303	3.14	584400.65	7554775.55	29.0275	68.0944
3.2	279912.82	7561579.60	21.7109	68.0833	3.14	529331.94	7571133.73	27.7094	68.2520
3.2	233875.22	7466329.41	20.8389	67.1950	3.14	506804.39	7570390.24	27.1645	68.2468
3.2	206456.88	7432599.38	20.2931	66.8690	3.14	453887.62	7602140.31	25.8711	68.5279
3.2	104024.88	7481694.14	17.8201	67.1883	3.14	410173.24	7559966.23	24.8379	68.1393
3.3	104024.88	7481694.14	17.8201	67.1883	3.15	506804.39	7570390.24	27.1645	68.2468
3.3	150288.52	7459520.38	18.9449	67.0489	3.15	529331.94	7571133.73	27.7094	68.2520
3.3	206456.88	7432599.38	20.2931	66.8690	3.15	584400.65	7554775.55	29.0275	68.0944
3.3	233875.22	7466329.41	20.8389	67.1950	3.15	525529.41	7485945.88	27.5975	67.4884
3.3	255540.56	7458421.00	21.3539	67.1429	3.15	437868.90	7383589.22	25.5999	66.5650

3.3	292793.97	7453764.32	22.2186	67.1293	3.15	424025.29	7402039.19	25.2767	66.7274
3.3	311420.67	7459056.00	22.6382	67.1889	3.15	394621.16	7420106.61	24.5945	66.8806
3.3	287850.33	7428229.34	22.1508	66.8976	3.15	443304.26	7499481.77	25.6664	67.6054
3.3	245015.74	7382554.88	21.2729	66.4571	3.15	506804.39	7570390.24	27.1645	68.2468
3.3	253020.94	7328037.34	21.5578	65.9767	3.16	729146.05	7505939.91	32.3894	67.5794
3.3	230848.84	7270065.16	21.1900	65.4413	3.16	594498.48	7374194.37	29.1217	66.4726
3.3	194201.93	7276399.36	20.3906	65.4655	3.16	496939.87	7279005.27	26.9335	65.6330
3.3	167341.02	7247173.25	19.8863	65.1789	3.16	451960.47	7235047.12	25.9722	65.2351
3.3	160415.01	7141063.28	19.9895	64.2271	3.16	434604.77	7253768.80	25.5921	65.4000
3.3	147126.47	7125443.27	19.7543	64.0747	3.16	392721.08	7306647.74	24.6485	65.8630
3.3	55874.25	7045261.76	18.1322	63.2593	3.16	389732.60	7327353.77	24.5655	66.0476
3.3	-14242.33	6983383.76	16.9480	62.6194	3.16	584400.65	7554775.55	29.0275	68.0944
3.3	-60657.00	6903070.12	16.3157	61.8439	3.16	617963.95	7592941.35	29.8754	68.4245
3.3	-166448.24	6962371.35	14.1329	62.1939	3.16	729146.05	7505939.91	32.3894	67.5794
3.3	-158633.06	7029027.61	14.0242	62.7909	3.17	522838.35	7118422.11	27.4701	64.1914
3.3	-123831.03	7072513.06	14.5261	63.2329	3.17	504158.64	7091079.21	27.0849	63.9467
3.3	-94640.86	7108986.43	14.9587	63.6026	3.17	481062.40	7154643.87	26.6055	64.5166
3.3	-57.63	7141402.23	16.7294	64.0354	3.17	451960.47	7235047.12	25.9722	65.2351
3.3	38968.48	7159923.10	17.4605	64.2533	3.17	496939.87	7279005.27	26.9335	65.6330
3.3	33015.35	7195641.92	17.2267	64.5612	3.17	584701.66	7208116.47	28.7954	64.9862
3.3	5234.04	7224746.14	16.5570	64.7788	3.17	682244.13	7306333.46	30.9904	65.8262
3.3	29708.05	7316689.03	16.7512	65.6261	3.17	594498.48	7374194.37	29.1217	66.4726
3.3	-8780.52	7343736.89	15.8272	65.8061	3.17	729146.71	7505939.91	32.3894	67.5794
3.3	-4549.80	7375326.22	15.7954	66.0908	3.17	763449.73	7466246.19	33.0994	67.1967
3.3	104024.88	7481694.14	17.8201	67.1883	3.17	804651.61	7404116.52	33.8869	66.6044
3.4	62224.79	6967702.12	18.4615	62.5789	3.17	522838.35	7118422.11	27.4701	64.1914
3.4	23969.23	6879651.20	17.9641	61.7514	3.18	496939.87	7279005.27	26.9335	65.6330
3.4	-11650.12	6834840.71	17.4229	61.3090	3.18	594498.48	7374194.37	29.1217	66.4726
3.4	-62866.76	6817782.92	16.5330	61.0880	3.18	682244.13	7306333.46	30.9904	65.8262
3.4	-106370.11	6830356.03	15.7018	61.1343	3.18	584701.66	7208116.47	28.7954	64.9862
3.4	-60657.00	6903070.12	16.3157	61.8439	3.18	496939.87	7279005.27	26.9335	65.6330
3.4	62224.79	6967702.12	18.4615	62.5789	3.19	490746.47	7071446.82	26.8124	63.7704
3.5	55874.25	7045261.76	18.1322	63.2593	3.19	522838.35	7118422.11	27.4701	64.1914
3.5	147126.47	7125443.27	19.7543	64.0747	3.19	804651.61	7404116.52	33.8869	66.6044
3.5	137846.01	7088424.32	19.6528	63.7357	3.19	839853.64	7326456.63	34.4662	65.8771
3.5	121247.36	7031926.64	19.4539	63.2156	3.19	860727.10	7249861.67	34.7146	65.1734
3.5	62224.79	6967702.12	18.4615	62.5789	3.19	866264.12	7206969.15	34.7203	64.7859
3.5	-60657.00	6903070.12	16.3157	61.8439	3.19	868511.79	7159612.81	34.6474	64.3624
3.5	-14242.33	6983383.76	16.9480	62.6194	3.19	864753.98	7098427.09	34.4229	63.8220
3.5	55874.25	7045261.76	18.1322	63.2593	3.19	850478.80	7026542.14	33.9763	63.1963
3.6	121247.36	7031926.64	19.4539	63.2156	3.19	812744.97	6930141.95	33.0510	62.3708
3.6	137846.01	7088424.32	19.6528	63.7357	3.19	721617.75	6805612.56	31.1413	61.3213
3.6	147126.47	7125443.27	19.7543	64.0747	3.19	548954.92	6975138.29	27.9633	62.9029
3.6	160415.01	7141063.28	19.9895	64.2271	3.19	510854.84	7003713.35	27.2155	63.1625
3.6	167341.02	7247173.25	19.8863	65.1789	3.19	490746.47	7071446.82	26.8124	63.7704
3.6	194201.93	7276399.36	20.3906	65.4655	3.20	346700.12	7190043.62	23.7722	64.7997
3.6	230848.84	7270065.16	21.1900	65.4413	3.20	345251.32	7253616.12	23.6713	65.3685
3.6	277424.76	7228820.40	22.2575	65.1077	3.20	383325.13	7216594.38	24.5204	65.0525

3.6	237994.12	7206635.96	21.4631	64.8807	3.20	434604.77	7253768.80	25.5921	65.4000
3.6	253377.63	7159226.17	21.8675	64.4687	3.20	451960.47	7235047.12	25.9722	65.2351
3.6	215722.41	7115218.40	21.1721	64.0466	3.20	481062.40	7154643.87	26.6055	64.5166
3.6	240755.55	7077750.52	21.7457	63.7314	3.20	504158.64	7091079.21	27.0849	63.9467
3.6	232126.61	7069180.81	21.5864	63.6483	3.20	490746.47	7071446.82	26.8124	63.7704
3.6	181831.00	7028705.10	20.6576	63.2456	3.20	510854.84	7003713.35	27.2155	63.1625
3.6	162805.64	7054364.11	20.2276	63.4570	3.20	548954.92	6975138.29	27.9633	62.9029
3.6	147213.57	7060181.38	19.9043	63.4937	3.20	721617.75	6805612.56	31.1413	61.3213
3.6	121247.36	7031926.64	19.4539	63.2156	3.20	638217.79	6738276.46	29.5365	60.7560
3.7	310773.73	7280989.31	22.8934	65.5954	3.20	610295.85	6770584.77	29.0430	61.0546
3.7	345251.32	7253616.12	23.6713	65.3685	3.20	554501.59	6785041.44	28.0140	61.1960
3.7	346700.12	7190043.62	23.7722	64.7997	3.20	527613.39	6806303.59	27.5169	61.3897
3.7	335801.46	7182142.79	23.5522	64.7238	3.20	493217.49	6793735.86	26.8735	61.2778
3.7	300362.94	7150943.24	22.8531	64.4254	3.20	445154.07	6766214.04	25.9851	61.0269
3.7	265967.04	7102788.98	22.2164	63.9730	3.20	431390.39	6706380.44	25.7515	60.4877
3.7	240755.55	7077750.52	21.7457	63.7314	3.20	445108.19	6677500.58	26.0090	60.2306
3.7	215722.41	7115218.40	21.1721	64.0466	3.20	470858.85	6670199.82	26.4749	60.1677
3.7	253377.63	7159226.17	21.8675	64.4687	3.20	360934.13	6659682.46	24.5026	60.0507
3.7	237994.12	7206635.96	21.4631	64.8807	3.20	158810.89	6704779.67	20.8143	60.3353
3.7	277424.76	7228820.40	22.2575	65.1077	3.20	33206.86	6790437.11	18.3598	60.9712
3.7	302102.22	7206967.57	22.8123	64.9278	3.20	-11650.12	6834840.71	17.4229	61.3090
3.7	310773.73	7280989.31	22.8934	65.5954	3.20	23969.23	6879651.20	17.9641	61.7514
3.8	302102.22	7206967.57	22.8123	64.9278	3.20	62224.79	6967702.12	18.4615	62.5789
3.8	230848.84	7270065.16	21.1900	65.4413	3.20	147213.57	7060181.38	19.9043	63.4937
3.8	253020.94	7328037.34	21.5578	65.9767	3.20	162805.64	7054364.11	20.2276	63.4570
3.8	313121.01	7327892.41	22.8775	66.0165	3.20	181831.00	7028705.10	20.6576	63.2456
3.8	310773.73	7280989.31	22.8934	65.5954	3.20	232126.61	7069180.81	21.5864	63.6483
3.8	302102.22	7206967.57	22.8123	64.9278	3.20	240755.55	7077750.52	21.7457	63.7314
3.9	313121.01	7327892.41	22.8775	66.0165	3.20	265967.04	7102788.98	22.2164	63.9730
3.9	389732.60	7327353.77	24.5655	66.0476	3.20	300362.94	7150943.24	22.8531	64.4254
3.9	392721.08	7306647.74	24.6485	65.8630	3.20	335801.46	7182142.79	23.5522	64.7238
3.9	434604.77	7253768.80	25.5921	65.4000	3.20	346700.12	7190043.62	23.7722	64.7997
3.9	383325.13	7216594.38	24.5204	65.0525	3.21	638217.79	6738276.46	29.5365	60.7560
3.9	345251.32	7253616.12	23.6713	65.3685	3.21	575225.24	6704344.16	28.3681	60.4683
3.9	310773.73	7280989.31	22.8934	65.5954	3.21	518056.31	6682156.56	27.3264	60.2757
3.9	313121.01	7327892.41	22.8775	66.0165	3.21	470858.85	6670199.82	26.4749	60.1677
3.10	394621.16	7420106.61	24.5945	66.8806	3.21	445108.19	6677500.58	26.0090	60.2306
3.10	424025.29	7402039.19	25.2767	66.7274	3.21	431390.39	6706380.44	25.7515	60.4877
3.10	437868.90	7383589.22	25.5999	66.5650	3.21	445154.07	6766214.04	25.9851	61.0269
3.10	389732.60	7327353.77	24.5655	66.0476	3.21	493217.49	6793735.86	26.8735	61.2778
3.10	313121.34	7327892.41	22.8775	66.0165	3.21	527613.39	6806303.59	27.5169	61.3897
3.10	394621.16	7420106.61	24.5945	66.8806	3.21	554501.59	6785041.44	28.0140	61.1960
3.11	287850.66	7428229.34	22.1508	66.8976	3.21	610295.85	6770584.77	29.0430	61.0546
3.11	311421.00	7459056.00	22.6382	67.1889	3.21	638217.79	6738276.46	29.5365	60.7560
3.11	363279.44	7514724.45	23.7679	67.7156					
3.11	453887.95	7602140.31	25.8712	68.5279					
3.11	506804.72	7570390.24	27.1645	68.2468					
3.11	443304.60	7499481.77	25.6664	67.6054					

3.11	394621.16	7420106.61	24.5945	66.8806
3.11	313121.34	7327892.41	22.8775	66.0165
3.11	253021.27	7328037.34	21.5578	65.9767
3.11	245016.07	7382554.88	21.2729	66.4571
3.11	287850.66	7428229.34	22.1508	66.8976
3.12	255540.56	7458421.00	21.3539	67.1429
3.12	233875.22	7466329.41	20.8389	67.1950
3.12	279912.82	7561579.60	21.7109	68.0833
3.12	303725.36	7621110.97	22.1687	68.6326
3.12	343412.94	7702073.63	23.0131	69.3821
3.12	404547.69	7787798.80	24.4771	70.1789
3.12	431399.55	7803844.90	25.1736	70.3313
3.12	483113.22	7777480.03	26.5554	70.1035
3.12	474469.24	7740586.71	26.3384	69.7720
3.12	431778.12	7690988.45	25.2688	69.3198
3.12	398215.48	7658729.72	24.4521	69.0202
3.12	380287.16	7611245.81	24.0608	68.5877
3.12	410173.24	7559966.23	24.8379	68.1393
3.12	363279.11	7514724.45	23.7679	67.7156
3.12	311420.67	7459056.00	22.6382	67.1889
3.12	292793.97	7453764.32	22.2186	67.1293
3.12	255540.56	7458421.00	21.3539	67.1429

ISSN 0357-3060
ISBN 978-952-10-9583-2 (PDF)
ISBN 978-952-10-5078-7 (Paperback)
Unigrafia
Helsinki 2015